Enclosure 4

Non-proprietary Reference Documents and Redacted Versions of Proprietary Reference Documents (Public Version)

(16 Attachments)

(558 Total Pages, including cover sheets)

Enclosure 4 Document List

Attachment 1 – Westinghouse Report LTR-REA-21-1-NP, Revision 1, St. Lucie Units 1 & 2 Subsequent License Renewal: Unit 1 Reactor Vessel, Vessel Support, and Bioshield Concrete Exposure Data, May 26, 2021

Attachment 2 – Westinghouse Report LTR-REA-21-2-NP, Revision 1, St. Lucie Units 1 & 2 Subsequent License Renewal: Unit 2 Reactor Vessel, Vessel Support, and Bioshield Concrete Exposure Data, June 7, 2021

Attachment 3 – Westinghouse Report LTR-SDA-21-021-NP, Revision 1, St. Lucie Units 1&2 Subsequent License Renewal: Reactor Pressure Vessel Supports Assessment, June 24, 2021

Attachment 4 – Westinghouse Report WCAP-18609-NP, Revision 2, St. Lucie Units 1 & 2 Subsequent License Renewal: Time-Limited Aging Analyses on Reactor Vessel Integrity, July 16, 2021

Attachment 5 – Westinghouse Report LTR-SDA-II-20-32-NP, Revision 3, St. Lucie Units 1 & 2 Subsequent License Renewal: 80-Year Projected Transient Cycles, July 15, 2021

Attachment 6 – Westinghouse Report LTR-SDA-II-20-31-NP, Rev. 2, St. Lucie Units 1 & 2 Subsequent License Renewal: Primary Equipment and Piping Environmentally Assisted Fatigue Evaluations, July 14, 2021

Attachment 7 – BWXT Report MSLEF-SR-01-NP, Revision 0, St. Lucie Unit 1 Replacement Steam Generator Environmentally Assisted Fatigue Report (Non-Proprietary), July 16, 2021

Attachment 8 – Framatome Document No. 86-9329647-000, St. Lucie SLR CUFen Evaluations Summary – Non Proprietary, July 15, 2021

Attachment 9 – Structural Integrity Report No. 2001262.403, Revision 0, Summary of Fatigue Usage for Charging Nozzle at St. Lucie, Units 1 and 2 for Subsequent License Renewal, June 25, 2021

Attachment 10 – Westinghouse Report WCAP-18617-NP, Revision 1, St. Lucie Units 1 & 2 Subsequent License Renewal: Technical Justification for Eliminating Large Primary Loop Pipe Rupture as the Structural Design Basis, June 3, 2021

Attachment 11 – Westinghouse Report LTR-SDA-20-097-NP, Revision 2, St. Lucie Units 1 & 2 Subsequent License Renewal: Alloy 600 Half Nozzle Repair Flaw Evaluation, May 5, 2021

Attachment 12 – Westinghouse Report LTR-SDA-20-104-NP, Rev. 2, St. Lucie Units 1&2 Subsequent License Renewal: Evaluation of Time-Limited Aging Analysis of the Reactor Vessel Internals, July 9, 2021

Attachment 13 – Westinghouse Report LTR-SDA-20-099-NP, Revision 1, St. Lucie Units 1&2 Subsequent License Renewal: Task 9E RCP Casing Code Case N-481 Evaluation, April 7, 2021

Attachment 14 – Structural Integrity Report No. 2001262.402, Revision 1, Flaw Tolerance Evaluation of St. Lucie Units 1 and 2 CASS Components for SLR, July 15, 2021

Attachment 15 – Framatome Document No. 86-9329648-000, St. Lucie SLR Crack Growth Analysis Summary - Non Proprietary, July 2, 2021

Attachment 16 – Structural Integrity Report No. 2001262.401, Revision 1, Flaw Tolerance Evaluation of St. Lucie, Units 1 and 2 Surge Line Using ASME Code, Section XI, Appendix L for Subsequent License Renewal, July 15, 2021

Enclosure 4

Non-proprietary Reference Documents and Redacted Versions of Proprietary Reference Documents (Public Version)

Attachment 1

Westinghouse Report LTR-REA-21-1-NP, Revision 1, St. Lucie Units 1 & 2 Subsequent License Renewal: Unit 1 Reactor Vessel, Vessel Support, and Bioshield Concrete Exposure Data,

May 26, 2021

(56 Total Pages, including cover sheets)

Westinghouse

To: John T. Ahearn Date: May 26, 2021
cc: Jay D. White

From: Radiation Engineering & Analysis (REA)
Phone: (412) 374-5851
Email: hawkae@westinghouse.com
Our Ref: **LTR-REA-21-1-NP, Revision 1**

Subject: **St. Lucie Units 1 & 2 Subsequent License Renewal: Unit 1 Reactor Vessel, Vessel Support, and Bioshield Concrete Exposure Data**

Attachment(s): 1. St. Lucie Units 1 & 2 Subsequent License Renewal: Unit 1 Reactor Vessel, Vessel Support, and Bioshield Concrete Exposure Data

Attachment 1 provides select exposure data applicable to the St. Lucie Unit 1 reactor pressure vessel (RPV), RPV support structure, concrete bioshield, and in-vessel dosimetry. These data are intended to be used in downstream evaluations of the RPV pressure-temperature limit (PT-limit) curves, RPV support structure embrittlement, and bioshield concrete degradation. In addition, the information in Attachment 1 needs to be provided to Florida Power and Light (FPL) in support of the St. Lucie subsequent license renewal (SLR) project.

Changes made in Revision 1 of this summary report are clearly identified in the document comment and resolution form (DCRF) that is electronically attached in PRIME and, as such, are not marked with change bars.

The information provided in Attachment 1 is applicable to St. Lucie Unit 1. Exposure data applicable to the St. Lucie Unit 2 RPV, RPV support structure, concrete bioshield, and in-vessel dosimetry will be provided in a separate summary report.

Please contact the undersigned if there are any questions regarding this information.

Author: *(Electronically Approved)**
Andrew E. Hawk
Radiation Engineering & Analysis

Reviewer: *(Electronically Approved)**
Greg A. Fischer
Radiation Engineering & Analysis

Approver: *(Electronically Approved)**
Jesse J Klingensmith
Radiation Engineering & Analysis

**Electronically approved records are authenticated in the electronic document management system.*

Attachment 1

St. Lucie Units 1 & 2 Subsequent License Renewal: Unit 1 Reactor Vessel, Vessel Support, and Bioshield Concrete Exposure Data

Table of Contents

1.0 Introduction 3
2.0 Discrete Ordinates Model 3
3.0 Dosimetry Comparisons 11
4.0 Exposure Results 13
4.1 Reactor Pressure Vessel 13
4.2 Surveillance Capsules 26
4.3 RPV Support Structure 35
4.4 Bioshield Concrete 46
5.0 References 53

1.0 Introduction

This attachment describes a discrete ordinates transport analysis that was performed for St. Lucie Unit 1. The results summarized in this attachment are intended to be used in downstream evaluations of the reactor pressure vessel (RPV) pressure-temperature limit (PT-limit) curves, RPV support structure embrittlement, and bioshield concrete degradation performed in support of the St. Lucie subsequent license renewal (SLR) project.

The neutron transport methodology used to generate the data provided in this attachment followed the guidance of Regulatory Guide 1.190 (Reference 1). It is also consistent with the methodology described in WCAP-18124-NP-A (Reference 2) that was approved by the United States Nuclear Regulatory Commission (USNRC). The methodology described Reference 2 has been generically approved for calculating exposures of the RPV beltline (i.e., in general, RPV materials opposite the active fuel). Presently, there are no generically-approved methods for calculating exposures of RPV extended beltline materials, RPV support structures, or bioshield concrete.

2.0 Discrete Ordinates Model

Discrete ordinates transport calculations were performed on a fuel-cycle-specific basis to determine the neutron and gamma ray environment within the reactor (and reactor cavity) geometry. The specific methods applied were consistent with those described in Reference 2.

All of the transport calculations were performed using the RAPTOR-M3G discrete ordinates computer code and the BUGLE-96 cross section library. The BUGLE-96 library provides a 67-group coupled neutron-gamma ray cross section data set produced specifically for light water reactor applications. The transport calculations treated anisotropic scattering with a P_3 Legendre expansion and modeled the angular discretization with an S_{16} order of angular quadrature. Energy- and space-dependent core power distributions as well as system operating temperatures were treated on a fuel-cycle-specific basis.

Top views of the model geometry at the core midplane with (applicable to Cycles 1–5) and without (applicable to Cycle 6 and beyond) a fully circumferential thermal shield are shown in Figure 2-1 and Figure 2-4. In these figures, a single quadrant is depicted showing the arrangement of the core, reactor internals, core barrel, downcomer, RPV cladding, RPV, reactor cavity, reflective insulation, RPV support structure, and bioshield. Depictions of the in-vessel surveillance capsules, including their associated support structures, are also shown.

From a neutronics standpoint, the inclusion of the surveillance capsules and associated support structures in the geometric model is significant. Since the presence of the capsules and support structures has a marked impact on the magnitude of the neutron fluence rate and relative neutron and gamma ray spectra at dosimetry locations within the capsules, a meaningful evaluation of the radiation environment internal to the capsules can be made only when these perturbation effects are accounted for in the transport calculations.

Top views of the reactor model geometry at the centerline of the inlet and outlet nozzles with (applicable to Cycles 1–5) and without (applicable to Cycle 6 and beyond) a fully circumferential thermal shield are shown in Figure 2-2 and Figure 2-5.

Oblique views of the model geometry with (applicable to Cycles 1–5) and without (applicable to Cycle 6 and beyond) a fully circumferential thermal shield are shown in Figure 2-3 and Figure 2-6. Note that the stainless steel girth ribs located between the core shroud and barrel regions are shown in these figures. The RPV support structure located between the reflective insulation and bioshield is also shown.

When developing the reactor model shown in Figure 2-1 through Figure 2-6, nominal dimensions were typically used for the various structural components. One significant exception to this was the RPV inner radius, where as-built dimensions (which were significantly different than the reference design dimensions) were used.

Water temperatures and coolant densities in the core and downcomer regions of the reactor were taken to be representative of full-power operating conditions. Coolant above the core was assumed to be at core outlet conditions and coolant below the active core was assumed to be at core inlet conditions. All coolant temperatures and densities were varied on a cycle-specific basis. The reactor core itself was treated as a homogeneous mixture of fuel, cladding, water, and miscellaneous core structures such as fuel assembly grids and guide tubes.

The geometric mesh description of the reactor models shown in Figure 2-1 through Figure 2-6 consisted of 323 radial by 203 azimuthal by 406 axial intervals. Mesh sizes were chosen to ensure sufficient resolution of the stair-step-shaped shroud plates and a sufficient number of meshes throughout the radial and axial regions of interest. The pointwise inner iteration convergence criterion utilized in the calculations was set at a value of 0.001.

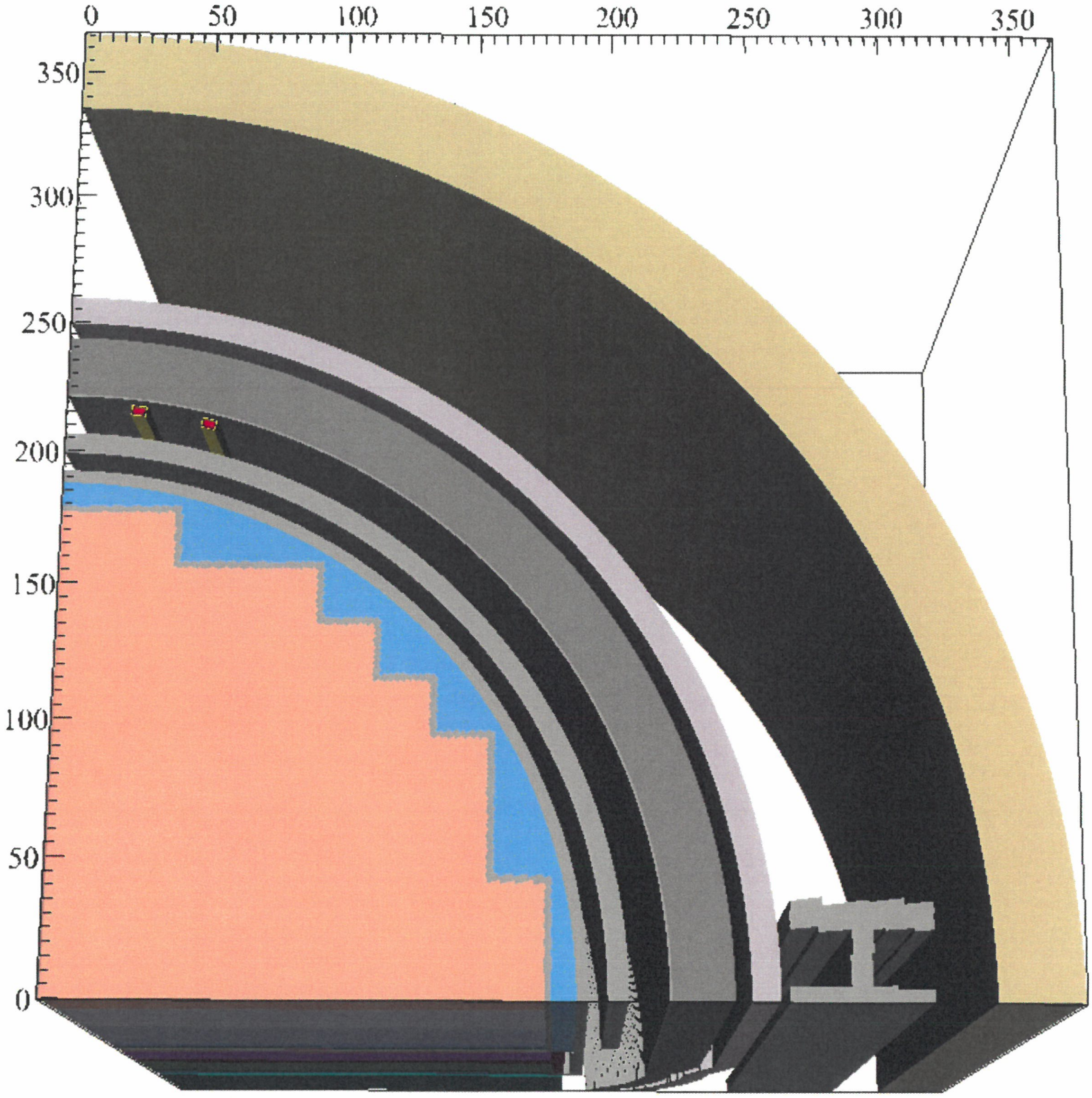

Dimensions shown are in centimeters.

Figure 2-1
Top View of the Reactor Geometry at the Core Midplane – with Thermal Shield (Cycles 1–5)

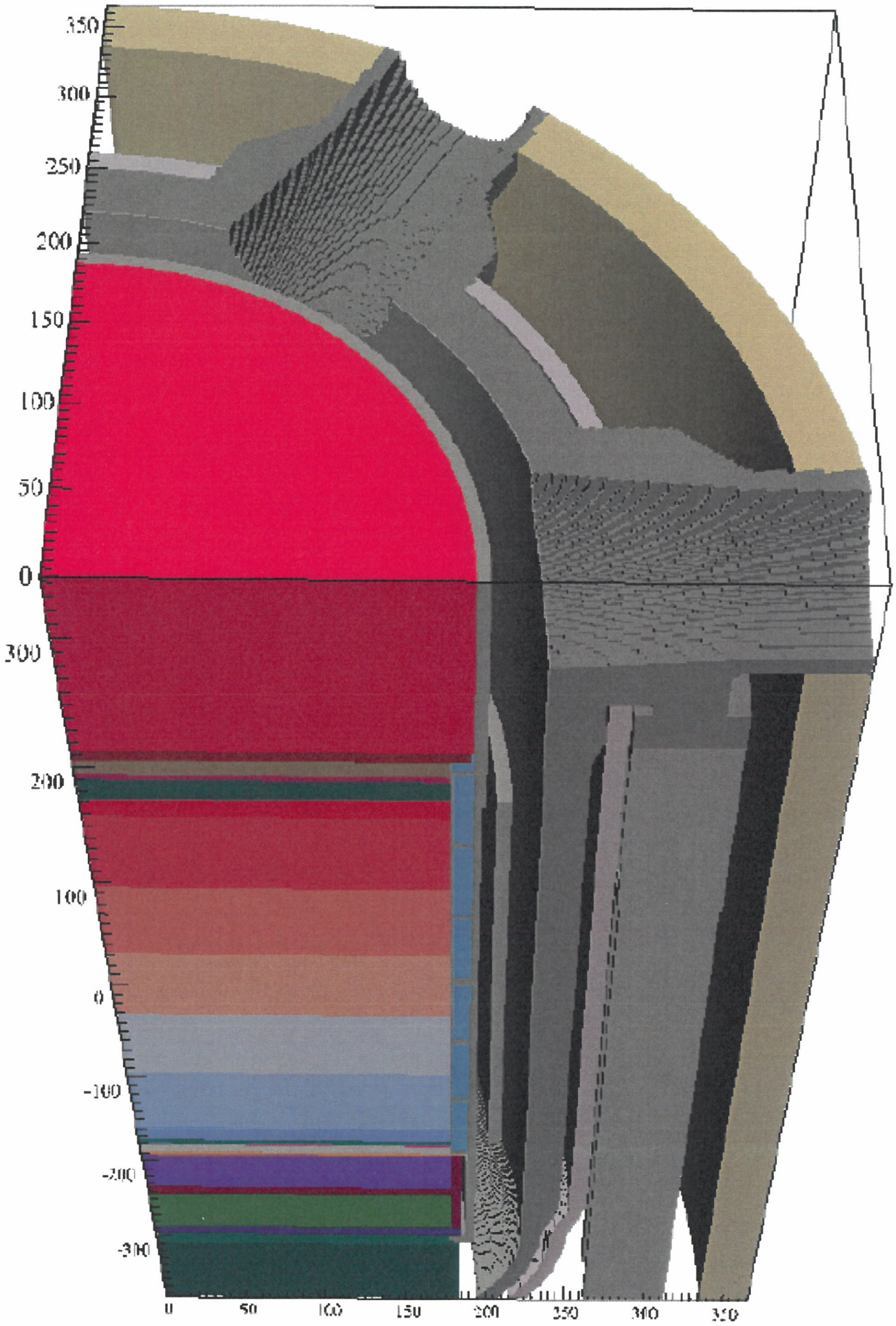

Dimensions shown are in centimeters.

Figure 2-2
Top View of the Reactor Geometry at the Nozzle Centerline – with Thermal Shield (Cycles 1–5)

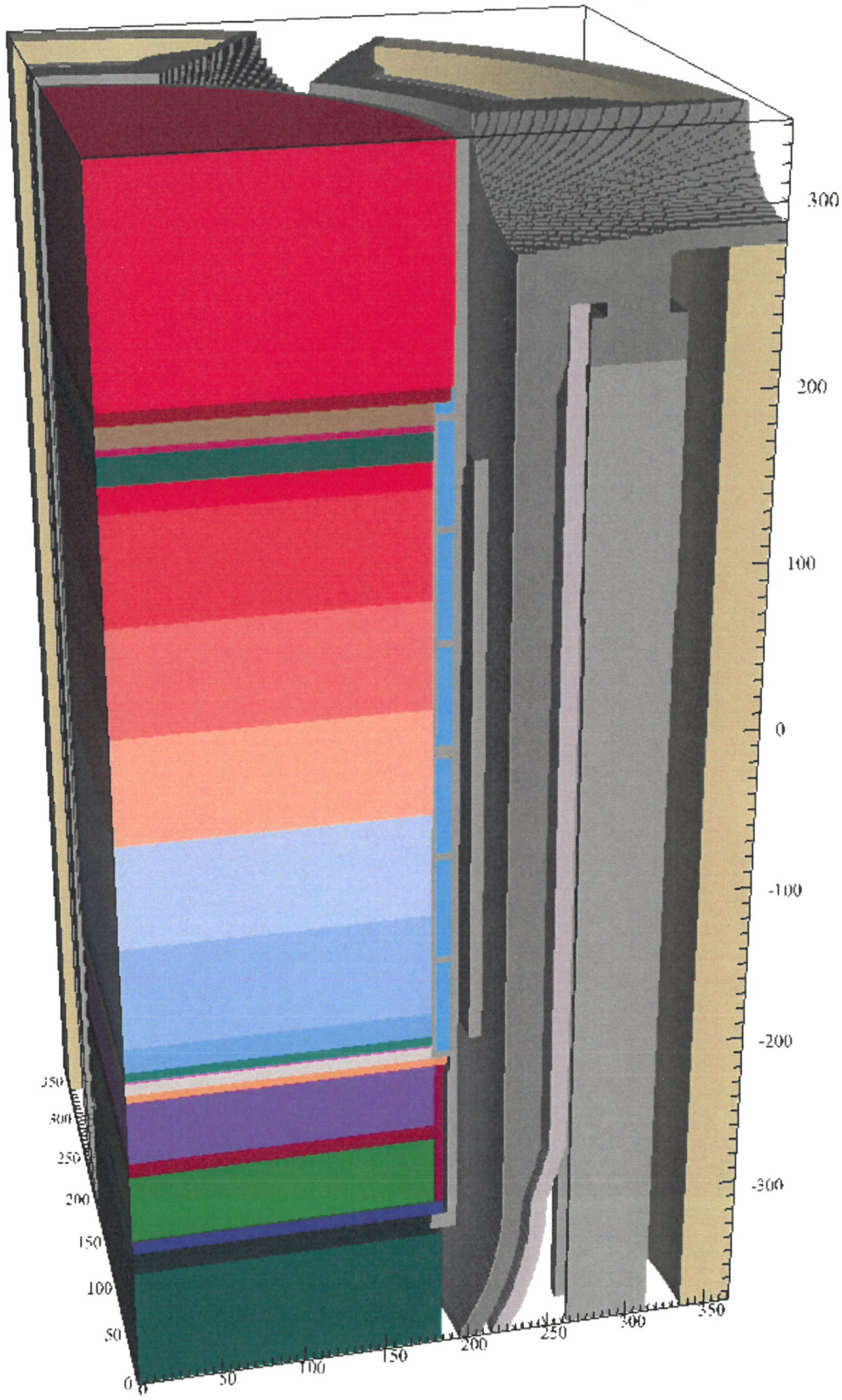

Dimensions shown are in centimeters.

Figure 2-3
Oblique View of the Reactor Geometry – with Thermal Shield (Cycles 1–5)

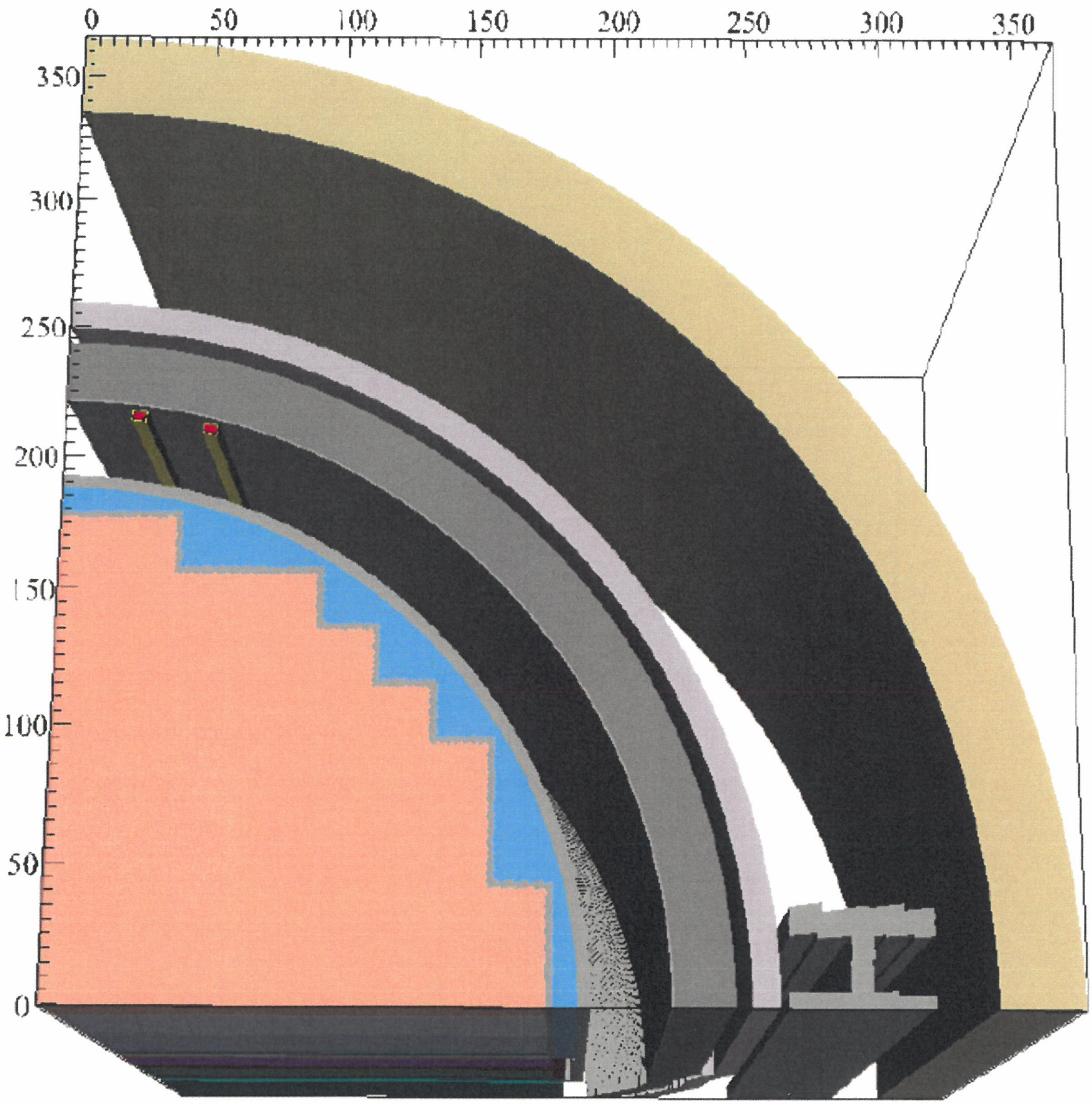

Dimensions shown are in centimeters.

Figure 2-4
Top View of the Reactor Geometry at the Core Midplane – Without Thermal Shield (Cycles 6+)

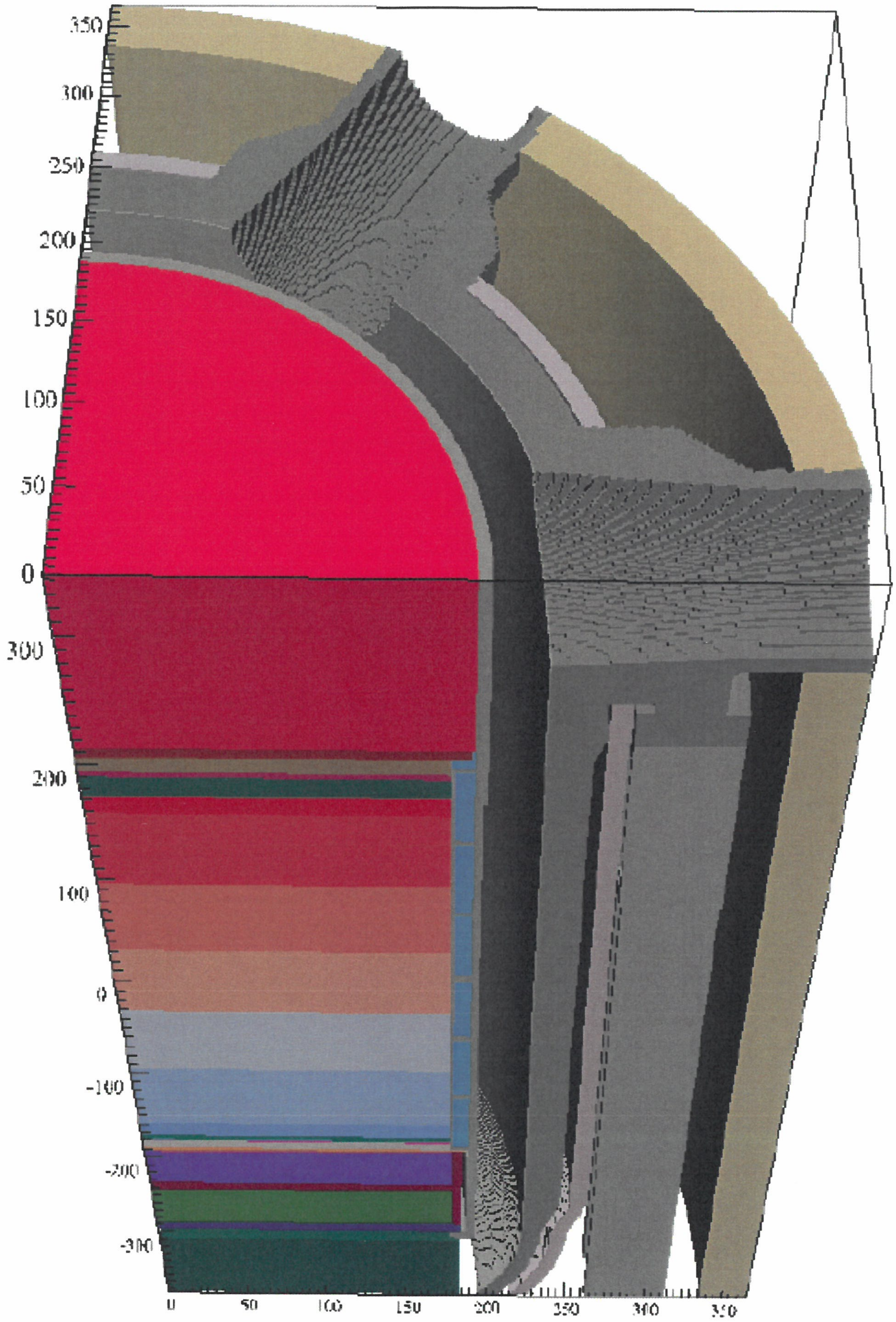

Dimensions shown are in centimeters.

Figure 2-5
Top View of the Reactor Geometry at the Nozzle Centerline – Without Thermal Shield (Cycles 6+)

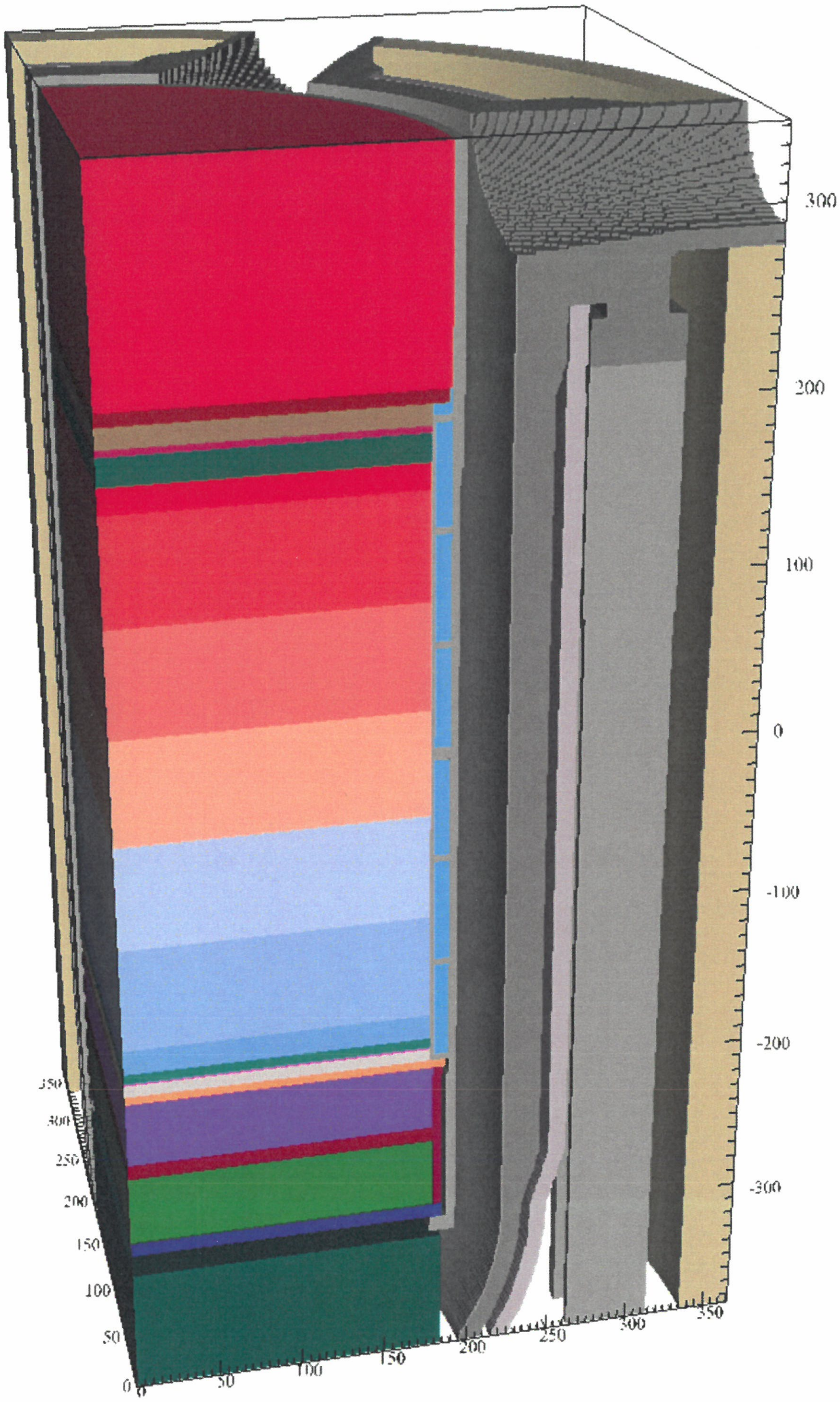

Dimensions shown are in centimeters.

Figure 2-6
Oblique View of the Reactor Geometry – Without Thermal Shield (Cycles 6+)

3.0 Dosimetry Comparisons

Six surveillance capsules for monitoring the effects of neutron exposure on the RPV core region (beltline) materials were inserted in the reactor vessel prior to initial plant startup. These capsules were placed in the reactor vessel, between the core barrel and the vessel wall, at azimuthal angles of 83°, 97°, 263°, and 277° (7° from the core cardinal axis) and 104° and 284° (14° from the core cardinal axis).

To date, the following in-vessel surveillance capsules have been withdrawn from reactor core and analyzed as part of the reactor vessel materials surveillance program:

- Capsule 97 was withdrawn from the 97° location following the completion of Cycle 5.
- Capsule 104 was withdrawn from the 104° location following the completion of Cycle 9.
- Capsule 284 was withdrawn from the 284° location following the completion of Cycle 15.

These capsules were re-analyzed to validate the results of the plant-specific neutron transport calculations. More specifically, the Capsule 97, 104, and 284 threshold sensor measurements were compared with the applicable results of the RAPTOR-M3G calculations to demonstrate that, at the in-vessel locations where the sensors were irradiated, the measurements and calculations agreed within the ±20% criterion of Reference 1. These measurement and calculation comparisons were performed on two levels. On the first level, calculations of individual sensor reaction rates were compared directly with the measurement data from the counting laboratory. This level of comparison was not impacted by the least-squares evaluation of the sensor sets. On the second level, calculated values of neutron exposure rates in terms of fast neutron (E > 1.0 MeV) fluence rate and iron atom displacement rate were compared with the best-estimate exposure rates obtained from the least-squares evaluation.

Table 3-1 provides comparisons of the measurement-to-calculation (M/C) ratios for the neutron dosimetry in the in-vessel surveillance capsules. For the individual threshold foils, the M/C ratios range from 0.75 to 1.40, with an overall average of 1.07 and standard deviation of 16.1%. In this case, the overall average was based on an equal weighting of each of the sensor types with no adjustments made to account for the spectral coverage of the individual sensors.

Table 3-2 provides comparisons of the best-estimate-to-calculation (BE/C) ratios for fast neutron (E > 1.0 MeV) fluence rate and iron atom displacement rate resulting from the least-squares evaluation of the neutron dosimetry in the in-vessel surveillance capsules. For these capsules, the average BE/C ratios are 1.00 with an associated standard deviation of 14.8% for fast neutron (E > 1.0 MeV) fluence rate, and 1.01 with an associated standard deviation of 13.7% for iron atom displacement rate.

The M/C and BE/C data comparisons in Table 3-1 and Table 3-2 provide a validation of the results of the plant-specific neutron transport calculations. Each of these data comparisons shows that the in-vessel measurements and calculations agree within the 20% criterion specified in Reference 1. In addition, the average M/C and BE/C results agree within the 13% (1σ) uncertainty assigned to the absolute transport calculations.

Table 3-1
Measurement-to-Calculation (M/C) Ratios for the Surveillance Capsules

Reaction	Capsule			Average	Std. Dev.
	97	104	284		
$^{63}Cu\ (n,\alpha)\ ^{60}Co$	1.40	1.11	1.17	1.23	12.5%
$^{46}Ti\ (n,p)\ ^{46}Sc$	1.22	0.96	--[1]	1.09	16.9%
$^{54}Fe\ (n,p)\ ^{54}Mn$	1.10	0.89	1.05	1.01	10.8%
$^{58}Ni\ (n,p)\ ^{58}Co$	1.14	0.85	1.15	1.05	16.3%
$^{238}U(Cd)\ (n,f)\ ^{137}Cs$	1.17	0.75	--[2]	0.96	30.9%
Average of M/C Ratios				1.07	16.1%

Note(s):

1. The normalized reaction rate for this sensor was not within three standard deviations of the Combustion Engineering (CE) in-vessel surveillance capsule database value. This sensor was therefore rejected.
2. The uranium powder in this fission monitor was contaminated with cadmium powder and could not be counted. This is not unusual for the type of surveillance capsules used at St. Lucie.

Table 3-2
Best-Estimate-to-Calculation (BE/C) Ratios for the Surveillance Capsules

Capsule	Fast (E > 1.0 MeV) Fluence Rate		Iron Atom Displacement Rate	
	BE/C	Std. Dev.	BE/C	Std. Dev.
97	1.09	6.0%	1.10	6.0%
104	0.83	6.0%	0.85	6.0%
284	1.08	7.0%	1.08	6.0%
Average	1.00	14.8%	1.01	13.7%

4.0 Exposure Results

4.1 Reactor Pressure Vessel

Neutron exposure data for the RPV at the clad/base metal interface are provided in Table 4-1 through Table 4-4. In particular, fast neutron (E > 1.0 MeV) fluence rates and fluences determined at the RPV clad/base metal interface are provided in Table 4-1 and Table 4-2 as a function of irradiation time. Similar data in terms of iron atom displacement rates (dpa/s) and iron atom displacements (dpa) are provided in Table 4-3 and Table 4-4.

Fast neutron (E > 1.0 MeV) fluence and iron atom displacement projections for the RPV welds and shells are provided in Table 4-5 and Table 4-6. The neutron exposure data provided in Table 4-5 and Table 4-6 are the maximum values at either the RPV clad/base metal interface or the RPV outer surface. Note that for regions and materials above and below the core (e.g., the inlet-nozzle-to-upper-shell weld and lower-shell-to-bottom-head circumferential weld), the neutron exposure values at the RPV outer surface can be greater than those at the clad/base metal interface (Reference 3).

Table 4-1
Fast Neutron (E > 1.0 MeV) Fluence Rate at the RPV Clad/Base Metal Interface

Cycle	Cycle Length (EFPY)	Cumulative Operating Time (EFPY)	Fast Neutron (E > 1.0 MeV) Fluence Rate (n/cm^2-s)							
			0°	15°	30°	45°	60°	75°	90°	Maximum
1	1.05	1.05	2.48E+10	1.51E+10	1.46E+10	1.08E+10	1.47E+10	1.48E+10	2.48E+10	2.48E+10
2	0.74	1.79	2.48E+10	1.51E+10	1.46E+10	1.08E+10	1.47E+10	1.48E+10	2.48E+10	2.48E+10
3	0.69	2.48	2.48E+10	1.51E+10	1.46E+10	1.08E+10	1.47E+10	1.48E+10	2.48E+10	2.48E+10
4	1.22	3.70	2.48E+10	1.51E+10	1.46E+10	1.08E+10	1.47E+10	1.48E+10	2.48E+10	2.48E+10
5	1.12	4.82	2.54E+10	1.32E+10	1.11E+10	7.89E+09	1.12E+10	1.29E+10	2.55E+10	2.55E+10
6	1.36	6.18	3.58E+10	2.04E+10	1.70E+10	1.25E+10	1.72E+10	1.98E+10	3.58E+10	3.58E+10
7	1.05	7.22	3.58E+10	2.04E+10	1.70E+10	1.25E+10	1.72E+10	1.98E+10	3.58E+10	3.58E+10
8	1.18	8.41	3.58E+10	2.04E+10	1.70E+10	1.25E+10	1.72E+10	1.98E+10	3.58E+10	3.58E+10
9	1.29	9.70	3.58E+10	2.04E+10	1.70E+10	1.25E+10	1.72E+10	1.98E+10	3.58E+10	3.58E+10
10	1.31	11.01	1.89E+10	1.48E+10	1.72E+10	1.32E+10	1.73E+10	1.44E+10	1.89E+10	1.89E+10
11	1.21	12.22	1.60E+10	1.29E+10	1.83E+10	1.36E+10	1.83E+10	1.26E+10	1.60E+10	1.89E+10
12	1.27	13.48	1.99E+10	1.51E+10	2.01E+10	1.43E+10	2.04E+10	1.49E+10	2.00E+10	2.10E+10
13	1.14	14.62	1.69E+10	1.31E+10	1.73E+10	1.33E+10	1.75E+10	1.29E+10	1.69E+10	1.81E+10
14	1.18	15.80	1.85E+10	1.44E+10	1.73E+10	1.35E+10	1.74E+10	1.41E+10	1.85E+10	1.85E+10
15	1.62	17.42	2.26E+10	1.51E+10	1.26E+10	1.01E+10	1.25E+10	1.46E+10	2.27E+10	2.27E+10
16	1.44	18.86	2.27E+10	1.49E+10	1.47E+10	1.28E+10	1.47E+10	1.45E+10	2.27E+10	2.27E+10
17	1.39	20.26	1.88E+10	1.33E+10	1.22E+10	1.13E+10	1.22E+10	1.29E+10	1.88E+10	1.88E+10
18	1.40	21.66	2.11E+10	1.34E+10	1.28E+10	1.09E+10	1.29E+10	1.30E+10	2.11E+10	2.11E+10
19	1.42	23.08	2.00E+10	1.33E+10	1.25E+10	1.12E+10	1.26E+10	1.29E+10	1.99E+10	2.00E+10
20	1.27	24.35	2.16E+10	1.46E+10	1.23E+10	1.11E+10	1.23E+10	1.41E+10	2.13E+10	2.16E+10
21	1.38	25.73	2.18E+10	1.43E+10	1.13E+10	1.02E+10	1.14E+10	1.37E+10	2.16E+10	2.18E+10
22	1.35	27.08	2.40E+10	1.53E+10	1.14E+10	1.03E+10	1.15E+10	1.47E+10	2.39E+10	2.40E+10
23	1.31	28.39	2.38E+10	1.56E+10	1.31E+10	1.15E+10	1.32E+10	1.51E+10	2.37E+10	2.38E+10
24	1.29	29.67	2.81E+10	1.72E+10	1.57E+10	1.39E+10	1.60E+10	1.66E+10	2.81E+10	2.81E+10
25	1.33	31.00	3.16E+10	1.96E+10	1.58E+10	1.36E+10	1.59E+10	1.91E+10	3.18E+10	3.18E+10
26	1.33	32.33	3.13E+10	1.94E+10	1.68E+10	1.47E+10	1.69E+10	1.88E+10	3.13E+10	3.13E+10

Table 4-1
Fast Neutron (E > 1.0 MeV) Fluence Rate at the RPV Clad/Base Metal Interface

Cycle	Cycle Length (EFPY)	Cumulative Operating Time (EFPY)	Fast Neutron (E > 1.0 MeV) Fluence Rate (n/cm^2-s)							
			0°	15°	30°	45°	60°	75°	90°	Maximum
27	1.30	33.64	2.96E+10	1.73E+10	1.29E+10	1.05E+10	1.32E+10	1.68E+10	2.97E+10	2.97E+10
28	1.30	34.94	2.59E+10	1.64E+10	1.42E+10	1.27E+10	1.41E+10	1.59E+10	2.59E+10	2.59E+10
29	1.37	36.31	2.89E+10	1.72E+10	1.34E+10	1.19E+10	1.35E+10	1.66E+10	2.90E+10	2.90E+10
30[1]	1.35	37.66	2.83E+10	1.71E+10	1.41E+10	1.27E+10	1.43E+10	1.66E+10	2.83E+10	2.83E+10

Note(s):

1. Cycle 30 was the current operating cycle at the time the exposures reported in this table were determined. Values listed are based on the projected EFPY for this cycle.

Table 4-2
Fast Neutron (E > 1.0 MeV) Fluence at the RPV Clad/Base Metal Interface

Cycle	Cycle Length (EFPY)	Cumulative Operating Time (EFPY)	Fast Neutron (E > 1.0 MeV) Fluence (n/cm^2)							
			0°	15°	30°	45°	60°	75°	90°	Maximum
1	1.05	1.05	8.23E+17	5.01E+17	4.83E+17	3.57E+17	4.87E+17	4.92E+17	8.24E+17	8.24E+17
2	0.74	1.79	1.40E+18	8.53E+17	8.21E+17	6.07E+17	8.29E+17	8.36E+17	1.40E+18	1.40E+18
3	0.69	2.48	1.94E+18	1.18E+18	1.14E+18	8.42E+17	1.15E+18	1.16E+18	1.94E+18	1.94E+18
4	1.22	3.70	2.90E+18	1.77E+18	1.70E+18	1.26E+18	1.72E+18	1.73E+18	2.90E+18	2.90E+18
5	1.12	4.82	3.77E+18	2.22E+18	2.08E+18	1.53E+18	2.10E+18	2.18E+18	3.78E+18	3.78E+18
6	1.36	6.18	5.29E+18	3.08E+18	2.80E+18	2.06E+18	2.83E+18	3.01E+18	5.29E+18	5.29E+18
7	1.05	7.22	6.46E+18	3.75E+18	3.36E+18	2.47E+18	3.39E+18	3.66E+18	6.46E+18	6.46E+18
8	1.18	8.41	7.78E+18	4.50E+18	3.98E+18	2.93E+18	4.02E+18	4.39E+18	7.78E+18	7.78E+18
9	1.29	9.70	9.23E+18	5.32E+18	4.67E+18	3.44E+18	4.72E+18	5.19E+18	9.24E+18	9.24E+18
10	1.31	11.01	1.00E+19	5.93E+18	5.38E+18	3.98E+18	5.43E+18	5.78E+18	1.00E+19	1.00E+19
11	1.21	12.22	1.06E+19	6.42E+18	6.08E+18	4.50E+18	6.13E+18	6.26E+18	1.06E+19	1.06E+19
12	1.27	13.48	1.14E+19	7.01E+18	6.86E+18	5.06E+18	6.93E+18	6.84E+18	1.14E+19	1.14E+19
13	1.14	14.62	1.20E+19	7.49E+18	7.49E+18	5.54E+18	7.56E+18	7.31E+18	1.20E+19	1.20E+19
14	1.18	15.80	1.27E+19	8.02E+18	8.13E+18	6.04E+18	8.20E+18	7.83E+18	1.27E+19	1.27E+19
15	1.62	17.42	1.38E+19	8.80E+18	8.77E+18	6.56E+18	8.84E+18	8.58E+18	1.39E+19	1.39E+19
16	1.44	18.86	1.49E+19	9.47E+18	9.44E+18	7.14E+18	9.51E+18	9.24E+18	1.49E+19	1.49E+19
17	1.39	20.26	1.57E+19	1.01E+19	9.97E+18	7.64E+18	1.01E+19	9.81E+18	1.57E+19	1.57E+19
18	1.40	21.66	1.66E+19	1.07E+19	1.05E+19	8.12E+18	1.06E+19	1.04E+19	1.66E+19	1.66E+19
19	1.42	23.08	1.75E+19	1.12E+19	1.11E+19	8.62E+18	1.12E+19	1.10E+19	1.75E+19	1.75E+19
20	1.27	24.35	1.84E+19	1.18E+19	1.16E+19	9.06E+18	1.17E+19	1.15E+19	1.84E+19	1.84E+19
21	1.38	25.73	1.93E+19	1.25E+19	1.21E+19	9.51E+18	1.22E+19	1.21E+19	1.93E+19	1.93E+19
22	1.35	27.08	2.04E+19	1.31E+19	1.26E+19	9.95E+18	1.27E+19	1.27E+19	2.04E+19	2.04E+19
23	1.31	28.39	2.13E+19	1.37E+19	1.31E+19	1.04E+19	1.32E+19	1.34E+19	2.13E+19	2.13E+19
24	1.29	29.67	2.25E+19	1.44E+19	1.38E+19	1.10E+19	1.39E+19	1.40E+19	2.25E+19	2.25E+19
25	1.33	31.00	2.38E+19	1.53E+19	1.44E+19	1.16E+19	1.45E+19	1.48E+19	2.38E+19	2.38E+19
26	1.33	32.33	2.51E+19	1.61E+19	1.51E+19	1.22E+19	1.52E+19	1.56E+19	2.51E+19	2.51E+19

Table 4-2
Fast Neutron (E > 1.0 MeV) Fluence at the RPV Clad/Base Metal Interface

Cycle	Cycle Length (EFPY)	Cumulative Operating Time (EFPY)	Fast Neutron (E > 1.0 MeV) Fluence (n/cm^2)							
			0°	15°	30°	45°	60°	75°	90°	Maximum
27	1.30	33.64	2.63E+19	1.68E+19	1.57E+19	1.26E+19	1.58E+19	1.63E+19	2.63E+19	2.63E+19
28	1.30	34.94	2.74E+19	1.75E+19	1.62E+19	1.31E+19	1.64E+19	1.70E+19	2.74E+19	2.74E+19
29	1.37	36.31	2.87E+19	1.82E+19	1.68E+19	1.36E+19	1.69E+19	1.77E+19	2.87E+19	2.87E+19
30[1]	1.35	37.66	2.99E+19	1.89E+19	1.74E+19	1.42E+19	1.75E+19	1.84E+19	2.99E+19	2.99E+19
Projections with no bias on the peripheral and re-entrant corner assembly relative powers										
Future[2]	--	42.00	3.38E+19	2.13E+19	1.93E+19	1.58E+19	1.94E+19	2.07E+19	3.38E+19	3.38E+19
Future[2]	--	48.00	3.93E+19	2.45E+19	2.18E+19	1.81E+19	2.20E+19	2.38E+19	3.93E+19	3.93E+19
Future[2]	--	54.00	4.48E+19	2.78E+19	2.44E+19	2.03E+19	2.45E+19	2.69E+19	4.48E+19	4.48E+19
Future[2]	--	60.00	5.03E+19	3.10E+19	2.69E+19	2.25E+19	2.71E+19	3.01E+19	5.03E+19	5.03E+19
Future[2]	--	66.00	5.58E+19	3.43E+19	2.94E+19	2.48E+19	2.96E+19	3.32E+19	5.58E+19	5.58E+19
Future[2]	--	72.00	6.12E+19	3.75E+19	3.20E+19	2.70E+19	3.22E+19	3.64E+19	6.12E+19	6.12E+19
Projections with a +10% bias on the peripheral and re-entrant corner assembly relative powers										
Future[2]	--	42.00	3.41E+19	2.15E+19	1.94E+19	1.60E+19	1.96E+19	2.09E+19	3.41E+19	3.41E+19
Future[2]	--	48.00	4.01E+19	2.50E+19	2.22E+19	1.84E+19	2.23E+19	2.43E+19	4.01E+19	4.01E+19
Future[2]	--	54.00	4.60E+19	2.85E+19	2.50E+19	2.08E+19	2.51E+19	2.76E+19	4.60E+19	4.60E+19
Future[2]	--	60.00	5.19E+19	3.20E+19	2.77E+19	2.33E+19	2.79E+19	3.10E+19	5.19E+19	5.19E+19
Future[2]	--	66.00	5.78E+19	3.55E+19	3.05E+19	2.57E+19	3.07E+19	3.44E+19	5.79E+19	5.79E+19
Future[2]	--	72.00	6.38E+19	3.91E+19	3.33E+19	2.82E+19	3.34E+19	3.78E+19	6.38E+19	6.38E+19

Note(s):

1. Cycle 30 was the current operating cycle at the time the exposures reported in this table were determined. Values listed are based on the projected EFPY for this cycle.
2. Values beyond Cycle 30 are based on the average core power distributions and reactor operating conditions of Cycle 29 and are determined both with and without a 1.1 bias on the peripheral and re-entrant corner assembly relative powers.

Table 4-3
Iron Atom Displacement Rate at the RPV Clad/Base Metal Interface

Cycle	Cycle Length (EFPY)	Cumulative Operating Time (EFPY)	Iron Atom Displacement Rate (dpa/s)							
			0°	15°	30°	45°	60°	75°	90°	Maximum
1	1.05	1.05	3.93E-11	2.41E-11	2.30E-11	1.71E-11	2.32E-11	2.39E-11	3.92E-11	3.93E-11
2	0.74	1.79	3.93E-11	2.41E-11	2.30E-11	1.71E-11	2.32E-11	2.39E-11	3.92E-11	3.93E-11
3	0.69	2.48	3.93E-11	2.41E-11	2.30E-11	1.71E-11	2.32E-11	2.39E-11	3.92E-11	3.93E-11
4	1.22	3.70	3.93E-11	2.41E-11	2.30E-11	1.71E-11	2.32E-11	2.39E-11	3.92E-11	3.93E-11
5	1.12	4.82	4.02E-11	2.11E-11	1.75E-11	1.25E-11	1.77E-11	2.09E-11	4.01E-11	4.02E-11
6	1.36	6.18	5.46E-11	3.14E-11	2.60E-11	1.94E-11	2.63E-11	3.06E-11	5.45E-11	5.46E-11
7	1.05	7.22	5.46E-11	3.14E-11	2.60E-11	1.94E-11	2.63E-11	3.06E-11	5.45E-11	5.46E-11
8	1.18	8.41	5.46E-11	3.14E-11	2.60E-11	1.94E-11	2.63E-11	3.06E-11	5.45E-11	5.46E-11
9	1.29	9.70	5.46E-11	3.14E-11	2.60E-11	1.94E-11	2.63E-11	3.06E-11	5.45E-11	5.46E-11
10	1.31	11.01	2.89E-11	2.28E-11	2.63E-11	2.03E-11	2.64E-11	2.22E-11	2.88E-11	2.89E-11
11	1.21	12.22	2.45E-11	1.99E-11	2.79E-11	2.09E-11	2.80E-11	1.96E-11	2.44E-11	2.89E-11
12	1.27	13.48	3.04E-11	2.33E-11	3.07E-11	2.21E-11	3.10E-11	2.30E-11	3.04E-11	3.21E-11
13	1.14	14.62	2.58E-11	2.03E-11	2.65E-11	2.04E-11	2.67E-11	2.00E-11	2.58E-11	2.76E-11
14	1.18	15.80	2.83E-11	2.22E-11	2.64E-11	2.08E-11	2.66E-11	2.19E-11	2.83E-11	2.83E-11
15	1.62	17.42	3.47E-11	2.33E-11	1.93E-11	1.56E-11	1.91E-11	2.26E-11	3.46E-11	3.47E-11
16	1.44	18.86	3.47E-11	2.30E-11	2.24E-11	1.97E-11	2.26E-11	2.24E-11	3.46E-11	3.47E-11
17	1.39	20.26	2.88E-11	2.04E-11	1.86E-11	1.74E-11	1.87E-11	1.99E-11	2.87E-11	2.88E-11
18	1.40	21.66	3.22E-11	2.07E-11	1.96E-11	1.68E-11	1.97E-11	2.01E-11	3.22E-11	3.22E-11
19	1.42	23.08	3.06E-11	2.06E-11	1.91E-11	1.72E-11	1.94E-11	2.00E-11	3.04E-11	3.06E-11
20	1.27	24.35	3.30E-11	2.25E-11	1.89E-11	1.71E-11	1.88E-11	2.17E-11	3.25E-11	3.30E-11
21	1.38	25.73	3.33E-11	2.19E-11	1.74E-11	1.57E-11	1.75E-11	2.13E-11	3.29E-11	3.33E-11
22	1.35	27.08	3.67E-11	2.35E-11	1.75E-11	1.59E-11	1.76E-11	2.28E-11	3.65E-11	3.67E-11
23	1.31	28.39	3.64E-11	2.40E-11	2.01E-11	1.77E-11	2.03E-11	2.33E-11	3.62E-11	3.64E-11
24	1.29	29.67	4.30E-11	2.64E-11	2.40E-11	2.14E-11	2.45E-11	2.58E-11	4.28E-11	4.30E-11
25	1.33	31.00	4.84E-11	3.02E-11	2.42E-11	2.09E-11	2.43E-11	2.95E-11	4.84E-11	4.84E-11
26	1.33	32.33	4.78E-11	2.98E-11	2.57E-11	2.27E-11	2.59E-11	2.90E-11	4.77E-11	4.78E-11

Table 4-3
Iron Atom Displacement Rate at the RPV Clad/Base Metal Interface

Cycle	Cycle Length (EFPY)	Cumulative Operating Time (EFPY)	Iron Atom Displacement Rate (dpa/s)							
			0°	15°	30°	45°	60°	75°	90°	Maximum
27	1.30	33.64	4.52E-11	2.66E-11	1.98E-11	1.62E-11	2.02E-11	2.60E-11	4.52E-11	4.52E-11
28	1.30	34.94	3.97E-11	2.53E-11	2.18E-11	1.95E-11	2.16E-11	2.46E-11	3.96E-11	3.97E-11
29	1.37	36.31	4.42E-11	2.64E-11	2.06E-11	1.83E-11	2.07E-11	2.57E-11	4.41E-11	4.42E-11
30[1]	1.35	37.66	4.32E-11	2.63E-11	2.16E-11	1.96E-11	2.19E-11	2.57E-11	4.31E-11	4.32E-11

Note(s):

1. Cycle 30 was the current operating cycle at the time the exposures reported in this table were determined. Values listed are based on the projected EFPY for this cycle.

Table 4-4
Iron Atom Displacements at the RPV Clad/Base Metal Interface

Cycle	Cycle Length (EFPY)	Cumulative Operating Time (EFPY)	Iron Atom Displacements (dpa)							
			0°	15°	30°	45°	60°	75°	90°	Maximum
1	1.05	1.05	1.30E-03	7.99E-04	7.63E-04	5.66E-04	7.69E-04	7.93E-04	1.30E-03	1.30E-03
2	0.74	1.79	2.21E-03	1.36E-03	1.30E-03	9.63E-04	1.31E-03	1.35E-03	2.21E-03	2.21E-03
3	0.69	2.48	3.07E-03	1.88E-03	1.80E-03	1.34E-03	1.81E-03	1.87E-03	3.06E-03	3.07E-03
4	1.22	3.70	4.59E-03	2.81E-03	2.68E-03	1.99E-03	2.71E-03	2.79E-03	4.58E-03	4.59E-03
5	1.12	4.82	5.98E-03	3.54E-03	3.29E-03	2.43E-03	3.32E-03	3.51E-03	5.97E-03	5.98E-03
6	1.36	6.18	8.29E-03	4.87E-03	4.39E-03	3.24E-03	4.43E-03	4.81E-03	8.27E-03	8.29E-03
7	1.05	7.22	1.01E-02	5.90E-03	5.24E-03	3.88E-03	5.29E-03	5.81E-03	1.00E-02	1.01E-02
8	1.18	8.41	1.21E-02	7.06E-03	6.20E-03	4.59E-03	6.26E-03	6.94E-03	1.21E-02	1.21E-02
9	1.29	9.70	1.43E-02	8.32E-03	7.25E-03	5.37E-03	7.32E-03	8.18E-03	1.43E-02	1.43E-02
10	1.31	11.01	1.55E-02	9.26E-03	8.34E-03	6.21E-03	8.41E-03	9.09E-03	1.54E-02	1.55E-02
11	1.21	12.22	1.64E-02	1.00E-02	9.40E-03	7.01E-03	9.48E-03	9.84E-03	1.64E-02	1.64E-02
12	1.27	13.48	1.76E-02	1.09E-02	1.06E-02	7.87E-03	1.07E-02	1.07E-02	1.76E-02	1.76E-02
13	1.14	14.62	1.85E-02	1.17E-02	1.16E-02	8.61E-03	1.17E-02	1.15E-02	1.85E-02	1.85E-02
14	1.18	15.80	1.96E-02	1.25E-02	1.25E-02	9.38E-03	1.26E-02	1.23E-02	1.95E-02	1.96E-02
15	1.62	17.42	2.14E-02	1.37E-02	1.35E-02	1.02E-02	1.36E-02	1.34E-02	2.13E-02	2.14E-02
16	1.44	18.86	2.29E-02	1.47E-02	1.45E-02	1.11E-02	1.46E-02	1.45E-02	2.29E-02	2.29E-02
17	1.39	20.26	2.42E-02	1.56E-02	1.54E-02	1.18E-02	1.55E-02	1.53E-02	2.41E-02	2.42E-02
18	1.40	21.66	2.56E-02	1.65E-02	1.62E-02	1.26E-02	1.63E-02	1.62E-02	2.56E-02	2.56E-02
19	1.42	23.08	2.70E-02	1.75E-02	1.71E-02	1.34E-02	1.72E-02	1.71E-02	2.69E-02	2.70E-02
20	1.27	24.35	2.83E-02	1.84E-02	1.78E-02	1.40E-02	1.80E-02	1.80E-02	2.82E-02	2.83E-02
21	1.38	25.73	2.98E-02	1.93E-02	1.86E-02	1.47E-02	1.87E-02	1.89E-02	2.97E-02	2.98E-02
22	1.35	27.08	3.13E-02	2.03E-02	1.93E-02	1.54E-02	1.95E-02	1.99E-02	3.12E-02	3.13E-02
23	1.31	28.39	3.28E-02	2.13E-02	2.02E-02	1.61E-02	2.03E-02	2.08E-02	3.27E-02	3.28E-02
24	1.29	29.67	3.46E-02	2.24E-02	2.11E-02	1.70E-02	2.13E-02	2.19E-02	3.45E-02	3.46E-02
25	1.33	31.00	3.66E-02	2.37E-02	2.22E-02	1.79E-02	2.23E-02	2.31E-02	3.65E-02	3.66E-02
26	1.33	32.33	3.86E-02	2.49E-02	2.32E-02	1.88E-02	2.34E-02	2.43E-02	3.85E-02	3.86E-02

Table 4-4
Iron Atom Displacements at the RPV Clad/Base Metal Interface

Cycle	Cycle Length (EFPY)	Cumulative Operating Time (EFPY)	Iron Atom Displacements (dpa)							
			0°	15°	30°	45°	60°	75°	90°	Maximum
27	1.30	33.64	4.05E-02	2.60E-02	2.41E-02	1.95E-02	2.42E-02	2.54E-02	4.03E-02	4.05E-02
28	1.30	34.94	4.21E-02	2.70E-02	2.49E-02	2.03E-02	2.51E-02	2.64E-02	4.20E-02	4.21E-02
29	1.37	36.31	4.40E-02	2.82E-02	2.58E-02	2.11E-02	2.60E-02	2.75E-02	4.39E-02	4.40E-02
30[1]	1.35	37.66	4.59E-02	2.93E-02	2.68E-02	2.19E-02	2.70E-02	2.86E-02	4.57E-02	4.59E-02
Projections with no bias on the peripheral and re-entrant corner assembly relative powers										
Future[2]	--	42.00	5.19E-02	3.29E-02	2.96E-02	2.44E-02	2.98E-02	3.21E-02	5.18E-02	5.19E-02
Future[2]	--	48.00	6.03E-02	3.79E-02	3.35E-02	2.79E-02	3.37E-02	3.70E-02	6.01E-02	6.03E-02
Future[2]	--	54.00	6.87E-02	4.29E-02	3.74E-02	3.14E-02	3.76E-02	4.19E-02	6.85E-02	6.87E-02
Future[2]	--	60.00	7.71E-02	4.79E-02	4.13E-02	3.48E-02	4.15E-02	4.67E-02	7.68E-02	7.71E-02
Future[2]	--	66.00	8.54E-02	5.30E-02	4.52E-02	3.83E-02	4.55E-02	5.16E-02	8.52E-02	8.54E-02
Future[2]	--	72.00	9.38E-02	5.80E-02	4.91E-02	4.17E-02	4.94E-02	5.64E-02	9.35E-02	9.38E-02
Projections with a +10% bias on the peripheral and re-entrant corner assembly relative powers										
Future[2]	--	42.00	5.24E-02	3.32E-02	2.98E-02	2.47E-02	3.00E-02	3.24E-02	5.23E-02	5.24E-02
Future[2]	--	48.00	6.15E-02	3.86E-02	3.41E-02	2.84E-02	3.43E-02	3.77E-02	6.13E-02	6.15E-02
Future[2]	--	54.00	7.05E-02	4.40E-02	3.83E-02	3.22E-02	3.85E-02	4.29E-02	7.03E-02	7.05E-02
Future[2]	--	60.00	7.96E-02	4.95E-02	4.26E-02	3.60E-02	4.28E-02	4.82E-02	7.93E-02	7.96E-02
Future[2]	--	66.00	8.86E-02	5.49E-02	4.68E-02	3.97E-02	4.71E-02	5.34E-02	8.84E-02	8.86E-02
Future[2]	--	72.00	9.77E-02	6.03E-02	5.11E-02	4.35E-02	5.13E-02	5.87E-02	9.74E-02	9.77E-02

Note(s):

1. Cycle 30 was the current operating cycle at the time the exposures reported in this table were determined. Values listed are based on the projected EFPY for this cycle.
2. Values beyond Cycle 30 are based on the average core power distributions and reactor operating conditions of Cycle 29 and are determined both with and without a 1.1 bias on the peripheral and re-entrant corner assembly relative powers.

Table 4-5
Fast Neutron (E > 1.0 MeV) Fluence at the RPV Welds and Shells

Projections with no bias on the peripheral and re-entrant corner assembly relative powers				
Material	**Fast Neutron (E > 1.0 MeV) Fluence (n/cm²)**			
	37.66 EFPY[1]	**42 EFPY**	**48 EFPY**	**54 EFPY**
Inlet-nozzle-to-upper-shell weld (lowest extent)	3.54E+16	3.97E+16	4.57E+16	5.16E+16
Outlet-nozzle-to-upper-shell weld (lowest extent)	3.94E+16	4.48E+16	5.23E+16	5.98E+16
Upper Shell	1.41E+18	1.60E+18	1.86E+18	2.12E+18
Upper-to-Middle-Shell Circumferential Weld	1.77E+18	2.01E+18	2.33E+18	2.66E+18
Middle Shell	2.99E+19	3.38E+19	3.93E+19	4.48E+19
Middle Shell Longitudinal Weld – 15°	1.89E+19	2.13E+19	2.45E+19	2.78E+19
Middle Shell Longitudinal Weld – 135°	1.42E+19	1.58E+19	1.81E+19	2.03E+19
Middle Shell Longitudinal Weld – 255°	1.84E+19	2.07E+19	2.38E+19	2.69E+19
Middle-to-Lower-Shell Circumferential Weld	2.96E+19	3.35E+19	3.89E+19	4.44E+19
Lower Shell	2.97E+19	3.36E+19	3.91E+19	4.45E+19
Lower Shell Longitudinal Weld – 15°	1.88E+19	2.11E+19	2.44E+19	2.76E+19
Lower Shell Longitudinal Weld – 135°	1.41E+19	1.57E+19	1.79E+19	2.02E+19
Lower Shell Longitudinal Weld – 255°	1.82E+19	2.05E+19	2.36E+19	2.68E+19
Lower-Shell-to-Bottom-Head Circumferential Weld	2.18E+16	2.45E+16	2.83E+16	3.21E+16

Projections with no bias on the peripheral and re-entrant corner assembly relative powers				
Material	**Fast Neutron (E > 1.0 MeV) Fluence (n/cm²)**			
	60 EFPY	**66 EFPY**	**72 EFPY**	
Inlet-nozzle-to-upper-shell weld (lowest extent)	5.76E+16	6.35E+16	6.95E+16	
Outlet-nozzle-to-upper-shell weld (lowest extent)	6.73E+16	7.49E+16	8.24E+16	
Upper Shell	2.39E+18	2.65E+18	2.91E+18	
Upper-to-Middle-Shell Circumferential Weld	2.99E+18	3.32E+18	3.64E+18	
Middle Shell	5.03E+19	5.58E+19	6.12E+19	
Middle Shell Longitudinal Weld – 15°	3.10E+19	3.43E+19	3.75E+19	
Middle Shell Longitudinal Weld – 135°	2.25E+19	2.48E+19	2.70E+19	
Middle Shell Longitudinal Weld – 255°	3.01E+19	3.32E+19	3.64E+19	
Middle-to-Lower-Shell Circumferential Weld	4.98E+19	5.52E+19	6.07E+19	
Lower Shell	5.00E+19	5.55E+19	6.09E+19	
Lower Shell Longitudinal Weld – 15°	3.08E+19	3.41E+19	3.73E+19	
Lower Shell Longitudinal Weld – 135°	2.24E+19	2.46E+19	2.69E+19	
Lower Shell Longitudinal Weld – 255°	2.99E+19	3.30E+19	3.61E+19	
Lower-Shell-to-Bottom-Head Circumferential Weld	3.59E+16	3.97E+16	4.35E+16	

Table 4-5
Fast Neutron (E > 1.0 MeV) Fluence at the RPV Welds and Shells

Projections with a +10% bias on the peripheral and re-entrant corner assembly relative powers				
Material	**Fast Neutron (E > 1.0 MeV) Fluence (n/cm^2)**			
	37.66 EFPY[1]	**42 EFPY**	**48 EFPY**	**54 EFPY**
Inlet-nozzle-to-upper-shell weld (lowest extent)	3.54E+16	4.01E+16	4.66E+16	5.30E+16
Outlet-nozzle-to-upper-shell weld (lowest extent)	3.94E+16	4.51E+16	5.29E+16	6.08E+16
Upper Shell	1.41E+18	1.61E+18	1.89E+18	2.17E+18
Upper-to-Middle-Shell Circumferential Weld	1.77E+18	2.02E+18	2.37E+18	2.72E+18
Middle Shell	2.99E+19	3.41E+19	4.01E+19	4.60E+19
Middle Shell Longitudinal Weld – 15°	1.89E+19	2.15E+19	2.50E+19	2.85E+19
Middle Shell Longitudinal Weld – 135°	1.42E+19	1.60E+19	1.84E+19	2.08E+19
Middle Shell Longitudinal Weld – 255°	1.84E+19	2.09E+19	2.42E+19	2.76E+19
Middle-to-Lower-Shell Circumferential Weld	2.96E+19	3.38E+19	3.97E+19	4.56E+19
Lower Shell	2.97E+19	3.39E+19	3.99E+19	4.58E+19
Lower Shell Longitudinal Weld – 15°	1.88E+19	2.13E+19	2.48E+19	2.83E+19
Lower Shell Longitudinal Weld – 135°	1.41E+19	1.58E+19	1.83E+19	2.07E+19
Lower Shell Longitudinal Weld – 255°	1.82E+19	2.07E+19	2.41E+19	2.75E+19
Lower-Shell-to-Bottom-Head Circumferential Weld	2.18E+16	2.47E+16	2.89E+16	3.30E+16

Projections with a +10% bias on the peripheral and re-entrant corner assembly relative powers				
Material	**Fast Neutron (E > 1.0 MeV) Fluence (n/cm^2)**			
	60 EFPY	**66 EFPY**	**72 EFPY**	
Inlet-nozzle-to-upper-shell weld (lowest extent)	5.95E+16	6.59E+16	7.24E+16	
Outlet-nozzle-to-upper-shell weld (lowest extent)	6.87E+16	7.65E+16	8.44E+16	
Upper Shell	2.45E+18	2.73E+18	3.01E+18	
Upper-to-Middle-Shell Circumferential Weld	3.07E+18	3.42E+18	3.77E+18	
Middle Shell	5.19E+19	5.79E+19	6.38E+19	
Middle Shell Longitudinal Weld – 15°	3.20E+19	3.55E+19	3.91E+19	
Middle Shell Longitudinal Weld – 135°	2.33E+19	2.57E+19	2.82E+19	
Middle Shell Longitudinal Weld – 255°	3.10E+19	3.44E+19	3.78E+19	
Middle-to-Lower-Shell Circumferential Weld	5.15E+19	5.73E+19	6.32E+19	
Lower Shell	5.17E+19	5.76E+19	6.35E+19	
Lower Shell Longitudinal Weld – 15°	3.18E+19	3.53E+19	3.88E+19	
Lower Shell Longitudinal Weld – 135°	2.31E+19	2.56E+19	2.80E+19	
Lower Shell Longitudinal Weld – 255°	3.08E+19	3.42E+19	3.76E+19	
Lower-Shell-to-Bottom-Head Circumferential Weld	3.71E+16	4.12E+16	4.53E+16	

Note(s):

1. Value listed is the projected EFPY at the end of Cycle 30.

Table 4-6
Iron Atom Displacements at the RPV Welds and Shells

Projections with no bias on the peripheral and re-entrant corner assembly relative powers				
Material	**Iron Atom Displacements (dpa)**			
	37.66 EFPY[1]	**42 EFPY**	**48 EFPY**	**54 EFPY**
Inlet-nozzle-to-upper-shell weld (lowest extent)	2.94E-04	3.29E-04	3.78E-04	4.26E-04
Outlet-nozzle-to-upper-shell weld (lowest extent)	3.39E-04	3.82E-04	4.42E-04	5.02E-04
Upper Shell	2.35E-03	2.67E-03	3.10E-03	3.54E-03
Upper-to-Middle-Shell Circumferential Weld	2.92E-03	3.31E-03	3.85E-03	4.38E-03
Middle Shell	4.59E-02	5.19E-02	6.03E-02	6.87E-02
Middle Shell Longitudinal Weld – 15°	2.93E-02	3.29E-02	3.79E-02	4.29E-02
Middle Shell Longitudinal Weld – 135°	2.19E-02	2.44E-02	2.79E-02	3.13E-02
Middle Shell Longitudinal Weld – 255°	2.86E-02	3.21E-02	3.70E-02	4.19E-02
Middle-to-Lower-Shell Circumferential Weld	4.55E-02	5.15E-02	5.98E-02	6.81E-02
Lower Shell	4.55E-02	5.16E-02	5.99E-02	6.83E-02
Lower Shell Longitudinal Weld – 15°	2.90E-02	3.26E-02	3.76E-02	4.26E-02
Lower Shell Longitudinal Weld – 135°	2.17E-02	2.42E-02	2.77E-02	3.11E-02
Lower Shell Longitudinal Weld – 255°	2.84E-02	3.19E-02	3.67E-02	4.15E-02
Lower-Shell-to-Bottom-Head Circumferential Weld	1.50E-04	1.69E-04	1.94E-04	2.20E-04

Projections with no bias on the peripheral and re-entrant corner assembly relative powers				
Material	**Iron Atom Displacements (dpa)**			
	60 EFPY	**66 EFPY**	**72 EFPY**	
Inlet-nozzle-to-upper-shell weld (lowest extent)	4.75E-04	5.23E-04	5.72E-04	
Outlet-nozzle-to-upper-shell weld (lowest extent)	5.61E-04	6.21E-04	6.80E-04	
Upper Shell	3.97E-03	4.41E-03	4.85E-03	
Upper-to-Middle-Shell Circumferential Weld	4.92E-03	5.46E-03	6.00E-03	
Middle Shell	7.70E-02	8.54E-02	9.38E-02	
Middle Shell Longitudinal Weld – 15°	4.79E-02	5.29E-02	5.80E-02	
Middle Shell Longitudinal Weld – 135°	3.48E-02	3.83E-02	4.17E-02	
Middle Shell Longitudinal Weld – 255°	4.67E-02	5.16E-02	5.64E-02	
Middle-to-Lower-Shell Circumferential Weld	7.64E-02	8.48E-02	9.31E-02	
Lower Shell	7.66E-02	8.49E-02	9.33E-02	
Lower Shell Longitudinal Weld – 15°	4.76E-02	5.26E-02	5.75E-02	
Lower Shell Longitudinal Weld – 135°	3.45E-02	3.80E-02	4.14E-02	
Lower Shell Longitudinal Weld – 255°	4.64E-02	5.12E-02	5.60E-02	
Lower-Shell-to-Bottom-Head Circumferential Weld	2.45E-04	2.71E-04	2.96E-04	

Table 4-6
Iron Atom Displacements at the RPV Welds and Shells

Projections with a +10% bias on the peripheral and re-entrant corner assembly relative powers				
Material	**Iron Atom Displacements (dpa)**			
	37.66 EFPY[1]	**42 EFPY**	**48 EFPY**	**54 EFPY**
Inlet-nozzle-to-upper-shell weld (lowest extent)	2.94E-04	3.32E-04	3.85E-04	4.38E-04
Outlet-nozzle-to-upper-shell weld (lowest extent)	3.39E-04	3.86E-04	4.51E-04	5.15E-04
Upper Shell	2.35E-03	2.69E-03	3.15E-03	3.62E-03
Upper-to-Middle-Shell Circumferential Weld	2.92E-03	3.33E-03	3.91E-03	4.49E-03
Middle Shell	4.59E-02	5.24E-02	6.15E-02	7.05E-02
Middle Shell Longitudinal Weld – 15°	2.93E-02	3.32E-02	3.86E-02	4.40E-02
Middle Shell Longitudinal Weld – 135°	2.19E-02	2.47E-02	2.84E-02	3.22E-02
Middle Shell Longitudinal Weld – 255°	2.86E-02	3.24E-02	3.77E-02	4.29E-02
Middle-to-Lower-Shell Circumferential Weld	4.55E-02	5.20E-02	6.10E-02	7.00E-02
Lower Shell	4.55E-02	5.21E-02	6.11E-02	7.01E-02
Lower Shell Longitudinal Weld – 15°	2.90E-02	3.29E-02	3.83E-02	4.37E-02
Lower Shell Longitudinal Weld – 135°	2.17E-02	2.44E-02	2.82E-02	3.19E-02
Lower Shell Longitudinal Weld – 255°	2.84E-02	3.22E-02	3.74E-02	4.26E-02
Lower-Shell-to-Bottom-Head Circumferential Weld	1.50E-04	1.70E-04	1.98E-04	2.26E-04

Projections with a +10% bias on the peripheral and re-entrant corner assembly relative powers				
Material	**Iron Atom Displacements (dpa)**			
	60 EFPY	**66 EFPY**	**72 EFPY**	
Inlet-nozzle-to-upper-shell weld (lowest extent)	4.90E-04	5.43E-04	5.96E-04	
Outlet-nozzle-to-upper-shell weld (lowest extent)	5.80E-04	6.44E-04	7.09E-04	
Upper Shell	4.08E-03	4.55E-03	5.01E-03	
Upper-to-Middle-Shell Circumferential Weld	5.06E-03	5.64E-03	6.21E-03	
Middle Shell	7.96E-02	8.86E-02	9.77E-02	
Middle Shell Longitudinal Weld – 15°	4.95E-02	5.49E-02	6.03E-02	
Middle Shell Longitudinal Weld – 135°	3.60E-02	3.97E-02	4.35E-02	
Middle Shell Longitudinal Weld – 255°	4.82E-02	5.34E-02	5.87E-02	
Middle-to-Lower-Shell Circumferential Weld	7.89E-02	8.79E-02	9.69E-02	
Lower Shell	7.91E-02	8.81E-02	9.72E-02	
Lower Shell Longitudinal Weld – 15°	4.91E-02	5.45E-02	5.99E-02	
Lower Shell Longitudinal Weld – 135°	3.57E-02	3.95E-02	4.32E-02	
Lower Shell Longitudinal Weld – 255°	4.78E-02	5.31E-02	5.83E-02	
Lower-Shell-to-Bottom-Head Circumferential Weld	2.53E-04	2.81E-04	3.09E-04	

Note(s):

1. Value listed is the projected EFPY at the end of Cycle 30.

4.2 Surveillance Capsules

Neutron exposure data for the surveillance capsules are provided in Table 4-7 through Table 4-10. In particular, fast neutron (E > 1.0 MeV) fluence rates and fluences determined at the core midplane and geometric center of the surveillance capsules are provided in Table 4-7 and Table 4-8 as a function of irradiation time. Similar data in terms of iron atom displacement rates (dpa/s) and iron atom displacements (dpa) are provided in Table 4-9 and Table 4-10.

Lead factors for the surveillance capsules are provided in Table 4-11. The lead factor is defined as the ratio of the calculated neutron fluence at the geometric center of the surveillance capsule to the maximum fluence at the RPV clad/base metal interface.

Table 4-7
Fast Neutron (E > 1.0 MeV) Fluence Rate at the Geometric Center of the Surveillance Capsules

Cycle	Cycle Length (EFPY)	Cumulative Operating Time (EFPY)	Fluence Rate (n/cm^2-s)	
			7°	14°
1	1.05	1.05	3.42E+10	2.32E+10
2	0.74	1.79	3.42E+10	2.32E+10
3	0.69	2.48	3.42E+10	2.32E+10
4	1.22	3.70	3.42E+10	2.32E+10
5	1.12	4.82	3.10E+10	1.94E+10
6	1.36	6.18	4.18E+10	2.80E+10
7	1.05	7.22	4.18E+10	2.80E+10
8	1.18	8.41	4.18E+10	2.80E+10
9	1.29	9.70	4.18E+10	2.80E+10
10	1.31	11.01	2.38E+10	1.94E+10
11	1.21	12.22	1.85E+10	1.59E+10
12	1.27	13.48	2.34E+10	1.92E+10
13	1.14	14.62	1.95E+10	1.64E+10
14	1.18	15.80	2.22E+10	1.85E+10
15	1.62	17.42	2.84E+10	2.08E+10
16	1.44	18.86	2.83E+10	2.05E+10
17	1.39	20.26	2.43E+10	1.83E+10
18	1.40	21.66	2.60E+10	1.85E+10
19	1.42	23.08	2.50E+10	1.83E+10
20	1.27	24.35	2.70E+10	2.00E+10
21	1.38	25.73	2.72E+10	1.97E+10
22	1.35	27.08	2.99E+10	2.12E+10
23	1.31	28.39	2.98E+10	2.16E+10
24	1.29	29.67	3.42E+10	2.37E+10
25	1.33	31.00	3.96E+10	2.76E+10
26	1.33	32.33	3.88E+10	2.70E+10
27	1.30	33.64	3.57E+10	2.41E+10
28	1.30	34.94	3.22E+10	2.27E+10
29	1.37	36.31	3.51E+10	2.38E+10
30[1]	1.35	37.66	3.46E+10	2.38E+10

Note(s):

1. Cycle 30 was the current operating cycle at the time the exposures reported in this table were determined. Values listed are based on the projected EFPY for this cycle.

Table 4-8
Fast Neutron (E > 1.0 MeV) Fluence at the Geometric Center of the Surveillance Capsules

Cycle	Cycle Length (EFPY)	Cumulative Operating Time (EFPY)	Fluence (n/cm^2)	
			7°	14°
1	1.05	1.05	1.14E+18	7.71E+17
2	0.74	1.79	1.93E+18	1.31E+18
3	0.69	2.48	2.68E+18	1.82E+18
4	1.22	3.70	4.00E+18	2.71E+18
5	1.12	4.82	5.09E+18[1]	3.40E+18
6	1.36	6.18	6.88E+18	4.60E+18
7	1.05	7.22	8.27E+18	5.52E+18
8	1.18	8.41	9.83E+18	6.56E+18
9	1.29	9.70	1.15E+19	7.70E+18[2]
10	1.31	11.01	1.25E+19	8.50E+18
11	1.21	12.22	1.32E+19	9.11E+18
12	1.27	13.48	1.42E+19	9.88E+18
13	1.14	14.62	1.49E+19	1.05E+19
14	1.18	15.80	1.57E+19	1.12E+19
15	1.62	17.42	1.71E+19	1.22E+19[3]
16	1.44	18.86	1.84E+19	1.32E+19
17	1.39	20.26	1.95E+19	1.40E+19
18	1.40	21.66	2.06E+19	1.48E+19
19	1.42	23.08	2.18E+19	1.56E+19
20	1.27	24.35	2.28E+19	1.64E+19
21	1.38	25.73	2.40E+19	1.73E+19
22	1.35	27.08	2.53E+19	1.82E+19
23	1.31	28.39	2.65E+19	1.90E+19
24	1.29	29.67	2.79E+19	2.00E+19
25	1.33	31.00	2.96E+19	2.12E+19
26	1.33	32.33	3.12E+19	2.23E+19
27	1.30	33.64	3.27E+19	2.33E+19
28	1.30	34.94	3.40E+19	2.42E+19
29	1.37	36.31	3.55E+19	2.53E+19
30[4]	1.35	37.66	3.70E+19	2.63E+19

Table 4-8
Fast Neutron (E > 1.0 MeV) Fluence at the Geometric Center of the Surveillance Capsules

No bias on the peripheral and re-entrant corner assembly relative powers				
Cycle	**Cycle Length (EFPY)**	**Cumulative Operating Time (EFPY)**	**Fluence (n/cm²)**	
			7°	**14°**
Future[5]	--	42.00	4.18E+19	2.95E+19
Future[5]	--	48.00	4.84E+19	3.41E+19
Future[5]	--	54.00	5.51E+19	3.86E+19
Future[5]	--	60.00	6.17E+19	4.31E+19
Future[5]	--	66.00	6.84E+19	4.76E+19
Future[5]	--	72.00	7.50E+19	5.21E+19

+10% bias on the peripheral and re-entrant corner assembly relative powers				
Cycle	**Cycle Length (EFPY)**	**Cumulative Operating Time (EFPY)**	**Fluence (n/cm²)**	
			7°	**14°**
Future[5]	--	42.00	4.22E+19	2.98E+19
Future[5]	--	48.00	4.94E+19	3.47E+19
Future[5]	--	54.00	5.66E+19	3.96E+19
Future[5]	--	60.00	6.38E+19	4.45E+19
Future[5]	--	66.00	7.10E+19	4.94E+19
Future[5]	--	72.00	7.81E+19	5.42E+19

Note(s):

1. This value is applicable to Capsule 97.
2. This value is applicable to Capsule 104.
3. This value is applicable to Capsule 284.
4. Cycle 30 was the current operating cycle at the time the exposures reported in this table were determined. Values listed are based on the projected EFPY for this cycle.
5. Values beyond Cycle 30 are based on the average core power distributions and reactor operating conditions of Cycle 29 and are determined both with and without a 1.1 bias on the peripheral and re-entrant corner assembly relative powers.

Table 4-9
Iron Atom Displacement Rate at the Geometric Center of the Surveillance Capsules

Cycle	Cycle Length (EFPY)	Cumulative Operating Time (EFPY)	Displacement Rate (dpa/s)	
			7°	14°
1	1.05	1.05	5.26E-11	3.58E-11
2	0.74	1.79	5.26E-11	3.58E-11
3	0.69	2.48	5.26E-11	3.58E-11
4	1.22	3.70	5.26E-11	3.58E-11
5	1.12	4.82	4.77E-11	3.00E-11
6	1.36	6.18	6.07E-11	4.09E-11
7	1.05	7.22	6.07E-11	4.09E-11
8	1.18	8.41	6.07E-11	4.09E-11
9	1.29	9.70	6.07E-11	4.09E-11
10	1.31	11.01	3.47E-11	2.84E-11
11	1.21	12.22	2.70E-11	2.34E-11
12	1.27	13.48	3.41E-11	2.83E-11
13	1.14	14.62	2.85E-11	2.41E-11
14	1.18	15.80	3.23E-11	2.71E-11
15	1.62	17.42	4.14E-11	3.04E-11
16	1.44	18.86	4.11E-11	3.01E-11
17	1.39	20.26	3.53E-11	2.68E-11
18	1.40	21.66	3.79E-11	2.71E-11
19	1.42	23.08	3.64E-11	2.69E-11
20	1.27	24.35	3.93E-11	2.92E-11
21	1.38	25.73	3.95E-11	2.88E-11
22	1.35	27.08	4.35E-11	3.10E-11
23	1.31	28.39	4.34E-11	3.15E-11
24	1.29	29.67	4.97E-11	3.47E-11
25	1.33	31.00	5.75E-11	4.03E-11
26	1.33	32.33	5.63E-11	3.95E-11
27	1.30	33.64	5.19E-11	3.53E-11
28	1.30	34.94	4.68E-11	3.33E-11
29	1.37	36.31	5.10E-11	3.49E-11
30[1]	1.35	37.66	5.03E-11	3.48E-11

Note(s):

1. Cycle 30 was the current operating cycle at the time the exposures reported in this table were determined. Values listed are based on the projected EFPY for this cycle.

Table 4-10
Iron Atom Displacements at the Geometric Center of the Surveillance Capsules

Cycle	Cycle Length (EFPY)	Cumulative Operating Time (EFPY)	Displacements (dpa)	
			7°	14°
1	1.05	1.05	1.74E-03	1.19E-03
2	0.74	1.79	2.96E-03	2.02E-03
3	0.69	2.48	4.11E-03	2.80E-03
4	1.22	3.70	6.14E-03	4.18E-03
5	1.12	4.82	7.82E-03[1]	5.24E-03
6	1.36	6.18	1.04E-02	6.99E-03
7	1.05	7.22	1.24E-02	8.35E-03
8	1.18	8.41	1.47E-02	9.87E-03
9	1.29	9.70	1.72E-02	1.15E-02[2]
10	1.31	11.01	1.86E-02	1.27E-02
11	1.21	12.22	1.96E-02	1.36E-02
12	1.27	13.48	2.10E-02	1.47E-02
13	1.14	14.62	2.20E-02	1.56E-02
14	1.18	15.80	2.32E-02	1.66E-02
15	1.62	17.42	2.53E-02	1.82E-02[3]
16	1.44	18.86	2.72E-02	1.95E-02
17	1.39	20.26	2.88E-02	2.07E-02
18	1.40	21.66	3.04E-02	2.19E-02
19	1.42	23.08	3.21E-02	2.31E-02
20	1.27	24.35	3.37E-02	2.43E-02
21	1.38	25.73	3.54E-02	2.55E-02
22	1.35	27.08	3.72E-02	2.69E-02
23	1.31	28.39	3.90E-02	2.82E-02
24	1.29	29.67	4.10E-02	2.96E-02
25	1.33	31.00	4.34E-02	3.13E-02
26	1.33	32.33	4.58E-02	3.29E-02
27	1.30	33.64	4.79E-02	3.44E-02
28	1.30	34.94	4.99E-02	3.57E-02
29	1.37	36.31	5.21E-02	3.73E-02
30[4]	1.35	37.66	5.42E-02	3.87E-02

Table 4-10
Iron Atom Displacements at the Geometric Center of the Surveillance Capsules

No bias on the peripheral and re-entrant corner assembly relative powers				
Cycle	**Cycle Length (EFPY)**	**Cumulative Operating Time (EFPY)**	**Displacements (dpa)**	
			7°	**14°**
Future[5]	--	42.00	6.12E-02	4.35E-02
Future[5]	--	48.00	7.09E-02	5.01E-02
Future[5]	--	54.00	8.05E-02	5.67E-02
Future[5]	--	60.00	9.02E-02	6.33E-02
Future[5]	--	66.00	9.98E-02	6.99E-02
Future[5]	--	72.00	1.09E-01	7.66E-02

+10% bias on the peripheral and re-entrant corner assembly relative powers				
Cycle	**Cycle Length (EFPY)**	**Cumulative Operating Time (EFPY)**	**Displacements (dpa)**	
			7°	**14°**
Future[5]	--	42.00	6.18E-02	4.39E-02
Future[5]	--	48.00	7.22E-02	5.11E-02
Future[5]	--	54.00	8.27E-02	5.82E-02
Future[5]	--	60.00	9.31E-02	6.54E-02
Future[5]	--	66.00	1.04E-01	7.25E-02
Future[5]	--	72.00	1.14E-01	7.97E-02

Note(s):

1. This value is applicable to Capsule 97.
2. This value is applicable to Capsule 104.
3. This value is applicable to Capsule 284.
4. Cycle 30 was the current operating cycle at the time the exposures reported in this table were determined. Values listed are based on the projected EFPY for this cycle.
5. Values beyond Cycle 30 are based on the average core power distributions and reactor operating conditions of Cycle 29 and are determined both with and without a 1.1 bias on the peripheral and re-entrant corner assembly relative powers.

Table 4-11
Surveillance Capsule Lead Factors

Cycle	Cycle Length (EFPY)	Cumulative Operating Time (EFPY)	Lead Factor	
			7°	14°
1	1.05	1.05	1.38	0.94
2	0.74	1.79	1.38	0.94
3	0.69	2.48	1.38	0.94
4	1.22	3.70	1.38	0.94
5	1.12	4.82	1.35[1]	0.90
6	1.36	6.18	1.30	0.87
7	1.05	7.22	1.28	0.85
8	1.18	8.41	1.26	0.84
9	1.29	9.70	1.25	0.83[2]
10	1.31	11.01	1.25	0.85
11	1.21	12.22	1.25	0.86
12	1.27	13.48	1.24	0.87
13	1.14	14.62	1.24	0.87
14	1.18	15.80	1.23	0.88
15	1.62	17.42	1.24	0.88[3]
16	1.44	18.86	1.24	0.88
17	1.39	20.26	1.24	0.89
18	1.40	21.66	1.24	0.89
19	1.42	23.08	1.24	0.89
20	1.27	24.35	1.24	0.89
21	1.38	25.73	1.24	0.89
22	1.35	27.08	1.24	0.89
23	1.31	28.39	1.24	0.89
24	1.29	29.67	1.24	0.89
25	1.33	31.00	1.24	0.89
26	1.33	32.33	1.24	0.89
27	1.30	33.64	1.24	0.88
28	1.30	34.94	1.24	0.88
29	1.37	36.31	1.24	0.88
30[4]	1.35	37.66	1.24	0.88

Table 4-11
Surveillance Capsule Lead Factors

No bias on the peripheral and re-entrant corner assembly relative powers				
Cycle	**Cycle Length (EFPY)**	**Cumulative Operating Time (EFPY)**	**Lead Factor**	
			7°	**14°**
Future[5]	--	42.00	1.24	0.87
Future[5]	--	48.00	1.23	0.87
Future[5]	--	54.00	1.23	0.86
Future[5]	--	60.00	1.23	0.86
Future[5]	--	66.00	1.23	0.85
Future[5]	--	72.00	1.22	0.85

+10% bias on the peripheral and re-entrant corner assembly relative powers				
Cycle	**Cycle Length (EFPY)**	**Cumulative Operating Time (EFPY)**	**Lead Factor**	
			7°	**14°**
Future[5]	--	42.00	1.24	0.87
Future[5]	--	48.00	1.23	0.87
Future[5]	--	54.00	1.23	0.86
Future[5]	--	60.00	1.23	0.86
Future[5]	--	66.00	1.23	0.85
Future[5]	--	72.00	1.23	0.85

Note(s):

1. This value is applicable to Capsule 97.
2. This value is applicable to Capsule 104
3. This value is applicable to Capsule 284.
4. Cycle 30 was the current operating cycle at the time the lead factors reported in this table were determined. Values listed are based on the projected EFPY for this cycle.
5. Values beyond Cycle 30 are based on the average core power distributions and reactor operating conditions of Cycle 29 and are determined both with and without a 1.1 bias on the peripheral and re-entrant corner assembly relative powers.

4.3 RPV Support Structure

Neutron exposure data for the RPV support structure are provided in Table 4-12 through Table 4-20. In particular:

- Table 4-12 provides the maximum neutron exposures, expressed as fast neutron (E > 1.0 MeV and E > 0.1 MeV) fluences and iron atom displacements (all energies and E > 0.1 MeV), at the RPV support structure. Note that each value reported in Table 4-12 was determined at the RPV support structure inner surface, 0° azimuth, and axial elevation where the maximum exposure occurred.
- Table 4-13 and Table 4-14 provide fast neutron (E > 1.0 MeV) fluence projections at the RPV support structure as a function of height. Note that each fluence value reported in Table 4-13 and Table 4-14 was determined at the RPV support structure inner surface, 0° azimuth, and axial elevation indicated.
- Table 4-15 and Table 4-16 provide fast neutron (E > 0.1 MeV) fluence projections at the RPV support structure as a function of height. Note that each fluence value reported in Table 4-15 and Table 4-16 was determined at the RPV support structure inner surface, 0° azimuth, and axial elevation indicated.
- Table 4-17 and Table 4-18 provide iron atom displacement (all energies) projections at the RPV support structure as a function of height. Note that each displacement value reported in Table 4-17 and Table 4-18 was determined at the RPV support structure inner surface, 0° azimuth, and axial elevation indicated.
- Table 4-19 and Table 4-20 provide iron atom displacement (E > 0.1 MeV) projections at the RPV support structure as a function of height. Note that each displacement value reported in Table 4-19 and Table 4-20 was determined at the RPV support structure inner surface, 0° azimuth, and axial elevation indicated.

Table 4-12
Maximum Neutron Exposures at the RPV Support Structure

Cycle	Cycle Length (EFPY)	Cumulative Operating Time (EFPY)	Fast Neutron Fluence (n/cm^2)		Iron Atom Displacements (dpa)	
			E > 1.0 MeV	E > 0.1 MeV	All Energies	E > 0.1 MeV
1	1.05	1.05	3.49E+16	5.00E+17	1.58E-04	1.44E-04
2	0.74	1.79	5.93E+16	8.49E+17	2.68E-04	2.45E-04
3	0.69	2.48	8.22E+16	1.18E+18	3.72E-04	3.39E-04
4	1.22	3.70	1.23E+17	1.76E+18	5.56E-04	5.07E-04
5	1.12	4.82	1.59E+17	2.27E+18	7.19E-04	6.55E-04
6	1.36	6.18	2.21E+17	3.01E+18	9.61E-04	8.78E-04
7	1.05	7.22	2.69E+17	3.58E+18	1.15E-03	1.05E-03
8	1.18	8.41	3.24E+17	4.22E+18	1.36E-03	1.24E-03
9	1.29	9.70	3.83E+17	4.93E+18	1.59E-03	1.46E-03
10	1.31	11.01	4.18E+17	5.35E+18	1.73E-03	1.59E-03
11	1.21	12.22	4.45E+17	5.68E+18	1.84E-03	1.68E-03
12	1.27	13.48	4.77E+17	6.07E+18	1.96E-03	1.80E-03
13	1.14	14.62	5.03E+17	6.38E+18	2.06E-03	1.89E-03
14	1.18	15.80	5.33E+17	6.72E+18	2.17E-03	1.99E-03
15	1.62	17.42	5.83E+17	7.30E+18	2.36E-03	2.17E-03
16	1.44	18.86	6.27E+17	7.83E+18	2.54E-03	2.33E-03
17	1.39	20.26	6.64E+17	8.28E+18	2.68E-03	2.46E-03
18	1.40	21.66	7.04E+17	8.76E+18	2.84E-03	2.61E-03
19	1.42	23.08	7.43E+17	9.24E+18	3.00E-03	2.75E-03
20	1.27	24.35	7.81E+17	9.69E+18	3.15E-03	2.89E-03
21	1.38	25.73	8.22E+17	1.02E+19	3.31E-03	3.04E-03
22	1.35	27.08	8.66E+17	1.07E+19	3.48E-03	3.20E-03
23	1.31	28.39	9.08E+17	1.12E+19	3.65E-03	3.35E-03
24	1.29	29.67	9.57E+17	1.18E+19	3.84E-03	3.53E-03
25	1.33	31.00	1.01E+18	1.25E+19	4.06E-03	3.73E-03
26	1.33	32.33	1.07E+18	1.32E+19	4.28E-03	3.93E-03
27	1.30	33.64	1.12E+18	1.38E+19	4.48E-03	4.12E-03
28	1.30	34.94	1.17E+18	1.43E+19	4.66E-03	4.28E-03
29	1.37	36.31	1.22E+18	1.50E+19	4.87E-03	4.47E-03
30[1]	1.35	37.66	1.27E+18	1.56E+19	5.07E-03	4.66E-03

Table 4-12
Maximum Neutron Exposures at the RPV Support Structure

Cycle	Cycle Length (EFPY)	Cumulative Operating Time (EFPY)	Fast Neutron Fluence (n/cm^2)		Iron Atom Displacements (dpa)	
			E > 1.0 MeV	E > 0.1 MeV	All Energies	E > 0.1 MeV
Projections with no bias on the peripheral and re-entrant corner assembly relative powers						
Future[2]	--	42.00	1.44E+18	1.76E+19	5.72E-03	5.26E-03
Future[2]	--	48.00	1.67E+18	2.03E+19	6.63E-03	6.09E-03
Future[2]	--	54.00	1.90E+18	2.31E+19	7.53E-03	6.93E-03
Future[2]	--	60.00	2.13E+18	2.58E+19	8.43E-03	7.76E-03
Future[2]	--	66.00	2.37E+18	2.86E+19	9.34E-03	8.59E-03
Future[2]	--	72.00	2.60E+18	3.14E+19	1.02E-02	9.42E-03
Projections with a +10% bias on the peripheral and re-entrant corner assembly relative powers						
Future[2]	--	42.00	1.45E+18	1.77E+19	5.78E-03	5.31E-03
Future[2]	--	48.00	1.70E+18	2.07E+19	6.76E-03	6.22E-03
Future[2]	--	54.00	1.95E+18	2.37E+19	7.74E-03	7.12E-03
Future[2]	--	60.00	2.20E+18	2.67E+19	8.72E-03	8.02E-03
Future[2]	--	66.00	2.45E+18	2.97E+19	9.70E-03	8.92E-03
Future[2]	--	72.00	2.71E+18	3.27E+19	1.07E-02	9.83E-03

Note(s):

1. Cycle 30 was the current operating cycle at the time the exposures reported in this table were determined. Values listed are based on the projected EFPY for this cycle.
2. Values beyond Cycle 30 are based on the average core power distributions and reactor operating conditions of Cycle 29 and are determined both with and without a 1.1 bias on the peripheral and re-entrant corner assembly relative powers.

Table 4-13
Fast Neutron (E > 1.0 MeV) Fluence at the RPV Support Structure –
No Bias on the Peripheral and Re-Entrant Corner Assembly Relative Powers

Elevation[1] (cm)	Fast Neutron (E > 1.0 MeV) Fluence (n/cm^2)						
	37.66 EFPY[2]	42 EFPY	48 EFPY	54 EFPY	60 EFPY	66 EFPY	72 EFPY
218.81[3]	9.90E+16	1.12E+17	1.31E+17	1.49E+17	1.67E+17	1.85E+17	2.04E+17
213.36	1.26E+17	1.43E+17	1.66E+17	1.90E+17	2.13E+17	2.36E+17	2.60E+17
198.12	2.22E+17	2.52E+17	2.94E+17	3.36E+17	3.77E+17	4.19E+17	4.60E+17
182.88	3.52E+17	4.00E+17	4.67E+17	5.34E+17	6.00E+17	6.67E+17	7.33E+17
167.64	5.22E+17	5.94E+17	6.93E+17	7.92E+17	8.91E+17	9.90E+17	1.09E+18
152.40	7.09E+17	8.06E+17	9.40E+17	1.07E+18	1.21E+18	1.34E+18	1.48E+18
137.16	8.83E+17	1.00E+18	1.17E+18	1.34E+18	1.50E+18	1.67E+18	1.83E+18
121.92	1.03E+18	1.17E+18	1.36E+18	1.55E+18	1.74E+18	1.93E+18	2.12E+18
106.68	1.13E+18	1.28E+18	1.49E+18	1.70E+18	1.91E+18	2.12E+18	2.32E+18
91.44	1.20E+18	1.36E+18	1.58E+18	1.80E+18	2.02E+18	2.25E+18	2.47E+18
76.20	1.23E+18	1.39E+18	1.61E+18	1.84E+18	2.06E+18	2.28E+18	2.51E+18
60.96	1.25E+18	1.42E+18	1.65E+18	1.88E+18	2.10E+18	2.33E+18	2.56E+18
45.72	1.26E+18	1.43E+18	1.66E+18	1.89E+18	2.11E+18	2.34E+18	2.57E+18
30.48	1.26E+18	1.43E+18	1.66E+18	1.88E+18	2.11E+18	2.34E+18	2.57E+18
15.24	1.25E+18	1.42E+18	1.65E+18	1.88E+18	2.10E+18	2.33E+18	2.56E+18
0.00	1.26E+18	1.42E+18	1.65E+18	1.88E+18	2.11E+18	2.34E+18	2.57E+18
-15.24	1.26E+18	1.43E+18	1.66E+18	1.89E+18	2.12E+18	2.35E+18	2.58E+18
-30.48	1.27E+18	1.44E+18	1.67E+18	1.90E+18	2.13E+18	2.36E+18	2.60E+18
-45.72	1.27E+18	1.44E+18	1.67E+18	1.90E+18	2.13E+18	2.36E+18	2.59E+18
-60.96	1.26E+18	1.43E+18	1.66E+18	1.89E+18	2.12E+18	2.35E+18	2.58E+18
-76.20	1.24E+18	1.41E+18	1.64E+18	1.86E+18	2.09E+18	2.32E+18	2.55E+18
-91.44	1.21E+18	1.37E+18	1.59E+18	1.82E+18	2.04E+18	2.26E+18	2.48E+18
-106.68	1.15E+18	1.30E+18	1.51E+18	1.72E+18	1.94E+18	2.15E+18	2.36E+18
-121.92	1.05E+18	1.19E+18	1.38E+18	1.58E+18	1.77E+18	1.97E+18	2.16E+18
-137.16	9.10E+17	1.03E+18	1.20E+18	1.37E+18	1.54E+18	1.71E+18	1.89E+18
-152.40	7.40E+17	8.41E+17	9.80E+17	1.12E+18	1.26E+18	1.40E+18	1.54E+18
-167.64	5.51E+17	6.26E+17	7.30E+17	8.35E+17	9.39E+17	1.04E+18	1.15E+18
-182.88	3.74E+17	4.25E+17	4.95E+17	5.66E+17	6.37E+17	7.07E+17	7.78E+17
-198.12	2.33E+17	2.65E+17	3.09E+17	3.53E+17	3.97E+17	4.40E+17	4.84E+17
-213.36	1.39E+17	1.58E+17	1.84E+17	2.10E+17	2.36E+17	2.61E+17	2.87E+17
-228.60	8.41E+16	9.52E+16	1.11E+17	1.26E+17	1.41E+17	1.57E+17	1.72E+17
-243.84	5.37E+16	6.06E+16	7.03E+16	7.99E+16	8.95E+16	9.92E+16	1.09E+17
-259.08	3.75E+16	4.23E+16	4.90E+16	5.56E+16	6.23E+16	6.89E+16	7.56E+16
-274.32	2.82E+16	3.17E+16	3.67E+16	4.17E+16	4.66E+16	5.16E+16	5.66E+16
-289.56	2.26E+16	2.55E+16	2.94E+16	3.34E+16	3.74E+16	4.14E+16	4.53E+16
-304.80	1.82E+16	2.05E+16	2.37E+16	2.69E+16	3.01E+16	3.33E+16	3.65E+16

Note(s):

1. Elevations are given with respect to the midplane of the active fuel.
2. Value listed is the projected EFPY at the end of Cycle 30.
3. This elevation corresponds to the top of the 6-inch-thick horizontal plate at the top-center of the RPV support structure.
4. Linear interpolation between the EFPY values listed in this table may be performed as necessary.

Table 4-14
Fast Neutron (E > 1.0 MeV) Fluence at the RPV Support Structure –
+10% Bias on the Peripheral and Re-Entrant Corner Assembly Relative Powers

Elevation[1] (cm)	Fast Neutron (E > 1.0 MeV) Fluence (n/cm^2)						
	37.66 EFPY[2]	42 EFPY	48 EFPY	54 EFPY	60 EFPY	66 EFPY	72 EFPY
218.81[3]	9.90E+16	1.13E+17	1.33E+17	1.53E+17	1.72E+17	1.92E+17	2.12E+17
213.36	1.26E+17	1.44E+17	1.70E+17	1.95E+17	2.20E+17	2.45E+17	2.70E+17
198.12	2.22E+17	2.55E+17	3.00E+17	3.45E+17	3.90E+17	4.35E+17	4.80E+17
182.88	3.52E+17	4.04E+17	4.76E+17	5.49E+17	6.21E+17	6.93E+17	7.65E+17
167.64	5.22E+17	6.00E+17	7.07E+17	8.14E+17	9.22E+17	1.03E+18	1.14E+18
152.40	7.09E+17	8.14E+17	9.59E+17	1.10E+18	1.25E+18	1.40E+18	1.54E+18
137.16	8.83E+17	1.01E+18	1.19E+18	1.37E+18	1.55E+18	1.73E+18	1.91E+18
121.92	1.03E+18	1.18E+18	1.38E+18	1.59E+18	1.80E+18	2.01E+18	2.21E+18
106.68	1.13E+18	1.29E+18	1.52E+18	1.75E+18	1.97E+18	2.20E+18	2.43E+18
91.44	1.20E+18	1.38E+18	1.61E+18	1.85E+18	2.09E+18	2.33E+18	2.57E+18
76.20	1.23E+18	1.40E+18	1.64E+18	1.89E+18	2.13E+18	2.37E+18	2.62E+18
60.96	1.25E+18	1.43E+18	1.68E+18	1.93E+18	2.18E+18	2.42E+18	2.67E+18
45.72	1.26E+18	1.44E+18	1.69E+18	1.94E+18	2.19E+18	2.43E+18	2.68E+18
30.48	1.26E+18	1.44E+18	1.69E+18	1.94E+18	2.18E+18	2.43E+18	2.68E+18
15.24	1.25E+18	1.43E+18	1.68E+18	1.93E+18	2.17E+18	2.42E+18	2.67E+18
0.00	1.26E+18	1.43E+18	1.68E+18	1.93E+18	2.18E+18	2.42E+18	2.67E+18
-15.24	1.26E+18	1.44E+18	1.69E+18	1.94E+18	2.19E+18	2.44E+18	2.69E+18
-30.48	1.27E+18	1.45E+18	1.70E+18	1.95E+18	2.20E+18	2.45E+18	2.70E+18
-45.72	1.27E+18	1.45E+18	1.70E+18	1.95E+18	2.20E+18	2.45E+18	2.70E+18
-60.96	1.26E+18	1.44E+18	1.69E+18	1.94E+18	2.19E+18	2.44E+18	2.68E+18
-76.20	1.24E+18	1.42E+18	1.67E+18	1.92E+18	2.16E+18	2.41E+18	2.65E+18
-91.44	1.21E+18	1.39E+18	1.63E+18	1.87E+18	2.11E+18	2.35E+18	2.59E+18
-106.68	1.15E+18	1.31E+18	1.54E+18	1.77E+18	2.00E+18	2.23E+18	2.46E+18
-121.92	1.05E+18	1.20E+18	1.41E+18	1.62E+18	1.83E+18	2.04E+18	2.25E+18
-137.16	9.10E+17	1.04E+18	1.23E+18	1.41E+18	1.60E+18	1.78E+18	1.97E+18
-152.40	7.40E+17	8.49E+17	1.00E+18	1.15E+18	1.30E+18	1.45E+18	1.60E+18
-167.64	5.51E+17	6.32E+17	7.45E+17	8.58E+17	9.71E+17	1.08E+18	1.20E+18
-182.88	3.74E+17	4.29E+17	5.05E+17	5.82E+17	6.58E+17	7.35E+17	8.11E+17
-198.12	2.33E+17	2.68E+17	3.15E+17	3.62E+17	4.10E+17	4.57E+17	5.04E+17
-213.36	1.39E+17	1.60E+17	1.87E+17	2.15E+17	2.43E+17	2.71E+17	2.99E+17
-228.60	8.41E+16	9.61E+16	1.13E+17	1.29E+17	1.46E+17	1.62E+17	1.79E+17
-243.84	5.37E+16	6.12E+16	7.16E+16	8.20E+16	9.24E+16	1.03E+17	1.13E+17
-259.08	3.75E+16	4.27E+16	4.99E+16	5.71E+16	6.43E+16	7.15E+16	7.87E+16
-274.32	2.82E+16	3.20E+16	3.74E+16	4.28E+16	4.82E+16	5.35E+16	5.89E+16
-289.56	2.26E+16	2.57E+16	3.00E+16	3.43E+16	3.86E+16	4.29E+16	4.72E+16
-304.80	1.82E+16	2.07E+16	2.42E+16	2.76E+16	3.11E+16	3.45E+16	3.80E+16

Note(s):

1. Elevations are given with respect to the midplane of the active fuel.
2. Value listed is the projected EFPY at the end of Cycle 30.
3. This elevation corresponds to the top of the 6-inch-thick horizontal plate at the top-center of the RPV support structure.
4. Linear interpolation between the EFPY values listed in this table may be performed as necessary.

Table 4-15
Fast Neutron (E > 0.1 MeV) Fluence at the RPV Support Structure –
No Bias on the Peripheral and Re-Entrant Corner Assembly Relative Powers

Elevation[1] (cm)	Fast Neutron (E > 0.1 MeV) Fluence (n/cm^2)						
	37.66 EFPY[2]	42 EFPY	48 EFPY	54 EFPY	60 EFPY	66 EFPY	72 EFPY
218.81[3]	2.56E+18	2.89E+18	3.35E+18	3.80E+18	4.26E+18	4.72E+18	5.18E+18
213.36	2.97E+18	3.35E+18	3.88E+18	4.41E+18	4.94E+18	5.48E+18	6.01E+18
198.12	4.12E+18	4.65E+18	5.39E+18	6.14E+18	6.88E+18	7.62E+18	8.36E+18
182.88	5.41E+18	6.11E+18	7.09E+18	8.07E+18	9.05E+18	1.00E+19	1.10E+19
167.64	7.07E+18	8.00E+18	9.28E+18	1.06E+19	1.18E+19	1.31E+19	1.44E+19
152.40	8.89E+18	1.01E+19	1.17E+19	1.33E+19	1.49E+19	1.65E+19	1.81E+19
137.16	1.06E+19	1.20E+19	1.40E+19	1.59E+19	1.78E+19	1.97E+19	2.16E+19
121.92	1.21E+19	1.37E+19	1.59E+19	1.81E+19	2.03E+19	2.24E+19	2.46E+19
106.68	1.33E+19	1.50E+19	1.74E+19	1.98E+19	2.22E+19	2.46E+19	2.69E+19
91.44	1.43E+19	1.62E+19	1.87E+19	2.13E+19	2.39E+19	2.64E+19	2.90E+19
76.20	1.56E+19	1.76E+19	2.03E+19	2.31E+19	2.58E+19	2.86E+19	3.14E+19
60.96	1.50E+19	1.69E+19	1.95E+19	2.22E+19	2.48E+19	2.74E+19	3.01E+19
45.72	1.48E+19	1.67E+19	1.93E+19	2.20E+19	2.46E+19	2.72E+19	2.98E+19
30.48	1.48E+19	1.66E+19	1.92E+19	2.18E+19	2.44E+19	2.70E+19	2.96E+19
15.24	1.47E+19	1.65E+19	1.91E+19	2.17E+19	2.43E+19	2.69E+19	2.95E+19
0.00	1.46E+19	1.65E+19	1.91E+19	2.16E+19	2.42E+19	2.68E+19	2.94E+19
-15.24	1.46E+19	1.65E+19	1.90E+19	2.16E+19	2.42E+19	2.68E+19	2.93E+19
-30.48	1.46E+19	1.64E+19	1.90E+19	2.15E+19	2.41E+19	2.67E+19	2.93E+19
-45.72	1.44E+19	1.63E+19	1.88E+19	2.14E+19	2.39E+19	2.65E+19	2.90E+19
-60.96	1.43E+19	1.61E+19	1.86E+19	2.11E+19	2.36E+19	2.62E+19	2.87E+19
-76.20	1.39E+19	1.57E+19	1.82E+19	2.07E+19	2.31E+19	2.56E+19	2.81E+19
-91.44	1.35E+19	1.52E+19	1.76E+19	2.00E+19	2.24E+19	2.47E+19	2.71E+19
-106.68	1.27E+19	1.43E+19	1.66E+19	1.89E+19	2.11E+19	2.34E+19	2.56E+19
-121.92	1.16E+19	1.31E+19	1.52E+19	1.73E+19	1.94E+19	2.14E+19	2.35E+19
-137.16	1.02E+19	1.15E+19	1.34E+19	1.52E+19	1.71E+19	1.89E+19	2.07E+19
-152.40	8.54E+18	9.66E+18	1.12E+19	1.27E+19	1.43E+19	1.58E+19	1.74E+19
-167.64	6.75E+18	7.63E+18	8.85E+18	1.01E+19	1.13E+19	1.25E+19	1.37E+19
-182.88	5.05E+18	5.71E+18	6.62E+18	7.53E+18	8.44E+18	9.35E+18	1.03E+19
-198.12	3.63E+18	4.10E+18	4.75E+18	5.40E+18	6.05E+18	6.70E+18	7.35E+18
-213.36	2.57E+18	2.90E+18	3.36E+18	3.81E+18	4.27E+18	4.73E+18	5.18E+18
-228.60	1.84E+18	2.07E+18	2.40E+18	2.72E+18	3.04E+18	3.37E+18	3.69E+18
-243.84	1.35E+18	1.52E+18	1.76E+18	1.99E+18	2.23E+18	2.47E+18	2.70E+18
-259.08	1.02E+18	1.15E+18	1.32E+18	1.50E+18	1.67E+18	1.85E+18	2.03E+18
-274.32	7.84E+17	8.81E+17	1.01E+18	1.15E+18	1.28E+18	1.42E+18	1.55E+18
-289.56	6.28E+17	7.06E+17	8.13E+17	9.20E+17	1.03E+18	1.13E+18	1.24E+18
-304.80	5.14E+17	5.77E+17	6.64E+17	7.51E+17	8.38E+17	9.25E+17	1.01E+18

Note(s):

1. Elevations are given with respect to the midplane of the active fuel.
2. Value listed is the projected EFPY at the end of Cycle 30.
3. This elevation corresponds to the top of the 6-inch-thick horizontal plate at the top-center of the RPV support structure.
4. Linear interpolation between the EFPY values listed in this table may be performed as necessary.

Table 4-16
Fast Neutron (E > 0.1 MeV) Fluence at the RPV Support Structure –
+10% Bias on the Peripheral and Re-Entrant Corner Assembly Relative Powers

Elevation[1] (cm)	Fast Neutron (E > 0.1 MeV) Fluence (n/cm^2)						
	37.66 EFPY[2]	42 EFPY	48 EFPY	54 EFPY	60 EFPY	66 EFPY	72 EFPY
218.81[3]	2.56E+18	2.92E+18	3.41E+18	3.91E+18	4.40E+18	4.90E+18	5.39E+18
213.36	2.97E+18	3.38E+18	3.96E+18	4.53E+18	5.11E+18	5.68E+18	6.26E+18
198.12	4.12E+18	4.70E+18	5.50E+18	6.30E+18	7.11E+18	7.91E+18	8.71E+18
182.88	5.41E+18	6.17E+18	7.24E+18	8.30E+18	9.36E+18	1.04E+19	1.15E+19
167.64	7.07E+18	8.07E+18	9.46E+18	1.09E+19	1.22E+19	1.36E+19	1.50E+19
152.40	8.89E+18	1.02E+19	1.19E+19	1.37E+19	1.54E+19	1.71E+19	1.89E+19
137.16	1.06E+19	1.22E+19	1.42E+19	1.63E+19	1.84E+19	2.05E+19	2.26E+19
121.92	1.21E+19	1.39E+19	1.62E+19	1.86E+19	2.10E+19	2.33E+19	2.57E+19
106.68	1.33E+19	1.52E+19	1.78E+19	2.04E+19	2.29E+19	2.55E+19	2.81E+19
91.44	1.43E+19	1.64E+19	1.91E+19	2.19E+19	2.47E+19	2.74E+19	3.02E+19
76.20	1.56E+19	1.77E+19	2.07E+19	2.37E+19	2.67E+19	2.97E+19	3.27E+19
60.96	1.50E+19	1.70E+19	1.99E+19	2.28E+19	2.56E+19	2.85E+19	3.14E+19
45.72	1.48E+19	1.69E+19	1.97E+19	2.26E+19	2.54E+19	2.82E+19	3.11E+19
30.48	1.48E+19	1.68E+19	1.96E+19	2.24E+19	2.52E+19	2.81E+19	3.09E+19
15.24	1.47E+19	1.67E+19	1.95E+19	2.23E+19	2.51E+19	2.79E+19	3.07E+19
0.00	1.46E+19	1.66E+19	1.94E+19	2.22E+19	2.50E+19	2.78E+19	3.06E+19
-15.24	1.46E+19	1.66E+19	1.94E+19	2.22E+19	2.50E+19	2.78E+19	3.05E+19
-30.48	1.46E+19	1.66E+19	1.93E+19	2.21E+19	2.49E+19	2.77E+19	3.05E+19
-45.72	1.44E+19	1.64E+19	1.92E+19	2.20E+19	2.47E+19	2.75E+19	3.02E+19
-60.96	1.43E+19	1.62E+19	1.90E+19	2.17E+19	2.44E+19	2.71E+19	2.99E+19
-76.20	1.39E+19	1.59E+19	1.86E+19	2.12E+19	2.39E+19	2.66E+19	2.93E+19
-91.44	1.35E+19	1.53E+19	1.79E+19	2.05E+19	2.31E+19	2.57E+19	2.83E+19
-106.68	1.27E+19	1.45E+19	1.69E+19	1.94E+19	2.18E+19	2.43E+19	2.67E+19
-121.92	1.16E+19	1.32E+19	1.55E+19	1.78E+19	2.00E+19	2.23E+19	2.45E+19
-137.16	1.02E+19	1.17E+19	1.36E+19	1.56E+19	1.76E+19	1.96E+19	2.16E+19
-152.40	8.54E+18	9.75E+18	1.14E+19	1.31E+19	1.48E+19	1.64E+19	1.81E+19
-167.64	6.75E+18	7.71E+18	9.03E+18	1.04E+19	1.17E+19	1.30E+19	1.43E+19
-182.88	5.05E+18	5.76E+18	6.75E+18	7.73E+18	8.72E+18	9.71E+18	1.07E+19
-198.12	3.63E+18	4.14E+18	4.84E+18	5.54E+18	6.25E+18	6.95E+18	7.66E+18
-213.36	2.57E+18	2.93E+18	3.42E+18	3.92E+18	4.41E+18	4.91E+18	5.40E+18
-228.60	1.84E+18	2.09E+18	2.44E+18	2.79E+18	3.14E+18	3.49E+18	3.84E+18
-243.84	1.35E+18	1.54E+18	1.79E+18	2.05E+18	2.30E+18	2.56E+18	2.81E+18
-259.08	1.02E+18	1.16E+18	1.35E+18	1.54E+18	1.73E+18	1.92E+18	2.11E+18
-274.32	7.84E+17	8.89E+17	1.03E+18	1.18E+18	1.33E+18	1.47E+18	1.62E+18
-289.56	6.28E+17	7.12E+17	8.28E+17	9.44E+17	1.06E+18	1.18E+18	1.29E+18
-304.80	5.14E+17	5.82E+17	6.77E+17	7.71E+17	8.65E+17	9.60E+17	1.05E+18

Note(s):

1. Elevations are given with respect to the midplane of the active fuel.
2. Value listed is the projected EFPY at the end of Cycle 30.
3. This elevation corresponds to the top of the 6-inch-thick horizontal plate at the top-center of the RPV support structure.
4. Linear interpolation between the EFPY values listed in this table may be performed as necessary.

Table 4-17
Iron Atom Displacements (All Neutron Energies) at the RPV Support Structure – No Bias on the Peripheral and Re-Entrant Corner Assembly Relative Powers

Elevation[1] (cm)	Iron Atom Displacements – All Neutron Energies (dpa)						
	37.66 EFPY[2]	42 EFPY	48 EFPY	54 EFPY	60 EFPY	66 EFPY	72 EFPY
218.81[3]	7.61E-04	8.60E-04	9.96E-04	1.13E-03	1.27E-03	1.40E-03	1.54E-03
213.36	8.89E-04	1.00E-03	1.16E-03	1.32E-03	1.48E-03	1.64E-03	1.80E-03
198.12	1.27E-03	1.43E-03	1.66E-03	1.89E-03	2.12E-03	2.35E-03	2.58E-03
182.88	1.71E-03	1.93E-03	2.24E-03	2.55E-03	2.86E-03	3.17E-03	3.48E-03
167.64	2.27E-03	2.57E-03	2.99E-03	3.40E-03	3.82E-03	4.24E-03	4.65E-03
152.40	2.90E-03	3.28E-03	3.81E-03	4.34E-03	4.86E-03	5.39E-03	5.92E-03
137.16	3.49E-03	3.95E-03	4.58E-03	5.22E-03	5.85E-03	6.49E-03	7.12E-03
121.92	4.00E-03	4.52E-03	5.24E-03	5.96E-03	6.68E-03	7.41E-03	8.13E-03
106.68	4.39E-03	4.96E-03	5.75E-03	6.53E-03	7.32E-03	8.11E-03	8.90E-03
91.44	4.71E-03	5.32E-03	6.16E-03	7.01E-03	7.85E-03	8.69E-03	9.53E-03
76.20	5.05E-03	5.70E-03	6.60E-03	7.50E-03	8.40E-03	9.30E-03	1.02E-02
60.96	4.91E-03	5.54E-03	6.42E-03	7.29E-03	8.16E-03	9.04E-03	9.91E-03
45.72	4.89E-03	5.51E-03	6.38E-03	7.25E-03	8.11E-03	8.98E-03	9.85E-03
30.48	4.86E-03	5.49E-03	6.35E-03	7.21E-03	8.08E-03	8.94E-03	9.80E-03
15.24	4.84E-03	5.46E-03	6.32E-03	7.17E-03	8.03E-03	8.89E-03	9.75E-03
0.00	4.83E-03	5.44E-03	6.30E-03	7.16E-03	8.01E-03	8.87E-03	9.73E-03
-15.24	4.83E-03	5.45E-03	6.30E-03	7.16E-03	8.02E-03	8.87E-03	9.73E-03
-30.48	4.82E-03	5.44E-03	6.29E-03	7.15E-03	8.01E-03	8.86E-03	9.72E-03
-45.72	4.79E-03	5.40E-03	6.25E-03	7.10E-03	7.96E-03	8.81E-03	9.66E-03
-60.96	4.73E-03	5.34E-03	6.18E-03	7.02E-03	7.87E-03	8.71E-03	9.55E-03
-76.20	4.64E-03	5.24E-03	6.06E-03	6.89E-03	7.72E-03	8.54E-03	9.37E-03
-91.44	4.48E-03	5.06E-03	5.86E-03	6.67E-03	7.47E-03	8.27E-03	9.07E-03
-106.68	4.23E-03	4.78E-03	5.54E-03	6.30E-03	7.06E-03	7.83E-03	8.59E-03
-121.92	3.87E-03	4.38E-03	5.08E-03	5.78E-03	6.48E-03	7.18E-03	7.88E-03
-137.16	3.40E-03	3.84E-03	4.46E-03	5.08E-03	5.69E-03	6.31E-03	6.93E-03
-152.40	2.83E-03	3.20E-03	3.72E-03	4.23E-03	4.75E-03	5.26E-03	5.78E-03
-167.64	2.21E-03	2.50E-03	2.91E-03	3.31E-03	3.71E-03	4.12E-03	4.52E-03
-182.88	1.63E-03	1.84E-03	2.14E-03	2.43E-03	2.73E-03	3.02E-03	3.32E-03
-198.12	1.14E-03	1.29E-03	1.50E-03	1.71E-03	1.91E-03	2.12E-03	2.33E-03
-213.36	7.94E-04	8.97E-04	1.04E-03	1.18E-03	1.32E-03	1.46E-03	1.60E-03
-228.60	5.58E-04	6.30E-04	7.28E-04	8.26E-04	9.25E-04	1.02E-03	1.12E-03
-243.84	4.06E-04	4.57E-04	5.28E-04	5.98E-04	6.69E-04	7.40E-04	8.10E-04
-259.08	3.04E-04	3.42E-04	3.95E-04	4.47E-04	5.00E-04	5.52E-04	6.05E-04
-274.32	2.34E-04	2.63E-04	3.03E-04	3.43E-04	3.83E-04	4.24E-04	4.64E-04
-289.56	1.88E-04	2.12E-04	2.44E-04	2.76E-04	3.08E-04	3.40E-04	3.72E-04
-304.80	1.55E-04	1.74E-04	2.00E-04	2.26E-04	2.52E-04	2.78E-04	3.05E-04

Note(s):
1. Elevations are given with respect to the midplane of the active fuel.
2. Value listed is the projected EFPY at the end of Cycle 30.
3. This elevation corresponds to the top of the 6-inch-thick horizontal plate at the top-center of the RPV support structure.
4. Linear interpolation between the EFPY values listed in this table may be performed as necessary.

Table 4-18
Iron Atom Displacements (All Neutron Energies) at the RPV Support Structure – +10% Bias on the Peripheral and Re-Entrant Corner Assembly Relative Powers

Elevation[1] (cm)	Iron Atom Displacements – All Neutron Energies (dpa)						
	37.66 EFPY[2]	42 EFPY	48 EFPY	54 EFPY	60 EFPY	66 EFPY	72 EFPY
218.81[3]	7.61E-04	8.68E-04	1.02E-03	1.16E-03	1.31E-03	1.46E-03	1.61E-03
213.36	8.89E-04	1.01E-03	1.19E-03	1.36E-03	1.53E-03	1.71E-03	1.88E-03
198.12	1.27E-03	1.45E-03	1.69E-03	1.94E-03	2.19E-03	2.44E-03	2.69E-03
182.88	1.71E-03	1.95E-03	2.29E-03	2.62E-03	2.96E-03	3.30E-03	3.63E-03
167.64	2.27E-03	2.60E-03	3.05E-03	3.50E-03	3.95E-03	4.40E-03	4.85E-03
152.40	2.90E-03	3.31E-03	3.88E-03	4.46E-03	5.03E-03	5.61E-03	6.18E-03
137.16	3.49E-03	3.99E-03	4.68E-03	5.37E-03	6.05E-03	6.74E-03	7.43E-03
121.92	4.00E-03	4.56E-03	5.35E-03	6.13E-03	6.91E-03	7.70E-03	8.48E-03
106.68	4.39E-03	5.01E-03	5.86E-03	6.72E-03	7.57E-03	8.43E-03	9.28E-03
91.44	4.71E-03	5.37E-03	6.29E-03	7.20E-03	8.12E-03	9.03E-03	9.95E-03
76.20	5.05E-03	5.75E-03	6.73E-03	7.71E-03	8.68E-03	9.66E-03	1.06E-02
60.96	4.91E-03	5.60E-03	6.54E-03	7.49E-03	8.44E-03	9.38E-03	1.03E-02
45.72	4.89E-03	5.57E-03	6.51E-03	7.45E-03	8.39E-03	9.33E-03	1.03E-02
30.48	4.86E-03	5.54E-03	6.48E-03	7.41E-03	8.35E-03	9.28E-03	1.02E-02
15.24	4.84E-03	5.51E-03	6.44E-03	7.37E-03	8.30E-03	9.23E-03	1.02E-02
0.00	4.83E-03	5.50E-03	6.42E-03	7.35E-03	8.28E-03	9.20E-03	1.01E-02
-15.24	4.83E-03	5.50E-03	6.42E-03	7.35E-03	8.28E-03	9.21E-03	1.01E-02
-30.48	4.82E-03	5.49E-03	6.42E-03	7.34E-03	8.27E-03	9.19E-03	1.01E-02
-45.72	4.79E-03	5.45E-03	6.37E-03	7.30E-03	8.22E-03	9.14E-03	1.01E-02
-60.96	4.73E-03	5.39E-03	6.30E-03	7.21E-03	8.12E-03	9.04E-03	9.95E-03
-76.20	4.64E-03	5.29E-03	6.18E-03	7.08E-03	7.97E-03	8.87E-03	9.76E-03
-91.44	4.48E-03	5.11E-03	5.98E-03	6.85E-03	7.72E-03	8.58E-03	9.45E-03
-106.68	4.23E-03	4.83E-03	5.65E-03	6.48E-03	7.30E-03	8.12E-03	8.95E-03
-121.92	3.87E-03	4.42E-03	5.18E-03	5.94E-03	6.69E-03	7.45E-03	8.21E-03
-137.16	3.40E-03	3.88E-03	4.55E-03	5.22E-03	5.88E-03	6.55E-03	7.22E-03
-152.40	2.83E-03	3.23E-03	3.79E-03	4.35E-03	4.91E-03	5.46E-03	6.02E-03
-167.64	2.21E-03	2.53E-03	2.96E-03	3.40E-03	3.84E-03	4.27E-03	4.71E-03
-182.88	1.63E-03	1.86E-03	2.18E-03	2.50E-03	2.82E-03	3.14E-03	3.46E-03
-198.12	1.14E-03	1.31E-03	1.53E-03	1.75E-03	1.98E-03	2.20E-03	2.42E-03
-213.36	7.94E-04	9.05E-04	1.06E-03	1.21E-03	1.36E-03	1.52E-03	1.67E-03
-228.60	5.58E-04	6.35E-04	7.42E-04	8.48E-04	9.55E-04	1.06E-03	1.17E-03
-243.84	4.06E-04	4.61E-04	5.38E-04	6.14E-04	6.91E-04	7.67E-04	8.44E-04
-259.08	3.04E-04	3.46E-04	4.02E-04	4.59E-04	5.16E-04	5.73E-04	6.30E-04
-274.32	2.34E-04	2.66E-04	3.09E-04	3.53E-04	3.96E-04	4.39E-04	4.83E-04
-289.56	1.88E-04	2.14E-04	2.48E-04	2.83E-04	3.18E-04	3.53E-04	3.88E-04
-304.80	1.55E-04	1.75E-04	2.04E-04	2.32E-04	2.60E-04	2.89E-04	3.17E-04

Note(s):

1. Elevations are given with respect to the midplane of the active fuel.
2. Value listed is the projected EFPY at the end of Cycle 30.
3. This elevation corresponds to the top of the 6-inch-thick horizontal plate at the top-center of the RPV support structure.
4. Linear interpolation between the EFPY values listed in this table may be performed as necessary.

Table 4-19
Iron Atom Displacements (E > 0.1 MeV) at the RPV Support Structure –
No Bias on the Peripheral and Re-Entrant Corner Assembly Relative Powers

Elevation[1] (cm)	Iron Atom Displacements – Neutron Energies > 0.1 MeV (dpa)						
	37.66 EFPY[2]	42 EFPY	48 EFPY	54 EFPY	60 EFPY	66 EFPY	72 EFPY
218.81[3]	6.57E-04	7.42E-04	8.60E-04	9.78E-04	1.10E-03	1.21E-03	1.33E-03
213.36	7.73E-04	8.74E-04	1.01E-03	1.15E-03	1.29E-03	1.43E-03	1.57E-03
198.12	1.12E-03	1.27E-03	1.47E-03	1.68E-03	1.88E-03	2.08E-03	2.29E-03
182.88	1.53E-03	1.74E-03	2.02E-03	2.30E-03	2.58E-03	2.86E-03	3.14E-03
167.64	2.06E-03	2.34E-03	2.72E-03	3.10E-03	3.48E-03	3.85E-03	4.23E-03
152.40	2.65E-03	3.00E-03	3.48E-03	3.97E-03	4.45E-03	4.94E-03	5.43E-03
137.16	3.20E-03	3.63E-03	4.21E-03	4.80E-03	5.38E-03	5.96E-03	6.55E-03
121.92	3.68E-03	4.16E-03	4.82E-03	5.49E-03	6.16E-03	6.82E-03	7.49E-03
106.68	4.04E-03	4.56E-03	5.29E-03	6.02E-03	6.75E-03	7.47E-03	8.20E-03
91.44	4.33E-03	4.90E-03	5.68E-03	6.45E-03	7.23E-03	8.01E-03	8.79E-03
76.20	4.63E-03	5.23E-03	6.06E-03	6.89E-03	7.72E-03	8.55E-03	9.37E-03
60.96	4.52E-03	5.10E-03	5.91E-03	6.71E-03	7.52E-03	8.32E-03	9.13E-03
45.72	4.50E-03	5.08E-03	5.88E-03	6.68E-03	7.48E-03	8.28E-03	9.08E-03
30.48	4.48E-03	5.06E-03	5.85E-03	6.65E-03	7.45E-03	8.24E-03	9.04E-03
15.24	4.46E-03	5.03E-03	5.82E-03	6.62E-03	7.41E-03	8.20E-03	8.99E-03
0.00	4.45E-03	5.02E-03	5.81E-03	6.60E-03	7.39E-03	8.18E-03	8.98E-03
-15.24	4.45E-03	5.02E-03	5.82E-03	6.61E-03	7.40E-03	8.19E-03	8.98E-03
-30.48	4.45E-03	5.02E-03	5.81E-03	6.60E-03	7.40E-03	8.19E-03	8.98E-03
-45.72	4.42E-03	4.99E-03	5.78E-03	6.57E-03	7.35E-03	8.14E-03	8.93E-03
-60.96	4.37E-03	4.94E-03	5.72E-03	6.50E-03	7.27E-03	8.05E-03	8.83E-03
-76.20	4.29E-03	4.84E-03	5.61E-03	6.38E-03	7.14E-03	7.91E-03	8.67E-03
-91.44	4.15E-03	4.68E-03	5.43E-03	6.17E-03	6.91E-03	7.66E-03	8.40E-03
-106.68	3.92E-03	4.43E-03	5.13E-03	5.84E-03	6.54E-03	7.25E-03	7.95E-03
-121.92	3.58E-03	4.05E-03	4.70E-03	5.35E-03	6.00E-03	6.64E-03	7.29E-03
-137.16	3.14E-03	3.55E-03	4.12E-03	4.69E-03	5.26E-03	5.83E-03	6.40E-03
-152.40	2.60E-03	2.95E-03	3.42E-03	3.90E-03	4.38E-03	4.85E-03	5.33E-03
-167.64	2.02E-03	2.29E-03	2.66E-03	3.03E-03	3.40E-03	3.77E-03	4.15E-03
-182.88	1.48E-03	1.67E-03	1.94E-03	2.21E-03	2.48E-03	2.75E-03	3.02E-03
-198.12	1.03E-03	1.16E-03	1.35E-03	1.53E-03	1.72E-03	1.91E-03	2.09E-03
-213.36	7.02E-04	7.93E-04	9.18E-04	1.04E-03	1.17E-03	1.30E-03	1.42E-03
-228.60	4.86E-04	5.48E-04	6.34E-04	7.20E-04	8.06E-04	8.92E-04	9.78E-04
-243.84	3.48E-04	3.93E-04	4.53E-04	5.14E-04	5.75E-04	6.36E-04	6.97E-04
-259.08	2.59E-04	2.91E-04	3.36E-04	3.81E-04	4.26E-04	4.71E-04	5.16E-04
-274.32	1.98E-04	2.23E-04	2.57E-04	2.91E-04	3.25E-04	3.59E-04	3.93E-04
-289.56	1.58E-04	1.78E-04	2.05E-04	2.32E-04	2.59E-04	2.86E-04	3.13E-04
-304.80	1.29E-04	1.45E-04	1.67E-04	1.89E-04	2.11E-04	2.33E-04	2.55E-04

Note(s):

1. Elevations are given with respect to the midplane of the active fuel.
2. Value listed is the projected EFPY at the end of Cycle 30.
3. This elevation corresponds to the top of the 6-inch-thick horizontal plate at the top-center of the RPV support structure.
4. Linear interpolation between the EFPY values listed in this table may be performed as necessary.

Table 4-20
Iron Atom Displacements (E > 0.1 MeV) at the RPV Support Structure –
+10% Bias on the Peripheral and Re-Entrant Corner Assembly Relative Powers

Elevation[1] (cm)	Iron Atom Displacements – Neutron Energies > 0.1 MeV (dpa)						
	37.66 EFPY[2]	42 EFPY	48 EFPY	54 EFPY	60 EFPY	66 EFPY	72 EFPY
218.81[3]	6.57E-04	7.49E-04	8.77E-04	1.00E-03	1.13E-03	1.26E-03	1.39E-03
213.36	7.73E-04	8.83E-04	1.03E-03	1.18E-03	1.34E-03	1.49E-03	1.64E-03
198.12	1.12E-03	1.28E-03	1.50E-03	1.72E-03	1.94E-03	2.16E-03	2.38E-03
182.88	1.53E-03	1.75E-03	2.06E-03	2.36E-03	2.66E-03	2.97E-03	3.27E-03
167.64	2.06E-03	2.36E-03	2.77E-03	3.18E-03	3.59E-03	4.01E-03	4.42E-03
152.40	2.65E-03	3.03E-03	3.56E-03	4.08E-03	4.61E-03	5.13E-03	5.66E-03
137.16	3.20E-03	3.66E-03	4.30E-03	4.93E-03	5.56E-03	6.20E-03	6.83E-03
121.92	3.68E-03	4.20E-03	4.92E-03	5.64E-03	6.37E-03	7.09E-03	7.81E-03
106.68	4.04E-03	4.61E-03	5.40E-03	6.19E-03	6.98E-03	7.77E-03	8.56E-03
91.44	4.33E-03	4.95E-03	5.79E-03	6.63E-03	7.48E-03	8.32E-03	9.16E-03
76.20	4.63E-03	5.28E-03	6.18E-03	7.08E-03	7.98E-03	8.88E-03	9.78E-03
60.96	4.52E-03	5.15E-03	6.03E-03	6.90E-03	7.77E-03	8.64E-03	9.52E-03
45.72	4.50E-03	5.13E-03	5.99E-03	6.86E-03	7.73E-03	8.60E-03	9.46E-03
30.48	4.48E-03	5.11E-03	5.97E-03	6.83E-03	7.70E-03	8.56E-03	9.42E-03
15.24	4.46E-03	5.08E-03	5.94E-03	6.79E-03	7.65E-03	8.51E-03	9.37E-03
0.00	4.45E-03	5.07E-03	5.92E-03	6.78E-03	7.64E-03	8.49E-03	9.35E-03
-15.24	4.45E-03	5.07E-03	5.93E-03	6.79E-03	7.64E-03	8.50E-03	9.36E-03
-30.48	4.45E-03	5.07E-03	5.92E-03	6.78E-03	7.64E-03	8.50E-03	9.35E-03
-45.72	4.42E-03	5.04E-03	5.89E-03	6.74E-03	7.59E-03	8.45E-03	9.30E-03
-60.96	4.37E-03	4.98E-03	5.83E-03	6.67E-03	7.51E-03	8.36E-03	9.20E-03
-76.20	4.29E-03	4.89E-03	5.72E-03	6.55E-03	7.38E-03	8.21E-03	9.04E-03
-91.44	4.15E-03	4.73E-03	5.53E-03	6.34E-03	7.14E-03	7.95E-03	8.75E-03
-106.68	3.92E-03	4.47E-03	5.23E-03	6.00E-03	6.76E-03	7.52E-03	8.29E-03
-121.92	3.58E-03	4.09E-03	4.79E-03	5.49E-03	6.20E-03	6.90E-03	7.60E-03
-137.16	3.14E-03	3.58E-03	4.20E-03	4.82E-03	5.44E-03	6.06E-03	6.68E-03
-152.40	2.60E-03	2.98E-03	3.49E-03	4.01E-03	4.52E-03	5.04E-03	5.55E-03
-167.64	2.02E-03	2.31E-03	2.72E-03	3.12E-03	3.52E-03	3.92E-03	4.32E-03
-182.88	1.48E-03	1.69E-03	1.98E-03	2.27E-03	2.56E-03	2.86E-03	3.15E-03
-198.12	1.03E-03	1.17E-03	1.37E-03	1.58E-03	1.78E-03	1.98E-03	2.18E-03
-213.36	7.02E-04	8.00E-04	9.36E-04	1.07E-03	1.21E-03	1.34E-03	1.48E-03
-228.60	4.86E-04	5.53E-04	6.46E-04	7.39E-04	8.32E-04	9.25E-04	1.02E-03
-243.84	3.48E-04	3.96E-04	4.62E-04	5.28E-04	5.94E-04	6.60E-04	7.26E-04
-259.08	2.59E-04	2.94E-04	3.43E-04	3.91E-04	4.40E-04	4.89E-04	5.37E-04
-274.32	1.98E-04	2.25E-04	2.61E-04	2.98E-04	3.35E-04	3.72E-04	4.09E-04
-289.56	1.58E-04	1.80E-04	2.09E-04	2.38E-04	2.68E-04	2.97E-04	3.27E-04
-304.80	1.29E-04	1.46E-04	1.70E-04	1.94E-04	2.18E-04	2.42E-04	2.66E-04

Note(s):

1. Elevations are given with respect to the midplane of the active fuel.
2. Value listed is the projected EFPY at the end of Cycle 30.
3. This elevation corresponds to the top of the 6-inch-thick horizontal plate at the top-center of the RPV support structure.
4. Linear interpolation between the EFPY values listed in this table may be performed as necessary.

4.4 Bioshield Concrete

Neutron and gamma exposure data for the bioshield concrete are provided in Table 4-21 through Table 4-23. In particular, fast neutron (E > 1.0 MeV) fluences are provided in Table 4-21 as a function of irradiation time. Similar data, but for energies greater than 0.1 MeV, are provided in Table 4-22. Calculated gamma doses for the bioshield concrete are provided in Table 4-23. In all cases, the data provided in Table 4-21 through Table 4-23 are the maximum exposures experienced by the bioshield concrete at the azimuthal angles listed and at the azimuthal location providing the maximum exposure relative to the core cardinal axes.

Table 4-23 shows that the concrete gamma dose threshold value for consideration of radiation exposure effects, 1×10^{8} Gy (1×10^{10} rad), is not projected to be exceeded prior to a cumulative operating time of 72 EFPY.

Table 4-21
Fast Neutron (E > 1.0 MeV) Fluence at the Bioshield Concrete

Cycle	Cycle Length (EFPY)	Cumulative Operating Time (EFPY)	Fast Neutron (E > 1.0 MeV) Fluence (n/cm^2)							
			0°	15°	30°	45°	60°	75°	90°	Maximum
1	1.05	1.05	3.87E+15	1.33E+16	1.27E+16	1.19E+16	1.28E+16	1.55E+16	1.80E+16	1.80E+16
2	0.74	1.79	6.57E+15	2.27E+16	2.17E+16	2.02E+16	2.17E+16	2.64E+16	3.07E+16	3.07E+16
3	0.69	2.48	9.11E+15	3.15E+16	3.00E+16	2.80E+16	3.01E+16	3.66E+16	4.25E+16	4.25E+16
4	1.22	3.70	1.36E+16	4.70E+16	4.49E+16	4.18E+16	4.50E+16	5.46E+16	6.35E+16	6.35E+16
5	1.12	4.82	1.74E+16	5.94E+16	5.59E+16	5.16E+16	5.60E+16	6.93E+16	8.13E+16	8.13E+16
6	1.36	6.18	2.43E+16	8.27E+16	7.70E+16	7.04E+16	7.71E+16	9.64E+16	1.13E+17	1.13E+17
7	1.05	7.22	2.97E+16	1.01E+17	9.33E+16	8.49E+16	9.34E+16	1.17E+17	1.38E+17	1.38E+17
8	1.18	8.41	3.57E+16	1.21E+17	1.12E+17	1.01E+17	1.12E+17	1.41E+17	1.66E+17	1.66E+17
9	1.29	9.70	4.23E+16	1.43E+17	1.32E+17	1.19E+17	1.32E+17	1.67E+17	1.96E+17	1.96E+17
10	1.31	11.01	4.67E+16	1.60E+17	1.50E+17	1.37E+17	1.50E+17	1.86E+17	2.16E+17	2.16E+17
11	1.21	12.22	5.04E+16	1.74E+17	1.67E+17	1.54E+17	1.67E+17	2.02E+17	2.32E+17	2.32E+17
12	1.27	13.48	5.48E+16	1.91E+17	1.86E+17	1.72E+17	1.86E+17	2.21E+17	2.51E+17	2.51E+17
13	1.14	14.62	5.83E+16	2.05E+17	2.02E+17	1.87E+17	2.02E+17	2.36E+17	2.66E+17	2.66E+17
14	1.18	15.80	6.21E+16	2.19E+17	2.18E+17	2.02E+17	2.18E+17	2.52E+17	2.82E+17	2.82E+17
15	1.62	17.42	6.78E+16	2.39E+17	2.36E+17	2.19E+17	2.36E+17	2.74E+17	3.08E+17	3.08E+17
16	1.44	18.86	7.31E+16	2.58E+17	2.55E+17	2.38E+17	2.55E+17	2.96E+17	3.32E+17	3.32E+17
17	1.39	20.26	7.75E+16	2.73E+17	2.71E+17	2.53E+17	2.71E+17	3.14E+17	3.52E+17	3.52E+17
18	1.40	21.66	8.22E+16	2.90E+17	2.87E+17	2.68E+17	2.87E+17	3.32E+17	3.74E+17	3.74E+17
19	1.42	23.08	8.68E+16	3.06E+17	3.03E+17	2.84E+17	3.03E+17	3.51E+17	3.94E+17	3.94E+17
20	1.27	24.35	9.12E+16	3.21E+17	3.18E+17	2.98E+17	3.18E+17	3.69E+17	4.14E+17	4.14E+17
21	1.38	25.73	9.60E+16	3.38E+17	3.33E+17	3.12E+17	3.33E+17	3.87E+17	4.36E+17	4.36E+17
22	1.35	27.08	1.01E+17	3.55E+17	3.49E+17	3.26E+17	3.49E+17	4.07E+17	4.59E+17	4.59E+17
23	1.31	28.39	1.06E+17	3.72E+17	3.65E+17	3.42E+17	3.65E+17	4.26E+17	4.82E+17	4.82E+17
24	1.29	29.67	1.11E+17	3.91E+17	3.83E+17	3.59E+17	3.84E+17	4.49E+17	5.07E+17	5.07E+17
25	1.33	31.00	1.18E+17	4.12E+17	4.04E+17	3.78E+17	4.04E+17	4.74E+17	5.37E+17	5.37E+17
26	1.33	32.33	1.24E+17	4.34E+17	4.24E+17	3.98E+17	4.25E+17	4.99E+17	5.66E+17	5.66E+17

Table 4-21
Fast Neutron (E > 1.0 MeV) Fluence at the Bioshield Concrete

Cycle	Cycle Length (EFPY)	Cumulative Operating Time (EFPY)	Fast Neutron (E > 1.0 MeV) Fluence (n/cm^2)							
			0°	15°	30°	45°	60°	75°	90°	Maximum
27	1.30	33.64	1.30E+17	4.53E+17	4.41E+17	4.13E+17	4.41E+17	5.21E+17	5.93E+17	5.93E+17
28	1.30	34.94	1.35E+17	4.71E+17	4.58E+17	4.29E+17	4.58E+17	5.42E+17	6.17E+17	6.17E+17
29	1.37	36.31	1.41E+17	4.91E+17	4.76E+17	4.46E+17	4.76E+17	5.65E+17	6.44E+17	6.44E+17
30[1]	1.35	37.66	1.47E+17	5.11E+17	4.95E+17	4.63E+17	4.95E+17	5.88E+17	6.71E+17	6.71E+17
Projections with no bias on the peripheral and re-entrant corner assembly relative powers										
Future[2]	--	42.00	1.66E+17	5.73E+17	5.52E+17	5.15E+17	5.52E+17	6.60E+17	7.57E+17	7.57E+17
Future[2]	--	48.00	1.92E+17	6.60E+17	6.31E+17	5.88E+17	6.30E+17	7.61E+17	8.76E+17	8.76E+17
Future[2]	--	54.00	2.17E+17	7.46E+17	7.10E+17	6.61E+17	7.09E+17	8.61E+17	9.95E+17	9.95E+17
Future[2]	--	60.00	2.43E+17	8.33E+17	7.89E+17	7.34E+17	7.88E+17	9.62E+17	1.11E+18	1.11E+18
Future[2]	--	66.00	2.69E+17	9.19E+17	8.68E+17	8.07E+17	8.66E+17	1.06E+18	1.23E+18	1.23E+18
Future[2]	--	72.00	2.95E+17	1.01E+18	9.47E+17	8.79E+17	9.45E+17	1.16E+18	1.35E+18	1.35E+18
Projections with a +10% bias on the peripheral and re-entrant corner assembly relative powers										
Future[2]	--	42.00	1.67E+17	5.79E+17	5.57E+17	5.20E+17	5.57E+17	6.66E+17	7.64E+17	7.64E+17
Future[2]	--	48.00	1.95E+17	6.72E+17	6.43E+17	5.99E+17	6.42E+17	7.75E+17	8.93E+17	8.93E+17
Future[2]	--	54.00	2.23E+17	7.66E+17	7.28E+17	6.78E+17	7.28E+17	8.84E+17	1.02E+18	1.02E+18
Future[2]	--	60.00	2.51E+17	8.60E+17	8.14E+17	7.58E+17	8.13E+17	9.93E+17	1.15E+18	1.15E+18
Future[2]	--	66.00	2.79E+17	9.54E+17	9.00E+17	8.37E+17	8.99E+17	1.10E+18	1.28E+18	1.28E+18
Future[2]	--	72.00	3.07E+17	1.05E+18	9.86E+17	9.16E+17	9.84E+17	1.21E+18	1.41E+18	1.41E+18

Note(s):

1. Cycle 30 was the current operating cycle at the time the exposures reported in this table were determined. Values listed are based on the projected EFPY for this cycle.
2. Values beyond Cycle 30 are based on the average core power distributions and reactor operating conditions of Cycle 29 and are determined both with and without a 1.1 bias on the peripheral and re-entrant corner assembly relative powers.

Table 4-22
Fast Neutron (E > 0.1 MeV) Fluence at the Bioshield Concrete

Cycle	Cycle Length (EFPY)	Cumulative Operating Time (EFPY)	Fast Neutron (E > 0.1 MeV) Fluence (n/cm^2)							
			0°	15°	30°	45°	60°	75°	90°	Maximum
1	1.05	1.05	1.03E+17	1.70E+17	1.57E+17	1.44E+17	1.50E+17	1.76E+17	1.97E+17	1.97E+17
2	0.74	1.79	1.76E+17	2.90E+17	2.67E+17	2.44E+17	2.55E+17	2.99E+17	3.35E+17	3.35E+17
3	0.69	2.48	2.43E+17	4.01E+17	3.70E+17	3.38E+17	3.54E+17	4.14E+17	4.65E+17	4.65E+17
4	1.22	3.70	3.63E+17	6.00E+17	5.53E+17	5.06E+17	5.28E+17	6.18E+17	6.94E+17	6.94E+17
5	1.12	4.82	4.63E+17	7.58E+17	6.92E+17	6.27E+17	6.60E+17	7.83E+17	8.85E+17	8.85E+17
6	1.36	6.18	6.16E+17	1.01E+18	9.11E+17	8.21E+17	8.67E+17	1.04E+18	1.17E+18	1.17E+18
7	1.05	7.22	7.35E+17	1.20E+18	1.08E+18	9.70E+17	1.03E+18	1.23E+18	1.40E+18	1.40E+18
8	1.18	8.41	8.68E+17	1.41E+18	1.27E+18	1.14E+18	1.21E+18	1.45E+18	1.65E+18	1.65E+18
9	1.29	9.70	1.01E+18	1.65E+18	1.48E+18	1.32E+18	1.40E+18	1.69E+18	1.92E+18	1.92E+18
10	1.31	11.01	1.11E+18	1.83E+18	1.66E+18	1.49E+18	1.58E+18	1.87E+18	2.10E+18	2.10E+18
11	1.21	12.22	1.19E+18	1.98E+18	1.82E+18	1.65E+18	1.74E+18	2.02E+18	2.25E+18	2.25E+18
12	1.27	13.48	1.29E+18	2.15E+18	2.01E+18	1.83E+18	1.91E+18	2.20E+18	2.43E+18	2.43E+18
13	1.14	14.62	1.37E+18	2.29E+18	2.16E+18	1.97E+18	2.06E+18	2.34E+18	2.57E+18	2.57E+18
14	1.18	15.80	1.45E+18	2.44E+18	2.31E+18	2.12E+18	2.21E+18	2.49E+18	2.72E+18	2.72E+18
15	1.62	17.42	1.57E+18	2.65E+18	2.50E+18	2.29E+18	2.39E+18	2.70E+18	2.96E+18	2.96E+18
16	1.44	18.86	1.69E+18	2.85E+18	2.69E+18	2.47E+18	2.57E+18	2.90E+18	3.17E+18	3.17E+18
17	1.39	20.26	1.79E+18	3.01E+18	2.85E+18	2.62E+18	2.72E+18	3.07E+18	3.36E+18	3.36E+18
18	1.40	21.66	1.89E+18	3.19E+18	3.01E+18	2.77E+18	2.88E+18	3.24E+18	3.55E+18	3.55E+18
19	1.42	23.08	2.00E+18	3.36E+18	3.18E+18	2.93E+18	3.03E+18	3.42E+18	3.74E+18	3.74E+18
20	1.27	24.35	2.09E+18	3.52E+18	3.33E+18	3.07E+18	3.18E+18	3.58E+18	3.92E+18	3.92E+18
21	1.38	25.73	2.20E+18	3.69E+18	3.49E+18	3.21E+18	3.33E+18	3.76E+18	4.12E+18	4.12E+18
22	1.35	27.08	2.31E+18	3.87E+18	3.65E+18	3.35E+18	3.48E+18	3.94E+18	4.33E+18	4.33E+18
23	1.31	28.39	2.42E+18	4.05E+18	3.81E+18	3.51E+18	3.64E+18	4.13E+18	4.53E+18	4.53E+18
24	1.29	29.67	2.54E+18	4.26E+18	4.00E+18	3.68E+18	3.82E+18	4.33E+18	4.76E+18	4.76E+18
25	1.33	31.00	2.68E+18	4.49E+18	4.21E+18	3.87E+18	4.02E+18	4.57E+18	5.03E+18	5.03E+18
26	1.33	32.33	2.83E+18	4.72E+18	4.43E+18	4.07E+18	4.22E+18	4.81E+18	5.30E+18	5.30E+18

Table 4-22
Fast Neutron (E > 0.1 MeV) Fluence at the Bioshield Concrete

Cycle	Cycle Length (EFPY)	Cumulative Operating Time (EFPY)	Fast Neutron (E > 0.1 MeV) Fluence (n/cm^2)							
			0°	15°	30°	45°	60°	75°	90°	Maximum
27	1.30	33.64	2.95E+18	4.92E+18	4.60E+18	4.23E+18	4.39E+18	5.02E+18	5.54E+18	5.54E+18
28	1.30	34.94	3.07E+18	5.12E+18	4.78E+18	4.39E+18	4.56E+18	5.21E+18	5.75E+18	5.75E+18
29	1.37	36.31	3.20E+18	5.33E+18	4.97E+18	4.56E+18	4.73E+18	5.43E+18	6.00E+18	6.00E+18
30[1]	1.35	37.66	3.33E+18	5.54E+18	5.16E+18	4.73E+18	4.91E+18	5.64E+18	6.24E+18	6.24E+18
Projections with no bias on the peripheral and re-entrant corner assembly relative powers										
Future[2]	--	42.00	3.74E+18	6.20E+18	5.75E+18	5.27E+18	5.48E+18	6.32E+18	7.02E+18	7.02E+18
Future[2]	--	48.00	4.31E+18	7.12E+18	6.58E+18	6.01E+18	6.25E+18	7.26E+18	8.09E+18	8.09E+18
Future[2]	--	54.00	4.88E+18	8.05E+18	7.40E+18	6.75E+18	7.03E+18	8.20E+18	9.16E+18	9.16E+18
Future[2]	--	60.00	5.45E+18	8.97E+18	8.22E+18	7.49E+18	7.81E+18	9.14E+18	1.02E+19	1.02E+19
Future[2]	--	66.00	6.02E+18	9.89E+18	9.04E+18	8.23E+18	8.58E+18	1.01E+19	1.13E+19	1.13E+19
Future[2]	--	72.00	6.60E+18	1.08E+19	9.86E+18	8.97E+18	9.36E+18	1.10E+19	1.24E+19	1.24E+19
Projections with a +10% bias on the peripheral and re-entrant corner assembly relative powers										
Future[2]	--	42.00	3.77E+18	6.26E+18	5.81E+18	5.32E+18	5.52E+18	6.38E+18	7.08E+18	7.08E+18
Future[2]	--	48.00	4.39E+18	7.26E+18	6.70E+18	6.12E+18	6.37E+18	7.40E+18	8.25E+18	8.25E+18
Future[2]	--	54.00	5.01E+18	8.26E+18	7.59E+18	6.93E+18	7.21E+18	8.42E+18	9.41E+18	9.41E+18
Future[2]	--	60.00	5.63E+18	9.26E+18	8.48E+18	7.73E+18	8.06E+18	9.44E+18	1.06E+19	1.06E+19
Future[2]	--	66.00	6.25E+18	1.03E+19	9.38E+18	8.54E+18	8.90E+18	1.05E+19	1.17E+19	1.17E+19
Future[2]	--	72.00	6.87E+18	1.13E+19	1.03E+19	9.34E+18	9.74E+18	1.15E+19	1.29E+19	1.29E+19

Note(s):

1. Cycle 30 was the current operating cycle at the time the exposures reported in this table were determined. Values listed are based on the projected EFPY for this cycle.
2. Values beyond Cycle 30 are based on the average core power distributions and reactor operating conditions of Cycle 29 and are determined both with and without a 1.1 bias on the peripheral and re-entrant corner assembly relative powers.

Table 4-23
Gamma Dose at the Bioshield Concrete

Cycle	Cycle Length (EFPY)	Cumulative Operating Time (EFPY)	Gamma Dose (Gy)							
			0°	15°	30°	45°	60°	75°	90°	Maximum
1	1.05	1.05	3.05E+05	5.45E+05	5.16E+05	4.99E+05	5.24E+05	5.81E+05	6.37E+05	6.38E+05
2	0.74	1.79	5.18E+05	9.27E+05	8.77E+05	8.49E+05	8.91E+05	9.88E+05	1.08E+06	1.09E+06
3	0.69	2.48	7.18E+05	1.29E+06	1.22E+06	1.18E+06	1.23E+06	1.37E+06	1.50E+06	1.50E+06
4	1.22	3.70	1.07E+06	1.92E+06	1.82E+06	1.76E+06	1.84E+06	2.05E+06	2.24E+06	2.25E+06
5	1.12	4.82	1.36E+06	2.42E+06	2.27E+06	2.18E+06	2.30E+06	2.58E+06	2.85E+06	2.86E+06
6	1.36	6.18	1.81E+06	3.73E+06	3.45E+06	3.26E+06	3.49E+06	3.95E+06	4.34E+06	4.35E+06
7	1.05	7.22	2.16E+06	4.75E+06	4.36E+06	4.10E+06	4.41E+06	5.00E+06	5.49E+06	5.50E+06
8	1.18	8.41	2.56E+06	5.89E+06	5.39E+06	5.04E+06	5.44E+06	6.18E+06	6.79E+06	6.81E+06
9	1.29	9.70	2.99E+06	7.15E+06	6.52E+06	6.07E+06	6.58E+06	7.48E+06	8.21E+06	8.23E+06
10	1.31	11.01	3.30E+06	8.07E+06	7.53E+06	7.05E+06	7.59E+06	8.44E+06	9.13E+06	9.15E+06
11	1.21	12.22	3.56E+06	8.88E+06	8.48E+06	7.99E+06	8.54E+06	9.27E+06	9.87E+06	9.89E+06
12	1.27	13.48	3.87E+06	9.83E+06	9.54E+06	9.01E+06	9.62E+06	1.02E+07	1.08E+07	1.08E+07
13	1.14	14.62	4.12E+06	1.06E+07	1.04E+07	9.85E+06	1.05E+07	1.10E+07	1.15E+07	1.15E+07
14	1.18	15.80	4.38E+06	1.14E+07	1.13E+07	1.07E+07	1.14E+07	1.19E+07	1.23E+07	1.23E+07
15	1.62	17.42	4.76E+06	1.25E+07	1.23E+07	1.17E+07	1.24E+07	1.30E+07	1.34E+07	1.35E+07
16	1.44	18.86	5.12E+06	1.35E+07	1.34E+07	1.27E+07	1.35E+07	1.40E+07	1.45E+07	1.46E+07
17	1.39	20.26	5.42E+06	1.44E+07	1.42E+07	1.36E+07	1.43E+07	1.49E+07	1.55E+07	1.55E+07
18	1.40	21.66	5.74E+06	1.52E+07	1.51E+07	1.45E+07	1.52E+07	1.58E+07	1.64E+07	1.65E+07
19	1.42	23.08	6.06E+06	1.61E+07	1.60E+07	1.53E+07	1.61E+07	1.68E+07	1.74E+07	1.74E+07
20	1.27	24.35	6.36E+06	1.70E+07	1.69E+07	1.61E+07	1.70E+07	1.76E+07	1.83E+07	1.83E+07
21	1.38	25.73	6.68E+06	1.79E+07	1.77E+07	1.69E+07	1.78E+07	1.86E+07	1.93E+07	1.93E+07
22	1.35	27.08	7.01E+06	1.88E+07	1.85E+07	1.77E+07	1.87E+07	1.95E+07	2.03E+07	2.04E+07
23	1.31	28.39	7.34E+06	1.97E+07	1.94E+07	1.86E+07	1.96E+07	2.05E+07	2.13E+07	2.14E+07
24	1.29	29.67	7.71E+06	2.08E+07	2.05E+07	1.96E+07	2.06E+07	2.16E+07	2.25E+07	2.26E+07
25	1.33	31.00	8.15E+06	2.20E+07	2.16E+07	2.07E+07	2.17E+07	2.28E+07	2.39E+07	2.39E+07
26	1.33	32.33	8.58E+06	2.32E+07	2.27E+07	2.18E+07	2.29E+07	2.41E+07	2.52E+07	2.53E+07

Table 4-23
Gamma Dose at the Bioshield Concrete

Cycle	Cycle Length (EFPY)	Cumulative Operating Time (EFPY)	Gamma Dose (Gy)							
			0°	15°	30°	45°	60°	75°	90°	Maximum
27	1.30	33.64	8.95E+06	2.42E+07	2.37E+07	2.27E+07	2.38E+07	2.52E+07	2.64E+07	2.65E+07
28	1.30	34.94	9.31E+06	2.52E+07	2.46E+07	2.36E+07	2.48E+07	2.62E+07	2.75E+07	2.76E+07
29	1.37	36.31	9.70E+06	2.63E+07	2.56E+07	2.45E+07	2.58E+07	2.73E+07	2.88E+07	2.88E+07
30[1]	1.35	37.66	1.01E+07	2.74E+07	2.66E+07	2.55E+07	2.68E+07	2.84E+07	3.00E+07	3.01E+07
Projections with no bias on the peripheral and re-entrant corner assembly relative powers										
Future[2]	--	42.00	1.13E+07	3.08E+07	2.98E+07	2.85E+07	2.99E+07	3.20E+07	3.39E+07	3.40E+07
Future[2]	--	48.00	1.30E+07	3.55E+07	3.41E+07	3.26E+07	3.43E+07	3.69E+07	3.93E+07	3.94E+07
Future[2]	--	54.00	1.47E+07	4.03E+07	3.85E+07	3.68E+07	3.87E+07	4.18E+07	4.48E+07	4.49E+07
Future[2]	--	60.00	1.65E+07	4.50E+07	4.28E+07	4.09E+07	4.30E+07	4.68E+07	5.02E+07	5.03E+07
Future[2]	--	66.00	1.82E+07	4.97E+07	4.72E+07	4.50E+07	4.74E+07	5.17E+07	5.56E+07	5.58E+07
Future[2]	--	72.00	1.99E+07	5.44E+07	5.15E+07	4.92E+07	5.18E+07	5.66E+07	6.10E+07	6.12E+07
Projections with a +10% bias on the peripheral and re-entrant corner assembly relative powers										
Future[2]	--	42.00	1.14E+07	3.11E+07	3.01E+07	2.88E+07	3.02E+07	3.23E+07	3.42E+07	3.43E+07
Future[2]	--	48.00	1.33E+07	3.62E+07	3.48E+07	3.33E+07	3.50E+07	3.77E+07	4.01E+07	4.03E+07
Future[2]	--	54.00	1.51E+07	4.14E+07	3.95E+07	3.78E+07	3.97E+07	4.30E+07	4.60E+07	4.62E+07
Future[2]	--	60.00	1.70E+07	4.65E+07	4.43E+07	4.23E+07	4.45E+07	4.84E+07	5.19E+07	5.21E+07
Future[2]	--	66.00	1.89E+07	5.17E+07	4.90E+07	4.68E+07	4.92E+07	5.37E+07	5.78E+07	5.80E+07
Future[2]	--	72.00	2.07E+07	5.68E+07	5.37E+07	5.13E+07	5.40E+07	5.91E+07	6.37E+07	6.39E+07

Note(s):

1. Cycle 30 was the current operating cycle at the time the exposures reported in this table were determined. Values listed are based on the projected EFPY for this cycle.
2. Values beyond Cycle 30 are based on the average core power distributions and reactor operating conditions of Cycle 29 and are determined both with and without a 1.1 bias on the peripheral and re-entrant corner assembly relative powers.

5.0 References

1. USNRC Regulatory Guide 1.190, "Calculational and Dosimetry Methods for Determining Pressure Vessel Neutron Fluence," Office of Nuclear Regulatory Research, March 2001.
2. Westinghouse Report WCAP-18124-NP-A, Revision 0, "Fluence Determination with RAPTOR-M3G and FERRET," July 2018.
3. Westinghouse InfoGram IG-13-2, "Fluence Attenuation Profile in Reactor Pressure Vessel Shell and Inlet/Outlet Nozzle Regions," July 2013.

Approval Information
Author Approval Hawk Andrew E May-26-2021 12:39:02
Reviewer Approval Fischer Greg A May-26-2021 13:15:35
Manager Approval Klingensmith Jesse J May-26-2021 13:32:42

Files approved on May-26-2021

Enclosure 4

Non-proprietary Reference Documents and Redacted Versions of Proprietary Reference Documents (Public Version)

Attachment 2

Westinghouse Report LTR-REA-21-2-NP, Revision 1, St. Lucie Units 1 & 2 Subsequent License Renewal: Unit 2 Reactor Vessel, Vessel Support, and Bioshield Concrete Exposure Data, June 7, 2021

(59 Total Pages, including cover sheets)

Westinghouse

To: John T. Ahearn
cc: Jay D. White

Date: June 7, 2021

From: Radiation Engineering & Analysis (REA)
Phone: (724) 940-8119
Email: nedwidfm@westinghouse.com
Our Ref: **LTR-REA-21-2-NP, Revision 1**

Subject: **St. Lucie Units 1 & 2 Subsequent License Renewal: Unit 2 Reactor Vessel, Vessel Support, and Bioshield Concrete Exposure Data**

Attachment(s): 1. St. Lucie Units 1 & 2 Subsequent License Renewal: Unit 2 Reactor Vessel, Vessel Support, and Bioshield Concrete Exposure Data

Attachment 1 provides select exposure data applicable to the St. Lucie Unit 2 reactor pressure vessel (RPV), RPV support structure, concrete bioshield, and in-vessel dosimetry. These data are intended to be used in downstream evaluations of the RPV pressure-temperature limit (PT-limit) curves, RPV support structure embrittlement, and bioshield concrete degradation. In addition, the information in Attachment 1 needs to be provided to Florida Power & Light Company (FPL) in support of the St. Lucie subsequent license renewal (SLR) project.

Changes made in Revision 1 of this summary report are clearly identified in the document comment and resolution form (DCRF) that is electronically attached in PRIME and, as such, are not marked with change bars.

Please contact the undersigned if there are any questions regarding this information.

Author: *(Electronically Approved)**
Frank M. Nedwidek
Nuclear Operations

Reviewer: *(Electronically Approved)**
Eugene T. Hayes
Radiation Engineering & Analysis

Approver: *(Electronically Approved)**
Jesse J Klingensmith
Radiation Engineering & Analysis

**Electronically approved records are authenticated in the electronic document management system.*

Attachment 1

St. Lucie Units 1 & 2 Subsequent License Renewal: Unit 2 Reactor Vessel, Vessel Support, and Bioshield Concrete Exposure Data

Table of Contents

1.0 Introduction ... 3
2.0 Discrete Ordinates Model ... 3
3.0 Dosimetry Comparisons ... 8
4.0 Exposure Results ... 10
4.1 Reactor Pressure Vessel ... 10
4.2 Surveillance Capsules ... 21
4.3 RPV Support Structure ... 30
4.4 Bioshield Concrete ... 49
5.0 References ... 56

1.0 Introduction

This attachment describes a discrete ordinates transport analysis that was performed for St. Lucie Unit 2. The results summarized in this attachment are intended to be used in downstream evaluations of the reactor pressure vessel (RPV) pressure-temperature limit (PT-limit) curves, RPV support structure embrittlement, and bioshield concrete degradation performed in support of the St. Lucie subsequent license renewal (SLR) project.

The neutron transport methodology used to generate the data provided in this attachment followed the guidance of Regulatory Guide 1.190 (Reference 1). It is also consistent with the methodology described in WCAP-18124-NP-A (Reference 2) that was approved by the United States Nuclear Regulatory Commission (USNRC). The methodology described Reference 2 has been generically-approved for calculating exposures of the RPV beltline (i.e., in general, RPV materials opposite the active fuel). Presently, there are no generically-approved methods for calculating exposures of RPV extended beltline materials, RPV support structures, or bioshield concrete.

2.0 Discrete Ordinates Model

Discrete ordinates transport calculations were performed on a fuel-cycle-specific basis to determine the neutron and gamma ray environment within the reactor (and reactor cavity) geometry. The specific methods applied were consistent with those described in Reference 2.

All of the transport calculations were performed using Version 3.0 of the RAPTOR-M3G discrete ordinates computer code and the BUGLE-96 cross section library. The BUGLE-96 library provides a 67-group coupled neutron-gamma ray cross section data set produced specifically for light water reactor applications. The transport calculations treated anisotropic scattering with a P_3 Legendre expansion and modeled the angular discretization with an S_{16} order of angular quadrature. Energy- and space-dependent core power distributions as well as system operating temperatures were treated on a fuel-cycle-specific basis.

A top view of the model geometry at the core midplane is shown in Figure 2-1. In this figure, a single quadrant is depicted showing the arrangement of the core, reactor internals, core barrel, RPV cladding, RPV, reactor cavity, reflective insulation, RPV support structure, and bioshield. Depictions of the in-vessel surveillance capsules, including their associated support structures, are also shown.

From a neutronics standpoint, the inclusion of the surveillance capsules and associated support structures in the geometric model is significant. Since the presence of the capsules and support structures has a marked impact on the magnitude of the neutron fluence rate and relative neutron and gamma ray spectra at dosimetry locations within the capsules, a meaningful evaluation of the radiation environment internal to the capsules can be made only when these perturbation effects are accounted for in the transport calculations.

A top view of the reactor model geometry at the nozzle centerline is shown in Figure 2-2.

An oblique view of the model geometry is shown in Figure 2-3. Note that the stainless steel girth ribs located between the core shroud and core barrel are shown in this figure. The RPV support structure located between the reflective insulation and bioshield is also shown.

When developing the reactor model shown in Figure 2-1 through Figure 2-3, nominal dimensions were typically used for the various structural components. Significant exceptions where as-built dimensions were used include the RPV inner radius (which is significantly different than the reference design dimensions) and surveillance capsule centerline and elevation.

Water temperatures and coolant densities in the core and downcomer regions of the reactor were taken to be representative of full-power operating conditions. Coolant above the core was assumed to be at core outlet conditions and coolant below the active core was assumed to be at core inlet conditions. All coolant temperatures and densities were varied on a cycle-specific basis. The reactor core itself was treated as a homogeneous mixture of fuel, cladding, water, and miscellaneous core structures such as fuel assembly grids and guide tubes.

The geometric mesh description of the reactor models shown in Figure 2-1 through Figure 2-3 consisted of 319 radial by 201 azimuthal by 408 axial intervals. Mesh sizes were chosen to ensure sufficient resolution of the stair-step-shaped shroud plates and a sufficient number of meshes throughout the radial and axial regions of interest. The pointwise inner iteration convergence criterion utilized in the calculations was set at a value of 0.001.

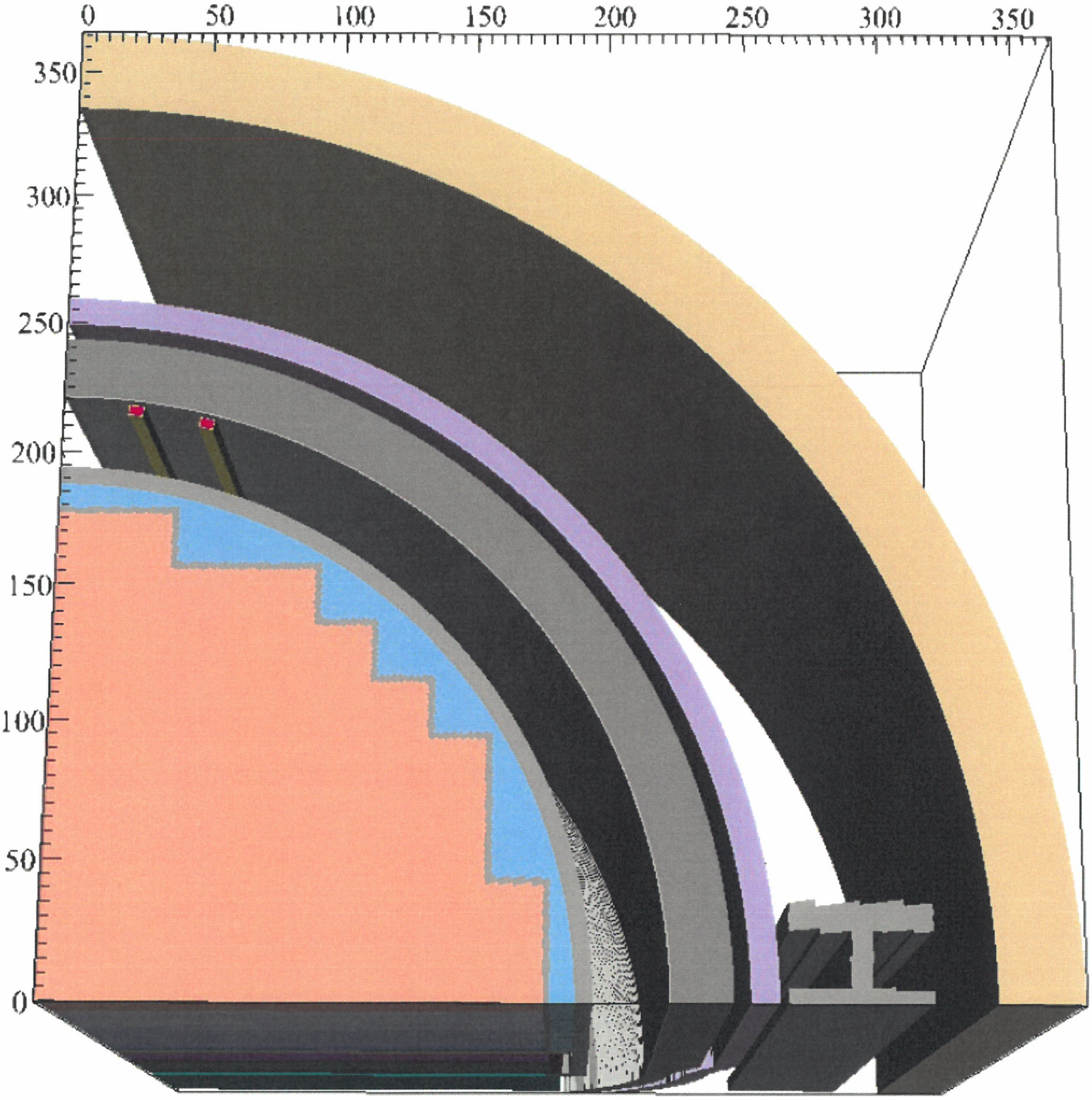

Dimensions shown are in centimeters.

Figure 2-1
Top View of the Reactor Geometry at the Core Midplane

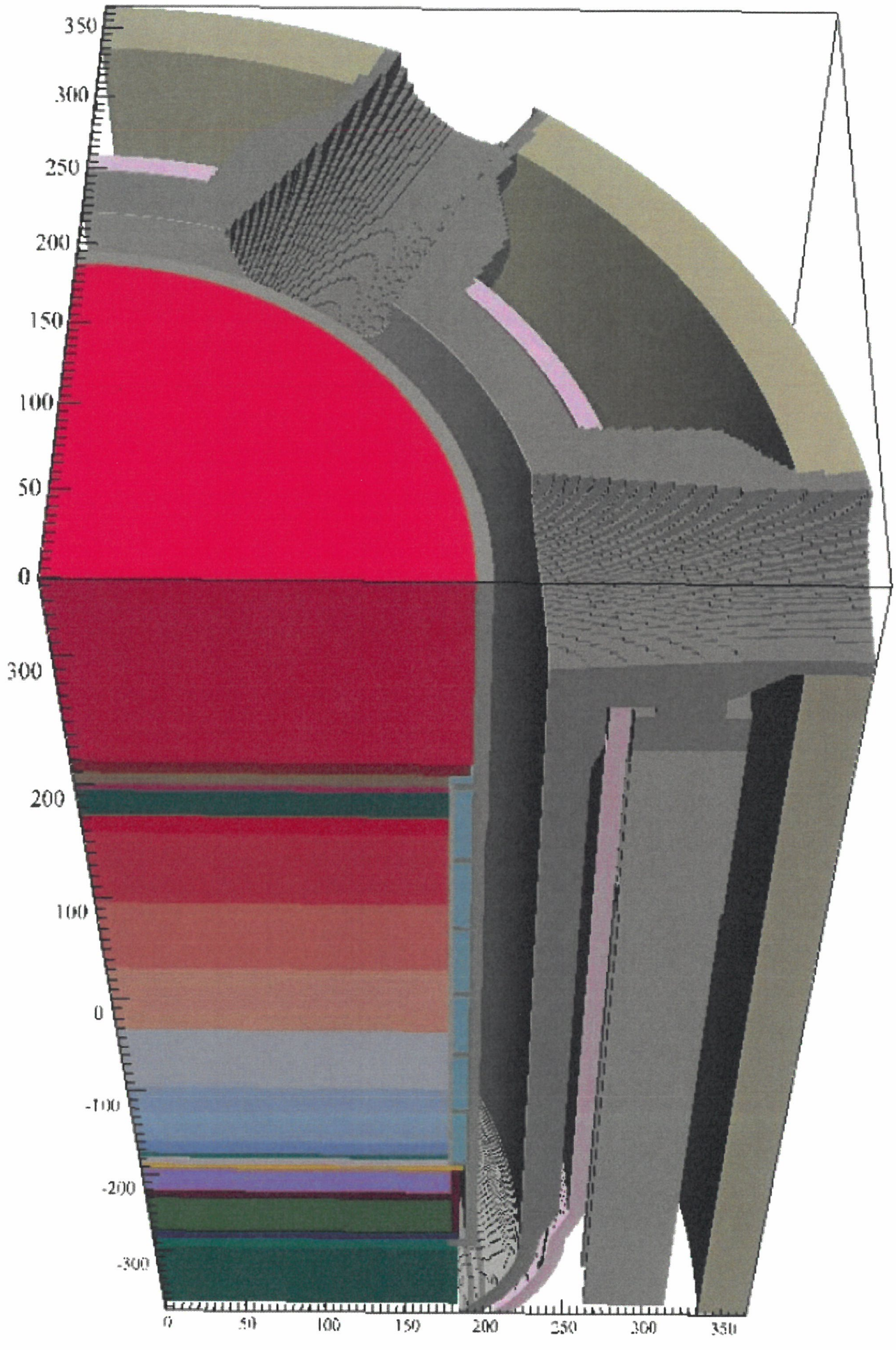

Dimensions shown are in centimeters.

Figure 2-2
Top View of the Reactor Geometry at the Nozzle Centerline

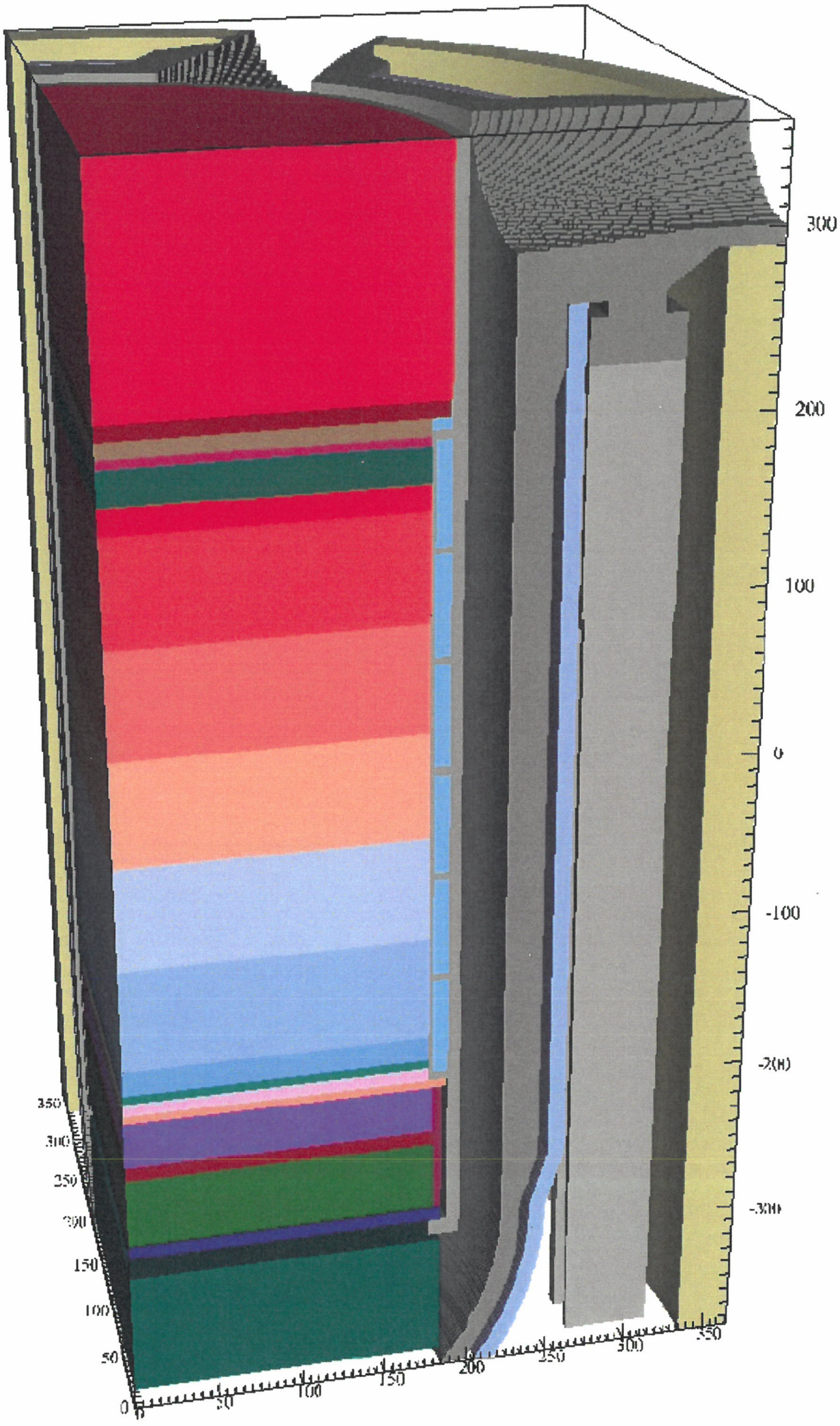

Dimensions shown are in centimeters.

Figure 2-3
Oblique View of the Reactor Geometry

3.0 Dosimetry Comparisons

Six surveillance capsules for monitoring the effects of neutron exposure on the RPV core region (beltline) materials were inserted in the reactor vessel prior to initial plant startup. These capsules were placed in the reactor vessel, between the core barrel and the vessel wall, at azimuthal angles of 83°, 97°, 263°, and 277° (7° from the core cardinal axis) and 104° and 284° (14° from the core cardinal axis).

To date, the following in-vessel surveillance capsules have been withdrawn from reactor core and analyzed as part of the reactor vessel materials surveillance program:

- Capsule 83° was withdrawn from the 83° location following the completion of Cycle 1.
- Capsule 263° was withdrawn from the 263° location following the completion of Cycle 9.
- Capsule 97° was withdrawn from the 97° location following the completion of Cycle 20.

These capsules were re-analyzed to validate the results of the plant-specific neutron transport calculations. More specifically, the Capsule 83°, 263°, and 97° threshold sensor measurements were compared with the applicable results of the RAPTOR-M3G calculations to demonstrate that, at the in-vessel locations where the sensors were irradiated, the measurements and calculations agreed within the ±20% criterion of Reference 1. These measurement and calculation comparisons were performed on two levels. On the first level, calculations of individual sensor reaction rates were compared directly with the measurement data from the counting laboratory. This level of comparison was not impacted by the least-squares evaluation of the sensor sets. On the second level, calculated values of neutron exposure rates in terms of fast neutron (E > 1.0 MeV) fluence rate and iron atom displacement rate were compared with the best-estimate exposure rates obtained from the least-squares evaluation.

Table 3-1 provides comparisons of the measurement-to-calculation (M/C) ratios for the neutron dosimetry in the in-vessel surveillance capsules. The overall average M/C ratio for the entire 13 sample data set is 1.06 with an associated standard deviation of 14%. The observed average M/C ratios range from 0.76 to 1.23 for the individual sensor types.

Table 3-2 provides comparisons of the best-estimate-to-calculation (BE/C) ratios for fast neutron (E > 1.0 MeV) fluence rate and iron atom displacement rate resulting from the least-squares evaluation of the neutron dosimetry in the in-vessel surveillance capsules. For these capsules, the average BE/C ratios are 1.01 with an associated standard deviation of 6.0% for fast neutron (E > 1.0 MeV) fluence rate, and 1.02 with an associated standard deviation of 5.5% for iron atom displacement rate.

The M/C and BE/C data comparisons in Table 3-1 and Table 3-2 provide a validation of the results of the plant-specific neutron transport calculations. Each of these data comparisons shows that the in-vessel measurements and calculations agree within the 20% criterion specified in Reference 1. In addition, the average M/C and BE/C results agree within the 13% (1σ) uncertainty assigned to the absolute transport calculations.

Table 3-1
Measurement-to-Calculation (M/C) Ratios for the Surveillance Capsules

Reaction	Capsule			Average	Std. Dev.
	83°	263°	97°		
$^{63}Cu\ (n,\alpha)\ ^{60}Co$	1.27	1.18	--[1]	1.23	5.2%
$^{46}Ti\ (n,p)\ ^{46}Sc$	1.13	1.13	1.10	1.12	1.5%
$^{54}Fe\ (n,p)\ ^{54}Mn$	1.11	1.11	1.02	1.08	4.8%
$^{58}Ni\ (n,p)\ ^{58}Co$	1.12	1.07	1.03	1.07	4.2%
$^{238}U(Cd)\ (n,f)\ ^{137}Cs$	0.75	--[1]	0.77	0.76	1.9%
Average of M/C Ratios				1.06	14%

Note(s):

1. The normalized reaction rate for this sensor was not within three standard deviations of the Combustion Engineering (CE) in-vessel surveillance capsule database value. This is indicative of a questionable measurement, and therefore is not included in measurement-to-calculation comparisons performed in accordance with Regulatory Guide 1.190.

Table 3-2
Best-Estimate-to-Calculation (BE/C) Ratios for the Surveillance Capsules

Capsule	Fast (E > 1.0 MeV) Fluence Rate		Iron Atom Displacement Rate	
	BE/C	Std. Dev.	BE/C	Std. Dev.
83°	1.00	6.0%	1.01	6.0%
263°	1.08	7.0%	1.08	6.0%
97°	0.96	6.0%	0.97	6.0%
Average	1.01	6.0%	1.02	5.5%

4.0 Exposure Results

4.1 Reactor Pressure Vessel

Neutron exposure data for the RPV at the clad/base metal interface are provided in Table 4-1 through Table 4-4. In particular, fast neutron (E > 1.0 MeV) fluence rates and fluences determined at the RPV clad/base metal interface are provided in Table 4-1 and Table 4-2 as a function of irradiation time. Similar data in terms of iron atom displacement rate and iron atom displacements are provided in Table 4-3 and Table 4-4.

Fast neutron (E > 1.0 MeV) fluence and iron atom displacement projections for the RPV welds and shells are provided in Table 4-5 and Table 4-6. The neutron exposure data provided in Table 4-5 and Table 4-6 are the maximum values at either the RPV clad/base metal interface or the RPV outer surface. Note that for regions and materials above and below the core (e.g., inlet-nozzle-to-upper-shell weld, outlet-nozzle-to-upper-shell weld, and lower-shell-to-bottom-head circumferential weld), the neutron exposure values at the RPV outer surface can be greater than those at the clad/base metal interface (Reference 3).

Table 4-1
Fast Neutron (E > 1.0 MeV) Fluence Rate at the RPV Clad/Base Metal Interface

Cycle	Cycle Length (EFPY)	Cumulative Operating Time (EFPY)	Fluence Rate (n/cm^2-s)							
			0°	15°	30°	45°	60°	75°	90°	Maximum
1	1.11	1.11	3.19E+10	2.03E+10	1.71E+10	1.26E+10	1.71E+10	1.97E+10	3.19E+10	3.19E+10
2	1.12	2.23	3.36E+10	1.98E+10	1.71E+10	1.28E+10	1.71E+10	1.93E+10	3.37E+10	3.37E+10
3	1.22	3.45	3.01E+10	1.80E+10	1.47E+10	1.07E+10	1.47E+10	1.75E+10	3.02E+10	3.02E+10
4	1.16	4.61	2.05E+10	1.61E+10	1.56E+10	1.18E+10	1.56E+10	1.58E+10	2.05E+10	2.05E+10
5	1.30	5.91	1.99E+10	1.61E+10	1.55E+10	1.13E+10	1.55E+10	1.57E+10	1.99E+10	2.00E+10
6	1.35	7.26	2.14E+10	1.37E+10	1.22E+10	9.79E+09	1.22E+10	1.34E+10	2.14E+10	2.14E+10
7	1.21	8.47	2.31E+10	1.44E+10	1.21E+10	1.02E+10	1.21E+10	1.40E+10	2.32E+10	2.32E+10
8	1.38	9.85	1.40E+10	1.10E+10	1.30E+10	1.01E+10	1.30E+10	1.08E+10	1.41E+10	1.41E+10
9	1.22	11.07	1.92E+10	1.58E+10	1.39E+10	1.00E+10	1.39E+10	1.55E+10	1.92E+10	1.98E+10
10	1.44	12.51	2.05E+10	1.59E+10	1.37E+10	1.06E+10	1.37E+10	1.55E+10	2.05E+10	2.09E+10
11	1.32	13.83	1.92E+10	1.42E+10	1.43E+10	1.16E+10	1.43E+10	1.39E+10	1.92E+10	1.92E+10
12	1.51	15.34	1.94E+10	1.25E+10	1.23E+10	1.07E+10	1.23E+10	1.22E+10	1.94E+10	1.94E+10
13	1.29	16.63	2.14E+10	1.41E+10	1.30E+10	1.14E+10	1.30E+10	1.38E+10	2.14E+10	2.14E+10
14	1.43	18.06	1.87E+10	1.27E+10	1.23E+10	1.06E+10	1.23E+10	1.24E+10	1.87E+10	1.87E+10
15	1.15	19.21	2.18E+10	1.41E+10	1.20E+10	9.78E+09	1.20E+10	1.37E+10	2.19E+10	2.19E+10
16	1.25	20.46	2.22E+10	1.46E+10	1.23E+10	9.93E+09	1.23E+10	1.42E+10	2.22E+10	2.22E+10
17	1.25	21.71	2.08E+10	1.40E+10	1.18E+10	9.70E+09	1.18E+10	1.38E+10	2.16E+10	2.16E+10
18	1.42	23.13	2.00E+10	1.42E+10	1.21E+10	1.00E+10	1.19E+10	1.39E+10	2.01E+10	2.02E+10
19	1.19	24.32	2.54E+10	1.75E+10	1.65E+10	1.29E+10	1.65E+10	1.68E+10	2.52E+10	2.54E+10
20	1.23	25.55	2.99E+10	1.95E+10	1.86E+10	1.54E+10	1.86E+10	1.90E+10	2.99E+10	2.99E+10
21	1.28	26.83	2.85E+10	1.89E+10	1.84E+10	1.50E+10	1.83E+10	1.84E+10	2.85E+10	2.85E+10
22	1.31	28.13	3.30E+10	2.13E+10	1.92E+10	1.68E+10	1.92E+10	2.07E+10	3.31E+10	3.31E+10
23	1.40	29.53	3.30E+10	2.14E+10	2.12E+10	1.70E+10	2.12E+10	2.09E+10	3.30E+10	3.30E+10
24	1.34	30.88	3.01E+10	1.95E+10	1.84E+10	1.46E+10	1.84E+10	1.90E+10	3.02E+10	3.02E+10
25[1]	1.43	32.30	2.88E+10	1.87E+10	1.79E+10	1.38E+10	1.80E+10	1.85E+10	2.92E+10	2.92E+10

Note(s):

1. Cycle 25 was the current operating cycle at the time this summary report was authored.

Table 4-2
Fast Neutron (E > 1.0 MeV) Fluence at the RPV Clad/Base Metal Interface

Cycle	Cycle Length (EFPY)	Cumulative Operating Time (EFPY)	Fast Neutron (E > 1.0 MeV) Fluence (n/cm^2)							
			0°	15°	30°	45°	60°	75°	90°	Maximum
1	1.11	1.11	1.12E+18	7.10E+17	5.99E+17	4.41E+17	5.99E+17	6.91E+17	1.12E+18	1.12E+18
2	1.12	2.23	2.30E+18	1.41E+18	1.20E+18	8.92E+17	1.20E+18	1.37E+18	2.30E+18	2.30E+18
3	1.22	3.45	3.46E+18	2.10E+18	1.77E+18	1.30E+18	1.77E+18	2.04E+18	3.46E+18	3.46E+18
4	1.16	4.61	4.20E+18	2.68E+18	2.33E+18	1.73E+18	2.33E+18	2.61E+18	4.20E+18	4.20E+18
5	1.30	5.91	5.00E+18	3.33E+18	2.96E+18	2.19E+18	2.96E+18	3.25E+18	5.00E+18	5.00E+18
6	1.35	7.26	5.90E+18	3.90E+18	3.47E+18	2.60E+18	3.47E+18	3.81E+18	5.91E+18	5.91E+18
7	1.21	8.47	6.78E+18	4.45E+18	3.93E+18	2.99E+18	3.93E+18	4.34E+18	6.79E+18	6.79E+18
8	1.38	9.85	7.37E+18	4.92E+18	4.48E+18	3.42E+18	4.48E+18	4.80E+18	7.38E+18	7.38E+18
9	1.22	11.07	8.11E+18	5.53E+18	5.02E+18	3.80E+18	5.02E+18	5.40E+18	8.13E+18	8.13E+18
10	1.44	12.51	9.05E+18	6.25E+18	5.64E+18	4.29E+18	5.64E+18	6.10E+18	9.06E+18	9.06E+18
11	1.32	13.83	9.84E+18	6.83E+18	6.23E+18	4.76E+18	6.23E+18	6.67E+18	9.85E+18	9.85E+18
12	1.51	15.34	1.08E+19	7.43E+18	6.81E+18	5.27E+18	6.81E+18	7.25E+18	1.08E+19	1.08E+19
13	1.29	16.63	1.16E+19	8.00E+18	7.34E+18	5.73E+18	7.34E+18	7.81E+18	1.16E+19	1.16E+19
14	1.43	18.06	1.25E+19	8.57E+18	7.89E+18	6.21E+18	7.89E+18	8.36E+18	1.25E+19	1.25E+19
15	1.15	19.21	1.32E+19	9.08E+18	8.33E+18	6.56E+18	8.32E+18	8.86E+18	1.33E+19	1.33E+19
16	1.25	20.46	1.41E+19	9.65E+18	8.81E+18	6.95E+18	8.81E+18	9.41E+18	1.41E+19	1.41E+19
17	1.25	21.71	1.49E+19	1.02E+19	9.27E+18	7.33E+18	9.27E+18	9.96E+18	1.50E+19	1.50E+19
18	1.42	23.13	1.58E+19	1.08E+19	9.81E+18	7.78E+18	9.80E+18	1.06E+19	1.59E+19	1.59E+19
19	1.19	24.32	1.68E+19	1.15E+19	1.04E+19	8.26E+18	1.04E+19	1.12E+19	1.68E+19	1.68E+19
20	1.23	25.55	1.79E+19	1.22E+19	1.12E+19	8.86E+18	1.11E+19	1.19E+19	1.80E+19	1.80E+19
21	1.28	26.83	1.91E+19	1.30E+19	1.19E+19	9.46E+18	1.19E+19	1.27E+19	1.91E+19	1.91E+19
22	1.31	28.13	2.04E+19	1.39E+19	1.27E+19	1.02E+19	1.27E+19	1.35E+19	2.05E+19	2.05E+19
23	1.40	29.53	2.19E+19	1.48E+19	1.36E+19	1.09E+19	1.36E+19	1.45E+19	2.19E+19	2.19E+19
24	1.34	30.88	2.32E+19	1.57E+19	1.44E+19	1.15E+19	1.44E+19	1.53E+19	2.32E+19	2.32E+19
25[1]	1.43	32.30	2.45E+19	1.65E+19	1.52E+19	1.21E+19	1.52E+19	1.61E+19	2.45E+19	2.45E+19

Table 4-2
Fast Neutron (E > 1.0 MeV) Fluence at the RPV Clad/Base Metal Interface

Cycle	Cycle Length (EFPY)	Cumulative Operating Time (EFPY)	Fast Neutron (E > 1.0 MeV) Fluence (n/cm^2)							
			0°	15°	30°	45°	60°	75°	90°	Maximum
Projections with no bias on the peripheral and re-entrant corner assembly relative powers										
Future[2]	--	36.00	2.80E+19	1.88E+19	1.74E+19	1.38E+19	1.73E+19	1.83E+19	2.81E+19	2.81E+19
Future[2]	--	42.00	3.37E+19	2.25E+19	2.08E+19	1.66E+19	2.08E+19	2.19E+19	3.38E+19	3.38E+19
Future[2]	--	48.00	3.94E+19	2.62E+19	2.43E+19	1.94E+19	2.43E+19	2.55E+19	3.95E+19	3.95E+19
Future[2]	--	54.00	4.51E+19	2.99E+19	2.78E+19	2.21E+19	2.78E+19	2.91E+19	4.52E+19	4.52E+19
Future[2]	--	60.00	5.08E+19	3.36E+19	3.13E+19	2.49E+19	3.12E+19	3.27E+19	5.09E+19	5.09E+19
Future[2]	--	66.00	5.65E+19	3.73E+19	3.48E+19	2.76E+19	3.47E+19	3.63E+19	5.66E+19	5.66E+19
Future[2]	--	72.00	6.22E+19	4.10E+19	3.82E+19	3.04E+19	3.82E+19	3.99E+19	6.23E+19	6.23E+19
Projections with a +10% bias on the peripheral and re-entrant corner assembly relative powers										
Future[2]	--	36.00	2.83E+19	1.90E+19	1.76E+19	1.40E+19	1.75E+19	1.85E+19	2.84E+19	2.84E+19
Future[2]	--	42.00	3.45E+19	2.30E+19	2.14E+19	1.70E+19	2.13E+19	2.24E+19	3.46E+19	3.46E+19
Future[2]	--	48.00	4.07E+19	2.70E+19	2.52E+19	2.01E+19	2.51E+19	2.64E+19	4.08E+19	4.08E+19
Future[2]	--	54.00	4.69E+19	3.11E+19	2.90E+19	2.31E+19	2.90E+19	3.03E+19	4.70E+19	4.70E+19
Future[2]	--	60.00	5.31E+19	3.51E+19	3.28E+19	2.61E+19	3.28E+19	3.42E+19	5.32E+19	5.32E+19
Future[2]	--	66.00	5.93E+19	3.91E+19	3.66E+19	2.91E+19	3.66E+19	3.81E+19	5.94E+19	5.94E+19
Future[2]	--	72.00	6.55E+19	4.31E+19	4.04E+19	3.22E+19	4.04E+19	4.21E+19	6.56E+19	6.56E+19

Note(s):

1. Cycle 25 was the current operating cycle at the time this summary report was authored.
2. Values beyond Cycle 25 are based on the average core power distributions and reactor operating conditions of Cycle 24 and are determined both with and without a 1.1 bias on the peripheral and re-entrant corner assembly relative powers.

Table 4-3
Iron Atom Displacement Rate at the RPV Clad/Base Metal Interface

Cycle	Cycle Length (EFPY)	Cumulative Operating Time (EFPY)	Iron Atom Displacement Rate (dpa/s)							
			0°	15°	30°	45°	60°	75°	90°	Maximum
1	1.11	1.11	4.86E-11	3.11E-11	2.61E-11	1.94E-11	2.61E-11	3.04E-11	4.86E-11	4.86E-11
2	1.12	2.23	5.13E-11	3.04E-11	2.61E-11	1.97E-11	2.61E-11	2.98E-11	5.12E-11	5.13E-11
3	1.22	3.45	4.59E-11	2.76E-11	2.25E-11	1.65E-11	2.25E-11	2.71E-11	4.58E-11	4.59E-11
4	1.16	4.61	3.13E-11	2.47E-11	2.38E-11	1.81E-11	2.38E-11	2.43E-11	3.13E-11	3.14E-11
5	1.30	5.91	3.05E-11	2.47E-11	2.37E-11	1.75E-11	2.37E-11	2.43E-11	3.04E-11	3.06E-11
6	1.35	7.26	3.27E-11	2.11E-11	1.86E-11	1.51E-11	1.86E-11	2.07E-11	3.26E-11	3.27E-11
7	1.21	8.47	3.53E-11	2.21E-11	1.86E-11	1.57E-11	1.86E-11	2.17E-11	3.53E-11	3.53E-11
8	1.38	9.85	2.15E-11	1.69E-11	1.99E-11	1.56E-11	1.99E-11	1.66E-11	2.14E-11	2.15E-11
9	1.22	11.07	2.94E-11	2.43E-11	2.12E-11	1.54E-11	2.12E-11	2.38E-11	2.93E-11	3.02E-11
10	1.44	12.51	3.14E-11	2.44E-11	2.09E-11	1.63E-11	2.09E-11	2.39E-11	3.13E-11	3.19E-11
11	1.32	13.83	2.94E-11	2.19E-11	2.18E-11	1.78E-11	2.18E-11	2.15E-11	2.93E-11	2.94E-11
12	1.51	15.34	2.97E-11	1.93E-11	1.89E-11	1.65E-11	1.89E-11	1.89E-11	2.96E-11	2.97E-11
13	1.29	16.63	3.27E-11	2.17E-11	2.00E-11	1.75E-11	2.00E-11	2.13E-11	3.26E-11	3.27E-11
14	1.43	18.06	2.86E-11	1.95E-11	1.88E-11	1.63E-11	1.88E-11	1.91E-11	2.85E-11	2.86E-11
15	1.15	19.21	3.34E-11	2.17E-11	1.84E-11	1.51E-11	1.84E-11	2.12E-11	3.33E-11	3.34E-11
16	1.25	20.46	3.40E-11	2.25E-11	1.88E-11	1.53E-11	1.88E-11	2.20E-11	3.39E-11	3.40E-11
17	1.25	21.71	3.19E-11	2.15E-11	1.81E-11	1.49E-11	1.81E-11	2.14E-11	3.29E-11	3.29E-11
18	1.42	23.13	3.06E-11	2.17E-11	1.85E-11	1.55E-11	1.83E-11	2.15E-11	3.08E-11	3.09E-11
19	1.19	24.32	3.89E-11	2.69E-11	2.52E-11	1.98E-11	2.52E-11	2.60E-11	3.84E-11	3.89E-11
20	1.23	25.55	4.57E-11	3.00E-11	2.84E-11	2.36E-11	2.84E-11	2.93E-11	4.56E-11	4.57E-11
21	1.28	26.83	4.36E-11	2.91E-11	2.81E-11	2.31E-11	2.79E-11	2.84E-11	4.35E-11	4.36E-11
22	1.31	28.13	5.05E-11	3.28E-11	2.93E-11	2.58E-11	2.93E-11	3.20E-11	5.04E-11	5.05E-11
23	1.40	29.53	5.04E-11	3.29E-11	3.23E-11	2.61E-11	3.23E-11	3.22E-11	5.03E-11	5.04E-11
24	1.34	30.88	4.60E-11	3.00E-11	2.81E-11	2.24E-11	2.80E-11	2.94E-11	4.60E-11	4.60E-11
25[1]	1.43	32.30	4.41E-11	2.87E-11	2.74E-11	2.12E-11	2.74E-11	2.86E-11	4.44E-11	4.44E-11

Note(s):
1. Cycle 25 was the current operating cycle at the time this summary report was authored.

Table 4-4
Iron Atom Displacements at the RPV Clad/Base Metal Interface

Cycle	Cycle Length (EFPY)	Cumulative Operating Time (EFPY)	Iron Atom Displacements (dpa)							
			0°	15°	30°	45°	60°	75°	90°	Maximum
1	1.11	1.11	1.70E-03	1.09E-03	9.14E-04	6.79E-04	9.14E-04	1.07E-03	1.70E-03	1.70E-03
2	1.12	2.23	3.51E-03	2.16E-03	1.83E-03	1.37E-03	1.83E-03	2.11E-03	3.50E-03	3.51E-03
3	1.22	3.45	5.28E-03	3.22E-03	2.70E-03	2.01E-03	2.70E-03	3.15E-03	5.27E-03	5.28E-03
4	1.16	4.61	6.40E-03	4.11E-03	3.56E-03	2.66E-03	3.55E-03	4.03E-03	6.39E-03	6.40E-03
5	1.30	5.91	7.63E-03	5.11E-03	4.52E-03	3.37E-03	4.52E-03	5.02E-03	7.62E-03	7.63E-03
6	1.35	7.26	9.01E-03	6.00E-03	5.30E-03	4.00E-03	5.29E-03	5.88E-03	8.99E-03	9.01E-03
7	1.21	8.47	1.04E-02	6.84E-03	6.00E-03	4.60E-03	6.00E-03	6.71E-03	1.03E-02	1.04E-02
8	1.38	9.85	1.13E-02	7.56E-03	6.84E-03	5.26E-03	6.84E-03	7.41E-03	1.12E-02	1.13E-02
9	1.22	11.07	1.24E-02	8.49E-03	7.66E-03	5.86E-03	7.66E-03	8.33E-03	1.24E-02	1.24E-02
10	1.44	12.51	1.38E-02	9.60E-03	8.61E-03	6.60E-03	8.61E-03	9.42E-03	1.38E-02	1.38E-02
11	1.32	13.83	1.50E-02	1.05E-02	9.52E-03	7.33E-03	9.51E-03	1.03E-02	1.50E-02	1.50E-02
12	1.51	15.34	1.64E-02	1.14E-02	1.04E-02	8.12E-03	1.04E-02	1.12E-02	1.64E-02	1.64E-02
13	1.29	16.63	1.78E-02	1.23E-02	1.12E-02	8.83E-03	1.12E-02	1.21E-02	1.77E-02	1.78E-02
14	1.43	18.06	1.91E-02	1.32E-02	1.21E-02	9.56E-03	1.21E-02	1.29E-02	1.90E-02	1.91E-02
15	1.15	19.21	2.03E-02	1.40E-02	1.27E-02	1.01E-02	1.27E-02	1.37E-02	2.02E-02	2.03E-02
16	1.25	20.46	2.16E-02	1.48E-02	1.35E-02	1.07E-02	1.35E-02	1.45E-02	2.15E-02	2.16E-02
17	1.25	21.71	2.28E-02	1.57E-02	1.42E-02	1.13E-02	1.42E-02	1.54E-02	2.28E-02	2.28E-02
18	1.42	23.13	2.42E-02	1.66E-02	1.50E-02	1.20E-02	1.50E-02	1.63E-02	2.42E-02	2.42E-02
19	1.19	24.32	2.57E-02	1.77E-02	1.59E-02	1.27E-02	1.59E-02	1.73E-02	2.56E-02	2.57E-02
20	1.23	25.55	2.74E-02	1.88E-02	1.70E-02	1.36E-02	1.70E-02	1.85E-02	2.74E-02	2.74E-02
21	1.28	26.83	2.92E-02	2.00E-02	1.82E-02	1.46E-02	1.82E-02	1.96E-02	2.92E-02	2.92E-02
22	1.31	28.13	3.13E-02	2.13E-02	1.94E-02	1.56E-02	1.94E-02	2.09E-02	3.12E-02	3.13E-02
23	1.40	29.53	3.35E-02	2.28E-02	2.08E-02	1.68E-02	2.08E-02	2.23E-02	3.34E-02	3.35E-02
24	1.34	30.88	3.54E-02	2.41E-02	2.20E-02	1.77E-02	2.20E-02	2.36E-02	3.54E-02	3.54E-02
25[1]	1.43	32.30	3.74E-02	2.54E-02	2.32E-02	1.87E-02	2.32E-02	2.49E-02	3.74E-02	3.74E-02

Table 4-4
Iron Atom Displacements at the RPV Clad/Base Metal Interface

Cycle	Cycle Length (EFPY)	Cumulative Operating Time (EFPY)	Iron Atom Displacements (dpa)							
			0°	15°	30°	45°	60°	75°	90°	Maximum
Projections with no bias on the peripheral and re-entrant corner assembly relative powers										
Future[2]	--	36.00	4.28E-02	2.89E-02	2.65E-02	2.13E-02	2.65E-02	2.83E-02	4.28E-02	4.28E-02
Future[2]	--	42.00	5.15E-02	3.45E-02	3.18E-02	2.55E-02	3.18E-02	3.39E-02	5.15E-02	5.15E-02
Future[2]	--	48.00	6.02E-02	4.02E-02	3.71E-02	2.98E-02	3.71E-02	3.94E-02	6.02E-02	6.02E-02
Future[2]	--	54.00	6.89E-02	4.59E-02	4.25E-02	3.40E-02	4.24E-02	4.50E-02	6.89E-02	6.89E-02
Future[2]	--	60.00	7.76E-02	5.16E-02	4.78E-02	3.83E-02	4.77E-02	5.06E-02	7.76E-02	7.76E-02
Future[2]	--	66.00	8.63E-02	5.73E-02	5.31E-02	4.25E-02	5.30E-02	5.61E-02	8.63E-02	8.63E-02
Future[2]	--	72.00	9.51E-02	6.29E-02	5.84E-02	4.68E-02	5.83E-02	6.17E-02	9.50E-02	9.51E-02
Projections with a +10% bias on the peripheral and re-entrant corner assembly relative powers										
Future[2]	--	36.00	4.32E-02	2.92E-02	2.68E-02	2.16E-02	2.68E-02	2.86E-02	4.32E-02	4.32E-02
Future[2]	--	42.00	5.27E-02	3.54E-02	3.26E-02	2.62E-02	3.26E-02	3.47E-02	5.27E-02	5.27E-02
Future[2]	--	48.00	6.22E-02	4.15E-02	3.85E-02	3.09E-02	3.84E-02	4.07E-02	6.21E-02	6.22E-02
Future[2]	--	54.00	7.17E-02	4.77E-02	4.43E-02	3.55E-02	4.42E-02	4.68E-02	7.16E-02	7.17E-02
Future[2]	--	60.00	8.11E-02	5.39E-02	5.01E-02	4.02E-02	5.00E-02	5.29E-02	8.11E-02	8.11E-02
Future[2]	--	66.00	9.06E-02	6.01E-02	5.59E-02	4.48E-02	5.58E-02	5.89E-02	9.05E-02	9.06E-02
Future[2]	--	72.00	1.00E-01	6.63E-02	6.17E-02	4.95E-02	6.16E-02	6.50E-02	1.00E-01	1.00E-01

Note(s):

1. Cycle 25 was the current operating cycle at the time this summary report was authored.
2. Values beyond Cycle 25 are based on the average core power distributions and reactor operating conditions of Cycle 24 and are determined both with and without a 1.1 bias on the peripheral and re-entrant corner assembly relative powers.

Table 4-5
Fast Neutron (E > 1.0 MeV) Fluence at the RPV Welds and Shells

Projections with no bias on the peripheral and re-entrant corner assembly relative powers				
Material	**Fast Neutron (E > 1.0 MeV) Fluence (n/cm^2)**			
	32.30 EFPY[1]	**36 EFPY**	**42 EFPY**	**48 EFPY**
Inlet-nozzle-to-upper-shell weld (lowest extent)	2.89E+16	3.29E+16	3.93E+16	4.58E+16
Outlet-nozzle-to-upper-shell weld (lowest extent)	3.97E+16	4.51E+16	5.39E+16	6.27E+16
Upper Shell[2]	6.47E+17	7.23E+17	8.47E+17	9.70E+17
Upper-to-Intermediate-Shell Circumferential Weld	7.46E+17	8.34E+17	9.77E+17	1.12E+18
Intermediate Shell	2.45E+19	2.81E+19	3.38E+19	3.95E+19
Intermediate Shell Longitudinal Weld – 15°	1.65E+19	1.88E+19	2.25E+19	2.62E+19
Intermediate Shell Longitudinal Weld – 135°	1.21E+19	1.38E+19	1.66E+19	1.94E+19
Intermediate Shell Longitudinal Weld – 255°[3]	1.65E+19	1.88E+19	2.25E+19	2.62E+19
Intermediate-to-Lower-Shell Circumferential Weld	2.44E+19	2.79E+19	3.35E+19	3.92E+19
Lower Shell	2.44E+19	2.79E+19	3.36E+19	3.93E+19
Lower Shell Longitudinal Weld – 15°	1.64E+19	1.86E+19	2.23E+19	2.60E+19
Lower Shell Longitudinal Weld – 135°	1.21E+19	1.37E+19	1.65E+19	1.92E+19
Lower Shell Longitudinal Weld – 255°[3]	1.64E+19	1.86E+19	2.23E+19	2.60E+19
Lower-Shell-to-Bottom-Head Circumferential Weld	2.41E+16	2.75E+16	3.29E+16	3.83E+16

Projections with no bias on the peripheral and re-entrant corner assembly relative powers				
Material	**Fast Neutron (E > 1.0 MeV) Fluence (n/cm^2)**			
	54 EFPY	**60 EFPY**	**66 EFPY**	**72 EFPY**
Inlet-nozzle-to-upper-shell weld (lowest extent)	5.22E+16	5.86E+16	6.50E+16	7.15E+16
Outlet-nozzle-to-upper-shell weld (lowest extent)	7.15E+16	8.03E+16	8.91E+16	9.79E+16
Upper Shell[2]	1.09E+18	1.22E+18	1.34E+18	1.46E+18
Upper-to-Intermediate-Shell Circumferential Weld	1.26E+18	1.41E+18	1.55E+18	1.69E+18
Intermediate Shell	4.52E+19	5.09E+19	5.66E+19	6.23E+19
Intermediate Shell Longitudinal Weld – 15°	2.99E+19	3.36E+19	3.73E+19	4.10E+19
Intermediate Shell Longitudinal Weld – 135°	2.21E+19	2.49E+19	2.76E+19	3.04E+19
Intermediate Shell Longitudinal Weld – 255°[3]	2.99E+19	3.36E+19	3.73E+19	4.10E+19
Intermediate-to-Lower-Shell Circumferential Weld	4.49E+19	5.06E+19	5.62E+19	6.19E+19
Lower Shell	4.50E+19	5.07E+19	5.64E+19	6.21E+19
Lower Shell Longitudinal Weld – 15°	2.97E+19	3.34E+19	3.70E+19	4.07E+19
Lower Shell Longitudinal Weld – 135°	2.20E+19	2.47E+19	2.75E+19	3.02E+19
Lower Shell Longitudinal Weld – 255°[3]	2.97E+19	3.34E+19	3.70E+19	4.07E+19
Lower-Shell-to-Bottom-Head Circumferential Weld	4.37E+16	4.92E+16	5.46E+16	6.00E+16

Table 4-5
Fast Neutron (E > 1.0 MeV) Fluence at the RPV Welds and Shells

Projections with a +10% bias on the peripheral and re-entrant corner assembly relative powers				
Material	**Fast Neutron (E > 1.0 MeV) Fluence (n/cm^2)**			
	32.30 EFPY[1]	**36 EFPY**	**42 EFPY**	**48 EFPY**
Inlet-nozzle-to-upper-shell weld (lowest extent)	2.89E+16	3.33E+16	4.03E+16	4.73E+16
Outlet-nozzle-to-upper-shell weld (lowest extent)	3.97E+16	4.56E+16	5.52E+16	6.48E+16
Upper Shell[2]	6.47E+17	7.28E+17	8.60E+17	9.92E+17
Upper-to-Intermediate-Shell Circumferential Weld	7.46E+17	8.40E+17	9.92E+17	1.14E+18
Intermediate Shell	2.45E+19	2.84E+19	3.46E+19	4.08E+19
Intermediate Shell Longitudinal Weld – 15°	1.65E+19	1.90E+19	2.30E+19	2.70E+19
Intermediate Shell Longitudinal Weld – 135°	1.21E+19	1.40E+19	1.70E+19	2.01E+19
Intermediate Shell Longitudinal Weld – 255°[3]	1.65E+19	1.90E+19	2.30E+19	2.70E+19
Intermediate-to-Lower-Shell Circumferential Weld	2.44E+19	2.82E+19	3.43E+19	4.05E+19
Lower Shell	2.44E+19	2.82E+19	3.44E+19	4.06E+19
Lower Shell Longitudinal Weld – 15°	1.64E+19	1.88E+19	2.29E+19	2.69E+19
Lower Shell Longitudinal Weld – 135°	1.21E+19	1.39E+19	1.69E+19	1.99E+19
Lower Shell Longitudinal Weld – 255°[3]	1.64E+19	1.88E+19	2.29E+19	2.69E+19
Lower-Shell-to-Bottom-Head Circumferential Weld	2.41E+16	2.78E+16	3.37E+16	3.96E+16

Projections with a +10% bias on the peripheral and re-entrant corner assembly relative powers				
Material	**Fast Neutron (E > 1.0 MeV) Fluence (n/cm^2)**			
	54 EFPY	**60 EFPY**	**66 EFPY**	**72 EFPY**
Inlet-nozzle-to-upper-shell weld (lowest extent)	5.43E+16	6.13E+16	6.84E+16	7.54E+16
Outlet-nozzle-to-upper-shell weld (lowest extent)	7.44E+16	8.40E+16	9.36E+16	1.03E+17
Upper Shell[2]	1.12E+18	1.26E+18	1.39E+18	1.52E+18
Upper-to-Intermediate-Shell Circumferential Weld	1.30E+18	1.45E+18	1.60E+18	1.75E+18
Intermediate Shell	4.70E+19	5.32E+19	5.94E+19	6.56E+19
Intermediate Shell Longitudinal Weld – 15°	3.11E+19	3.51E+19	3.91E+19	4.31E+19
Intermediate Shell Longitudinal Weld – 135°	2.31E+19	2.61E+19	2.91E+19	3.22E+19
Intermediate Shell Longitudinal Weld – 255°[3]	3.11E+19	3.51E+19	3.91E+19	4.31E+19
Intermediate-to-Lower-Shell Circumferential Weld	4.67E+19	5.28E+19	5.90E+19	6.52E+19
Lower Shell	4.68E+19	5.29E+19	5.91E+19	6.53E+19
Lower Shell Longitudinal Weld – 15°	3.09E+19	3.49E+19	3.89E+19	4.29E+19
Lower Shell Longitudinal Weld – 135°	2.29E+19	2.59E+19	2.89E+19	3.20E+19
Lower Shell Longitudinal Weld – 255°[3]	3.09E+19	3.49E+19	3.89E+19	4.29E+19
Lower-Shell-to-Bottom-Head Circumferential Weld	4.55E+16	5.14E+16	5.73E+16	6.32E+16

Note(s):

1. Value listed is the projected EFPY at the end of Cycle 25.
2. Exposure values for the upper shell longitudinal welds are bounded by the exposure values for the upper shell.
3. Exposure values for the intermediate shell and lower shell 255° longitudinal welds are bounded by the exposure values for the intermediate shell and lower shell 15° longitudinal welds.

Table 4-6
Iron Atom Displacements at the RPV Welds and Shells

Projections with no bias on the peripheral and re-entrant corner assembly relative powers				
Material	**Iron Atom Displacements (dpa)**			
	32.30 EFPY[1]	**36 EFPY**	**42 EFPY**	**48 EFPY**
Inlet-nozzle-to-upper-shell weld (lowest extent)	2.42E-04	2.75E-04	3.29E-04	3.84E-04
Outlet-nozzle-to-upper-shell weld (lowest extent)	3.16E-04	3.59E-04	4.29E-04	5.00E-04
Upper Shell[2]	1.11E-03	1.25E-03	1.46E-03	1.68E-03
Upper-to-Intermediate-Shell Circumferential Weld	1.27E-03	1.43E-03	1.67E-03	1.92E-03
Intermediate Shell	3.74E-02	4.28E-02	5.15E-02	6.02E-02
Intermediate Shell Longitudinal Weld – 15°	2.54E-02	2.89E-02	3.45E-02	4.02E-02
Intermediate Shell Longitudinal Weld – 135°	1.87E-02	2.13E-02	2.55E-02	2.98E-02
Intermediate Shell Longitudinal Weld – 255°[3]	2.54E-02	2.89E-02	3.45E-02	4.02E-02
Intermediate-to-Lower-Shell Circumferential Weld	3.72E-02	4.25E-02	5.12E-02	5.98E-02
Lower Shell	3.72E-02	4.25E-02	5.12E-02	5.99E-02
Lower Shell Longitudinal Weld – 15°	2.52E-02	2.86E-02	3.43E-02	3.99E-02
Lower Shell Longitudinal Weld – 135°	1.85E-02	2.11E-02	2.53E-02	2.96E-02
Lower Shell Longitudinal Weld – 255°[3]	2.52E-02	2.86E-02	3.43E-02	3.99E-02
Lower-Shell-to-Bottom-Head Circumferential Weld	1.58E-04	1.80E-04	2.16E-04	2.52E-04

Projections with no bias on the peripheral and re-entrant corner assembly relative powers				
Material	**Iron Atom Displacements (dpa)**			
	54 EFPY	**60 EFPY**	**66 EFPY**	**72 EFPY**
Inlet-nozzle-to-upper-shell weld (lowest extent)	4.38E-04	4.92E-04	5.46E-04	6.00E-04
Outlet-nozzle-to-upper-shell weld (lowest extent)	5.70E-04	6.41E-04	7.11E-04	7.81E-04
Upper Shell[2]	1.89E-03	2.11E-03	2.33E-03	2.54E-03
Upper-to-Intermediate-Shell Circumferential Weld	2.17E-03	2.41E-03	2.66E-03	2.91E-03
Intermediate Shell	6.89E-02	7.76E-02	8.63E-02	9.51E-02
Intermediate Shell Longitudinal Weld – 15°	4.59E-02	5.16E-02	5.73E-02	6.30E-02
Intermediate Shell Longitudinal Weld – 135°	3.40E-02	3.83E-02	4.25E-02	4.68E-02
Intermediate Shell Longitudinal Weld – 255°[3]	4.59E-02	5.16E-02	5.73E-02	6.30E-02
Intermediate-to-Lower-Shell Circumferential Weld	6.85E-02	7.71E-02	8.58E-02	9.44E-02
Lower Shell	6.85E-02	7.72E-02	8.59E-02	9.46E-02
Lower Shell Longitudinal Weld – 15°	4.56E-02	5.12E-02	5.69E-02	6.25E-02
Lower Shell Longitudinal Weld – 135°	3.38E-02	3.80E-02	4.22E-02	4.64E-02
Lower Shell Longitudinal Weld – 255°[3]	4.56E-02	5.12E-02	5.69E-02	6.25E-02
Lower-Shell-to-Bottom-Head Circumferential Weld	2.87E-04	3.23E-04	3.59E-04	3.95E-04

Table 4-6
Iron Atom Displacements at the RPV Welds and Shells

Projections with a +10% bias on the peripheral and re-entrant corner assembly relative powers				
Material	**Iron Atom Displacements (dpa)**			
	32.30 EFPY[1]	**36 EFPY**	**42 EFPY**	**48 EFPY**
Inlet-nozzle-to-upper-shell weld (lowest extent)	2.42E-04	2.79E-04	3.38E-04	3.97E-04
Outlet-nozzle-to-upper-shell weld (lowest extent)	3.16E-04	3.63E-04	4.40E-04	5.17E-04
Upper Shell[2]	1.11E-03	1.26E-03	1.49E-03	1.72E-03
Upper-to-Intermediate-Shell Circumferential Weld	1.27E-03	1.44E-03	1.70E-03	1.96E-03
Intermediate Shell	3.74E-02	4.32E-02	5.27E-02	6.22E-02
Intermediate Shell Longitudinal Weld – 15°	2.54E-02	2.92E-02	3.54E-02	4.16E-02
Intermediate Shell Longitudinal Weld – 135°	1.87E-02	2.16E-02	2.62E-02	3.09E-02
Intermediate Shell Longitudinal Weld – 255°[3]	2.54E-02	2.92E-02	3.54E-02	4.16E-02
Intermediate-to-Lower-Shell Circumferential Weld	3.72E-02	4.30E-02	5.24E-02	6.18E-02
Lower Shell	3.72E-02	4.30E-02	5.24E-02	6.18E-02
Lower Shell Longitudinal Weld – 15°	2.52E-02	2.89E-02	3.51E-02	4.12E-02
Lower Shell Longitudinal Weld – 135°	1.85E-02	2.14E-02	2.60E-02	3.06E-02
Lower Shell Longitudinal Weld – 255°[3]	2.52E-02	2.89E-02	3.51E-02	4.12E-02
Lower-Shell-to-Bottom-Head Circumferential Weld	1.58E-04	1.82E-04	2.21E-04	2.60E-04

Projections with a +10% bias on the peripheral and re-entrant corner assembly relative powers				
Material	**Iron Atom Displacements (dpa)**			
	54 EFPY	**60 EFPY**	**66 EFPY**	**72 EFPY**
Inlet-nozzle-to-upper-shell weld (lowest extent)	4.56E-04	5.15E-04	5.74E-04	6.33E-04
Outlet-nozzle-to-upper-shell weld (lowest extent)	5.93E-04	6.70E-04	7.47E-04	8.24E-04
Upper Shell[2]	1.95E-03	2.18E-03	2.41E-03	2.64E-03
Upper-to-Intermediate-Shell Circumferential Weld	2.23E-03	2.49E-03	2.76E-03	3.02E-03
Intermediate Shell	7.17E-02	8.11E-02	9.06E-02	1.00E-01
Intermediate Shell Longitudinal Weld – 15°	4.77E-02	5.39E-02	6.01E-02	6.63E-02
Intermediate Shell Longitudinal Weld – 135°	3.55E-02	4.02E-02	4.48E-02	4.95E-02
Intermediate Shell Longitudinal Weld – 255°[3]	4.77E-02	5.39E-02	6.01E-02	6.63E-02
Intermediate-to-Lower-Shell Circumferential Weld	7.12E-02	8.06E-02	9.00E-02	9.94E-02
Lower Shell	7.12E-02	8.07E-02	9.01E-02	9.95E-02
Lower Shell Longitudinal Weld – 15°	4.74E-02	5.35E-02	5.97E-02	6.58E-02
Lower Shell Longitudinal Weld – 135°	3.52E-02	3.99E-02	4.45E-02	4.91E-02
Lower Shell Longitudinal Weld – 255°[3]	4.74E-02	5.35E-02	5.97E-02	6.58E-02
Lower-Shell-to-Bottom-Head Circumferential Weld	2.99E-04	3.38E-04	3.77E-04	4.16E-04

Note(s):

1. Value listed is the projected EFPY at the end of Cycle 25.
2. Exposure values for the upper shell longitudinal welds are bounded by the exposure values for the upper shell.
3. Exposure values for the intermediate shell and lower shell 255° longitudinal welds are bounded by the exposure values for the intermediate shell and lower shell 15° longitudinal welds.

4.2 Surveillance Capsules

Neutron exposure data for the surveillance capsules are provided in Table 4-7 through Table 4-10. In particular, fast neutron (E > 1.0 MeV) fluence rates and fluences determined at the core midplane and geometric center of the surveillance capsules are provided in Table 4-7 and Table 4-8 as a function of irradiation time. Similar data in terms of iron atom displacement rate and iron atom displacements are provided in Table 4-9 and Table 4-10.

Lead factors for the surveillance capsules are provided in Table 4-11. The lead factor is defined as the ratio of the calculated neutron fluence at the geometric center of the surveillance capsule to the maximum fluence at the RPV clad/base metal interface.

Table 4-7
Fast Neutron (E > 1.0 MeV) Fluence Rate at the Geometric Center of the Surveillance Capsules

Cycle	Cycle Length (EFPY)	Cumulative Operating Time (EFPY)	Fluence Rate (n/cm^2-s)	
			7°	14°
1	1.11	1.11	4.06E+10	2.86E+10
2	1.12	2.23	4.01E+10	2.72E+10
3	1.22	3.45	3.62E+10	2.49E+10
4	1.16	4.61	2.66E+10	2.16E+10
5	1.30	5.91	2.62E+10	2.17E+10
6	1.35	7.26	2.58E+10	1.86E+10
7	1.21	8.47	2.79E+10	1.96E+10
8	1.38	9.85	1.72E+10	1.40E+10
9	1.22	11.07	2.62E+10	2.16E+10
10	1.44	12.51	2.78E+10	2.21E+10
11	1.32	13.83	2.49E+10	1.95E+10
12	1.51	15.34	2.42E+10	1.74E+10
13	1.29	16.63	2.70E+10	1.97E+10
14	1.43	18.06	2.37E+10	1.76E+10
15	1.15	19.21	2.77E+10	1.98E+10
16	1.25	20.46	2.85E+10	2.06E+10
17	1.25	21.71	2.78E+10	2.01E+10
18	1.42	23.13	2.66E+10	2.01E+10
19	1.19	24.32	3.26E+10	2.41E+10
20	1.23	25.55	3.78E+10	2.72E+10
21	1.28	26.83	3.63E+10	2.64E+10
22	1.31	28.13	4.25E+10	3.03E+10
23	1.40	29.53	4.18E+10	3.00E+10
24	1.34	30.88	3.81E+10	2.73E+10
25[1]	1.43	32.30	3.69E+10	2.66E+10

Note(s):

1. Cycle 25 was the current operating cycle at the time this summary report was authored.

Table 4-8
Fast Neutron (E > 1.0 MeV) Fluence at the Geometric Center of the Surveillance Capsules

Cycle	Cycle Length (EFPY)	Cumulative Operating Time (EFPY)	Fluence (n/cm^2)	
			7°	14°
1	1.11	1.11	1.42E+18[1]	1.00E+18
2	1.12	2.23	2.84E+18	1.97E+18
3	1.22	3.45	4.23E+18	2.92E+18
4	1.16	4.61	5.20E+18	3.72E+18
5	1.30	5.91	6.28E+18	4.60E+18
6	1.35	7.26	7.38E+18	5.39E+18
7	1.21	8.47	8.44E+18	6.14E+18
8	1.38	9.85	9.19E+18	6.75E+18
9	1.22	11.07	1.02E+19[2]	7.59E+18
10	1.44	12.51	1.15E+19	8.59E+18
11	1.32	13.83	1.25E+19	9.40E+18
12	1.51	15.34	1.37E+19	1.02E+19
13	1.29	16.63	1.48E+19	1.10E+19
14	1.43	18.06	1.58E+19	1.18E+19
15	1.15	19.21	1.68E+19	1.25E+19
16	1.25	20.46	1.80E+19	1.34E+19
17	1.25	21.71	1.91E+19	1.42E+19
18	1.42	23.13	2.02E+19	1.51E+19
19	1.19	24.32	2.15E+19	1.60E+19
20	1.23	25.55	2.29E+19[3]	1.70E+19
21	1.28	26.83	2.44E+19	1.81E+19
22	1.31	28.13	2.61E+19	1.93E+19
23	1.40	29.53	2.80E+19	2.06E+19
24	1.34	30.88	2.96E+19	2.18E+19
25[4]	1.43	32.30	3.13E+19	2.30E+19

Table 4-8
Fast Neutron (E > 1.0 MeV) Fluence at the Geometric Center of the Surveillance Capsules

No bias on the peripheral and re-entrant corner assembly relative powers				
Cycle	**Cycle Length (EFPY)**	**Cumulative Operating Time (EFPY)**	**Fluence (n/cm^2)**	
			7°	**14°**
Future[5]	--	36.00	3.57E+19	2.62E+19
Future[5]	--	42.00	4.29E+19	3.14E+19
Future[5]	--	48.00	5.01E+19	3.65E+19
Future[5]	--	54.00	5.74E+19	4.17E+19
Future[5]	--	60.00	6.46E+19	4.69E+19
Future[5]	--	66.00	7.18E+19	5.21E+19
Future[5]	--	72.00	7.90E+19	5.72E+19

+10% bias on the peripheral and re-entrant corner assembly relative powers				
Cycle	**Cycle Length (EFPY)**	**Cumulative Operating Time (EFPY)**	**Fluence (n/cm^2)**	
			7°	**14°**
Future[5]	--	36.00	3.61E+19	2.65E+19
Future[5]	--	42.00	4.40E+19	3.21E+19
Future[5]	--	48.00	5.18E+19	3.78E+19
Future[5]	--	54.00	5.97E+19	4.34E+19
Future[5]	--	60.00	6.75E+19	4.90E+19
Future[5]	--	66.00	7.54E+19	5.47E+19
Future[5]	--	72.00	8.33E+19	6.03E+19

Note(s):

1. This value is applicable to Capsule 83°.
2. This value is applicable to Capsule 263°.
3. This value is applicable to Capsule 97°.
4. Cycle 25 was the current operating cycle at the time this summary report was authored.
5. Values beyond Cycle 25 are based on the average core power distributions and reactor operating conditions of Cycle 24 and are determined both with and without a 1.1 bias on the peripheral and re-entrant corner assembly relative powers.

Table 4-9
Iron Atom Displacement Rate at the Geometric Center of the Surveillance Capsules

Cycle	Cycle Length (EFPY)	Cumulative Operating Time (EFPY)	Displacement Rate (dpa/s)	
			7°	14°
1	1.11	1.11	5.91E-11	4.19E-11
2	1.12	2.23	5.84E-11	3.99E-11
3	1.22	3.45	5.27E-11	3.64E-11
4	1.16	4.61	3.88E-11	3.17E-11
5	1.30	5.91	3.82E-11	3.18E-11
6	1.35	7.26	3.76E-11	2.72E-11
7	1.21	8.47	4.07E-11	2.88E-11
8	1.38	9.85	2.51E-11	2.06E-11
9	1.22	11.07	3.82E-11	3.16E-11
10	1.44	12.51	4.05E-11	3.24E-11
11	1.32	13.83	3.63E-11	2.86E-11
12	1.51	15.34	3.53E-11	2.55E-11
13	1.29	16.63	3.94E-11	2.89E-11
14	1.43	18.06	3.46E-11	2.58E-11
15	1.15	19.21	4.04E-11	2.90E-11
16	1.25	20.46	4.16E-11	3.02E-11
17	1.25	21.71	4.06E-11	2.94E-11
18	1.42	23.13	3.87E-11	2.94E-11
19	1.19	24.32	4.75E-11	3.53E-11
20	1.23	25.55	5.51E-11	3.99E-11
21	1.28	26.83	5.28E-11	3.86E-11
22	1.31	28.13	6.19E-11	4.43E-11
23	1.40	29.53	6.08E-11	4.39E-11
24	1.34	30.88	5.55E-11	4.00E-11
25[1]	1.43	32.30	5.38E-11	3.89E-11

Note(s):

1. Cycle 25 was the current operating cycle at the time this summary report was authored.

Table 4-10
Iron Atom Displacements at the Geometric Center of the Surveillance Capsules

Cycle	Cycle Length (EFPY)	Cumulative Operating Time (EFPY)	Displacements (dpa)	
			7°	14°
1	1.11	1.11	2.07E-03[1]	1.47E-03
2	1.12	2.23	4.13E-03	2.88E-03
3	1.22	3.45	6.16E-03	4.28E-03
4	1.16	4.61	7.58E-03	5.44E-03
5	1.30	5.91	9.15E-03	6.74E-03
6	1.35	7.26	1.08E-02	7.90E-03
7	1.21	8.47	1.23E-02	9.00E-03
8	1.38	9.85	1.34E-02	9.90E-03
9	1.22	11.07	1.49E-02[2]	1.11E-02
10	1.44	12.51	1.67E-02	1.26E-02
11	1.32	13.83	1.82E-02	1.38E-02
12	1.51	15.34	1.99E-02	1.50E-02
13	1.29	16.63	2.15E-02	1.62E-02
14	1.43	18.06	2.31E-02	1.73E-02
15	1.15	19.21	2.45E-02	1.84E-02
16	1.25	20.46	2.62E-02	1.96E-02
17	1.25	21.71	2.78E-02	2.07E-02
18	1.42	23.13	2.95E-02	2.21E-02
19	1.19	24.32	3.13E-02	2.34E-02
20	1.23	25.55	3.34E-02[3]	2.49E-02
21	1.28	26.83	3.56E-02	2.65E-02
22	1.31	28.13	3.81E-02	2.83E-02
23	1.40	29.53	4.08E-02	3.02E-02
24	1.34	30.88	4.32E-02	3.19E-02
25[4]	1.43	32.30	4.56E-02	3.37E-02

Table 4-10
Iron Atom Displacements at the Geometric Center of the Surveillance Capsules

No bias on the peripheral and re-entrant corner assembly relative powers				
Cycle	**Cycle Length (EFPY)**	**Cumulative Operating Time (EFPY)**	**Displacements (dpa)**	
			7°	**14°**
Future[5]	--	36.00	5.21E-02	3.84E-02
Future[5]	--	42.00	6.26E-02	4.59E-02
Future[5]	--	48.00	7.31E-02	5.35E-02
Future[5]	--	54.00	8.36E-02	6.11E-02
Future[5]	--	60.00	9.41E-02	6.87E-02
Future[5]	--	66.00	1.05E-01	7.62E-02
Future[5]	--	72.00	1.15E-01	8.38E-02

+10% bias on the peripheral and re-entrant corner assembly relative powers				
Cycle	**Cycle Length (EFPY)**	**Cumulative Operating Time (EFPY)**	**Displacements (dpa)**	
			7°	**14°**
Future[5]	--	36.00	5.26E-02	3.88E-02
Future[5]	--	42.00	6.41E-02	4.70E-02
Future[5]	--	48.00	7.55E-02	5.53E-02
Future[5]	--	54.00	8.70E-02	6.36E-02
Future[5]	--	60.00	9.84E-02	7.18E-02
Future[5]	--	66.00	1.10E-01	8.01E-02
Future[5]	--	72.00	1.21E-01	8.83E-02

Note(s):

1. This value is applicable to Capsule 83°.
2. This value is applicable to Capsule 263°.
3. This value is applicable to Capsule 97°.
4. Cycle 25 was the current operating cycle at the time this summary report was authored.
5. Values beyond Cycle 25 are based on the average core power distributions and reactor operating conditions of Cycle 24 and are determined both with and without a 1.1 bias on the peripheral and re-entrant corner assembly relative powers.

Table 4-11
Surveillance Capsule Lead Factors

Cycle	Cycle Length (EFPY)	Cumulative Operating Time (EFPY)	Lead Factor	
			7°	14°
1	1.11	1.11	1.27[1]	0.90
2	1.12	2.23	1.23	0.85
3	1.22	3.45	1.22	0.84
4	1.16	4.61	1.24	0.88
5	1.30	5.91	1.25	0.92
6	1.35	7.26	1.25	0.91
7	1.21	8.47	1.24	0.90
8	1.38	9.85	1.24	0.91
9	1.22	11.07	1.26[2]	0.93
10	1.44	12.51	1.27	0.95
11	1.32	13.83	1.27	0.95
12	1.51	15.34	1.27	0.95
13	1.29	16.63	1.27	0.95
14	1.43	18.06	1.27	0.95
15	1.15	19.21	1.27	0.95
16	1.25	20.46	1.27	0.95
17	1.25	21.71	1.27	0.94
18	1.42	23.13	1.28	0.95
19	1.19	24.32	1.28	0.95
20	1.23	25.55	1.28[3]	0.95
21	1.28	26.83	1.28	0.95
22	1.31	28.13	1.28	0.94
23	1.40	29.53	1.28	0.94
24	1.34	30.88	1.27	0.94
25[4]	1.43	32.30	1.27	0.94

Table 4-11
Surveillance Capsule Lead Factors

No bias on the peripheral and re-entrant corner assembly relative powers				
Cycle	**Cycle Length (EFPY)**	**Cumulative Operating Time (EFPY)**	**Lead Factor**	
			7°	**14°**
Future[5]	--	36.00	1.27	0.93
Future[5]	--	42.00	1.27	0.93
Future[5]	--	48.00	1.27	0.93
Future[5]	--	54.00	1.27	0.92
Future[5]	--	60.00	1.27	0.92
Future[5]	--	66.00	1.27	0.92
Future[5]	--	72.00	1.27	0.92

+10% bias on the peripheral and re-entrant corner assembly relative powers				
Cycle	**Cycle Length (EFPY)**	**Cumulative Operating Time (EFPY)**	**Lead Factor**	
			7°	**14°**
Future[5]	--	36.00	1.27	0.93
Future[5]	--	42.00	1.27	0.93
Future[5]	--	48.00	1.27	0.93
Future[5]	--	54.00	1.27	0.92
Future[5]	--	60.00	1.27	0.92
Future[5]	--	66.00	1.27	0.92
Future[5]	--	72.00	1.27	0.92

Note(s):

1. This value is applicable to Capsule 83°.
2. This value is applicable to Capsule 263°
3. This value is applicable to Capsule 97°.
4. Cycle 25 was the current operating cycle at the time this summary report was authored.
5. Values beyond Cycle 25 are based on the average core power distributions and reactor operating conditions of Cycle 24 and are determined both with and without a 1.1 bias on the peripheral and re-entrant corner assembly relative powers.

4.3 RPV Support Structure

Neutron exposure data for the RPV support structure are provided in Table 4-12 through Table 4-20. In particular:

- Table 4-12 provides the maximum neutron exposures, expressed as fast neutron (E > 1.0 MeV and E > 0.1 MeV) fluences and iron atom displacements (all energies and E > 0.1 MeV), at the RPV support structure. Note that each value reported in Table 4-12 was determined at the RPV support structure inner surface, 0° azimuth, and axial elevation where the maximum exposure of interest occurred.
- Table 4-13 and Table 4-14 provide fast neutron (E > 1.0 MeV) fluence projections at the RPV support structure as a function of height. Note that each fluence value reported in Table 4-13 and Table 4-14 was determined at the RPV support structure inner surface, 0° azimuth, and axial elevation indicated.
- Table 4-15 and Table 4-16 provide fast neutron (E > 0.1 MeV) fluence projections at the RPV support structure as a function of height. Note that each fluence value reported in Table 4-15 and Table 4-16 was determined at the RPV support structure inner surface, 0° azimuth, and axial elevation indicated.
- Table 4-17 and Table 4-18 provide iron atom displacement (all energies) projections at the RPV support structure as a function of height. Note that each displacement value reported in Table 4-17 and Table 4-18 was determined at the RPV support structure inner surface, 0° azimuth, and axial elevation indicated.
- Table 4-19 and Table 4-20 provide iron atom displacement (E > 0.1 MeV) projections at the RPV support structure as a function of height. Note that each displacement value reported in Table 4-19 and Table 4-20 was determined at the RPV support structure inner surface, 0° azimuth, and axial elevation indicated.

Table 4-12
Maximum Neutron Exposures at the RPV Support Structure

Cycle	Cycle Length (EFPY)	Cumulative Operating Time (EFPY)	Fast Neutron Fluence (n/cm^2)		Iron Atom Displacements (dpa)	
			E > 1.0 MeV	E > 0.1 MeV	All Energies	E > 0.1 MeV
1	1.11	1.11	4.86E+16	5.63E+17	1.84E-04	1.69E-04
2	1.12	2.23	9.85E+16	1.17E+18	3.82E-04	3.51E-04
3	1.22	3.45	1.47E+17	1.74E+18	5.69E-04	5.24E-04
4	1.16	4.61	1.81E+17	2.13E+18	6.96E-04	6.41E-04
5	1.30	5.91	2.18E+17	2.56E+18	8.36E-04	7.69E-04
6	1.35	7.26	2.57E+17	3.04E+18	9.92E-04	9.13E-04
7	1.21	8.47	2.94E+17	3.48E+18	1.14E-03	1.05E-03
8	1.38	9.85	3.21E+17	3.82E+18	1.25E-03	1.15E-03
9	1.22	11.07	3.55E+17	4.22E+18	1.38E-03	1.27E-03
10	1.44	12.51	3.97E+17	4.74E+18	1.55E-03	1.42E-03
11	1.32	13.83	4.33E+17	5.17E+18	1.69E-03	1.55E-03
12	1.51	15.34	4.74E+17	5.65E+18	1.84E-03	1.70E-03
13	1.29	16.63	5.12E+17	6.10E+18	1.99E-03	1.83E-03
14	1.43	18.06	5.49E+17	6.54E+18	2.14E-03	1.96E-03
15	1.15	19.21	5.84E+17	6.94E+18	2.27E-03	2.09E-03
16	1.25	20.46	6.22E+17	7.39E+18	2.42E-03	2.22E-03
17	1.25	21.71	6.59E+17	7.82E+18	2.56E-03	2.35E-03
18	1.42	23.13	6.99E+17	8.30E+18	2.71E-03	2.49E-03
19	1.19	24.32	7.41E+17	8.81E+18	2.88E-03	2.65E-03
20	1.23	25.55	7.92E+17	9.40E+18	3.07E-03	2.82E-03
21	1.28	26.83	8.42E+17	9.99E+18	3.27E-03	3.00E-03
22	1.31	28.13	9.02E+17	1.07E+19	3.50E-03	3.22E-03
23	1.40	29.53	9.66E+17	1.15E+19	3.74E-03	3.44E-03
24	1.34	30.88	1.02E+18	1.21E+19	3.96E-03	3.64E-03
25[1]	1.43	32.30	1.08E+18	1.28E+19	4.18E-03	3.84E-03

Table 4-12
Maximum Neutron Exposures at the RPV Support Structure

Cycle	Cycle Length (EFPY)	Cumulative Operating Time (EFPY)	Fast Neutron Fluence (n/cm^2)		Iron Atom Displacements (dpa)	
			E > 1.0 MeV	E > 0.1 MeV	All Energies	E > 0.1 MeV
Projections with no bias on the peripheral and re-entrant corner assembly relative powers						
Future[2]	--	36.00	1.23E+18	1.46E+19	4.77E-03	4.38E-03
Future[2]	--	42.00	1.48E+18	1.75E+19	5.72E-03	5.27E-03
Future[2]	--	48.00	1.73E+18	2.04E+19	6.68E-03	6.15E-03
Future[2]	--	54.00	1.98E+18	2.34E+19	7.64E-03	7.03E-03
Future[2]	--	60.00	2.23E+18	2.63E+19	8.59E-03	7.91E-03
Future[2]	--	66.00	2.48E+18	2.92E+19	9.55E-03	8.79E-03
Future[2]	--	72.00	2.73E+18	3.22E+19	1.05E-02	9.67E-03
Projections with a +10% bias on the peripheral and re-entrant corner assembly relative powers						
Future[2]	--	36.00	1.25E+18	1.48E+19	4.82E-03	4.43E-03
Future[2]	--	42.00	1.52E+18	1.79E+19	5.86E-03	5.39E-03
Future[2]	--	48.00	1.79E+18	2.11E+19	6.91E-03	6.35E-03
Future[2]	--	54.00	2.06E+18	2.43E+19	7.95E-03	7.31E-03
Future[2]	--	60.00	2.33E+18	2.75E+19	8.99E-03	8.27E-03
Future[2]	--	66.00	2.60E+18	3.07E+19	1.00E-02	9.23E-03
Future[2]	--	72.00	2.87E+18	3.39E+19	1.11E-02	1.02E-02

Note(s):

1. Cycle 25 was the current operating cycle at the time this summary report was authored.
2. Values beyond Cycle 25 are based on the average core power distributions and reactor operating conditions of Cycle 24 and are determined both with and without a 1.1 bias on the peripheral and re-entrant corner assembly relative powers.

Table 4-13
Fast Neutron (E > 1.0 MeV) Fluence at the RPV Support Structure –
No Bias on the Peripheral and Re-Entrant Corner Assembly Relative Powers

Elevation[1] (cm)	Fast Neutron (E > 1.0 MeV) Fluence (n/cm^2)							
	32.30 EFPY[2]	36 EFPY	42 EFPY	48 EFPY	54 EFPY	60 EFPY	66 EFPY	72 EFPY
231.16[3]	6.31E+16	7.14E+16	8.48E+16	9.83E+16	1.12E+17	1.25E+17	1.39E+17	1.52E+17
228.60	6.98E+16	7.90E+16	9.38E+16	1.09E+17	1.23E+17	1.38E+17	1.53E+17	1.68E+17
213.36	1.26E+17	1.43E+17	1.69E+17	1.96E+17	2.23E+17	2.49E+17	2.76E+17	3.03E+17
198.12	2.05E+17	2.32E+17	2.76E+17	3.20E+17	3.64E+17	4.07E+17	4.51E+17	4.95E+17
182.88	3.25E+17	3.68E+17	4.38E+17	5.08E+17	5.78E+17	6.48E+17	7.18E+17	7.88E+17
167.64	4.77E+17	5.41E+17	6.46E+17	7.50E+17	8.55E+17	9.59E+17	1.06E+18	1.17E+18
152.40	6.37E+17	7.25E+17	8.67E+17	1.01E+18	1.15E+18	1.29E+18	1.43E+18	1.58E+18
137.16	7.82E+17	8.91E+17	1.07E+18	1.24E+18	1.42E+18	1.60E+18	1.77E+18	1.95E+18
121.92	8.96E+17	1.02E+18	1.23E+18	1.43E+18	1.63E+18	1.84E+18	2.04E+18	2.25E+18
106.68	9.80E+17	1.12E+18	1.34E+18	1.57E+18	1.79E+18	2.02E+18	2.24E+18	2.46E+18
91.44	1.06E+18	1.21E+18	1.45E+18	1.70E+18	1.94E+18	2.19E+18	2.43E+18	2.67E+18
76.20	1.05E+18	1.20E+18	1.44E+18	1.68E+18	1.93E+18	2.17E+18	2.41E+18	2.65E+18
60.96	1.06E+18	1.21E+18	1.46E+18	1.70E+18	1.94E+18	2.19E+18	2.43E+18	2.68E+18
45.72	1.07E+18	1.22E+18	1.47E+18	1.72E+18	1.96E+18	2.21E+18	2.46E+18	2.70E+18
30.48	1.07E+18	1.23E+18	1.47E+18	1.72E+18	1.97E+18	2.22E+18	2.46E+18	2.71E+18
15.24	1.07E+18	1.22E+18	1.47E+18	1.72E+18	1.97E+18	2.21E+18	2.46E+18	2.71E+18
0.00	1.07E+18	1.23E+18	1.47E+18	1.72E+18	1.97E+18	2.22E+18	2.47E+18	2.71E+18
-15.24	1.08E+18	1.23E+18	1.48E+18	1.73E+18	1.98E+18	2.23E+18	2.48E+18	2.73E+18
-30.48	1.08E+18	1.23E+18	1.48E+18	1.73E+18	1.98E+18	2.23E+18	2.48E+18	2.73E+18
-45.72	1.07E+18	1.23E+18	1.47E+18	1.72E+18	1.97E+18	2.22E+18	2.47E+18	2.71E+18
-60.96	1.06E+18	1.22E+18	1.46E+18	1.71E+18	1.95E+18	2.20E+18	2.45E+18	2.69E+18
-76.20	1.05E+18	1.20E+18	1.44E+18	1.69E+18	1.93E+18	2.17E+18	2.42E+18	2.66E+18
-91.44	1.02E+18	1.17E+18	1.40E+18	1.64E+18	1.88E+18	2.12E+18	2.35E+18	2.59E+18
-106.68	9.69E+17	1.11E+18	1.33E+18	1.56E+18	1.78E+18	2.01E+18	2.23E+18	2.46E+18
-121.92	8.88E+17	1.01E+18	1.22E+18	1.43E+18	1.63E+18	1.84E+18	2.04E+18	2.25E+18

Table 4-13
Fast Neutron (E > 1.0 MeV) Fluence at the RPV Support Structure –
No Bias on the Peripheral and Re-Entrant Corner Assembly Relative Powers

Elevation[1] (cm)	Fast Neutron (E > 1.0 MeV) Fluence (n/cm^2)							
	32.30 EFPY[2]	36 EFPY	42 EFPY	48 EFPY	54 EFPY	60 EFPY	66 EFPY	72 EFPY
-137.16	7.76E+17	8.86E+17	1.07E+18	1.24E+18	1.42E+18	1.60E+18	1.78E+18	1.96E+18
-152.40	6.36E+17	7.25E+17	8.70E+17	1.02E+18	1.16E+18	1.31E+18	1.45E+18	1.60E+18
-167.64	4.78E+17	5.44E+17	6.51E+17	7.59E+17	8.66E+17	9.74E+17	1.08E+18	1.19E+18
-182.88	3.25E+17	3.69E+17	4.42E+17	5.14E+17	5.86E+17	6.58E+17	7.31E+17	8.03E+17
-198.12	2.02E+17	2.30E+17	2.74E+17	3.19E+17	3.63E+17	4.08E+17	4.52E+17	4.97E+17
-213.36	1.20E+17	1.36E+17	1.62E+17	1.89E+17	2.15E+17	2.41E+17	2.67E+17	2.94E+17
-228.60	7.20E+16	8.17E+16	9.76E+16	1.13E+17	1.29E+17	1.45E+17	1.61E+17	1.77E+17
-243.84	4.58E+16	5.21E+16	6.23E+16	7.24E+16	8.26E+16	9.27E+16	1.03E+17	1.13E+17
-259.08	3.20E+16	3.64E+16	4.36E+16	5.07E+16	5.79E+16	6.50E+16	7.22E+16	7.93E+16
-274.32	2.50E+16	2.84E+16	3.40E+16	3.96E+16	4.52E+16	5.08E+16	5.64E+16	6.20E+16
-289.56	2.04E+16	2.33E+16	2.78E+16	3.24E+16	3.70E+16	4.16E+16	4.61E+16	5.07E+16

Note(s):

1. Elevations are given with respect to the midplane of the active fuel.
2. Value listed is the projected EFPY at the end of Cycle 25.
3. This elevation corresponds to the top of the 6-inch-thick horizontal plate at the top-center of the RPV support structure.
4. Linear interpolation between the EFPY values listed in this table may be performed as necessary.

Table 4-14
Fast Neutron (E > 1.0 MeV) Fluence at the RPV Support Structure –
+10% Bias on the Peripheral and Re-Entrant Corner Assembly Relative Powers

Elevation[1] (cm)	Fast Neutron (E > 1.0 MeV) Fluence (n/cm^2)							
	32.30 EFPY[2]	36 EFPY	42 EFPY	48 EFPY	54 EFPY	60 EFPY	66 EFPY	72 EFPY
231.16[3]	6.31E+16	7.21E+16	8.67E+16	1.01E+17	1.16E+17	1.30E+17	1.45E+17	1.60E+17
228.60	6.98E+16	7.98E+16	9.59E+16	1.12E+17	1.28E+17	1.44E+17	1.60E+17	1.76E+17
213.36	1.26E+17	1.44E+17	1.73E+17	2.02E+17	2.31E+17	2.60E+17	2.89E+17	3.18E+17
198.12	2.05E+17	2.35E+17	2.82E+17	3.30E+17	3.77E+17	4.25E+17	4.72E+17	5.20E+17
182.88	3.25E+17	3.72E+17	4.48E+17	5.24E+17	6.00E+17	6.77E+17	7.53E+17	8.29E+17
167.64	4.77E+17	5.47E+17	6.60E+17	7.74E+17	8.88E+17	1.00E+18	1.12E+18	1.23E+18
152.40	6.37E+17	7.32E+17	8.87E+17	1.04E+18	1.20E+18	1.35E+18	1.51E+18	1.66E+18
137.16	7.82E+17	9.00E+17	1.09E+18	1.28E+18	1.48E+18	1.67E+18	1.86E+18	2.05E+18
121.92	8.96E+17	1.03E+18	1.26E+18	1.48E+18	1.70E+18	1.92E+18	2.14E+18	2.37E+18
106.68	9.80E+17	1.13E+18	1.37E+18	1.62E+18	1.86E+18	2.11E+18	2.35E+18	2.60E+18
91.44	1.06E+18	1.22E+18	1.49E+18	1.76E+18	2.02E+18	2.29E+18	2.55E+18	2.82E+18
76.20	1.05E+18	1.21E+18	1.48E+18	1.74E+18	2.00E+18	2.27E+18	2.53E+18	2.79E+18
60.96	1.06E+18	1.23E+18	1.49E+18	1.76E+18	2.02E+18	2.29E+18	2.55E+18	2.82E+18
45.72	1.07E+18	1.24E+18	1.51E+18	1.77E+18	2.04E+18	2.31E+18	2.58E+18	2.85E+18
30.48	1.07E+18	1.24E+18	1.51E+18	1.78E+18	2.05E+18	2.32E+18	2.59E+18	2.86E+18
15.24	1.07E+18	1.24E+18	1.51E+18	1.78E+18	2.05E+18	2.32E+18	2.58E+18	2.85E+18
0.00	1.07E+18	1.24E+18	1.51E+18	1.78E+18	2.05E+18	2.32E+18	2.59E+18	2.86E+18
-15.24	1.08E+18	1.24E+18	1.52E+18	1.79E+18	2.06E+18	2.33E+18	2.60E+18	2.87E+18
-30.48	1.08E+18	1.24E+18	1.52E+18	1.79E+18	2.06E+18	2.33E+18	2.60E+18	2.87E+18
-45.72	1.07E+18	1.24E+18	1.51E+18	1.78E+18	2.05E+18	2.32E+18	2.59E+18	2.86E+18
-60.96	1.06E+18	1.23E+18	1.50E+18	1.76E+18	2.03E+18	2.30E+18	2.57E+18	2.84E+18
-76.20	1.05E+18	1.21E+18	1.48E+18	1.74E+18	2.01E+18	2.27E+18	2.54E+18	2.80E+18
-91.44	1.02E+18	1.18E+18	1.44E+18	1.70E+18	1.95E+18	2.21E+18	2.47E+18	2.73E+18
-106.68	9.69E+17	1.12E+18	1.36E+18	1.61E+18	1.85E+18	2.10E+18	2.34E+18	2.58E+18
-121.92	8.88E+17	1.03E+18	1.25E+18	1.47E+18	1.70E+18	1.92E+18	2.14E+18	2.37E+18

Table 4-14
Fast Neutron (E > 1.0 MeV) Fluence at the RPV Support Structure –
+10% Bias on the Peripheral and Re-Entrant Corner Assembly Relative Powers

Elevation[1] (cm)	Fast Neutron (E > 1.0 MeV) Fluence (n/cm^2)							
	32.30 EFPY[2]	36 EFPY	42 EFPY	48 EFPY	54 EFPY	60 EFPY	66 EFPY	72 EFPY
-137.16	7.76E+17	8.96E+17	1.09E+18	1.28E+18	1.48E+18	1.67E+18	1.87E+18	2.06E+18
-152.40	6.36E+17	7.33E+17	8.91E+17	1.05E+18	1.21E+18	1.36E+18	1.52E+18	1.68E+18
-167.64	4.78E+17	5.50E+17	6.66E+17	7.83E+17	9.00E+17	1.02E+18	1.13E+18	1.25E+18
-182.88	3.25E+17	3.73E+17	4.52E+17	5.30E+17	6.09E+17	6.87E+17	7.65E+17	8.44E+17
-198.12	2.02E+17	2.32E+17	2.80E+17	3.29E+17	3.77E+17	4.26E+17	4.74E+17	5.22E+17
-213.36	1.20E+17	1.37E+17	1.66E+17	1.94E+17	2.23E+17	2.52E+17	2.80E+17	3.09E+17
-228.60	7.20E+16	8.26E+16	9.98E+16	1.17E+17	1.34E+17	1.51E+17	1.69E+17	1.86E+17
-243.84	4.58E+16	5.26E+16	6.37E+16	7.47E+16	8.57E+16	9.68E+16	1.08E+17	1.19E+17
-259.08	3.20E+16	3.68E+16	4.46E+16	5.24E+16	6.02E+16	6.79E+16	7.57E+16	8.35E+16
-274.32	2.50E+16	2.87E+16	3.48E+16	4.09E+16	4.70E+16	5.31E+16	5.92E+16	6.53E+16
-289.56	2.04E+16	2.35E+16	2.85E+16	3.35E+16	3.85E+16	4.34E+16	4.84E+16	5.34E+16

Note(s):

1. Elevations are given with respect to the midplane of the active fuel.
2. Value listed is the projected EFPY at the end of Cycle 25.
3. This elevation corresponds to the top of the 6-inch-thick horizontal plate at the top-center of the RPV support structure.
4. Linear interpolation between the EFPY values listed in this table may be performed as necessary.

Table 4-15
Fast Neutron (E > 0.1 MeV) Fluence at the RPV Support Structure –
No Bias on the Peripheral and Re-Entrant Corner Assembly Relative Powers

Elevation[1] (cm)	Fast Neutron (E > 0.1 MeV) Fluence (n/cm^2)							
	32.30 EFPY[2]	36 EFPY	42 EFPY	48 EFPY	54 EFPY	60 EFPY	66 EFPY	72 EFPY
231.16[3]	1.77E+18	2.01E+18	2.40E+18	2.79E+18	3.17E+18	3.56E+18	3.95E+18	4.33E+18
228.60	1.90E+18	2.15E+18	2.56E+18	2.98E+18	3.39E+18	3.80E+18	4.22E+18	4.63E+18
213.36	2.70E+18	3.06E+18	3.65E+18	4.24E+18	4.82E+18	5.41E+18	6.00E+18	6.59E+18
198.12	3.54E+18	4.01E+18	4.79E+18	5.56E+18	6.33E+18	7.10E+18	7.88E+18	8.65E+18
182.88	4.73E+18	5.37E+18	6.41E+18	7.45E+18	8.49E+18	9.53E+18	1.06E+19	1.16E+19
167.64	6.19E+18	7.04E+18	8.41E+18	9.78E+18	1.12E+19	1.25E+19	1.39E+19	1.53E+19
152.40	7.74E+18	8.80E+18	1.05E+19	1.23E+19	1.40E+19	1.57E+19	1.75E+19	1.92E+19
137.16	9.17E+18	1.04E+19	1.25E+19	1.46E+19	1.67E+19	1.87E+19	2.08E+19	2.29E+19
121.92	1.04E+19	1.18E+19	1.42E+19	1.65E+19	1.89E+19	2.12E+19	2.36E+19	2.60E+19
106.68	1.14E+19	1.30E+19	1.56E+19	1.82E+19	2.08E+19	2.34E+19	2.60E+19	2.86E+19
91.44	1.26E+19	1.44E+19	1.73E+19	2.01E+19	2.30E+19	2.59E+19	2.88E+19	3.17E+19
76.20	1.24E+19	1.42E+19	1.70E+19	1.98E+19	2.27E+19	2.55E+19	2.84E+19	3.12E+19
60.96	1.23E+19	1.41E+19	1.69E+19	1.97E+19	2.26E+19	2.54E+19	2.82E+19	3.10E+19
45.72	1.23E+19	1.41E+19	1.69E+19	1.98E+19	2.26E+19	2.54E+19	2.83E+19	3.11E+19
30.48	1.23E+19	1.41E+19	1.69E+19	1.97E+19	2.26E+19	2.54E+19	2.82E+19	3.11E+19
15.24	1.23E+19	1.40E+19	1.69E+19	1.97E+19	2.25E+19	2.53E+19	2.82E+19	3.10E+19
0.00	1.23E+19	1.40E+19	1.68E+19	1.96E+19	2.25E+19	2.53E+19	2.81E+19	3.09E+19
-15.24	1.22E+19	1.40E+19	1.68E+19	1.96E+19	2.24E+19	2.53E+19	2.81E+19	3.09E+19
-30.48	1.22E+19	1.39E+19	1.67E+19	1.95E+19	2.23E+19	2.51E+19	2.79E+19	3.07E+19
-45.72	1.21E+19	1.38E+19	1.66E+19	1.93E+19	2.21E+19	2.49E+19	2.77E+19	3.05E+19
-60.96	1.19E+19	1.36E+19	1.63E+19	1.91E+19	2.18E+19	2.46E+19	2.73E+19	3.00E+19
-76.20	1.16E+19	1.33E+19	1.60E+19	1.87E+19	2.13E+19	2.40E+19	2.67E+19	2.94E+19
-91.44	1.12E+19	1.28E+19	1.54E+19	1.80E+19	2.06E+19	2.32E+19	2.58E+19	2.84E+19
-106.68	1.06E+19	1.21E+19	1.46E+19	1.70E+19	1.95E+19	2.19E+19	2.44E+19	2.68E+19
-121.92	9.73E+18	1.11E+19	1.34E+19	1.56E+19	1.78E+19	2.01E+19	2.23E+19	2.46E+19

Table 4-15
Fast Neutron (E > 0.1 MeV) Fluence at the RPV Support Structure –
No Bias on the Peripheral and Re-Entrant Corner Assembly Relative Powers

Elevation[1] (cm)	Fast Neutron (E > 0.1 MeV) Fluence (n/cm^2)							
	32.30 EFPY[2]	36 EFPY	42 EFPY	48 EFPY	54 EFPY	60 EFPY	66 EFPY	72 EFPY
-137.16	8.59E+18	9.81E+18	1.18E+19	1.38E+19	1.57E+19	1.77E+19	1.97E+19	2.17E+19
-152.40	7.24E+18	8.26E+18	9.91E+18	1.16E+19	1.32E+19	1.49E+19	1.65E+19	1.82E+19
-167.64	5.75E+18	6.55E+18	7.86E+18	9.16E+18	1.05E+19	1.18E+19	1.31E+19	1.44E+19
-182.88	4.32E+18	4.91E+18	5.88E+18	6.85E+18	7.82E+18	8.79E+18	9.76E+18	1.07E+19
-198.12	3.10E+18	3.53E+18	4.22E+18	4.92E+18	5.61E+18	6.30E+18	7.00E+18	7.69E+18
-213.36	2.19E+18	2.49E+18	2.98E+18	3.46E+18	3.95E+18	4.44E+18	4.93E+18	5.42E+18
-228.60	1.56E+18	1.77E+18	2.12E+18	2.47E+18	2.82E+18	3.17E+18	3.51E+18	3.86E+18
-243.84	1.13E+18	1.29E+18	1.54E+18	1.80E+18	2.05E+18	2.30E+18	2.56E+18	2.81E+18
-259.08	8.44E+17	9.61E+17	1.15E+18	1.34E+18	1.53E+18	1.72E+18	1.91E+18	2.10E+18
-274.32	6.64E+17	7.56E+17	9.06E+17	1.06E+18	1.21E+18	1.35E+18	1.50E+18	1.65E+18
-289.56	5.42E+17	6.17E+17	7.39E+17	8.61E+17	9.83E+17	1.11E+18	1.23E+18	1.35E+18

Note(s):

1. Elevations are given with respect to the midplane of the active fuel.
2. Value listed is the projected EFPY at the end of Cycle 25.
3. This elevation corresponds to the top of the 6-inch-thick horizontal plate at the top-center of the RPV support structure.
4. Linear interpolation between the EFPY values listed in this table may be performed as necessary.

Table 4-16
Fast Neutron (E > 0.1 MeV) Fluence at the RPV Support Structure –
+10% Bias on the Peripheral and Re-Entrant Corner Assembly Relative Powers

Elevation[1] (cm)	Fast Neutron (E > 0.1 MeV) Fluence (n/cm^2)							
	32.30 EFPY[2]	36 EFPY	42 EFPY	48 EFPY	54 EFPY	60 EFPY	66 EFPY	72 EFPY
231.16[3]	1.77E+18	2.03E+18	2.45E+18	2.88E+18	3.30E+18	3.72E+18	4.14E+18	4.56E+18
228.60	1.90E+18	2.17E+18	2.62E+18	3.07E+18	3.52E+18	3.97E+18	4.42E+18	4.87E+18
213.36	2.70E+18	3.09E+18	3.73E+18	4.37E+18	5.01E+18	5.65E+18	6.29E+18	6.93E+18
198.12	3.54E+18	4.06E+18	4.90E+18	5.74E+18	6.58E+18	7.42E+18	8.26E+18	9.10E+18
182.88	4.73E+18	5.43E+18	6.56E+18	7.69E+18	8.83E+18	9.96E+18	1.11E+19	1.22E+19
167.64	6.19E+18	7.11E+18	8.61E+18	1.01E+19	1.16E+19	1.31E+19	1.46E+19	1.61E+19
152.40	7.74E+18	8.90E+18	1.08E+19	1.27E+19	1.46E+19	1.64E+19	1.83E+19	2.02E+19
137.16	9.17E+18	1.06E+19	1.28E+19	1.51E+19	1.73E+19	1.96E+19	2.18E+19	2.41E+19
121.92	1.04E+19	1.20E+19	1.45E+19	1.71E+19	1.97E+19	2.22E+19	2.48E+19	2.74E+19
106.68	1.14E+19	1.31E+19	1.60E+19	1.88E+19	2.16E+19	2.45E+19	2.73E+19	3.01E+19
91.44	1.26E+19	1.45E+19	1.77E+19	2.08E+19	2.40E+19	2.71E+19	3.03E+19	3.34E+19
76.20	1.24E+19	1.43E+19	1.74E+19	2.05E+19	2.36E+19	2.67E+19	2.98E+19	3.29E+19
60.96	1.23E+19	1.42E+19	1.73E+19	2.04E+19	2.35E+19	2.66E+19	2.96E+19	3.27E+19
45.72	1.23E+19	1.42E+19	1.73E+19	2.04E+19	2.35E+19	2.66E+19	2.97E+19	3.28E+19
30.48	1.23E+19	1.42E+19	1.73E+19	2.04E+19	2.35E+19	2.66E+19	2.97E+19	3.28E+19
15.24	1.23E+19	1.42E+19	1.73E+19	2.04E+19	2.34E+19	2.65E+19	2.96E+19	3.27E+19
0.00	1.23E+19	1.42E+19	1.72E+19	2.03E+19	2.34E+19	2.65E+19	2.95E+19	3.26E+19
-15.24	1.22E+19	1.41E+19	1.72E+19	2.03E+19	2.33E+19	2.64E+19	2.95E+19	3.26E+19
-30.48	1.22E+19	1.41E+19	1.71E+19	2.02E+19	2.32E+19	2.63E+19	2.93E+19	3.24E+19
-45.72	1.21E+19	1.39E+19	1.70E+19	2.00E+19	2.30E+19	2.60E+19	2.91E+19	3.21E+19
-60.96	1.19E+19	1.37E+19	1.67E+19	1.97E+19	2.27E+19	2.57E+19	2.87E+19	3.16E+19
-76.20	1.16E+19	1.34E+19	1.63E+19	1.93E+19	2.22E+19	2.51E+19	2.80E+19	3.10E+19
-91.44	1.12E+19	1.30E+19	1.58E+19	1.86E+19	2.14E+19	2.42E+19	2.71E+19	2.99E+19
-106.68	1.06E+19	1.22E+19	1.49E+19	1.76E+19	2.02E+19	2.29E+19	2.56E+19	2.82E+19
-121.92	9.73E+18	1.12E+19	1.37E+19	1.61E+19	1.86E+19	2.10E+19	2.34E+19	2.59E+19

Table 4-16
Fast Neutron (E > 0.1 MeV) Fluence at the RPV Support Structure –
+10% Bias on the Peripheral and Re-Entrant Corner Assembly Relative Powers

Elevation[1] (cm)	Fast Neutron (E > 0.1 MeV) Fluence (n/cm^2)							
	32.30 EFPY[2]	36 EFPY	42 EFPY	48 EFPY	54 EFPY	60 EFPY	66 EFPY	72 EFPY
-137.16	8.59E+18	9.92E+18	1.21E+19	1.42E+19	1.64E+19	1.85E+19	2.07E+19	2.28E+19
-152.40	7.24E+18	8.35E+18	1.01E+19	1.19E+19	1.37E+19	1.55E+19	1.73E+19	1.91E+19
-167.64	5.75E+18	6.63E+18	8.04E+18	9.46E+18	1.09E+19	1.23E+19	1.37E+19	1.51E+19
-182.88	4.32E+18	4.97E+18	6.02E+18	7.08E+18	8.13E+18	9.19E+18	1.02E+19	1.13E+19
-198.12	3.10E+18	3.57E+18	4.32E+18	5.08E+18	5.83E+18	6.58E+18	7.34E+18	8.09E+18
-213.36	2.19E+18	2.51E+18	3.05E+18	3.58E+18	4.11E+18	4.64E+18	5.17E+18	5.70E+18
-228.60	1.56E+18	1.79E+18	2.17E+18	2.55E+18	2.93E+18	3.31E+18	3.69E+18	4.07E+18
-243.84	1.13E+18	1.30E+18	1.58E+18	1.86E+18	2.13E+18	2.41E+18	2.69E+18	2.96E+18
-259.08	8.44E+17	9.71E+17	1.18E+18	1.38E+18	1.59E+18	1.80E+18	2.01E+18	2.21E+18
-274.32	6.64E+17	7.65E+17	9.28E+17	1.09E+18	1.25E+18	1.42E+18	1.58E+18	1.74E+18
-289.56	5.42E+17	6.24E+17	7.57E+17	8.90E+17	1.02E+18	1.16E+18	1.29E+18	1.42E+18

Note(s):

1. Elevations are given with respect to the midplane of the active fuel.
2. Value listed is the projected EFPY at the end of Cycle 25.
3. This elevation corresponds to the top of the 6-inch-thick horizontal plate at the top-center of the RPV support structure.
4. Linear interpolation between the EFPY values listed in this table may be performed as necessary.

Table 4-17
Iron Atom Displacements (All Neutron Energies) at the RPV Support Structure –
No Bias on the Peripheral and Re-Entrant Corner Assembly Relative Powers

Elevation[1] (cm)	Iron Atom Displacements – All Neutron Energies (dpa)							
	32.30 EFPY[2]	36 EFPY	42 EFPY	48 EFPY	54 EFPY	60 EFPY	66 EFPY	72 EFPY
231.16[3]	5.25E-04	5.95E-04	7.09E-04	8.23E-04	9.38E-04	1.05E-03	1.17E-03	1.28E-03
228.60	5.62E-04	6.37E-04	7.60E-04	8.82E-04	1.00E-03	1.13E-03	1.25E-03	1.37E-03
213.36	8.17E-04	9.26E-04	1.10E-03	1.28E-03	1.46E-03	1.64E-03	1.81E-03	1.99E-03
198.12	1.10E-03	1.25E-03	1.49E-03	1.72E-03	1.96E-03	2.20E-03	2.44E-03	2.68E-03
182.88	1.50E-03	1.71E-03	2.04E-03	2.37E-03	2.70E-03	3.02E-03	3.35E-03	3.68E-03
167.64	2.00E-03	2.28E-03	2.72E-03	3.16E-03	3.61E-03	4.05E-03	4.49E-03	4.94E-03
152.40	2.53E-03	2.88E-03	3.45E-03	4.02E-03	4.58E-03	5.15E-03	5.71E-03	6.28E-03
137.16	3.02E-03	3.44E-03	4.12E-03	4.81E-03	5.49E-03	6.17E-03	6.85E-03	7.53E-03
121.92	3.43E-03	3.91E-03	4.68E-03	5.46E-03	6.24E-03	7.02E-03	7.80E-03	8.58E-03
106.68	3.76E-03	4.29E-03	5.14E-03	6.00E-03	6.86E-03	7.71E-03	8.57E-03	9.43E-03
91.44	4.14E-03	4.72E-03	5.67E-03	6.62E-03	7.56E-03	8.51E-03	9.46E-03	1.04E-02
76.20	4.08E-03	4.66E-03	5.59E-03	6.53E-03	7.46E-03	8.40E-03	9.34E-03	1.03E-02
60.96	4.07E-03	4.65E-03	5.58E-03	6.51E-03	7.45E-03	8.38E-03	9.32E-03	1.02E-02
45.72	4.08E-03	4.66E-03	5.60E-03	6.53E-03	7.47E-03	8.41E-03	9.35E-03	1.03E-02
30.48	4.08E-03	4.66E-03	5.60E-03	6.53E-03	7.47E-03	8.41E-03	9.35E-03	1.03E-02
15.24	4.07E-03	4.65E-03	5.58E-03	6.52E-03	7.46E-03	8.39E-03	9.33E-03	1.03E-02
0.00	4.06E-03	4.64E-03	5.57E-03	6.51E-03	7.45E-03	8.38E-03	9.32E-03	1.03E-02
-15.24	4.06E-03	4.63E-03	5.57E-03	6.51E-03	7.44E-03	8.38E-03	9.31E-03	1.02E-02
-30.48	4.04E-03	4.62E-03	5.55E-03	6.48E-03	7.41E-03	8.34E-03	9.28E-03	1.02E-02
-45.72	4.01E-03	4.58E-03	5.50E-03	6.43E-03	7.35E-03	8.27E-03	9.20E-03	1.01E-02
-60.96	3.96E-03	4.52E-03	5.43E-03	6.34E-03	7.26E-03	8.17E-03	9.08E-03	1.00E-02
-76.20	3.88E-03	4.43E-03	5.32E-03	6.22E-03	7.11E-03	8.01E-03	8.91E-03	9.80E-03
-91.44	3.75E-03	4.28E-03	5.15E-03	6.01E-03	6.88E-03	7.75E-03	8.61E-03	9.48E-03
-106.68	3.54E-03	4.05E-03	4.87E-03	5.68E-03	6.50E-03	7.32E-03	8.14E-03	8.96E-03
-121.92	3.25E-03	3.71E-03	4.46E-03	5.21E-03	5.96E-03	6.71E-03	7.46E-03	8.21E-03

Table 4-17
Iron Atom Displacements (All Neutron Energies) at the RPV Support Structure – No Bias on the Peripheral and Re-Entrant Corner Assembly Relative Powers

Elevation[1] (cm)	**Iron Atom Displacements – All Neutron Energies (dpa)**							
	32.30 EFPY[2]	**36 EFPY**	**42 EFPY**	**48 EFPY**	**54 EFPY**	**60 EFPY**	**66 EFPY**	**72 EFPY**
-137.16	2.87E-03	3.27E-03	3.93E-03	4.59E-03	5.25E-03	5.91E-03	6.57E-03	7.23E-03
-152.40	2.40E-03	2.74E-03	3.29E-03	3.84E-03	4.38E-03	4.93E-03	5.48E-03	6.03E-03
-167.64	1.89E-03	2.15E-03	2.58E-03	3.01E-03	3.43E-03	3.86E-03	4.29E-03	4.72E-03
-182.88	1.39E-03	1.59E-03	1.90E-03	2.21E-03	2.52E-03	2.84E-03	3.15E-03	3.46E-03
-198.12	9.80E-04	1.11E-03	1.33E-03	1.55E-03	1.77E-03	1.99E-03	2.21E-03	2.43E-03
-213.36	6.76E-04	7.69E-04	9.19E-04	1.07E-03	1.22E-03	1.37E-03	1.52E-03	1.67E-03
-228.60	4.73E-04	5.38E-04	6.43E-04	7.49E-04	8.55E-04	9.60E-04	1.07E-03	1.17E-03
-243.84	3.40E-04	3.87E-04	4.63E-04	5.39E-04	6.15E-04	6.91E-04	7.67E-04	8.43E-04
-259.08	2.53E-04	2.87E-04	3.44E-04	4.01E-04	4.58E-04	5.14E-04	5.71E-04	6.28E-04
-274.32	1.99E-04	2.27E-04	2.72E-04	3.17E-04	3.62E-04	4.07E-04	4.51E-04	4.96E-04
-289.56	1.63E-04	1.86E-04	2.23E-04	2.59E-04	2.96E-04	3.33E-04	3.70E-04	4.07E-04

Note(s):

1. Elevations are given with respect to the midplane of the active fuel.
2. Value listed is the projected EFPY at the end of Cycle 25.
3. This elevation corresponds to the top of the 6-inch-thick horizontal plate at the top-center of the RPV support structure.
4. Linear interpolation between the EFPY values listed in this table may be performed as necessary.

Table 4-18
Iron Atom Displacements (All Neutron Energies) at the RPV Support Structure –
+10% Bias on the Peripheral and Re-Entrant Corner Assembly Relative Powers

Elevation[1] (cm)	Iron Atom Displacements – All Neutron Energies (dpa)							
	32.30 EFPY[2]	36 EFPY	42 EFPY	48 EFPY	54 EFPY	60 EFPY	66 EFPY	72 EFPY
231.16[3]	5.25E-04	6.01E-04	7.26E-04	8.50E-04	9.74E-04	1.10E-03	1.22E-03	1.35E-03
228.60	5.62E-04	6.44E-04	7.77E-04	9.10E-04	1.04E-03	1.18E-03	1.31E-03	1.44E-03
213.36	8.17E-04	9.36E-04	1.13E-03	1.32E-03	1.52E-03	1.71E-03	1.90E-03	2.09E-03
198.12	1.10E-03	1.26E-03	1.52E-03	1.78E-03	2.04E-03	2.30E-03	2.56E-03	2.82E-03
182.88	1.50E-03	1.73E-03	2.08E-03	2.44E-03	2.80E-03	3.16E-03	3.52E-03	3.88E-03
167.64	2.00E-03	2.30E-03	2.79E-03	3.27E-03	3.75E-03	4.23E-03	4.72E-03	5.20E-03
152.40	2.53E-03	2.91E-03	3.53E-03	4.15E-03	4.77E-03	5.38E-03	6.00E-03	6.62E-03
137.16	3.02E-03	3.48E-03	4.22E-03	4.97E-03	5.71E-03	6.45E-03	7.20E-03	7.94E-03
121.92	3.43E-03	3.95E-03	4.80E-03	5.65E-03	6.50E-03	7.34E-03	8.19E-03	9.04E-03
106.68	3.76E-03	4.33E-03	5.27E-03	6.20E-03	7.14E-03	8.07E-03	9.01E-03	9.94E-03
91.44	4.14E-03	4.77E-03	5.81E-03	6.84E-03	7.87E-03	8.90E-03	9.94E-03	1.10E-02
76.20	4.08E-03	4.71E-03	5.73E-03	6.75E-03	7.77E-03	8.79E-03	9.81E-03	1.08E-02
60.96	4.07E-03	4.70E-03	5.72E-03	6.73E-03	7.75E-03	8.77E-03	9.79E-03	1.08E-02
45.72	4.08E-03	4.71E-03	5.73E-03	6.75E-03	7.77E-03	8.80E-03	9.82E-03	1.08E-02
30.48	4.08E-03	4.71E-03	5.73E-03	6.75E-03	7.77E-03	8.80E-03	9.82E-03	1.08E-02
15.24	4.07E-03	4.70E-03	5.72E-03	6.74E-03	7.76E-03	8.78E-03	9.80E-03	1.08E-02
0.00	4.06E-03	4.69E-03	5.71E-03	6.73E-03	7.75E-03	8.77E-03	9.78E-03	1.08E-02
-15.24	4.06E-03	4.69E-03	5.70E-03	6.72E-03	7.74E-03	8.76E-03	9.78E-03	1.08E-02
-30.48	4.04E-03	4.67E-03	5.68E-03	6.70E-03	7.71E-03	8.72E-03	9.74E-03	1.08E-02
-45.72	4.01E-03	4.63E-03	5.63E-03	6.64E-03	7.65E-03	8.65E-03	9.66E-03	1.07E-02
-60.96	3.96E-03	4.57E-03	5.56E-03	6.55E-03	7.55E-03	8.54E-03	9.54E-03	1.05E-02
-76.20	3.88E-03	4.48E-03	5.45E-03	6.43E-03	7.40E-03	8.37E-03	9.35E-03	1.03E-02
-91.44	3.75E-03	4.33E-03	5.27E-03	6.21E-03	7.16E-03	8.10E-03	9.04E-03	9.98E-03
-106.68	3.54E-03	4.09E-03	4.98E-03	5.87E-03	6.76E-03	7.65E-03	8.55E-03	9.44E-03
-121.92	3.25E-03	3.75E-03	4.57E-03	5.38E-03	6.20E-03	7.02E-03	7.83E-03	8.65E-03

Table 4-18
Iron Atom Displacements (All Neutron Energies) at the RPV Support Structure – +10% Bias on the Peripheral and Re-Entrant Corner Assembly Relative Powers

Elevation[1] (cm)	Iron Atom Displacements – All Neutron Energies (dpa)							
	32.30 EFPY[2]	36 EFPY	42 EFPY	48 EFPY	54 EFPY	60 EFPY	66 EFPY	72 EFPY
-137.16	2.87E-03	3.31E-03	4.02E-03	4.74E-03	5.46E-03	6.18E-03	6.89E-03	7.61E-03
-152.40	2.40E-03	2.77E-03	3.37E-03	3.96E-03	4.56E-03	5.15E-03	5.75E-03	6.35E-03
-167.64	1.89E-03	2.18E-03	2.64E-03	3.11E-03	3.57E-03	4.04E-03	4.50E-03	4.96E-03
-182.88	1.39E-03	1.60E-03	1.94E-03	2.28E-03	2.62E-03	2.96E-03	3.30E-03	3.64E-03
-198.12	9.80E-04	1.13E-03	1.36E-03	1.60E-03	1.84E-03	2.08E-03	2.32E-03	2.55E-03
-213.36	6.76E-04	7.77E-04	9.41E-04	1.10E-03	1.27E-03	1.43E-03	1.60E-03	1.76E-03
-228.60	4.73E-04	5.44E-04	6.58E-04	7.73E-04	8.88E-04	1.00E-03	1.12E-03	1.23E-03
-243.84	3.40E-04	3.91E-04	4.74E-04	5.57E-04	6.40E-04	7.22E-04	8.05E-04	8.88E-04
-259.08	2.53E-04	2.91E-04	3.52E-04	4.14E-04	4.76E-04	5.38E-04	6.00E-04	6.62E-04
-274.32	1.99E-04	2.29E-04	2.78E-04	3.27E-04	3.76E-04	4.25E-04	4.74E-04	5.23E-04
-289.56	1.63E-04	1.88E-04	2.28E-04	2.68E-04	3.08E-04	3.48E-04	3.88E-04	4.28E-04

Note(s):

1. Elevations are given with respect to the midplane of the active fuel.
2. Value listed is the projected EFPY at the end of Cycle 25.
3. This elevation corresponds to the top of the 6-inch-thick horizontal plate at the top-center of the RPV support structure.
4. Linear interpolation between the EFPY values listed in this table may be performed as necessary.

Table 4-19
Iron Atom Displacements (E > 0.1 MeV) at the RPV Support Structure –
No Bias on the Peripheral and Re-Entrant Corner Assembly Relative Powers

Elevation[1] (cm)	Iron Atom Displacements – Neutron Energies > 0.1 MeV (dpa)							
	32.30 EFPY[2]	36 EFPY	42 EFPY	48 EFPY	54 EFPY	60 EFPY	66 EFPY	72 EFPY
231.16[3]	4.49E-04	5.09E-04	6.06E-04	7.04E-04	8.01E-04	8.99E-04	9.96E-04	1.09E-03
228.60	4.82E-04	5.47E-04	6.52E-04	7.56E-04	8.61E-04	9.66E-04	1.07E-03	1.18E-03
213.36	7.15E-04	8.11E-04	9.66E-04	1.12E-03	1.28E-03	1.43E-03	1.59E-03	1.74E-03
198.12	9.78E-04	1.11E-03	1.32E-03	1.53E-03	1.75E-03	1.96E-03	2.17E-03	2.38E-03
182.88	1.36E-03	1.54E-03	1.84E-03	2.13E-03	2.43E-03	2.73E-03	3.02E-03	3.32E-03
167.64	1.83E-03	2.08E-03	2.48E-03	2.88E-03	3.29E-03	3.69E-03	4.09E-03	4.50E-03
152.40	2.32E-03	2.64E-03	3.16E-03	3.68E-03	4.20E-03	4.72E-03	5.24E-03	5.76E-03
137.16	2.78E-03	3.17E-03	3.79E-03	4.42E-03	5.05E-03	5.67E-03	6.30E-03	6.93E-03
121.92	3.16E-03	3.60E-03	4.31E-03	5.03E-03	5.75E-03	6.46E-03	7.18E-03	7.90E-03
106.68	3.46E-03	3.95E-03	4.74E-03	5.53E-03	6.32E-03	7.11E-03	7.90E-03	8.69E-03
91.44	3.81E-03	4.35E-03	5.22E-03	6.09E-03	6.97E-03	7.84E-03	8.71E-03	9.59E-03
76.20	3.76E-03	4.29E-03	5.15E-03	6.01E-03	6.87E-03	7.74E-03	8.60E-03	9.46E-03
60.96	3.75E-03	4.28E-03	5.14E-03	6.00E-03	6.86E-03	7.72E-03	8.58E-03	9.45E-03
45.72	3.76E-03	4.30E-03	5.16E-03	6.02E-03	6.89E-03	7.75E-03	8.62E-03	9.48E-03
30.48	3.76E-03	4.30E-03	5.16E-03	6.03E-03	6.89E-03	7.76E-03	8.62E-03	9.49E-03
15.24	3.75E-03	4.29E-03	5.15E-03	6.01E-03	6.88E-03	7.74E-03	8.61E-03	9.47E-03
0.00	3.75E-03	4.28E-03	5.14E-03	6.01E-03	6.87E-03	7.73E-03	8.60E-03	9.46E-03
-15.24	3.75E-03	4.28E-03	5.14E-03	6.01E-03	6.87E-03	7.73E-03	8.60E-03	9.46E-03
-30.48	3.73E-03	4.26E-03	5.12E-03	5.98E-03	6.85E-03	7.71E-03	8.57E-03	9.43E-03
-45.72	3.70E-03	4.23E-03	5.08E-03	5.94E-03	6.79E-03	7.65E-03	8.50E-03	9.35E-03
-60.96	3.66E-03	4.18E-03	5.02E-03	5.87E-03	6.71E-03	7.55E-03	8.40E-03	9.24E-03
-76.20	3.58E-03	4.10E-03	4.92E-03	5.75E-03	6.58E-03	7.41E-03	8.24E-03	9.07E-03
-91.44	3.47E-03	3.96E-03	4.76E-03	5.57E-03	6.37E-03	7.17E-03	7.97E-03	8.77E-03
-106.68	3.28E-03	3.74E-03	4.50E-03	5.26E-03	6.02E-03	6.78E-03	7.54E-03	8.29E-03
-121.92	3.01E-03	3.43E-03	4.13E-03	4.82E-03	5.52E-03	6.21E-03	6.90E-03	7.60E-03

Table 4-19
Iron Atom Displacements (E > 0.1 MeV) at the RPV Support Structure –
No Bias on the Peripheral and Re-Entrant Corner Assembly Relative Powers

Elevation[1] (cm)	Iron Atom Displacements – Neutron Energies > 0.1 MeV (dpa)							
	32.30 EFPY[2]	36 EFPY	42 EFPY	48 EFPY	54 EFPY	60 EFPY	66 EFPY	72 EFPY
-137.16	2.65E-03	3.02E-03	3.63E-03	4.24E-03	4.85E-03	5.46E-03	6.07E-03	6.68E-03
-152.40	2.21E-03	2.52E-03	3.03E-03	3.53E-03	4.04E-03	4.54E-03	5.05E-03	5.55E-03
-167.64	1.73E-03	1.97E-03	2.36E-03	2.76E-03	3.15E-03	3.54E-03	3.93E-03	4.32E-03
-182.88	1.27E-03	1.44E-03	1.73E-03	2.01E-03	2.29E-03	2.58E-03	2.86E-03	3.15E-03
-198.12	8.80E-04	1.00E-03	1.20E-03	1.39E-03	1.59E-03	1.79E-03	1.98E-03	2.18E-03
-213.36	5.98E-04	6.80E-04	8.13E-04	9.46E-04	1.08E-03	1.21E-03	1.35E-03	1.48E-03
-228.60	4.12E-04	4.69E-04	5.61E-04	6.53E-04	7.44E-04	8.36E-04	9.28E-04	1.02E-03
-243.84	2.93E-04	3.33E-04	3.98E-04	4.64E-04	5.29E-04	5.95E-04	6.60E-04	7.26E-04
-259.08	2.15E-04	2.45E-04	2.94E-04	3.42E-04	3.90E-04	4.39E-04	4.87E-04	5.35E-04
-274.32	1.69E-04	1.92E-04	2.30E-04	2.68E-04	3.06E-04	3.44E-04	3.82E-04	4.20E-04
-289.56	1.38E-04	1.57E-04	1.88E-04	2.19E-04	2.49E-04	2.80E-04	3.11E-04	3.42E-04

Note(s):

1. Elevations are given with respect to the midplane of the active fuel.
2. Value listed is the projected EFPY at the end of Cycle 25.
3. This elevation corresponds to the top of the 6-inch-thick horizontal plate at the top-center of the RPV support structure.
4. Linear interpolation between the EFPY values listed in this table may be performed as necessary.

Table 4-20
Iron Atom Displacements (E > 0.1 MeV) at the RPV Support Structure –
+10% Bias on the Peripheral and Re-Entrant Corner Assembly Relative Powers

Elevation[1] (cm)	Iron Atom Displacements – Neutron Energies > 0.1 MeV (dpa)							
	32.30 EFPY[2]	36 EFPY	42 EFPY	48 EFPY	54 EFPY	60 EFPY	66 EFPY	72 EFPY
231.16[3]	4.49E-04	5.14E-04	6.20E-04	7.26E-04	8.32E-04	9.38E-04	1.04E-03	1.15E-03
228.60	4.82E-04	5.53E-04	6.67E-04	7.81E-04	8.95E-04	1.01E-03	1.12E-03	1.24E-03
213.36	7.15E-04	8.19E-04	9.88E-04	1.16E-03	1.33E-03	1.49E-03	1.66E-03	1.83E-03
198.12	9.78E-04	1.12E-03	1.35E-03	1.58E-03	1.81E-03	2.05E-03	2.28E-03	2.51E-03
182.88	1.36E-03	1.56E-03	1.88E-03	2.20E-03	2.53E-03	2.85E-03	3.17E-03	3.50E-03
167.64	1.83E-03	2.10E-03	2.54E-03	2.98E-03	3.42E-03	3.86E-03	4.30E-03	4.74E-03
152.40	2.32E-03	2.67E-03	3.24E-03	3.80E-03	4.37E-03	4.93E-03	5.50E-03	6.06E-03
137.16	2.78E-03	3.20E-03	3.88E-03	4.57E-03	5.25E-03	5.94E-03	6.62E-03	7.30E-03
121.92	3.16E-03	3.64E-03	4.42E-03	5.20E-03	5.98E-03	6.76E-03	7.55E-03	8.33E-03
106.68	3.46E-03	3.99E-03	4.85E-03	5.71E-03	6.58E-03	7.44E-03	8.30E-03	9.16E-03
91.44	3.81E-03	4.40E-03	5.35E-03	6.30E-03	7.25E-03	8.20E-03	9.15E-03	1.01E-02
76.20	3.76E-03	4.34E-03	5.28E-03	6.22E-03	7.16E-03	8.09E-03	9.03E-03	9.97E-03
60.96	3.75E-03	4.33E-03	5.27E-03	6.20E-03	7.14E-03	8.08E-03	9.02E-03	9.96E-03
45.72	3.76E-03	4.34E-03	5.28E-03	6.23E-03	7.17E-03	8.11E-03	9.05E-03	9.99E-03
30.48	3.76E-03	4.34E-03	5.29E-03	6.23E-03	7.17E-03	8.11E-03	9.06E-03	1.00E-02
15.24	3.75E-03	4.33E-03	5.27E-03	6.22E-03	7.16E-03	8.10E-03	9.04E-03	9.98E-03
0.00	3.75E-03	4.33E-03	5.27E-03	6.21E-03	7.15E-03	8.09E-03	9.03E-03	9.97E-03
-15.24	3.75E-03	4.32E-03	5.27E-03	6.21E-03	7.15E-03	8.09E-03	9.03E-03	9.97E-03
-30.48	3.73E-03	4.31E-03	5.25E-03	6.18E-03	7.12E-03	8.06E-03	8.99E-03	9.93E-03
-45.72	3.70E-03	4.27E-03	5.20E-03	6.13E-03	7.06E-03	7.99E-03	8.92E-03	9.85E-03
-60.96	3.66E-03	4.22E-03	5.14E-03	6.06E-03	6.98E-03	7.90E-03	8.82E-03	9.73E-03
-76.20	3.58E-03	4.14E-03	5.04E-03	5.94E-03	6.84E-03	7.75E-03	8.65E-03	9.55E-03
-91.44	3.47E-03	4.00E-03	4.88E-03	5.75E-03	6.62E-03	7.49E-03	8.37E-03	9.24E-03
-106.68	3.28E-03	3.79E-03	4.61E-03	5.44E-03	6.26E-03	7.08E-03	7.91E-03	8.73E-03
-121.92	3.01E-03	3.47E-03	4.23E-03	4.98E-03	5.74E-03	6.49E-03	7.25E-03	8.00E-03

Table 4-20
Iron Atom Displacements (E > 0.1 MeV) at the RPV Support Structure –
+10% Bias on the Peripheral and Re-Entrant Corner Assembly Relative Powers

Elevation[1] (cm)	Iron Atom Displacements – Neutron Energies > 0.1 MeV (dpa)							
	32.30 EFPY[2]	36 EFPY	42 EFPY	48 EFPY	54 EFPY	60 EFPY	66 EFPY	72 EFPY
-137.16	2.65E-03	3.06E-03	3.72E-03	4.38E-03	5.04E-03	5.70E-03	6.37E-03	7.03E-03
-152.40	2.21E-03	2.55E-03	3.10E-03	3.65E-03	4.20E-03	4.75E-03	5.30E-03	5.85E-03
-167.64	1.73E-03	1.99E-03	2.42E-03	2.85E-03	3.27E-03	3.70E-03	4.12E-03	4.55E-03
-182.88	1.27E-03	1.46E-03	1.77E-03	2.08E-03	2.38E-03	2.69E-03	3.00E-03	3.31E-03
-198.12	8.80E-04	1.01E-03	1.23E-03	1.44E-03	1.65E-03	1.87E-03	2.08E-03	2.29E-03
-213.36	5.98E-04	6.87E-04	8.32E-04	9.77E-04	1.12E-03	1.27E-03	1.41E-03	1.56E-03
-228.60	4.12E-04	4.74E-04	5.74E-04	6.74E-04	7.74E-04	8.74E-04	9.74E-04	1.07E-03
-243.84	2.93E-04	3.36E-04	4.08E-04	4.79E-04	5.50E-04	6.22E-04	6.93E-04	7.64E-04
-259.08	2.15E-04	2.48E-04	3.01E-04	3.53E-04	4.06E-04	4.59E-04	5.11E-04	5.64E-04
-274.32	1.69E-04	1.94E-04	2.36E-04	2.77E-04	3.19E-04	3.60E-04	4.01E-04	4.43E-04
-289.56	1.38E-04	1.58E-04	1.92E-04	2.26E-04	2.60E-04	2.93E-04	3.27E-04	3.61E-04

Note(s):

1. Elevations are given with respect to the midplane of the active fuel.
2. Value listed is the projected EFPY at the end of Cycle 25.
3. This elevation corresponds to the top of the 6-inch-thick horizontal plate at the top-center of the RPV support structure.
4. Linear interpolation between the EFPY values listed in this table may be performed as necessary.

4.4 Bioshield Concrete

Neutron and gamma exposure data for the bioshield concrete are provided in Table 4-21 through Table 4-23. In particular, fast neutron (E > 1.0 MeV) fluences are provided in Table 4-21 as a function of irradiation time. Similar data, but for energies greater than 0.1 MeV, are provided in Table 4-22. Calculated gamma doses for the bioshield concrete are provided in Table 4-23. In all cases, the data provided in Table 4-21 through Table 4-23 are the maximum exposures experienced by the bioshield concrete at the azimuthal angles listed relative to the core cardinal axes and at the axial elevation providing the maximum exposure.

Table 4-23 shows that the concrete gamma dose threshold value for consideration of radiation exposure effects, 1×10^{8} Gy (1×10^{10} rad), is not projected to be exceeded prior to a cumulative operating time of 72 EFPY.

Table 4-21
Fast Neutron (E > 1.0 MeV) Fluence at the Bioshield Concrete

Cycle	Cycle Length (EFPY)	Cumulative Operating Time (EFPY)	Fast Neutron (E > 1.0 MeV) Fluence (n/cm²)							
			0°	15°	30°	45°	60°	75°	90°	Maximum
1	1.11	1.11	5.56E+15	1.90E+16	1.73E+16	1.57E+16	1.73E+16	2.18E+16	2.55E+16	2.55E+16
2	1.12	2.23	1.13E+16	3.84E+16	3.52E+16	3.18E+16	3.50E+16	4.42E+16	5.19E+16	5.19E+16
3	1.22	3.45	1.69E+16	5.71E+16	5.20E+16	4.68E+16	5.18E+16	6.59E+16	7.74E+16	7.74E+16
4	1.16	4.61	2.11E+16	7.26E+16	6.77E+16	6.13E+16	6.74E+16	8.34E+16	9.63E+16	9.63E+16
5	1.30	5.91	2.57E+16	8.99E+16	8.50E+16	7.74E+16	8.48E+16	1.03E+17	1.17E+17	1.17E+17
6	1.35	7.26	3.04E+16	1.06E+17	1.00E+17	9.16E+16	1.00E+17	1.21E+17	1.38E+17	1.38E+17
7	1.21	8.47	3.48E+16	1.21E+17	1.14E+17	1.05E+17	1.14E+17	1.38E+17	1.58E+17	1.58E+17
8	1.38	9.85	3.84E+16	1.34E+17	1.29E+17	1.19E+17	1.29E+17	1.54E+17	1.74E+17	1.74E+17
9	1.22	11.07	4.26E+16	1.50E+17	1.44E+17	1.33E+17	1.44E+17	1.71E+17	1.93E+17	1.93E+17
10	1.44	12.51	4.78E+16	1.69E+17	1.62E+17	1.49E+17	1.62E+17	1.93E+17	2.17E+17	2.17E+17
11	1.32	13.83	5.24E+16	1.85E+17	1.79E+17	1.65E+17	1.79E+17	2.11E+17	2.37E+17	2.37E+17
12	1.51	15.34	5.72E+16	2.02E+17	1.96E+17	1.82E+17	1.96E+17	2.31E+17	2.59E+17	2.59E+17
13	1.29	16.63	6.18E+16	2.18E+17	2.12E+17	1.97E+17	2.11E+17	2.49E+17	2.80E+17	2.80E+17
14	1.43	18.06	6.64E+16	2.34E+17	2.28E+17	2.12E+17	2.27E+17	2.67E+17	3.00E+17	3.00E+17
15	1.15	19.21	7.04E+16	2.48E+17	2.41E+17	2.24E+17	2.40E+17	2.83E+17	3.18E+17	3.18E+17
16	1.25	20.46	7.49E+16	2.63E+17	2.55E+17	2.37E+17	2.55E+17	3.01E+17	3.39E+17	3.39E+17
17	1.25	21.71	7.92E+16	2.78E+17	2.69E+17	2.50E+17	2.69E+17	3.18E+17	3.59E+17	3.59E+17
18	1.42	23.13	8.40E+16	2.95E+17	2.85E+17	2.65E+17	2.85E+17	3.37E+17	3.81E+17	3.81E+17
19	1.19	24.32	8.91E+16	3.13E+17	3.03E+17	2.82E+17	3.02E+17	3.58E+17	4.04E+17	4.04E+17
20	1.23	25.55	9.51E+16	3.34E+17	3.24E+17	3.01E+17	3.23E+17	3.82E+17	4.31E+17	4.31E+17
21	1.28	26.83	1.01E+17	3.55E+17	3.45E+17	3.21E+17	3.44E+17	4.06E+17	4.58E+17	4.58E+17
22	1.31	28.13	1.08E+17	3.80E+17	3.68E+17	3.43E+17	3.67E+17	4.34E+17	4.90E+17	4.90E+17
23	1.40	29.53	1.16E+17	4.06E+17	3.94E+17	3.68E+17	3.93E+17	4.64E+17	5.25E+17	5.25E+17
24	1.34	30.88	1.23E+17	4.29E+17	4.16E+17	3.89E+17	4.15E+17	4.90E+17	5.55E+17	5.55E+17
25[1]	1.43	32.30	1.29E+17	4.52E+17	4.39E+17	4.10E+17	4.38E+17	5.17E+17	5.86E+17	5.86E+17

Table 4-21
Fast Neutron (E > 1.0 MeV) Fluence at the Bioshield Concrete

Cycle	Cycle Length (EFPY)	Cumulative Operating Time (EFPY)	Fast Neutron (E > 1.0 MeV) Fluence (n/cm^2)							
			0°	15°	30°	45°	60°	75°	90°	Maximum
Projections with no bias on the peripheral and re-entrant corner assembly relative powers										
Future[2]	--	36.00	1.47E+17	5.16E+17	5.01E+17	4.68E+17	4.99E+17	5.89E+17	6.68E+17	6.68E+17
Future[2]	--	42.00	1.77E+17	6.18E+17	6.00E+17	5.61E+17	5.98E+17	7.07E+17	8.02E+17	8.02E+17
Future[2]	--	48.00	2.07E+17	7.20E+17	6.99E+17	6.54E+17	6.97E+17	8.24E+17	9.35E+17	9.35E+17
Future[2]	--	54.00	2.36E+17	8.23E+17	7.99E+17	7.47E+17	7.96E+17	9.41E+17	1.07E+18	1.07E+18
Future[2]	--	60.00	2.66E+17	9.25E+17	8.98E+17	8.40E+17	8.96E+17	1.06E+18	1.20E+18	1.20E+18
Future[2]	--	66.00	2.95E+17	1.03E+18	9.98E+17	9.33E+17	9.95E+17	1.18E+18	1.34E+18	1.34E+18
Future[2]	--	72.00	3.25E+17	1.13E+18	1.10E+18	1.03E+18	1.09E+18	1.29E+18	1.47E+18	1.47E+18
Projections with a +10% bias on the peripheral and re-entrant corner assembly relative powers										
Future[2]	--	36.00	1.49E+17	5.21E+17	5.06E+17	4.73E+17	5.05E+17	5.96E+17	6.75E+17	6.75E+17
Future[2]	--	42.00	1.81E+17	6.33E+17	6.15E+17	5.75E+17	6.13E+17	7.24E+17	8.21E+17	8.21E+17
Future[2]	--	48.00	2.13E+17	7.45E+17	7.24E+17	6.77E+17	7.22E+17	8.52E+17	9.66E+17	9.66E+17
Future[2]	--	54.00	2.46E+17	8.56E+17	8.32E+17	7.79E+17	8.30E+17	9.79E+17	1.11E+18	1.11E+18
Future[2]	--	60.00	2.78E+17	9.68E+17	9.41E+17	8.81E+17	9.38E+17	1.11E+18	1.26E+18	1.26E+18
Future[2]	--	66.00	3.10E+17	1.08E+18	1.05E+18	9.83E+17	1.05E+18	1.23E+18	1.40E+18	1.40E+18
Future[2]	--	72.00	3.42E+17	1.19E+18	1.16E+18	1.08E+18	1.15E+18	1.36E+18	1.55E+18	1.55E+18

Note(s):

1. Cycle 25 was the current operating cycle at the time this summary report was authored.
2. Values beyond Cycle 25 are based on the average core power distributions and reactor operating conditions of Cycle 24 and are determined both with and without a 1.1 bias on the peripheral and re-entrant corner assembly relative powers.

Table 4-22
Fast Neutron (E > 0.1 MeV) Fluence at the Bioshield Concrete

Cycle	Cycle Length (EFPY)	Cumulative Operating Time (EFPY)	Fast Neutron (E > 0.1 MeV) Fluence (n/cm^2)							
			0°	15°	30°	45°	60°	75°	90°	Maximum
1	1.11	1.11	1.23E+17	2.02E+17	1.80E+17	1.61E+17	1.71E+17	2.06E+17	2.32E+17	2.32E+17
2	1.12	2.23	2.51E+17	4.10E+17	3.66E+17	3.28E+17	3.47E+17	4.17E+17	4.72E+17	4.72E+17
3	1.22	3.45	3.74E+17	6.09E+17	5.41E+17	4.82E+17	5.13E+17	6.20E+17	7.02E+17	7.02E+17
4	1.16	4.61	4.67E+17	7.71E+17	6.97E+17	6.26E+17	6.62E+17	7.83E+17	8.76E+17	8.76E+17
5	1.30	5.91	5.70E+17	9.52E+17	8.71E+17	7.85E+17	8.28E+17	9.65E+17	1.07E+18	1.07E+18
6	1.35	7.26	6.72E+17	1.12E+18	1.03E+18	9.29E+17	9.78E+17	1.14E+18	1.26E+18	1.26E+18
7	1.21	8.47	7.69E+17	1.28E+18	1.17E+18	1.06E+18	1.11E+18	1.30E+18	1.44E+18	1.44E+18
8	1.38	9.85	8.49E+17	1.42E+18	1.32E+18	1.20E+18	1.26E+18	1.44E+18	1.59E+18	1.59E+18
9	1.22	11.07	9.42E+17	1.59E+18	1.47E+18	1.34E+18	1.40E+18	1.61E+18	1.77E+18	1.77E+18
10	1.44	12.51	1.06E+18	1.79E+18	1.66E+18	1.51E+18	1.58E+18	1.81E+18	1.99E+18	1.99E+18
11	1.32	13.83	1.16E+18	1.96E+18	1.82E+18	1.66E+18	1.74E+18	1.99E+18	2.17E+18	2.17E+18
12	1.51	15.34	1.27E+18	2.14E+18	2.00E+18	1.82E+18	1.90E+18	2.17E+18	2.37E+18	2.37E+18
13	1.29	16.63	1.37E+18	2.31E+18	2.16E+18	1.97E+18	2.06E+18	2.34E+18	2.56E+18	2.56E+18
14	1.43	18.06	1.47E+18	2.48E+18	2.32E+18	2.12E+18	2.21E+18	2.51E+18	2.75E+18	2.75E+18
15	1.15	19.21	1.56E+18	2.62E+18	2.45E+18	2.24E+18	2.34E+18	2.66E+18	2.91E+18	2.91E+18
16	1.25	20.46	1.65E+18	2.79E+18	2.60E+18	2.38E+18	2.48E+18	2.82E+18	3.10E+18	3.10E+18
17	1.25	21.71	1.75E+18	2.94E+18	2.74E+18	2.51E+18	2.61E+18	2.99E+18	3.28E+18	3.28E+18
18	1.42	23.13	1.86E+18	3.12E+18	2.91E+18	2.66E+18	2.77E+18	3.17E+18	3.48E+18	3.48E+18
19	1.19	24.32	1.97E+18	3.31E+18	3.09E+18	2.82E+18	2.94E+18	3.36E+18	3.69E+18	3.69E+18
20	1.23	25.55	2.10E+18	3.54E+18	3.30E+18	3.02E+18	3.14E+18	3.59E+18	3.94E+18	3.94E+18
21	1.28	26.83	2.24E+18	3.76E+18	3.51E+18	3.22E+18	3.34E+18	3.81E+18	4.19E+18	4.19E+18
22	1.31	28.13	2.39E+18	4.02E+18	3.75E+18	3.44E+18	3.57E+18	4.08E+18	4.48E+18	4.48E+18
23	1.40	29.53	2.56E+18	4.30E+18	4.02E+18	3.69E+18	3.83E+18	4.37E+18	4.80E+18	4.80E+18
24	1.34	30.88	2.71E+18	4.55E+18	4.25E+18	3.90E+18	4.05E+18	4.61E+18	5.07E+18	5.07E+18
25[1]	1.43	32.30	2.86E+18	4.80E+18	4.48E+18	4.11E+18	4.27E+18	4.87E+18	5.36E+18	5.36E+18

Table 4-22
Fast Neutron (E > 0.1 MeV) Fluence at the Bioshield Concrete

Cycle	Cycle Length (EFPY)	Cumulative Operating Time (EFPY)	Fast Neutron (E > 0.1 MeV) Fluence (n/cm^2)							
			0°	15°	30°	45°	60°	75°	90°	Maximum
Projections with no bias on the peripheral and re-entrant corner assembly relative powers										
Future[2]	--	36.00	3.26E+18	5.47E+18	5.11E+18	4.69E+18	4.86E+18	5.55E+18	6.11E+18	6.11E+18
Future[2]	--	42.00	3.91E+18	6.56E+18	6.12E+18	5.62E+18	5.83E+18	6.65E+18	7.33E+18	7.33E+18
Future[2]	--	48.00	4.57E+18	7.65E+18	7.14E+18	6.56E+18	6.80E+18	7.76E+18	8.55E+18	8.55E+18
Future[2]	--	54.00	5.22E+18	8.74E+18	8.15E+18	7.49E+18	7.77E+18	8.86E+18	9.77E+18	9.77E+18
Future[2]	--	60.00	5.88E+18	9.83E+18	9.17E+18	8.42E+18	8.73E+18	9.97E+18	1.10E+19	1.10E+19
Future[2]	--	66.00	6.53E+18	1.09E+19	1.02E+19	9.36E+18	9.70E+18	1.11E+19	1.22E+19	1.22E+19
Future[2]	--	72.00	7.18E+18	1.20E+19	1.12E+19	1.03E+19	1.07E+19	1.22E+19	1.34E+19	1.34E+19
Projections with a +10% bias on the peripheral and re-entrant corner assembly relative powers										
Future[2]	--	36.00	3.30E+18	5.53E+18	5.16E+18	4.74E+18	4.92E+18	5.61E+18	6.18E+18	6.18E+18
Future[2]	--	42.00	4.01E+18	6.72E+18	6.27E+18	5.76E+18	5.98E+18	6.82E+18	7.51E+18	7.51E+18
Future[2]	--	48.00	4.72E+18	7.91E+18	7.39E+18	6.79E+18	7.03E+18	8.02E+18	8.84E+18	8.84E+18
Future[2]	--	54.00	5.44E+18	9.10E+18	8.50E+18	7.81E+18	8.09E+18	9.23E+18	1.02E+19	1.02E+19
Future[2]	--	60.00	6.15E+18	1.03E+19	9.61E+18	8.83E+18	9.15E+18	1.04E+19	1.15E+19	1.15E+19
Future[2]	--	66.00	6.86E+18	1.15E+19	1.07E+19	9.85E+18	1.02E+19	1.16E+19	1.28E+19	1.28E+19
Future[2]	--	72.00	7.57E+18	1.27E+19	1.18E+19	1.09E+19	1.13E+19	1.28E+19	1.42E+19	1.42E+19

Note(s):

1. Cycle 25 was the current operating cycle at the time this summary report was authored.
2. Values beyond Cycle 25 are based on the average core power distributions and reactor operating conditions of Cycle 24 and are determined both with and without a 1.1 bias on the peripheral and re-entrant corner assembly relative powers.

Table 4-23
Gamma Dose at the Bioshield Concrete

Cycle	Cycle Length (EFPY)	Cumulative Operating Time (EFPY)	Gamma Dose (Gy)							
			0°	15°	30°	45°	60°	75°	90°	Maximum
1	1.11	1.11	3.68E+05	9.74E+05	8.88E+05	8.31E+05	8.92E+05	1.01E+06	1.11E+06	1.11E+06
2	1.12	2.23	7.50E+05	1.96E+06	1.79E+06	1.68E+06	1.80E+06	2.05E+06	2.25E+06	2.25E+06
3	1.22	3.45	1.11E+06	2.91E+06	2.64E+06	2.45E+06	2.65E+06	3.03E+06	3.34E+06	3.35E+06
4	1.16	4.61	1.40E+06	3.70E+06	3.43E+06	3.19E+06	3.44E+06	3.85E+06	4.15E+06	4.16E+06
5	1.30	5.91	1.72E+06	4.57E+06	4.30E+06	4.00E+06	4.32E+06	4.76E+06	5.04E+06	5.05E+06
6	1.35	7.26	2.03E+06	5.37E+06	5.07E+06	4.73E+06	5.09E+06	5.59E+06	5.94E+06	5.95E+06
7	1.21	8.47	2.31E+06	6.12E+06	5.77E+06	5.39E+06	5.79E+06	6.37E+06	6.78E+06	6.80E+06
8	1.38	9.85	2.57E+06	6.80E+06	6.50E+06	6.11E+06	6.53E+06	7.07E+06	7.46E+06	7.48E+06
9	1.22	11.07	2.85E+06	7.58E+06	7.25E+06	6.80E+06	7.29E+06	7.88E+06	8.28E+06	8.30E+06
10	1.44	12.51	3.21E+06	8.53E+06	8.17E+06	7.66E+06	8.21E+06	8.87E+06	9.29E+06	9.32E+06
11	1.32	13.83	3.52E+06	9.35E+06	9.01E+06	8.47E+06	9.05E+06	9.72E+06	1.02E+07	1.02E+07
12	1.51	15.34	3.84E+06	1.02E+07	9.84E+06	9.30E+06	9.89E+06	1.06E+07	1.11E+07	1.11E+07
13	1.29	16.63	4.15E+06	1.10E+07	1.06E+07	1.01E+07	1.07E+07	1.14E+07	1.19E+07	1.20E+07
14	1.43	18.06	4.45E+06	1.18E+07	1.14E+07	1.08E+07	1.15E+07	1.22E+07	1.28E+07	1.28E+07
15	1.15	19.21	4.71E+06	1.24E+07	1.21E+07	1.14E+07	1.21E+07	1.29E+07	1.36E+07	1.36E+07
16	1.25	20.46	5.01E+06	1.32E+07	1.28E+07	1.21E+07	1.28E+07	1.37E+07	1.44E+07	1.45E+07
17	1.25	21.71	5.29E+06	1.39E+07	1.35E+07	1.28E+07	1.35E+07	1.45E+07	1.53E+07	1.53E+07
18	1.42	23.13	5.61E+06	1.48E+07	1.43E+07	1.35E+07	1.43E+07	1.54E+07	1.62E+07	1.62E+07
19	1.19	24.32	5.96E+06	1.57E+07	1.51E+07	1.44E+07	1.52E+07	1.63E+07	1.72E+07	1.72E+07
20	1.23	25.55	6.36E+06	1.67E+07	1.62E+07	1.54E+07	1.62E+07	1.74E+07	1.83E+07	1.84E+07
21	1.28	26.83	6.77E+06	1.78E+07	1.72E+07	1.64E+07	1.73E+07	1.85E+07	1.95E+07	1.95E+07
22	1.31	28.13	7.24E+06	1.90E+07	1.84E+07	1.76E+07	1.85E+07	1.98E+07	2.09E+07	2.09E+07
23	1.40	29.53	7.75E+06	2.04E+07	1.97E+07	1.89E+07	1.98E+07	2.12E+07	2.23E+07	2.24E+07
24	1.34	30.88	8.20E+06	2.15E+07	2.08E+07	1.99E+07	2.09E+07	2.24E+07	2.36E+07	2.37E+07
25[1]	1.43	32.30	8.64E+06	2.27E+07	2.20E+07	2.10E+07	2.21E+07	2.36E+07	2.49E+07	2.50E+07

Table 4-23
Gamma Dose at the Bioshield Concrete

Cycle	Cycle Length (EFPY)	Cumulative Operating Time (EFPY)	Gamma Dose (Gy)							
			0°	15°	30°	45°	60°	75°	90°	Maximum
Projections with no bias on the peripheral and re-entrant corner assembly relative powers										
Future[2]	--	36.00	9.86E+06	2.58E+07	2.50E+07	2.40E+07	2.51E+07	2.69E+07	2.84E+07	2.85E+07
Future[2]	--	42.00	1.18E+07	3.10E+07	3.00E+07	2.88E+07	3.01E+07	3.22E+07	3.41E+07	3.42E+07
Future[2]	--	48.00	1.38E+07	3.61E+07	3.50E+07	3.35E+07	3.51E+07	3.76E+07	3.98E+07	3.99E+07
Future[2]	--	54.00	1.58E+07	4.12E+07	3.99E+07	3.83E+07	4.01E+07	4.29E+07	4.55E+07	4.56E+07
Future[2]	--	60.00	1.77E+07	4.63E+07	4.49E+07	4.31E+07	4.51E+07	4.82E+07	5.12E+07	5.13E+07
Future[2]	--	66.00	1.97E+07	5.14E+07	4.99E+07	4.79E+07	5.00E+07	5.36E+07	5.69E+07	5.70E+07
Future[2]	--	72.00	2.17E+07	5.66E+07	5.48E+07	5.27E+07	5.50E+07	5.89E+07	6.25E+07	6.27E+07
Projections with a +10% bias on the peripheral and re-entrant corner assembly relative powers										
Future[2]	--	36.00	9.97E+06	2.61E+07	2.53E+07	2.43E+07	2.54E+07	2.72E+07	2.88E+07	2.88E+07
Future[2]	--	42.00	1.21E+07	3.17E+07	3.08E+07	2.95E+07	3.09E+07	3.30E+07	3.50E+07	3.51E+07
Future[2]	--	48.00	1.43E+07	3.73E+07	3.62E+07	3.47E+07	3.63E+07	3.89E+07	4.12E+07	4.13E+07
Future[2]	--	54.00	1.64E+07	4.29E+07	4.16E+07	4.00E+07	4.18E+07	4.47E+07	4.74E+07	4.75E+07
Future[2]	--	60.00	1.86E+07	4.85E+07	4.71E+07	4.52E+07	4.73E+07	5.05E+07	5.36E+07	5.38E+07
Future[2]	--	66.00	2.07E+07	5.41E+07	5.25E+07	5.05E+07	5.27E+07	5.63E+07	5.98E+07	6.00E+07
Future[2]	--	72.00	2.29E+07	5.97E+07	5.79E+07	5.57E+07	5.82E+07	6.22E+07	6.60E+07	6.62E+07

Note(s):

1. Cycle 25 was the current operating cycle at the time this summary report was authored.
2. Values beyond Cycle 25 are based on the average core power distributions and reactor operating conditions of Cycle 24 and are determined both with and without a 1.1 bias on the peripheral and re-entrant corner assembly relative powers.

5.0 References

1. USNRC Regulatory Guide 1.190, "Calculational and Dosimetry Methods for Determining Pressure Vessel Neutron Fluence," Office of Nuclear Regulatory Research, March 2001.

2. Westinghouse Report WCAP-18124-NP-A, Revision 0, "Fluence Determination with RAPTOR-M3G and FERRET," July 2018.

3. Westinghouse InfoGram IG-13-2, "Fluence Attenuation Profile in Reactor Pressure Vessel Shell and Inlet/Outlet Nozzle Regions," July 2013.

Approval Information
Author Approval Nedwidek Frank M Jun-07-2021 10:28:01
Reviewer Approval Hayes Eugene Jun-07-2021 10:32:51
Approver Approval Klingensmith Jesse J Jun-07-2021 16:21:01
Hold to Release Approval Nedwidek Frank M Jun-08-2021 11:36:44

Files approved on Jun-08-2021

Enclosure 4

Non-proprietary Reference Documents and Redacted Versions of Proprietary Reference Documents (Public Version)

Attachment 3

Westinghouse Report LTR-SDA-21-021-NP, Revision 1, St. Lucie Units 1&2 Subsequent License Renewal: Reactor Pressure Vessel Supports Assessment, June 24, 2021

(27 Total Pages, including cover sheets)

LTR-SDA-21-021-NP, Revision 1

St. Lucie Units 1&2 Subsequent License Renewal: Reactor Pressure Vessel Supports Assessment

June 2021

Authors: Gordon Z. Hall*, Structural Design & Analysis
Jay D. White*, Structural Design & Analysis

Verifier: Xiaolan Song*, RV/CV Design & Analysis
J. Brian Hall*, Material and Chemistry
Justin D. Webb*, Structural Design & Analysis
Nicholas Bisceglia*, Reactor Mechanical Products

Reviewer: Anees Udyawar*, RV/CV Design & Analysis

Manager: Stephen P. Rigby*, Structural Design & Analysis

Foreword

This document contains Westinghouse Electric Company LLC proprietary information and data which has been identified by brackets. Coding (a,c,e) associated with the brackets sets forth information which is considered proprietary.

The proprietary information and data contained within the brackets in this report were obtained at considerable Westinghouse expense and its release could seriously affect our competitive position. This information is to be withheld from public disclosure in accordance with the Rules of Practice 10 CFR 2.390 and the information presented herein is safeguarded in accordance with 10 CFR 2.390. Withholding of this information does not adversely affect the public interest.

This information has been provided for your internal use only and should not be released to persons or organizations outside the Directorate of Regulation and the Advisory Committee on Reactor Safeguards (ACRS) without the express written approval of Westinghouse Electric Company LLC. Should it become necessary to release this information to such persons as part of the review procedure, please contact Westinghouse Electric Company LLC, which will make the necessary arrangements required to protect the Company's proprietary interests.

Several locations in this topical report contain proprietary information. Proprietary information is identified and bracketed. For each of the bracketed locations, the reason for the proprietary classification is provided, using a standardized system. The proprietary brackets are labeled with three (3) different letters, "a", "c", and "e" per Westinghouse policy procedure BMS-LGL-84, which stand for:

a. The information reveals the distinguishing aspects of a process or component, structure, tool, method, etc. The prevention of its use by Westinghouse's competitors, without license from Westinghouse, gives Westinghouse a competitive economic advantage.

c. The information, if used by a competitor, would reduce the competitor's expenditure of resources or improve the competitor's advantage in the design, manufacture, shipment, installation, assurance of quality, or licensing of a similar product.

e. The information reveals aspects of past, present, or future Westinghouse- or customer-funded development plans and programs of potential commercial value to Westinghouse.

1.0 Background and Executive Summary

The purpose of this letter report is to document the qualitative fracture mechanics assessment of the St. Lucie (PSL) Units 1 and 2 structural steel reactor pressure vessel (RPV) supports, as it pertains to the irradiation aging effects for the 80-year subsequent license renewal (SLR). This assessment provides the technical justification to support an inspection-based approach as permitted by the pre-decisional draft interim staff guidance (ISG) [1] as an appropriate means of managing the irradiation aging concerns through the subsequent period of extended operation (SPEO).

The qualitative assessment is a comparative analysis to the Point Beach Nuclear (PBN) RPV supports analysis [4]. For PBN, it is concluded that the ASME Section XI In-Service Inspection (ISI) program is a sufficient approach to manage the radiation embrittlement effects of the RPV support for 80 calendar years (72 effective full power year (EFPY)). Furthermore, the PBN analysis deemed the RPV supports to be flaw tolerant based on the fracture mechanics analysis and review of fabrication records. The comparison assessment herein assumes that the fabrication requirements for PSL and PBN are similar since the plant-specific AISC (American Institute of Steel Construction) and AWS (American Welding Society) Code years for PSL are later than PBN, indicating the fabrication inspection requirements for PSL is at least as stringent as PBN. The comparison of the inputs for the critical flaw size calculation indicates favorable results for PSL RPV supports compared to PBN. Therefore, the conclusions in the PBN RPV support fracture mechanics analysis [4] are applicable to PSL1 and PSL2 RPV supports. Continued inspections in accordance with the ASME Section XI [20] ISI program to address the irradiation aging effects for the RPV supports is justifiable for SPEO. No additional inspection is required beyond the current ASME Section XI ISI program at PSL1 and PSL2.

Revision 1 of this letter report addresses Florida Power & Light Company (FPL) comments. Changes are marked by change bars on the right.

2.0 Methodology

This assessment reviews key parameters that affect the flaw tolerance of the structural steel RPV supports, as well as the ability to inspect the RPV supports. The primary inputs to such an evaluation are geometry, fracture toughness, and the stress of the RPV supports, which determine either the ductility of the material or the flaw stability in the support components. Each of these parameters for the PSL RPV supports is compared to PBN for which Westinghouse has previously performed the detailed RPV support fracture mechanics critical flaw evaluation. Favorable comparative assessment results between PSL and PBN would lead to the PBN conclusions being applicable to PSL RPV supports. [

]^{a,c,e} Thus, with favorable comparison of stresses and fracture toughness, the critical flaw sizes for PSL would be larger than those calculated for PBN, indicating at least the same level of flaw tolerance.

The PSL and PBN RPV supports are classified as long-column type, and are primarily made of welded and bolted plates. Both feature long slender members with support structure at the top, which consists of welded and bolted plates. Therefore, PBN is selected as the analogous plant for comparison.

The comparative assessment is presented as follows:

- Section 4.0 Geometry and Material Comparison
    - Column
    - Horizontal Support Plate
    - Base Plate
    - Support Shoe Socket/Slide Assembly
    - Bolts
- Section 5.0 Fracture Toughness Comparison for 72 EFPY
- Section 6.0 Estimated Loads and Stresses
    - 6.1 Branch Line Pipe Break Load Development for RPV Support Assessment
    - 6.2 RPV Support Finite Element Stress Analysis
- Section 7.0 Fracture Toughness and Stress Comparison
    - 7.1 Top Horizontal Support Plate
    - 7.2 Bottom Horizontal Support Plate
    - 7.3 Support Shoe Socket/Slide Assembly
    - 7.4 Bolts Connecting Column and Horizontal Support
    - 7.5 Column and Base Plate
    - 7.6 Anchor Bolts
- Section 8.0 Inspection
- Section 9.0 Analysis Conservatisms
- Section 10.0 Conclusions
- Section 11.0 References

3.0 Open Items

There are no open items in this letter report.

4.0 Geometry and Material Comparison

The purpose of the geometry comparison is to identify an analogous PBN component for each PSL component of interest. For the purpose of fracture mechanics evaluation, all components are categorized into two basic geometries: plates and round bars. Component materials are identified in this section. Both PSL and PBN RPV support configurations are "long column" type defined in NUREG/CR-5320 [3] and WCAP-12345 [5].

Table 4-1: RPV Support Column Length Comparison

		Column Length (in)
PSL [9]	Support A, Hot Leg Support B, Cold Leg	279.5 286.5
PBN [13]		242

As shown in Figure 4-1 and Figure 4-2, the PSL RPV supports are three "T-shaped" structures (two cold legs and one hot leg) made of plates that are joined by welds and bolts. The ends of the horizontal "T" are embedded in concrete. The bottom plate of the column is bolted to the concrete floor. The PBN RPV supports are illustrated in Figure 4-3. The six-sided hexagonal box ring girder are made of plates and beams with either welded or bolted joints. The shear braces are embedded in concrete. The box ring girder is supported vertically by six vertical tubular columns which are pinned and bolted to the concrete floor. Since both PSL and PBN RPV supports are categorized as the long column type with similar design features, the geometry and material comparison are appropriate for the purpose of this assessment. [

]^{a,c,e}

The following discussion goes through the PSL RPV support components of interest and compare to the analogous PBN RPV support fracture mechanics assessment in WCAP-18554-P [4] for a qualitative assessment. Fracture toughness comparisons between PSL and PBN materials are discussed in Section 5.0. The thickness of the components considered herein are relevant to the margins for the critical flaw sizes, which is further discussed in detail in Section 7.0.

Column

The PBN evaluation in WCAP-18554-P [4] reported that [

]^{a,c,e} which is consistent with the stipulation in WCAP-12345 [5] that the long column stresses are in compression. [

]^{a,c,e} the columns are not a limiting region for both PBN units and this conclusion can be extended to PSL. Therefore, the columns are excluded from further evaluation herein. The column materials are listed below for information.

PSL

- Material: ASTM A-441 [9]

PBN

- Material: ASTM A-53-63T Type S Grade B [4]

Horizontal Support Plate

Figure 4-1 and Figure 4-2 illustrates the PSL RPV support. The horizontal support structure (horizontal part of the T-structure) is at an elevation just below the RPV nozzles. The PSL horizontal supports and the PBN box ring girder are at an elevation just below RPV nozzles. [

]^{a,c,e}

Detailed evaluations of fracture toughness for PSL materials and the comparison between PSL and PBN is in Section 5.0. The materials and plate thicknesses are summarized below for the PSL horizontal support plates, PBN box ring girder and shear brace.

PSL Horizontal Support: Composed of multiple flanges and webs

- Material: ASTM A-441 and A-533 Cl. 2 Gr. B [9]
- Horizontal Flange Thickness: 4" and 6"
- Vertical Plate Thickness: 3" and 5"
- Web Thickness = 3"

PBN Box Ring Girder, composed of 4 steel plates welded into a box shape.

- Material: U. S. Steel T-1[1] [4]
- Flange Thickness = 3"
- Web Thickness = 1.5"

Base Plate

The PSL RPV support base plates are thicker and have larger footprints than PBN RPV support base plates. Given the same critical flaw size as PBN, PSL would have more margin.

PSL RPV Support Base Plate

- Material: ASTM A-441 [9]
- Thickness = 4"

PBN RPV Support Base Plate

- Material: U. S. Steel T-1 [4]
- Thickness = 2"

Support Shoe Socket/Slide Assembly

The flaws postulated on the plates were considered for the fracture mechanics evaluation of PBN RPV support shoes at the nozzle supports. As shown in Figure 4-1 and Figure 4-4, the PSL RPV nozzle support shoe region has a different design. The socket plate of the PSL socket/slide assembly is bolted on the nozzle support foot and sits on the dome-shaped slide. The slide is held in place on the support structure by two restraining plates on the side as illustrated in Figure 4-4 and is lubricated on both sides. The restraining plates are bolted onto the 6" structural plate. The socket/slide assembly is in compression and does not need to be evaluated.

The PSL socket/slide assembly bolts experience primarily shear loads due to friction between the components. Axial and bending tensile loads are not significant for these bolts. These bolts are addressed below.

Bolts

Bolts and screws (herein referred to interchangeably) are represented as round bars for fracture mechanics evaluations. The postulated flaws for PBN bolts are also applicable to all PSL bolts and screws. Therefore, it is appropriate to compare the stresses and dimensions of the bolts and screws directly. [

[1] U.S. Steel T-1 are ASTM A-514-65 or A517-65, Type F for 4" thick components and under [4].

]^{a,c,e} Further discussion about fracture toughness is contained in Section 5.0. Anchor bolts in the RPV support design are addressed in Section 7.6.

PSL Socket Head Cap Screw for the Socket/Slide Assembly
- Material: Allenoy [9.c, 9.d]
- Outside Diameter = 1.5625" [9.e and 9.f]

PSL Bolts for the Socket/Slide Retaining Plates
- Material not specified [9.a]
- 7/8" Countersunk Flat Head Bolt [9.a]

PSL Bolts connecting column and horizontal support
- Material: A-325 [9.a and 9.b]
- Outside Diameter = 1.25" [9.a and 9.b]

PBN Bolts at Shear Brace and Box Ring Girder
- Material: ASTM A-490
- Outside Diameter = 1.6012"

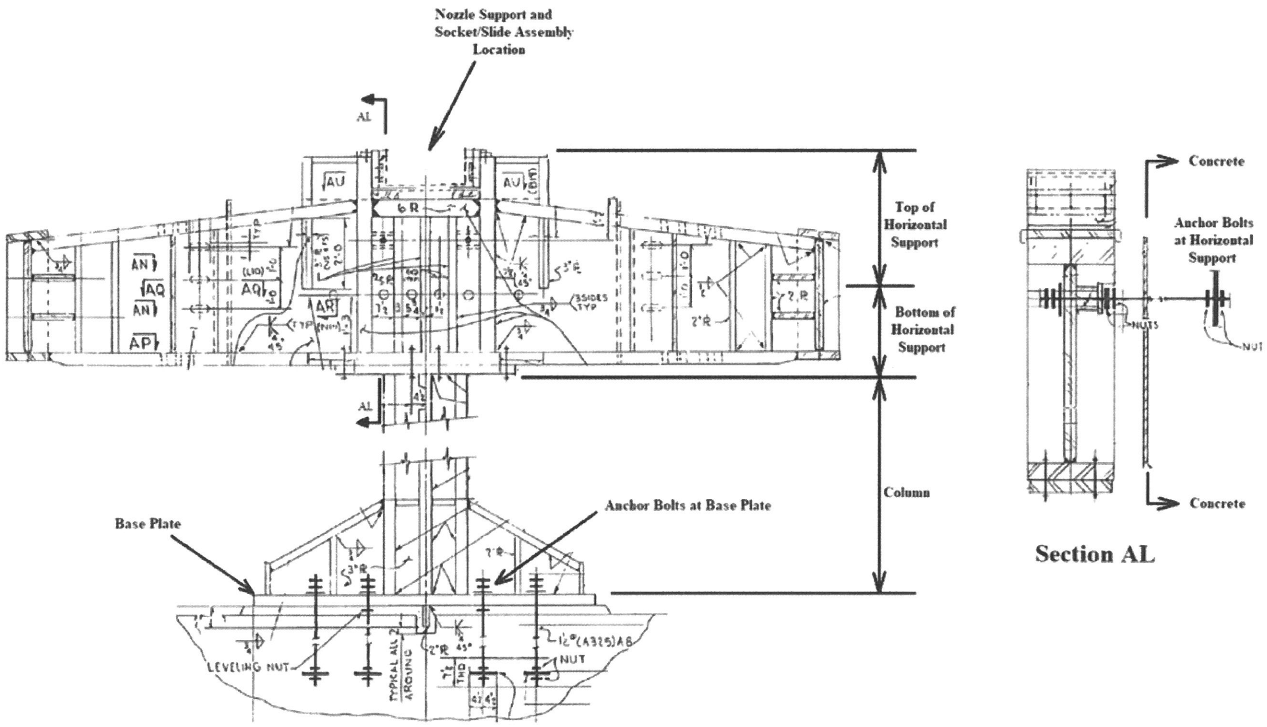

Figure 4-1: St. Lucie RPV Support [9.a and 9.b]

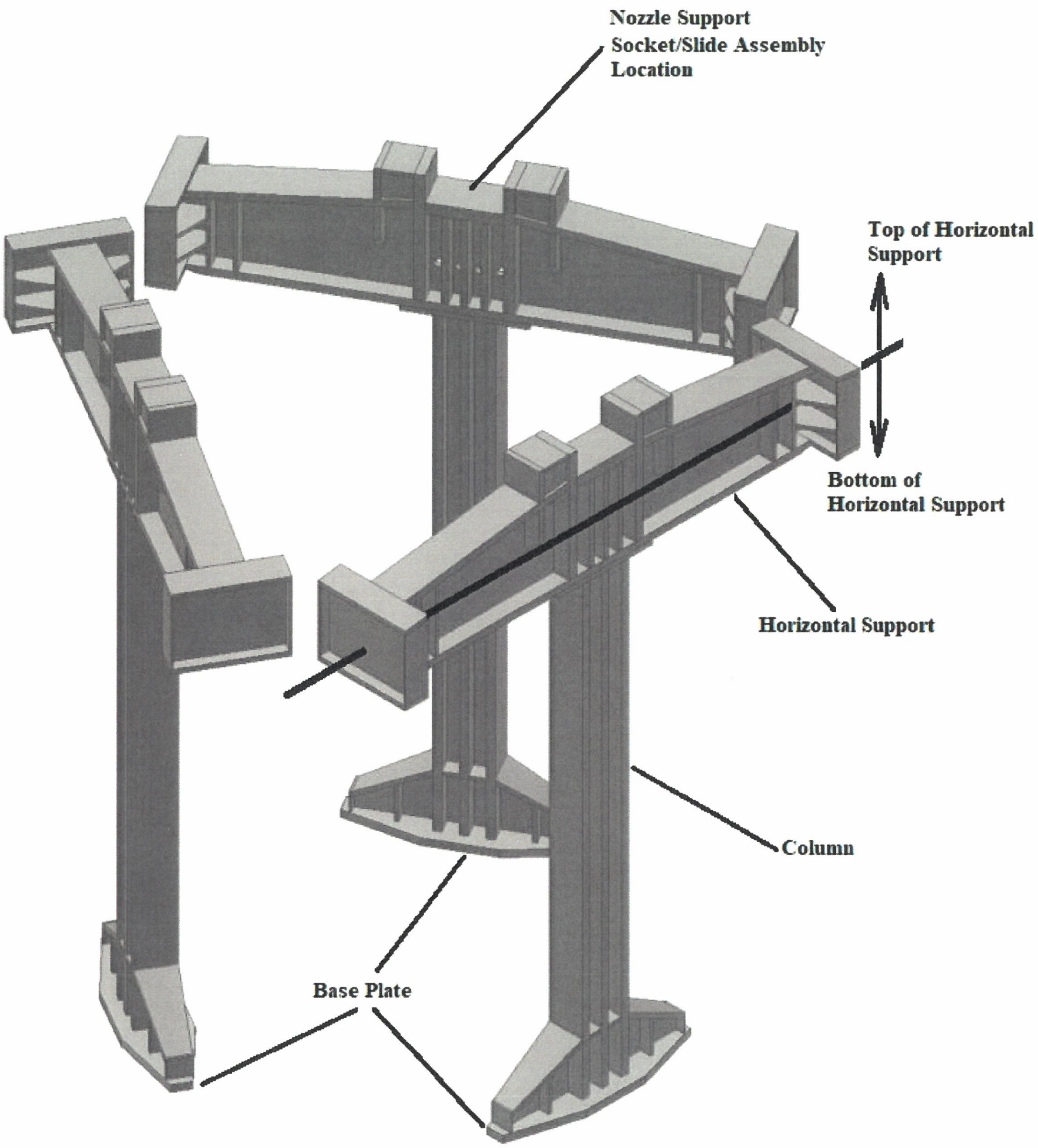

Figure 4-2: St. Lucie RPV Supports Arrangement Illustration

a,c,e

Figure 4-3: Point Beach Units 1 and 2 RPV Support Assembly

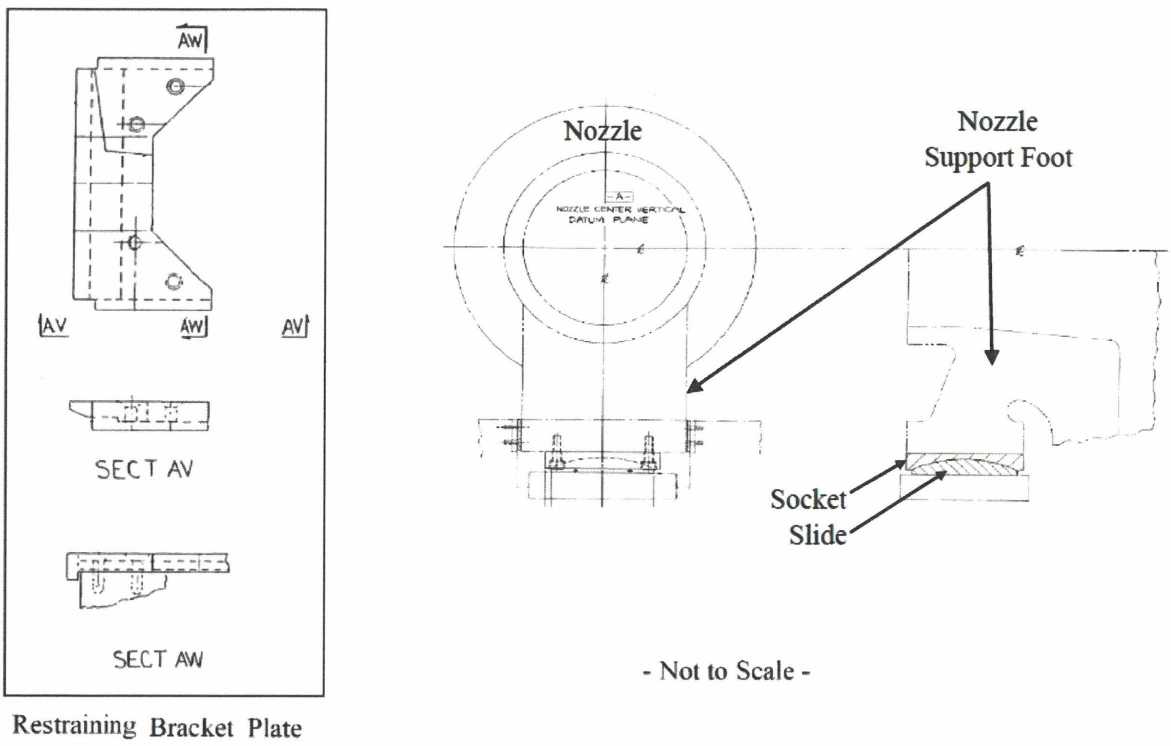

Figure 4-4: St. Lucie RPV Support Shoe Socket and Slide at Nozzle Support [9.a, 9.b, 9.d, 9.c]

5.0 Fracture Toughness Comparison for 72 EFPY

The plant-specific PSL component fracture toughness for 72 EFPY is calculated and compared to the analogous PBN components identified in Section 4.0. The methodology for fracture toughness determination for PSL is consistent with the PBN evaluation in WCAP-18554-P [4]. PSL unit-specific fluence values are taken into consideration for the embrittlement using Figure 3-1 of NUREG-1509 [2] upper bound curve. [

]a,c,e

There is no CVN test requirement per the PSL1 specification [8.a] and no CVN data is available in the certified material test reports (CMTR) as provided in FPL design input transmittal [14], Item 6b-c-6. [

]a,c,e

The normal operating temperature of the RPV supports is an input for the fracture toughness calculation. The PSL1 UFSAR Appendix 3H [11], Figure 1 provides a temperature distribution during steady-state normal operating conditions for the hot leg support. The temperature distribution during steady-state normal operating conditions for the cold leg RPV supports is not available. As illustrated in Figure 5-1, the hot leg support reactor support foot location is 189°F. [

]a,c,e The limiting cold leg RPV support is conservatively used for the comparison evaluation herein.

There is no available thermal analysis of normal operating conditions for the PSL2 RPV supports. [

]a,c,e The PBN RPV supports operating temperatures listed in Table 5-2 of WCAP-18554-P [4] are higher than PSL1 and PSL2 RPV support temperatures used in this assessment.

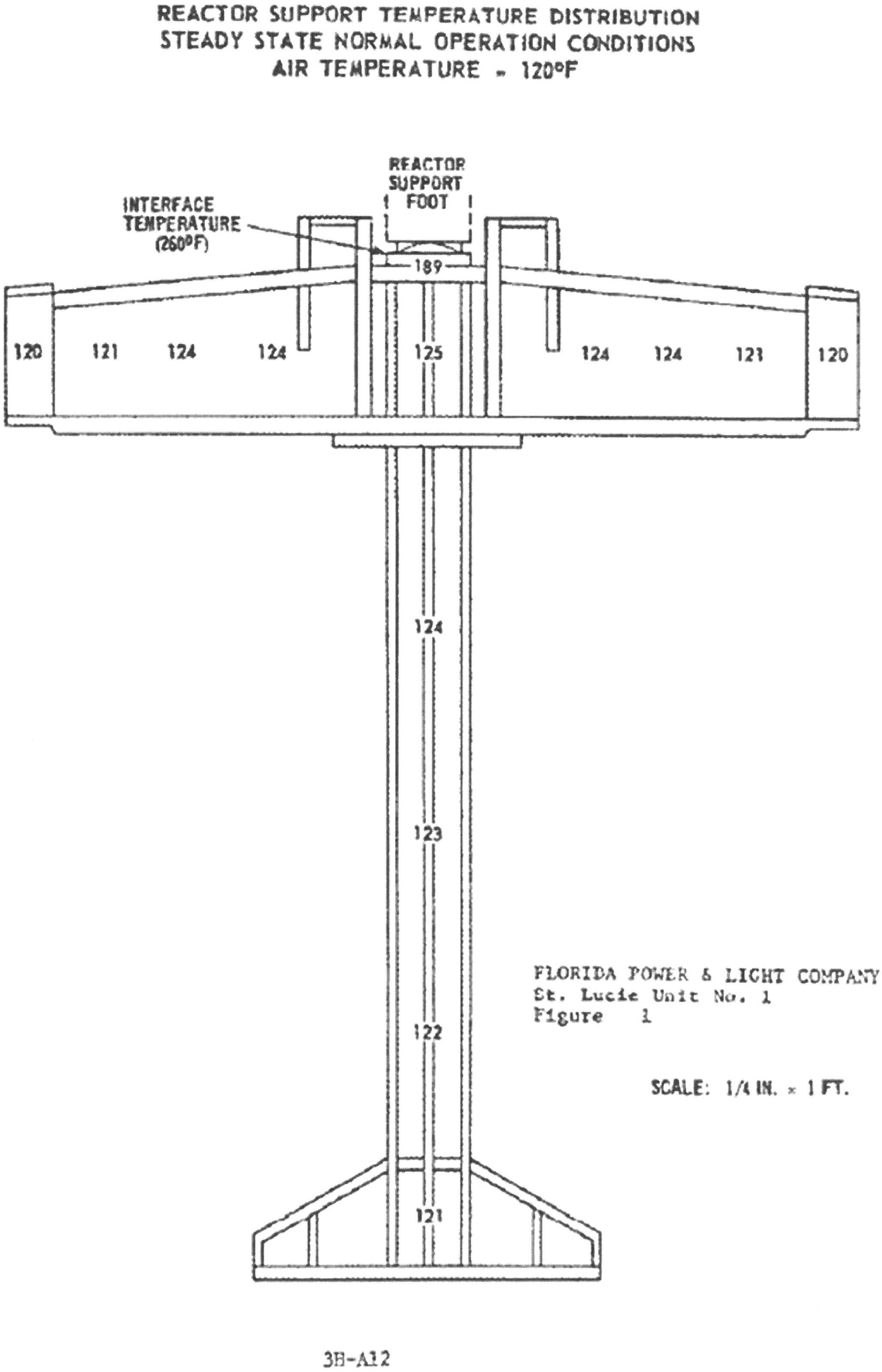

Figure 5-1: St. Lucie Unit 1 RPV Support Normal Operation Temperature [11]

The fracture toughness of the corresponding components of PBN and PSL RPV supports are summarized in Table 5-1. The comparison of the fracture toughness is mixed between PSL and PBN.

Table 5-1: Fracture Toughness Summary (ksi√in)

<table>
<tr><th>PBN</th><th colspan="2">PSL1</th><th colspan="2">PSL2</th></tr>
<tr><td rowspan="9">Box ring girder
$K_{Ic} = 57$</td><td colspan="4">Top Horizontal Support Plates</td></tr>
<tr><td>A-441</td><td>Cold Leg $K_{Ic} = [\quad]^{a,c,e}$</td><td>A-441</td><td>$K_{Ic} = [\quad]^{a,c,e}$</td></tr>
<tr><td>A-533
Cl.2 Gr. B</td><td>Cold Leg $K_{Ic} = [\quad]^{a,c,e}$</td><td>A-533
Cl.2 Gr. B</td><td>$K_{Ic} = [\quad]^{a,c,e}$</td></tr>
<tr><td>Weld</td><td>Cold Leg $K_{Ic} = [\quad]^{a,c,e}$</td><td>Weld</td><td>$K_{Ic} = [\quad]^{a,c,e}$</td></tr>
<tr><td colspan="4">Bottom Horizontal Support Plates</td></tr>
<tr><td>A-441</td><td>$K_{Ic} = [\quad]^{a,c,e}$</td><td>A-441</td><td>$K_{Ic} = [\quad]^{a,c,e}$</td></tr>
<tr><td>A-533
Cl.2 Gr. B</td><td>$K_{Ic} = [\quad]^{a,c,e}$</td><td>A-533
Cl.2 Gr. B</td><td>$K_{Ic} = [\quad]^{a,c,e}$</td></tr>
<tr><td>Weld</td><td>$K_{Ic} = [\quad]^{a,c,e}$</td><td>Weld</td><td>$K_{Ic} = [\quad]^{a,c,e}$</td></tr>
<tr style="display:none"></tr>
<tr><td rowspan="2">Base plate
$K_{Ic} = 70$</td><td colspan="4">Base plate / column bottom</td></tr>
<tr><td colspan="2">$K_{Ic} = [\quad]^{a,c,e}$</td><td colspan="2">$K_{Ic} = [\quad]^{a,c,e}$</td></tr>
<tr><td>Bolts at shear brace
and box ring girder
$K_{Ic} = 32$</td><td colspan="4">K_{Ic} for A-325 bolt (high strength bolt material)
is applicable to all bolts for St. Lucie
$K_{Ic} = [\quad]^{a,c,e}$</td></tr>
<tr><td>Support shoe</td><td colspan="4">Socket/Slide Assembly is in compression only, therefore, it is not considered for this comparison.</td></tr>
</table>

6.0 Estimated Loads and Stresses

The faulted load combination for the RPV supports consist of the absolute sum of deadweight, thermal, safe shutdown earthquake (SSE) and branch line pipe break (BLPB). The deadweight, thermal and SSE are PSL unit-specific loads from AORs [10]. The following sections discuss the load development and the stress analysis.

6.1 Branch Line Pipe Break Load Development for RPV Support Assessment

Based on the historic RPV supports fracture mechanics evaluations, including the PBN evaluation in WCAP-18554-P [4], the faulted conditions (Level D) are the most limiting for stress. All other design conditions are bounded by the faulted conditions. Therefore, faulted stresses are considered for the purpose of this assessment. [

]a,c,e

The NRC accepted the topical report, CEN-367-A [22], an LBB evaluation for Combustion Engineering (CE) designed nuclear steam supply systems for the CE owners group (CEOG). FPL was a participating CEOG member and PSL1 and PSL2 were included in the bounding analyses in CEN-367-A. Per L-2017-071 [23] and L-2016-088 [24], NRC staff concluded PSL1 and PSL2 units are bounded by the CEOG analysis in [22], and the LBB remains valid for PSL1 and PSL2 under EPU conditions. Therefore, in order to perform the comparison assessment with PBN RPV support evaluation in WCAP-18554-P [4], BLPB loads for PSL are required and were calculated.

To develop the BLPB loads for PSL1 and PSL2, the reactor coolant system (RCS) models from the analyses of record (AOR) need to be updated to reflect the current configurations. However, inputs for the PSL BLPB load development are not complete at the time of this assessment, therefore, conservative estimated loads are used instead. Inputs for the BLPB load cases are composed of:

- Thrust loads at the break location, e.g., safety injection nozzle guillotine break.
- Reactor vessel internals (RVI) blowdown loads due to propagation of the pressure wave developed from the break location
- Sub-compartment pressures emanating from the break location that push on the steam generators and reactor coolant pumps

[

]a,c,e

6.2 RPV Support Finite Element Stress Analysis

The ANSYS FEM representing the PSL RPV support structures is illustrated in Figure 6-1. There are minor differences between the RPV supports for PSL1 and PSL2, hot leg and cold leg, e.g., a 7" height difference between the hot and cold leg supports [9.a and 9.b], and scallop cut outs of the bottom horizontal support plates. These differences were reviewed and the limiting condition among all support geometries was incorporated into the model; therefore, a single model representing both units was employed.

The estimated BLPB loads discussed in Section 6.1 are used. Figure 6-2 illustrates the load application of the model. The combined vertical and lateral loads are applied to footprint area of the interfacing shim and/or load bearing plates. Two faulted cases, namely the 12" BLPB, and the 2" and 3" BLPB cases are run for PSL1 and PSL2 separately. The finite element analysis (FEA) deformation and stress intensity contour plots are illustrated in Figure 6-3. [

]a,c,e Stress paths shown in Figure 6-4 are created at the high stress region for post-processing. The paths are a few elements away from geometric and mesh discontinuities to avoid modeling artifacts. [

]a,c,e

a,c,e

Figure 6-1: St. Lucie RPV Support Finite Element Model

a,c,e

Figure 6-2: St. Lucie RPV Support Load Application

a,c,e

Figure 6-3: St. Lucie RPV Support FEA Result Contour Plots

a,c,e

Figure 6-4: St. Lucie RPV Support FEA Stress Location, Viewed from Concrete Side

The stresses for PSL1 and PSL 2 are summarized in Table 6-1. The stress comparison between PSL and PBN RPV supports is mixed. Therefore, for PSL vs. PBN fracture toughness and stresses are normalized for a more comprehensive comparison in Section 7.0.

Table 6-1: RPV Supports Stress Comparison

PBN [4] [ ]a,c,e	**PSL1**		**PSL2**	
	Top Horizontal Support Plates			
	12" BLPB	**2"& 3" BLPB**	**12" BLPB**	**2"& 3" BLPB**
Box Ring Girder: [ ]a,c,e Web t = 1.5" Flange t = 3"	A-441: [ ]a,c,e t = 4"	A-441: [ ]a,c,e t = 4"	A-441: [ ]a,c,e t = 4"	A-441: [ ]a,c,e t = 4"
	A-533: [ ]a,c,e t = 5"	A-533: [ ]a,c,e t = 5"	A-533: [ ]a,c,e t = 5"	A-533: [ ]a,c,e t = 5"

Note: t = thickness

7.0 Fracture Toughness and Stress Comparison

The PSL plant-specific fracture toughnesses were determined in Section 5.0. Likewise, PSL plant-specific faulted loads and stresses with estimated BLPB loads were determined in Section 6.1 and 6.2, respectively. These inputs to critical flaw size determination for PSL plants are compared to that for PBN plants. [

]a,c,e

7.1 Top Horizontal Support Plate

As illustrated in Figure 6-3, the highest stress region is the top horizonal support plates. [

]a,c,e The PBN box ring girder is constructed with full penetration welds at four corners of the box. As discussed in WCAP-18554-P, the PBN specification and drawing did not specify the box ring girder welds as having had post weld heat treatment (PWHT), thus the flange weld residual stress (WRS) was conservatively assumed to be [

]a,c,e. WRS is added to the calculated stresses for the PBN RPV support fracture mechanics evaluation.

Similarly, the PSL RPV supports are constructed with welded steel plates. WRS needs to be considered in addition to the FEA stresses. The PSL1 Ebasco specification [8.a] specifies that all field connections to be friction type, i.e., bolt joints, unless otherwise noted on drawings. The PSL1 drawing in [9.a] has no indication or notes of any field welding. Therefore, all welds for the PSL1 RPV supports were performed at fabrication facility (i.e., shop welds) and the Ebasco specification and addendum [8.a and 8.b] are applicable. The Ebasco specification addendum [8.b] requires PWHT be performed in accordance with AWS Specification D2.0 [18]. Per AWS D2.0, welded assemblies shall be stress relieved by heat treating where required by specification. Based on these specification requirements, it is evident that the PSL1 RPV supports had been stress relieved by PWHT. The PSL2 Ebasco specification [8.c] requires PWHT for weld joints of base metal thickness greater than 1.5". Per the FPL input transmittal [14], the PSL2 CMTRs and stress relief reports indicated that PWHT were performed for the PSL2 RPV supports. Since the PSL1 and PSL2 are stress relieved by PWHT, the applicable WRS is [

]a,c,e

Since the combined effect of fracture toughness and stress comparison is not straightforward, input parameters for the critical flaw size calculation are reviewed for a more comprehensive comparison. The general form of stress intensity factor, K_I solution is:

$$K_I = F * \sigma \sqrt{\frac{\pi a}{Q}}$$

where:

K_I = Mode I stress intensity factor (ksi√in)

F = Factor to account for flaw size, aspect ratio, geometry (wall thickness) and flaw location

σ = Membrane stress normal to the crack face (ksi)

a = Flaw depth (inch)

Q = Flaw shape parameter

[

]a,c,e

The normalized fracture toughness and stress comparison ratios are summarized in Table 7-1 for the top horizontal support plates. All cases have normalized comparison ratios greater than 1, which infer these PSL plates at the top of the horizontal supports have critical flaw sizes greater than PBN. [

]a,c,e

Table 7-1: Normalized Ratio Comparison for Top Horizontal Support Plates

	PSL1		PSL2	
Plate Material	A-441	A-533 Cl.2 Gr. B	A-441	A-533 Cl.2 Gr. B
Faulted Load with 12" BLBP	4.34	2.56	7.09	7.30
Faulted Load with 2" and 3" BLPB	9.83	3.43	19.62	12.43

7.2 Bottom Horizontal Support Plate

As shown in Table 5-1, [

]a,c,e Therefore, the bottom horizontal support plates were investigated. The bottom horizontal support plate is 56" from the top horizontal support. The analogous dimension is 13.5" for the Point Beach, i.e., the box ring girder height. Therefore, the bottom of the PSL horizontal support is closer to the reactor core compared to the PBN box ring girder, and irradiation embrittlement is more pronounced. For conservatism, the fracture toughness for the PSL bottom horizontal support location used the maximum iron displacements per atom (dpa) of the entire height of the column. Additionally, the normal operating temperature at the bottom horizontal support plate is conservatively assumed to be [

]a,c,e

The maximum FEA stress for the bottom horizontal support plates is [ ]a,c,e for both PSL1 and PSL2. As discussed in Section 7.1, WRS is added to the FEA stress for the comparison. The normalized comparison ratios are summarized in Table 7-2 for the bottom horizontal support plates. All ratios are greater than 1, which infers that the PSL bottom horizontal support plates have greater critical flaw sizes than the PBN. [

]a,c,e

Table 7-2: Normalized Ratio Comparison for Bottom Horizontal Support Plates

	PSL1		PSL2	
Plate Material	A-441 3" Plate	A-533 Cl.2 Gr. B 5" Plate	A-441 3" Plate	A-533 Cl.2 Gr. B 5" Plate
Faulted Load with 12" BLBP	4.07	2.52	4.31	2.58
Faulted Load with 2" and 3" BLPB	9.30	4.63	8.45	4.26

7.3 Support Shoe Socket/Slide Assembly

As illustrated in Figure 4-4, the PSL reactor vessel nozzle support sits on the socket and slide assembly. The socket plate is bolted onto the forged nozzle support foot. The dome shape slide sits on the RPV support plate and restrained by the restraining bracket plates to the left and right. This support design at PSL is different from the PBN support shoe illustrated in Figures 3-4 and 3-5 of WCAP-18554-P [4]. The PSL socket and slide assembly as well as the restraining bracket plates only experience the vertical load "A" as illustrated in Figure 6-2. Since these components are only in compression, they are not considered in the FEA. The bolts for the socket and the restraining bracket plates experience mainly a shear load due to friction. [

]a,c,e Therefore, the PBN support bolts conclusions in WCAP-18554-P [4] is applicable to the PSL socket/slide bolts.

As discussed in Section 4.0, the slide is held in place on the support structure by two restraining plates on the side as illustrated in Figure 4-4 and is lubricated on both sides. PSL1 and PSL2 drawings E-19367-340-002 and E-13172-340-002 (electronically attached to [14]) defines the lubricant as "Bonded Dry Film Lubricant." The drawings specifies that the lubricant shall meet the design requirements of reactor vessel sliding bearings design specification [25 and 26]. The following paragraph briefly discusses the effects of the lubricant at the socket/slide assembly on the fracture mechanics assessment of the RPV supports. The structural and design basis aspects of the effect of lubricant on the RPV supports is beyond the scope of this assessment.

Per the load input in [10], the radial friction load is only applicable to normal operating conditions. The faulted condition does not include the friction load. As discussed in Section 6.1, the faulted stresses are selected for the assessment because it bounds all design conditions including normal operating conditions. In order to assess the irradiation effect of lubricant degradation for the fracture mechanics assessment, [

]a,c,e Therefore, any increase of normal operating stresses due to degradation or loss of the lubricant is bounded by the faulted stresses for the fracture mechanics assessment in this letter report.

7.4 Bolts Connecting Column and Horizontal Support

The bolt loads for the A-325 1.25" bolts that connects the top of the column and the horizontal support are extracted from the FEA and reviewed. [

]a,c,e Therefore, the PBN support bolts conclusions in WCAP-18554-P [4] bound PSL bolts connecting the column and horizontal supports.

7.5 Column and Base Plate

The column is in compression; therefore, it is not the limiting component for this assessment, as was the case for PBN. [

]a,c,e Therefore, the base plates are not limiting.

7.6 Anchor Bolts

Anchor bolts at the base plates are embedded in concrete. Additionally, the fluence at the base plate is relatively low. The irradiation embrittlement effect is insignificant for the base plate anchor bolts. These anchor bolts are included in the FEA model, and the boundary conditions are set up such that the anchor bolts resist any lateral loads that would cause the baseplate to slide along the concrete. Due to the rigidity of the upper part of the support, the anchor bolts at the base experience insignificant shear load. Stresses for the base plate anchor bolts are bounded by the bolts connecting the top of the column and the horizontal support.

As shown in Figure 4-1, anchor bolts at the horizontal supports are not entirely embedded in concrete but partially exposed. The embedded anchor bolts in the support upper portion were not modeled in the FEA. Due to their relative flexibility compared to the rest of the upper support, which is embedded in concrete at its ends, and the clearance holes, these anchor bolts will not provide any significant load resistance in the directions normal to the bolt axis. They were conservatively omitted from the FEA model so that any stiffness contribution from those bolts is not represented in the model. All of the loads are transmitted through the body of the support to the concrete embedment at the ends of the upper support and to the column. As a result, the PSL RPV support anchor bolts are not limiting.

8.0 Inspection

St. Lucie Unit 1 reactor vessel supports were inspected in April 2021 based on VT-3 per 2007 Edition and 2008 addenda ASME Section XI, IWF requirements [15]. The Unit 1 RPV supports were also inspected in 2012 [15]. Based on the visual examination, all Unit 1 accessible support components were acceptable, there were no deformation or structural degradation, there were no cracks in welds, there were no loose/missing/detached items, and no recordable corrosion was observed (except for light rust). In addition, the Unit 1 RPV support at the "B" hot leg was examined in 2018 with VT-3 and magnetic particle examination (MT) of the nozzle support foot. The results were also acceptable [21].

The St. Lucie Unit 2 RPV supports were inspected in 2012. Based on the visual examination, all Unit 2 accessible support components were acceptable, there were no deformation or structural degradation, there were no cracks in welds, there were no loose/missing/detached items, and no recordable corrosion was observed. The Unit 2 inspection report identified boric acid residue on the supports [15]; however, the structural integrity of the supports was not impacted. In addition, all Unit 2 RPV supports are scheduled for examination in the fall of 2021 [21].

The following describes the current PSL ISI program pertaining to the RPV supports per [15 and 21]. PSL1 and PSL2 have similar configurations and accessibility regarding inspection of the RPV supports. For the upper support area where stress is limiting, VT-3 is performed for the A1 cold leg and the A2 cold leg. Additionally, MT is required for one of the three RPV supports. VT-3 and MT are performed for the "B" hot leg RPV support [21]. These inspections are implemented once every ten years as part of the ISI program.

To date, PSL1 and PSL2 have acceptable inspection results over the past inspection intervals; no gross deformation has been detected at the RPV support locations.

9.0 Analysis Conservatisms

Uncertainties in the analysis of this qualitative assessment are reduced or mitigated by using bounding, conservative assumptions as detailed below:

a. The iron displacements per atom (dpa) values include contributions of fast neutrons above 0.1 MeV as well as thermal neutrons below 0.1 MeV (all energies) and include a +10% bias on the peripheral and re-entrant corner assembly relative powers. [

]a,c,e It should be noted that fluence uncertainties are bounded by the large margins available in the fracture mechanics comparison between PSL and PBN.

b. [

]a,c,e

c. [

]a,c,e

d. [

]a,c,e

e. [

]a,c,e

f. [

]a,c,e

g. [

]a,c,e

10.0 Conclusions

The PBN RPV support analysis, WCAP-18554-P [4] concluded that the ASME Section XI ISI program is a sufficient approach to manage the radiation embrittlement effects of the RPV support for 80 calendar years (72 EFPY). Furthermore, the PBN analysis concluded the RPV supports to be flaw tolerant based on the fracture analysis and review of fabrication records.

Plant-specific fracture toughness, including irradiation and strain effects are calculated for PSL. The PSL1 and PSL2 BLPB loads are conservatively estimated for the detailed plant-specific RPV supports FEA analyses. The combined effect of fracture toughness and stresses are considered to compare PSL to PBN. As shown in Section 7.0, all comparisons are favorable, which infer PSL RPV support plates will have greater critical flaw sizes than PBN. All PSL bolts are bounded by PBN conclusions. Also, any increase of normal operating stresses due to degradation or loss of the lubricant is bounded by the faulted stresses for the fracture mechanics assessment herein.

Therefore, the conclusions in the PBN RPV support fracture mechanics analysis [4] are applicable to PSL1 and PSL2 RPV supports. The PSL RPV supports are structurally stable considering 80 calendar years (72 EFPY) of radiation embrittlement effects, as a sufficient level of flaw tolerance is demonstrated. The continued inspections in accordance with the current PSL ASME Section XI [20] ISI program to address the irradiation aging effects for the RPV supports is justifiable for SPEO. No additional inspection is required beyond the current ASME Section XI ISI program at PSL1 and PSL2.

11.0 References

1. NRC ADAMS Accession Number ML20049H359, SLR Document Changes: Add FE Section 3.5.2.2.2.7 and AMR Items for Irradiation Embrittlement of Reactor Vessel (RV) Steel Supports and Other Steel Structural Support Components near RV, February 18, 2020.
2. NUREG-1509, "Radiation Effects on Reactor Pressure Vessel Supports," May 1996.
3. NUREG/CR-5320, "Impact of Radiation Embrittlement on Integrity of Pressure Vessel Supports for Two PWR Plants." January 1989.
4. Westinghouse Report, WCAP-18554-P, Rev. 1, "Fracture Mechanics Assessment of Reactor Pressure Vessel Structural Steel Supports for Point Beach Units 1 and 2," September 2020.
5. Westinghouse Report, WCAP-12345, Rev. 1, "Westinghouse Owners Group Irradiation Effects on Reactor Vessel Supports," October, 1989.
6. [

   ]a,c,e
7. [

   ]a,c,e
8. EBASCO Structural Steel Specifications
   a. FLO-8770-761, Rev. 2, "Structural Steel - Saint Lucie Unit No. 1," February 15, 1970. (Electronically attached to [14] as FLO 8770.761 R2.pdf.)
   b. FLO-8770-761, Rev. 2, Addendum, "Addendum to EBASCO FLO-8770-761 For Class I Structures and Components," January 11, 1971. (Electronically attached to [14] as 00000001.pdf, page 88.)
   c. FLO-2998-761, Rev. 6, "Structural Steel - Saint Lucie Unit No. 2," February 18, 1987. (Electronically attached to [14] as FLO 2998.761 R6.pdf.)
9. St. Lucie Units 1 and 2 Drawings
   a. EBASCO Drawing, 8770-G-794, Rev. 5, "St Lucie Plant Unit 1 Reactor Building Equipment Supports." (Electronically attached to [14] as 8770-G-794 SH 2 REV 005.pdf.)
   b. EBASCO Drawing, 2998-G-794, Rev. 3, "St Lucie Plant Unit 2 Reactor Building Equipment Supports." (Electronically attached to [14] as 2998-G-794 SH 2 REV 003.pdf.)
   c. FPL Drawing, 8770-370, Rev. 0 (a.k.a., Combustion Engineering, E-STD-220-003)
   d. FPL Drawing, 2998-3854, Rev. 0 (a.k.a., Combustion Engineering, E-13172-340-003)
   e. FPL Drawing, 8770-369, Rev.0 (a.k.a., Combustion Engineering, E-STD-220-002)
   f. FPL Drawing, 2998-3853, Rev. 0 (a.k.a., Combustion Engineering, E-13172-340-002)
10. Load Input Drawings:
    a. Combustion Engineering Drawing, E-19367-220-001, Rev. 02, "Reactor Coolant System Support Design Loads."
    b. Combustion Engineering Drawing, E-13172-220-001, Rev. 03, "Reactor Coolant System Support Design Loads."

11. St. Lucie Unit 1 Updated Final Safety Assessment Report (UFSAR), Appendix 3H, "Analysis of Reactor Support Structure, St. Lucie Plant," Amendment 22, May 2007.

12. American Petroleum Institute, API-579-1/ASME FFS-1, "Fitness-For-Service," June 2016.

13. Point Beach Units 1 and 2 Drawings:

    a. Bechtel #C-320, "Unit 1 Reactor Steel Supports," Rev. 12.

    b. Bechtel #C-2320, "Unit 2 Reactor Steel Supports," Rev. 4.

14. FPL Letter, PSLWEC-21-0066, Rev. 0, "Design Input Transmittal for WS06b-c RPV Supports to Support the St. Lucie Unit 1 and Unit 2 Subsequent License Renewal Rev.1," June 15, 2021.

15. FPL Letter, PSLWEC-21-0039, Rev. 0, "Design Input Transmittal for WS10 RPV Support Assessment to Support the St. Lucie Unit 1 and Unit 2 Subsequent License Renewal," May 10, 2021.

16. FPL Letter, PSLWEC-21-0005, Rev. 0, "Design Input Transmittal for WS09a Alloy 600 Locations to Support the St. Lucie Unit 1 and Unit 2 Subsequent License Renewal," February 4, 2021.

17. Specification, 19367-31-5, Rev. 16, "Engineering Specification for Reactor Coolant Pipe and Fittings for Florida Power and Light Company St. Lucie Plant Unit No. 1 1973-890 MW Installation," June 12, 2013. (Electronically attached to [16] as "19367-31-5, Rev 16.pdf".)

18. AWS D2.0-66, Seventh Edition, "Specifications for Welded Highway and Railway Bridges," 1966.

19. [

    ]a,c,e

20. ASME Boiler and Pressure Vessel Code, 2007 Edition with 2008 Addenda, Section XI, "Rules for Inservice Inspection of Nuclear Power Plant Components."

21. FPL Comments Transmitted by Email, electronically attached in PRIME as "FPL_comments.zip"

    a. From Pennicooke McFarlane, Denise to Ahearn John T., May 28, 2021, 5:01PM, "RE: WEC-FPL-PSL-SLR-21-020: Initial RPV Supports Assessment Letter Report (WS10)."

    b. Comment Form, "LTR-SDA-21-021-P Rev 0 - DCRF Rev F (signed).pdf"

    c. Comment Form, "LTR-SDA-21-021-NP Rev 0 – DCRF Rev C (signed).pdf"

22. Combustion Engineering Owners Group Topical Report, CEN-367-A, Rev. 0, "Leak-Before-Break Evaluation of Primary Coolant Loop Piping in Combustion Engineering Designed Nuclear Steam Supply Systems," February, 1991.

23. NRC ADAMS Accession Number ML17129A599, FPL Letter, L-2017-071, "Re: St. Lucie Unit 1 Docket Nos. 50-335 Report of 10 CFR 50.59 Plant Changes," May 04, 2017.

24. NRC ADAMS Accession Number ML16113A329, FPL Letter, L-2016-088, "Re: St. Lucie Unit 2 Docket Nos. 50-389 Report of 10 CFR 50.59 Plant Changes," April 19, 2016.

25. Combustion Engineering Specification, 19367-PE-501, Rev. 0, "Project Specification for Reactor Vessel Sliding Bearings," February 15, 1973.

26. Combustion Engineering Specification, 13172-PE-501, Rev. 0, "Project Specification for Reactor Vessel Sliding Bearings," January 24, 1978.

This page was added to the quality record by the PRIME system upon its validation and shall not be considered in the page numbering of this document.

Approval Information
Author Approval Hall Gordon Z Jun-24-2021 16:43:59
Author Approval White Jay D Jun-24-2021 16:53:44
Verifier Approval Patterson Lynn Jun-24-2021 16:57:59
Verifier Approval Hall J Brian Jun-24-2021 16:58:35
Verifier Approval Song Xiaolan Jun-24-2021 17:00:35
Verifier Approval Webb Justin D Jun-24-2021 17:01:55
Verifier Approval Bisceglia Nicholas M Jun-24-2021 17:10:06
Manager Approval Rigby Stephen Jun-24-2021 17:29:34

Files approved on Jun-24-2021

*** This record was final approved on 6/24/2021 5:29:34 PM. (This statement was added by the PRIME system upon its validation)

Enclosure 4

Non-proprietary Reference Documents and Redacted Versions of Proprietary Reference Documents (Public Version)

Attachment 4

Westinghouse Report WCAP-18609-NP, Revision 2, St. Lucie Units 1 & 2 Subsequent License Renewal: Time-Limited Aging Analyses on Reactor Vessel Integrity, July 16, 2021

(141 Total Pages, including cover sheets)

WCAP-18609-NP
Revision 2

July 2021

St. Lucie Units 1 & 2 Subsequent License Renewal: Time-Limited Aging Analyses on Reactor Vessel Integrity

Westinghouse

WCAP-18609-NP
Revision 2

St. Lucie Units 1 & 2 Subsequent License Renewal: Time-Limited Aging Analyses on Reactor Vessel Integrity

D. Brett Lynch*
Reactor Vessel/Containment Vessel (RV/CV) Design and Analysis

July 2021

Reviewers: Benjamin E. Mays*
License Renewal, Radiation Analysis, and Nuclear Operations

Andrew E. Hawk*
Radiation Engineering and Analysis

Approvers: Lynn A. Patterson*, Manager
RV/CV Design and Analysis

Jesse J Klingensmith*, Manager
Radiation Engineering and Analysis

*Electronically approved records are authenticated in the electronic document management system.

Westinghouse Electric Company LLC
1000 Westinghouse Dr.
Cranberry Township, PA 16066

RECORD OF REVISIONS

Revision 0: Original Issue

Revision 1: This revision is issued to correct cited reference numbers in various locations. No technical changes or updates to the references themselves are made as a part of this revision. Changes are marked with change bars.

Revision 2: This revision is issued to correct the footnote placement in Tables 9-1 and 9-2. No technical changes are made as a part of this revision. Changes are marked with change bars.

TABLE OF CONTENTS

LIST OF TABLES iv

LIST OF FIGURES vii

1 TIME-LIMITED AGING ANALYSIS 1-1

2 CALCULATED NEUTRON FLUENCE FOR ST. LUCIE UNITS 1 AND 2 2-1
- 2.1 INTRODUCTION 2-1
- 2.2 DISCRETE ORDINATES ANALYSIS 2-1
- 2.3 CALCULATIONAL UNCERTAINTIES 2-4
- 2.4 ST. LUCIE UNIT 1 NEUTRON FLUENCE DATA TABLES AND FIGURES 2-6
- 2.5 ST. LUCIE UNIT 2 NEUTRON FLUENCE DATA TABLES AND FIGURES 2-32

3 FRACTURE TOUGHNESS PROPERTIES 3-1

4 SURVEILLANCE DATA 4-1

5 CHEMISTRY FACTORS 5-1

6 PRESSURIZED THERMAL SHOCK EVALUATION 6-1

7 UPPER-SHELF ENERGY 7-1

8 HEATUP AND COOLDOWN PRESSURE-TEMPERATURE LIMIT CURVES 8-1
- 8.1 ADJUSTED REFERENCE TEMPERATURES CALCULATION 8-1
- 8.2 P-T LIMIT CURVES APPLICABILITY 8-24

9 SURVEILLANCE CAPSULE WITHDRAWAL SCHEDULES 9-1

10 REFERENCES 10-1

APPENDIX A VALIDATION OF THE RADIATION TRANSPORT MODELS BASED ON NEUTRON DOSIMETRY MEASUREMENTS A-1

APPENDIX B ST. LUCIE UNITS 1 AND 2 SURVEILLANCE PROGRAM CREDIBILITY EVALUATION B-1

LIST OF TABLES

Table 1-1 Evaluation of Time-Limited Aging Analyses Per the Criteria of 10 CFR 54.3 1-1

Table 2.4-1 St. Lucie Unit 1 Fast Neutron Fluence Rate (E > 1.0 MeV) at the RPV Clad/Base Metal Interface 2-6

Table 2.4-2 St. Lucie Unit 1 Fast Neutron Fluence (E > 1.0 MeV) at the RPV Clad/Base Metal Interface 2-8

Table 2.4-3 St. Lucie Unit 1 Iron Atom Displacement Rate at the RPV Clad/Base Metal Interface 2-10

Table 2.4-4 St. Lucie Unit 1 Iron Atom Displacements at the RPV Clad/Base Metal Interface.......2-12

Table 2.4-5 St. Lucie Unit 1 Fast Neutron Fluence (E > 1.0 MeV) at RPV Welds and Shells 2-14

Table 2.4-6 St. Lucie Unit 1 Iron Atom Displacements at RPV Welds and Shells 2-16

Table 2.4-7 St. Lucie Unit 1 Fast Neutron (E > 1.0 MeV) Fluence Rate at the Geometric Center of the Surveillance Capsule Locations 2-18

Table 2.4-8 St. Lucie Unit 1 Fast Neutron (E > 1.0 MeV) Fluence at the Geometric Center of the Surveillance Capsules 2-19

Table 2.4-9 St. Lucie Unit 1 Iron Atom Displacement Rate at the Geometric Center of the Surveillance Capsules 2-21

Table 2.4-10 St. Lucie Unit 1 Iron Atom Displacements at the Geometric Center of the Surveillance Capsules 2-22

Table 2.4-11 St. Lucie Unit 1 Surveillance Capsule Lead Factors 2-24

Table 2.5-1 St. Lucie Unit 2 Fast Neutron (E > 1.0 MeV) Fluence Rate at the RPV Clad/Base Metal Interface 2-32

Table 2.5-2 St. Lucie Unit 2 Fast Neutron (E > 1.0 MeV) Fluence at the RPV Clad/Base Metal Interface 2-33

Table 2.5-3 St. Lucie Unit 2 Calculated Maximum Iron Atom Displacement Rate at the RPV Clad/Base Metal Interface 2-35

Table 2.5-4 St. Lucie Unit 2 Iron Atom Displacements at the RPV Clad/Base Metal Interface.......2-36

Table 2.5-5 St. Lucie Unit 2 Fast Neutron Fluence (E > 1.0 MeV) at RPV Welds and Shells 2-38

Table 2.5-6 St. Lucie Unit 2 Iron Atom Displacements at the RPV Welds and Shells 2-40

Table 2.5-7 St. Lucie Unit 2 Fast Neutron (E > 1.0 MeV) Fluence Rate at the Geometric Center of the Surveillance Capsules 2-42

Table 2.5-8 St. Lucie Unit 2 Fast Neutron (E > 1.0 MeV) Fluence at the Geometric Center of the Surveillance Capsules 2-43

Table 2.5-9 St. Lucie Unit 2 Iron Atom Displacement Rate at the Geometric Center of the Surveillance Capsules 2-45

Table 2.5-10 St. Lucie Unit 2 Iron Atom Displacements at the Geometric Center of the Surveillance Capsules 2-46

Table 2.5-11 St. Lucie Unit 2 Surveillance Capsule Lead Factors 2-48

Table 3-1 St. Lucie Unit 1 Reactor Vessel Beltline, Extended Beltline, and Surveillance Material Properties and Chemistry 3-3

Table 3-2 St. Lucie Unit 2 Reactor Vessel Beltline, Extended Beltline, and Surveillance Material Properties and Chemistry 3-5

Table 4-1 St. Lucie Unit 1 Surveillance Program Results 4-2

Table 4-2 St. Lucie Unit 2 Surveillance Program Results 4-2

Table 4-3 Sister-Plant Surveillance Capsule Data for Heat # 305424 from Beaver Valley Unit 1 .. 4-3

Table 5-1 Calculation of Chemistry Factors Using St. Lucie Unit 1 Surveillance Capsule Data 5-2

Table 5-2 Calculation of Chemistry Factors Using St. Lucie Unit 2 Surveillance Capsule Data 5-3

Table 5-3 Calculation of Chemistry Factor Using Sister-Plant Surveillance Capsule Data for Heat # 305424 from Beaver Valley Unit 1 5-4

Table 5-4 Position 1.1 and 2.1 Chemistry Factors for St. Lucie Unit 1 5-5

Table 5-5 Position 1.1 and 2.1 Chemistry Factors for St. Lucie Unit 2 5-6

Table 6-1 RT_{PTS} Calculations for St. Lucie Unit 1 Reactor Vessel Beltline Materials at 72 EFPY 6-2

Table 6-2 RT_{PTS} Calculations for St. Lucie Unit 2 Reactor Vessel Beltline Materials at 72 EFPY 6-4

Table 7-1 Predicted USE Values for the St. Lucie Unit 1 Beltline and Extended Beltline Materials at SLR (72 EFPY) 7-3

Table 7-2 Predicted USE Values for the St. Lucie Unit 2 Beltline and Extended Beltline Materials at 72 EFPY 7-4

Table 8-1 St. Lucie Unit 1 Fluence and Fluence Factor Values for the Surface, 1/4T, and 3/4T Locations at 54 EFPY 8-3

Table 8-2 St. Lucie Unit 2 Fluence and Fluence Factor Values for the Surface, 1/4T, and 3/4T Locations at 55 EFPY 8-4

Table 8-3 St. Lucie Unit 1 Fluence and Fluence Factor Values for the Surface, 1/4T, and 3/4T Locations at 72 EFPY 8-5

Table 8-4 St. Lucie Unit 2 Fluence and Fluence Factor Values for the Surface, 1/4T, and 3/4T Locations at 72 EFPY 8-6

Table 8-5 Calculation of the St. Lucie Unit 1 ART Values at the 1/4T Location for the Reactor Vessel Beltline and Extended Beltline Materials at EOLE (54 EFPY) 8-7

Table 8-6 Calculation of the St. Lucie Unit 1 ART Values at the 3/4T Location for the Reactor Vessel Beltline and Extended Beltline Materials at EOLE (54 EFPY) 8-9

Table 8-7 Calculation of the St. Lucie Unit 2 ART Values at the 1/4T Location for the Reactor Vessel Beltline and Extended Beltline Materials at EOLE (55 EFPY) 8-11

Table 8-8 Calculation of the St. Lucie Unit 2 ART Values at the 3/4T Location for the Reactor Vessel Beltline and Extended Beltline Materials at EOLE (55 EFPY) 8-13

Table 8-9 Calculation of the St. Lucie Unit 1 ART Values at the 1/4T Location for the Reactor Vessel Beltline and Extended Beltline Materials at SLR (72 EFPY) 8-15

Table 8-10 Calculation of the St. Lucie Unit 1 ART Values at the 3/4T Location for the Reactor Vessel Beltline and Extended Beltline Materials at SLR (72 EFPY) 8-17

Table 8-11 Calculation of the St. Lucie Unit 2 ART Values at the 1/4T Location for the Reactor Vessel Beltline and Extended Beltline Materials at SLR (72 EFPY) 8-19

Table 8-12 Calculation of the St. Lucie Unit 2 ART Values at the 3/4T Location for the Reactor Vessel Beltline and Extended Beltline Materials at SLR (72 EFPY) 8-21

Table 8-13 Calculation of the St. Lucie Unit 2 ART Values For the Hot Leg Nozzle Materials at SLR (72 EFPY) 8-23

Table 8-14 Summary of the Limiting ART Values 8-24

Table 9-1 St. Lucie Unit 1 Recommended Surveillance Capsule Withdrawal Schedule 9-3

Table 9-2 St. Lucie Unit 2 Recommended Surveillance Capsule Withdrawal Schedule 9-3

Table A-1 Measurement-to-Calculation (M/C) Ratios for the Surveillance Capsules – Unit 1 .... A-2

Table A-2 Best-Estimate-to-Calculation (BE/C) Ratios for the Surveillance Capsules – Unit 1 .... A-2

Table A-3 Measurement-to-Calculation (M/C) Ratios for the Surveillance Capsules – Unit 2 .... A-4

Table A-4 Best-Estimate-to-Calculation (BE/C) Ratios for the Surveillance Capsules A-4

Table B-1 Regulatory Guide 1.99, Revision 2, Credibility Criteria B-1

Table B-2 Calculation of Interim Chemistry Factors for the Credibility Evaluation Using St. Lucie Unit 1 Surveillance Capsule Data B-3

Table B-3 St. Lucie Unit 1 Surveillance Capsule Data Scatter about the Best-Fit Line B-4

Table B-4 St. Lucie Unit 1 Calculation of Residual versus Fast Fluence B-5

Table B-5 Calculation of Interim Chemistry Factors for the Credibility Evaluation Using St. Lucie Unit 2 Surveillance Capsule Data B-8

Table B-6 St. Lucie Unit 2 Surveillance Capsule Data Scatter about the Best-Fit Line Using All Available Surveillance Data B-9

Table B-7 St. Lucie Unit 2 Calculation of Residual versus Fast Fluence B-10

LIST OF FIGURES

Figure 2.4-1 Top View of the Reactor Geometry at the Core Midplane – with Thermal Shield (Unit 1, Cycles 1–5) 2-26

Figure 2.4-2 Top View of the Reactor Geometry at the Nozzle Centerline – with Thermal Shield (Unit 1, Cycles 1–5) 2-27

Figure 2.4-3 Oblique View of the Reactor Geometry – with Thermal Shield (Unit 1, Cycles 1–5) ..2-28

Figure 2.4-4 Top View of the Reactor Geometry at the Core Midplane – Without Thermal Shield (Unit 1, Cycles 6+) 2-29

Figure 2.4-5 Top View of the Reactor Geometry at the Nozzle Centerline – Without Thermal Shield (Unit 1, Cycles 6+) 2-30

Figure 2.4-6 Oblique View of the Reactor Geometry – Without Thermal Shield (Unit 1, Cycles 6+) 2-31

Figure 2.5-1 Top View of the Reactor Geometry at the Core Midplane (Unit 2) 2-50

Figure 2.5-2 Top View of the Reactor Geometry at the Nozzle Centerline (Unit 2) 2-51

Figure 2.5-3 Oblique View of the Reactor Geometry (Unit 2) 2-52

Figure 3-1 Generic RPV Material Identifications 3-2

Figure 7-1 Regulatory Guide 1.99, Revision 2, St. Lucie Unit 1 Predicted Decrease in USE at 72 EFPY as a Function of Copper and Fluence 7-6

Figure 7-2 Regulatory Guide 1.99, Revision 2, St. Lucie Unit 2 Predicted Decrease in USE at 72 EFPY as a Function of Copper and Fluence 7-7

EXECUTIVE SUMMARY

This report presents the time-limited aging analyses (TLAAs) for the St. Lucie Units 1 and 2 reactor pressure vessels (RPVs) with respect to reactor vessel integrity (RVI) in accordance with the requirements of the License Renewal Rule, 10 CFR Part 54. TLAAs are calculations that address safety-related aspects of the RPV within the bounds of the current 60-year license. These calculations must also be evaluated to account for an extended period of operation (80 years) also termed subsequent (or second) license renewal (SLR) period.

St. Lucie Units 1 and 2 are currently licensed through 60 years of operation; therefore, with a 20-year license extension, the SLR term is applicable through 80 years of operation. The evaluations in this report for 60 years of operation are applicable through 54 effective full-power years (EFPY) for Unit 1 and 55 EFPY for Unit 2, which are deemed end-of-license extension (EOLE). These EOLE determinations are consistent with the pressure-temperature (P-T) limit curves currently implemented in the plants' Technical Specifications. Similarly, evaluations in this report performed at 80 years of operation are applicable through 72 EFPY, which is deemed the SLR. Updated neutron fluence evaluations were used to identify the St. Lucie Units 1 and 2 beltline materials, i.e., materials with a SLR fluence $\geq 10^{17}$ n/cm^2 (E < 1.0 MeV), and as input to the reactor vessel (RV) integrity evaluations in support of current plant operations and SLR.

A summary of the St. Lucie Units 1 and 2 RVI TLAAs follows. Based on the results presented herein, it is concluded that the St. Lucie Units 1 and 2 RPVs will continue to meet RPV integrity regulatory requirements through SLR.

Fluence

The RV beltline neutron fluence values applicable to a postulated subsequent 20-year license renewal period were calculated for the St. Lucie Units 1 and 2 materials. The analysis methodologies used to calculate the St. Lucie Units 1 and 2 vessel fluence values satisfy the requirements set forth in Regulatory Guide 1.190. See Section 2 for more details.

Pressurized Thermal Shock

The RT_{PTS} values of all of the beltline materials in the St. Lucie Units 1 and 2 RPVs are below the RT_{PTS} screening criteria of 270°F for base metal and/or longitudinal welds, and 300°F for circumferentially oriented welds (per 10 CFR 50.61), through SLR (72 EFPY). See Section 6 for more details.

Upper-Shelf Energy

The upper-shelf energy (USE) values of all of the beltline and extended beltline materials in the St. Lucie Units 1 and 2 RVs are projected to remain above the USE screening criterion of 50 ft-lb (per 10 CFR 50, Appendix G) through SLR (72 EFPY). See Section 7 for more details.

Determination of Adjusted Reference Temperatures and Pressure-Temperature Limit Curve Applicability

Adjusted reference temperatures (ARTs) are calculated at EOLE and SLR. The ART values are used to perform an applicability check on the St. Lucie Units 1 and 2 P-T limit curves currently implemented in the Technical Specifications. With the consideration of the St. Lucie Units 1 and 2 updated fluence projections

and revised Position 2.1 chemistry factor (CF) values, the existing EOLE P-T limit curves for St. Lucie Unit 1 continue to remain valid through at least EOLE (54 EFPY), specifically through 63.8 EFPY. In addition, the current P-T limit curves for St. Lucie Unit 2 could be extended through 72 EFPY if desired. These conclusions consider the reactor vessel inlet/outlet nozzles, as required by Regulatory Issue Summary (RIS) 2014-11. Section 4.2.3.1.4 of NUREG-2192 does not require that P-T limit curves be provided for the SLR application. Therefore, the 72 EFPY ART values are presented herein for information, consistent with standard practice for reactor vessel integrity TLAAs. See Section 8 for more details.

Surveillance Capsule Withdrawal Schedule

With consideration of a subsequent 20-year license renewal to 80 years (72 EFPY), changes to the capsule withdrawal schedules are recommended for St. Lucie Units 1 and 2. See Section 9 for more details.

Appendix A provides the validation of the radiation transport calculation models based on neutron dosimetry measurements.

Appendix B contains a credibility evaluation for surveillance materials considering the updated fluence analysis.

1 TIME-LIMITED AGING ANALYSIS

Time-limited aging analyses (TLAAs) are those licensee calculations that:

1. Consider the effects of aging
2. Involve time-limited assumptions defined by the current operating term (e.g., 60 years)
3. Involve structures, systems, and components (SSCs) within the scope of license renewal
4. Involve conclusions or provide the basis for conclusions related to the capability of the SSCs to perform its intended functions
5. Were determined to be relevant by the licensee in making a safety determination
6. Are contained or incorporated by reference in the current licensing basis (CLB)

The potential TLAAs for the reactor pressure vessel (RPV) for subsequent license renewal (SLR) are identified in Table 1-1 along with indication of whether or not they meet the six criteria of 10 CFR 54.3 [Ref. 1] for TLAAs. The purpose of this report is to evaluate beltline materials with respect to reactor vessel integrity (RVI) TLAAs.

Table 1-1 Evaluation of Time-Limited Aging Analyses Per the Criteria of 10 CFR 54.3

Time-Limited Aging Analysis	Calculated Fluence	Pressurized Thermal Shock	Upper-Shelf Energy	Pressure-Temperature Limits for Heatup and Cooldown
Considers the Effects of Aging	YES	YES	YES	YES
Involves Time-Limited Assumptions Defined by the Current Operating Term	YES	YES	YES	YES
Involves SSC Within the Scope of License Renewal	YES	YES	YES	YES
Involves Conclusions or Provides the Basis for Conclusions Related to the Capability of SSC to Perform Its Intended Function	YES	YES	YES	YES
Determined to be Relevant by the Licensee in Making a Safety Determination	YES	YES	YES	YES
Contained or Incorporated by Reference in the CLB	YES	YES	YES	YES

2 CALCULATED NEUTRON FLUENCE FOR ST. LUCIE UNITS 1 AND 2

2.1 INTRODUCTION

This section describes a discrete ordinates (S_n) transport analysis performed for the St. Lucie Units 1 and 2 reactors to determine the neutron radiation environment within the reactor pressure vessels (RPVs) and surveillance capsules. In this analysis, fast neutron exposure parameters in terms of fast neutron fluence (E > 1.0 MeV) and iron atom displacements (dpa) were established on a fuel-cycle-specific basis. Comparisons of the results from the dosimetry evaluations with the analytical predictions served to validate the plant-specific neutron transport calculations. These validated calculations subsequently form the basis for projections of the neutron exposure of the RPV for operating periods extending to 72 EFPY.

The use of fast neutron fluence (E > 1.0 MeV) to correlate measured material property changes to the neutron exposure of the material has traditionally been accepted for the development of damage trend curves as well as for the implementation of trend curve data to assess the condition of the vessel. However, it has been suggested that an exposure model that accounts for differences in neutron energy spectra between surveillance capsule locations and positions within the vessel wall could lead to an improvement in the uncertainties associated with damage trend curves and improved accuracy in the evaluation of damage gradients through the reactor vessel wall.

Because of this potential shift away from a threshold fluence toward an energy-dependent damage function for data correlation, ASTM Standard Practice E853-18, "Standard Practice for Analysis and Interpretation of Light-Water Reactor Surveillance Neutron Exposure Results" [Ref. 2] recommends reporting displacements per iron atom along with fluence (E > 1.0 MeV) to provide a database for future reference. The energy-dependent dpa function to be used for this evaluation is specified in ASTM Standard Practice E693-94, "Standard Practice for Characterizing Neutron Exposures in Iron and Low Alloy Steels in Terms of Displacements per Atom" [Ref. 3]. The application of the dpa parameter to the assessment of embrittlement gradients through the thickness of the reactor vessel wall has been promulgated in Revision 2 to Regulatory Guide (RG) 1.99, "Radiation Embrittlement of Reactor Vessel Materials" [Ref. 4].

All calculations and dosimetry evaluations described in this section were based on nuclear cross-section data derived from ENDF/B-VI. Furthermore, the neutron transport and dosimetry evaluation methodologies follow the guidance of Regulatory Guide 1.190 [Ref. 5]. Additionally, the methods used to develop the calculated pressure vessel fluence are consistent with the NRC-approved methodology described in WCAP-18124-NP-A [Ref. 6].

2.2 DISCRETE ORDINATES ANALYSIS

Discrete ordinates transport calculations were performed on a fuel-cycle-specific basis to determine the neutron and gamma ray environment within the reactor geometry. The specific methods applied are consistent with those described in WCAP-18124-NP-A. The specific methods applied were consistent with those described in Reference 4. In the application of this methodology to the analysis performed herein, plant-specific forward transport calculations were used to directly solve for the space- and energy-dependent scalar flux, $\phi(r, \theta, z, E)$.

All transport calculations were carried out using the three-dimensional discrete ordinates code RAPTOR-M3G and the BUGLE-96 cross-section library. The BUGLE-96 library provides a 67-group-coupled neutron-gamma ray cross-section data set produced specifically for light water reactor applications. In these analyses, anisotropic scattering was treated with a P_3 Legendre expansion and the angular discretization was modeled with an S_{16} order of angular quadrature. Energy- and space-dependent core power distributions, as well as system operating temperatures, were treated on a fuel-cycle-specific basis.

Top views of the model geometry at the core midplane for Unit 1 with (applicable to Unit 1, Cycles 1–5) and without (applicable to Unit 1, Cycle 6 and beyond) a fully circumferential thermal shield are shown in Figure 2.4-1 and Figure 2.4-4, respectively. A top view of the model geometry at the core midplane for Unit 2 is shown in Figure 2.5-1. In these figures, a single quadrant is depicted showing the arrangement of the core, reactor internals, core barrel, downcomer, RPV cladding, RPV, reactor cavity, reflective insulation, RPV support structure, and bioshield. Depictions of the in-vessel surveillance capsules, including their associated support structures, are also shown.

From a neutronics standpoint, the inclusion of the surveillance capsules and associated support structures in the analytical model is significant. Since the presence of the capsules and support structures has a marked impact on the magnitude of the neutron fluence rate as well as on the relative neutron and gamma ray spectra at dosimetry locations within the capsules, a meaningful evaluation of the radiation environment internal to the capsules can be made only when these perturbation effects are properly accounted for in the analysis.

Top views of the reactor model geometry at the centerline of the inlet and outlet nozzles for Unit 1 with (applicable to Unit 1, Cycles 1–5) and without (applicable to Unit 1, Cycle 6 and beyond) a fully circumferential thermal shield are shown in Figure 2.4-2 and Figure 2.4-5, respectively. A top view of the reactor model geometry at the centerline of the inlet and outlet nozzles for Unit 2 is shown in Figure 2.5-2.

Oblique views of the model geometry for Unit 1 with (applicable to Unit 1, Cycles 1–5) and without (applicable to Unit 1, Cycle 6 and beyond; Unit 2 Cycle 1 and beyond) a fully circumferential thermal shield are shown in Figure 2.4-3 and Figure 2.4-6, respectively. An oblique view of the model geometry for Unit 2 is shown in Figure 2.5-3. Note that the stainless steel girth ribs located between the core shroud and barrel regions are shown in these figures. The RPV support structure located between the reflective insulation and bioshield is also shown.

In developing the RAPTOR-M3G model of the reactor geometry shown in the figures, nominal design dimensions were employed for the various structural components. However, for the RPV inner radius, as-built dimensions were used.

Water temperatures and coolant densities in the core and downcomer regions of the reactor were taken to be representative of full-power operating conditions. These coolant temperatures were varied on a cycle-specific basis. The reactor core itself was treated as a homogeneous mixture of fuel, cladding, water, and miscellaneous core structures such as fuel assembly grids and guide tubes.

The geometric mesh description of the reactor models shown in the figures consisted of 323 radial by 203 azimuthal by 406 axial intervals. Mesh sizes were chosen to ensure sufficient resolution of the stair-step-shaped shroud plates and a sufficient number of meshes throughout the radial and axial regions of interest. The pointwise inner iteration convergence criterion utilized in the calculations was set at a value of 0.001.

For St. Lucie Unit 1, neutron exposure data pertinent to the RPV clad/base metal interface are given in Tables 2.4-1 and 2.4-2 for neutron fluence rate (E > 1.0 MeV) and fluence (E > 1.0 MeV), respectively, and in Tables 2.4-3 and 2.4-4 for dpa/s and dpa, respectively. In each case, the data are provided for each operating cycle of the St. Lucie Unit 1 reactor. Neutron fluence (E > 1.0 MeV) and dpa are also projected to future operating times extending to 72 EFPY. The projections use Cycle 29 as the basis for future projections with and without a 10% positive bias on the peripheral and re-entrant corner assembly relative powers. The RPV exposure data are presented in terms of the maximum exposure experienced by the pressure vessel at azimuthal angles of 0°, 15°, 30°, 45°, 60°, 75°, and 90°, and at the azimuthal location providing the maximum exposure relative to the core cardinal axes.

For St. Lucie Unit 2, neutron exposure data pertinent to the RPV clad/base metal interface are given in Tables 2.5-1 and 2.5-2 for neutron fluence rate (E > 1.0 MeV) and fluence (E > 1.0 MeV), respectively, and in Tables 2.5-3 and 2.5-4 for dpa/s and dpa, respectively. In each case, the data are provided for each operating cycle of the St. Lucie Unit 2 reactor. Neutron fluence (E > 1.0 MeV) and dpa are also projected to future operating times extending to 72 EFPY. The projections use Cycle 24 as the basis for future projections with and without a 10% positive bias on the peripheral and re-entrant corner assembly relative powers. The RPV exposure data are presented in terms of the maximum exposure experienced by the pressure vessel at azimuthal angles of 0°, 15°, 30°, 45°, 60°, 75°, and 90°, and at the azimuthal location providing the maximum exposure relative to the core cardinal axes.

The maximum projected fast neutron fluence (E > 1.0 MeV) and dpa of the various RPV materials are given in Tables 2.4-5 and 2.4-6, respectively, for St. Lucie Unit 1. Similarly, the maximum projected fast neutron fluence (E > 1.0 MeV) and dpa of the various RPV materials are given in Tables 2.5-5 and 2.5-6, respectively, for St. Lucie Unit 2. These neutron exposure data are the maximum values at either the RPV clad/base metal interface or the RPV outer surface. Note that for regions and materials above and below the core (e.g., outlet nozzle to nozzle belt forging weld and lower shell to lower head ring circumferential weld), the neutron exposure values at the RPV outer surface can be greater than those at the clad/base metal interface as described in Westinghouse InfoGram IG-13-2 [Ref. 7].

Results of the discrete ordinates transport analyses pertinent to the surveillance capsule evaluations are provided in Tables 2.4-7 through 2.4-11 for St. Lucie Unit 1, and Tables 2.5-7 through 2.5-11 for St. Lucie Unit 2. In Tables 2.4-7 and 2.5-7, the calculated fast neutron fluence rate (E > 1.0 MeV) is provided at the geometric center of capsule locations as a function of irradiation time for St. Lucie Units 1 and 2, respectively. In Tables 2.4-8 and 2.5-8, the calculated fast neutron fluence (E > 1.0 MeV) is provided for the individual capsules for St. Lucie Units 1 and 2, respectively. Similar data presented in terms of iron atom displacement rate and integrated iron atom displacements are given in Tables 2.4-9 and 2.4-10, respectively, for Unit 1, and Tables 2.5-9 and 2.5-10, respectively, for Unit 2.

In Tables 2.4-11 and 2.5-11, lead factors associated with surveillance capsules are provided as a function of operating time for St. Lucie Units 1 and 2, respectively. The lead factor is defined as the ratio of the neutron fluence (E > 1.0 MeV) at the geometric center of the surveillance capsule to the maximum neutron fluence (E > 1.0 MeV) at the RPV clad/base metal interface.

2.3 CALCULATIONAL UNCERTAINTIES

The uncertainty associated with the calculated neutron exposure of the St. Lucie Units 1 and 2 surveillance capsule and reactor pressure vessel beltline is based on the recommended approach provided in Regulatory Guide 1.190. In particular, the qualification of the methodology was carried out in the following four stages:

1. **Simulator Benchmark Comparisons:** Comparisons of calculations with measurements from simulator benchmarks, including the pool critical assembly (PCA) simulator at the Oak Ridge National Laboratory (ORNL) and the VENUS-1 Experiment.

2. **Operating Reactor and Calculational Benchmarks:** Comparisons of calculations with surveillance capsule and reactor cavity measurements from the H.B. Robinson power reactor benchmark experiment. Also considered are comparisons of calculations to results published in the NRC fluence calculation benchmark.

3. **Analytic Uncertainty Analysis:** An analytical sensitivity study addressing the uncertainty components resulting from important input parameters applicable to the plant-specific transport calculations used in the neutron exposure assessments.

4. **Plant-Specific Benchmarking:** Comparisons of the plant-specific calculations with all available dosimetry results from the St. Lucie surveillance program.

The first phase of the methods qualification (simulator benchmark comparisons) addressed the adequacy of basic transport calculation and dosimetry evaluation techniques and associated cross-sections. This phase, however, did not test the accuracy of commercial core neutron source calculations nor did it address uncertainties in operational or geometric variables that impact power reactor calculations. The second phase of the qualification (operating reactor and calculational benchmark comparisons) addressed uncertainties in these additional areas that are primarily methods-related and would tend to apply generically to all fast neutron exposure evaluations. The third phase of the qualification (analytical sensitivity study) identified the potential uncertainties introduced into the overall evaluation due to calculational methods approximations, as well as to a lack of knowledge relative to various plant-specific input parameters. The overall calculational uncertainty applicable to the St. Lucie analysis was established from results of these three phases of the methods qualification.

The fourth phase of the uncertainty assessment (comparisons with St. Lucie Units 1 and 2 measurements) was used solely to demonstrate the validity of the transport calculations and to confirm the uncertainty estimates associated with the analytical results. The comparison was used only as a check and was not used in any way to modify the calculated surveillance capsule and pressure vessel neutron exposures described in Section 2.2. As such, the validation of the analytical model based on the measured plant dosimetry is provided in Appendix A.

The following summarizes the uncertainties developed from the first three phases of the methodology qualification. Additional information pertinent to these evaluations is provided in Westinghouse Report WCAP-18124-NP-A, "Fluence Determination with RAPTOR-M3G and FERRET" [Ref. 6].

Description	**Capsule and Vessel IR**
Simulator Benchmark Comparisons	3%
Operating Reactor and Calculational Benchmarks	5%
Analytic Uncertainty Analysis	11%
Additional Uncertainty for Factors not Explicitly Evaluated	5%
Net Calculational Uncertainty	**13%**

The net calculational uncertainty was determined by combining the individual components in quadrature. Therefore, the resultant uncertainty was treated as random, and no systematic bias was applied to the analytical results. The results of the plant-specific measurement comparisons provided in Appendix A support these uncertainty assessments for St. Lucie Units 1 and 2.

2.4 ST. LUCIE UNIT 1 NEUTRON FLUENCE DATA TABLES AND FIGURES

Table 2.4-1 St. Lucie Unit 1 Fast Neutron Fluence Rate (E > 1.0 MeV) at the RPV Clad/Base Metal Interface

Cycle	Cycle Length (EFPY)	Cumulative Operating Time (EFPY)	Fast Neutron (E > 1.0 MeV) Fluence Rate (n/cm²-s)							
			0°	15°	30°	45°	60°	75°	90°	Maximum
1	1.05	1.05	2.48E+10	1.51E+10	1.46E+10	1.08E+10	1.47E+10	1.48E+10	2.48E+10	2.48E+10
2	0.74	1.79	2.48E+10	1.51E+10	1.46E+10	1.08E+10	1.47E+10	1.48E+10	2.48E+10	2.48E+10
3	0.69	2.48	2.48E+10	1.51E+10	1.46E+10	1.08E+10	1.47E+10	1.48E+10	2.48E+10	2.48E+10
4	1.22	3.70	2.48E+10	1.51E+10	1.46E+10	1.08E+10	1.47E+10	1.48E+10	2.48E+10	2.48E+10
5	1.12	4.82	2.54E+10	1.32E+10	1.11E+10	7.89E+09	1.12E+10	1.29E+10	2.55E+10	2.55E+10
6	1.36	6.18	3.58E+10	2.04E+10	1.70E+10	1.25E+10	1.72E+10	1.98E+10	3.58E+10	3.58E+10
7	1.05	7.22	3.58E+10	2.04E+10	1.70E+10	1.25E+10	1.72E+10	1.98E+10	3.58E+10	3.58E+10
8	1.18	8.41	3.58E+10	2.04E+10	1.70E+10	1.25E+10	1.72E+10	1.98E+10	3.58E+10	3.58E+10
9	1.29	9.70	3.58E+10	2.04E+10	1.70E+10	1.25E+10	1.72E+10	1.98E+10	3.58E+10	3.58E+10
10	1.31	11.01	1.89E+10	1.48E+10	1.72E+10	1.32E+10	1.73E+10	1.44E+10	1.89E+10	1.89E+10
11	1.21	12.22	1.60E+10	1.29E+10	1.83E+10	1.36E+10	1.83E+10	1.26E+10	1.60E+10	1.89E+10
12	1.27	13.48	1.99E+10	1.51E+10	2.01E+10	1.43E+10	2.04E+10	1.49E+10	2.00E+10	2.10E+10
13	1.14	14.62	1.69E+10	1.31E+10	1.73E+10	1.33E+10	1.75E+10	1.29E+10	1.69E+10	1.81E+10
14	1.18	15.80	1.85E+10	1.44E+10	1.73E+10	1.35E+10	1.74E+10	1.41E+10	1.85E+10	1.85E+10
15	1.62	17.42	2.26E+10	1.51E+10	1.26E+10	1.01E+10	1.25E+10	1.46E+10	2.27E+10	2.27E+10
16	1.44	18.86	2.27E+10	1.49E+10	1.47E+10	1.28E+10	1.47E+10	1.45E+10	2.27E+10	2.27E+10
17	1.39	20.26	1.88E+10	1.33E+10	1.22E+10	1.13E+10	1.22E+10	1.29E+10	1.88E+10	1.88E+10
18	1.40	21.66	2.11E+10	1.34E+10	1.28E+10	1.09E+10	1.29E+10	1.30E+10	2.11E+10	2.11E+10
19	1.42	23.08	2.00E+10	1.33E+10	1.25E+10	1.12E+10	1.26E+10	1.29E+10	1.99E+10	2.00E+10
20	1.27	24.35	2.16E+10	1.46E+10	1.23E+10	1.11E+10	1.23E+10	1.41E+10	2.13E+10	2.16E+10
21	1.38	25.73	2.18E+10	1.43E+10	1.13E+10	1.02E+10	1.14E+10	1.37E+10	2.16E+10	2.18E+10
22	1.35	27.08	2.40E+10	1.53E+10	1.14E+10	1.03E+10	1.15E+10	1.47E+10	2.39E+10	2.40E+10
23	1.31	28.39	2.38E+10	1.56E+10	1.31E+10	1.15E+10	1.32E+10	1.51E+10	2.37E+10	2.38E+10
24	1.29	29.67	2.81E+10	1.72E+10	1.57E+10	1.39E+10	1.60E+10	1.66E+10	2.81E+10	2.81E+10

Table 2.4-1 St. Lucie Unit 1 Fast Neutron Fluence Rate (E > 1.0 MeV) at the RPV Clad/Base Metal Interface (Continued)

Cycle	Cycle Length (EFPY)	Cumulative Operating Time (EFPY)	Fast Neutron (E > 1.0 MeV) Fluence Rate (n/cm^2-s)							
			0°	15°	30°	45°	60°	75°	90°	Maximum
25	1.33	31.00	3.16E+10	1.96E+10	1.58E+10	1.36E+10	1.59E+10	1.91E+10	3.18E+10	3.18E+10
26	1.33	32.33	3.13E+10	1.94E+10	1.68E+10	1.47E+10	1.69E+10	1.88E+10	3.13E+10	3.13E+10
27	1.30	33.64	2.96E+10	1.73E+10	1.29E+10	1.05E+10	1.32E+10	1.68E+10	2.97E+10	2.97E+10
28	1.30	34.94	2.59E+10	1.64E+10	1.42E+10	1.27E+10	1.41E+10	1.59E+10	2.59E+10	2.59E+10
29	1.37	36.31	2.89E+10	1.72E+10	1.34E+10	1.19E+10	1.35E+10	1.66E+10	2.90E+10	2.90E+10
30[(a)]	1.35	37.66	2.83E+10	1.71E+10	1.41E+10	1.27E+10	1.43E+10	1.66E+10	2.83E+10	2.83E+10

Notes:

(a) Cycle 30 was the current operating cycle at the time the exposures reported in this table were determined. Values listed are based on the projected EFPY for this cycle.

Table 2.4-2 St. Lucie Unit 1 Fast Neutron Fluence (E > 1.0 MeV) at the RPV Clad/Base Metal Interface

Cycle	Cycle Length (EFPY)	Cumulative Operating Time (EFPY)	Fast Neutron (E > 1.0 MeV) Fluence (n/cm^2)							
			0°	15°	30°	45°	60°	75°	90°	Maximum
1	1.05	1.05	8.23E+17	5.01E+17	4.83E+17	3.57E+17	4.87E+17	4.92E+17	8.24E+17	8.24E+17
2	0.74	1.79	1.40E+18	8.53E+17	8.21E+17	6.07E+17	8.29E+17	8.36E+17	1.40E+18	1.40E+18
3	0.69	2.48	1.94E+18	1.18E+18	1.14E+18	8.42E+17	1.15E+18	1.16E+18	1.94E+18	1.94E+18
4	1.22	3.70	2.90E+18	1.77E+18	1.70E+18	1.26E+18	1.72E+18	1.73E+18	2.90E+18	2.90E+18
5	1.12	4.82	3.77E+18	2.22E+18	2.08E+18	1.53E+18	2.10E+18	2.18E+18	3.78E+18	3.78E+18
6	1.36	6.18	5.29E+18	3.08E+18	2.80E+18	2.06E+18	2.83E+18	3.01E+18	5.29E+18	5.29E+18
7	1.05	7.22	6.46E+18	3.75E+18	3.36E+18	2.47E+18	3.39E+18	3.66E+18	6.46E+18	6.46E+18
8	1.18	8.41	7.78E+18	4.50E+18	3.98E+18	2.93E+18	4.02E+18	4.39E+18	7.78E+18	7.78E+18
9	1.29	9.70	9.23E+18	5.32E+18	4.67E+18	3.44E+18	4.72E+18	5.19E+18	9.24E+18	9.24E+18
10	1.31	11.01	1.00E+19	5.93E+18	5.38E+18	3.98E+18	5.43E+18	5.78E+18	1.00E+19	1.00E+19
11	1.21	12.22	1.06E+19	6.42E+18	6.08E+18	4.50E+18	6.13E+18	6.26E+18	1.06E+19	1.06E+19
12	1.27	13.48	1.14E+19	7.01E+18	6.86E+18	5.06E+18	6.93E+18	6.84E+18	1.14E+19	1.14E+19
13	1.14	14.62	1.20E+19	7.49E+18	7.49E+18	5.54E+18	7.56E+18	7.31E+18	1.20E+19	1.20E+19
14	1.18	15.80	1.27E+19	8.02E+18	8.13E+18	6.04E+18	8.20E+18	7.83E+18	1.27E+19	1.27E+19
15	1.62	17.42	1.38E+19	8.80E+18	8.77E+18	6.56E+18	8.84E+18	8.58E+18	1.39E+19	1.39E+19
16	1.44	18.86	1.49E+19	9.47E+18	9.44E+18	7.14E+18	9.51E+18	9.24E+18	1.49E+19	1.49E+19
17	1.39	20.26	1.57E+19	1.01E+19	9.97E+18	7.64E+18	1.01E+19	9.81E+18	1.57E+19	1.57E+19
18	1.40	21.66	1.66E+19	1.07E+19	1.05E+19	8.12E+18	1.06E+19	1.04E+19	1.66E+19	1.66E+19
19	1.42	23.08	1.75E+19	1.12E+19	1.11E+19	8.62E+18	1.12E+19	1.10E+19	1.75E+19	1.75E+19
20	1.27	24.35	1.84E+19	1.18E+19	1.16E+19	9.06E+18	1.17E+19	1.15E+19	1.84E+19	1.84E+19
21	1.38	25.73	1.93E+19	1.25E+19	1.21E+19	9.51E+18	1.22E+19	1.21E+19	1.93E+19	1.93E+19
22	1.35	27.08	2.04E+19	1.31E+19	1.26E+19	9.95E+18	1.27E+19	1.27E+19	2.04E+19	2.04E+19
23	1.31	28.39	2.13E+19	1.37E+19	1.31E+19	1.04E+19	1.32E+19	1.34E+19	2.13E+19	2.13E+19
24	1.29	29.67	2.25E+19	1.44E+19	1.38E+19	1.10E+19	1.39E+19	1.40E+19	2.25E+19	2.25E+19
25	1.33	31.00	2.38E+19	1.53E+19	1.44E+19	1.16E+19	1.45E+19	1.48E+19	2.38E+19	2.38E+19
26	1.33	32.33	2.51E+19	1.61E+19	1.51E+19	1.22E+19	1.52E+19	1.56E+19	2.51E+19	2.51E+19

Table 2.4-2 St. Lucie Unit 1 Fast Neutron Fluence (E > 1.0 MeV) at the RPV Clad/Base Metal Interface (Continued)

Cycle	Cycle Length (EFPY)	Cumulative Operating Time (EFPY)	Fast Neutron (E > 1.0 MeV) Fluence (n/cm^2)							
			0°	15°	30°	45°	60°	75°	90°	Maximum
27	1.30	33.64	2.63E+19	1.68E+19	1.57E+19	1.26E+19	1.58E+19	1.63E+19	2.63E+19	2.63E+19
28	1.30	34.94	2.74E+19	1.75E+19	1.62E+19	1.31E+19	1.64E+19	1.70E+19	2.74E+19	2.74E+19
29	1.37	36.31	2.87E+19	1.82E+19	1.68E+19	1.36E+19	1.69E+19	1.77E+19	2.87E+19	2.87E+19
30(a)	1.35	37.66	2.99E+19	1.89E+19	1.74E+19	1.42E+19	1.75E+19	1.84E+19	2.99E+19	2.99E+19
Projections with no bias on the peripheral and re-entrant corner assembly relative powers										
Future(b)	--	42.00	3.38E+19	2.13E+19	1.93E+19	1.58E+19	1.94E+19	2.07E+19	3.38E+19	3.38E+19
Future(b)	--	48.00	3.93E+19	2.45E+19	2.18E+19	1.81E+19	2.20E+19	2.38E+19	3.93E+19	3.93E+19
Future(b)\	--	54.00	4.48E+19	2.78E+19	2.44E+19	2.03E+19	2.45E+19	2.69E+19	4.48E+19	4.48E+19
Future(b)	--	60.00	5.03E+19	3.10E+19	2.69E+19	2.25E+19	2.71E+19	3.01E+19	5.03E+19	5.03E+19
Future(b)	--	66.00	5.58E+19	3.43E+19	2.94E+19	2.48E+19	2.96E+19	3.32E+19	5.58E+19	5.58E+19
Future(b)	--	72.00	6.12E+19	3.75E+19	3.20E+19	2.70E+19	3.22E+19	3.64E+19	6.12E+19	6.12E+19
Projections with a +10% bias on the peripheral and re-entrant corner assembly relative powers										
Future(b)	--	42.00	3.41E+19	2.15E+19	1.94E+19	1.60E+19	1.96E+19	2.09E+19	3.41E+19	3.41E+19
Future(b)	--	48.00	4.01E+19	2.50E+19	2.22E+19	1.84E+19	2.23E+19	2.43E+19	4.01E+19	4.01E+19
Future(b)	--	54.00	4.60E+19	2.85E+19	2.50E+19	2.08E+19	2.51E+19	2.76E+19	4.60E+19	4.60E+19
Future(b)	--	60.00	5.19E+19	3.20E+19	2.77E+19	2.33E+19	2.79E+19	3.10E+19	5.19E+19	5.19E+19
Future(b)	--	66.00	5.78E+19	3.55E+19	3.05E+19	2.57E+19	3.07E+19	3.44E+19	5.79E+19	5.79E+19
Future(b)	--	72.00	6.38E+19	3.91E+19	3.33E+19	2.82E+19	3.34E+19	3.78E+19	6.38E+19	6.38E+19

Notes:

(a) Cycle 30 was the current operating cycle at the time the exposures reported in this table were determined. Values listed are based on the projected EFPY for this cycle.

(b) Values beyond Cycle 30 are based on the average core power distributions and reactor operating conditions of Cycle 29 and are determined both with and without a 1.1 bias on the peripheral and re-entrant corner assembly relative powers.

Table 2.4-3 St. Lucie Unit 1 Iron Atom Displacement Rate at the RPV Clad/Base Metal Interface

Cycle	Cycle Length (EFPY)	Cumulative Operating Time (EFPY)	Iron Atom Displacement Rate (dpa/s)							
			0°	15°	30°	45°	60°	75°	90°	Maximum
1	1.05	1.05	3.93E-11	2.41E-11	2.30E-11	1.71E-11	2.32E-11	2.39E-11	3.92E-11	3.93E-11
2	0.74	1.79	3.93E-11	2.41E-11	2.30E-11	1.71E-11	2.32E-11	2.39E-11	3.92E-11	3.93E-11
3	0.69	2.48	3.93E-11	2.41E-11	2.30E-11	1.71E-11	2.32E-11	2.39E-11	3.92E-11	3.93E-11
4	1.22	3.70	3.93E-11	2.41E-11	2.30E-11	1.71E-11	2.32E-11	2.39E-11	3.92E-11	3.93E-11
5	1.12	4.82	4.02E-11	2.11E-11	1.75E-11	1.25E-11	1.77E-11	2.09E-11	4.01E-11	4.02E-11
6	1.36	6.18	5.46E-11	3.14E-11	2.60E-11	1.94E-11	2.63E-11	3.06E-11	5.45E-11	5.46E-11
7	1.05	7.22	5.46E-11	3.14E-11	2.60E-11	1.94E-11	2.63E-11	3.06E-11	5.45E-11	5.46E-11
8	1.18	8.41	5.46E-11	3.14E-11	2.60E-11	1.94E-11	2.63E-11	3.06E-11	5.45E-11	5.46E-11
9	1.29	9.70	5.46E-11	3.14E-11	2.60E-11	1.94E-11	2.63E-11	3.06E-11	5.45E-11	5.46E-11
10	1.31	11.01	2.89E-11	2.28E-11	2.63E-11	2.03E-11	2.64E-11	2.22E-11	2.88E-11	2.89E-11
11	1.21	12.22	2.45E-11	1.99E-11	2.79E-11	2.09E-11	2.80E-11	1.96E-11	2.44E-11	2.89E-11
12	1.27	13.48	3.04E-11	2.33E-11	3.07E-11	2.21E-11	3.10E-11	2.30E-11	3.04E-11	3.21E-11
13	1.14	14.62	2.58E-11	2.03E-11	2.65E-11	2.04E-11	2.67E-11	2.00E-11	2.58E-11	2.76E-11
14	1.18	15.80	2.83E-11	2.22E-11	2.64E-11	2.08E-11	2.66E-11	2.19E-11	2.83E-11	2.83E-11
15	1.62	17.42	3.47E-11	2.33E-11	1.93E-11	1.56E-11	1.91E-11	2.26E-11	3.46E-11	3.47E-11
16	1.44	18.86	3.47E-11	2.30E-11	2.24E-11	1.97E-11	2.26E-11	2.24E-11	3.46E-11	3.47E-11
17	1.39	20.26	2.88E-11	2.04E-11	1.86E-11	1.74E-11	1.87E-11	1.99E-11	2.87E-11	2.88E-11
18	1.40	21.66	3.22E-11	2.07E-11	1.96E-11	1.68E-11	1.97E-11	2.01E-11	3.22E-11	3.22E-11
19	1.42	23.08	3.06E-11	2.06E-11	1.91E-11	1.72E-11	1.94E-11	2.00E-11	3.04E-11	3.06E-11
20	1.27	24.35	3.30E-11	2.25E-11	1.89E-11	1.71E-11	1.88E-11	2.17E-11	3.25E-11	3.30E-11
21	1.38	25.73	3.33E-11	2.19E-11	1.74E-11	1.57E-11	1.75E-11	2.13E-11	3.29E-11	3.33E-11
22	1.35	27.08	3.67E-11	2.35E-11	1.75E-11	1.59E-11	1.76E-11	2.28E-11	3.65E-11	3.67E-11
23	1.31	28.39	3.64E-11	2.40E-11	2.01E-11	1.77E-11	2.03E-11	2.33E-11	3.62E-11	3.64E-11
24	1.29	29.67	4.30E-11	2.64E-11	2.40E-11	2.14E-11	2.45E-11	2.58E-11	4.28E-11	4.30E-11
25	1.33	31.00	4.84E-11	3.02E-11	2.42E-11	2.09E-11	2.43E-11	2.95E-11	4.84E-11	4.84E-11
26	1.33	32.33	4.78E-11	2.98E-11	2.57E-11	2.27E-11	2.59E-11	2.90E-11	4.77E-11	4.78E-11

Table 2.4-3 St. Lucie Unit 1 Iron Atom Displacement Rate at the RPV Clad/Base Metal Interface (Continued)

Cycle	Cycle Length (EFPY)	Cumulative Operating Time (EFPY)	Iron Atom Displacement Rate (dpa/s)							
			0°	15°	30°	45°	60°	75°	90°	Maximum
27	1.30	33.64	4.52E-11	2.66E-11	1.98E-11	1.62E-11	2.02E-11	2.60E-11	4.52E-11	4.52E-11
28	1.30	34.94	3.97E-11	2.53E-11	2.18E-11	1.95E-11	2.16E-11	2.46E-11	3.96E-11	3.97E-11
29	1.37	36.31	4.42E-11	2.64E-11	2.06E-11	1.83E-11	2.07E-11	2.57E-11	4.41E-11	4.42E-11
30[a]	1.35	37.66	4.32E-11	2.63E-11	2.16E-11	1.96E-11	2.19E-11	2.57E-11	4.31E-11	4.32E-11

Note:

(a) Cycle 30 was the current operating cycle at the time the exposures reported in this table were determined. Values listed are based on the projected EFPY for this cycle.

Table 2.4-4 St. Lucie Unit 1 Iron Atom Displacements at the RPV Clad/Base Metal Interface

Cycle	Cycle Length (EFPY)	Cumulative Operating Time (EFPY)	Iron Atom Displacements (dpa)							
			0°	15°	30°	45°	60°	75°	90°	Maximum
1	1.05	1.05	1.30E-03	7.99E-04	7.63E-04	5.66E-04	7.69E-04	7.93E-04	1.30E-03	1.30E-03
2	0.74	1.79	2.21E-03	1.36E-03	1.30E-03	9.63E-04	1.31E-03	1.35E-03	2.21E-03	2.21E-03
3	0.69	2.48	3.07E-03	1.88E-03	1.80E-03	1.34E-03	1.81E-03	1.87E-03	3.06E-03	3.07E-03
4	1.22	3.70	4.59E-03	2.81E-03	2.68E-03	1.99E-03	2.71E-03	2.79E-03	4.58E-03	4.59E-03
5	1.12	4.82	5.98E-03	3.54E-03	3.29E-03	2.43E-03	3.32E-03	3.51E-03	5.97E-03	5.98E-03
6	1.36	6.18	8.29E-03	4.87E-03	4.39E-03	3.24E-03	4.43E-03	4.81E-03	8.27E-03	8.29E-03
7	1.05	7.22	1.01E-02	5.90E-03	5.24E-03	3.88E-03	5.29E-03	5.81E-03	1.00E-02	1.01E-02
8	1.18	8.41	1.21E-02	7.06E-03	6.20E-03	4.59E-03	6.26E-03	6.94E-03	1.21E-02	1.21E-02
9	1.29	9.70	1.43E-02	8.32E-03	7.25E-03	5.37E-03	7.32E-03	8.18E-03	1.43E-02	1.43E-02
10	1.31	11.01	1.55E-02	9.26E-03	8.34E-03	6.21E-03	8.41E-03	9.09E-03	1.54E-02	1.55E-02
11	1.21	12.22	1.64E-02	1.00E-02	9.40E-03	7.01E-03	9.48E-03	9.84E-03	1.64E-02	1.64E-02
12	1.27	13.48	1.76E-02	1.09E-02	1.06E-02	7.87E-03	1.07E-02	1.07E-02	1.76E-02	1.76E-02
13	1.14	14.62	1.85E-02	1.17E-02	1.16E-02	8.61E-03	1.17E-02	1.15E-02	1.85E-02	1.85E-02
14	1.18	15.80	1.96E-02	1.25E-02	1.25E-02	9.38E-03	1.26E-02	1.23E-02	1.95E-02	1.96E-02
15	1.62	17.42	2.14E-02	1.37E-02	1.35E-02	1.02E-02	1.36E-02	1.34E-02	2.13E-02	2.14E-02
16	1.44	18.86	2.29E-02	1.47E-02	1.45E-02	1.11E-02	1.46E-02	1.45E-02	2.29E-02	2.29E-02
17	1.39	20.26	2.42E-02	1.56E-02	1.54E-02	1.18E-02	1.55E-02	1.53E-02	2.41E-02	2.42E-02
18	1.40	21.66	2.56E-02	1.65E-02	1.62E-02	1.26E-02	1.63E-02	1.62E-02	2.56E-02	2.56E-02
19	1.42	23.08	2.70E-02	1.75E-02	1.71E-02	1.34E-02	1.72E-02	1.71E-02	2.69E-02	2.70E-02
20	1.27	24.35	2.83E-02	1.84E-02	1.78E-02	1.40E-02	1.80E-02	1.80E-02	2.82E-02	2.83E-02
21	1.38	25.73	2.98E-02	1.93E-02	1.86E-02	1.47E-02	1.87E-02	1.89E-02	2.97E-02	2.98E-02
22	1.35	27.08	3.13E-02	2.03E-02	1.93E-02	1.54E-02	1.95E-02	1.99E-02	3.12E-02	3.13E-02
23	1.31	28.39	3.28E-02	2.13E-02	2.02E-02	1.61E-02	2.03E-02	2.08E-02	3.27E-02	3.28E-02
24	1.29	29.67	3.46E-02	2.24E-02	2.11E-02	1.70E-02	2.13E-02	2.19E-02	3.45E-02	3.46E-02
25	1.33	31.00	3.66E-02	2.37E-02	2.22E-02	1.79E-02	2.23E-02	2.31E-02	3.65E-02	3.66E-02
26	1.33	32.33	3.86E-02	2.49E-02	2.32E-02	1.88E-02	2.34E-02	2.43E-02	3.85E-02	3.86E-02

Table 2.4-4 St. Lucie Unit 1 Iron Atom Displacements at the RPV Clad/Base Metal Interface (Continued)

Cycle	Cycle Length (EFPY)	Cumulative Operating Time (EFPY)	Iron Atom Displacements (dpa)							
			0°	15°	30°	45°	60°	75°	90°	Maximum
27	1.30	33.64	4.05E-02	2.60E-02	2.41E-02	1.95E-02	2.42E-02	2.54E-02	4.03E-02	4.05E-02
28	1.30	34.94	4.21E-02	2.70E-02	2.49E-02	2.03E-02	2.51E-02	2.64E-02	4.20E-02	4.21E-02
29	1.37	36.31	4.40E-02	2.82E-02	2.58E-02	2.11E-02	2.60E-02	2.75E-02	4.39E-02	4.40E-02
30[(a)]	1.35	37.66	4.59E-02	2.93E-02	2.68E-02	2.19E-02	2.70E-02	2.86E-02	4.57E-02	4.59E-02
Projections with no bias on the peripheral and re-entrant corner assembly relative powers										
Future[(b)]	--	42.00	5.19E-02	3.29E-02	2.96E-02	2.44E-02	2.98E-02	3.21E-02	5.18E-02	5.19E-02
Future[(b)]	--	48.00	6.03E-02	3.79E-02	3.35E-02	2.79E-02	3.37E-02	3.70E-02	6.01E-02	6.03E-02
Future[(b)]	--	54.00	6.87E-02	4.29E-02	3.74E-02	3.14E-02	3.76E-02	4.19E-02	6.85E-02	6.87E-02
Future[(b)]	--	60.00	7.71E-02	4.79E-02	4.13E-02	3.48E-02	4.15E-02	4.67E-02	7.68E-02	7.71E-02
Future[(b)]	--	66.00	8.54E-02	5.30E-02	4.52E-02	3.83E-02	4.55E-02	5.16E-02	8.52E-02	8.54E-02
Future[(b)]	--	72.00	9.38E-02	5.80E-02	4.91E-02	4.17E-02	4.94E-02	5.64E-02	9.35E-02	9.38E-02
Projections with a +10% bias on the peripheral and re-entrant corner assembly relative powers										
Future[(b)]	--	42.00	5.24E-02	3.32E-02	2.98E-02	2.47E-02	3.00E-02	3.24E-02	5.23E-02	5.24E-02
Future[(b)]	--	48.00	6.15E-02	3.86E-02	3.41E-02	2.84E-02	3.43E-02	3.77E-02	6.13E-02	6.15E-02
Future[(b)]	--	54.00	7.05E-02	4.40E-02	3.83E-02	3.22E-02	3.85E-02	4.29E-02	7.03E-02	7.05E-02
Future[(b)]	--	60.00	7.96E-02	4.95E-02	4.26E-02	3.60E-02	4.28E-02	4.82E-02	7.93E-02	7.96E-02
Future[(b)]	--	66.00	8.86E-02	5.49E-02	4.68E-02	3.97E-02	4.71E-02	5.34E-02	8.84E-02	8.86E-02
Future[(b)]	--	72.00	9.77E-02	6.03E-02	5.11E-02	4.35E-02	5.13E-02	5.87E-02	9.74E-02	9.77E-02

Notes:

(a) Cycle 30 was the current operating cycle at the time the exposures reported in this table were determined. Values listed are based on the projected EFPY for this cycle.

(b) Values beyond Cycle 30 are based on the average core power distributions and reactor operating conditions of Cycle 29 and are determined both with and without a 1.1 bias on the peripheral and re-entrant corner assembly relative powers.

Table 2.4-5 St. Lucie Unit 1 Fast Neutron Fluence (E > 1.0 MeV) at RPV Welds and Shells

Projections with no bias on the peripheral and re-entrant corner assembly relative powers

Material	Fast Neutron (E > 1.0 MeV) Fluence (n/cm²)			
	37.66 EFPY[a]	42 EFPY	48 EFPY	54 EFPY
Inlet (Cold Leg)-Nozzle-to-Upper-Shell Weld (lowest extent)	3.54E+16	3.97E+16	4.57E+16	5.16E+16
Outlet (Hot Leg)-Nozzle-to-Upper-Shell Weld (lowest extent)	3.94E+16	4.48E+16	5.23E+16	5.98E+16
Upper Shell	1.41E+18	1.60E+18	1.86E+18	2.12E+18
Upper-to-Intermediate-Shell Circumferential Weld	1.77E+18	2.01E+18	2.33E+18	2.66E+18
Intermediate Shell	2.99E+19	3.38E+19	3.93E+19	4.48E+19
Intermediate Shell Longitudinal Weld – 15°	1.89E+19	2.13E+19	2.45E+19	2.78E+19
Intermediate Shell Longitudinal Weld – 135°	1.42E+19	1.58E+19	1.81E+19	2.03E+19
Intermediate Shell Longitudinal Weld – 255°	1.84E+19	2.07E+19	2.38E+19	2.69E+19
Intermediate-to-Lower-Shell Circumferential Weld	2.96E+19	3.35E+19	3.89E+19	4.44E+19
Lower Shell	2.97E+19	3.36E+19	3.91E+19	4.45E+19
Lower Shell Longitudinal Weld – 15°	1.88E+19	2.11E+19	2.44E+19	2.76E+19
Lower Shell Longitudinal Weld – 135°	1.41E+19	1.57E+19	1.79E+19	2.02E+19
Lower Shell Longitudinal Weld – 255°	1.82E+19	2.05E+19	2.36E+19	2.68E+19
Lower-Shell-to-Bottom-Head Circumferential Weld	2.18E+16	2.45E+16	2.83E+16	3.21E+16

Projections with no bias on the peripheral and re-entrant corner assembly relative powers

Material	Fast Neutron (E > 1.0 MeV) Fluence (n/cm²)			
	60 EFPY	66 EFPY	72 EFPY	
Inlet (Cold Leg)-Nozzle-to-Upper-Shell Weld (lowest extent)	5.76E+16	6.35E+16	6.95E+16	
Outlet (Hot Leg)-Nozzle-to-Upper-Shell Weld (lowest extent)	6.73E+16	7.49E+16	8.24E+16	
Upper Shell	2.39E+18	2.65E+18	2.91E+18	
Upper-to-Intermediate-Shell Circumferential Weld	2.99E+18	3.32E+18	3.64E+18	
Intermediate Shell	5.03E+19	5.58E+19	6.12E+19	
Intermediate Shell Longitudinal Weld – 15°	3.10E+19	3.43E+19	3.75E+19	
Intermediate Shell Longitudinal Weld – 135°	2.25E+19	2.48E+19	2.70E+19	
Intermediate Shell Longitudinal Weld – 255°	3.01E+19	3.32E+19	3.64E+19	
Intermediate-to-Lower-Shell Circumferential Weld	4.98E+19	5.52E+19	6.07E+19	
Lower Shell	5.00E+19	5.55E+19	6.09E+19	
Lower Shell Longitudinal Weld – 15°	3.08E+19	3.41E+19	3.73E+19	
Lower Shell Longitudinal Weld – 135°	2.24E+19	2.46E+19	2.69E+19	
Lower Shell Longitudinal Weld – 255°	2.99E+19	3.30E+19	3.61E+19	
Lower-Shell-to-Bottom-Head Circumferential Weld	3.59E+16	3.97E+16	4.35E+16	

Table 2.4-5 St. Lucie Unit 1 Fast Neutron Fluence (E > 1.0 MeV) at RPV Welds and Shells (Continued)

Projections with a +10% bias on the peripheral and re-entrant corner assembly relative powers				
Material	**Fast Neutron (E > 1.0 MeV) Fluence (n/cm^2)**			
	37.66 EFPY[(a)]	**42 EFPY**	**48 EFPY**	**54 EFPY**
Inlet (Cold Leg)-Nozzle-to-Upper-Shell Weld (lowest extent)	3.54E+16	4.01E+16	4.66E+16	5.30E+16
Outlet (Hot Leg)-Nozzle-to-Upper-Shell Weld (lowest extent)	3.94E+16	4.51E+16	5.29E+16	6.08E+16
Upper Shell	1.41E+18	1.61E+18	1.89E+18	2.17E+18
Upper-to-Intermediate-Shell Circumferential Weld	1.77E+18	2.02E+18	2.37E+18	2.72E+18
Intermediate Shell	2.99E+19	3.41E+19	4.01E+19	4.60E+19
Intermediate Shell Longitudinal Weld – 15°	1.89E+19	2.15E+19	2.50E+19	2.85E+19
Intermediate Shell Longitudinal Weld – 135°	1.42E+19	1.60E+19	1.84E+19	2.08E+19
Intermediate Shell Longitudinal Weld – 255°	1.84E+19	2.09E+19	2.42E+19	2.76E+19
Intermediate-to-Lower-Shell Circumferential Weld	2.96E+19	3.38E+19	3.97E+19	4.56E+19
Lower Shell	2.97E+19	3.39E+19	3.99E+19	4.58E+19
Lower Shell Longitudinal Weld – 15°	1.88E+19	2.13E+19	2.48E+19	2.83E+19
Lower Shell Longitudinal Weld – 135°	1.41E+19	1.58E+19	1.83E+19	2.07E+19
Lower Shell Longitudinal Weld – 255°	1.82E+19	2.07E+19	2.41E+19	2.75E+19
Lower-Shell-to-Bottom-Head Circumferential Weld	2.18E+16	2.47E+16	2.89E+16	3.30E+16

Projections with a +10% bias on the peripheral and re-entrant corner assembly relative powers				
Material	**Fast Neutron (E > 1.0 MeV) Fluence (n/cm^2)**			
	60 EFPY	**66 EFPY**	**72 EFPY**	
Inlet (Cold Leg)-Nozzle-to-Upper-Shell Weld (lowest extent)	5.95E+16	6.59E+16	7.24E+16	
Outlet (Hot Leg)-Nozzle-to-Upper-Shell Weld (lowest extent)	6.87E+16	7.65E+16	8.44E+16	
Upper Shell	2.45E+18	2.73E+18	3.01E+18	
Upper-to-Intermediate-Shell Circumferential Weld	3.07E+18	3.42E+18	3.77E+18	
Intermediate Shell	5.19E+19	5.79E+19	6.38E+19	
Intermediate Shell Longitudinal Weld – 15°	3.20E+19	3.55E+19	3.91E+19	
Intermediate Shell Longitudinal Weld – 135°	2.33E+19	2.57E+19	2.82E+19	
Intermediate Shell Longitudinal Weld – 255°	3.10E+19	3.44E+19	3.78E+19	
Intermediate-to-Lower-Shell Circumferential Weld	5.15E+19	5.73E+19	6.32E+19	
Lower Shell	5.17E+19	5.76E+19	6.35E+19	
Lower Shell Longitudinal Weld – 15°	3.18E+19	3.53E+19	3.88E+19	
Lower Shell Longitudinal Weld – 135°	2.31E+19	2.56E+19	2.80E+19	
Lower Shell Longitudinal Weld – 255°	3.08E+19	3.42E+19	3.76E+19	
Lower-Shell-to-Bottom-Head Circumferential Weld	3.71E+16	4.12E+16	4.53E+16	

Note:

(a) Value listed is the projected EFPY at the end of Cycle 30.

Table 2.4-6 St. Lucie Unit 1 Iron Atom Displacements at RPV Welds and Shells

Projections with no bias on the peripheral and re-entrant corner assembly relative powers				
Material	**Iron Atom Displacements (dpa)**			
	37.66 EFPY(a)	**42 EFPY**	**48 EFPY**	**54 EFPY**
Inlet (Cold Leg)-Nozzle-to-Upper-Shell Weld (lowest extent)	2.94E-04	3.29E-04	3.78E-04	4.26E-04
Outlet (Hot Leg)-Nozzle-to-Upper-Shell Weld (lowest extent)	3.39E-04	3.82E-04	4.42E-04	5.02E-04
Upper Shell	2.35E-03	2.67E-03	3.10E-03	3.54E-03
Upper-to-Intermediate-Shell Circumferential Weld	2.92E-03	3.31E-03	3.85E-03	4.38E-03
Intermediate Shell	4.59E-02	5.19E-02	6.03E-02	6.87E-02
Intermediate Shell Longitudinal Weld – 15°	2.93E-02	3.29E-02	3.79E-02	4.29E-02
Intermediate Shell Longitudinal Weld – 135°	2.19E-02	2.44E-02	2.79E-02	3.13E-02
Intermediate Shell Longitudinal Weld – 255°	2.86E-02	3.21E-02	3.70E-02	4.19E-02
Intermediate-to-Lower-Shell Circumferential Weld	4.55E-02	5.15E-02	5.98E-02	6.81E-02
Lower Shell	4.55E-02	5.16E-02	5.99E-02	6.83E-02
Lower Shell Longitudinal Weld – 15°	2.90E-02	3.26E-02	3.76E-02	4.26E-02
Lower Shell Longitudinal Weld – 135°	2.17E-02	2.42E-02	2.77E-02	3.11E-02
Lower Shell Longitudinal Weld – 255°	2.84E-02	3.19E-02	3.67E-02	4.15E-02
Lower-Shell-to-Bottom-Head Circumferential Weld	1.50E-04	1.69E-04	1.94E-04	2.20E-04

Projections with no bias on the peripheral and re-entrant corner assembly relative powers				
Material	**Iron Atom Displacements (dpa)**			
	60 EFPY	**66 EFPY**	**72 EFPY**	
Inlet (Cold Leg)-Nozzle-to-Upper-Shell Weld (lowest extent)	4.75E-04	5.23E-04	5.72E-04	
Outlet (Hot Leg)-Nozzle-to-Upper-Shell Weld (lowest extent)	5.61E-04	6.21E-04	6.80E-04	
Upper Shell	3.97E-03	4.41E-03	4.85E-03	
Upper-to-Intermediate-Shell Circumferential Weld	4.92E-03	5.46E-03	6.00E-03	
Intermediate Shell	7.70E-02	8.54E-02	9.38E-02	
Intermediate Shell Longitudinal Weld – 15°	4.79E-02	5.29E-02	5.80E-02	
Intermediate Shell Longitudinal Weld – 135°	3.48E-02	3.83E-02	4.17E-02	
Intermediate Shell Longitudinal Weld – 255°	4.67E-02	5.16E-02	5.64E-02	
Intermediate-to-Lower-Shell Circumferential Weld	7.64E-02	8.48E-02	9.31E-02	
Lower Shell	7.66E-02	8.49E-02	9.33E-02	
Lower Shell Longitudinal Weld – 15°	4.76E-02	5.26E-02	5.75E-02	
Lower Shell Longitudinal Weld – 135°	3.45E-02	3.80E-02	4.14E-02	
Lower Shell Longitudinal Weld – 255°	4.64E-02	5.12E-02	5.60E-02	
Lower-Shell-to-Bottom-Head Circumferential Weld	2.45E-04	2.71E-04	2.96E-04	

Table 2.4-6 St. Lucie Unit 1 Iron Atom Displacements at RPV Welds and Shells (Continued)

Projections with a +10% bias on the peripheral and re-entrant corner assembly relative powers

Material	Iron Atom Displacements (dpa)			
	37.66 EFPY[(a)]	42 EFPY	48 EFPY	54 EFPY
Inlet (Cold Leg)-Nozzle-to-Upper-Shell Weld (lowest extent)	2.94E-04	3.32E-04	3.85E-04	4.38E-04
Outlet (Hot Leg)-Nozzle-to-Upper-Shell Weld (lowest extent)	3.39E-04	3.86E-04	4.51E-04	5.15E-04
Upper Shell	2.35E-03	2.69E-03	3.15E-03	3.62E-03
Upper-to-Intermediate-Shell Circumferential Weld	2.92E-03	3.33E-03	3.91E-03	4.49E-03
Intermediate Shell	4.59E-02	5.24E-02	6.15E-02	7.05E-02
Intermediate Shell Longitudinal Weld – 15°	2.93E-02	3.32E-02	3.86E-02	4.40E-02
Intermediate Shell Longitudinal Weld – 135°	2.19E-02	2.47E-02	2.84E-02	3.22E-02
Intermediate Shell Longitudinal Weld – 255°	2.86E-02	3.24E-02	3.77E-02	4.29E-02
Intermediate-to-Lower-Shell Circumferential Weld	4.55E-02	5.20E-02	6.10E-02	7.00E-02
Lower Shell	4.55E-02	5.21E-02	6.11E-02	7.01E-02
Lower Shell Longitudinal Weld – 15°	2.90E-02	3.29E-02	3.83E-02	4.37E-02
Lower Shell Longitudinal Weld – 135°	2.17E-02	2.44E-02	2.82E-02	3.19E-02
Lower Shell Longitudinal Weld – 255°	2.84E-02	3.22E-02	3.74E-02	4.26E-02
Lower-Shell-to-Bottom-Head Circumferential Weld	1.50E-04	1.70E-04	1.98E-04	2.26E-04

Projections with a +10% bias on the peripheral and re-entrant corner assembly relative powers

Material	Iron Atom Displacements (dpa)			
	60 EFPY	66 EFPY	72 EFPY	
Inlet (Cold Leg)-Nozzle-to-Upper-Shell Weld (lowest extent)	4.90E-04	5.43E-04	5.96E-04	
Outlet (Hot Leg)-Nozzle-to-Upper-Shell Weld (lowest extent)	5.80E-04	6.44E-04	7.09E-04	
Upper Shell	4.08E-03	4.55E-03	5.01E-03	
Upper-to-Intermediate-Shell Circumferential Weld	5.06E-03	5.64E-03	6.21E-03	
Intermediate Shell	7.96E-02	8.86E-02	9.77E-02	
Intermediate Shell Longitudinal Weld – 15°	4.95E-02	5.49E-02	6.03E-02	
Intermediate Shell Longitudinal Weld – 135°	3.60E-02	3.97E-02	4.35E-02	
Intermediate Shell Longitudinal Weld – 255°	4.82E-02	5.34E-02	5.87E-02	
Intermediate-to-Lower-Shell Circumferential Weld	7.89E-02	8.79E-02	9.69E-02	
Lower Shell	7.91E-02	8.81E-02	9.72E-02	
Lower Shell Longitudinal Weld – 15°	4.91E-02	5.45E-02	5.99E-02	
Lower Shell Longitudinal Weld – 135°	3.57E-02	3.95E-02	4.32E-02	
Lower Shell Longitudinal Weld – 255°	4.78E-02	5.31E-02	5.83E-02	
Lower-Shell-to-Bottom-Head Circumferential Weld	2.53E-04	2.81E-04	3.09E-04	

Note:

(a) Value listed is the projected EFPY at the end of Cycle 30.

Table 2.4-7 St. Lucie Unit 1 Fast Neutron (E > 1.0 MeV) Fluence Rate at the Geometric Center of the Surveillance Capsule Locations

Cycle	Cycle Length (EFPY)	Cumulative Operating Time (EFPY)	Fluence Rate (n/cm^2-s)	
			7°	14°
1	1.05	1.05	3.42E+10	2.32E+10
2	0.74	1.79	3.42E+10	2.32E+10
3	0.69	2.48	3.42E+10	2.32E+10
4	1.22	3.70	3.42E+10	2.32E+10
5	1.12	4.82	3.10E+10	1.94E+10
6	1.36	6.18	4.18E+10	2.80E+10
7	1.05	7.22	4.18E+10	2.80E+10
8	1.18	8.41	4.18E+10	2.80E+10
9	1.29	9.70	4.18E+10	2.80E+10
10	1.31	11.01	2.38E+10	1.94E+10
11	1.21	12.22	1.85E+10	1.59E+10
12	1.27	13.48	2.34E+10	1.92E+10
13	1.14	14.62	1.95E+10	1.64E+10
14	1.18	15.80	2.22E+10	1.85E+10
15	1.62	17.42	2.84E+10	2.08E+10
16	1.44	18.86	2.83E+10	2.05E+10
17	1.39	20.26	2.43E+10	1.83E+10
18	1.40	21.66	2.60E+10	1.85E+10
19	1.42	23.08	2.50E+10	1.83E+10
20	1.27	24.35	2.70E+10	2.00E+10
21	1.38	25.73	2.72E+10	1.97E+10
22	1.35	27.08	2.99E+10	2.12E+10
23	1.31	28.39	2.98E+10	2.16E+10
24	1.29	29.67	3.42E+10	2.37E+10
25	1.33	31.00	3.96E+10	2.76E+10
26	1.33	32.33	3.88E+10	2.70E+10
27	1.30	33.64	3.57E+10	2.41E+10
28	1.30	34.94	3.22E+10	2.27E+10
29	1.37	36.31	3.51E+10	2.38E+10
30[(a)]	1.35	37.66	3.46E+10	2.38E+10

Note:

(a) Cycle 30 was the current operating cycle at the time the exposures reported in this table were determined. Values listed are based on the projected EFPY for this cycle.

Table 2.4-8 St. Lucie Unit 1 Fast Neutron (E > 1.0 MeV) Fluence at the Geometric Center of the Surveillance Capsules

Cycle	Cycle Length (EFPY)	Cumulative Operating Time (EFPY)	Fluence (n/cm^2)	
			7°	14°
1	1.05	1.05	1.14E+18	7.71E+17
2	0.74	1.79	1.93E+18	1.31E+18
3	0.69	2.48	2.68E+18	1.82E+18
4	1.22	3.70	4.00E+18	2.71E+18
5	1.12	4.82	5.09E+18[a]	3.40E+18
6	1.36	6.18	6.88E+18	4.60E+18
7	1.05	7.22	8.27E+18	5.52E+18
8	1.18	8.41	9.83E+18	6.56E+18
9	1.29	9.70	1.15E+19	7.70E+18[b]
10	1.31	11.01	1.25E+19	8.50E+18
11	1.21	12.22	1.32E+19	9.11E+18
12	1.27	13.48	1.42E+19	9.88E+18
13	1.14	14.62	1.49E+19	1.05E+19
14	1.18	15.80	1.57E+19	1.12E+19
15	1.62	17.42	1.71E+19	1.22E+19[c]
16	1.44	18.86	1.84E+19	1.32E+19
17	1.39	20.26	1.95E+19	1.40E+19
18	1.40	21.66	2.06E+19	1.48E+19
19	1.42	23.08	2.18E+19	1.56E+19
20	1.27	24.35	2.28E+19	1.64E+19
21	1.38	25.73	2.40E+19	1.73E+19
22	1.35	27.08	2.53E+19	1.82E+19
23	1.31	28.39	2.65E+19	1.90E+19
24	1.29	29.67	2.79E+19	2.00E+19
25	1.33	31.00	2.96E+19	2.12E+19
26	1.33	32.33	3.12E+19	2.23E+19
27	1.30	33.64	3.27E+19	2.33E+19
28	1.30	34.94	3.40E+19	2.42E+19
29	1.37	36.31	3.55E+19	2.53E+19
30[d]	1.35	37.66	3.70E+19	2.63E+19

Table 2.4-8 St. Lucie Unit 1 Fast Neutron (E > 1.0 MeV) Fluence at the Geometric Center of the Surveillance Capsules (Continued)

No bias on the peripheral and re-entrant corner assembly relative powers				
Cycle	**Cycle Length (EFPY)**	**Cumulative Operating Time (EFPY)**	**Fluence (n/cm²)**	
			7°	**14°**
Future[(e)]	--	42.00	4.18E+19	2.95E+19
Future[(e)]	--	48.00	4.84E+19	3.41E+19
Future[(e)]	--	54.00	5.51E+19	3.86E+19
Future[(e)]	--	60.00	6.17E+19	4.31E+19
Future[(e)]	--	66.00	6.84E+19	4.76E+19
Future[(e)]	--	72.00	7.50E+19	5.21E+19

+10% bias on the peripheral and re-entrant corner assembly relative powers				
Cycle	**Cycle Length (EFPY)**	**Cumulative Operating Time (EFPY)**	**Fluence (n/cm²)**	
			7°	**14°**
Future[(e)]	--	42.00	4.22E+19	2.98E+19
Future[(e)]	--	48.00	4.94E+19	3.47E+19
Future[(e)]	--	54.00	5.66E+19	3.96E+19
Future[(e)]	--	60.00	6.38E+19	4.45E+19
Future[(e)]	--	66.00	7.10E+19	4.94E+19
Future[(e)]	--	72.00	7.81E+19	5.42E+19

Note:

(a) This value is applicable to Capsule 97.

(b) This value is applicable to Capsule 104.

(c) This value is applicable to Capsule 284.

(d) Cycle 30 was the current operating cycle at the time the exposures reported in this table were determined. Values listed are based on the projected EFPY for this cycle.

(e) Values beyond Cycle 30 are based on the average core power distributions and reactor operating conditions of Cycle 29 and are determined both with and without a 1.1 bias on the peripheral and re-entrant corner assembly relative powers.

Table 2.4-9 St. Lucie Unit 1 Iron Atom Displacement Rate at the Geometric Center of the Surveillance Capsules

Cycle	Cycle Length (EFPY)	Cumulative Operating Time (EFPY)	Displacement Rate (dpa/s)	
			7°	14°
1	1.05	1.05	5.26E-11	3.58E-11
2	0.74	1.79	5.26E-11	3.58E-11
3	0.69	2.48	5.26E-11	3.58E-11
4	1.22	3.70	5.26E-11	3.58E-11
5	1.12	4.82	4.77E-11	3.00E-11
6	1.36	6.18	6.07E-11	4.09E-11
7	1.05	7.22	6.07E-11	4.09E-11
8	1.18	8.41	6.07E-11	4.09E-11
9	1.29	9.70	6.07E-11	4.09E-11
10	1.31	11.01	3.47E-11	2.84E-11
11	1.21	12.22	2.70E-11	2.34E-11
12	1.27	13.48	3.41E-11	2.83E-11
13	1.14	14.62	2.85E-11	2.41E-11
14	1.18	15.80	3.23E-11	2.71E-11
15	1.62	17.42	4.14E-11	3.04E-11
16	1.44	18.86	4.11E-11	3.01E-11
17	1.39	20.26	3.53E-11	2.68E-11
18	1.40	21.66	3.79E-11	2.71E-11
19	1.42	23.08	3.64E-11	2.69E-11
20	1.27	24.35	3.93E-11	2.92E-11
21	1.38	25.73	3.95E-11	2.88E-11
22	1.35	27.08	4.35E-11	3.10E-11
23	1.31	28.39	4.34E-11	3.15E-11
24	1.29	29.67	4.97E-11	3.47E-11
25	1.33	31.00	5.75E-11	4.03E-11
26	1.33	32.33	5.63E-11	3.95E-11
27	1.30	33.64	5.19E-11	3.53E-11
28	1.30	34.94	4.68E-11	3.33E-11
29	1.37	36.31	5.10E-11	3.49E-11
30[(a)]	1.35	37.66	5.03E-11	3.48E-11

Note:

(a) Cycle 30 was the current operating cycle at the time the exposures reported in this table were determined. Values listed are based on the projected EFPY for this cycle.

Table 2.4-10 St. Lucie Unit 1 Iron Atom Displacements at the Geometric Center of the Surveillance Capsules

Cycle	Cycle Length (EFPY)	Cumulative Operating Time (EFPY)	Displacements (dpa)	
			7°	14°
1	1.05	1.05	1.74E-03	1.19E-03
2	0.74	1.79	2.96E-03	2.02E-03
3	0.69	2.48	4.11E-03	2.80E-03
4	1.22	3.70	6.14E-03	4.18E-03
5	1.12	4.82	7.82E-03[(a)]	5.24E-03
6	1.36	6.18	1.04E-02	6.99E-03
7	1.05	7.22	1.24E-02	8.35E-03
8	1.18	8.41	1.47E-02	9.87E-03
9	1.29	9.70	1.72E-02	1.15E-02[(b)]
10	1.31	11.01	1.86E-02	1.27E-02
11	1.21	12.22	1.96E-02	1.36E-02
12	1.27	13.48	2.10E-02	1.47E-02
13	1.14	14.62	2.20E-02	1.56E-02
14	1.18	15.80	2.32E-02	1.66E-02
15	1.62	17.42	2.53E-02	1.82E-02[(c)]
16	1.44	18.86	2.72E-02	1.95E-02
17	1.39	20.26	2.88E-02	2.07E-02
18	1.40	21.66	3.04E-02	2.19E-02
19	1.42	23.08	3.21E-02	2.31E-02
20	1.27	24.35	3.37E-02	2.43E-02
21	1.38	25.73	3.54E-02	2.55E-02
22	1.35	27.08	3.72E-02	2.69E-02
23	1.31	28.39	3.90E-02	2.82E-02
24	1.29	29.67	4.10E-02	2.96E-02
25	1.33	31.00	4.34E-02	3.13E-02
26	1.33	32.33	4.58E-02	3.29E-02
27	1.30	33.64	4.79E-02	3.44E-02
28	1.30	34.94	4.99E-02	3.57E-02
29	1.37	36.31	5.21E-02	3.73E-02
30[(d)]	1.35	37.66	5.42E-02	3.87E-02

Table 2.4-10 St. Lucie Unit 1 Iron Atom Displacements at the Geometric Center of the Surveillance Capsules (Continued)

No bias on the peripheral and re-entrant corner assembly relative powers				
Cycle	Cycle Length (EFPY)	Cumulative Operating Time (EFPY)	Displacements (dpa)	
			7°	14°
Future(e)	--	42.00	6.12E-02	4.35E-02
Future(e)	--	48.00	7.09E-02	5.01E-02
Future(e)	--	54.00	8.05E-02	5.67E-02
Future(e)	--	60.00	9.02E-02	6.33E-02
Future(e)	--	66.00	9.98E-02	6.99E-02
Future(e)	--	72.00	1.09E-01	7.66E-02

+10% bias on the peripheral and re-entrant corner assembly relative powers				
Cycle	Cycle Length (EFPY)	Cumulative Operating Time (EFPY)	Displacements (dpa)	
			7°	14°
Future(e)	--	42.00	6.18E-02	4.39E-02
Future(e)	--	48.00	7.22E-02	5.11E-02
Future(e)	--	54.00	8.27E-02	5.82E-02
Future(e)	--	60.00	9.31E-02	6.54E-02
Future(e)	--	66.00	1.04E-01	7.25E-02
Future(e)	--	72.00	1.14E-01	7.97E-02

Note:

(a) This value is applicable to Capsule 97.

(b) This value is applicable to Capsule 104.

(c) This value is applicable to Capsule 284.

(d) Cycle 30 was the current operating cycle at the time the exposures reported in this table were determined. Values listed are based on the projected EFPY for this cycle.

(e) Values beyond Cycle 30 are based on the average core power distributions and reactor operating conditions of Cycle 29 and are determined both with and without a 1.1 bias on the peripheral and re-entrant corner assembly relative powers.

Table 2.4-11 St. Lucie Unit 1 Surveillance Capsule Lead Factors

Cycle	Cycle Length (EFPY)	Cumulative Operating Time (EFPY)	Lead Factor	
			7°	14°
1	1.05	1.05	1.38	0.94
2	0.74	1.79	1.38	0.94
3	0.69	2.48	1.38	0.94
4	1.22	3.70	1.38	0.94
5	1.12	4.82	1.35[a]	0.90
6	1.36	6.18	1.30	0.87
7	1.05	7.22	1.28	0.85
8	1.18	8.41	1.26	0.84
9	1.29	9.70	1.25	0.83[b]
10	1.31	11.01	1.25	0.85
11	1.21	12.22	1.25	0.86
12	1.27	13.48	1.24	0.87
13	1.14	14.62	1.24	0.87
14	1.18	15.80	1.23	0.88
15	1.62	17.42	1.24	0.88[c]
16	1.44	18.86	1.24	0.88
17	1.39	20.26	1.24	0.89
18	1.40	21.66	1.24	0.89
19	1.42	23.08	1.24	0.89
20	1.27	24.35	1.24	0.89
21	1.38	25.73	1.24	0.89
22	1.35	27.08	1.24	0.89
23	1.31	28.39	1.24	0.89
24	1.29	29.67	1.24	0.89
25	1.33	31.00	1.24	0.89
26	1.33	32.33	1.24	0.89
27	1.30	33.64	1.24	0.88
28	1.30	34.94	1.24	0.88
29	1.37	36.31	1.24	0.88
30[d]	1.35	37.66	1.24	0.88

Table 2.4-11 St. Lucie Unit 1 Surveillance Capsule Lead Factors (Continued)

No bias on the peripheral and re-entrant corner assembly relative powers				
Cycle	**Cycle Length (EFPY)**	**Cumulative Operating Time (EFPY)**	**Lead Factor**	
			7°	**14°**
Future[(e)]	--	42.00	1.24	0.87
Future[(e)]	--	48.00	1.23	0.87
Future[(e)]	--	54.00	1.23	0.86
Future[(e)]	--	60.00	1.23	0.86
Future[(e)]	--	66.00	1.23	0.85
Future[(e)]	--	72.00	1.22	0.85

+10% bias on the peripheral and re-entrant corner assembly relative powers				
Cycle	**Cycle Length (EFPY)**	**Cumulative Operating Time (EFPY)**	**Lead Factor**	
			7°	**14°**
Future[(e)]	--	42.00	1.24	0.87
Future[(e)]	--	48.00	1.23	0.87
Future[(e)]	--	54.00	1.23	0.86
Future[(e)]	--	60.00	1.23	0.86
Future[(e)]	--	66.00	1.23	0.85
Future[(e)]	--	72.00	1.23	0.85

Note:

(a) This value is applicable to Capsule 97.

(b) This value is applicable to Capsule 104

(c) This value is applicable to Capsule 284.

(d) Cycle 30 was the current operating cycle at the time the lead factors reported in this table were determined. Values listed are based on the projected EFPY for this cycle.

(e) Values beyond Cycle 30 are based on the average core power distributions and reactor operating conditions of Cycle 29 and are determined both with and without a 1.1 bias on the peripheral and re-entrant corner assembly relative powers.

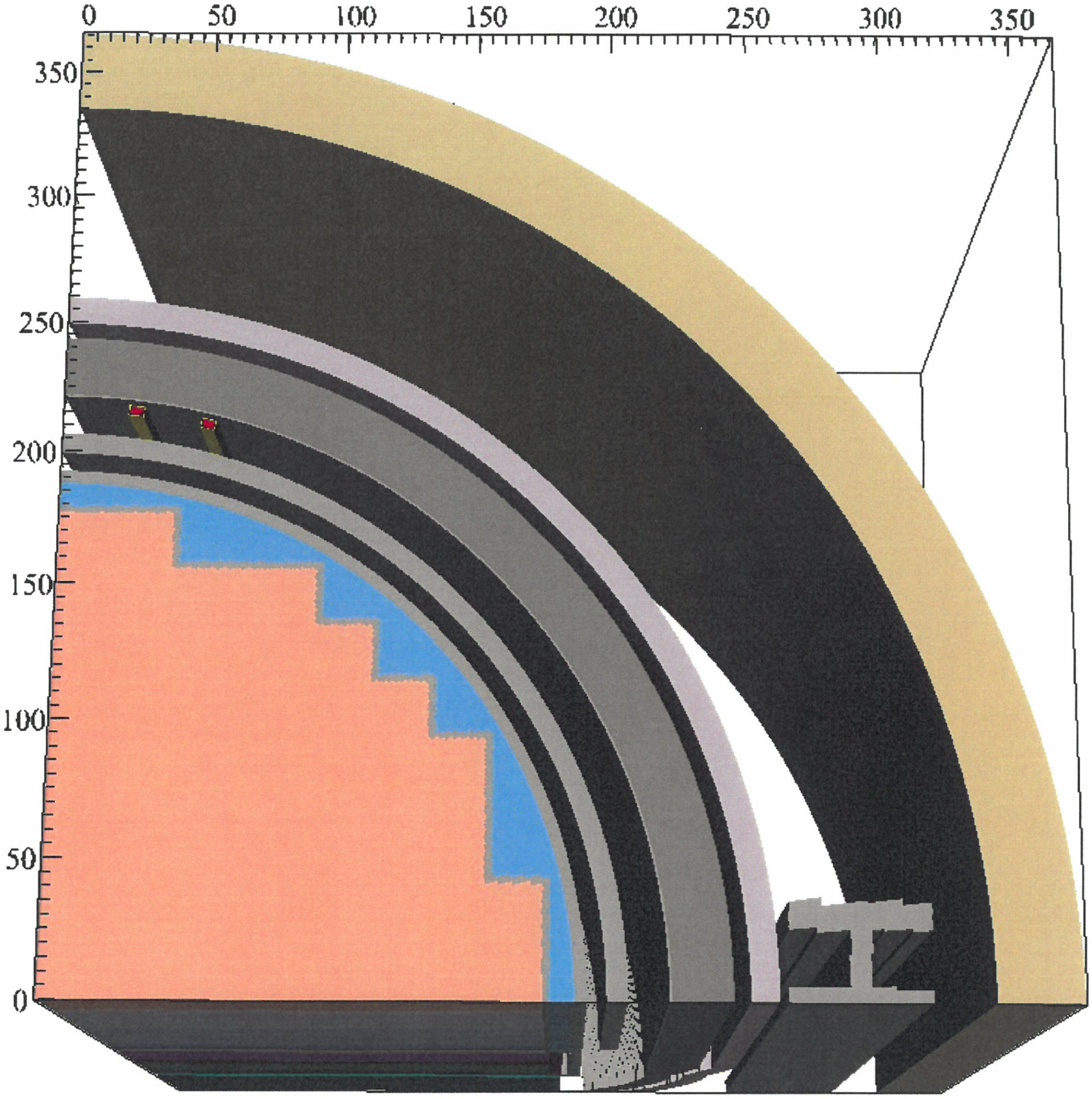

Figure 2.4-1 Top View of the Reactor Geometry at the Core Midplane – with Thermal Shield (Unit 1, Cycles 1–5)

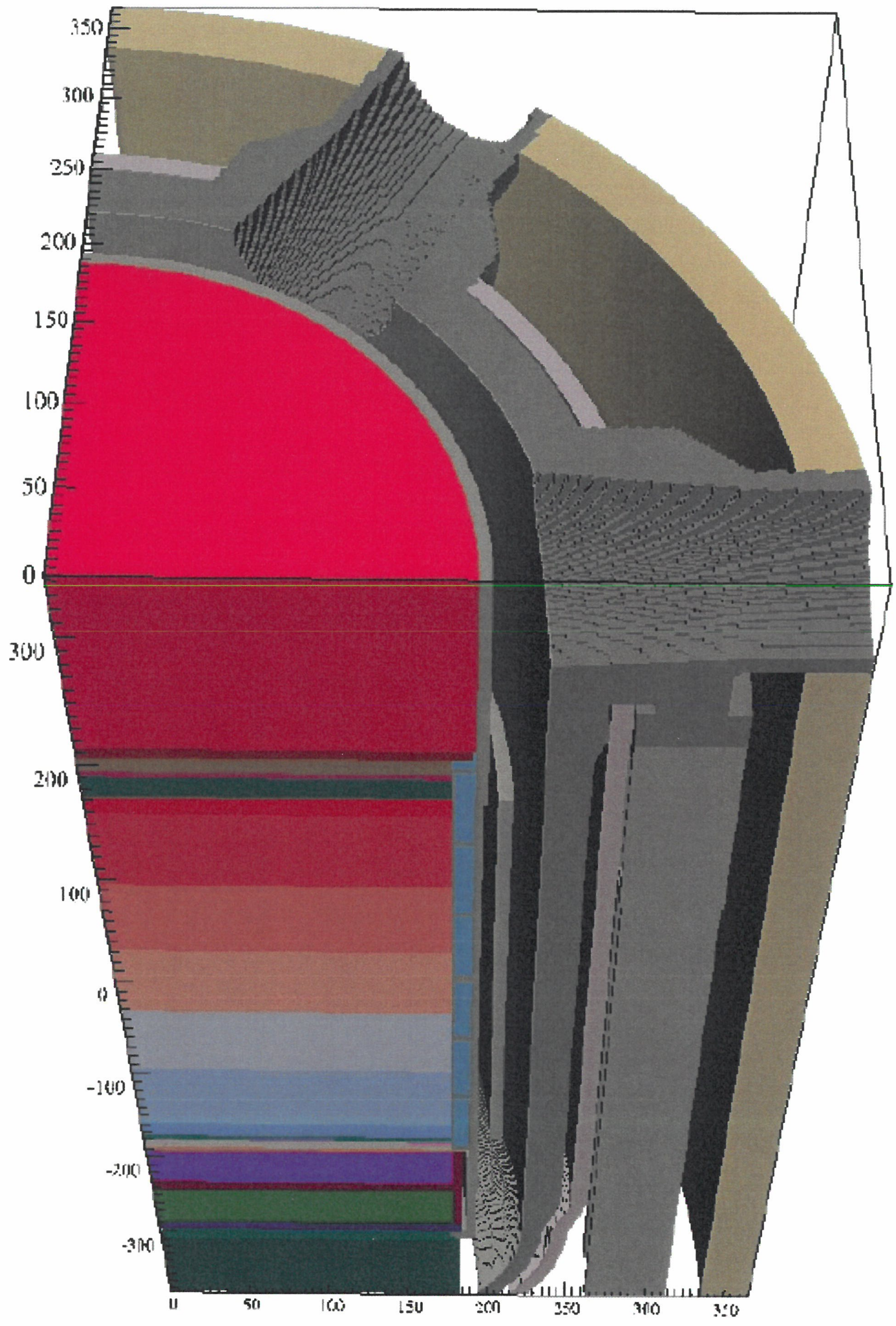

Figure 2.4-2 Top View of the Reactor Geometry at the Nozzle Centerline – with Thermal Shield (Unit 1, Cycles 1–5)

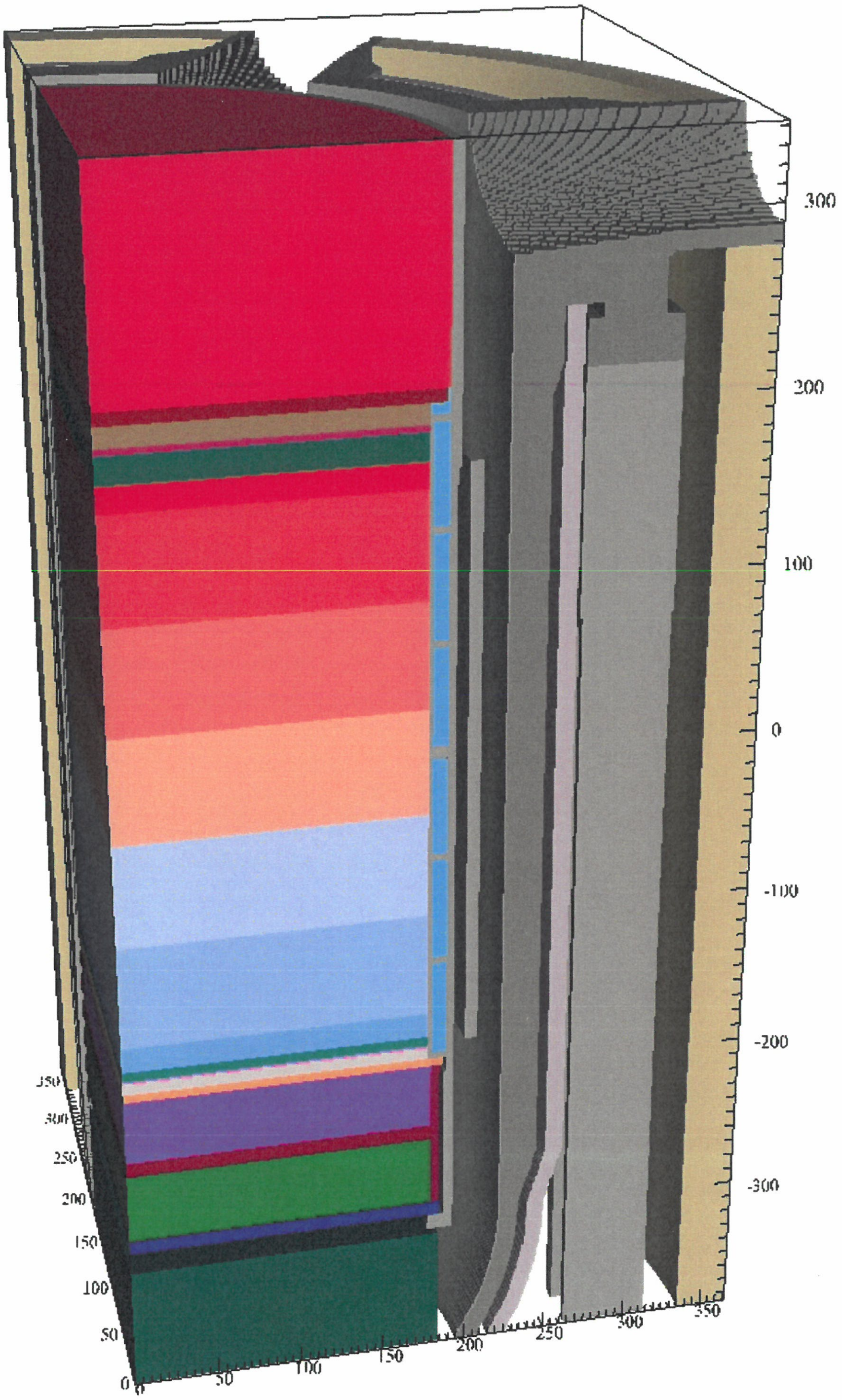

Figure 2.4-3 Oblique View of the Reactor Geometry – with Thermal Shield (Unit 1, Cycles 1–5)

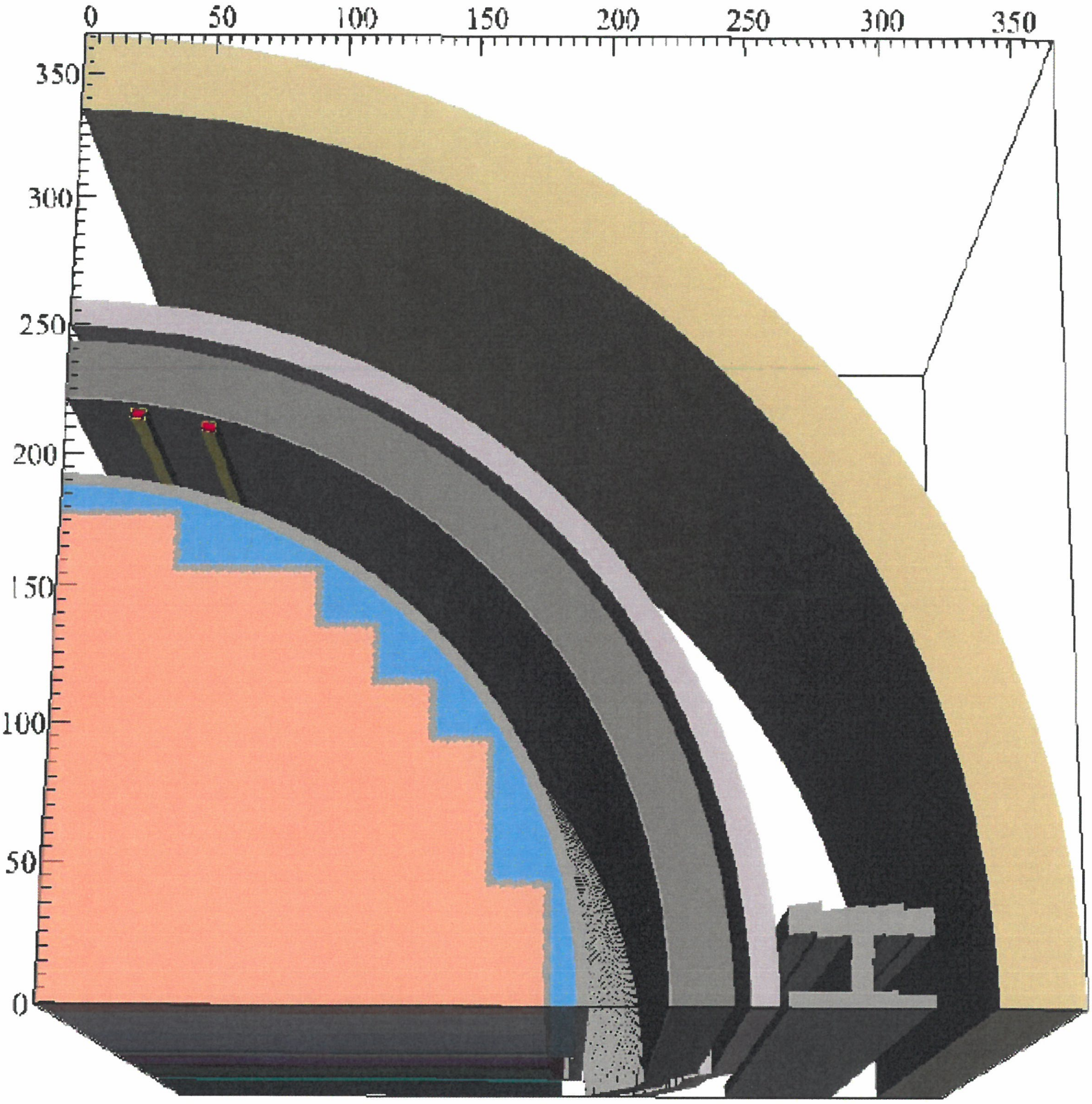

Figure 2.4-4 Top View of the Reactor Geometry at the Core Midplane – Without Thermal Shield (Unit 1, Cycles 6+)

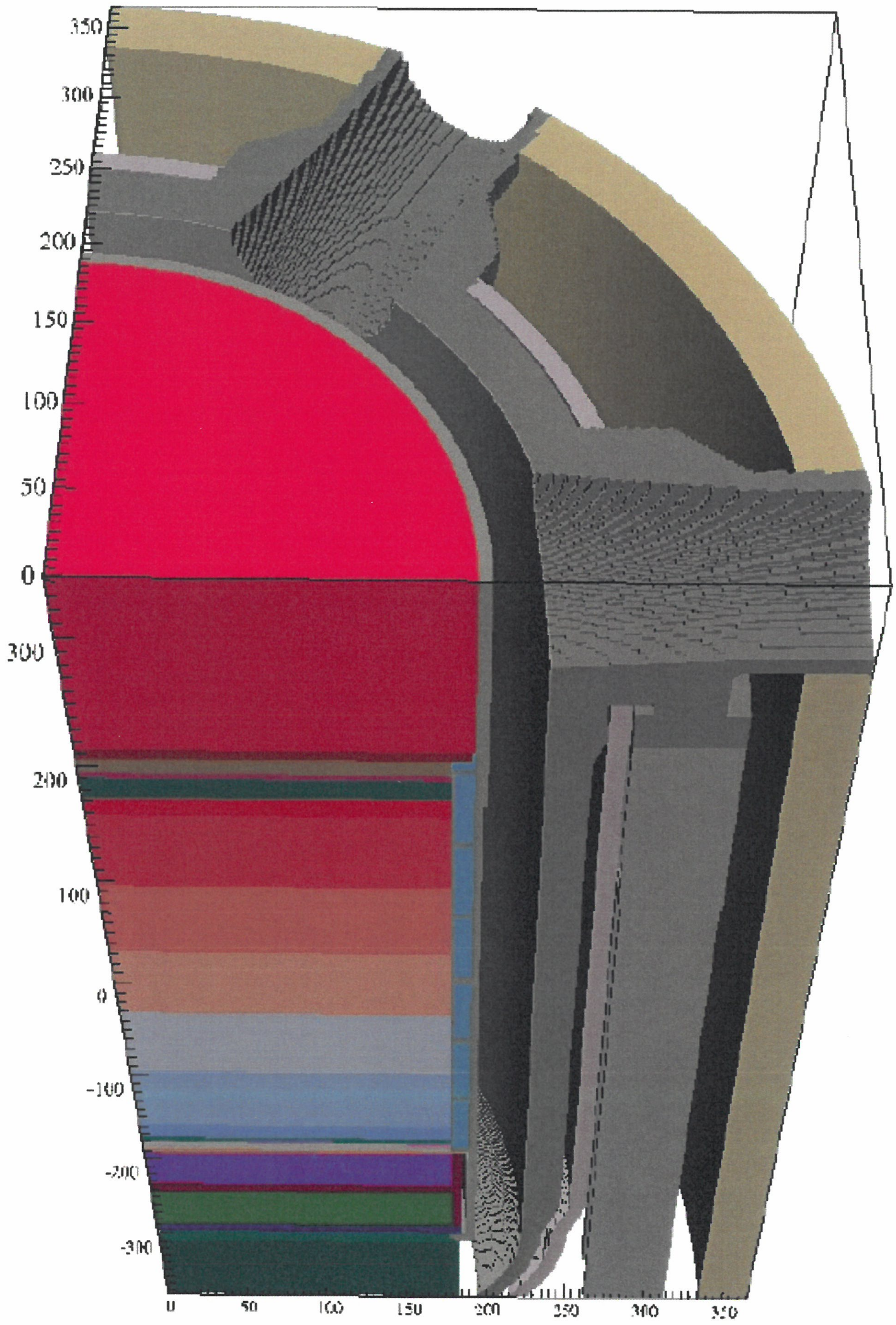

Figure 2.4-5 Top View of the Reactor Geometry at the Nozzle Centerline – Without Thermal Shield (Unit 1, Cycles 6+)

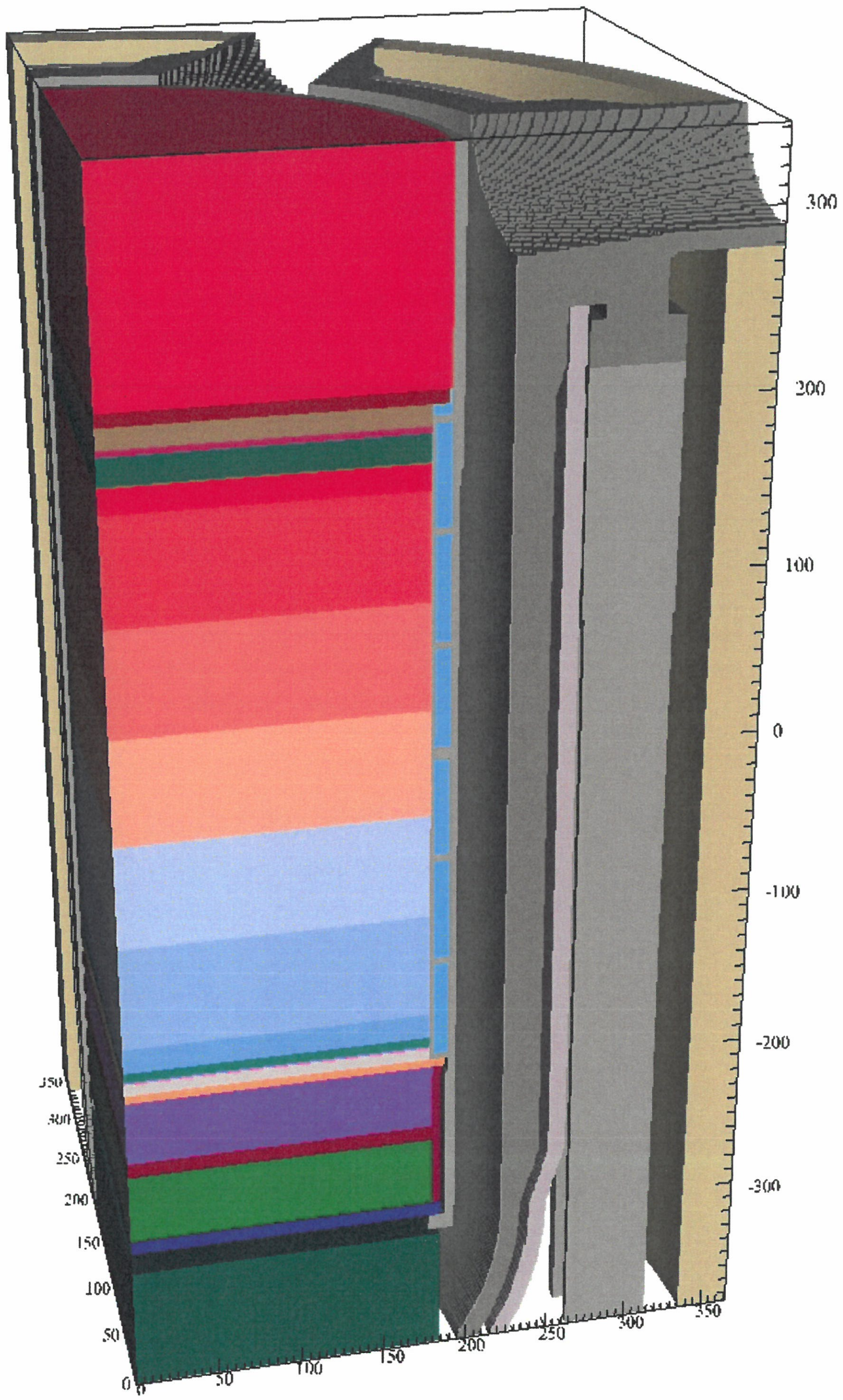

Figure 2.4-6 Oblique View of the Reactor Geometry – Without Thermal Shield (Unit 1, Cycles 6+)

2.5 ST. LUCIE UNIT 2 NEUTRON FLUENCE DATA TABLES AND FIGURES

Table 2.5-1 St. Lucie Unit 2 Fast Neutron (E > 1.0 MeV) Fluence Rate at the RPV Clad/Base Metal Interface

Cycle	Cycle Length (EFPY)	Cumulative Operating Time (EFPY)	Fluence Rate (n/cm²-s)							
			0°	15°	30°	45°	60°	75°	90°	Maximum
1	1.11	1.11	3.19E+10	2.03E+10	1.71E+10	1.26E+10	1.71E+10	1.97E+10	3.19E+10	3.19E+10
2	1.12	2.23	3.36E+10	1.98E+10	1.71E+10	1.28E+10	1.71E+10	1.93E+10	3.37E+10	3.37E+10
3	1.22	3.45	3.01E+10	1.80E+10	1.47E+10	1.07E+10	1.47E+10	1.75E+10	3.02E+10	3.02E+10
4	1.16	4.61	2.05E+10	1.61E+10	1.56E+10	1.18E+10	1.56E+10	1.58E+10	2.05E+10	2.05E+10
5	1.30	5.91	1.99E+10	1.61E+10	1.55E+10	1.13E+10	1.55E+10	1.57E+10	1.99E+10	2.00E+10
6	1.35	7.26	2.14E+10	1.37E+10	1.22E+10	9.79E+09	1.22E+10	1.34E+10	2.14E+10	2.14E+10
7	1.21	8.47	2.31E+10	1.44E+10	1.21E+10	1.02E+10	1.21E+10	1.40E+10	2.32E+10	2.32E+10
8	1.38	9.85	1.40E+10	1.10E+10	1.30E+10	1.01E+10	1.30E+10	1.08E+10	1.41E+10	1.41E+10
9	1.22	11.07	1.92E+10	1.58E+10	1.39E+10	1.00E+10	1.39E+10	1.55E+10	1.92E+10	1.98E+10
10	1.44	12.51	2.05E+10	1.59E+10	1.37E+10	1.06E+10	1.37E+10	1.55E+10	2.05E+10	2.09E+10
11	1.32	13.83	1.92E+10	1.42E+10	1.43E+10	1.16E+10	1.43E+10	1.39E+10	1.92E+10	1.92E+10
12	1.51	15.34	1.94E+10	1.25E+10	1.23E+10	1.07E+10	1.23E+10	1.22E+10	1.94E+10	1.94E+10
13	1.29	16.63	2.14E+10	1.41E+10	1.30E+10	1.14E+10	1.30E+10	1.38E+10	2.14E+10	2.14E+10
14	1.43	18.06	1.87E+10	1.27E+10	1.23E+10	1.06E+10	1.23E+10	1.24E+10	1.87E+10	1.87E+10
15	1.15	19.21	2.18E+10	1.41E+10	1.20E+10	9.78E+09	1.20E+10	1.37E+10	2.19E+10	2.19E+10
16	1.25	20.46	2.22E+10	1.46E+10	1.23E+10	9.93E+09	1.23E+10	1.42E+10	2.22E+10	2.22E+10
17	1.25	21.71	2.08E+10	1.40E+10	1.18E+10	9.70E+09	1.18E+10	1.38E+10	2.16E+10	2.16E+10
18	1.42	23.13	2.00E+10	1.42E+10	1.21E+10	1.00E+10	1.19E+10	1.39E+10	2.01E+10	2.02E+10
19	1.19	24.32	2.54E+10	1.75E+10	1.65E+10	1.29E+10	1.65E+10	1.68E+10	2.52E+10	2.54E+10
20	1.23	25.55	2.99E+10	1.95E+10	1.86E+10	1.54E+10	1.86E+10	1.90E+10	2.99E+10	2.99E+10
21	1.28	26.83	2.85E+10	1.89E+10	1.84E+10	1.50E+10	1.83E+10	1.84E+10	2.85E+10	2.85E+10
22	1.31	28.13	3.30E+10	2.13E+10	1.92E+10	1.68E+10	1.92E+10	2.07E+10	3.31E+10	3.31E+10
23	1.40	29.53	3.30E+10	2.14E+10	2.12E+10	1.70E+10	2.12E+10	2.09E+10	3.30E+10	3.30E+10
24	1.34	30.88	3.01E+10	1.95E+10	1.84E+10	1.46E+10	1.84E+10	1.90E+10	3.02E+10	3.02E+10
25[(a)]	1.43	32.30	2.88E+10	1.87E+10	1.79E+10	1.38E+10	1.80E+10	1.85E+10	2.92E+10	2.92E+10

Note:

(a) Cycle 25 was the current operating cycle at the time the exposures reported in this table were determined. Values listed are based on the projected EFPY for this cycle.

Table 2.5-2 St. Lucie Unit 2 Fast Neutron (E > 1.0 MeV) Fluence at the RPV Clad/Base Metal Interface

Cycle	Cycle Length (EFPY)	Cumulative Operating Time (EFPY)	Fast Neutron (E > 1.0 MeV) Fluence (n/cm^2)							
			0°	15°	30°	45°	60°	75°	90°	Maximum
1	1.11	1.11	1.12E+18	7.10E+17	5.99E+17	4.41E+17	5.99E+17	6.91E+17	1.12E+18	1.12E+18
2	1.12	2.23	2.30E+18	1.41E+18	1.20E+18	8.92E+17	1.20E+18	1.37E+18	2.30E+18	2.30E+18
3	1.22	3.45	3.46E+18	2.10E+18	1.77E+18	1.30E+18	1.77E+18	2.04E+18	3.46E+18	3.46E+18
4	1.16	4.61	4.20E+18	2.68E+18	2.33E+18	1.73E+18	2.33E+18	2.61E+18	4.20E+18	4.20E+18
5	1.30	5.91	5.00E+18	3.33E+18	2.96E+18	2.19E+18	2.96E+18	3.25E+18	5.00E+18	5.00E+18
6	1.35	7.26	5.90E+18	3.90E+18	3.47E+18	2.60E+18	3.47E+18	3.81E+18	5.91E+18	5.91E+18
7	1.21	8.47	6.78E+18	4.45E+18	3.93E+18	2.99E+18	3.93E+18	4.34E+18	6.79E+18	6.79E+18
8	1.38	9.85	7.37E+18	4.92E+18	4.48E+18	3.42E+18	4.48E+18	4.80E+18	7.38E+18	7.38E+18
9	1.22	11.07	8.11E+18	5.53E+18	5.02E+18	3.80E+18	5.02E+18	5.40E+18	8.13E+18	8.13E+18
10	1.44	12.51	9.05E+18	6.25E+18	5.64E+18	4.29E+18	5.64E+18	6.10E+18	9.06E+18	9.06E+18
11	1.32	13.83	9.84E+18	6.83E+18	6.23E+18	4.76E+18	6.23E+18	6.67E+18	9.85E+18	9.85E+18
12	1.51	15.34	1.08E+19	7.43E+18	6.81E+18	5.27E+18	6.81E+18	7.25E+18	1.08E+19	1.08E+19
13	1.29	16.63	1.16E+19	8.00E+18	7.34E+18	5.73E+18	7.34E+18	7.81E+18	1.16E+19	1.16E+19
14	1.43	18.06	1.25E+19	8.57E+18	7.89E+18	6.21E+18	7.89E+18	8.36E+18	1.25E+19	1.25E+19
15	1.15	19.21	1.32E+19	9.08E+18	8.33E+18	6.56E+18	8.32E+18	8.86E+18	1.33E+19	1.33E+19
16	1.25	20.46	1.41E+19	9.65E+18	8.81E+18	6.95E+18	8.81E+18	9.41E+18	1.41E+19	1.41E+19
17	1.25	21.71	1.49E+19	1.02E+19	9.27E+18	7.33E+18	9.27E+18	9.96E+18	1.50E+19	1.50E+19
18	1.42	23.13	1.58E+19	1.08E+19	9.81E+18	7.78E+18	9.80E+18	1.06E+19	1.59E+19	1.59E+19
19	1.19	24.32	1.68E+19	1.15E+19	1.04E+19	8.26E+18	1.04E+19	1.12E+19	1.68E+19	1.68E+19
20	1.23	25.55	1.79E+19	1.22E+19	1.12E+19	8.86E+18	1.11E+19	1.19E+19	1.80E+19	1.80E+19
21	1.28	26.83	1.91E+19	1.30E+19	1.19E+19	9.46E+18	1.19E+19	1.27E+19	1.91E+19	1.91E+19
22	1.31	28.13	2.04E+19	1.39E+19	1.27E+19	1.02E+19	1.27E+19	1.35E+19	2.05E+19	2.05E+19
23	1.40	29.53	2.19E+19	1.48E+19	1.36E+19	1.09E+19	1.36E+19	1.45E+19	2.19E+19	2.19E+19
24	1.34	30.88	2.32E+19	1.57E+19	1.44E+19	1.15E+19	1.44E+19	1.53E+19	2.32E+19	2.32E+19
25[a]	1.43	32.30	2.45E+19	1.65E+19	1.52E+19	1.21E+19	1.52E+19	1.61E+19	2.45E+19	2.45E+19

Table 2.5-2 St. Lucie Unit 2 Fast Neutron (E > 1.0 MeV) Fluence at the RPV Clad/Base Metal Interface (Continued)

Projections with no bias on the peripheral and re-entrant corner assembly relative powers										
Future(b)	--	36.00	2.80E+19	1.88E+19	1.74E+19	1.38E+19	1.73E+19	1.83E+19	2.81E+19	2.81E+19
Future(b)	--	42.00	3.37E+19	2.25E+19	2.08E+19	1.66E+19	2.08E+19	2.19E+19	3.38E+19	3.38E+19
Future(b)	--	48.00	3.94E+19	2.62E+19	2.43E+19	1.94E+19	2.43E+19	2.55E+19	3.95E+19	3.95E+19
Future(b)	--	54.00	4.51E+19	2.99E+19	2.78E+19	2.21E+19	2.78E+19	2.91E+19	4.52E+19	4.52E+19
Future(b)	--	60.00	5.08E+19	3.36E+19	3.13E+19	2.49E+19	3.12E+19	3.27E+19	5.09E+19	5.09E+19
Future(b)	--	66.00	5.65E+19	3.73E+19	3.48E+19	2.76E+19	3.47E+19	3.63E+19	5.66E+19	5.66E+19
Future(b)	--	72.00	6.22E+19	4.10E+19	3.82E+19	3.04E+19	3.82E+19	3.99E+19	6.23E+19	6.23E+19
Projections with a +10% bias on the peripheral and re-entrant corner assembly relative powers										
Future(b)	--	36.00	2.83E+19	1.90E+19	1.76E+19	1.40E+19	1.75E+19	1.85E+19	2.84E+19	2.84E+19
Future(b)	--	42.00	3.45E+19	2.30E+19	2.14E+19	1.70E+19	2.13E+19	2.24E+19	3.46E+19	3.46E+19
Future(b)	--	48.00	4.07E+19	2.70E+19	2.52E+19	2.01E+19	2.51E+19	2.64E+19	4.08E+19	4.08E+19
Future(b)	--	54.00	4.69E+19	3.11E+19	2.90E+19	2.31E+19	2.90E+19	3.03E+19	4.70E+19	4.70E+19
Future(b)	--	60.00	5.31E+19	3.51E+19	3.28E+19	2.61E+19	3.28E+19	3.42E+19	5.32E+19	5.32E+19
Future(b)	--	66.00	5.93E+19	3.91E+19	3.66E+19	2.91E+19	3.66E+19	3.81E+19	5.94E+19	5.94E+19
Future(b)	--	72.00	6.55E+19	4.31E+19	4.04E+19	3.22E+19	4.04E+19	4.21E+19	6.56E+19	6.56E+19

Notes:

(a) Cycle 25 was the current operating cycle at the time the exposures reported in this table were determined. Values listed are based on the projected EFPY for this cycle.

(b) Values beyond Cycle 25 are based on the average core power distributions and reactor operating conditions of Cycle 24 and are determined both with and without a 1.1 bias on the peripheral and re-entrant corner assembly relative powers.

Table 2.5-3 St. Lucie Unit 2 Calculated Maximum Iron Atom Displacement Rate at the RPV Clad/Base Metal Interface

Cycle	Cycle Length (EFPY)	Cumulative Operating Time (EFPY)	Iron Atom Displacement Rate (dpa/s)							
			0°	15°	30°	45°	60°	75°	90°	Maximum
1	1.11	1.11	4.86E-11	3.11E-11	2.61E-11	1.94E-11	2.61E-11	3.04E-11	4.86E-11	4.86E-11
2	1.12	2.23	5.13E-11	3.04E-11	2.61E-11	1.97E-11	2.61E-11	2.98E-11	5.12E-11	5.13E-11
3	1.22	3.45	4.59E-11	2.76E-11	2.25E-11	1.65E-11	2.25E-11	2.71E-11	4.58E-11	4.59E-11
4	1.16	4.61	3.13E-11	2.47E-11	2.38E-11	1.81E-11	2.38E-11	2.43E-11	3.13E-11	3.14E-11
5	1.30	5.91	3.05E-11	2.47E-11	2.37E-11	1.75E-11	2.37E-11	2.43E-11	3.04E-11	3.06E-11
6	1.35	7.26	3.27E-11	2.11E-11	1.86E-11	1.51E-11	1.86E-11	2.07E-11	3.26E-11	3.27E-11
7	1.21	8.47	3.53E-11	2.21E-11	1.86E-11	1.57E-11	1.86E-11	2.17E-11	3.53E-11	3.53E-11
8	1.38	9.85	2.15E-11	1.69E-11	1.99E-11	1.56E-11	1.99E-11	1.66E-11	2.14E-11	2.15E-11
9	1.22	11.07	2.94E-11	2.43E-11	2.12E-11	1.54E-11	2.12E-11	2.38E-11	2.93E-11	3.02E-11
10	1.44	12.51	3.14E-11	2.44E-11	2.09E-11	1.63E-11	2.09E-11	2.39E-11	3.13E-11	3.19E-11
11	1.32	13.83	2.94E-11	2.19E-11	2.18E-11	1.78E-11	2.18E-11	2.15E-11	2.93E-11	2.94E-11
12	1.51	15.34	2.97E-11	1.93E-11	1.89E-11	1.65E-11	1.89E-11	1.89E-11	2.96E-11	2.97E-11
13	1.29	16.63	3.27E-11	2.17E-11	2.00E-11	1.75E-11	2.00E-11	2.13E-11	3.26E-11	3.27E-11
14	1.43	18.06	2.86E-11	1.95E-11	1.88E-11	1.63E-11	1.88E-11	1.91E-11	2.85E-11	2.86E-11
15	1.15	19.21	3.34E-11	2.17E-11	1.84E-11	1.51E-11	1.84E-11	2.12E-11	3.33E-11	3.34E-11
16	1.25	20.46	3.40E-11	2.25E-11	1.88E-11	1.53E-11	1.88E-11	2.20E-11	3.39E-11	3.40E-11
17	1.25	21.71	3.19E-11	2.15E-11	1.81E-11	1.49E-11	1.81E-11	2.14E-11	3.29E-11	3.29E-11
18	1.42	23.13	3.06E-11	2.17E-11	1.85E-11	1.55E-11	1.83E-11	2.15E-11	3.08E-11	3.09E-11
19	1.19	24.32	3.89E-11	2.69E-11	2.52E-11	1.98E-11	2.52E-11	2.60E-11	3.84E-11	3.89E-11
20	1.23	25.55	4.57E-11	3.00E-11	2.84E-11	2.36E-11	2.84E-11	2.93E-11	4.56E-11	4.57E-11
21	1.28	26.83	4.36E-11	2.91E-11	2.81E-11	2.31E-11	2.79E-11	2.84E-11	4.35E-11	4.36E-11
22	1.31	28.13	5.05E-11	3.28E-11	2.93E-11	2.58E-11	2.93E-11	3.20E-11	5.04E-11	5.05E-11
23	1.40	29.53	5.04E-11	3.29E-11	3.23E-11	2.61E-11	3.23E-11	3.22E-11	5.03E-11	5.04E-11
24	1.34	30.88	4.60E-11	3.00E-11	2.81E-11	2.24E-11	2.80E-11	2.94E-11	4.60E-11	4.60E-11
25[(a)]	1.43	32.30	4.41E-11	2.87E-11	2.74E-11	2.12E-11	2.74E-11	2.86E-11	4.44E-11	4.44E-11

Note:

(a) Cycle 25 was the current operating cycle at the time the exposures reported in this table were determined. Values listed are based on the projected EFPY for this cycle.

Table 2.5-4 St. Lucie Unit 2 Iron Atom Displacements at the RPV Clad/Base Metal Interface

Cycle	Cycle Length (EFPY)	Cumulative Operating Time (EFPY)	Iron Atom Displacements (dpa)							
			0°	15°	30°	45°	60°	75°	90°	Maximum
1	1.11	1.11	1.70E-03	1.09E-03	9.14E-04	6.79E-04	9.14E-04	1.07E-03	1.70E-03	1.70E-03
2	1.12	2.23	3.51E-03	2.16E-03	1.83E-03	1.37E-03	1.83E-03	2.11E-03	3.50E-03	3.51E-03
3	1.22	3.45	5.28E-03	3.22E-03	2.70E-03	2.01E-03	2.70E-03	3.15E-03	5.27E-03	5.28E-03
4	1.16	4.61	6.40E-03	4.11E-03	3.56E-03	2.66E-03	3.55E-03	4.03E-03	6.39E-03	6.40E-03
5	1.30	5.91	7.63E-03	5.11E-03	4.52E-03	3.37E-03	4.52E-03	5.02E-03	7.62E-03	7.63E-03
6	1.35	7.26	9.01E-03	6.00E-03	5.30E-03	4.00E-03	5.29E-03	5.88E-03	8.99E-03	9.01E-03
7	1.21	8.47	1.04E-02	6.84E-03	6.00E-03	4.60E-03	6.00E-03	6.71E-03	1.03E-02	1.04E-02
8	1.38	9.85	1.13E-02	7.56E-03	6.84E-03	5.26E-03	6.84E-03	7.41E-03	1.12E-02	1.13E-02
9	1.22	11.07	1.24E-02	8.49E-03	7.66E-03	5.86E-03	7.66E-03	8.33E-03	1.24E-02	1.24E-02
10	1.44	12.51	1.38E-02	9.60E-03	8.61E-03	6.60E-03	8.61E-03	9.42E-03	1.38E-02	1.38E-02
11	1.32	13.83	1.50E-02	1.05E-02	9.52E-03	7.33E-03	9.51E-03	1.03E-02	1.50E-02	1.50E-02
12	1.51	15.34	1.64E-02	1.14E-02	1.04E-02	8.12E-03	1.04E-02	1.12E-02	1.64E-02	1.64E-02
13	1.29	16.63	1.78E-02	1.23E-02	1.12E-02	8.83E-03	1.12E-02	1.21E-02	1.77E-02	1.78E-02
14	1.43	18.06	1.91E-02	1.32E-02	1.21E-02	9.56E-03	1.21E-02	1.29E-02	1.90E-02	1.91E-02
15	1.15	19.21	2.03E-02	1.40E-02	1.27E-02	1.01E-02	1.27E-02	1.37E-02	2.02E-02	2.03E-02
16	1.25	20.46	2.16E-02	1.48E-02	1.35E-02	1.07E-02	1.35E-02	1.45E-02	2.15E-02	2.16E-02
17	1.25	21.71	2.28E-02	1.57E-02	1.42E-02	1.13E-02	1.42E-02	1.54E-02	2.28E-02	2.28E-02
18	1.42	23.13	2.42E-02	1.66E-02	1.50E-02	1.20E-02	1.50E-02	1.63E-02	2.42E-02	2.42E-02
19	1.19	24.32	2.57E-02	1.77E-02	1.59E-02	1.27E-02	1.59E-02	1.73E-02	2.56E-02	2.57E-02
20	1.23	25.55	2.74E-02	1.88E-02	1.70E-02	1.36E-02	1.70E-02	1.85E-02	2.74E-02	2.74E-02
21	1.28	26.83	2.92E-02	2.00E-02	1.82E-02	1.46E-02	1.82E-02	1.96E-02	2.92E-02	2.92E-02
22	1.31	28.13	3.13E-02	2.13E-02	1.94E-02	1.56E-02	1.94E-02	2.09E-02	3.12E-02	3.13E-02
23	1.40	29.53	3.35E-02	2.28E-02	2.08E-02	1.68E-02	2.08E-02	2.23E-02	3.34E-02	3.35E-02
24	1.34	30.88	3.54E-02	2.41E-02	2.20E-02	1.77E-02	2.20E-02	2.36E-02	3.54E-02	3.54E-02
25[(a)]	1.43	32.30	3.74E-02	2.54E-02	2.32E-02	1.87E-02	2.32E-02	2.49E-02	3.74E-02	3.74E-02

Table 2.5-4 St. Lucie Unit 2 Iron Atom Displacements at the RPV Clad/Base Metal Interface (Continued)

Projections with no bias on the peripheral and re-entrant corner assembly relative powers										
Future(b)	--	36.00	4.28E-02	2.89E-02	2.65E-02	2.13E-02	2.65E-02	2.83E-02	4.28E-02	4.28E-02
Future(b)	--	42.00	5.15E-02	3.45E-02	3.18E-02	2.55E-02	3.18E-02	3.39E-02	5.15E-02	5.15E-02
Future(b)	--	48.00	6.02E-02	4.02E-02	3.71E-02	2.98E-02	3.71E-02	3.94E-02	6.02E-02	6.02E-02
Future(b)	--	54.00	6.89E-02	4.59E-02	4.25E-02	3.40E-02	4.24E-02	4.50E-02	6.89E-02	6.89E-02
Future(b)	--	60.00	7.76E-02	5.16E-02	4.78E-02	3.83E-02	4.77E-02	5.06E-02	7.76E-02	7.76E-02
Future(b)	--	66.00	8.63E-02	5.73E-02	5.31E-02	4.25E-02	5.30E-02	5.61E-02	8.63E-02	8.63E-02
Future(b)	--	72.00	9.51E-02	6.29E-02	5.84E-02	4.68E-02	5.83E-02	6.17E-02	9.50E-02	9.51E-02
Projections with a +10% bias on the peripheral and re-entrant corner assembly relative powers										
Future(b)	--	36.00	4.32E-02	2.92E-02	2.68E-02	2.16E-02	2.68E-02	2.86E-02	4.32E-02	4.32E-02
Future(b)	--	42.00	5.27E-02	3.54E-02	3.26E-02	2.62E-02	3.26E-02	3.47E-02	5.27E-02	5.27E-02
Future(b)	--	48.00	6.22E-02	4.15E-02	3.85E-02	3.09E-02	3.84E-02	4.07E-02	6.21E-02	6.22E-02
Future(b)	--	54.00	7.17E-02	4.77E-02	4.43E-02	3.55E-02	4.42E-02	4.68E-02	7.16E-02	7.17E-02
Future(b)	--	60.00	8.11E-02	5.39E-02	5.01E-02	4.02E-02	5.00E-02	5.29E-02	8.11E-02	8.11E-02
Future(b)	--	66.00	9.06E-02	6.01E-02	5.59E-02	4.48E-02	5.58E-02	5.89E-02	9.05E-02	9.06E-02
Future(b)	--	72.00	1.00E-01	6.63E-02	6.17E-02	4.95E-02	6.16E-02	6.50E-02	1.00E-01	1.00E-01

Notes:

(a) Cycle 25 was the current operating cycle at the time the exposures reported in this table were determined. Values listed are based on the projected EFPY for this cycle.

(b) Values beyond Cycle 25 are based on the average core power distributions and reactor operating conditions of Cycle 24 and are determined both with and without a 1.1 bias on the peripheral and re-entrant corner assembly relative powers.

Table 2.5-5 St. Lucie Unit 2 Fast Neutron Fluence (E > 1.0 MeV) at RPV Welds and Shells

Projections with no bias on the peripheral and re-entrant corner assembly relative powers				
Material	**Fast Neutron (E > 1.0 MeV) Fluence (n/cm²)**			
	32.30 EFPY[a]	**36 EFPY**	**42 EFPY**	**48 EFPY**
Inlet (Cold Leg)-Nozzle-to-Upper-Shell Weld (lowest extent)	2.89E+16	3.29E+16	3.93E+16	4.58E+16
Outlet (Hot Leg)-Nozzle-to-Upper-Shell Weld (lowest extent)	3.97E+16	4.51E+16	5.39E+16	6.27E+16
Upper Shell[b]	6.47E+17	7.23E+17	8.47E+17	9.70E+17
Upper-to-Intermediate-Shell Circumferential Weld	7.46E+17	8.34E+17	9.77E+17	1.12E+18
Intermediate Shell	2.45E+19	2.81E+19	3.38E+19	3.95E+19
Intermediate Shell Longitudinal Weld – 15°	1.65E+19	1.88E+19	2.25E+19	2.62E+19
Intermediate Shell Longitudinal Weld – 135°	1.21E+19	1.38E+19	1.66E+19	1.94E+19
Intermediate Shell Longitudinal Weld – 255°[c]	1.65E+19	1.88E+19	2.25E+19	2.62E+19
Intermediate-to-Lower-Shell Circumferential Weld	2.44E+19	2.79E+19	3.35E+19	3.92E+19
Lower Shell	2.44E+19	2.79E+19	3.36E+19	3.93E+19
Lower Shell Longitudinal Weld – 15°	1.64E+19	1.86E+19	2.23E+19	2.60E+19
Lower Shell Longitudinal Weld – 135°	1.21E+19	1.37E+19	1.65E+19	1.92E+19
Lower Shell Longitudinal Weld – 255°[c]	1.64E+19	1.86E+19	2.23E+19	2.60E+19
Lower-Shell-to-Bottom-Head Circumferential Weld	2.41E+16	2.75E+16	3.29E+16	3.83E+16

Projections with no bias on the peripheral and re-entrant corner assembly relative powers				
Material	**Fast Neutron (E > 1.0 MeV) Fluence (n/cm²)**			
	54 EFPY	**60 EFPY**	**66 EFPY**	**72 EFPY**
Inlet (Cold Leg)-Nozzle-to-Upper-Shell Weld (lowest extent)	5.22E+16	5.86E+16	6.50E+16	7.15E+16
Outlet (Hot Leg)-Nozzle-to-Upper-Shell Weld (lowest extent)	7.15E+16	8.03E+16	8.91E+16	9.79E+16
Upper Shell[b]	1.09E+18	1.22E+18	1.34E+18	1.46E+18
Upper-to-Intermediate-Shell Circumferential Weld	1.26E+18	1.41E+18	1.55E+18	1.69E+18
Intermediate Shell	4.52E+19	5.09E+19	5.66E+19	6.23E+19
Intermediate Shell Longitudinal Weld – 15°	2.99E+19	3.36E+19	3.73E+19	4.10E+19
Intermediate Shell Longitudinal Weld – 135°	2.21E+19	2.49E+19	2.76E+19	3.04E+19
Intermediate Shell Longitudinal Weld – 255°[c]	2.99E+19	3.36E+19	3.73E+19	4.10E+19
Intermediate-to-Lower-Shell Circumferential Weld	4.49E+19	5.06E+19	5.62E+19	6.19E+19
Lower Shell	4.50E+19	5.07E+19	5.64E+19	6.21E+19
Lower Shell Longitudinal Weld – 15°	2.97E+19	3.34E+19	3.70E+19	4.07E+19
Lower Shell Longitudinal Weld – 135°	2.20E+19	2.47E+19	2.75E+19	3.02E+19
Lower Shell Longitudinal Weld – 255°[c]	2.97E+19	3.34E+19	3.70E+19	4.07E+19
Lower-Shell-to-Bottom-Head Circumferential Weld	4.37E+16	4.92E+16	5.46E+16	6.00E+16

Table 2.5-5 St. Lucie Unit 2 Fast Neutron Fluence (E > 1.0 MeV) at RPV Welds and Shells (Continued)

Projections with a +10% bias on the peripheral and re-entrant corner assembly relative powers				
Material	**Fast Neutron (E > 1.0 MeV) Fluence (n/cm²)**			
	32.30 EFPY[(a)]	**36 EFPY**	**42 EFPY**	**48 EFPY**
Inlet (Cold Leg)-Nozzle-to-Upper-Shell Weld (lowest extent)	2.89E+16	3.33E+16	4.03E+16	4.73E+16
Outlet (Hot Leg)-Nozzle-to-Upper-Shell Weld (lowest extent)	3.97E+16	4.56E+16	5.52E+16	6.48E+16
Upper Shell[(b)]	6.47E+17	7.28E+17	8.60E+17	9.92E+17
Upper-to-Intermediate-Shell Circumferential Weld	7.46E+17	8.40E+17	9.92E+17	1.14E+18
Intermediate Shell	2.45E+19	2.84E+19	3.46E+19	4.08E+19
Intermediate Shell Longitudinal Weld – 15°	1.65E+19	1.90E+19	2.30E+19	2.70E+19
Intermediate Shell Longitudinal Weld – 135°	1.21E+19	1.40E+19	1.70E+19	2.01E+19
Intermediate Shell Longitudinal Weld – 255°[(c)]	1.65E+19	1.90E+19	2.30E+19	2.70E+19
Intermediate-to-Lower-Shell Circumferential Weld	2.44E+19	2.82E+19	3.43E+19	4.05E+19
Lower Shell	2.44E+19	2.82E+19	3.44E+19	4.06E+19
Lower Shell Longitudinal Weld – 15°	1.64E+19	1.88E+19	2.29E+19	2.69E+19
Lower Shell Longitudinal Weld – 135°	1.21E+19	1.39E+19	1.69E+19	1.99E+19
Lower Shell Longitudinal Weld – 255°[(c)]	1.64E+19	1.88E+19	2.29E+19	2.69E+19
Lower-Shell-to-Bottom-Head Circumferential Weld	2.41E+16	2.78E+16	3.37E+16	3.96E+16

Projections with a +10% bias on the peripheral and re-entrant corner assembly relative powers				
Material	**Fast Neutron (E > 1.0 MeV) Fluence (n/cm²)**			
	54 EFPY	**60 EFPY**	**66 EFPY**	**72 EFPY**
Inlet (Cold Leg)-Nozzle-to-Upper-Shell Weld (lowest extent)	5.43E+16	6.13E+16	6.84E+16	7.54E+16
Outlet (Hot Leg)-Nozzle-to-Upper-Shell Weld (lowest extent)	7.44E+16	8.40E+16	9.36E+16	1.03E+17
Upper Shell[(b)]	1.12E+18	1.26E+18	1.39E+18	1.52E+18
Upper-to-Intermediate-Shell Circumferential Weld	1.30E+18	1.45E+18	1.60E+18	1.75E+18
Intermediate Shell	4.70E+19	5.32E+19	5.94E+19	6.56E+19
Intermediate Shell Longitudinal Weld – 15°	3.11E+19	3.51E+19	3.91E+19	4.31E+19
Intermediate Shell Longitudinal Weld – 135°	2.31E+19	2.61E+19	2.91E+19	3.22E+19
Intermediate Shell Longitudinal Weld – 255°[(c)]	3.11E+19	3.51E+19	3.91E+19	4.31E+19
Intermediate-to-Lower-Shell Circumferential Weld	4.67E+19	5.28E+19	5.90E+19	6.52E+19
Lower Shell	4.68E+19	5.29E+19	5.91E+19	6.53E+19
Lower Shell Longitudinal Weld – 15°	3.09E+19	3.49E+19	3.89E+19	4.29E+19
Lower Shell Longitudinal Weld – 135°	2.29E+19	2.59E+19	2.89E+19	3.20E+19
Lower Shell Longitudinal Weld – 255°[(c)]	3.09E+19	3.49E+19	3.89E+19	4.29E+19
Lower-Shell-to-Bottom-Head Circumferential Weld	4.55E+16	5.14E+16	5.73E+16	6.32E+16

Notes:

(a) Value listed is the projected EFPY at the end of Cycle 25.

(b) Exposure values for the upper shell longitudinal welds are bounded by the exposure values for the upper shell.

(c) Exposure values for the intermediate shell and lower shell 255° longitudinal welds are bounded by the exposure values for the intermediate shell and lower shell 15° longitudinal welds.

Table 2.5-6 St. Lucie Unit 2 Iron Atom Displacements at the RPV Welds and Shells

Projections with no bias on the peripheral and re-entrant corner assembly relative powers				
Material	**Iron Atom Displacements (dpa)**			
	32.30 EFPY[(a)]	**36 EFPY**	**42 EFPY**	**48 EFPY**
Inlet (Cold Leg)-Nozzle-to-Upper-Shell Weld (lowest extent)	2.42E-04	2.75E-04	3.29E-04	3.84E-04
Outlet (Hot Leg)-Nozzle-to-Upper-Shell Weld (lowest extent)	3.16E-04	3.59E-04	4.29E-04	5.00E-04
Upper Shell[(b)]	1.11E-03	1.25E-03	1.46E-03	1.68E-03
Upper-to-Intermediate-Shell Circumferential Weld	1.27E-03	1.43E-03	1.67E-03	1.92E-03
Intermediate Shell	3.74E-02	4.28E-02	5.15E-02	6.02E-02
Intermediate Shell Longitudinal Weld – 15°	2.54E-02	2.89E-02	3.45E-02	4.02E-02
Intermediate Shell Longitudinal Weld – 135°	1.87E-02	2.13E-02	2.55E-02	2.98E-02
Intermediate Shell Longitudinal Weld – 255°[(c)]	2.54E-02	2.89E-02	3.45E-02	4.02E-02
Intermediate-to-Lower-Shell Circumferential Weld	3.72E-02	4.25E-02	5.12E-02	5.98E-02
Lower Shell	3.72E-02	4.25E-02	5.12E-02	5.99E-02
Lower Shell Longitudinal Weld – 15°	2.52E-02	2.86E-02	3.43E-02	3.99E-02
Lower Shell Longitudinal Weld – 135°	1.85E-02	2.11E-02	2.53E-02	2.96E-02
Lower Shell Longitudinal Weld – 255°[(c)]	2.52E-02	2.86E-02	3.43E-02	3.99E-02
Lower-Shell-to-Bottom-Head Circumferential Weld	1.58E-04	1.80E-04	2.16E-04	2.52E-04

Projections with no bias on the peripheral and re-entrant corner assembly relative powers				
Material	**Iron Atom Displacements (dpa)**			
	54 EFPY	**60 EFPY**	**66 EFPY**	**72 EFPY**
Inlet (Cold Leg)-Nozzle-to-Upper-Shell Weld (lowest extent)	4.38E-04	4.92E-04	5.46E-04	6.00E-04
Outlet (Hot Leg)-Nozzle-to-Upper-Shell Weld (lowest extent)	5.70E-04	6.41E-04	7.11E-04	7.81E-04
Upper Shell[(b)]	1.89E-03	2.11E-03	2.33E-03	2.54E-03
Upper-to-Intermediate-Shell Circumferential Weld	2.17E-03	2.41E-03	2.66E-03	2.91E-03
Intermediate Shell	6.89E-02	7.76E-02	8.63E-02	9.51E-02
Intermediate Shell Longitudinal Weld – 15°	4.59E-02	5.16E-02	5.73E-02	6.30E-02
Intermediate Shell Longitudinal Weld – 135°	3.40E-02	3.83E-02	4.25E-02	4.68E-02
Intermediate Shell Longitudinal Weld – 255°[(c)]	4.59E-02	5.16E-02	5.73E-02	6.30E-02
Intermediate-to-Lower-Shell Circumferential Weld	6.85E-02	7.71E-02	8.58E-02	9.44E-02
Lower Shell	6.85E-02	7.72E-02	8.59E-02	9.46E-02
Lower Shell Longitudinal Weld – 15°	4.56E-02	5.12E-02	5.69E-02	6.25E-02
Lower Shell Longitudinal Weld – 135°	3.38E-02	3.80E-02	4.22E-02	4.64E-02
Lower Shell Longitudinal Weld – 255°[(c)]	4.56E-02	5.12E-02	5.69E-02	6.25E-02
Lower-Shell-to-Bottom-Head Circumferential Weld	2.87E-04	3.23E-04	3.59E-04	3.95E-04

Table 2.5-6 St. Lucie Unit 2 Iron Atom Displacements at the RPV Welds and Shells (Continued)

Projections with a +10% bias on the peripheral and re-entrant corner assembly relative powers				
Material	**Iron Atom Displacements (dpa)**			
	32.30 EFPY[(a)]	**36 EFPY**	**42 EFPY**	**48 EFPY**
Inlet (Cold Leg)-Nozzle-to-Upper-Shell Weld (lowest extent)	2.42E-04	2.79E-04	3.38E-04	3.97E-04
Outlet (Hot Leg)-Nozzle-to-Upper-Shell Weld (lowest extent)	3.16E-04	3.63E-04	4.40E-04	5.17E-04
Upper Shell[(b)]	1.11E-03	1.26E-03	1.49E-03	1.72E-03
Upper-to-Intermediate-Shell Circumferential Weld	1.27E-03	1.44E-03	1.70E-03	1.96E-03
Intermediate Shell	3.74E-02	4.32E-02	5.27E-02	6.22E-02
Intermediate Shell Longitudinal Weld – 15°	2.54E-02	2.92E-02	3.54E-02	4.16E-02
Intermediate Shell Longitudinal Weld – 135°	1.87E-02	2.16E-02	2.62E-02	3.09E-02
Intermediate Shell Longitudinal Weld – 255°[(c)]	2.54E-02	2.92E-02	3.54E-02	4.16E-02
Intermediate-to-Lower-Shell Circumferential Weld	3.72E-02	4.30E-02	5.24E-02	6.18E-02
Lower Shell	3.72E-02	4.30E-02	5.24E-02	6.18E-02
Lower Shell Longitudinal Weld – 15°	2.52E-02	2.89E-02	3.51E-02	4.12E-02
Lower Shell Longitudinal Weld – 135°	1.85E-02	2.14E-02	2.60E-02	3.06E-02
Lower Shell Longitudinal Weld – 255°[(c)]	2.52E-02	2.89E-02	3.51E-02	4.12E-02
Lower-Shell-to-Bottom-Head Circumferential Weld	1.58E-04	1.82E-04	2.21E-04	2.60E-04

Projections with a +10% bias on the peripheral and re-entrant corner assembly relative powers				
Material	**Iron Atom Displacements (dpa)**			
	54 EFPY	**60 EFPY**	**66 EFPY**	**72 EFPY**
Inlet (Cold Leg)-Nozzle-to-Upper-Shell Weld (lowest extent)	4.56E-04	5.15E-04	5.74E-04	6.33E-04
Outlet (Hot Leg)-Nozzle-to-Upper-Shell Weld (lowest extent)	5.93E-04	6.70E-04	7.47E-04	8.24E-04
Upper Shell[(b)]	1.95E-03	2.18E-03	2.41E-03	2.64E-03
Upper-to-Intermediate-Shell Circumferential Weld	2.23E-03	2.49E-03	2.76E-03	3.02E-03
Intermediate Shell	7.17E-02	8.11E-02	9.06E-02	1.00E-01
Intermediate Shell Longitudinal Weld – 15°	4.77E-02	5.39E-02	6.01E-02	6.63E-02
Intermediate Shell Longitudinal Weld – 135°	3.55E-02	4.02E-02	4.48E-02	4.95E-02
Intermediate Shell Longitudinal Weld – 255°[(c)]	4.77E-02	5.39E-02	6.01E-02	6.63E-02
Intermediate-to-Lower-Shell Circumferential Weld	7.12E-02	8.06E-02	9.00E-02	9.94E-02
Lower Shell	7.12E-02	8.07E-02	9.01E-02	9.95E-02
Lower Shell Longitudinal Weld – 15°	4.74E-02	5.35E-02	5.97E-02	6.58E-02
Lower Shell Longitudinal Weld – 135°	3.52E-02	3.99E-02	4.45E-02	4.91E-02
Lower Shell Longitudinal Weld – 255°[(c)]	4.74E-02	5.35E-02	5.97E-02	6.58E-02
Lower-Shell-to-Bottom-Head Circumferential Weld	2.99E-04	3.38E-04	3.77E-04	4.16E-04

Notes:

(a) Value listed is the projected EFPY at the end of Cycle 25.

(b) Exposure values for the upper shell longitudinal welds are bounded by the exposure values for the upper shell.

(c) Exposure values for the intermediate shell and lower shell 255° longitudinal welds are bounded by the exposure values for the intermediate shell and lower shell 15° longitudinal welds.

Table 2.5-7 St. Lucie Unit 2 Fast Neutron (E > 1.0 MeV) Fluence Rate at the Geometric Center of the Surveillance Capsules

Cycle	Cycle Length (EFPY)	Cumulative Operating Time (EFPY)	Fluence Rate (n/cm^2-s)	
			7°	14°
1	1.11	1.11	4.06E+10	2.86E+10
2	1.12	2.23	4.01E+10	2.72E+10
3	1.22	3.45	3.62E+10	2.49E+10
4	1.16	4.61	2.66E+10	2.16E+10
5	1.30	5.91	2.62E+10	2.17E+10
6	1.35	7.26	2.58E+10	1.86E+10
7	1.21	8.47	2.79E+10	1.96E+10
8	1.38	9.85	1.72E+10	1.40E+10
9	1.22	11.07	2.62E+10	2.16E+10
10	1.44	12.51	2.78E+10	2.21E+10
11	1.32	13.83	2.49E+10	1.95E+10
12	1.51	15.34	2.42E+10	1.74E+10
13	1.29	16.63	2.70E+10	1.97E+10
14	1.43	18.06	2.37E+10	1.76E+10
15	1.15	19.21	2.77E+10	1.98E+10
16	1.25	20.46	2.85E+10	2.06E+10
17	1.25	21.71	2.78E+10	2.01E+10
18	1.42	23.13	2.66E+10	2.01E+10
19	1.19	24.32	3.26E+10	2.41E+10
20	1.23	25.55	3.78E+10	2.72E+10
21	1.28	26.83	3.63E+10	2.64E+10
22	1.31	28.13	4.25E+10	3.03E+10
23	1.40	29.53	4.18E+10	3.00E+10
24	1.34	30.88	3.81E+10	2.73E+10
25[a]	1.43	32.30	3.69E+10	2.66E+10

Note:

(a) Cycle 25 was the current operating cycle at the time the exposures reported in this table were determined. Values listed are based on the projected EFPY for this cycle.

Table 2.5-8 St. Lucie Unit 2 Fast Neutron (E > 1.0 MeV) Fluence at the Geometric Center of the Surveillance Capsules

Cycle	Cycle Length (EFPY)	Cumulative Operating Time (EFPY)	Fluence (n/cm^2)	
			7°	14°
1	1.11	1.11	1.42E+18[a]	1.00E+18
2	1.12	2.23	2.84E+18	1.97E+18
3	1.22	3.45	4.23E+18	2.92E+18
4	1.16	4.61	5.20E+18	3.72E+18
5	1.30	5.91	6.28E+18	4.60E+18
6	1.35	7.26	7.38E+18	5.39E+18
7	1.21	8.47	8.44E+18	6.14E+18
8	1.38	9.85	9.19E+18	6.75E+18
9	1.22	11.07	1.02E+19[b]	7.59E+18
10	1.44	12.51	1.15E+19	8.59E+18
11	1.32	13.83	1.25E+19	9.40E+18
12	1.51	15.34	1.37E+19	1.02E+19
13	1.29	16.63	1.48E+19	1.10E+19
14	1.43	18.06	1.58E+19	1.18E+19
15	1.15	19.21	1.68E+19	1.25E+19
16	1.25	20.46	1.80E+19	1.34E+19
17	1.25	21.71	1.91E+19	1.42E+19
18	1.42	23.13	2.02E+19	1.51E+19
19	1.19	24.32	2.15E+19	1.60E+19
20	1.23	25.55	2.29E+19[c]	1.70E+19
21	1.28	26.83	2.44E+19	1.81E+19
22	1.31	28.13	2.61E+19	1.93E+19
23	1.40	29.53	2.80E+19	2.06E+19
24	1.34	30.88	2.96E+19	2.18E+19
25[d]	1.43	32.30	3.13E+19	2.30E+19

Table 2.5-8 St. Lucie Unit 2 Fast Neutron (E > 1.0 MeV) Fluence at the Geometric Center of the Surveillance Capsules (Continued)

No bias on the peripheral and re-entrant corner assembly relative powers				
Cycle	**Cycle Length (EFPY)**	**Cumulative Operating Time (EFPY)**	**Fluence (n/cm²)**	
			7°	**14°**
Future[e]	--	36.00	3.57E+19	2.62E+19
Future[e]	--	42.00	4.29E+19	3.14E+19
Future[e]	--	48.00	5.01E+19	3.65E+19
Future[e]	--	54.00	5.74E+19	4.17E+19
Future[e]	--	60.00	6.46E+19	4.69E+19
Future[e]	--	66.00	7.18E+19	5.21E+19
Future[e]	--	72.00	7.90E+19	5.72E+19

+10% bias on the peripheral and re-entrant corner assembly relative powers				
Cycle	**Cycle Length (EFPY)**	**Cumulative Operating Time (EFPY)**	**Fluence (n/cm²)**	
			7°	**14°**
Future[e]	--	36.00	3.61E+19	2.65E+19
Future[e]	--	42.00	4.40E+19	3.21E+19
Future[e]	--	48.00	5.18E+19	3.78E+19
Future[e]	--	54.00	5.97E+19	4.34E+19
Future[e]	--	60.00	6.75E+19	4.90E+19
Future[e]	--	66.00	7.54E+19	5.47E+19
Future[e]	--	72.00	8.33E+19	6.03E+19

Notes:

(a) This value is applicable to Capsule 83°.

(b) This value is applicable to Capsule 263°.

(c) This value is applicable to Capsule 97°.

(d) Cycle 25 was the current operating cycle at the time the exposures reported in this table were determined. Values listed are based on the projected EFPY for this cycle.

(e) Values beyond Cycle 25 are based on the average core power distributions and reactor operating conditions of Cycle 24 and are determined both with and without a 1.1 bias on the peripheral and re-entrant corner assembly relative powers.

Table 2.5-9 St. Lucie Unit 2 Iron Atom Displacement Rate at the Geometric Center of the Surveillance Capsules

Cycle	Cycle Length (EFPY)	Cumulative Operating Time (EFPY)	Displacement Rate (dpa/s)	
			7°	14°
1	1.11	1.11	5.91E-11	4.19E-11
2	1.12	2.23	5.84E-11	3.99E-11
3	1.22	3.45	5.27E-11	3.64E-11
4	1.16	4.61	3.88E-11	3.17E-11
5	1.30	5.91	3.82E-11	3.18E-11
6	1.35	7.26	3.76E-11	2.72E-11
7	1.21	8.47	4.07E-11	2.88E-11
8	1.38	9.85	2.51E-11	2.06E-11
9	1.22	11.07	3.82E-11	3.16E-11
10	1.44	12.51	4.05E-11	3.24E-11
11	1.32	13.83	3.63E-11	2.86E-11
12	1.51	15.34	3.53E-11	2.55E-11
13	1.29	16.63	3.94E-11	2.89E-11
14	1.43	18.06	3.46E-11	2.58E-11
15	1.15	19.21	4.04E-11	2.90E-11
16	1.25	20.46	4.16E-11	3.02E-11
17	1.25	21.71	4.06E-11	2.94E-11
18	1.42	23.13	3.87E-11	2.94E-11
19	1.19	24.32	4.75E-11	3.53E-11
20	1.23	25.55	5.51E-11	3.99E-11
21	1.28	26.83	5.28E-11	3.86E-11
22	1.31	28.13	6.19E-11	4.43E-11
23	1.40	29.53	6.08E-11	4.39E-11
24	1.34	30.88	5.55E-11	4.00E-11
25[(a)]	1.43	32.30	5.38E-11	3.89E-11

Note:

(a) Cycle 25 was the current operating cycle at the time the exposures reported in this table were determined. Values listed are based on the projected EFPY for this cycle.

Table 2.5-10 St. Lucie Unit 2 Iron Atom Displacements at the Geometric Center of the Surveillance Capsules

Cycle	Cycle Length (EFPY)	Cumulative Operating Time (EFPY)	Displacements (dpa)	
			7°	14°
1	1.11	1.11	2.07E-03[(a)]	1.47E-03
2	1.12	2.23	4.13E-03	2.88E-03
3	1.22	3.45	6.16E-03	4.28E-03
4	1.16	4.61	7.58E-03	5.44E-03
5	1.30	5.91	9.15E-03	6.74E-03
6	1.35	7.26	1.08E-02	7.90E-03
7	1.21	8.47	1.23E-02	9.00E-03
8	1.38	9.85	1.34E-02	9.90E-03
9	1.22	11.07	1.49E-02[(b)]	1.11E-02
10	1.44	12.51	1.67E-02	1.26E-02
11	1.32	13.83	1.82E-02	1.38E-02
12	1.51	15.34	1.99E-02	1.50E-02
13	1.29	16.63	2.15E-02	1.62E-02
14	1.43	18.06	2.31E-02	1.73E-02
15	1.15	19.21	2.45E-02	1.84E-02
16	1.25	20.46	2.62E-02	1.96E-02
17	1.25	21.71	2.78E-02	2.07E-02
18	1.42	23.13	2.95E-02	2.21E-02
19	1.19	24.32	3.13E-02	2.34E-02
20	1.23	25.55	3.34E-02[(c)]	2.49E-02
21	1.28	26.83	3.56E-02	2.65E-02
22	1.31	28.13	3.81E-02	2.83E-02
23	1.40	29.53	4.08E-02	3.02E-02
24	1.34	30.88	4.32E-02	3.19E-02
25[(d)]	1.43	32.30	4.56E-02	3.37E-02

Table 2.5-10 St. Lucie Unit 2 Iron Atom Displacements at the Geometric Center of the Surveillance Capsules (Continued)

No bias on the peripheral and re-entrant corner assembly relative powers				
Cycle	Cycle Length (EFPY)	Cumulative Operating Time (EFPY)	Displacements (dpa)	
			7°	14°
Future(e)	--	36.00	5.21E-02	3.84E-02
Future(e)	--	42.00	6.26E-02	4.59E-02
Future(e)	--	48.00	7.31E-02	5.35E-02
Future(e)	--	54.00	8.36E-02	6.11E-02
Future(e)	--	60.00	9.41E-02	6.87E-02
Future(e)	--	66.00	1.05E-01	7.62E-02
Future(e)	--	72.00	1.15E-01	8.38E-02

+10% bias on the peripheral and re-entrant corner assembly relative powers				
Cycle	Cycle Length (EFPY)	Cumulative Operating Time (EFPY)	Displacements (dpa)	
			7°	14°
Future(e)	--	36.00	5.26E-02	3.88E-02
Future(e)	--	42.00	6.41E-02	4.70E-02
Future(e)	--	48.00	7.55E-02	5.53E-02
Future(e)	--	54.00	8.70E-02	6.36E-02
Future(e)	--	60.00	9.84E-02	7.18E-02
Future(e)	--	66.00	1.10E-01	8.01E-02
Future(e)	--	72.00	1.21E-01	8.83E-02

Notes:

(a) This value is applicable to Capsule 83°.

(b) This value is applicable to Capsule 263°.

(c) This value is applicable to Capsule 97°.

(d) Cycle 25 was the current operating cycle at the time the exposures reported in this table were determined. Values listed are based on the projected EFPY for this cycle.

(e) Values beyond Cycle 25 are based on the average core power distributions and reactor operating conditions of Cycle 24 and are determined both with and without a 1.1 bias on the peripheral and re-entrant corner assembly relative powers.

Table 2.5-11 St. Lucie Unit 2 Surveillance Capsule Lead Factors

Cycle	Cycle Length (EFPY)	Cumulative Operating Time (EFPY)	Lead Factor	
			7°	14°
1	1.11	1.11	1.27[a]	0.90
2	1.12	2.23	1.23	0.85
3	1.22	3.45	1.22	0.84
4	1.16	4.61	1.24	0.88
5	1.30	5.91	1.25	0.92
6	1.35	7.26	1.25	0.91
7	1.21	8.47	1.24	0.90
8	1.38	9.85	1.24	0.91
9	1.22	11.07	1.26[b]	0.93
10	1.44	12.51	1.27	0.95
11	1.32	13.83	1.27	0.95
12	1.51	15.34	1.27	0.95
13	1.29	16.63	1.27	0.95
14	1.43	18.06	1.27	0.95
15	1.15	19.21	1.27	0.95
16	1.25	20.46	1.27	0.95
17	1.25	21.71	1.27	0.94
18	1.42	23.13	1.28	0.95
19	1.19	24.32	1.28	0.95
20	1.23	25.55	1.28[c]	0.95
21	1.28	26.83	1.28	0.95
22	1.31	28.13	1.28	0.94
23	1.40	29.53	1.28	0.94
24	1.34	30.88	1.27	0.94
25[d]	1.43	32.30	1.27	0.94

Table 2.5-11 St. Lucie Unit 2 Surveillance Capsule Lead Factors (Continued)

No bias on the peripheral and re-entrant corner assembly relative powers				
Cycle	**Cycle Length (EFPY)**	**Cumulative Operating Time (EFPY)**	**Lead Factor**	
			7°	**14°**
Future[(e)]	--	36.00	1.27	0.93
Future[(e)]	--	42.00	1.27	0.93
Future[(e)]	--	48.00	1.27	0.93
Future[(e)]	--	54.00	1.27	0.92
Future[(e)]	--	60.00	1.27	0.92
Future[(e)]	--	66.00	1.27	0.92
Future[(e)]	--	72.00	1.27	0.92

+10% bias on the peripheral and re-entrant corner assembly relative powers				
Cycle	**Cycle Length (EFPY)**	**Cumulative Operating Time (EFPY)**	**Lead Factor**	
			7°	**14°**
Future[(e)]	--	36.00	1.27	0.93
Future[(e)]	--	42.00	1.27	0.93
Future[(e)]	--	48.00	1.27	0.93
Future[(e)]	--	54.00	1.27	0.92
Future[(e)]	--	60.00	1.27	0.92
Future[(e)]	--	66.00	1.27	0.92
Future[(e)]	--	72.00	1.27	0.92

Notes:

(a) This value is applicable to Capsule 83°.

(b) This value is applicable to Capsule 263°

(c) This value is applicable to Capsule 97°.

(d) Cycle 25 was the current operating cycle at the time the lead factors reported in this table were determined. Values listed are based on the projected EFPY for this cycle.

(e) Values beyond Cycle 25 are based on the average core power distributions and reactor operating conditions of Cycle 24 and are determined both with and without a 1.1 bias on the peripheral and re-entrant corner assembly relative powers.

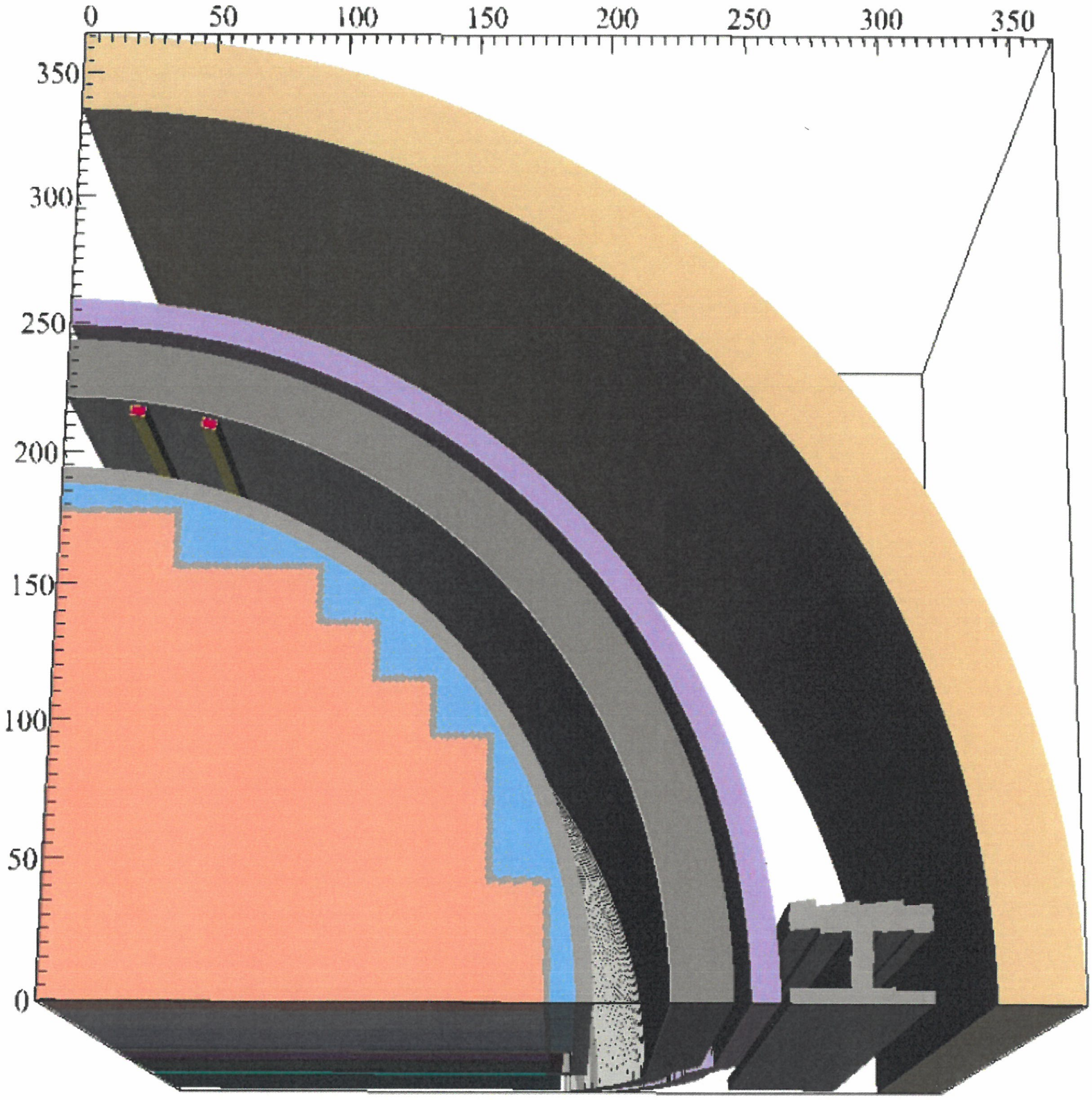

Figure 2.5-1 Top View of the Reactor Geometry at the Core Midplane (Unit 2)

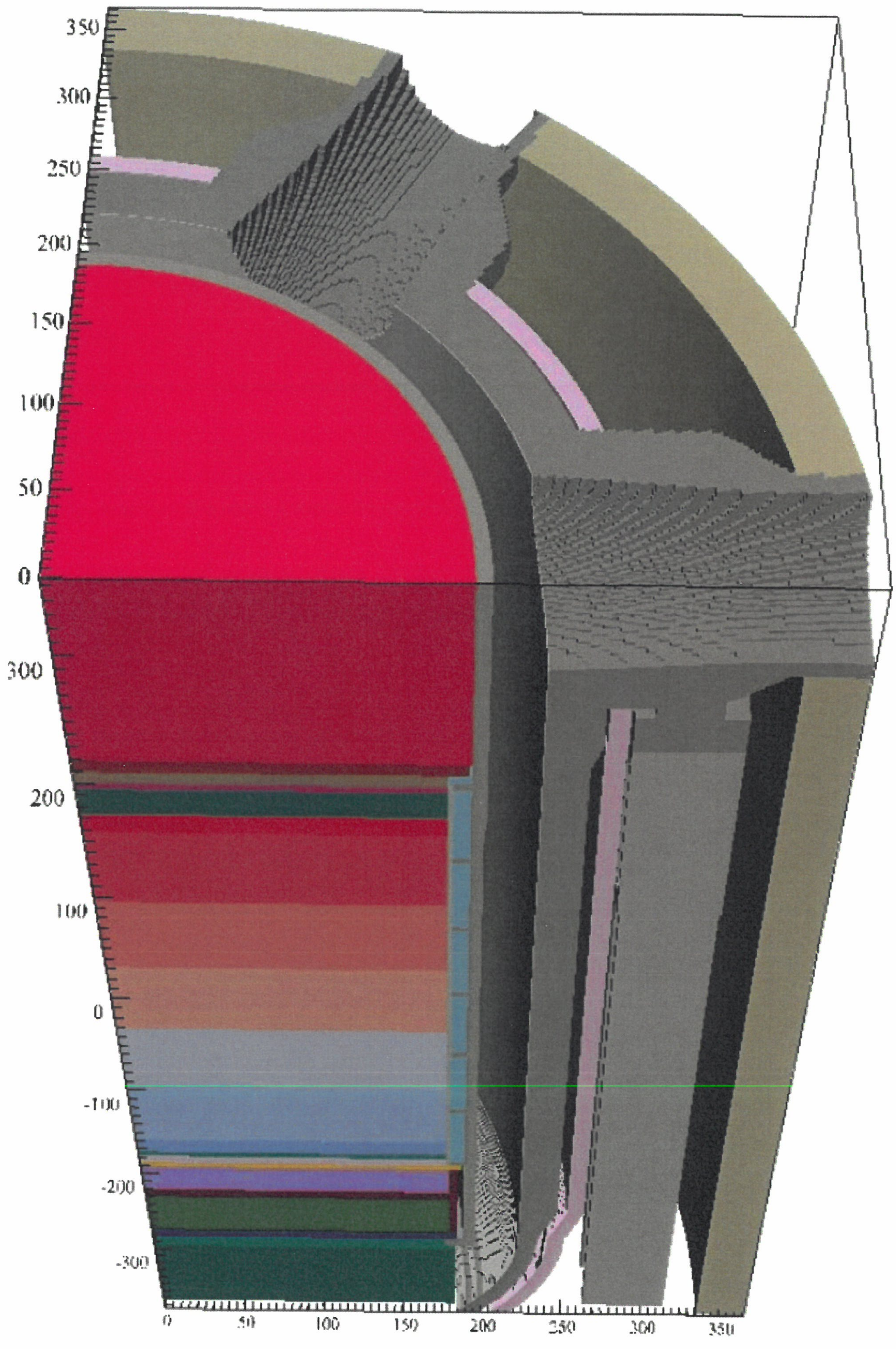

Figure 2.5-2 Top View of the Reactor Geometry at the Nozzle Centerline (Unit 2)

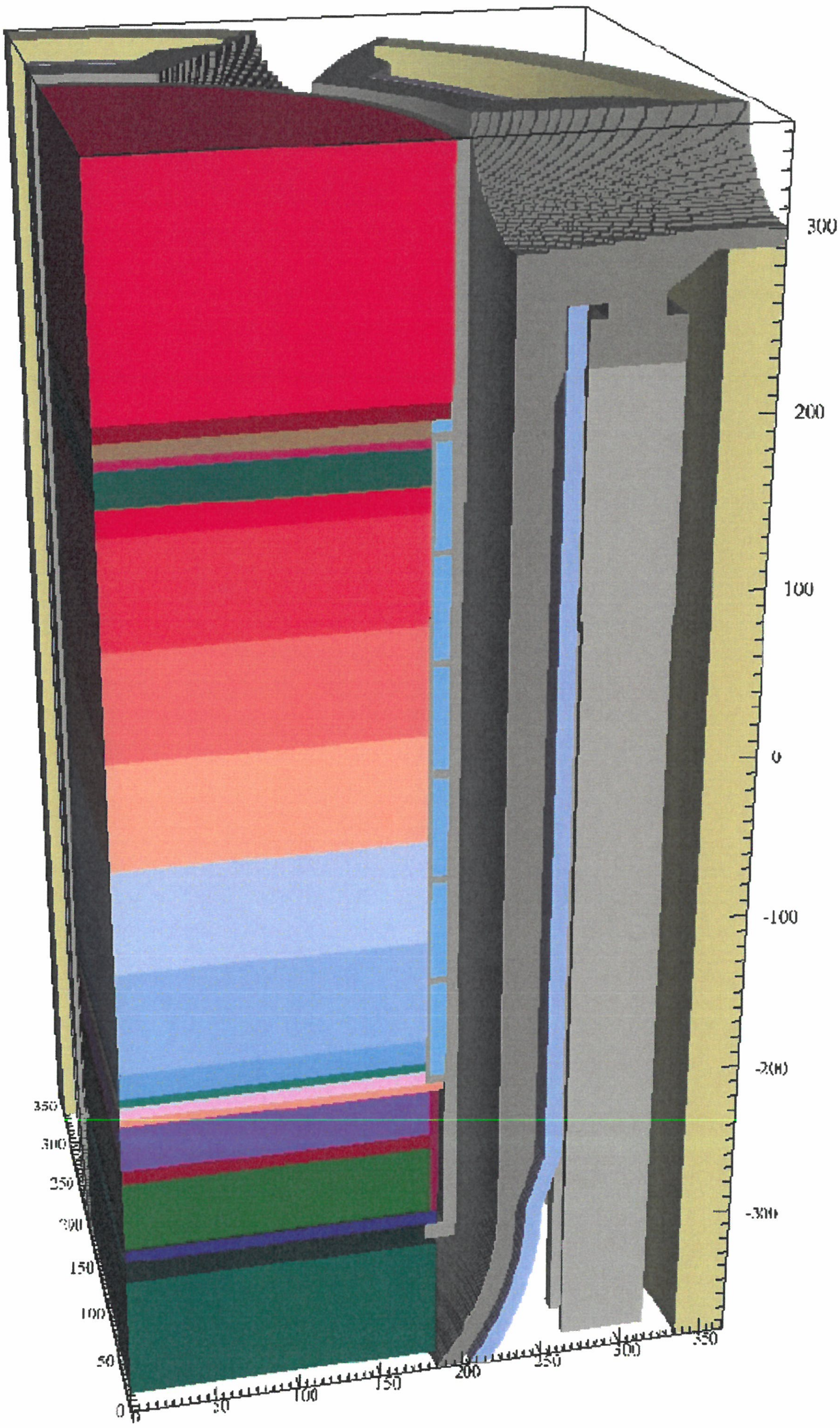

Figure 2.5-3 Oblique View of the Reactor Geometry (Unit 2)

3 FRACTURE TOUGHNESS PROPERTIES

The requirements for RVI are specified in 10 CFR 50, Appendix G [Ref. 8] and 10 CFR 50.61 [Ref. 9]. The beltline region of the reactor vessel is defined as the following in 10 CFR 50, Appendix G:

> *... the region of the reactor vessel (shell material including welds, heat affected zones, and plates or forgings) that directly surrounds the effective height of the active core and adjacent regions of the reactor vessel that are predicted to experience sufficient neutron radiation damage to be considered in the selection of the most limiting material with regard to radiation damage.*

As described in NRC Regulatory Issue Summary (RIS) 2014-11 [Ref. 10], any reactor vessel materials that are predicted to experience a neutron fluence exposure greater than 1.0 x 10^{17} n/cm^2 (E > 1.0 MeV) at the end of the licensed operating period should be considered to experience neutron embrittlement. The materials that exceed this fluence threshold are referred to as the "beltline" materials herein and are evaluated to ensure that the applicable neutron embrittlement effects are considered. The term "extended beltline" is used for materials that were not originally considered to be a part of the beltline region, but have projected fluence values greater than 1.0 x 10^{17} n/cm^2 (E > 1.0 MeV) at the end of the SLR period.

As seen from Tables 2.4-5 and 2.5-5, the beltline materials include the upper shell (also termed the "nozzle shell"), the intermediate shell, the lower shell, and the longitudinal and girth welds connecting these components. (Note that for reactor vessel welds, the terms "girth" and "circumferential" are used interchangeably, and "longitudinal" and "axial" are used interchangeably; herein, these welds shall be referred to as girth and axial welds.)

For Unit 1, the fluence for the inlet (also termed the "cold leg") and outlet (also termed the "hot leg") nozzle to upper shell plate welds are less than 1.0 x 10^{17} n/cm^2 (E > 1.0 MeV) at 72 EFPY. Therefore, the materials of the inlet/outlet nozzle forgings and the associated welds to the upper shell plates do **<u>not</u>** need to be considered in the beltline.

For Unit 2, the fluence for the outlet nozzle to upper shell plate welds are greater than 1.0 x 10^{17} n/cm^2 (E > 1.0 MeV) at 72 EFPY; however, the fluence for the inlet nozzle to upper shell plate welds are less than 1.0 x 10^{17} n/cm^2 (E > 1.0 MeV) at 72 EFPY. Therefore, the materials of the outlet nozzle forgings and the associated welds to the upper shell plate are considered in the beltline, while the inlet nozzle forgings and the associated welds to the upper shell plate do **<u>not</u>** need to be considered in the beltline.

Regardless of whether the reactor vessel nozzle forgings are part of the extended beltline, per NRC RIS 2014-11, the nozzle forging materials must be evaluated for their potential effect on P-T limit curves due to the higher stresses in the nozzle corner region. These higher stresses can potentially result in more restrictive P-T limits, even if the RT_{NDT} values for these components are not as high as those of the reactor vessel beltline shell materials that have simpler geometries. The effect of these higher stresses is addressed in Section 8.2.

A summary of the best-estimate copper (Cu) and nickel (Ni) contents in units of weight percent (wt. %), as well as initial RT_{NDT}, and USE for the reactor vessel beltline and extended beltline materials are provided in Table 3-1 for Unit 1 and Table 3-2 for Unit 2. Figure 3-1 provides a schematic of a generic RPV.

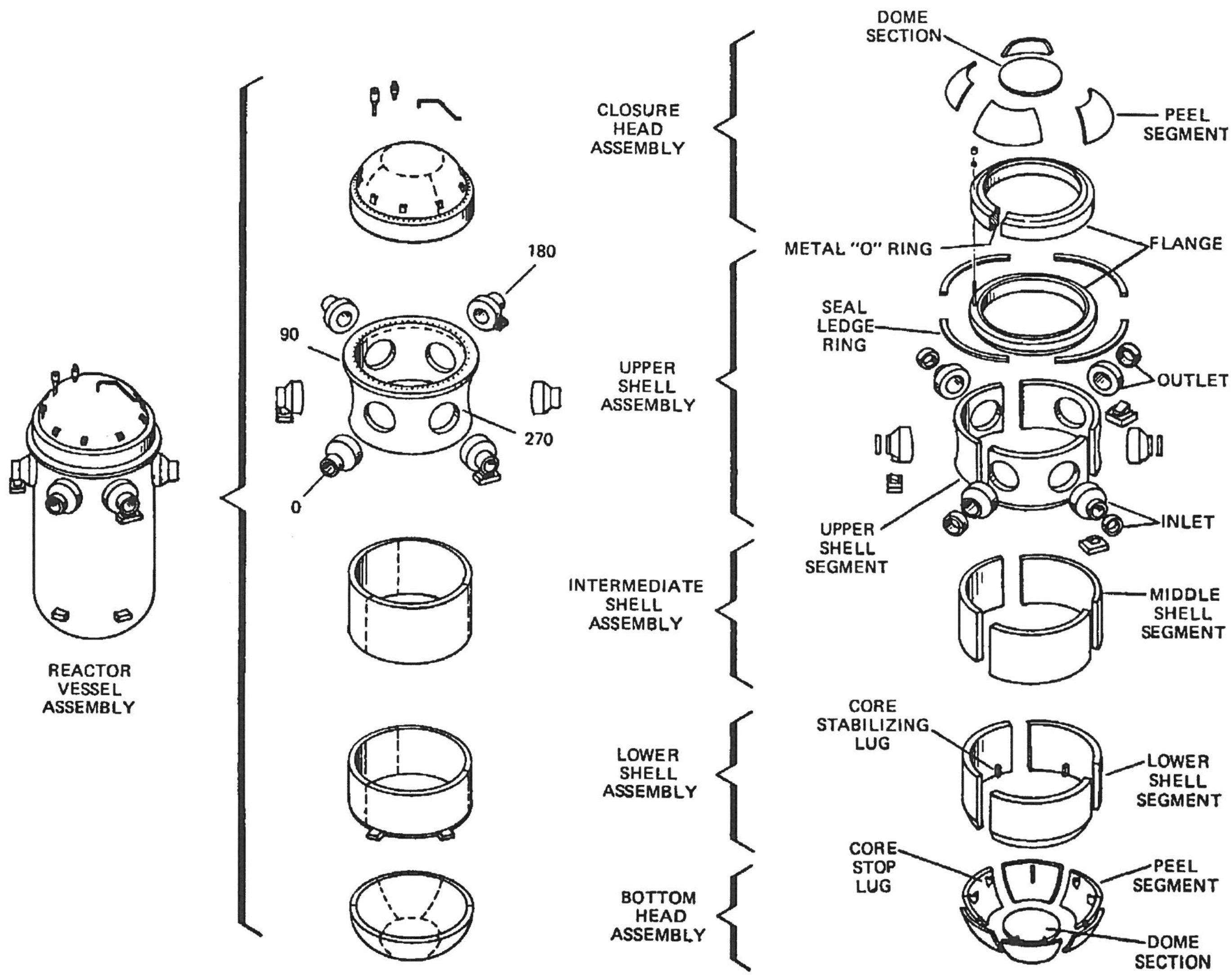

Figure 3-1 Generic RPV Material Identifications

Note: This figure is intended for information only to aid in visualization of the St. Lucie Units 1 and 2 RPVs. This schematic may not represent the exact configuration of the St. Lucie Units 1 and 2 RPVs, particularly outside of the beltline region.

Table 3-1 St. Lucie Unit 1 Reactor Vessel Beltline, Extended Beltline, and Surveillance Material Properties and Chemistry[(a)]

Material Description	Heat Number	Flux Type (Lot)	Wt. % Cu	Wt. % Ni	$RT_{NDT(U)}$ (°F)	σ_I[(b)] (°F)	Initial USE (ft-lb)
Beltline							
Intermediate Shell Plate C-7-1	A-4567-1	-	0.11	0.64	0	0	81.9
Intermediate Shell Plate C-7-2	B-9427-1	-	0.11	0.64	-10	0	81.9
Intermediate Shell Plate C-7-3	A-4567-2	-	0.11	0.58	10	0	76.05
Lower Shell Plate C-8-1	C-5935-1	-	0.15	0.56	20	0	81.9
Lower Shell Plate C-8-2	C-5935-2	-	0.15	0.57	20	0	103
Lower Shell Plate C-8-3	C-5935-3	-	0.12	0.58	0	0	88.4
Intermediate to Lower Shell Girth Weld Seam 9-203	90136	Linde 0091 (3999)	0.27	0.07	-60	0	144
Intermediate Shell Axial Weld Seams 2-203 A, B, & C	34B009 / A-8746	Linde 124 (3688 / 3878)	0.19	0.09	-56[(e)]	17[(e)]	102.3
Lower Shell Axial Weld Seams 3-203 A, B, & C	305424	Linde 1092 (3889)	0.27	0.63	-60	0	112
Extended Beltline[(c)]							
Upper Shell Plate C-6-1	A-4516-1	-	0.16[(f)]	0.53	33	0	68
Upper Shell Plate C-6-2	C-5313-2	-	0.16[(f)]	0.53	15	0	80
Upper Shell Plate C-6-3	C-5313-1	-	0.16[(f)]	0.53	15	0	84
Upper to Intermediate Shell Girth Weld Seam 8-203	21935	Linde 1092 (3889)	0.183[(d)]	0.704[(d)]	-56[(e)]	17[(e)]	109[(g)]
Upper Shell Axial Weld Seams 1-203 A, B, & C	21935 / 12008	Linde 1092 (3869)	0.213[(d)]	0.867[(d)]	-50[(h)]	0	118[(i)]
Surveillance Material							
Lower Shell Plate C-8-2[(j)]	C-5935-2	-	0.15	0.57	-	-	-
St. Lucie 1 Surveillance Weld[(j)]	90136	Linde 0091 (3999)	0.23	0.07	-	-	-
Beaver Valley 1 Surveillance Weld[(k)]	305424	Linde 1092 (3889)	0.26	0.61	-	-	-

Notes contained on following page.

Notes:

(a) Material properties extracted from WCAP-17389-P [Ref. 15], unless otherwise noted.

(b) $RT_{NDT(U)}$ values with a σ_I = 0°F are based on material-specific measured data. $RT_{NDT(U)}$ values with a σ_I = 17°F are based on generic data.

(c) Extended beltline material chemistry and the material properties ($RT_{NDT(U)}$ & USE) were defined from the reactor vessel certified material test reports (CMTRs) and fabrication records, unless otherwise noted. Base metal $RT_{NDT(U)}$ values were determined by reducing the "strong" direction orientation Charpy data to 65% of the value consistent with Branch Technical Position (BTP) 5-3 [Ref. 31] Position 1.1(3) and fitting the data using a hyperbolic tangent curve-fit. Base metal initial USE values are the average of all data points from the CMTRs with ≥ 95% shear reduced to 65% of the value consistent with BTP 5-3 [Ref. 31], because the specimens were oriented in the strong direction.

(d) Cu and Ni from CE-NPSD-1119 [Ref. 14], Table 5.

(e) 10 CFR 50.61 [Ref. 9] generic value.

(f) The St. Lucie Unit 1 upper shell plates supplied by Lukens did not have reported Cu values. A review of CMTRs with copper values for all Lukens plates supplied for St. Lucie Units 1 and 2 reactor vessels (14 plates total), identified a maximum value of 0.16% Cu. This maximum Cu value is greater than the mean +1σ which, per Regulatory Guide 1.99, Revision 2, provides a conservative chemistry estimate.

(g) USE for Heat # 21935 is from Diablo Canyon 1 (WCAP-17315-NP [Ref. 16]), Intermediate to Lower Shell Weld Seam 9-442. Both materials were made with Heat #21935 and Linde 1092 flux.

(h) $RT_{NDT(U)}$ for Heat # 21935/12008, Linde 1092, Lot 3869 is from identical material at Diablo Canyon 2 (WCAP-17315-NP [Ref. 16]).

(i) USE for Heat # 21935/12008, Linde 1092, Lot 3869 is from identical material at Diablo Canyon 2 (WCAP-17315-NP [Ref. 16]), specifically Intermediate Shell Axial Welds 2-201A/B/C.

(j) The surveillance weld flux type and lot are identified in WCAP-15446 [Ref. 17] and CE-NPSD-1119 [Ref. 14]. Lower Shell Plates C-8-1 and C-8-3 share a heat number (Heat # C-5935) with the surveillance plate taken from Lower Shell Plate C-8-2. Therefore, surveillance data applies to all lower shell plates that share this heat number.

(k) Surveillance data for Heat # 305424 taken from WCAP-18102-NP [Ref. 28].

Table 3-2 St. Lucie Unit 2 Reactor Vessel Beltline, Extended Beltline, and Surveillance Material Properties and Chemistry[a]

Material Description	Heat Number	Flux Type (Lot)	Wt. % Cu	Wt. % Ni	$RT_{NDT(U)}$ (°F)	σ_I[b] (°F)	Initial USE[c] (ft-lb)
Beltline							
Intermediate Shell Plate M-605-1	A-8490-2	-	0.11	0.61	30	0	105
Intermediate Shell Plate M-605-2	B-3416-2	-	0.13	0.62	10	0	113
Intermediate Shell Plate M-605-3	A-8490-1	-	0.11	0.61	0	0	113
Lower Shell Plate M-4116-1	B-8307-2	-	0.06	0.57	20	0	91
Lower Shell Plate M-4116-2	A-3131-1	-	0.07	0.60	20	0	105
Lower Shell Plate M-4116-3	A-3131-2	-	0.07	0.60	20	0	100
Intermediate to Lower Shell Girth Weld Seam 101-171	83637 / 3P7317	Linde 124 (0951)	0.07	0.07	-50	0	96
Intermediate Shell Axial Weld Seams 101-124A, B, & C	83642	Linde 0091 (3536)	0.05	0.09	-56	17	116
Intermediate Shell Axial Weld Seam 101-124C Repair	83637	Linde 0091 (1122)	0.05	0.07	-50	0	136
Lower Shell Axial Weld Seams 101-142A, B, & C	83637	Linde 0091 (1122)	0.05	0.07	-50	0	136
Extended Beltline							
Upper Shell Plate M-604-1	B-3493-1	-	0.16[d]	0.60	50	0	90[f]
Upper Shell Plate M-604-2	C-9632-2	-	0.16[d]	0.61	50	0	82[f]
Upper Shell Plate M-604-3	A-8524-1	-	0.16[d]	0.58	10	0	106[f]
Upper to Intermediate Shell Girth Weld Seam 106-121	83637	Linde 0091 (1122)	0.05[l]	0.07[l]	-50	0	136
Upper Shell Axial Weld Seams 101-122A & C	5P5622	Linde 0091 (1122)	0.153[e]	0.077[e]	-40	0	102[g]
Upper Shell Axial Weld Seams 101-122A & C	2P5755	Linde 0091 (0831)	0.21[e]	0.058[e]	-50	0	109[g]
Upper Shell Axial Weld Seam 101-122B	5P5622	Linde 0091 (1122 & 0831)	0.153[e]	0.077[e]	-40	0	102[g]
Hot Leg Nozzle A M-4103-2	124K630VA2W	-	0.127[j]	0.66	-30	0	107[j]
Hot Leg Nozzle B M-4103-1	124K630VA1W	-	0.127[j]	0.68	-20	0	111[j]
Hot Leg Nozzle to Shell Weld Seam 105-121A	4P6519	Linde 0091 (0145)	0.131[e]	0.06[e]	-60	0	107[g]
Hot Leg Nozzle to Shell Weld Seam 105-121B	Various SMAWs	-	0.05[k]	1.08[k]	-60[k]	0[k]	128[k]
Surveillance Material							
Intermediate Shell Plate M-605-1[h]	A-8490-2	-	0.11	0.61	-	-	-
St. Lucie 2 Surveillance Weld[i]	83637	Linde 124 (0951)	0.05	0.07	-	-	-

Notes contained on following page.

Notes:

(a) Information extracted from WCAP-18275-NP [Ref. 18], unless otherwise noted.

(b) All $RT_{NDT(U)}$ values are based on material-specific measured data with a σ_I = 0°F with the exception of Heat # 83642, which is based on a generic value and has a corresponding σ_I = 17°F.

(c) USE values from WCAP-17939-NP [Ref. 19] Table E-1, unless otherwise noted.

(d) The St. Lucie Unit 2 upper shell plates supplied by Lukens did not have reported Cu values. A review of CMTRs with copper values for all Lukens plates supplied for St. Lucie Units 1 and 2 reactor vessels (14 plates total), identified a maximum value of 0.16% Cu. This maximum Cu value is greater than the mean +1σ which, per Regulatory Guide 1.99, Revision 2, provides a conservative chemistry estimate.

(e) Cu and Ni from CE-NPSD-1119 [Ref. 14], Table 5.

(f) Values are the average of all Charpy V-notch energy data points in the transverse/axial direction with shear ≥ 95% from the CMTRs.

(g) The weld fabrication records contain no shear data for these materials. For Heat # 5P5622 and Heat # 4P6519, the USE is the average of all available Charpy V-notch energy data points. For Heat # 2P5755, the USE is the average of all data points tested at 10°F.

(h) Intermediate Shell Plate M-605-3 shares a heat number (Heat # A-8490) with the surveillance plate taken from Intermediate Shell Plate M-605-1. Therefore, surveillance data applies to the intermediate shell plates that share this heat number.

(i) The reactor vessel Intermediate to Lower Shell Girth Weld Seam 101-171 uses the same heat and flux type as the surveillance weld material; however, since another weld was also used in the girth weld fabrication, the surveillance weld Charpy data is not directly applicable to the vessel weld and will not be applied to this material. The surveillance weld data will be used to evaluate Intermediate Shell Axial Weld Seam 101-124C Repair and Lower Shell Axial Weld Seams 101-142A, B, & C since they share the same heat # as the surveillance weld, despite having a different flux type and lot number consistent with WCAP-18275-NP [Ref. 18].

(j) Cu value generic value for SA-508 Class 2 nozzle forgings from PWROG-15109-NP-A [Ref. 13]. USE values are the average of all data points from the CMTRs with ≥ 95% shear conservatively reduced to 65% of the value consistent with BTP 5-3 [Ref. 31], because the orientation of the specimens could not be determined with certainty.

(k) This nozzle weld material was fabricated with six distinct shielded metal arc welds (SMAWs), specifically Heat #'s EACAE, FAOJE, GABFE, HABIE, IAOCE, and KAOCE. The reported chemistry, RT_{NDT}, and USE reported are the maximum values taken from the weld fabrication records for each of the welds. σ_I = 0°F because RT_{NDT} is based on measured data for each weld.

(l) The upper to intermediate shell girth weld 106-121 was fabricated using the same weld material as the lower shell axial welds (101-142A/B/C). Therefore, for consistency with the lower shell axial welds, the chemistry for weld seam 106-121 is based on that previously reported and used for the lower shell axial welds (101-142A/B/C). These chemistry values are slightly conservative compared to the values for Heat # 83637 from CE-NPSD-1119, Revision 1 [Ref. 14], i.e., Cu = 0.048 wt.% and Ni = 0.066 wt.%.

4 SURVEILLANCE DATA

Per Regulatory Guide 1.99, Revision 2 [Ref. 4], calculation of Position 2.1 chemistry factors (CFs) requires data from the plant-specific surveillance program. In addition to the plant-specific surveillance data, data from surveillance programs at other plants, which include a St. Lucie Units 1 and 2 reactor vessel beltline material, may also need to be considered when calculating Position 2.1 CFs. Data from a surveillance program at another plant is often called 'sister-plant' data.

The St. Lucie Unit 1 surveillance capsules contain shell material from the Lower Shell C-8-2 Surveillance Plate. Lower Shell Plates C-8-1 and C-8-3 share a heat number (Heat # C-5935) with the surveillance plate; therefore, the surveillance data applies to all lower shell plates. The St. Lucie Unit 1 surveillance weld material was fabricated with the same material heat, flux type, and flux lot number as the Intermediate to Lower Shell Girth Weld Seam 9-203, which is weld wire Heat # 90136, Flux Type Linde 0091, and Lot # 3999. Table 4-1 summarizes the surveillance data available from the St. Lucie Unit 1 reactor vessel surveillance program that will be used in the calculation of the Position 2.1 CF values. Per Appendix B, the St. Lucie Unit 1 surveillance data for the Lower Shell Plate C-8-2 and Heat # 90136 materials are deemed credible. Therefore, a reduced margin term will be utilized in the Position 2.1 PTS and ART calculations contained in Sections 6 and 8 for these materials.

The St. Lucie Unit 2 surveillance capsules contain shell material from Intermediate Shell Plate M-605-1. Intermediate Shell Plate M-605-3 shares a heat number (Heat # A-8490) with the surveillance plate; therefore, surveillance data applies to this intermediate shell plate sharing this heat number. The St. Lucie Unit 2 surveillance weld material was fabricated from weld wire Heat # 83637, Flux Type Linde 124, and Lot # 0951. Reactor vessel Intermediate to Lower Shell Girth Weld Seam 101-171 uses the same heat and flux type as the surveillance weld material; however, since another weld heat (Heat # 3P7317) was also used in the girth weld fabrication, the surveillance weld Charpy data is not directly applicable to this vessel weld and will not be applied to this material. (It is noted that the Position 1.1 CF used for this weld is greater than, i.e., more conservative, than the resulting Position 2.1 CF based on the surveillance weld including the chemistry ratio adjustment.) The surveillance weld data will be used to evaluate Intermediate Shell Axial Weld Seam 101-124C Repair and Lower Shell Axial Weld Seams 101-142A, B, and C since they share the same heat # as the surveillance weld, despite having a different flux type and lot number. Table 4-2 summarizes the surveillance data available from the St. Lucie Unit 2 reactor vessel surveillance program that will be used in the calculation of the Position 2.1 CF values. Per Appendix B, St. Lucie Unit 2 surveillance data for the Intermediate Shell Plate M-605-1 and Heat # 83637 are deemed credible. Therefore, a reduced margin term will be utilized in the Position 2.1 PTS and ART calculations for these materials contained in Sections 6 and 8.

Sister-plant surveillance weld data is available for St. Lucie Unit 1 from Millstone 2 (Heat # 90136), Diablo Canyon 2 (Heat #'s 21935 / 12008) and Beaver Valley 1 (Heat # 305424), and for St. Lucie Unit 2 from Beaver Valley 2 (Heat # 83642). Since the Position 2.1 CF from sister-plant surveillance data is bounded by the Position 1.1 CF or the Position 2.1 CF with only plant-specific surveillance data, the Position 2.1 CF from sister-plant surveillance data does not need to be considered in the ΔRT_{NDT} calculations performed herein.

However, the surveillance data available for Heat # 305424 from the Beaver Valley Unit 1 surveillance data is used in Section 8.2 to justify the continued use of the current P-T limit curves through EOLE. The surveillance data for Heat # 305424 was determined to be non-credible in WCAP-18102-NP [Ref. 28]; thus, it must be used with a full margin term. The surveillance data for Heat # 305424 is provided in Table 4-3.

Table 4-1 St. Lucie Unit 1 Surveillance Program Results

Material	Capsule	Withdrawal (EOC)	Fluence(a) (n/cm^2, E > 1.0 MeV)	Measured ΔRT_{NDT}(b) (°F)	Measured USE %-Decrease(b) (%)	Average Irradiation Temperature (°F)
Lower Shell C-8-2 Surveillance Plate (Longitudinal)	97°	5	5.09E+18	68.7	23	541
	104°	9	7.70E+18	79.87	17	545
	284°	15	1.22E+19	87.93	21	547
Lower Shell C-8-2 Surveillance Plate (Transverse)	97°	5	5.09E+18	63.83	24	541
	284°	15	1.22E+19	84.99	15	547
Surveillance Weld (Heat # 90136)	97°	5	5.09E+18	72.34	31	541
	104°	9	7.70E+18	67.4	25	545
	284°	15	1.22E+19	68.0	24	547

Notes:

(a) The fluence values are taken from Table 2.4-8.

(b) Information is extracted from WCAP-15446-NP [Ref. 17].

Table 4-2 St. Lucie Unit 2 Surveillance Program Results

Material	Capsule	Withdrawal (EOC)	Fluence(a) (n/cm^2, E > 1.0 MeV)	Measured ΔRT_{NDT}(b) (°F)	Measured USE %-Decrease(b) (%)	Average Irradiation Temperature (°F)
Intermediate Shell M-605-1 Surveillance Plate (Longitudinal)	83°	1	1.42E+18	45.1	11	548
	97°	20	2.29E+19	132.7	19	549
Intermediate Shell M-605-1 Surveillance Plate (Transverse)	83°	1	1.42E+18	29.4	1	548
	263°	9	1.02E+19	102.7	23	549
	97°	20	2.29E+19	127.6	24	549
Surveillance Program Weld Metal (Heat # 83637)	83°	1	1.42E+18	15.8	13	548
	263°	9	1.02E+19	26.5	9	549
	97°	20	2.29E+19	24.8	17	549

Notes:

(a) The fluence values are taken from Table 2.5-8.

(b) Information is extracted from WCAP-17939-NP [Ref. 19].

Table 4-3 Sister-Plant Surveillance Capsule Data for Heat # 305424 from Beaver Valley Unit 1

Capsule	Capsule Fluence[(a)] (x 10^{19} n/cm², E > 1.0 MeV)	Measured 30 ft-lb Transition Temp. Shift[(a)] (°F)	Average Irradiation Temperature (°F)	Cu Wt. %[(a)]	Ni Wt. %[(a)]	Credible / Non-Credible[(a)]
V	0.297	159.8	543.0	0.26	0.61	Non-Credible
U	0.618	164.9	543.0			
W	0.952	186.3	543.0			
Y	2.10	178.5	543.0			
X	4.99	237.8	543.1			

Notes

(a) Information taken from WCAP-18102-NP [Ref. 28].

5 CHEMISTRY FACTORS

The chemistry factors (CFs) were calculated using Regulatory Guide (RG) 1.99, Revision 2, Positions 1.1 and 2.1. Position 1.1 CFs for each reactor vessel material are calculated using the best-estimate copper and nickel weight percent of the material and Tables 1 and 2 of RG 1.99, Revision 2. The best-estimate copper and nickel weight percent values for the St. Lucie Units 1 and 2 reactor vessel materials and the surveillance materials are provided in Tables 3-1 and 3-2.

The Position 2.1 CFs are calculated for the materials that have available surveillance data from the plant-specific or a sister-plant surveillance program. The Position 2.1 CF calculation is performed using the method described in RG 1.99, Revision 2. The St. Lucie Units 1 and 2 surveillance data are summarized in Section 4 and are utilized in the Position 2.1 CF calculations in this section. The Position 2.1 CF calculations for the St. Lucie Unit 1 surveillance materials are presented in Table 5-1. The Position 2.1 CF calculations for the St. Lucie Unit 2 surveillance materials are presented in Table 5-2. The Position 2.1 CF calculation for the Heat # 305424 surveillance material from Beaver Valley Unit 1 is presented in Table 5-3.

No adjustments of the measured ΔRT_{NDT} values from the St. Lucie Unit 1 or 2 surveillance program are required for these materials due to temperature differences since all data is from the plant-specific program. However, measured ΔRT_{NDT} values from the Beaver Valley Unit 1 surveillance program are adjusted to account for the different operating temperatures. In some cases, adjustment of the measured ΔRT_{NDT} values were required per RG 1.99 [Ref. 4] due to chemistry differences between the surveillance material and the corresponding vessel weld/plate. The chemistry adjustment factors based on the differences between the RG 1.99, Position 1.1 chemistry factors are shown below. All chemistry adjustment factors have been rounded to 2 decimal places.

Lower Shell Plate C-8-1

$CF_{\text{Beltline Plate (St. Lucie-1, C-8-1)}} = 107.80°F$

$CF_{\text{Surv. Plate (St. Lucie-1, C-8-2)}} = 108.35°F$

Ratio = 107.80 ÷ 108.35 = 0.99

Lower Shell Plate C-8-3

$CF_{\text{Beltline Plate (St. Lucie-1, C-8-3)}} = 82.60°F$

$CF_{\text{Surv. Plate (St. Lucie-1, C-8-2)}} = 108.35°F$

Ratio = 82.60 ÷ 108.35 = 0.76

Heat # 90136

$CF_{\text{Beltline Weld (St. Lucie-1)}} = 124.25°F$

$CF_{\text{Surv. Weld (St. Lucie-1)}} = 106.60°F$

Ratio = 124.25 ÷ 106.60 = 1.17

Heat # 305424

$CF_{\text{Beltline Weld (St. Lucie-1)}} = 188.80°F$

$CF_{\text{Surv. Weld (BV-1)}} = 181.60°F$

Ratio = 188.80 ÷ 181.60 = 1.04

The Position 1.1 and Position 2.1 CFs are summarized in Tables 5-4 and 5-5 for St. Lucie Units 1 and 2, respectively.

Table 5-1 Calculation of Chemistry Factors Using St. Lucie Unit 1 Surveillance Capsule Data

Material	Capsule	Capsule Fluence[(a)] (x 10^{19} n/cm^2, E > 1.0 MeV)	FF[(b)]	Measured ΔRT_{NDT}[(a)] (°F)	FF * ΔRT_{NDT} (°F)	FF^2
Lower Shell Plate C-8-2 (Longitudinal)	97°	0.509	0.811	68.70	55.75	0.659
	104°	0.770	0.927	79.87	74.01	0.859
	284°	1.22	1.055	87.93	92.81	1.114
Lower Shell Plate C-8-2 (Transverse)	97°	0.509	0.811	63.83	51.80	0.659
	284°	1.22	1.055	84.99	89.70	1.114
				SUM:	364.07	4.404
	$CF_{C\text{-}8\text{-}2} = \Sigma(FF * \Delta RT_{NDT}) \div \Sigma(FF^2) = (364.07) \div (4.404) = 82.67°F$					
Surveillance Weld (Heat # 90136)	97°	0.509	0.811	84.64 (72.34)	68.68	0.659
	104°	0.770	0.927	78.86 (67.40)	73.08	0.859
	284°	1.22	1.055	79.56 (68.00)	83.97	1.114
				SUM:	225.73	2.631
	$CF_{90136} = \Sigma(FF * \Delta RT_{NDT}) \div \Sigma(FF^2) = (225.73) \div (2.631) = 85.79°F$					

Notes:

(a) The fluence and ΔRT_{NDT} values are taken from Table 4-1. The St. Lucie Unit 1 surveillance weld measured ΔRT_{NDT} results have been adjusted by a ratio of 1.17 to account for chemistry differences between the Heat # 90136 surveillance weld and reactor vessel weld. The unadjusted measured ΔRT_{NDT} values are listed in parentheses.

(b) FF = fluence factor = $f^{(0.28 - 0.10 * \log(f))}$.

Table 5-2 Calculation of Chemistry Factors Using St. Lucie Unit 2 Surveillance Capsule Data

Material	Capsule	Capsule Fluence[a] (x 10^{19} n/cm^2, E > 1.0 MeV)	FF[b]	Measured ΔRT_{NDT}[a] (°F)	FF * ΔRT_{NDT} (°F)	FF^2
Intermediate Shell M-605-1 Surveillance Plate (Longitudinal)	83°	0.142	0.491	45.1	22.13	0.241
	97°	2.29	1.224	132.7	162.43	1.498
Intermediate Shell M-605-1 Surveillance Plate (Transverse)	83°	0.142	0.491	29.4	14.43	0.241
	263°	1.02	1.006	102.7	103.27	1.011
	97°	2.29	1.224	127.6	156.19	1.498
				SUM:	458.45	4.489
	$CF_{M\text{-}605\text{-}1} = \Sigma(FF * \Delta RT_{NDT}) \div \Sigma(FF^2) = (458.45) \div (4.489) = 102.12$°F					
Surveillance Weld Metal (Heat # 83637)	83°	0.142	0.491	15.8	7.75	0.241
	263°	1.02	1.006	26.5	26.65	1.011
	97°	2.29	1.224	24.8	30.36	1.498
				SUM:	64.76	2.750
	$CF_{83637} = \Sigma(FF * \Delta RT_{NDT}) \div \Sigma(FF^2) = (64.76) \div (2.750) = 23.55$°F					

Notes:

(a) The fluence and ΔRT_{NDT} values are taken from Table 4-2.

(b) FF = fluence factor = $f^{(0.28 - 0.10 * \log(f))}$.

Table 5-3 Calculation of Chemistry Factor Using Sister-Plant Surveillance Capsule Data for Heat # 305424 from Beaver Valley Unit 1

Capsule	Capsule Fluence[(a)] ($x\ 10^{19}\ n/cm^2$, E > 1.0 MeV)	FF[(b)]	Measured ΔRT_{NDT}[(a)] (°F)	Average Irradiation Temperature[(a)]	Adjusted ΔRT_{NDT}[(c)] (°F)	FF*Adjusted ΔRT_{NDT} (°F)	FF^2
V	0.297	0.668	159.8	543.0	158.91	106.10	0.446
U	0.618	0.865	164.9	543.0	164.22	142.08	0.749
W	0.952	0.986	186.3	543.0	186.47	183.90	0.973
Y	2.10	1.202	178.5	543.0	178.36	214.36	1.444
X	4.99	1.402	237.8	543.1	240.14	336.66	1.965
					SUM:	983.10	5.577
$CF_{305424} = \Sigma(FF * \Delta RT_{NDT}) \div \Sigma(FF^2) = (983.10) \div (5.577) = 176.28°F$							

Notes:

(a) The fluence, ΔRT_{NDT}, and irradiation temperature values are taken from Table 4-3.

(b) FF = fluence factor = $f^{(0.28 - 0.10 * \log(f))}$.

(c) Measured ΔRT_{NDT} values have been adjusted first by the difference in temperature between the capsule irradiation temperature from Table 4-3 and the St. Lucie Unit 1 average vessel inlet temperature through 72 EFPY (550°F). Then, the values are adjusted by the CF ratio of the St. Lucie Unit 1 vessel weld and the surveillance weld (1.04). For example:

Capsule V adjusted ΔRT_{NDT} = 1.04* [159.8°F + (543°F - 550°F)] = 158.91°F

Table 5-4 Position 1.1 and 2.1 Chemistry Factors for St. Lucie Unit 1

Material Description	Chemistry Factor	
	Position 1.1[(a)] (°F)	Position 2.1[(b)] (°F)
Beltline		
Intermediate Shell Plate C-7-1	74.60	-
Intermediate Shell Plate C-7-2	74.60	-
Intermediate Shell Plate C-7-3	73.80	-
Lower Shell Plate C-8-1	107.80	81.84[(c)]
Lower Shell Plate C-8-2	108.35	82.67
Lower Shell Plate C-8-3	82.60	62.83[(c)]
Intermediate to Lower Shell Girth Weld Seam 9-203 (Heat # 90136)	124.25	85.79
Intermediate Shell Axial Weld Seams 2-203 A, B, & C (Heat #'s 34B009 / A-8746)	90.65	-
Lower Shell Axial Weld Seams 3-203 A, B, & C (Heat # 305424)	188.80	176.28[(d)]
Extended Beltline		
Upper Shell Plate C-6-1	113.10	-
Upper Shell Plate C-6-2	113.10	-
Upper Shell Plate C-6-3	113.10	-
Upper to Intermediate Shell Girth Weld Seam 8-203 (Heat # 21935)	172.22	-
Upper Shell Axial Seams 1-203 A, B, and C (Heat #'s 21935 / 12008)	208.62	-
Surveillance Weld Materials		
St. Lucie 1 Surveillance Weld (Heat # 90136)	106.60	-
Beaver Valley 1 Surveillance Weld (Heat # 305424)	181.60	-

Notes:

(a) All values are based on Tables 1 and 2 of Regulatory Guide 1.99, Revision 2 (Position 1.1) using the Cu and Ni weight percent values given in Table 3-1.

(b) Values are from Tables 5-1 or 5-3, unless otherwise noted.

(c) Lower Shell Plates C-8-1 and C-8-3 share a heat number (Heat # C-5935) with the surveillance material taken from Lower Shell Plate C-8-2. Since the Cu and Ni values for these non-surveillance plates are lower than the surveillance plate, the Position 2.1 CF determined in Table 5-1 can be adjusted by the ratio of plates' Position 1.1 CFs.

(d) The surveillance data for Heat # 305424 from the Beaver Valley Unit 1 surveillance program was determined to be non-credible in WCAP 18102-NP [Ref.28]; thus, it must be used with a full margin term. However, the results demonstrate that the Position 1.1 CF is conservative for Heat # 305424.

Table 5-5 Position 1.1 and 2.1 Chemistry Factors for St. Lucie Unit 2

Material Description	Chemistry Factor	
	Position 1.1[(a)] (°F)	Position 2.1[(b)] (°F)
Beltline		
Intermediate Shell Plate M-605-1	74.15	102.12
Intermediate Shell Plate M-605-2	91.50	-
Intermediate Shell Plate M-605-3	74.15	102.12[(c)]
Lower Shell Plate M-4116-1	37.00	-
Lower Shell Plate M-4116-2	44.00	-
Lower Shell Plate M-4116-3	44.00	-
Intermediate to Lower Shell Girth Weld Seam 101-171 (Heat #'s 83637 / 3P7317)	40.05	-
Intermediate Shell Axial Weld Seams 101-124A, B, & C (Heat # 83642)	36.35	-
Intermediate Shell Axial Weld Seam 101-124C Repair (Heat # 83637)	34.05	23.55
Lower Shell Axial Weld Seams 101-142A, B, & C (Heat # 83637)	34.05	23.55
Extended Beltline		
Upper Shell Plate M-604-1	118.00	-
Upper Shell Plate M-604-2	118.25	-
Upper Shell Plate M-604-3	116.60	-
Upper Shell to Intermediate Shell Girth Weld Seam 106-121 (Heat # 83637)	34.05	23.55
Upper Shell Axial Weld Seams 101-122 A and C (Heat # 5P5622)	74.13	-
Upper Shell Axial Weld Seams 101-122 A and C (Heat # 2P5755)	96.64	-
Upper Shell Axial Weld Seam 101-122 B (Heat # 5P5622)	74.13	-
Hot Leg Nozzle A M-4103-2	89.92	-
Hot Leg Nozzle B M-4103-1	90.36	-
Hot Leg Nozzle to Shell Weld Seam 105-121A	63.70	-
Hot Leg Nozzle to Shell Weld Seam 105-121B	68.00	-
Surveillance Weld Material		
St. Lucie Unit 2 Surveillance Weld (Heat # 83637)	34.05	-

Notes contained on following page.

Notes:

(a) All values are based on Tables 1 and 2 of Regulatory Guide 1.99, Revision 2 (Position 1.1) using the Cu and Ni weight percent values given in Table 3-2.

(b) Values are from Table 5-2.

(c) Intermediate Shell Plate M-605-3 shares a heat number (Heat # A-8490) with the surveillance plate taken from Intermediate Shell Plate M-605-1. Since the Cu and Ni values for this non-surveillance plate are identical to the surveillance plate, the Position 2.1 CF determined in Table 5-2 is also applicable to Intermediate Shell Plate M-605-3.

6 PRESSURIZED THERMAL SHOCK EVALUATION

Pressurized thermal shock (PTS) may occur during a severe system transient, such as a loss-of-coolant accident (LOCA) or steam line break. Such transients may challenge the integrity of the RPV under the following conditions: severe overcooling of the inside surface of the vessel wall followed by high pressurization, significant degradation of vessel material toughness caused by radiation embrittlement, and the presence of a critical-size defect anywhere within the vessel wall.

In 1985, the U.S. Nuclear Regulatory Commission (NRC) issued a formal ruling on PTS (10 CFR 50.61 [Ref. 9]) that established screening criteria on PWR vessel embrittlement, as measured by the maximum reference nil-ductility transition temperature in the limiting beltline component at the end of license, termed RT_{PTS}. RT_{PTS} screening values were set by the NRC for beltline axial welds, forgings or plates, and for beltline circumferential weld seams for plant operation to the end-of-plant license. All domestic PWR vessels have been required to evaluate vessel embrittlement in accordance with the criteria through the end of license. The NRC revised 10 CFR 50.61 in 1991 and 1995 to change the procedure for calculating radiation embrittlement. These revisions make the procedure for calculating the reference temperature for pressurized thermal shock (RT_{PTS}) values consistent with the methods given in RG 1.99, Revision 2 [Ref. 4].

These accepted methods were used with the maximum fluence values of Section 2 to calculate the following RT_{PTS} values for the St. Lucie Units 1 and 2 RPV materials at 72 EFPY (SLR). Only those projected fluence values with a 1.1 bias on the peripheral and re-entrant corner assembly relative powers are considered in this section. The RT_{PTS} calculations are summarized in Tables 6-1 and 6-2 for St. Lucie Units 1 and 2, respectively.

PTS Conclusion

All of the beltline reactor vessel materials for St. Lucie Units 1 and 2 are projected to remain below the RT_{PTS} screening criteria values of 270°F for plates, forgings, and longitudinal welds, and 300°F for circumferentially-oriented welds (per 10 CFR 50.61) at SLR.

The St. Lucie Unit 1 limiting RT_{PTS} value for base metal or longitudinal weld materials at 72 EFPY is 250.8°F (see Table 6-1), which corresponds to Lower Shell Axial Weld Seams 3-203 A, B, & C (Heat # 305424). The St. Lucie Unit 1 limiting RT_{PTS} value for circumferentially-oriented weld materials at 72 EFPY is 135.3°F (see Table 6-1), which corresponds to the Upper to Intermediate Shell Girth Weld Seam 8-203 (Heat # 21935). The Intermediate to Lower Shell Girth Weld Seam 9-203 (Heat # 90136) result without the use of surveillance data is higher; however, use of credible surveillance data makes this material non-limiting.

The St. Lucie Unit 2 limiting RT_{PTS} value for base metal or longitudinal weld materials at 72 EFPY is 195.3°F (see Table 6-2), which corresponds to Intermediate Shell Plate M-605-1 with credible surveillance data. The St. Lucie Unit 2 limiting RT_{PTS} value for circumferentially-oriented weld materials at 72 EFPY is 64.1°F (see Table 6-2), which corresponds to the Intermediate to Lower Shell Girth Weld Seam 101-171 (Heat #'s 83637 / 3P7317).

Table 6-1 RT_{PTS} Calculations for St. Lucie Unit 1 Reactor Vessel Beltline Materials at 72 EFPY

Material	CF[a]	Fluence[b] (x 10^{19} n/cm^2, E > 1.0 MeV)	FF[c]	$RT_{NDT(U)}$[d] (°F)	Predicted ΔRT_{NDT} (°F)	σ_U (°F)	σ_Δ[e] (°F)	M (°F)	RT_{PTS} (°F)
Beltline									
Intermediate Shell Plate C-7-1	74.60	6.38	1.447	0	108.0	0	17.0	34.0	142.0
Intermediate Shell Plate C-7-2	74.60	6.38	1.447	-10	108.0	0	17.0	34.0	132.0
Intermediate Shell Plate C-7-3	73.80	6.38	1.447	10	106.8	0	17.0	34.0	150.8
Lower Shell Plate C-8-1	107.80	6.35	1.447	20	155.9	0	17.0	34.0	209.9
with **credible** surveillance data[f]	81.84	6.35	1.447	20	118.4	0	8.5	17.0	155.4
Lower Shell Plate C-8-2	108.35	6.35	1.447	20	156.7	0	17.0	34.0	210.7
with **credible** surveillance data[f]	82.67	6.35	1.447	20	119.6	0	8.5	17.0	156.6
Lower Shell Plate C-8-3	82.60	6.35	1.447	0	119.5	0	17.0	34.0	153.5
with **credible** surveillance data[f]	62.83	6.35	1.447	0	90.9	0	8.5	17.0	107.9
Intermediate to Lower Shell Girth Weld Seam 9-203 (Heat # 90136)	124.25	6.32	1.446	-60	179.6	0	28.0	56.0	175.6
with **credible** surveillance data[f]	85.79	6.32	1.446	-60	124.0	0	14.0	28.0	92.0
Intermediate Shell Axial Weld Seams 2-203 A, B, & C (Heat #'s 34B009 / A-8746)	90.65	3.91	1.351	-56	122.5	17	28.0	65.5	132.0
Lower Shell Axial Weld Seams 3-203 A, B, & C (Heat # 305424)	188.80	3.88	1.350	-60	254.8	0	28.0	56.0	250.8
with **non-credible** Beaver Valley Unit 1 surveillance data[f]	176.28	3.88	1.350	-60	237.9	0	28.0	56.0	233.9
Extended Beltline									
Upper Shell Plate C-6-1	113.10	0.301	0.671	33	75.9	0	17.0	34.0	142.9
Upper Shell Plate C-6-2	113.10	0.301	0.671	15	75.9	0	17.0	34.0	124.9
Upper Shell Plate C-6-3	113.10	0.301	0.671	15	75.9	0	17.0	34.0	124.9
Upper to Intermediate Shell Girth Weld Seam 8-203 (Heat # 21935)	172.22	0.377	0.730	-56	125.8	17	28.0	65.5	135.3
Upper Shell Axial Seams 1-203 A, B, and C (Heat #'s 21935 / 12008)	208.62	0.377	0.730	-50	152.3	0	28.0	56.0	158.3

Notes contained on the following page.

Notes:

(a) Chemistry factors (CFs) are taken from Table 5-4.

(b) The 72 EFPY maximum fluence values for the reactor vessel materials were taken from Table 2.4-5. Only those projected fluence values with a 1.1 bias on the peripheral and re-entrant corner assembly relative powers are considered.

(c) FF = fluence factor = $f^{(0.28 - 0.10 * \log(f))}$.

(d) $RT_{NDT(U)}$ values taken from Table 3-1.

(e) Per 10 CFR 50.61, the base metal σ_{Δ} = 17°F when surveillance data is non-credible or not used to determine the CF, and the base metal σ_{Δ} = 8.5°F when credible surveillance data is used to determine the CF. Also, per 10 CFR 50.61, the weld metal σ_{Δ} = 28°F when surveillance data are non-credible or not used to determine the CF, and the weld metal σ_{Δ} = 14°F when credible surveillance data are used to determine the CF. However, σ_{Δ} need not exceed 0.5 * ΔRT_{NDT}.

(f) The credibility evaluation for the St. Lucie Unit 1 surveillance data in Appendix B determined that the St. Lucie Unit 1 surveillance data for the Lower Shell Plate C-8-2 and Heat # 90136 materials are deemed credible. Therefore, the Position 2.1 CF can be used with a reduced margin term in lieu of the Position 1.1 CF. The Beaver Valley Unit 1 Heat # 305424 surveillance weld was determined to be non-credible in WCAP-18102-NP [Ref. 28].

Table 6-2 RT_{PTS} Calculations for St. Lucie Unit 2 Reactor Vessel Beltline Materials at 72 EFPY

Material	CF[(a)]	Fluence[(b)] (x 10^{19} n/cm^2, E > 1.0 MeV)	FF[(c)]	$RT_{NDT(U)}$[(d)] (°F)	Predicted ΔRT_{NDT} (°F)	σ_U (°F)	σ_Δ[(e)] (°F)	M (°F)	RT_{PTS} (°F)
Beltline									
Intermediate Shell Plate M-605-1	74.15	6.56	1.452	30	107.7	0	17.0	34.0	171.7
with **credible** surveillance data[(f)]	102.12	6.56	1.452	30	148.3	0	8.5	17.0	195.3
Intermediate Shell Plate M-605-2	91.50	6.56	1.452	10	132.9	0	17.0	34.0	176.9
Intermediate Shell Plate M-605-3	74.15	6.56	1.452	0	107.7	0	17.0	34.0	141.7
with **credible** surveillance data[(f)]	102.12	6.56	1.452	0	148.3	0	8.5	17.0	165.3
Lower Shell Plate M-4116-1	37.00	6.53	1.451	20	53.7	0	17.0	34.0	107.7
Lower Shell Plate M-4116-2	44.00	6.53	1.451	20	63.9	0	17.0	34.0	117.9
Lower Shell Plate M-4116-3	44.00	6.53	1.451	20	63.9	0	17.0	34.0	117.9
Intermediate to Lower Shell Girth Weld Seam 101-171 (Heat #'s 83637 / 3P7317)	40.05	6.52	1.451	-50	58.1	0	28.0	56.0	64.1
Intermediate Shell Axial Weld Seams 101-124A, B, & C (Heat # 83642)	36.35	4.31	1.372	-56	49.9	17	24.9	60.4	54.2
Intermediate Shell Axial Weld Seam 101-124C Repair (Heat # 83637)	34.05	4.31	1.372	-50	46.7	0	23.4	46.7	43.4
with **credible** surveillance data[(f)]	23.55	4.31	1.372	-50	32.3	0	14.0	28.0	10.3
Lower Shell Axial Welds Seams 101-142A, B, & C (Heat # 83637)	34.05	4.29	1.371	-50	46.7	0	23.3	46.7	43.4
with **credible** surveillance data[(f)]	23.55	4.29	1.371	-50	32.3	0	14.0	28.0	10.3

Table 6-2 RT_{PTS} Calculations for St. Lucie Unit 2 Reactor Vessel Beltline Materials at 72 EFPY (Continued)

Material	CF[(a)]	Fluence[(b)] (x 10^{19} n/cm^2, E > 1.0 MeV)	FF[(c)]	$RT_{NDT(U)}$[(d)] (°F)	Predicted ΔRT_{NDT} (°F)	σ_U (°F)	σ_Δ[(e)] (°F)	M (°F)	RT_{PTS} (°F)
Extended Beltline									
Upper Shell Plate M-604-1	118.00	0.152	0.506	50	59.7	0	17.0	34.0	143.7
Upper Shell Plate M-604-2	118.25	0.152	0.506	50	59.8	0	17.0	34.0	143.8
Upper Shell Plate M-604-3	116.60	0.152	0.506	10	59.0	0	17.0	34.0	103.0
Upper to Intermediate Shell Girth Weld Seam 106-121 (Heat # 83637)	34.05	0.175	0.538	-50	18.3	0	9.2	18.3	-13.4
with **credible** surveillance data[(f)]	23.55	0.175	0.538	-50	12.7	0	6.3	12.7	-24.7
Upper Shell Axial Weld Seams 101-122A & C (Heat # 5P5622)	74.13	0.175	0.538	-40	39.9	0	19.9	39.9	39.8
Upper Shell Axial Weld Seams 101-122A & C (Heat # 2P5755)	96.64	0.175	0.538	-50	52.0	0	26.0	52.0	54.0
Upper Shell Axial Weld Seam 101-122B (Heat # 5P5622)	74.13	0.175	0.538	-40	39.9	0	19.9	39.9	39.8
Hot Leg Nozzle A M-4103-2	89.92	0.0103	0.112	-30	10.1	0	5.0	10.1	-9.9
Hot Leg Nozzle B M-4103-1	90.36	0.0103	0.112	-20	10.1	0	5.1	10.1	0.2
Hot Leg Nozzle to Shell Weld Seam 105-121A (Heat # 4P6519)	63.70	0.0103	0.112	-60	7.1	0	3.6	7.1	-45.7
Hot Leg Nozzle to Shell Weld Seam 105-121B (Various SMAWs)	68.00	0.0103	0.112	-60	7.6	0	3.8	7.6	-44.8

Notes contained on the following page.

Notes:

(a) Chemistry factors (CFs) are taken from Table 5-5.

(b) The 72 EFPY maximum fluence values for the reactor vessel materials were taken from Table 2.5-5. Only those projected fluence values with a 1.1 bias on the peripheral and re-entrant corner assembly relative powers are considered.

(c) FF = fluence factor = $f^{(0.28 - 0.10 * \log(f))}$.

(d) $RT_{NDT(U)}$ values taken from Table 3-2.

(e) Per 10 CFR 50.61, the base metal σ_{Δ} = 17°F when surveillance data is non-credible or not used to determine the CF, and the base metal σ_{Δ} = 8.5°F when credible surveillance data is used to determine the CF. Also, per 10 CFR 50.61, the weld metal σ_{Δ} = 28°F when surveillance data are non-credible or not used to determine the CF, and the weld metal σ_{Δ} = 14°F when credible surveillance data are used to determine the CF. However, σ_{Δ} need not exceed 0.5 * ΔRT_{NDT}.

(f) The credibility evaluation for the St. Lucie Unit 2 surveillance data in Appendix B determined that the St. Lucie Unit 2 surveillance data for the Intermediate Shell Plate M-605-1 and Heat # 83637 are deemed credible.

7 UPPER-SHELF ENERGY

The decrease in Charpy upper-shelf energy (USE) is associated with the determination of acceptable RPV toughness during the license renewal period when the vessel is exposed to additional irradiation.

The requirements on USE are included in 10 CFR 50, Appendix G [Ref. 8]. 10 CFR 50, Appendix G requires utilities to submit an analysis at least three years prior to the time that the USE of any RPV material is predicted to drop below 50 ft-lb, as measured by Charpy V-notch specimen testing.

There are two methods that can be used to predict the decrease in USE with irradiation, depending on the availability of credible surveillance capsule data as defined in RG 1.99, Revision 2 [Ref. 4]. For vessel beltline materials that are not in the surveillance program or have non-credible data, the Charpy USE (Position 1.2) is assumed to decrease as a function of fluence and copper content, as indicated in RG 1.99, Revision 2.

When two or more credible surveillance sets become available from the reactor, they may be used to determine the Charpy USE of the surveillance material. The surveillance data are then used in conjunction with the Regulatory Guide to predict the change in USE (Position 2.2) of the RPV material due to irradiation. Per RG 1.99, Revision 2, when credible data exist, the Position 2.2 projected USE value should be used in preference to the Position 1.2 projected USE value.

The 72 EFPY Position 1.2 USE values of the vessel materials can be predicted using the corresponding 1/4T fluence projections, the copper content of the materials, and Figure 2 in RG 1.99, Revision 2 (see Figures 7-1 and 7-2 of this report). Only those projected fluence values with a 1.1 bias on the peripheral and re-entrant corner assembly relative powers are considered.

The predicted Position 2.2 USE values are determined for the reactor vessel materials that are contained in the surveillance program by using the reduced plant surveillance data along with the corresponding 1/4T fluence projection. The surveillance data from Tables 4-1 and 4-2 was plotted in RG 1.99, Revision 2, Figure 2 (see Figures 7-1 and 7-2 of this report). This data was fitted by drawing a line parallel to the existing lines as the upper bound of all the surveillance data. These reduced lines were used instead of the existing lines to determine the Position 2.2 USE values. Note, Position 2.2 USE projections are performed only for those St. Lucie Units 1 and 2 vessel base metal materials from which the surveillance materials were extracted and weld metal materials with the same heat and flux type as the surveillance weld.

The projected USE values were calculated to determine if the St. Lucie Units 1 and 2 beltline and extended beltline materials remain above the 50 ft-lb criterion at 72 EFPY (SLR). These calculations are summarized in Tables 7-1 and 7-2.

USE Conclusion

As shown in Tables 7-1 and 7-2, all of the St. Lucie Units 1 and 2 reactor vessel beltline materials are projected to remain above the USE screening criterion of 50 ft-lb (per 10 CFR 50, Appendix G) at 72 EFPY (SLR). The limiting projected USE value at SLR for St. Lucie Unit 1 is Intermediate Shell Plate C-7-3 with a projected USE of 54.8 ft-lb. The limiting projected USE value at SLR for St. Lucie Unit 2 is Lower Shell Plate M-4116-1 with a projected USE of 66.4 ft-lb.

Table 7-1 Predicted USE Values for the St. Lucie Unit 1 Beltline and Extended Beltline Materials at SLR (72 EFPY)

Material	Weight % Cu[(a)]	1/4T Fluence[(b)] (x 10^{19} n/cm^2, E > 1.0 MeV)	Unirradiated USE[(a)] (ft-lb)	Projected USE Decrease[(c)] (%)	Projected USE (ft-lb)
Beltline Materials Position 1.2 Results					
Intermediate Shell Plate C-7-1	0.11	3.80	81.9	28	59.0
Intermediate Shell Plate C-7-2	0.11	3.80	81.9	28	59.0
Intermediate Shell Plate C-7-3	0.11	3.80	76.05	28	54.8
Lower Shell Plate C-8-1	0.15	3.78	81.9	33	54.9
Lower Shell Plate C-8-2	0.15	3.78	103	33	69.0
Lower Shell Plate C-8-3	0.12	3.78	88.4	29	62.8
Intermediate to Lower Shell Girth Weld Seam 9-203 (Heat # 90136)	0.27	3.77	144	52	69.1
Intermediate Shell Axial Weld Seams 2-203 A, B, & C (Heat #'s 34B009 / A-8746)	0.19	2.33	102.3	41	60.4
Lower Shell Axial Weld Seams 3-203 A, B, & C (Heat # 305424)	0.27	2.31	112	49	57.1
Extended Beltline Materials Position 1.2 Results					
Upper Shell Plate C-6-1	0.16	0.179	68	17	56.4
Upper Shell Plate C-6-2	0.16	0.179	80	17	66.4
Upper Shell Plate C-6-3	0.16	0.179	84	17	69.7
Upper to Intermediate Shell Girth Weld Seam 8-203 (Heat # 21935)	0.183	0.225	109	24	82.8
Upper Shell Axial Seams 1-203 A, B, and C (Heat #'s 21935 / 12008)	0.213	0.225	118	26	87.3
Beltline Materials Position 2.2 Results					
Lower Shell Plate C-8-2	0.15	3.78	103	39	62.8
Intermediate to Lower Shell Girth Weld Seam 9-203 (Heat # 90136)	0.27	3.77	144	49	73.4

Notes:

(a) Copper weight percent values and unirradiated USE values were taken from Table 3-1.

(b) Values taken from Table 8-3. Only those projected fluence values with a 1.1 bias on the peripheral and re-entrant corner assembly relative powers are considered.

(c) Position 1.2 percentage USE decrease values were calculated by plotting the 1/4T fluence values on RG 1.99, Figure 2 and using the material-specific Cu wt. % values. Position 2.2 percentage USE decrease values were determined by drawing an upper-bound line parallel to the existing RG 1.99, Figure 2 lines through the applicable surveillance data points. These results should be used in preference to the existing graph lines for determining the decrease in USE, because the surveillance data is credible. The St. Lucie Unit 1 surveillance data use for the RG 1.99, Position 2.2 projection can be found in Table 4-1.

Table 7-2 Predicted USE Values for the St. Lucie Unit 2 Beltline and Extended Beltline Materials at 72 EFPY

Material	Weight % Cu[(a)]	1/4T Fluence[(b)] (x 10^{19} n/cm^2, E > 1.0 MeV)	Unirradiated USE[(a)] (ft-lb)	Projected USE Decrease[(c)] (%)	Projected USE (ft-lb)
Beltline Materials Position 1.2 Results					
Intermediate Shell Plate M-605-1	0.11	3.91	105	29	74.6
Intermediate Shell Plate M-605-2	0.13	3.91	113	31	78.0
Intermediate Shell Plate M-605-3	0.11	3.91	113	29	80.2
Lower Shell Plate M-4116-1	0.06	3.89	91	27	66.4
Lower Shell Plate M-4116-2	0.07	3.89	105	27	76.7
Lower Shell Plate M-4116-3	0.07	3.89	100	27	73.0
Intermediate to Lower Shell Girth Weld Seam 101-171 (Heat #'s 83637 / 3P7317)	0.07	3.89	96	30	67.2
Intermediate Shell Axial Weld Seams 101-124A, B, & C (Heat # 83642)	0.05	2.57	116	24	88.2
Intermediate Shell Axial Weld Seam 101-124C Repair (Heat # 83637)	0.05	2.57	136	24	103.4
Lower Shell Axial Welds Seams 101-142A, B, & C (Heat # 83637)	0.05	2.56	136	24	103.4
Extended Beltline Materials Position 1.2 Results					
Upper Shell Plate M-604-1	0.16	0.0906	90	15	76.5
Upper Shell Plate M-604-2	0.16	0.0906	82	15	69.7
Upper Shell Plate M-604-3	0.16	0.0906	106	15	90.1
Upper to Intermediate Shell Girth Weld Seam 106-121 (Heat # 83637)	0.05	0.104	136	12	119.7
Upper Shell Axial Weld Seams 101-122A & C (Heat # 5P5622)	0.153	0.104	102	18	83.6
Upper Shell Axial Weld Seams 101-122A & C (Heat # 2P5755)	0.21	0.104	109	22	85.0
Upper Shell Axial Weld Seam 101-122B (Heat # 5P5622)	0.153	0.104	102	18	83.6
Hot Leg Nozzle A M-4103-2	0.127	0.0103[(d)]	107	9	97.4
Hot Leg Nozzle B M-4103-1	0.127	0.0103[(d)]	111	9	101.0
Hot Leg Nozzle to Shell Weld Seam 105-121A (Heat # 4P6519)	0.131	0.0103[(d)]	107	11	95.2
Hot Leg Nozzle to Shell Weld Seam 105-121B (Various SMAWs)	0.05	0.0103[(d)]	128	8	117.8
Beltline Materials Position 2.2 Results					
Intermediate Shell Plate M-605-1	0.11	3.91	105	32	71.4

Notes contained on the following page.

Notes:

(a) Copper (Cu) weight percent values and unirradiated USE values were taken from Table 3-2. If the base metal or weld Cu weight percentages are below the minimum value presented in Figure 2 of RG 1.99, Revision 2 [Ref. 4] (0.1 for base metal and 0.05 for welds), then the Cu weight percentages were conservatively rounded up to the minimum value for projected USE decrease determination.

(b) Values taken from Table 8-4. Fluence values above 10^{17} n/cm^2 (E > 1.0 MeV) but below 2 x 10^{17} n/cm^2 (E > 1.0 MeV) were rounded to 2 x 10^{17} n/cm^2 (E > 1.0 MeV) when determining the % decrease because 2 x 10^{17} n/cm^2 is the lowest fluence displayed in Figure 2 of RG 1.99. Only those projected fluence values with a 1.1 bias on the peripheral and re-entrant corner assembly relative powers are considered.

(c) Position 1.2 percentage USE decrease values were calculated by plotting the 1/4T fluence values on RG 1.99, Figure 2 and using the material-specific Cu wt. % values. The percent-loss lines were extended into the low fluence area of RG 1.99, Figure 2, i.e., below 10^{18} n/cm^2, in order to determine the USE percent decrease, as needed. Position 2.2 percentage USE decrease values were determined by drawing an upper-bound line parallel to the existing RG 1.99, Figure 2 lines through the applicable surveillance data points. These results should be used in preference to the existing graph lines for determining the decrease in USE, because the surveillance data is credible. The St. Lucie Unit 2 surveillance data used for the RG 1.99, Position 2.2 projection can be found in Table 4-2.

(d) Values are the maximum fluence values instead of the 1/4T fluence values.

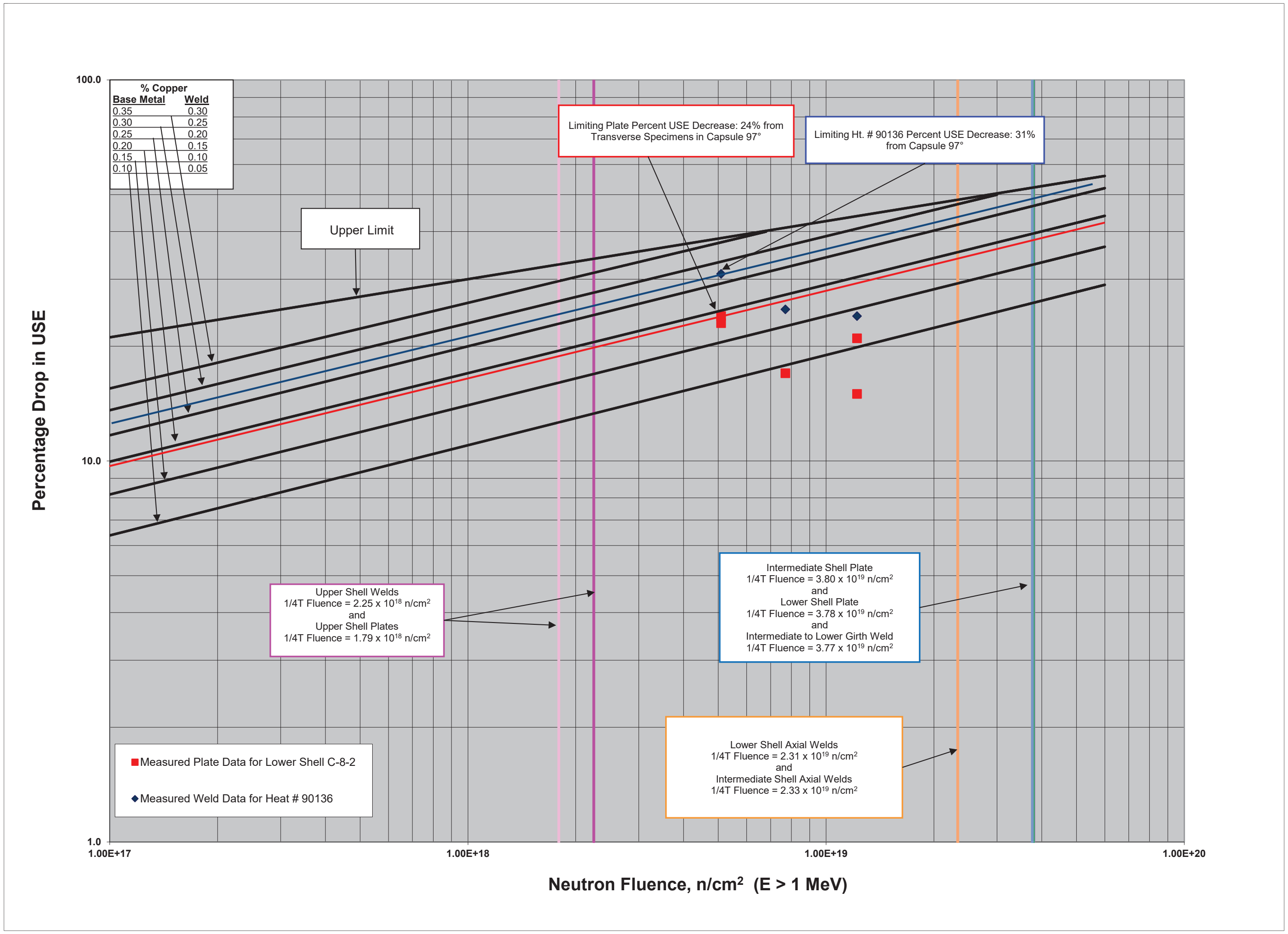

Figure 7-1 Regulatory Guide 1.99, Revision 2, St. Lucie Unit 1 Predicted Decrease in USE at 72 EFPY as a Function of Copper and Fluence

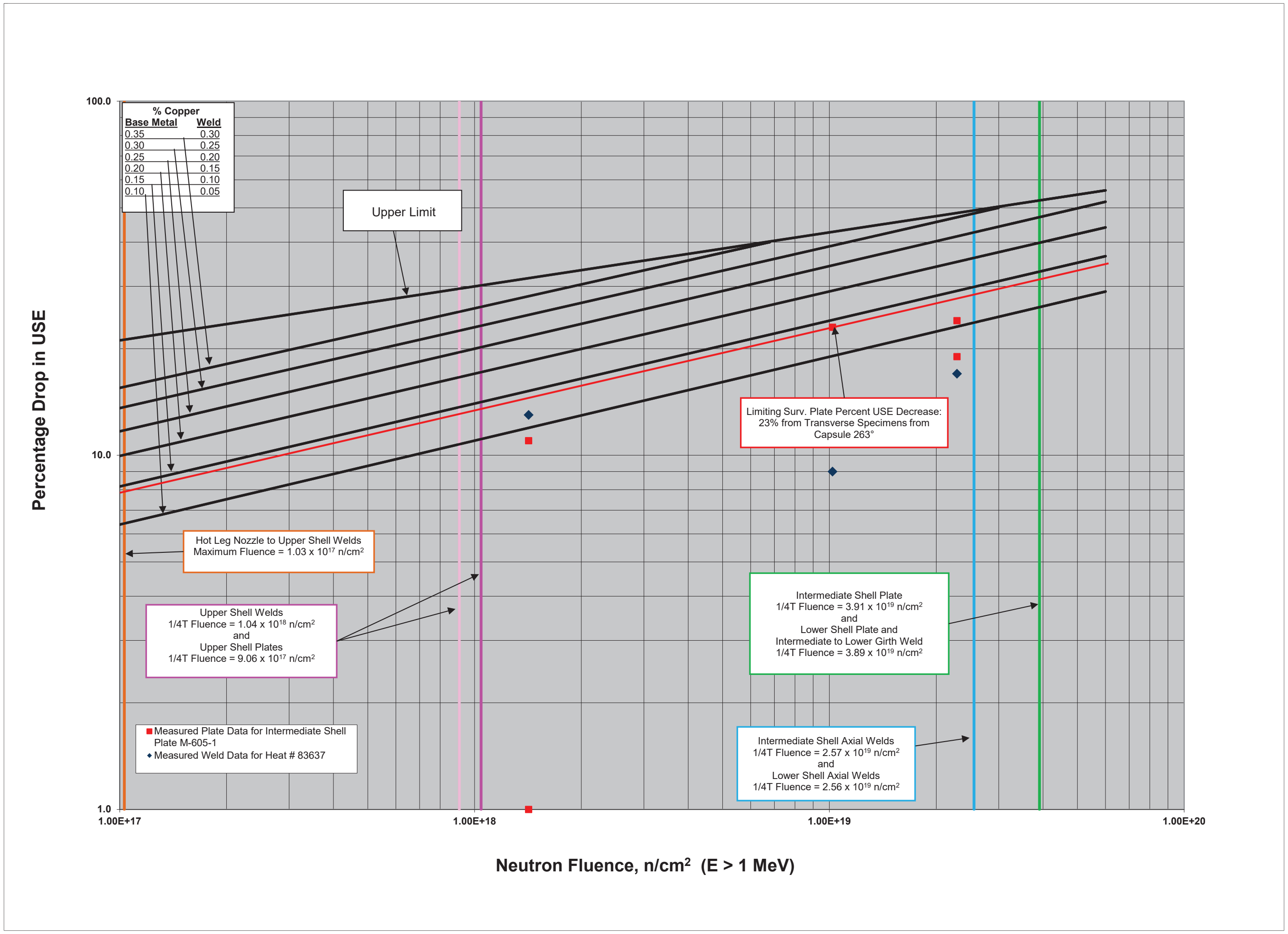

Figure 7-2 Regulatory Guide 1.99, Revision 2, St. Lucie Unit 2 Predicted Decrease in USE at 72 EFPY as a Function of Copper and Fluence

8 HEATUP AND COOLDOWN PRESSURE-TEMPERATURE LIMIT CURVES

Heatup and cooldown limit curves, also known as pressure-temperature (P-T) limit curves, are calculated using the most limiting value of RT_{NDT} (reference nil-ductility transition temperature) corresponding to the limiting material in the RPV. The most limiting RT_{NDT} of the material in the RPV is determined by using the unirradiated RPV material fracture toughness properties and estimating the irradiation-induced shift (ΔRT_{NDT}) per RG 1.99 [Ref. 4].

8.1 ADJUSTED REFERENCE TEMPERATURES CALCULATION

RT_{NDT} increases as the material is exposed to fast-neutron irradiation; therefore, to find the most limiting RT_{NDT} at any time period in the reactor's life, ΔRT_{NDT} due to the radiation exposure associated with that time period must be added to the original unirradiated RT_{NDT}. Using the adjusted reference temperature (ART) values, P-T limit curves are determined in accordance with the requirements of 10 CFR Part 50, Appendix G [Ref. 8], as augmented by Appendix G to Section XI of the ASME Boiler and Pressure Vessel Code [Ref. 11].

P-T limit curves through SLR (72 EFPY) do not need to be submitted as part of the St. Lucie Units 1 and 2 License Renewal Application (LRA) since P-T limit curves are available as a part of the current license. However, new P-T limit curve development or an extension of the applicability of the current curves must be completed prior to the expiration of the current curves as specified in the St. Lucie Units 1 and 2 licensing basis.

For St. Lucie Unit 1, the P-T limit curves implemented in the Technical Specification for normal heatup and cooldown of the primary reactor coolant system assume an EOLE of 54 EFPY, and the P-T limit curves were developed in WCAP-17197-NP [Ref. 20]. For St. Lucie Unit 2, the Technical Specification P-T limit curves assume an EOLE of 55 EFPY that were developed in WCAP-18275-NP [Ref. 18]. As a result of updated fluence data for license renewal, an applicability check of the current P-T limit curves is appropriate.

To confirm or update the applicability of the EOLE P-T limit curves, the updated reactor vessel ART values from the beltline materials must be shown to be less than or equal to the limiting beltline material ART values used in the P-T limits analysis. The RG 1.99, Revision 2 [Ref. 4] methodology was used along with the fluence values of Section 2 to calculate ART values for the St. Lucie Units 1 and 2 reactor vessel materials at EOLE and SLR. Note, the Unit 2 hot leg nozzles and associated welds will experience a fluence of 1×10^{17} n/cm^2 (E > 1.0 MeV) between 60 and 80 years of operation; therefore, these materials are only evaluated for SLR.

Tables 8-1 and 8-2 provide the surface, 1/4T, and 3/4T fluence and fluence factor (FF) values for St. Lucie Units 1 and 2 at 54 EFPY and 55 EFPY, respectively. Tables 8-3 and 8-4 provide the surface, 1/4T, and 3/4T fluence and FF values for St. Lucie Units 1 and 2 at 72 EFPY. These data are needed to calculate ART values. The Unit 1 ART calculations for EOLE are summarized in Table 8-5 for 1/4T and Table 8-6 for 3/4T. The Unit 2 ART calculations for EOLE are summarized in Table 8-7 for 1/4T and Table 8-8 for 3/4T. The Unit 1 ART calculations for SLR are summarized in Table 8-9 for 1/4T and Table 8-10 for 3/4T. The Unit 2 ART calculations for SLR are summarized in Table 8-11 for 1/4T and Table 8-12 for 3/4T.

Table 8-13 provides the ART values for the Unit 2 hot leg nozzles at SLR. This table is segregated because attenuation for the hot leg nozzle materials is not considered; thus, ART calculations are only needed at one location, i.e., the location of maximum fluence.

ART projections contained herein are based on those projected fluence values with a 1.1 bias on the peripheral and re-entrant corner assembly relative powers.

Table 8-1 St. Lucie Unit 1 Fluence and Fluence Factor Values for the Surface, 1/4T, and 3/4T Locations at 54 EFPY

Material	Surface Fluence[(a)] (x 10^{19} n/cm^2, E> 1.0 MeV)	1/4T Fluence[(b)] (x 10^{19} n/cm^2, E > 1.0 MeV)	1/4T FF[(c)]	3/4T Fluence[(b)] (x 10^{19} n/cm^2, E> 1.0 MeV)	3/4T FF[(c)]
Beltline					
Intermediate Shell Plate C-7-1	4.60	2.74	1.269	0.974	0.993
Intermediate Shell Plate C-7-2	4.60	2.74	1.269	0.974	0.993
Intermediate Shell Plate C-7-3	4.60	2.74	1.269	0.974	0.993
Lower Shell Plate C-8-1	4.58	2.73	1.268	0.970	0.991
Lower Shell Plate C-8-2	4.58	2.73	1.268	0.970	0.991
Lower Shell Plate C-8-3	4.58	2.73	1.268	0.970	0.991
Intermediate to Lower Shell Girth Weld Seam 9-203	4.56	2.72	1.267	0.965	0.990
Intermediate Shell Axial Weld Seams 2-203 A, B, & C	2.85	1.70	1.146	0.603	0.859
Lower Shell Axial Weld Seams 3-203 A, B, & C	2.83	1.69	1.144	0.599	0.857
Extended Beltline					
Upper Shell Plate C-6-1	0.217	0.129	0.470	0.0459	0.280
Upper Shell Plate C-6-2	0.217	0.129	0.470	0.0459	0.280
Upper Shell Plate C-6-3	0.217	0.129	0.470	0.0459	0.280
Upper to Intermediate Shell Girth Weld Seam 8-203	0.272	0.162	0.520	0.0576	0.316
Upper Shell Axial Weld Seams 1-203 A, B, & C	0.272	0.162	0.520	0.0576	0.316

Notes:

(a) The 54 EFPY surface fluence values for the reactor vessel materials were taken from Table 2.4-5. Only those projected fluence values with a 1.1 bias on the peripheral and re-entrant corner assembly relative powers are considered.

(b) The 1/4T and 3/4T fluence values were calculated from the surface fluence, the reactor vessel beltline thickness (8.625 inches) and equation $f = f_{surf} * e^{-0.24\,(x)}$ from RG 1.99, Revision 2, where x = the depth into the vessel wall (inches).

(c) FF = fluence factor = $f^{(0.28 - 0.10*\log(f))}$.

Table 8-2 St. Lucie Unit 2 Fluence and Fluence Factor Values for the Surface, 1/4T, and 3/4T Locations at 55 EFPY

Material	Surface Fluence[(a)] (x 10^{19} n/cm^2, E> 1.0 MeV)	1/4T Fluence[(b)] (x 10^{19} n/cm^2, E > 1.0 MeV)	1/4T FF[(c)]	3/4T Fluence[(b)] (x 10^{19} n/cm^2, E> 1.0 MeV)	3/4T FF[(c)]
Beltline					
Intermediate Shell Plate M-605-1	4.80	2.86	1.279	1.02	1.005
Intermediate Shell Plate M-605-2	4.80	2.86	1.279	1.02	1.005
Intermediate Shell Plate M-605-3	4.80	2.86	1.279	1.02	1.005
Lower Shell Plate M-4116-1	4.78	2.85	1.278	1.01	1.003
Lower Shell Plate M-4116-2	4.78	2.85	1.278	1.01	1.003
Lower Shell Plate M-4116-3	4.78	2.85	1.278	1.01	1.003
Intermediate to Lower Shell Girth Weld Seam 101-171	4.77	2.84	1.278	1.01	1.003
Intermediate Shell Axial Weld Seams 101-124A, B, & C	3.18	1.90	1.175	0.673	0.889
Lower Shell Axial Welds Seams 101-142A, B, & C	3.16	1.88	1.173	0.669	0.887
Extended Beltline					
Upper Shell Plate M-604-1	0.114	0.0679	0.344	0.0241	0.193
Upper Shell Plate M-604-2	0.114	0.0679	0.344	0.0241	0.193
Upper Shell Plate M-604-3	0.114	0.0679	0.344	0.0241	0.193
Upper to Intermediate Shell Girth Weld Seam 106-121	0.133	0.0793	0.372	0.0282	0.212
Upper Shell Axial Weld Seams 101-122A, B, & C	0.133	0.0793	0.372	0.0282	0.212

Notes:

(a) The 55 EFPY surface fluence values for the reactor vessel materials were interpolated from the 54 EFPY and 72 EFPY values in Table 2.5-5. Only those projected fluence values with a 1.1 bias on the peripheral and re-entrant corner assembly relative powers are considered.

(b) The 1/4T and 3/4T fluence values were calculated from the surface fluence, the reactor vessel beltline thickness (8.625 inches) and equation $f = f_{surf} * e^{-0.24\,(x)}$ from RG 1.99, Revision 2, where x = the depth into the vessel wall (inches).

(c) FF = fluence factor = $f^{(0.28 - 0.10*\log(f))}$.

Table 8-3 St. Lucie Unit 1 Fluence and Fluence Factor Values for the Surface, 1/4T, and 3/4T Locations at 72 EFPY

Material	Surface Fluence[a] (x 10^{19} n/cm^2, E> 1.0 MeV)	1/4T Fluence[b] (x 10^{19} n/cm^2, E > 1.0 MeV)	1/4T FF[c]	3/4T Fluence[b] (x 10^{19} n/cm^2, E> 1.0 MeV)	3/4T FF[c]
Beltline					
Intermediate Shell Plate C-7-1	6.38	3.80	1.345	1.35	1.084
Intermediate Shell Plate C-7-2	6.38	3.80	1.345	1.35	1.084
Intermediate Shell Plate C-7-3	6.38	3.80	1.345	1.35	1.084
Lower Shell Plate C-8-1	6.35	3.78	1.344	1.34	1.082
Lower Shell Plate C-8-2	6.35	3.78	1.344	1.34	1.082
Lower Shell Plate C-8-3	6.35	3.78	1.344	1.34	1.082
Intermediate to Lower Shell Girth Weld Seam 9-203	6.32	3.77	1.343	1.34	1.081
Intermediate Shell Axial Weld Seams 2-203 A, B, & C	3.91	2.33	1.229	0.828	0.947
Lower Shell Axial Weld Seams 3-203 A, B, & C	3.88	2.31	1.227	0.821	0.945
Extended Beltline					
Upper Shell Plate C-6-1	0.301	0.179	0.544	0.0637	0.333
Upper Shell Plate C-6-2	0.301	0.179	0.544	0.0637	0.333
Upper Shell Plate C-6-3	0.301	0.179	0.544	0.0637	0.333
Upper to Intermediate Shell Girth Weld Seam 8-203	0.377	0.225	0.598	0.0798	0.373
Upper Shell Axial Weld Seams 1-203 A, B, & C	0.377	0.225	0.598	0.0798	0.373

Notes:

(a) The 72 EFPY surface fluence values for the reactor vessel materials were taken from Table 2.4-5. Only those projected fluence values with a 1.1 bias on the peripheral and re-entrant corner assembly relative powers are considered.

(b) The 1/4T and 3/4T fluence values were calculated from the surface fluence, the reactor vessel beltline thickness (8.625 inches) and equation $f = f_{surf} * e^{-0.24 (x)}$ from RG 1.99, Revision 2, where x = the depth into the vessel wall (inches).

(c) FF = fluence factor = $f^{(0.28 - 0.10*\log (f))}$.

Table 8-4 St. Lucie Unit 2 Fluence and Fluence Factor Values for the Surface, 1/4T, and 3/4T Locations at 72 EFPY

Material	Surface Fluence(a) (x 10^{19} n/cm^2, E> 1.0 MeV)	1/4T Fluence(b) (x 10^{19} n/cm^2, E > 1.0 MeV)	1/4T FF(c)	3/4T Fluence(b) (x 10^{19} n/cm^2, E> 1.0 MeV)	3/4T FF(c)
Beltline					
Intermediate Shell Plate M-605-1	6.56	3.91	1.351	1.39	1.091
Intermediate Shell Plate M-605-2	6.56	3.91	1.351	1.39	1.091
Intermediate Shell Plate M-605-3	6.56	3.91	1.351	1.39	1.091
Lower Shell Plate M-4116-1	6.53	3.89	1.350	1.38	1.090
Lower Shell Plate M-4116-2	6.53	3.89	1.350	1.38	1.090
Lower Shell Plate M-4116-3	6.53	3.89	1.350	1.38	1.090
Intermediate to Lower Shell Girth Weld Seam 101-171	6.52	3.89	1.350	1.38	1.090
Intermediate Shell Axial Weld Seams 101-124A, B, & C	4.31	2.57	1.253	0.913	0.974
Lower Shell Axial Welds Seams 101-142A, B, & C	4.29	2.56	1.252	0.908	0.973
Extended Beltline					
Upper Shell Plate M-604-1	0.152	0.0906	0.397	0.0322	0.229
Upper Shell Plate M-604-2	0.152	0.0906	0.397	0.0322	0.229
Upper Shell Plate M-604-3	0.152	0.0906	0.397	0.0322	0.229
Upper to Intermediate Shell Girth Weld Seam 106-121	0.175	0.104	0.425	0.0371	0.248
Upper Shell Axial Weld Seams 101-122A, B, & C	0.175	0.104	0.425	0.0371	0.248
Hot Leg Nozzle A M-4103-2	0.0103	Note (d)	0.112(d)	Note (d)	
Hot Leg Nozzle B M-4103-1	0.0103		0.112(d)		
Hot Leg Nozzle to Shell Weld Seam 105-121A	0.0103		0.112(d)		
Hot Leg Nozzle to Shell Weld Seam 105-121B	0.0103		0.112(d)		

Notes:

(a) The 72 EFPY surface fluence values for the reactor vessel materials were taken from Table 2.5-5. Only those projected fluence values with a 1.1 bias on the peripheral and re-entrant corner assembly relative powers are considered.

(b) The 1/4T and 3/4T fluence values were calculated from the surface fluence, the reactor vessel beltline thickness (8.625 inches) and equation $f = f_{surf} * e^{-0.24\,(x)}$ from RG 1.99, Revision 2, where x = the depth into the vessel wall (inches).

(c) FF = fluence factor = $f^{(0.28 - 0.10*\log(f))}$.

(d) For conservatism, only the maximum fluence for the lowest extent of the hot leg nozzle to upper shell plate weld is considered. The FF shown in this table corresponds to the maximum fluence.

Table 8-5 Calculation of the St. Lucie Unit 1 ART Values at the 1/4T Location for the Reactor Vessel Beltline and Extended Beltline Materials at EOLE (54 EFPY)

Material	R.G. 1.99, Rev. 2 Position	CF[(a)]	1/4T Fluence[(b)] (x 10^{19} n/cm^2, E > 1.0 MeV)	1/4T FF[(b)]	$RT_{NDT(U)}$[(c)] (°F)	Predicted ΔRT_{NDT} (°F)	σ_I (°F)	σ_Δ[(d)] (°F)	M (°F)	ART (°F)
Beltline										
Intermediate Shell Plate C-7-1	1.1	74.60	2.74	1.269	0	94.7	0	17.0	34.0	128.7
Intermediate Shell Plate C-7-2	1.1	74.60	2.74	1.269	-10	94.7	0	17.0	34.0	118.7
Intermediate Shell Plate C-7-3	1.1	73.80	2.74	1.269	10	93.7	0	17.0	34.0	137.7
Lower Shell Plate C-8-1	1.1	107.80	2.73	1.268	20	136.7	0	17.0	34.0	190.7
with **credible** surveillance data[(e)]	2.1	81.84	2.73	1.268	20	103.8	0	8.5	17.0	140.8
Lower Shell Plate C-8-2	1.1	108.35	2.73	1.268	20	137.4	0	17.0	34.0	191.4
with **credible** surveillance data[(e)]	2.1	82.67	2.73	1.268	20	104.8	0	8.5	17.0	141.8
Lower Shell Plate C-8-3	1.1	82.60	2.73	1.268	0	104.7	0	17.0	34.0	138.7
with **credible** surveillance data[(e)]	2.1	62.83	2.73	1.268	0	79.7	0	8.5	17.0	96.7
Intermediate to Lower Shell Girth Weld Seam 9-203 (Heat # 90136)	1.1	124.25	2.72	1.267	-60	157.4	0	28.0	56.0	153.4
with **credible** surveillance data[(e)]	2.1	85.79	2.72	1.267	-60	108.7	0	14.0	28.0	76.7
Intermediate Shell Axial Weld Seams 2-203 A, B, & C (Heat #'s 34B009 / A-8746)	1.1	90.65	1.70	1.146	-56	103.9	17	28.0	65.5	113.4
Lower Shell Axial Weld Seams 3-203 A, B, & C (Heat # 305424)	1.1	188.80	1.69	1.144	-60	216.0	0	28.0	56.0	212.0
with **non-credible** Beaver Valley Unit 1 surveillance data[(e)]	2.1	176.28	1.69	1.144	-60	201.7	0	28.0	56.0	197.7

Table 8-5 Calculation of the St. Lucie Unit 1 ART Values at the 1/4T Location for the Reactor Vessel Beltline and Extended Beltline Materials at EOLE (54 EFPY) (Continued)

Material	R.G. 1.99, Rev. 2 Position	CF[(a)]	1/4T Fluence[(b)] (x 10^{19} n/cm^2, E > 1.0 MeV)	1/4T FF[(b)]	$RT_{NDT(U)}$[(c)] (°F)	Predicted ΔRT_{NDT} (°F)	σ_I (°F)	σ_Δ[(d)] (°F)	M (°F)	ART (°F)
Extended Beltline										
Upper Shell Plate C-6-1	1.1	113.10	0.129	0.470	33	53.2	0	17.0	34.0	120.2
Upper Shell Plate C-6-2	1.1	113.10	0.129	0.470	15	53.2	0	17.0	34.0	102.2
Upper Shell Plate C-6-3	1.1	113.10	0.129	0.470	15	53.2	0	17.0	34.0	102.2
Upper to Intermediate Shell Girth Weld Seam 8-203 (Heat # 21935)	1.1	172.22	0.162	0.520	-56	89.6	17	28.0	65.5	99.1
Upper Shell Axial Seams 1-203 A, B, and C (Heat #'s 21935 / 12008)	1.1	208.62	0.162	0.520	-50	108.6	0	28.0	56.0	114.6

Notes:

(a) Chemistry factors are taken from Table 5-4.

(b) Fluence and fluence factors taken from Table 8-1.

(c) $RT_{NDT(U)}$ values taken from Table 3-1.

(d) Per the guidance of RG 1.99, Revision 2 [Ref. 4], the base metal σ_Δ = 17°F for Position 1.1 and Position 2.1 with non-credible surveillance data, and the base metal σ_Δ = 8.5°F for Position 2.1 with credible surveillance data. Also, per RG 1.99, Revision 2, the weld metal σ_Δ = 28°F for Position 1.1 and Position 2.1 with non-credible surveillance data, and the weld metal σ_Δ = 14°F for Position 2.1 with credible surveillance data. However, σ_Δ need not exceed 0.5*ΔRT_{NDT} for either base metals or welds, with or without surveillance data.

(e) The credibility evaluation for the St. Lucie Unit 1 surveillance data in Appendix B determined that the St. Lucie Unit 1 surveillance data for the Lower Shell Plate C-8-2 and Heat # 90136 materials are deemed credible. Therefore, the Position 2.1 CF can be used with a reduced margin term in lieu of the Position 1.1 CF. The Beaver Valley Unit 1 Heat # 305424 surveillance weld was determined to be non-credible in WCAP-18102-NP [Ref. 28].

Table 8-6 Calculation of the St. Lucie Unit 1 ART Values at the 3/4T Location for the Reactor Vessel Beltline and Extended Beltline Materials at EOLE (54 EFPY)

Material	R.G. 1.99, Rev. 2 Position	CF[(a)]	3/4T Fluence[(b)] (x 10^{19} n/cm^2, E > 1.0 MeV)	3/4T FF[(b)]	$RT_{NDT(U)}$[(c)] (°F)	Predicted ΔRT_{NDT} (°F)	σ_I (°F)	σ_Δ[(d)] (°F)	M (°F)	ART (°F)
Beltline										
Intermediate Shell Plate C-7-1	1.1	74.60	0.974	0.993	0	74.0	0	17.0	34.0	108.0
Intermediate Shell Plate C-7-2	1.1	74.60	0.974	0.993	-10	74.0	0	17.0	34.0	98.0
Intermediate Shell Plate C-7-3	1.1	73.80	0.974	0.993	10	73.3	0	17.0	34.0	117.3
Lower Shell Plate C-8-1	1.1	107.80	0.970	0.991	20	106.9	0	17.0	34.0	160.9
with **credible** surveillance data[(e)]	2.1	81.84	0.970	0.991	20	81.1	0	8.5	17.0	118.1
Lower Shell Plate C-8-2	1.1	108.35	0.970	0.991	20	107.4	0	17.0	34.0	161.4
with **credible** surveillance data[(e)]	2.1	82.67	0.970	0.991	20	82.0	0	8.5	17.0	119.0
Lower Shell Plate C-8-3	1.1	82.60	0.970	0.991	0	81.9	0	17.0	34.0	115.9
with **credible** surveillance data[(e)]	2.1	62.83	0.970	0.991	0	62.3	0	8.5	17.0	79.3
Intermediate to Lower Shell Girth Weld Seam 9-203 (Heat # 90136)	1.1	124.25	0.965	0.990	-60	123.0	0	28.0	56.0	119.0
with **credible** surveillance data[(e)]	2.1	85.79	0.965	0.990	-60	84.9	0	14.0	28.0	52.9
Intermediate Shell Axial Weld Seams 2-203 A, B, & C (Heat #'s 34B009 / A-8746)	1.1	90.65	0.603	0.859	-56	77.8	17	28.0	65.5	87.3
Lower Shell Axial Weld Seams 3-203 A, B, & C (Heat # 305424)	1.1	188.80	0.599	0.857	-60	161.7	0	28.0	56.0	157.7
with **non-credible** Beaver Valley Unit 1 surveillance data[(e)]	2.1	176.28	0.599	0.857	-60	151.0	0	28.0	56.0	147.0

Table 8-6 Calculation of the St. Lucie Unit 1 ART Values at the 3/4T Location for the Reactor Vessel Beltline and Extended Beltline Materials at EOLE (54 EFPY) (Continued)

Material	R.G. 1.99, Rev. 2 Position	CF(a)	3/4T Fluence(b) (x 10^{19} n/cm^2, E > 1.0 MeV)	3/4T FF(b)	$RT_{NDT(U)}$(c) (°F)	Predicted ΔRT_{NDT} (°F)	σ_I (°F)	σ_Δ(d) (°F)	M (°F)	ART (°F)
Extended Beltline										
Upper Shell Plate C-6-1	1.1	113.10	0.0459	0.280	33	31.6	0	15.8	31.6	96.2
Upper Shell Plate C-6-2	1.1	113.10	0.0459	0.280	15	31.6	0	15.8	31.6	78.2
Upper Shell Plate C-6-3	1.1	113.10	0.0459	0.280	15	31.6	0	15.8	31.6	78.2
Upper to Intermediate Shell Girth Weld Seam 8-203 (Heat # 21935)	1.1	172.22	0.0576	0.316	-56	54.4	17	27.2	64.1	62.5
Upper Shell Axial Seams 1-203 A, B, and C (Heat #'s 21935 / 12008)	1.1	208.62	0.0576	0.316	-50	65.9	0	28.0	56.0	71.9

Notes:

(a) Chemistry factors are taken from Table 5-4.

(b) Fluence and fluence factors taken from Table 8-1.

(c) $RT_{NDT(U)}$ values taken from Table 3-1.

(d) Per the guidance of RG 1.99, Revision 2 [Ref. 4], the base metal σ_Δ = 17°F for Position 1.1 and Position 2.1 with non-credible surveillance data, and the base metal σ_Δ = 8.5°F for Position 2.1 with credible surveillance data. Also, per RG 1.99, Revision 2, the weld metal σ_Δ = 28°F for Position 1.1 and Position 2.1 with non-credible surveillance data, and the weld metal σ_Δ = 14°F for Position 2.1 with credible surveillance data. However, σ_Δ need not exceed 0.5*ΔRT_{NDT} for either base metals or welds, with or without surveillance data.

(e) The credibility evaluation for the St. Lucie Unit 1 surveillance data in Appendix B determined that the St. Lucie Unit 1 surveillance data for the Lower Shell Plate C-8-2 and Heat # 90136 materials are deemed credible. Therefore, the Position 2.1 CF can be used with a reduced margin term in lieu of the Position 1.1 CF. The Beaver Valley Unit 1 Heat # 305424 surveillance weld was determined to be non-credible in WCAP-18102-NP [Ref. 28].

Table 8-7 Calculation of the St. Lucie Unit 2 ART Values at the 1/4T Location for the Reactor Vessel Beltline and Extended Beltline Materials at EOLE (55 EFPY)

Material	R.G. 1.99, Rev. 2 Position	CF[a]	1/4T Fluence[b] (x 10^{19} n/cm^2, E > 1.0 MeV)	1/4T FF[b]	$RT_{NDT(U)}$[c] (°F)	Predicted ΔRT_{NDT} (°F)	σ_I (°F)	σ_Δ[d] (°F)	M (°F)	ART (°F)
Beltline										
Intermediate Shell Plate M-605-1	1.1	74.15	2.86	1.279	30	94.9	0	17.0	34.0	158.9
with **credible** surveillance data[e]	2.1	102.12	2.86	1.279	30	130.6	0	8.5	17.0	177.6
Intermediate Shell Plate M-605-2	1.1	91.50	2.86	1.279	10	117.1	0	17.0	34.0	161.1
Intermediate Shell Plate M-605-3	1.1	74.15	2.86	1.279	0	94.9	0	17.0	34.0	128.9
with **credible** surveillance data[e]	2.1	102.12	2.86	1.279	0	130.6	0	8.5	17.0	147.6
Lower Shell Plate M-4116-1	1.1	37.00	2.85	1.278	20	47.3	0	17.0	34.0	101.3
Lower Shell Plate M-4116-2	1.1	44.00	2.85	1.278	20	56.2	0	17.0	34.0	110.2
Lower Shell Plate M-4116-3	1.1	44.00	2.85	1.278	20	56.2	0	17.0	34.0	110.2
Intermediate to Lower Shell Girth Weld Seam 101-171 (Heat #'s 83637 / 3P7317)	1.1	40.05	2.84	1.278	-50	51.2	0	25.6	51.2	52.4
Intermediate Shell Axial Weld Seams 101-124A, B, & C (Heat # 83642)	1.1	36.35	1.90	1.175	-56	42.7	17	21.4	54.6	41.3
Intermediate Shell Axial Weld Seam 101-124C Repair (Heat # 83637)	1.1	34.05	1.90	1.175	-50	40.0	0	20.0	40.0	30.0
with **credible** surveillance data[e]	2.1	23.55	1.90	1.175	-50	27.7	0	13.8	27.7	5.3
Lower Shell Axial Welds Seams 101-142A, B, & C (Heat # 83637)	1.1	34.05	1.88	1.173	-50	40.0	0	20.0	39.9	29.9
with **credible** surveillance data[e]	2.1	23.55	1.88	1.173	-50	27.6	0	13.8	27.6	5.3

Table 8-7 Calculation of the St. Lucie Unit 2 ART Values at the 1/4T Location for the Reactor Vessel Beltline and Extended Beltline Materials at EOLE (55 EFPY) (Continued)

Material	R.G. 1.99, Rev. 2 Position	CF(a)	1/4T Fluence(b) (x 10^{19} n/cm^2, E > 1.0 MeV)	1/4T FF(b)	$RT_{NDT(U)}$(c) (°F)	Predicted ΔRT_{NDT} (°F)	σ_I (°F)	σ_Δ(d) (°F)	M (°F)	ART (°F)
Extended Beltline										
Upper Shell Plate M-604-1	1.1	118.00	0.0679	0.344	50	40.6	0	17.0	34.0	124.6
Upper Shell Plate M-604-2	1.1	118.25	0.0679	0.344	50	40.7	0	17.0	34.0	124.7
Upper Shell Plate M-604-3	1.1	116.60	0.0679	0.344	10	40.1	0	17.0	34.0	84.1
Upper to Intermediate Shell Girth Weld Seam 106-121 (Heat # 83637)	1.1	34.05	0.0793	0.372	-50	12.7	0	6.3	12.7	-24.7
with **credible** surveillance data(e)	2.1	23.55	0.0793	0.372	-50	8.8	0	4.4	8.8	-32.5
Upper Shell Axial Weld Seams 101-122A & C (Heat # 5P5622)	1.1	74.13	0.0793	0.372	-40	27.6	0	13.8	27.6	15.2
Upper Shell Axial Weld Seams 101-122A & C (Heat # 2P5755)	1.1	96.64	0.0793	0.372	-50	36.0	0	18.0	36.0	21.9
Upper Shell Axial Weld Seam 101-122B (Heat # 5P5622)	1.1	74.13	0.0793	0.372	-40	27.6	0	13.8	27.6	15.2

Notes:

(a) Chemistry factors are taken from Table 5-5.

(b) Fluence and fluence factors taken from Table 8-2.

(c) $RT_{NDT(U)}$ values taken from Table 3-2.

(d) Per the guidance of RG 1.99, Revision 2 [Ref. 4], the base metal σ_Δ = 17°F for Position 1.1 and Position 2.1 with non-credible surveillance data, and the base metal σ_Δ = 8.5°F for Position 2.1 with credible surveillance data. Also, per RG 1.99, Revision 2, the weld metal σ_Δ = 28°F for Position 1.1 and Position 2.1 with non-credible surveillance data, and the weld metal σ_Δ = 14°F for Position 2.1 with credible surveillance data. However, σ_Δ need not exceed 0.5*ΔRT_{NDT} for either base metals or welds, with or without surveillance data.

(e) The credibility evaluation for the St. Lucie Unit 2 surveillance data in Appendix B determined that the St. Lucie Unit 2 surveillance data for the Intermediate Shell Plate M-605-1 and Heat # 83637 are deemed credible.

Table 8-8 Calculation of the St. Lucie Unit 2 ART Values at the 3/4T Location for the Reactor Vessel Beltline and Extended Beltline Materials at EOLE (55 EFPY)

Material	R.G. 1.99, Rev. 2 Position	CF[(a)]	3/4T Fluence[(b)] (x 10^{19} n/cm^2, E > 1.0 MeV)	3/4T FF[(b)]	$RT_{NDT(U)}$[(c)] (°F)	Predicted ΔRT_{NDT} (°F)	σ_I (°F)	σ_Δ[(d)] (°F)	M (°F)	ART (°F)
Beltline										
Intermediate Shell Plate M-605-1	1.1	74.15	1.02	1.005	30	74.5	0	17.0	34.0	138.5
with **credible** surveillance data[(e)]	2.1	102.12	1.02	1.005	30	102.6	0	8.5	17.0	149.6
Intermediate Shell Plate M-605-2	1.1	91.50	1.02	1.005	10	91.9	0	17.0	34.0	135.9
Intermediate Shell Plate M-605-3	1.1	74.15	1.02	1.005	0	74.5	0	17.0	34.0	108.5
with **credible** surveillance data[(e)]	2.1	102.12	1.02	1.005	0	102.6	0	8.5	17.0	119.6
Lower Shell Plate M-4116-1	1.1	37.00	1.01	1.003	20	37.1	0	17.0	34.0	91.1
Lower Shell Plate M-4116-2	1.1	44.00	1.01	1.003	20	44.1	0	17.0	34.0	98.1
Lower Shell Plate M-4116-3	1.1	44.00	1.01	1.003	20	44.1	0	17.0	34.0	98.1
Intermediate to Lower Shell Girth Weld Seam 101-171 (Heat #'s 83637 / 3P7317)	1.1	40.05	1.01	1.003	-50	40.2	0	20.1	40.2	30.3
Intermediate Shell Axial Weld Seams 101-124A, B, & C (Heat # 83642)	1.1	36.35	0.673	0.889	-56	32.3	17	16.2	46.9	23.2
Intermediate Shell Axial Weld Seam 101-124C Repair (Heat # 83637)	1.1	34.05	0.673	0.889	-50	30.3	0	15.1	30.3	10.5
with **credible** surveillance data[(e)]	2.1	23.55	0.673	0.889	-50	20.9	0	10.5	20.9	-8.1
Lower Shell Axial Welds Seams 101-142A, B, & C (Heat # 83637)	1.1	34.05	0.669	0.887	-50	30.2	0	15.1	30.2	10.4
with **credible** surveillance data[(e)]	2.1	23.55	0.669	0.887	-50	20.9	0	10.4	20.9	-8.2

Table 8-8 Calculation of the St. Lucie Unit 2 ART Values at the 3/4T Location for the Reactor Vessel Beltline and Extended Beltline Materials at EOLE (55 EFPY) (Continued)

Material	R.G. 1.99, Rev. 2 Position	CF[(a)]	3/4T Fluence[(b)] (x 10^{19} n/cm^2, E > 1.0 MeV)	3/4T FF[(b)]	$RT_{NDT(U)}$[(c)] (°F)	Predicted ΔRT_{NDT} (°F)	σ_I (°F)	σ_Δ[(d)] (°F)	M (°F)	ART (°F)
Extended Beltline										
Upper Shell Plate M-604-1	1.1	118.00	0.0241	0.193	50	22.8	0	11.4	22.8	95.5
Upper Shell Plate M-604-2	1.1	118.25	0.0241	0.193	50	22.8	0	11.4	22.8	95.6
Upper Shell Plate M-604-3	1.1	116.60	0.0241	0.193	10	22.5	0	11.3	22.5	55.0
Upper to Intermediate Shell Girth Weld Seam 106-121 (Heat # 83637)	1.1	34.05	0.0282	0.212	-50	7.2	0	3.6	7.2	-35.6
with **credible** surveillance data[(e)]	2.1	23.55	0.0282	0.212	-50	5.0	0	2.5	5.0	-40.0
Upper Shell Axial Weld Seams 101-122A & C (Heat # 5P5622)	1.1	74.13	0.0282	0.212	-40	15.7	0	7.8	15.7	-8.6
Upper Shell Axial Weld Seams 101-122A & C (Heat # 2P5755)	1.1	96.64	0.0282	0.212	-50	20.4	0	10.2	20.4	-9.1
Upper Shell Axial Weld Seam 101-122B (Heat # 5P5622)	1.1	74.13	0.0282	0.212	-40	15.7	0	7.8	15.7	-8.6

Notes:

(a) Chemistry factors are taken from Table 5-5.

(b) Fluence and fluence factors taken from Table 8-2.

(c) $RT_{NDT(U)}$ values taken from Table 3-2.

(d) Per the guidance of RG 1.99, Revision 2 [Ref. 4], the base metal σ_Δ = 17°F for Position 1.1 and Position 2.1 with non-credible surveillance data, and the base metal σ_Δ = 8.5°F for Position 2.1 with credible surveillance data. Also, per RG 1.99, Revision 2, the weld metal σ_Δ = 28°F for Position 1.1 and Position 2.1 with non-credible surveillance data, and the weld metal σ_Δ = 14°F for Position 2.1 with credible surveillance data. However, σ_Δ need not exceed 0.5*ΔRT_{NDT} for either base metals or welds, with or without surveillance data.

(e) The credibility evaluation for the St. Lucie Unit 2 surveillance data in Appendix B determined that the St. Lucie Unit 2 surveillance data for the Intermediate Shell Plate M-605-1 and Heat # 83637 are deemed credible.

Table 8-9 Calculation of the St. Lucie Unit 1 ART Values at the 1/4T Location for the Reactor Vessel Beltline and Extended Beltline Materials at SLR (72 EFPY)

Material	R.G. 1.99, Rev. 2 Position	CF[(a)]	1/4T Fluence[(b)] (x 10^{19} n/cm^2, E > 1.0 MeV)	1/4T FF[(b)]	$RT_{NDT(U)}$[(c)] (°F)	Predicted ΔRT_{NDT} (°F)	σ_I (°F)	σ_Δ[(d)] (°F)	M (°F)	ART (°F)
Beltline										
Intermediate Shell Plate C-7-1	1.1	74.60	3.80	1.345	0	100.3	0	17.0	34.0	134.3
Intermediate Shell Plate C-7-2	1.1	74.60	3.80	1.345	-10	100.3	0	17.0	34.0	124.3
Intermediate Shell Plate C-7-3	1.1	73.80	3.80	1.345	10	99.3	0	17.0	34.0	143.3
Lower Shell Plate C-8-1	1.1	107.80	3.78	1.344	20	144.9	0	17.0	34.0	198.9
with **credible** surveillance data[(e)]	2.1	81.84	3.78	1.344	20	110.0	0	8.5	17.0	147.0
Lower Shell Plate C-8-2	1.1	108.35	3.78	1.344	20	145.6	0	17.0	34.0	199.6
with **credible** surveillance data[(e)]	2.1	82.67	3.78	1.344	20	111.1	0	8.5	17.0	148.1
Lower Shell Plate C-8-3	1.1	82.60	3.78	1.344	0	111.0	0	17.0	34.0	145.0
with **credible** surveillance data[(e)]	2.1	62.83	3.78	1.344	0	84.5	0	8.5	17.0	101.5
Intermediate to Lower Shell Girth Weld Seam 9-203 (Heat # 90136)	1.1	124.25	3.77	1.343	-60	166.9	0	28.0	56.0	162.9
with **credible** surveillance data[(e)]	2.1	85.79	3.77	1.343	-60	115.2	0	14.0	28.0	83.2
Intermediate Shell Axial Weld Seams 2-203 A, B, & C (Heat #'s 34B009 / A-8746)	1.1	90.65	2.33	1.229	-56	111.4	17	28.0	65.5	120.9
Lower Shell Axial Weld Seams 3-203 A, B, & C (Heat # 305424)	1.1	188.80	2.31	1.227	-60	231.6	0	28.0	56.0	227.6
with **non-credible** Beaver Valley Unit 1 surveillance data[(e)]	2.1	176.28	2.31	1.227	-60	216.2	0	28.0	56.0	212.2

Table 8-9 Calculation of the St. Lucie Unit 1 ART Values at the 1/4T Location for the Reactor Vessel Beltline and Extended Beltline Materials at SLR (72 EFPY) (Continued)

Material	R.G. 1.99, Rev. 2 Position	CF[(a)]	1/4T Fluence[(b)] (x 10^{19} n/cm^2, E > 1.0 MeV)	1/4T FF[(b)]	$RT_{NDT(U)}$[(c)] (°F)	Predicted ΔRT_{NDT} (°F)	σ_I (°F)	σ_Δ[(d)] (°F)	M (°F)	ART (°F)
Extended Beltline										
Upper Shell Plate C-6-1	1.1	113.10	0.179	0.544	33	61.5	0	17.0	34.0	128.5
Upper Shell Plate C-6-2	1.1	113.10	0.179	0.544	15	61.5	0	17.0	34.0	110.5
Upper Shell Plate C-6-3	1.1	113.10	0.179	0.544	15	61.5	0	17.0	34.0	110.5
Upper to Intermediate Shell Girth Weld Seam 8-203 (Heat # 21935)	1.1	172.22	0.225	0.598	-56	102.9	17	28.0	65.5	112.4
Upper Shell Axial Seams 1-203 A, B, and C (Heat #'s 21935 / 12008)	1.1	208.62	0.225	0.598	-50	124.7	0	28.0	56.0	130.7

Notes:

(a) Chemistry factors are taken from Table 5-4.

(b) Fluence and fluence factors taken from Table 8-3.

(c) $RT_{NDT(U)}$ values taken from Table 3-1.

(d) Per the guidance of RG 1.99, Revision 2 [Ref. 4], the base metal σ_Δ = 17°F for Position 1.1 and Position 2.1 with non-credible surveillance data, and the base metal σ_Δ = 8.5°F for Position 2.1 with credible surveillance data. Also, per RG 1.99, Revision 2, the weld metal σ_Δ = 28°F for Position 1.1 and Position 2.1 with non-credible surveillance data, and the weld metal σ_Δ = 14°F for Position 2.1 with credible surveillance data. However, σ_Δ need not exceed 0.5*ΔRT_{NDT} for either base metals or welds, with or without surveillance data.

(e) The credibility evaluation for the St. Lucie Unit 1 surveillance data in Appendix B determined that the St. Lucie Unit 1 surveillance data for the Lower Shell Plate C-8-2 and Heat # 90136 materials are deemed credible. Therefore, the Position 2.1 CF can be used with a reduced margin term in lieu of the Position 1.1 CF. The Beaver Valley Unit 1 Heat # 305424 surveillance weld was determined to be non-credible in WCAP-18102-NP [Ref. 28].

Table 8-10 Calculation of the St. Lucie Unit 1 ART Values at the 3/4T Location for the Reactor Vessel Beltline and Extended Beltline Materials at SLR (72 EFPY)

Material	R.G. 1.99, Rev. 2 Position	CF[(a)]	3/4T Fluence[(b)] (x 10^{19} n/cm^2, E > 1.0 MeV)	3/4T FF[(b)]	$RT_{NDT(U)}$[(c)] (°F)	Predicted ΔRT_{NDT} (°F)	σ_I (°F)	σ_Δ[(d)] (°F)	M (°F)	ART (°F)
Beltline										
Intermediate Shell Plate C-7-1	1.1	74.60	1.35	1.084	0	80.8	0	17.0	34.0	114.8
Intermediate Shell Plate C-7-2	1.1	74.60	1.35	1.084	-10	80.8	0	17.0	34.0	104.8
Intermediate Shell Plate C-7-3	1.1	73.80	1.35	1.084	10	80.0	0	17.0	34.0	124.0
Lower Shell Plate C-8-1	1.1	107.80	1.34	1.082	20	116.7	0	17.0	34.0	170.7
with **credible** surveillance data[(e)]	2.1	81.84	1.34	1.082	20	88.6	0	8.5	17.0	125.6
Lower Shell Plate C-8-2	1.1	108.35	1.34	1.082	20	117.3	0	17.0	34.0	171.3
with **credible** surveillance data[(e)]	2.1	82.67	1.34	1.082	20	89.5	0	8.5	17.0	126.5
Lower Shell Plate C-8-3	1.1	82.60	1.34	1.082	0	89.4	0	17	34.0	123.4
with **credible** surveillance data[(e)]	2.1	62.83	1.34	1.082	0	68.0	0	8.5	17.0	85.0
Intermediate to Lower Shell Girth Weld Seam 9-203 (Heat # 90136)	1.1	124.25	1.34	1.081	-60	134.3	0	28.0	56.0	130.3
with **credible** surveillance data[(e)]	2.1	85.79	1.34	1.081	-60	92.7	0	14.0	28.0	60.7
Intermediate Shell Axial Weld Seams 2-203 A, B, & C (Heat #'s 34B009 / A-8746)	1.1	90.65	0.828	0.947	-56	85.8	17	28.0	65.5	95.4
Lower Shell Axial Weld Seams 3-203 A, B, & C (Heat # 305424)	1.1	188.80	0.821	0.945	-60	178.4	0	28.0	56.0	174.4
with **non-credible** Beaver Valley Unit 1 surveillance data[(e)]	2.1	176.28	0.821	0.945	-60	166.6	0	28.0	56.0	162.6

Table 8-10 Calculation of the St. Lucie Unit 1 ART Values at the 3/4T Location for the Reactor Vessel Beltline and Extended Beltline Materials at SLR (72 EFPY) (Continued)

Material	R.G. 1.99, Rev. 2 Position	CF[(a)]	3/4T Fluence[(b)] (x 10^{19} n/cm^2, E > 1.0 MeV)	3/4T FF[(b)]	$RT_{NDT(U)}$[(c)] (°F)	Predicted ΔRT_{NDT} (°F)	σ_I (°F)	σ_Δ[(d)] (°F)	M (°F)	ART (°F)
Extended Beltline										
Upper Shell Plate C-6-1	1.1	113.10	0.0637	0.333	33	37.6	0	17.0	34.0	104.6
Upper Shell Plate C-6-2	1.1	113.10	0.0637	0.333	15	37.6	0	17.0	34.0	86.6
Upper Shell Plate C-6-3	1.1	113.10	0.0637	0.333	15	37.6	0	17.0	34.0	86.6
Upper to Intermediate Shell Girth Weld Seam 8-203 (Heat # 21935)	1.1	172.22	0.0798	0.373	-56	64.3	17	28.0	65.5	73.8
Upper Shell Axial Seams 1-203 A, B, and C (Heat #'s 21935 / 12008)	1.1	208.62	0.0798	0.373	-50	77.9	0	28.0	56.0	83.9

Notes:

(a) Chemistry factors are taken from Table 5-4.

(b) Fluence and fluence factors taken from Table 8-3.

(c) $RT_{NDT(U)}$ values taken from Table 3-1.

(d) Per the guidance of RG 1.99, Revision 2 [Ref. 4], the base metal σ_Δ = 17°F for Position 1.1 and Position 2.1 with non-credible surveillance data, and the base metal σ_Δ = 8.5°F for Position 2.1 with credible surveillance data. Also, per RG 1.99, Revision 2, the weld metal σ_Δ = 28°F for Position 1.1 and Position 2.1 with non-credible surveillance data, and the weld metal σ_Δ = 14°F for Position 2.1 with credible surveillance data. However, σ_Δ need not exceed 0.5*ΔRT_{NDT} for either base metals or welds, with or without surveillance data.

(e) The credibility evaluation for the St. Lucie Unit 1 surveillance data in Appendix B determined that the St. Lucie Unit 1 surveillance data for the Lower Shell Plate C-8-2 and Heat # 90136 materials are deemed credible. Therefore, the Position 2.1 CF can be used with a reduced margin term in lieu of the Position 1.1 CF. The Beaver Valley Unit 1 Heat # 305424 surveillance weld was determined to be non-credible in WCAP-18102-NP [Ref. 28].

Table 8-11 Calculation of the St. Lucie Unit 2 ART Values at the 1/4T Location for the Reactor Vessel Beltline and Extended Beltline Materials at SLR (72 EFPY)

Material	R.G. 1.99, Rev. 2 Position	CF[(a)]	1/4T Fluence[(b)] (x 10^{19} n/cm^2, E > 1.0 MeV)	1/4T FF[(b)]	$RT_{NDT(U)}$[(c)] (°F)	Predicted ΔRT_{NDT} (°F)	σ_I (°F)	σ_Δ[(d)] (°F)	M (°F)	ART (°F)
Beltline										
Intermediate Shell Plate M-605-1	1.1	74.15	3.91	1.351	30	100.2	0	17.0	34.0	164.2
with **credible** surveillance data[(e)]	2.1	102.12	3.91	1.351	30	138.0	0	8.5	17.0	185.0
Intermediate Shell Plate M-605-2	1.1	91.50	3.91	1.351	10	123.6	0	17.0	34.0	167.6
Intermediate Shell Plate M-605-3	1.1	74.15	3.91	1.351	0	100.2	0	17.0	34.0	134.2
with **credible** surveillance data[(e)]	2.1	102.12	3.91	1.351	0	138.0	0	8.5	17.0	155.0
Lower Shell Plate M-4116-1	1.1	37.00	3.89	1.350	20	50.0	0	17.0	34.0	104.0
Lower Shell Plate M-4116-2	1.1	44.00	3.89	1.350	20	59.4	0	17.0	34.0	113.4
Lower Shell Plate M-4116-3	1.1	44.00	3.89	1.350	20	59.4	0	17.0	34.0	113.4
Intermediate to Lower Shell Girth Weld Seam 101-171 (Heat #'s 83637 / 3P7317)	1.1	40.05	3.89	1.350	-50	54.1	0	27.0	54.1	58.1
Intermediate Shell Axial Weld Seams 101-124A, B, & C (Heat # 83642)	1.1	36.35	2.57	1.253	-56	45.5	17	22.8	56.8	46.4
Intermediate Shell Axial Weld Seam 101-124C Repair (Heat # 83637)	1.1	34.05	2.57	1.253	-50	42.7	0	21.3	42.7	35.3
with **credible** surveillance data[(e)]	2.1	23.55	2.57	1.253	-50	29.5	0	14.0	28.0	7.5
Lower Shell Axial Welds Seams 101-142A, B, & C (Heat # 83637)	1.1	34.05	2.56	1.252	-50	42.6	0	21.3	42.6	35.2
with **credible** surveillance data[(e)]	2.1	23.55	2.56	1.252	-50	29.5	0	14.0	28.0	7.5

Table 8-11 Calculation of the St. Lucie Unit 2 ART Values at the 1/4T Location for the Reactor Vessel Beltline and Extended Beltline Materials at SLR (72 EFPY) (Continued)

Material	R.G. 1.99, Rev. 2 Position	CF(a)	1/4T Fluence(b) (x 10^{19} n/cm^2, E > 1.0 MeV)	1/4T FF(b)	$RT_{NDT(U)}$(c) (°F)	Predicted ΔRT_{NDT} (°F)	σ_I (°F)	σ_Δ(d) (°F)	M (°F)	ART (°F)
Extended Beltline										
Upper Shell Plate M-604-1	1.1	118.00	0.0906	0.397	50	46.9	0	17.0	34.0	130.9
Upper Shell Plate M-604-2	1.1	118.25	0.0906	0.397	50	47.0	0	17.0	34.0	131.0
Upper Shell Plate M-604-3	1.1	116.60	0.0906	0.397	10	46.3	0	17.0	34.0	90.3
Upper to Intermediate Shell Girth Weld Seam 106-121 (Heat # 83637)	1.1	34.05	0.104	0.425	-50	14.5	0	7.2	14.5	-21.0
with **credible** surveillance data(e)	2.1	23.55	0.104	0.425	-50	10.0	0	5.0	10.0	-30.0
Upper Shell Axial Weld Seams 101-122A & C (Heat # 5P5622)	1.1	74.13	0.104	0.425	-40	31.5	0	15.8	31.5	23.1
Upper Shell Axial Weld Seams 101-122A & C (Heat # 2P5755)	1.1	96.64	0.104	0.425	-50	41.1	0	20.6	41.1	32.2
Upper Shell Axial Weld Seam 101-122B (Heat # 5P5622)	1.1	74.13	0.104	0.425	-40	31.5	0	15.8	31.5	23.1

Notes:

(a) Chemistry factors are taken from Table 5-5.

(b) Fluence and fluence factors taken from Table 8-4.

(c) $RT_{NDT(U)}$ values taken from Table 3-2.

(d) Per the guidance of RG 1.99, Revision 2 [Ref. 4], the base metal σ_Δ = 17°F for Position 1.1 and Position 2.1 with non-credible surveillance data, and the base metal σ_Δ = 8.5°F for Position 2.1 with credible surveillance data. Also, per RG 1.99, Revision 2, the weld metal σ_Δ = 28°F for Position 1.1 and Position 2.1 with non-credible surveillance data, and the weld metal σ_Δ = 14°F for Position 2.1 with credible surveillance data. However, σ_Δ need not exceed 0.5*ΔRT_{NDT} for either base metals or welds, with or without surveillance data.

(e) The credibility evaluation for the St. Lucie Unit 2 surveillance data in Appendix B determined that the St. Lucie Unit 2 surveillance data for the Intermediate Shell Plate M-605-1 and Heat # 83637 are deemed credible.

Table 8-12 Calculation of the St. Lucie Unit 2 ART Values at the 3/4T Location for the Reactor Vessel Beltline and Extended Beltline Materials at SLR (72 EFPY)

Material	R.G. 1.99, Rev. 2 Position	CF[(a)]	3/4T Fluence[(b)] (x 10^{19} n/cm^2, E > 1.0 MeV)	3/4T FF[(b)]	$RT_{NDT(U)}$[(c)] (°F)	Predicted ΔRT_{NDT} (°F)	σ_I (°F)	σ_Δ[(d)] (°F)	M (°F)	ART (°F)
Beltline										
Intermediate Shell Plate M-605-1	1.1	74.15	1.39	1.091	30	80.9	0	17.0	34.0	144.9
with **credible** surveillance data[(e)]	2.1	102.12	1.39	1.091	30	111.4	0	8.5	17.0	158.4
Intermediate Shell Plate M-605-2	1.1	91.50	1.39	1.091	10	99.8	0	17.0	34.0	143.8
Intermediate Shell Plate M-605-3	1.1	74.15	1.39	1.091	0	80.9	0	17.0	34.0	114.9
with **credible** surveillance data[(e)]	2.1	102.12	1.39	1.091	0	111.4	0	8.5	17.0	128.4
Lower Shell Plate M-4116-1	1.1	37.00	1.38	1.090	20	40.3	0	17.0	34.0	94.3
Lower Shell Plate M-4116-2	1.1	44.00	1.38	1.090	20	48.0	0	17.0	34.0	102.0
Lower Shell Plate M-4116-3	1.1	44.00	1.38	1.090	20	48.0	0	17.0	34.0	102.0
Intermediate to Lower Shell Girth Weld Seam 101-171 (Heat #'s 83637 / 3P7317)	1.1	40.05	1.38	1.090	-50	43.6	0	21.8	43.6	37.3
Intermediate Shell Axial Weld Seams 101-124A, B, & C (Heat # 83642)	1.1	36.35	0.913	0.974	-56	35.4	17	17.7	49.1	28.5
Intermediate Shell Axial Weld Seam 101-124C Repair (Heat # 83637)	1.1	34.05	0.913	0.974	-50	33.2	0	16.6	33.2	16.4
with **credible** surveillance data[(e)]	2.1	23.55	0.913	0.974	-50	22.9	0	11.5	22.9	-4.1
Lower Shell Axial Welds Seams 101-142A, B, & C (Heat # 83637)	1.1	34.05	0.908	0.973	-50	33.1	0	16.6	33.1	16.3
with **credible** surveillance data[(e)]	2.1	23.55	0.908	0.973	-50	22.9	0	11.5	22.9	-4.2

Table 8-12 Calculation of the St. Lucie Unit 2 ART Values at the 3/4T Location for the Reactor Vessel Beltline and Extended Beltline Materials at SLR (72 EFPY) (Continued)

Material	R.G. 1.99, Rev. 2 Position	CF(a)	3/4T Fluence(b) (x 10^{19} n/cm², E > 1.0 MeV)	3/4T FF(b)	$RT_{NDT(U)}$(c) (°F)	Predicted ΔRT_{NDT} (°F)	σ_I (°F)	σ_Δ(d) (°F)	M (°F)	ART (°F)
Extended Beltline										
Upper Shell Plate M-604-1	1.1	118.00	0.0322	0.229	50	27.0	0	13.5	27.0	104.0
Upper Shell Plate M-604-2	1.1	118.25	0.0322	0.229	50	27.1	0	13.5	27.1	104.1
Upper Shell Plate M-604-3	1.1	116.60	0.0322	0.229	10	26.7	0	13.3	26.7	63.3
Upper to Intermediate Shell Girth Weld Seam 106-121 (Heat # 83637)	1.1	34.05	0.0371	0.248	-50	8.4	0	4.2	8.4	-33.1
with **credible** surveillance data(e)	2.1	23.55	0.0371	0.248	-50	5.8	0	2.9	5.8	-38.3
Upper Shell Axial Weld Seams 101-122A & C (Heat # 5P5622)	1.1	74.13	0.0371	0.248	-40	18.4	0	9.2	18.4	-3.2
Upper Shell Axial Weld Seams 101-122A & C (Heat # 2P5755)	1.1	96.64	0.0371	0.248	-50	24.0	0	12.0	24.0	-2.1
Upper Shell Axial Weld Seam 101-122B (Heat # 5P5622)	1.1	74.13	0.0371	0.248	-40	18.4	0	9.2	18.4	-3.2

Notes:

(a) Chemistry factors are taken from Table 5-5.

(b) Fluence and fluence factors taken from Table 8-4.

(c) $RT_{NDT(U)}$ values taken from Table 3-2.

(d) Per the guidance of RG 1.99, Revision 2 [Ref. 4], the base metal σ_Δ = 17°F for Position 1.1 and Position 2.1 with non-credible surveillance data, and the base metal σ_Δ = 8.5°F for Position 2.1 with credible surveillance data. Also, per RG 1.99, Revision 2, the weld metal σ_Δ = 28°F for Position 1.1 and Position 2.1 with non-credible surveillance data, and the weld metal σ_Δ = 14°F for Position 2.1 with credible surveillance data. However, σ_Δ need not exceed 0.5*ΔRT_{NDT} for either base metals or welds, with or without surveillance data.

(e) The credibility evaluation for the St. Lucie Unit 2 surveillance data in Appendix B determined that the St. Lucie Unit 2 surveillance data for the Intermediate Shell Plate M-605-1 and Heat # 83637 are deemed credible.

Table 8-13 Calculation of the St. Lucie Unit 2 ART Values For the Hot Leg Nozzle Materials at SLR (72 EFPY)

Material	R.G. 1.99, Rev. 2 Position	CF(a)	Maximum Fluence(b) (x 10^{19} n/cm^2, E > 1.0 MeV)	FF(b)	$RT_{NDT(U)}$(c) (°F)	Predicted ΔRT_{NDT} (°F)	σ_I (°F)	σ_Δ(d) (°F)	M (°F)	ART (°F)
Hot Leg Nozzle A M-4103-2	1.1	89.92	0.0103	0.112	-30	10.1	0	5.0	10.1	-9.9
Hot Leg Nozzle B M-4103-1	1.1	90.36	0.0103	0.112	-20	10.1	0	5.1	10.1	0.2
Hot Leg Nozzle to Shell Weld Seam 105-121A (Heat # 4P6519)	1.1	63.70	0.0103	0.112	-60	7.1	0	3.6	7.1	-45.7
Hot Leg Nozzle to Shell Weld Seam 105-121B (Various SMAWs)	1.1	68.00	0.0103	0.112	-60	7.6	0	3.8	7.6	-44.8

Notes:

(a) Chemistry factors are taken from Table 5-5.

(b) Fluence and fluence factors taken from Table 8-4.

(c) $RT_{NDT(U)}$ values taken from Table 3-2.

(d) Per the guidance of Regulatory Guide 1.99, Revision 2 [Ref. 4], the base metal σ_Δ = 17°F for Position 1.1 and Position 2.1 with non-credible surveillance data, and the base metal σ_Δ = 8.5°F for Position 2.1 with credible surveillance data. Also, per Regulatory Guide 1.99, Revision 2, the weld metal σ_Δ = 28°F for Position 1.1 and Position 2.1 with non-credible surveillance data, and the weld metal σ_Δ = 14°F for Position 2.1 with credible surveillance data. However, σ_Δ need not exceed 0.5*ΔRT_{NDT} for either base metals or welds, with or without surveillance data.

8.2 P-T LIMIT CURVES APPLICABILITY

This section determines the applicability term of the current EOLE P-T limit curves by comparing the ART values contained in the analysis of record (AOR) with the ART values calculated using the updated fluence projections and materials information contained herein. If the ART values used in the previous analysis are *higher* or *equal* to the ART values calculated using the updated fluence, then the applicability term of the current curves will remain unchanged or possibly can be extended. If the ART values used in the previous analysis are *lower* than the ART values calculated using the updated fluence, then the applicability term of the current curves may need to be shortened. This new period of applicability can be calculated based on a comparison of the ART values and linear interpolation using the fluence projections. Tables 8-5 through 8-12 calculate the beltline and extended beltline 1/4T and 3/4T ART values for St. Lucie Units 1 and 2 at EOLE and SLR. Table 8-13 calculates the maximum ART values for St. Lucie Unit 2 hot leg nozzle and hot leg nozzle to upper shell plate weld materials at SLR.

Table 8-14 compares the TLAA limiting ART values at EOLE and SLR to the limiting ART values used in development of the existing EOLE P-T limit curves implemented in the Technical Specifications.

Table 8-14 Summary of the Limiting ART Values

Vessel Wall Location	Unit 1 Limiting ART (°F)			Unit 2 Limiting ART (°F)		
	P-T Limit Curves AOR[(a)]	EOLE[(c)]	SLR[(c)]	P-T Limit Curves AOR[(a)]	EOLE	SLR
1/4T	210	212.0 (197.7)	227.6 (212.2)	190.1	177.6	185.0
3/4T	156	157.7[(b)] (147.0)	174.4 (162.6)	158.7	149.6	158.4

Note:

(a) Limiting 1/4T and 3/4T ART values for Unit 1 P-T limit curves are from WCAP-17197-NP [Ref. 20]. Limiting 1/4T and 3/4T ART values for Unit 2 P-T limit curves from WCAP-18275-NP [Ref. 18].

(b) It is noted that Unit 1 Lower Shell Plates C-8-1 & C-8-2 have higher ART values when calculated with Regulatory Guide 1.99, Revision 2, Position 1.1; however, the availability of credible surveillance data allows the results calculated with Position 1.1 to be superseded by the results calculated with Position 2.1.

(c) The values in parentheses were generated using non-credible surveillance data for Heat # 305424 from the Beaver Valley Unit 1 surveillance data.

P-T Limit Curves Applicability Conclusion

For Unit 1, the results show that the limiting ART values at the 1/4T and 3/4T locations **exceed** the ART values used in the EOLE P-T limit curves when sister-plant data is **not** considered. Therefore, the existing EOLE P-T limit curves generated in WCAP-17197-NP would be valid for less than 54 EFPY. A 1/4T ART value of 210°F for the Lower Shell Axial Weld Seams 3-203 A, B, & C results from a surface fluence of 2.72 x 10^{19} n/cm^2 (E > 1.0 MeV). A 3/4T ART value of 156°F for the Lower Shell Axial Weld Seams 3-203 A, B, & C results from a surface fluence of 2.74 x 10^{19} n/cm^2 (E > 1.0 MeV). Using these fluence values and Table 2.4-5, it can be interpolated that the current P-T limit curves, and the associated LTOP enable temperatures, are only applicable until 52.1 EFPY. However, there is surveillance data available for Heat # 305424 from the Beaver Valley Unit 1 surveillance data. The use of this sister-plant data would allow the current P-T limit curves, and the associated LTOP enable temperatures, to remain valid through EOLE, specifically through 63.8 EFPY. The use of the lower RG1.99 Position 2.1 CF (compared to RG1.99 Position 1.1 CF) based on non-credible surveillance with a full margin term is justified since WCAP-18102-NP [Ref. 28], Table D-6 shows that the predicted to measured results are all within 2σ, i.e., ±56°F. This position is consistent with the NRC-approved conclusions of ML112870050 [Ref. 29] and ML113480303 [Ref. 30] for Heat # W5214 surveillance weld data. It is also noted that in WCAP-18102-NP [Ref. 28], Table D-6, the ΔRT_{NDT} is overpredicted for higher fluence data points, which have fluence values similar to that of the St. Lucie Unit 1 sister-weld. This observation further confirms that it is appropriate to use the sister-plant data.

For Unit 2, the results show that the limiting ART values at the 1/4T and 3/4T locations will **NOT be exceeded** during EOLE nor SLR. Therefore, the existing EOLE P-T limit curves, and the associated LTOP enable temperatures, generated in WCAP-18275-NP can be extended through SLR, i.e., 72 EFPY. More precisely, a 1/4T ART value of 190.1°F for Intermediate Shell Plate M-605-1 results from a surface fluence of 8.34 x 10^{19} n/cm^2 (E > 1.0 MeV). A 3/4T ART value of 158.7°F for Intermediate Shell Plate M-605-1 results from a surface fluence of 6.62 x 10^{19} n/cm^2 (E > 1.0 MeV). Using these fluence values and Table 2.5-5, it can be extrapolated that the current P-T limit curves are applicable until 72.6 EFPY.

Note that the terms of applicability for the P-T limits also implicitly confirm the bolt up temperature, lowest service temperature, and flange temperature limits. The bolt up temperature, lowest service temperature and flange-notch temperature limit are not affected by embrittlement; thus, they are unaffected by license renewal and may remain the same.

Nozzle P-T Limit Curves

NRC Regulatory Issue Summary (RIS) 2014-11 [Ref. 10] requires that the P-T limit curves account for the higher stresses in the nozzle corner region due to the potential for more restrictive P-T limits, even if the RT_{NDT} for these components are not as high as those of the reactor vessel beltline shell materials that have simpler geometries.

Pressurized Water Reactor Owners Group Report PWROG-15109-NP-A [Ref. 13] addresses this concern generically for the U.S. pressurized water reactor (PWR) operating fleet. The results of PWROG-15109-NP-A demonstrate that P-T limit curves developed with current NRC-approved methods bound the generic nozzle P-T limit curves. This document has been approved by the NRC as an acceptable means to address the concerns of RIS 2014-11. The results and conclusions of PWROG-15109-NP-A are applicable as long as the plant-specific St. Lucie Units 1 and 2 fluence at the nozzle corners remain less than the screening criterion of 4.28 x 10^{17} n/cm^2, as described in PWROG-15109-NP-A. Sections 2.4 and 2.5 demonstrate St. Lucie Units 1 and 2 adherence to this screening criterion. Thus PWROG-15109-NP-A is applicable, and nozzle P-T limit curves need no further consideration.

Low Temperature Overpressure Protection (LTOP) Controls Applicability Conclusion

For Unit 1, an evaluation was performed to validate that the current Low Temperature Overpressure Protection (LTOP) controls remain valid to at least 54 EFPY and reconcile any changes to the applicability term. This license renewal evaluation determined that there have been no adverse changes to the key input parameters used in the analysis. Therefore, similar to the P-T limits, the current LTOP controls remain valid to at least 54 EFPY. Since the LTOP evaluation is based on the P-T limit data, if there are no adverse changes to the LTOP input data, the LTOP setpoints and the enable temperature value will remain valid for the extended period of applicability of the P-T limit curves. Specifically, the existing Technical Specification power operated relief valve (PORV) setpoints of 350 psia at or below 200°F and 530 psia between 200°F and 300°F remain valid. The Technical Specification LTOP enable temperature value of 300°F for heatup and cooldown also remains valid since it is bounding of the enable temperature determined based on an ART value considering operation through 54 EFPY. The current bolt-up and lowest service temperature limits are unchanged. Technical Specification limiting conditions for operation (LCOs) and procedures for operation of reactor coolant, high pressure safety injection (HPSI) and charging pumps are unchanged. The evaluation of LTOP controls will need to be updated when new P-T curves are generated through SLR and/or if plant changes are made that affect the LTOP transients or mitigation capabilities.

For Unit 2, an evaluation was performed to validate that the current LTOP controls remain valid to at least 55 EFPY and reconcile any changes to the applicability term. This license renewal evaluation determined that there have been no changes to the key input parameters used in the analysis. Therefore, similar to the P-T limits, the current LTOP controls remain valid to at least 55 EFPY and may be extended through 72 EFPY. Since the LTOP evaluation is based on the P-T limit data, if there are no adverse changes to the LTOP input data, the LTOP setpoints and the enable temperature value will remain valid for the extended period of applicability of the P-T limit curves. Specifically, the existing shutdown cooling relief valve setpoint of 350 psia and the PORV setpoint of 490 psia remain valid. The Technical Specification LTOP enable temperature values of 252°F for heatup and 240°F for cooldown also remain valid since they are bounding of the enable temperature values determined based on an ART value considering operation through 72 EFPY. The current bolt-up and lowest service temperature limits are unchanged. Technical Specification LCOs and procedures for operation of reactor coolant, HPSI and charging pumps are unchanged. The evaluation of LTOP controls will need to be updated if new P-T curves are generated through SLR and/or if plant changes are made that affect the LTOP transients or mitigation capabilities.

9 SURVEILLANCE CAPSULE WITHDRAWAL SCHEDULES

This section provides recommended capsule withdrawal schedules for St. Lucie Units 1 and 2 in order to ensure compliance with 10 CFR 50, Appendix H [Ref. 21] and consideration of NUREG-1801, Revision 2 (GALL [Ref. 22]) and NUREG-2191 (GALL-SLR [Ref. 23]).

10 CFR 50, Appendix H [Ref. 21] states:

> *The design of the surveillance program and the withdrawal schedule must meet the requirements of the edition of ASTM E 185 that is current on the issue date of the ASME Code to which the reactor vessel was purchased; for reactor vessels purchased after 1982, the design of the surveillance program and the withdrawal schedule must meet the requirements of ASTM E 185-82. For reactor vessels purchased in or before 1982, later editions of ASTM E 185 may be used, but including only those editions through 1982. For each capsule withdrawal, the test procedures and reporting requirements must meet the requirements of ASTM E 185-82 to the extent practicable for the configuration of the specimens in the capsule.*

The St. Lucie Unit 1 reactor vessel was designed and constructed to ASME Section III, 1965 Edition through Winter 1967 Addenda per UFSAR Table 5.2-1 [Ref. 24]. The St. Lucie Unit 2 reactor vessel was designed and constructed to ASME Section III, 1971 Edition through Summer 1972 Addenda per UFSAR Table 5.2-1 [Ref. 25]. Thus, per 10 CFR 50, Appendix H, the St. Lucie Units 1 and 2 surveillance program withdrawal schedules may meet the requirements of any version of the ASTM E185 standard from the 1966 version for Unit 1 and the 1970 version for Unit 2 (the versions which were current on the issue date of the ASME Codes to which the reactor vessels were purchased) through the 1982 version. Per WCAP-15446 [Ref. 17] and WCAP-17939-NP [Ref. 19], the St. Lucie Units 1 and 2 surveillance capsule programs were designed to the ASTM E185-70 and ASTM E185-73 standards, respectively, which were the versions active at that time the programs were developed. Therefore, the requirements of 10 CFR 50, Appendix H were met at the time of the design of the reactor vessel surveillance programs.

Since that time, St. Lucie has implemented capsule withdrawal schedules in Unit 1 UFSAR [Ref. 24] Table 5.4-3 and Unit 2 UFSAR [Ref. 25] Table 5.3-9 to support license renewal (LR) to 60 years and comply with ASTM E185-82 [Ref. 27]. To date, St. Lucie Units 1 and 2 have withdrawn and tested three capsules from each unit. Unit 1 currently has two capsules (Capsule 263° and 83°) scheduled to be pulled and tested. Unit 2 currently has one capsule (Capsule 277°) currently scheduled to be pulled and tested. Per the LR SER [Ref. 26], each unit is required to test one capsule with a fluence greater than or equal to the EOLE RV fluence. The remaining in-vessel capsules (St. Lucie Unit 1 Capsule 277°, and Unit 2 Capsules 104° and 284°) are standby. Because ASTM E185-82 is based on plant operation during the original 40-year license term, the requirements are supplemented using NUREG-1801, Revision 2 (GALL [Ref. 22]) and NUREG-2191 (GALL-SLR [Ref. 23]). The latest recommended surveillance capsule withdrawal schedules for St. Lucie Units 1 and 2 are provided in Tables 9-1 and 9-2, respectively. It is noted that St. Lucie Unit 2 only has one remaining capsule with a lead factor greater than 1. Thus, in the recommended schedule, this capsule is utilized to provide data with SLR fluence as expeditiously as possible.

Surveillance Capsule Withdrawal Schedule Conclusion

The recommended surveillance capsule withdrawal schedules are provided in Tables 9-1 and 9-2 for St. Lucie Units 1 and 2, respectively. The schedules are in accordance with ASTM E185-82 [Ref. 27] and 10 CFR 50, Appendix H [Ref. 21] and consider the guidance contained in the GALL [Ref. 22] and GALL-SLR [Ref. 23]. Specifically, the withdrawn and tested capsules will meet the following GALL and GALL-SLR guidance:

- At least one capsule is withdrawn and tested with a fluence of between one and two times the 60-year peak reactor vessel wall neutron fluence.
- At least one capsule is withdrawn and tested with a fluence of between one and two times the 80-year peak reactor vessel wall neutron fluence.

It is noted that the capsule fluence should be used to determine when the capsule is withdrawn, and the EFPY is an approximation based on the unbiased capsule projections. The capsule should be withdrawn at the outage nearest to, but following, when the capsule fluence is met.

Table 9-1 St. Lucie Unit 1 Recommended Surveillance Capsule Withdrawal Schedule[d]

Vessel Location	Capsule Withdrawal EFPY[e]	Capsule Fluence (n/cm^2, E > 1.0 MeV)	Lead Factor[b]
97° [a]	4.82	5.09×10^{18}	1.35
104° [a]	9.70	7.70×10^{18}	0.83
284° [a]	17.42	1.22×10^{19}	0.88
263° [f]	46	4.60×10^{19}	1.23
83°	62	6.38×10^{19}	1.23
277°[c]	Standby[c]	------	1.23

Notes:

(a) Numbers for these capsules are actual. Fluence values reflect the most recent analysis.

(b) Lead factor is defined as the capsule fluence divided by RV base metal peak fluence.

(c) The capsule at 277° was found to be missing its ACME threaded top during a 1996 vessel inspection (Condition Report 96-1064). Without the top, a special removal tool will be required to retrieve the 277° capsule. This capsule may be substituted for either Capsule 83° or 263° if tooling capable of removing this capsule is developed, since it is considered to be radiologically equivalent to Capsules 83° and 263° (also at the 7° azimuthal location).

(d) Capsule removal schedule changes require NRC approval per 10 CFR 50, Appendix H.

(e) For capsules not yet withdrawn, the capsule will be withdrawn at the outage nearest to but following the stated EFPY.

(f) Based on Unit 1 UFSAR [Ref. 24] Table 5.4-2, Capsule 263° contains Standard Reference Material (SRM) in lieu of the transverse base metal Charpy specimens. It is recommended that this capsule be withdrawn prior to achieving the SLR in order for the SLR capsule to contain as many specimens as possible which are representative of St. Lucie Unit 1 reactor vessel material.

Table 9-2 St. Lucie Unit 2 Recommended Surveillance Capsule Withdrawal Schedule[c]

Vessel Location	Capsule Withdrawal EFPY[d]	Capsule Fluence (n/cm^2, E > 1.0 MeV)	Lead Factor[b]
83° [a]	1.11	1.42×10^{18}	1.27
263° [a]	11.07	1.02×10^{19}	1.26
97° [a]	25.55	2.29×10^{19}	1.28
277°	61	6.56×10^{19}	1.27
104°	Standby[e]	------	0.92
284°	Standby[e]	------	0.92

Note:

(a) Numbers for these capsules are actual. Fluence values reflect the most recent analysis.

(b) Lead factor is defined as the capsule fluence divided by RV base metal peak fluence.

(c) Capsule removal schedule changes require NRC approval per 10 CFR 50, Appendix H.

(d) For capsules not yet withdrawn, the capsule will be withdrawn at the outage nearest to but following the stated EFPY.

(e) Capsule will reach the EOLE fluence of 4.80×10^{19} n/cm^2 at 62 EFPY.

10 REFERENCES

1. Code of Federal Regulations, 10 CFR Part 54.3, "Definitions," U.S. Nuclear Regulatory Commission, Washington, D.C., Federal Register, dated August 28, 2007.
2. ASTM E853-18, "Standard Practice for Analysis and Interpretation of Light-Water Reactor Surveillance Neutron Exposure Results," 2018.
3. ASTM E693-94, "Standard Practice for Characterizing Neutron Exposures in Iron and Low Alloy Steels in Terms of Displacements Per Atom (DPA), E706 (ID)," 1994.
4. U.S. Nuclear Regulatory Commission, Office of Nuclear Regulatory Research, Regulatory Guide 1.99, Revision 2, "Radiation Embrittlement of Reactor Vessel Materials," May 1988. *[Agencywide Documents Access and Management System (ADAMS) Accession Number ML003740284]*
5. U.S. Nuclear Regulatory Commission, Office of Nuclear Regulatory Research, Regulatory Guide 1.190, Revision 0, "Calculational and Dosimetry Methods for Determining Pressure Vessel Neutron Fluence," March 2001. *[ADAMS Accession Number ML010890301]*
6. Westinghouse Report WCAP-18124-NP-A, Revision 0, "Fluence Determination with RAPTOR-M3G and FERRET," July 2018. *[ADAMS Accession Number ML18204A010]*
7. Westinghouse InfoGram IG-13-2, "Fluence Attenuation Profile in Reactor Pressure Vessel Shell and Inlet/Outlet Nozzle Regions," July 1, 2013.
8. Code of Federal Regulations 10 CFR 50, Appendix G, "Fracture Toughness Requirements," U.S. Nuclear Regulatory Commission, Federal Register, December 12, 2013.
9. Code of Federal Regulations 10 CFR 50.61, "Fracture Toughness Requirements for Protection Against Pressurized Thermal Shock Events," U.S. Nuclear Regulatory Commission, Federal Register, January 4, 2010.
10. U.S. Nuclear Regulatory Commission, Regulatory Issue Summary 2014-11, "Information on Licensing Applications for Fracture Toughness Requirements for Ferritic Reactor Coolant Pressure Boundary Components," October 2014. *[ADAMS Accession Number ML14149A165]*
11. Appendix G to the 1998 through the 2000 Addenda Edition of the ASME Boiler and Pressure Vessel (B&PV) Code, Section XI, Division 1, "Fracture Toughness Criteria for Protection Against Failure."
12. Westinghouse Report WCAP-14040-A, Revision 4, "Methodology Used to Develop Cold Overpressure Mitigating System Setpoints and RCS Heatup and Cooldown Limit Curves," May 2004.
13. Pressurized Water Reactor Owners Group (PWROG) Report PWROG-15109-NP-A, Revision 0, "PWR Pressure Vessel Nozzle Appendix G Evaluation," January 2020. *[ADAMS Accession Number ML20024E573]*
14. Combustion Engineering Report CE-NPSD-1119, Revision 1, "Updated Analysis for Combustion Engineering Fabricated Reactor Vessel Welds Best Estimate Copper and Nickel Content," July 1998.
15. Westinghouse Report WCAP-17389-P, Revision 0, "St. Lucie Unit 1 Extended Power Uprate (EPU) Engineering Report," February 2011.
16. Westinghouse Report WCAP-17315-NP, Revision 0, "Diablo Canyon Units 1 and 2 Pressurized Thermal Shock and Upper-Shelf Energy Evaluations," July 2011.
17. Westinghouse Report WCAP-15446, Revision 1, "Analysis of Capsule 284° from the Florida Power and Light St. Lucie Unit 1 Reactor Vessel Radiation Surveillance Program," January 2002.

18. Westinghouse Report WCAP-18275-NP, Revision 0, "St. Lucie Unit 2 Heatup and Cooldown Limit Curves for Normal Operation through End of License Extension," November 2019.

19. Westinghouse Report WCAP-17939-NP, Revision 0, "Analysis of Capsule 97° from the Florida Power & Light Company St. Lucie Unit 2 Reactor Vessel Radiation Surveillance Program," May 2015.

20. Westinghouse Report WCAP-17197-NP, Revision 1, "St. Lucie Unit 1 RCS Pressure and Temperature Limits and Low-Temperature Overpressure Protection Report for 54 Effective Full Power Years," January 2012.

21. Code of Federal Regulations 10 CFR 50, Appendix H, "Reactor Vessel Material Surveillance Program Requirements," U.S. Nuclear Regulatory Commission, Federal Register, October 2, 2020.

22. NUREG-1801, Revision 2, "Generic Aging Lessons Learned (GALL) Report," U.S. Nuclear Regulatory Commission, December 2010. *[ADAMS Accession Number ML103490041]*

23. NUREG-2191, Volume 2, "Generic Aging Lessons Learned for Subsequent License Renewal (GALL-SLR) Report," U.S. Nuclear Regulatory Commission, July 2017. *[ADAMS Accession Number ML17187A204]*

24. St. Lucie Unit 1 Updated Final Safety Analysis Report (UFSAR), Amendment No. 30, May 2020.

25. St. Lucie Unit 2 Updated Final Safety Analysis Report (UFSAR), Amendment No. 26, September 2020.

26. NRC Safety Evaluation Report (SER) NUREG-1779, Revision 0, "Safety Evaluation Report Related to the License Renewal of St. Lucie Nuclear Plant, Units 1 and 2," September 2003. *[ADAMS Accession Number ML032940205]*

27. ASTM E185-82, "Standard Practice for Conducting Surveillance Tests for Light-Water Cooled Nuclear Power Reactor Vessels," American Society for Testing and Materials, 1982.

28. Westinghouse Report WCAP-18102-NP, Revision 2, "Beaver Valley Unit 1 Heatup and Cooldown Limit Curves for Normal Operation," March 2021.

29. NRC Letter "Updated Reactor Pressure Vessel Pressurized Thermal Shock Evaluation for Palisades Nuclear Plant (TAC No. ME5263)," December 7, 2011. *[ADAMS Accession Number ML112870050]*

30. NRC Letter "Palisades Nuclear Plant – Issuance of Amendment RE: Primary Coolant System Pressure-Temperature Limits (TAC No. ME5806)," January 19, 2012. *[ADAMS Accession Number ML113480303]*

31. NUREG-0800, Standard Review Plan for the Review of Safety Analysis Reports for Nuclear Power Plants, Chapter 5 of LWR Edition, Branch Technical Position 5-3, "Fracture Toughness Requirements," Revision 4, U.S. Nuclear Regulatory Commission, March 2019. *[ADAMS Accession Number ML18338A516]*

APPENDIX A VALIDATION OF THE RADIATION TRANSPORT MODELS BASED ON NEUTRON DOSIMETRY MEASUREMENTS

A.1 ST. LUCIE UNIT 1 NEUTRON DOSIMETRY COMPARISONS

Six surveillance capsules for monitoring the effects of neutron exposure on the RPV core region (beltline) materials were inserted in the reactor vessel prior to initial plant startup. These capsules were placed in the reactor vessel, between the core barrel and the vessel wall, at azimuthal angles of 83°, 97°, 263°, and 277° (7° from the core cardinal axis) and 104° and 284° (14° from the core cardinal axis).

To date, the following in-vessel surveillance capsules have been withdrawn from the reactor core and analyzed as part of the reactor vessel materials surveillance program:

- Capsule 97 was withdrawn from the 97° location following the completion of Cycle 5.
- Capsule 104 was withdrawn from the 104° location following the completion of Cycle 9.
- Capsule 284 was withdrawn from the 284° location following the completion of Cycle 15.

These capsules were re-analyzed to validate the results of the plant-specific neutron transport calculations. More specifically, the Capsule 97, 104, and 284 threshold sensor measurements were compared with the applicable results of the RAPTOR-M3G calculations to demonstrate that, at the in-vessel locations where the sensors were irradiated, the measurements and calculations agreed within the ±20% criterion of RG 1.190 [Ref. A-1]. These measurement and calculation comparisons were performed on two levels. On the first level, calculations of individual sensor reaction rates were compared directly with the measurement data from the counting laboratory. This level of comparison was not impacted by the least-squares evaluation of the sensor sets. On the second level, calculated values of neutron exposure rates in terms of fast neutron (E > 1.0 MeV) fluence rate and iron atom displacement rate were compared with the best-estimate exposure rates obtained from the least-squares evaluation.

Table A-1 provides comparisons of the measurement-to-calculation (M/C) ratios for the neutron dosimetry in the in-vessel surveillance capsules. For the individual threshold foils, the M/C ratios range from 0.75 to 1.40, with an overall average of 1.07 and standard deviation of 16.1%. In this case, the overall average was based on an equal weighting of each of the sensor types with no adjustments made to account for the spectral coverage of the individual sensors.

Table A-2 provides comparisons of the best-estimate-to-calculation (BE/C) ratios for fast neutron (E > 1.0 MeV) fluence rate and iron atom displacement rate resulting from the least-squares evaluation of the neutron dosimetry in the in-vessel surveillance capsules. For these capsules, the average BE/C ratios are 1.00 with an associated standard deviation of 14.8% for fast neutron (E > 1.0 MeV) fluence rate, and 1.01 with an associated standard deviation of 13.7% for iron atom displacement rate.

The M/C and BE/C data comparisons in Table A-1 and Table A-2 provide a validation of the results of the plant-specific neutron transport calculations. Each of these data comparisons shows that the in-vessel measurements and calculations agree within the 20% criterion specified in RG 1.190 [Ref. A-1]. In addition, the average M/C and BE/C results agree within the 13% (1σ) uncertainty assigned to the absolute transport calculations.

Table A-1 Measurement-to-Calculation (M/C) Ratios for the Surveillance Capsules – Unit 1

Reaction	Capsule			Average	Std. Dev.
	97	104	284		
$^{63}Cu\ (n,\alpha)\ ^{60}Co$	1.40	1.11	1.17	1.23	12.5%
$^{46}Ti\ (n,p)\ ^{46}Sc$	1.22	0.96	--[(a)]	1.09	16.9%
$^{54}Fe\ (n,p)\ ^{54}Mn$	1.10	0.89	1.05	1.01	10.8%
$^{58}Ni\ (n,p)\ ^{58}Co$	1.14	0.85	1.15	1.05	16.3%
$^{238}U(Cd)\ (n,f)\ ^{137}Cs$	1.17	0.75	--[(b)]	0.96	30.9%
Average of M/C Ratios				1.07	16.1%

Notes:
(a) The normalized reaction rate for this sensor was not within three standard deviations of the Combustion Engineering (CE) in-vessel surveillance capsule database value. This sensor was therefore rejected.
(b) The uranium powder in this fission monitor was contaminated with cadmium powder and could not be counted. This is not unusual for the type of surveillance capsules used at St. Lucie.

Table A-2 Best-Estimate-to-Calculation (BE/C) Ratios for the Surveillance Capsules – Unit 1

Capsule	Fast (E > 1.0 MeV) Fluence Rate		Iron Atom Displacement Rate	
	BE/C	Std. Dev.	BE/C	Std. Dev.
97	1.09	6.0%	1.10	6.0%
104	0.83	6.0%	0.85	6.0%
284	1.08	7.0%	1.08	6.0%
Average	1.00	14.8%	1.01	13.7%

A.2 ST. LUCIE UNIT 2 NEUTRON DOSIMETRY COMPARISONS

Six surveillance capsules for monitoring the effects of neutron exposure on the RPV core region (beltline) materials were inserted in the reactor vessel prior to initial plant startup. These capsules were placed in the reactor vessel, between the core barrel and the vessel wall, at azimuthal angles of 83°, 97°, 263°, and 277° (7° from the core cardinal axis) and 104° and 284° (14° from the core cardinal axis).

To date, the following in-vessel surveillance capsules have been withdrawn from the reactor core and analyzed as part of the reactor vessel materials surveillance program:

- Capsule 83° was withdrawn from the 83° location following the completion of Cycle 1.
- Capsule 263° was withdrawn from the 263° location following the completion of Cycle 9.
- Capsule 97° was withdrawn from the 97° location following the completion of Cycle 20.

These capsules were re-analyzed to validate the results of the plant-specific neutron transport calculations. More specifically, the Capsule 83°, 263°, and 97° threshold sensor measurements were compared with the applicable results of the RAPTOR-M3G calculations to demonstrate that, at the in-vessel locations where the sensors were irradiated, the measurements and calculations agreed within the ±20% criterion of RG 1.190 [Ref. A-1]. These measurement and calculation comparisons were performed on two levels. On the first level, calculations of individual sensor reaction rates were compared directly with the measurement data from the counting laboratory. This level of comparison was not impacted by the least-squares evaluation of the sensor sets. On the second level, calculated values of neutron exposure rates in terms of fast neutron (E > 1.0 MeV) fluence rate and iron atom displacement rate were compared with the best-estimate exposure rates obtained from the least-squares evaluation.

Table A-3 provides comparisons of the measurement-to-calculation (M/C) ratios for the neutron dosimetry in the in-vessel surveillance capsules. The overall average M/C ratio for the entire 13 sample data set is 1.06 with an associated standard deviation of 14%. The observed average M/C ratios range from 0.76 to 1.23 for the individual sensor types.

Table A-4 provides comparisons of the best-estimate-to-calculation (BE/C) ratios for fast neutron (E > 1.0 MeV) fluence rate and iron atom displacement rate resulting from the least-squares evaluation of the neutron dosimetry in the in-vessel surveillance capsules. For these capsules, the average BE/C ratios are 1.01 with an associated standard deviation of 6.0% for fast neutron (E > 1.0 MeV) fluence rate, and 1.02 with an associated standard deviation of 5.5% for iron atom displacement rate.

The M/C and BE/C data comparisons in Table A-3 and Table A-4 provide a validation of the results of the plant-specific neutron transport calculations. Each of these data comparisons shows that the in-vessel measurements and calculations agree within the 20% criterion specified in RG 1.190 [Ref. A-1]. In addition, the average M/C and BE/C results agree within the 13% (1σ) uncertainty assigned to the absolute transport calculations.

Table A-3 Measurement-to-Calculation (M/C) Ratios for the Surveillance Capsules – Unit 2

Reaction	Capsule			Average	Std. Dev.
	83°	263°	97°		
$^{63}Cu\ (n,\alpha)\ ^{60}Co$	1.27	1.18	--(a)	1.23	5.2%
$^{46}Ti\ (n,p)\ ^{46}Sc$	1.13	1.13	1.10	1.12	1.5%
$^{54}Fe\ (n,p)\ ^{54}Mn$	1.11	1.11	1.02	1.08	4.8%
$^{58}Ni\ (n,p)\ ^{58}Co$	1.12	1.07	1.03	1.07	4.2%
$^{238}U(Cd)\ (n,f)\ ^{137}Cs$	0.75	--(a)	0.77	0.76	1.9%
Average of M/C Ratios				1.06	14%

Note:

(a) The normalized reaction rate for this sensor was not within three standard deviations of the Combustion Engineering (CE) in-vessel surveillance capsule database value. This sensor was therefore rejected.

Table A-4 Best-Estimate-to-Calculation (BE/C) Ratios for the Surveillance Capsules

Capsule	Fast (E > 1.0 MeV) Fluence Rate		Iron Atom Displacement Rate	
	BE/C	Std. Dev.	BE/C	Std. Dev.
83°	1.00	6.0%	1.01	6.0%
263°	1.08	7.0%	1.08	6.0%
97°	0.96	6.0%	0.97	6.0%
Average	1.01	6.0%	1.02	5.5%

A.3 REFERENCES

A-1. U.S. NRC Regulatory Guide (RG) 1.190, "Calculational and Dosimetry Methods for Determining Pressure Vessel Neutron Fluence," March 2001.

APPENDIX B ST. LUCIE UNITS 1 AND 2 SURVEILLANCE PROGRAM CREDIBILITY EVALUATION

B.1 INTRODUCTION

Regulatory Guide (RG) 1.99, Revision 2 [Ref. B-1] describes general procedures acceptable to the NRC staff for calculating the effects of neutron radiation embrittlement of the low-alloy steels currently used for light-water-cooled reactor vessels. Positions 2.1 and 2.2 of RG 1.99, Revision 2, describe the method for calculating the adjusted reference temperature and Charpy upper-shelf energy of reactor vessel beltline materials using surveillance capsule data. The methods of Positions 2.1 and 2.2 can only be applied when two or more credible surveillance data sets become available from the reactor in question.

To date, there have been three surveillance capsules removed and tested from each of the St. Lucie Units 1 and 2 reactor vessels. In accordance with RG 1.99, Revision 2, the credibility of the surveillance data will be judged based on five criteria.

Table B-1 reviews the five criteria in Regulatory Guide 1.99, Revision 2. The following subsections evaluate each of these five criteria for St. Lucie Units 1 and 2 in order to determine the credibility of the surveillance data for use in neutron radiation embrittlement calculations.

Table B-1 Regulatory Guide 1.99, Revision 2, Credibility Criteria

Criterion No.	Description
1	Materials in the capsules should be those judged most likely to be controlling with regard to radiation embrittlement.
2	Scatter in the plots of Charpy energy versus temperature for the irradiated and unirradiated conditions should be small enough to permit the determination of the 30 ft-lb temperature and upper-shelf energy unambiguously.
3	When there are two or more sets of surveillance data from one reactor, the scatter of ΔRT_{NDT} values about a best-fit line drawn as described in Regulatory Position 2.1 normally should be less than 28°F for welds and 17°F for base metal. Even if the fluence range is large (two or more orders of magnitude), the scatter should not exceed twice those values. Even if the data fail this criterion for use in shift calculations, they may be credible for determining decrease in upper-shelf energy if the upper shelf can be clearly determined, following the definition given in ASTM E185-82 [Ref. B-4].
4	The irradiation temperature of the Charpy specimens in the capsule should match the vessel wall temperature at the cladding/base metal interface within +/- 25°F.
5	The surveillance data for the correlation monitor material in the capsule should fall within the scatter band of the database for that material.

B.2 ST. LUCIE UNIT 1 CREDIBILITY EVALUATION

Criterion 1: Materials in the capsules should be those judged most likely to be controlling with regard to radiation embrittlement.

The beltline region of the reactor vessel is defined in Appendix G to 10 CFR Part 50, "Fracture Toughness Requirements" [Ref. B-2], as follows:

> *the region of the reactor vessel (shell material including welds, heat affected zones, and plates or forgings) that directly surrounds the effective height of the active core and adjacent regions of the reactor vessel that are predicted to experience sufficient neutron radiation damage to be considered in the selection of the most limiting material with regard to radiation damage.*

The St. Lucie Unit 1 reactor vessel consists of the following beltline region materials, which likely would have been considered at the time the surveillance program was designed and licensed:

- Intermediate Shell Plates C-7-1, C-7-2, and C-7-3
- Lower Shell Plates C-8-1, C-8-2, and C-8-3
- Intermediate to Lower Shell Girth Weld Seam 9-203
  (Heat # 90136, flux type Linde 0091, Lot # 3999)
- Intermediate shell plate axial weld seams 2-203A, B, & C
  (Heats # 34B009 & # A-8746, flux type Linde 124, Lots # 3688 & # 3878)
- Lower shell plate axial weld seams 3-203A, B & C
  (Heat # 305424, flux type Linde 1092, Lot # 3889)

Per WCAP-15446 [Ref. B-5], CENPD-39 [Ref. B-6] evaluated the surveillance materials in the surveillance program and judged those to be the most limiting. Lower Shell Plate C-8-2 was selected as the base metal surveillance material. This material is applicable to each of the lower shell plates, as they share a heat number. Additionally, this plate has the highest Cu and initial RT_{NDT} value of the beltline materials. Weld material corresponding to the Intermediate to Lower Shell Girth Weld 9-203 (Heat # 90136) was selected as the weld surveillance material. This weld is in the highest fluence location for a St. Lucie Unit 1 weld and also has a high Cu value.

<u>Based on the discussion, Criterion 1 is met for the St. Lucie Unit 1 surveillance program.</u>

Criterion 2: Scatter in the plots of Charpy energy versus temperature for the irradiated and unirradiated conditions should be small enough to permit the determination of the 30 ft-lb temperature and upper-shelf energy unambiguously.

Based on engineering judgment, the scatter in the data presented in these plots, as documented in WCAP-15446 [Ref. B-5], is small enough to permit the determination of the 30 ft-lb temperature and the upper-shelf energy of the St. Lucie Unit 1 surveillance materials unambiguously.

<u>Hence, the St. Lucie Unit 1 surveillance program meets Criterion 2.</u>

Criterion 3: When there are two or more sets of surveillance data from one reactor, the scatter of ΔRT_{NDT} values about a best-fit line drawn as described in Regulatory Position 2.1 normally should be less than 28°F for welds and 17°F for base metal. Even if the fluence range is large (two or more orders of magnitude), the scatter should not exceed twice those values. Even if the data fail this criterion for use in shift calculations, they may be credible for determining decrease in upper-shelf energy if the upper shelf can be clearly determined, following the definition given in ASTM E185-82.

The functional form of the least squares method as described in Regulatory Position 2.1 will be utilized to determine a best-fit line for this data and to determine if the scatter of these ΔRT_{NDT} values about this line is less than 28°F for welds and less than 17°F for plates or forgings.

Following is the calculation of the best-fit line as described in Regulatory Position 2.1 of Regulatory Guide 1.99, Revision 2. In addition, the recommended NRC methods for determining credibility will be followed. The NRC methods were presented to the industry at a meeting held by the NRC on February 12 and 13, 1998 [Ref. B-3]. At this meeting the NRC presented five cases. Of the five cases, Case 1 ("Surveillance Data Available from Plant but No Other Source") most closely represents the situation for the St. Lucie Unit 1 surveillance plate and weld materials.

Evaluation of St. Lucie Unit 1 Data Only (Case 1)

Following the NRC Case 1 guidelines, the St. Lucie Unit 1 surveillance plate and weld will be evaluated using the St. Lucie Unit 1 data. Table B-2 provides the calculation of the interim CFs for St. Lucie Unit 1. Since only St. Lucie Unit 1 data is being considered, no temperature or chemistry adjustments are required.

Table B-2 Calculation of Interim Chemistry Factors for the Credibility Evaluation Using St. Lucie Unit 1 Surveillance Capsule Data

Material	Capsule	Capsule Fluence[(a)] ($x 10^{19}$ n/cm², E > 1.0 MeV)	FF[(b)]	Measured ΔRT_{NDT}[(c)] (°F)	FF*ΔRT_{NDT} (°F)	FF^2
Lower Shell Plate C-8-2 (Longitudinal)	97°	0.509	0.811	68.70	55.75	0.659
	104°	0.770	0.927	79.87	74.01	0.859
	284°	1.22	1.055	87.93	92.81	1.114
Lower Shell Plate C-8-2 (Transverse)	97°	0.509	0.811	63.83	51.80	0.659
	284°	1.22	1.055	84.99	89.70	1.114
				SUM:	364.07	4.404
	$CF_{C\text{-}8\text{-}2} = \Sigma(FF * \Delta RT_{NDT}) \div \Sigma(FF^2) = (364.07) \div (4.404) = 82.67°F$					
Surveillance Weld (Heat # 90136)	97°	0.509	0.811	72.34	58.70	0.659
	104°	0.770	0.927	67.40	62.46	0.859
	284°	1.22	1.055	68.00	71.77	1.114
				SUM:	192.93	2.631
	$CF_{Surv.\ Weld} = \Sigma(FF * \Delta RT_{NDT}) \div \Sigma(FF^2) = (192.93) \div (2.631) = 73.32°F$					

Notes:

(a) Fluence taken from Table 2.4-8.

(b) FF = fluence factor = $f^{(0.28 - 0.10*\log(f))}$.

(c) Measured ΔRT_{NDT} taken from WCAP-15446-NP [Ref. B-5].

The scatter of ΔRT_{NDT} values about the functional form of a best-fit line drawn as described in Regulatory Guide 1.99, Revision 2, Position 2.1 is presented in Table B-3.

Table B-3 St. Lucie Unit 1 Surveillance Capsule Data Scatter about the Best-Fit Line

Material	Capsule	CF(a) (Slope$_{best-fit}$) (°F)	Capsule Fluence(b) (x 10^{19} n/cm^2)	FF(c)	Measured ΔRT_{NDT}(d) (°F)	Predicted ΔRT_{NDT}(e) (°F)	Scatter ΔRT_{NDT}(f) (°F)	<17°F (Plate) <28°F (Weld)
Lower Shell Plate C-8-2 (Longitudinal)	97°	82.67	0.509	0.811	68.70	67.1	1.6	Yes
	104°	82.67	0.770	0.927	79.87	76.6	3.3	Yes
	284°	82.67	1.22	1.055	87.93	87.3	0.7	Yes
Lower Shell Plate C-8-2 (Transverse)	97°	82.67	0.509	0.811	63.83	67.1	3.3	Yes
	284°	82.67	1.22	1.055	84.99	87.3	2.3	Yes
Surveillance Weld (Heat # 90136)	97°	73.32	0.509	0.811	72.34	59.5	12.8	Yes
	104°	73.32	0.770	0.927	67.40	67.9	0.5	Yes
	284°	73.32	1.22	1.055	68.00	77.4	9.4	Yes

Notes:

(a) CF calculated in Table B-2.

(b) Fluence taken from Table 2.4-8.

(c) FF = fluence factor = $f^{(0.28 - 0.10*\log(f))}$.

(d) Measured ΔRT_{NDT} taken from WCAP-15446-NP [Ref. B-5].

(e) Predicted ΔRT_{NDT} = CF x FF

(f) Scatter ΔRT_{NDT} = Absolute Value [Predicted ΔRT_{NDT} – Measured ΔRT_{NDT}.

The scatter of ΔRT_{NDT} values about the best-fit line, drawn as described in Regulatory Guide 1.99, Rev. 2, Position 2.1, should be less than 17°F for base metal and 28°F for welds. From a statistical point of view, +/- 1σ would be expected to encompass 68% of the data. Table B-3 indicates that the Lower Shell Plate C-8-2 has five of the five surveillance data points falling inside the +/- 1σ of 17°F scatter band for surveillance plate materials. Therefore, 100% of the data are bounded and the surveillance plate data are deemed "credible" per the third criterion.

Table B-3 indicates that the surveillance weld has three of the three surveillance data points falling inside the +/- 1σ of 28°F scatter band for surveillance weld materials. Therefore, 100% of the data are bounded and the surveillance weld data are deemed "credible" per the third criterion.

Criterion 4: The irradiation temperature of the Charpy specimens in the capsule should match the vessel wall temperature at the cladding/base metal interface within +/- 25°F.

The capsule specimens are located in the reactor between the thermal shield and the vessel wall and are positioned opposite the center of the core. The test capsules are in baskets attached to the reactor vessel. The location of the specimens with respect to the reactor vessel beltline provides assurance that the reactor vessel wall and the specimens experience equivalent operating conditions such that the temperatures will not differ by more than 25°F. Hence, this criterion is met.

Criterion 4 is met for the St. Lucie Unit 1 surveillance program.

Criterion 5: The surveillance data for the correlation monitor material in the capsule should fall within the scatter band of the database for that material.

The St. Lucie Unit 1 surveillance program does contain Standard Reference Material (SRM). As shown in NUREG/CR-6413, ORNL/TM-13133 [Ref. B-7], the material is A533 Grade B, Class 1 plate (HSST Plate 01) correlation monitor material. Figure 11 of NUREG/CR-6413, ORNL/TM-13133 contains a plot of residual versus fast fluence for the correlation monitor material. This figure shows a 2σ uncertainty of 50°F. The data used in Figure 11 is contained in Table 14 of NUREG/CR-6413 (identified as product SRM). SRM was contained only in the 104° capsule that has been removed and tested from St. Lucie Unit 1; however, the fluence value for this capsule has been updated. Table B-4 contains an updated calculation of the residual versus fast fluence.

Table B-4 St. Lucie Unit 1 Calculation of Residual versus Fast Fluence

Capsule	Capsule Fluence[(a)] (x 10^{19} n/cm^2, E > 1.0 MeV)	FF	Measured Shift[(b)] (°F)	RG 1.99 Shift (CF*FF)[(c)] (°F)	Residual Measured Shift (°F)
104°	0.770	0.927	121.0	126.1	5.1

Notes:

(a) Value taken from Table 4-1.

(b) Value taken from WCAP-15466 [Ref. B-5] Table D-3.

(c) Per WCAP-15466 [Ref. B-5] Table D-3, the Cu and Ni weight percent values for the St. Lucie Unit 1 correlation monitor material are 0.18 Cu and 0.66 Ni. This equates to a CF of 136.1°F from Regulatory Guide 1.99, Revision 2.

Table B-4 shows a 2σ uncertainty of less than 50°F, which is the allowable scatter in Figure 11 of NUREG/CR-6413. Hence, this criterion is met.

Conclusion

Based on the preceding responses to the five criteria of Regulatory Guide 1.99, Revision 2, Section B, the St. Lucie Unit 1 surveillance data for the Lower Shell Plate C-8-2 and Heat # 90136 materials are deemed credible.

B.3 ST. LUCIE UNIT 2 CREDIBILITY EVALUATION

Criterion 1: Materials in the capsules should be those judged most likely to be controlling with regard to radiation embrittlement.

The beltline region of the reactor vessel is defined in Appendix G to 10 CFR Part 50, "Fracture Toughness Requirements" [Ref. B-2], as follows:

> *the region of the reactor vessel (shell material including welds, heat affected zones, and plates or forgings) that directly surrounds the effective height of the active core and adjacent regions of the reactor vessel that are predicted to experience sufficient neutron radiation damage to be considered in the selection of the most limiting material with regard to radiation damage.*

The St. Lucie Unit 2 reactor vessel consists of the following beltline region materials, which likely would have been considered at the time the surveillance program was designed and licensed:

- Intermediate Shell Plates M-605-1, M-605-2, and M-605-3
- Lower Shell Plates M-4116-1, M-4116-2, and M-4116-3
- Intermediate to Lower Shell Girth Weld Seam 101-171 (Heat # 83637 and 3P7317, Flux Type Linde 124, Lot # 0951)
- Intermediate Shell Axial Weld Seams 101-124A, B, & C (Heat # 83642, Flux Type Linde 0091, Lot # 3536)
- Intermediate Shell Axial Weld Seam 101-124C Repair (Heat # 83637, Flux Type Linde 0091, Lot # 1122)
- Lower Shell Axial Weld Seams 101-142A, B, & C (Heat # 83637, Flux Type Linde 0091, Lot # 1122)

Per WCAP-17939-NP [Ref. B-8], the St. Lucie Unit 2 surveillance program was developed to the requirements of ASTM E185-73. Intermediate Shell Plate M-605-1 had the highest initial RT_{NDT} value and the second highest Cu wt. % value. This plate is also the same heat of material as the Intermediate Shell Plate M-605-3; therefore, it is also representative of a second beltline plate. Intermediate Shell Plate M-605-2 has a higher wt. % Cu value; however, it has superior fracture toughness properties (Initial USE and RT_{NDT}) as compared to Intermediate Shell Plate M-605-1. Lastly, all three lower shell plates, while having less than or equivalent initial USE values, have lower initial RT_{NDT} values and significantly better wt. % Cu values when compared to Intermediate Shell Plate M-605-1. Hence, the Intermediate Shell Plate M-605-1 was chosen as the most limiting plate material.

The surveillance weld metal was selected as Heat # 83637, Flux Type Linde 124, Lot # 0951. The selection of this weld material was the general practice for Combustion Engineering surveillance programs because it was considered representative material, even though this material is not directly applicable to any of the reactor vessel beltline welds. The vessel welds fabricated using the same weld wire heat, # 83637, are the intermediate shell axial weld repair, and the lower shell axial welds. However, these welds used a different flux type: Linde 0091 for the reactor vessel and Linde 124 for the surveillance weld. The intermediate to lower shell girth weld seam used the same heat and flux type; however, this weld was made with a second weld wire, Heat # 3P7317, making the surveillance weld only partially applicable to this vessel weld. Hence, weld wire Heat # 83637, Flux Type Linde 124 (Flux Lot # 0951) was utilized in the surveillance program.

Based on the discussion, Criterion 1 is met for the St. Lucie Unit 2 surveillance program.

Criterion 2: Scatter in the plots of Charpy energy versus temperature for the irradiated and unirradiated conditions should be small enough to permit the determination of the 30 ft-lb temperature and upper-shelf energy unambiguously.

Based on engineering judgment, the scatter in the data presented in these plots, as documented in WCAP-17939-NP [Ref. B-8], is small enough to permit the determination of the 30 ft-lb temperature and the upper-shelf energy of the St. Lucie Unit 2 surveillance materials unambiguously.

Hence, Criterion 2 is met for the St. Lucie Unit 2 surveillance program.

Criterion 3: When there are two or more sets of surveillance data from one reactor, the scatter of ΔRT_{NDT} values about a best-fit line drawn as described in Regulatory Position 2.1 normally should be less than 28°F for welds and 17°F for base metal. Even if the fluence range is large (two or more orders of magnitude), the scatter should not exceed twice those values. Even if the data fail this criterion for use in shift calculations, they may be credible for determining decrease in upper-shelf energy if the upper shelf can be clearly determined, following the definition given in ASTM E185-82.

The functional form of the least squares method as described in Regulatory Position 2.1 will be utilized to determine a best-fit line for this data and to determine if the scatter of these ΔRT_{NDT} values about this line is less than 28°F for welds and less than 17°F for plates or forgings.

Following is the calculation of the best-fit line as described in Regulatory Position 2.1 of Regulatory Guide 1.99, Revision 2. In addition, the recommended NRC methods for determining credibility will be followed. The NRC methods were presented to the industry at a meeting held by the NRC on February 12 and 13, 1998 [Ref. B-3]. At this meeting the NRC presented five cases. Of the five cases, Case 1 ("Surveillance Data Available from Plant but No Other Source") most closely represents the situation for the St. Lucie Unit 2 surveillance plate and weld materials.

Evaluation of St. Lucie Unit 2 Data Only (Case 1)

Following the NRC Case 1 guidelines, the St. Lucie Unit 2 surveillance data will be evaluated using the St. Lucie Unit 2 data. Table B-5 provides the calculation of the interim CFs for St. Lucie Unit 2. Since only St. Lucie Unit 2 data is being considered, no temperature or chemistry adjustments are required.

Table B-5 Calculation of Interim Chemistry Factors for the Credibility Evaluation Using St. Lucie Unit 2 Surveillance Capsule Data

Material	Capsule	Capsule Fluence[(a)] (x 10^{19} n/cm^2, E > 1.0 MeV)	FF[(b)]	Measured ΔRT_{NDT}[(c)] (°F)	FF*ΔRT_{NDT} (°F)	FF^2
Intermediate Shell Plate M-605-1 (Longitudinal)	83°	0.142	0.491	45.1	22.13	0.241
	97°	2.29	1.224	132.7	162.43	1.498
Intermediate Shell Plate M-605-1 (Transverse)	83°	0.142	0.491	29.40	14.43	0.241
	263°	1.02	1.006	102.7	103.27	1.011
	97°	2.29	1.224	127.6	156.19	1.498
				SUM:	458.45	4.489
	$CF_{M\text{-}605\text{-}1} = \Sigma(FF * \Delta RT_{NDT}) \div \Sigma(FF^2) = (458.45) \div (4.489) = 102.12°F$					
Surveillance Weld (Heat # 83637)	83°	0.142	0.491	15.8	7.75	0.241
	263°	1.02	1.006	26.5	26.65	1.011
	97°	2.29	1.224	24.8	30.36	1.498
				SUM:	64.76	2.750
	$CF_{Surv\ Weld} = \Sigma(FF * \Delta RT_{NDT}) \div \Sigma(FF^2) = (64.76) \div (2.750) = 23.55°F$					

Notes:

(a) Fluence taken from Table 2.5-8.

(b) FF = fluence factor = $f^{(0.28 - 0.10*\log(f))}$.

(c) Measured ΔRT_{NDT} taken from WCAP-17939-NP [Ref. B-8].

The scatter of ΔRT_{NDT} values about the functional form of a best-fit line drawn as described in Regulatory Guide 1.99, Revision 2, Position 2.1 is presented in Table B-6.

Table B-6 St. Lucie Unit 2 Surveillance Capsule Data Scatter about the Best-Fit Line Using All Available Surveillance Data

Material	Capsule	CF[a] ($Slope_{best-fit}$) (°F)	Capsule Fluence[b] (x 10^{19} n/cm^2)	FF[c]	Measured ΔRT_{NDT}[d] (°F)	Predicted ΔRT_{NDT}[e] (°F)	Scatter ΔRT_{NDT}[f] (°F)	<17°F (Plate) <28°F (Weld)
Intermediate Shell Plate M-605-1 (Longitudinal)	83°	102.12	0.142	0.491	45.1	50.1	5.0	Yes
	97°	102.12	2.29	1.224	132.7	125.0	7.7	Yes
Intermediate Shell Plate M-605-1 (Transverse)	83°	102.12	0.142	0.491	29.4	50.1	20.7	No
	263°	102.12	1.02	1.006	102.7	102.7	0.0	Yes
	97°	102.12	2.29	1.224	127.6	125.0	2.6	Yes
Surveillance Weld (Heat # 83637)	83°	23.55	0.142	0.491	15.8	11.6	4.2	Yes
	263°	23.55	1.02	1.006	26.5	23.7	2.8	Yes
	97°	23.55	2.29	1.224	24.8	28.8	4.0	Yes

Notes:

(a) CF calculated in Table B-5.

(b) Fluence taken from Table 2.5-8.

(c) FF = fluence factor = $f^{(0.28 - 0.10*\log(f))}$.

(d) Measured ΔRT_{NDT} taken from WCAP-17939-NP [Ref. B-8].

(e) Predicted ΔRT_{NDT} = CF x FF

(f) Scatter ΔRT_{NDT} = Absolute Value [Predicted ΔRT_{NDT} – Measured ΔRT_{NDT}].

The scatter of ΔRT_{NDT} values about the best-fit line, drawn as described in Regulatory Guide 1.99, Rev. 2, Position 2.1, should be less than 17°F for base metal and 28°F for welds. From a statistical point of view, +/- 1σ would be expected to encompass 68% of the data. Table B-6 indicates that the Intermediate Shell Plate M-605-1 has four of the five surveillance data points falling inside the +/- 1σ of 17°F scatter band for surveillance plate materials. Therefore, 80% of the data are bounded (4/5 x 100%) and the surveillance plate data are deemed "credible" per the third criterion.

Table B-6 indicates that the surveillance weld has three of the three surveillance data points falling inside the +/- 1σ of 28°F scatter band for surveillance weld materials. Therefore, 100% of the data are bounded and the surveillance weld data are deemed "credible" per the third criterion.

Criterion 4: The irradiation temperature of the Charpy specimens in the capsule should match the vessel wall temperature at the cladding/base metal interface within +/- 25°F.

The surveillance materials are contained in capsules positioned near the reactor vessel inside wall so that the irradiation conditions (fluence, flux spectrum, temperature) of the test specimens resemble, as closely as possible, the irradiation conditions of the reactor vessel. The capsules are bisected by the midplane of the core and are placed in capsule holders positioned circumferentially about the core at locations near the regions of maximum flux. The location of the specimens with respect to the reactor vessel beltline provides assurance that the reactor vessel wall and the specimens experience equivalent operating conditions such that the temperatures will not differ by more than 25°F.

Criterion 4 is met for the St. Lucie Unit 2 surveillance program.

Criterion 5: The surveillance data for the correlation monitor material in the capsule should fall within the scatter band of the database for that material.

The St. Lucie Unit 2 surveillance program does contain Standard Reference Material (SRM). As shown in NUREG/CR-6413, ORNL/TM-13133 [Ref. B-7], the material is A533 Grade B, Class 1 plate (HSST Plate 01) correlation monitor material. Figure 11 of NUREG/CR-6413, ORNL/TM-13133 contains a plot of residual versus fast fluence for the correlation monitor material. This figure shows a 2σ uncertainty of 50°F. The data used in Figure 11 is contained in Table 14 of NUREG/CR-6413 (identified as product SRM). SRM was contained only in the 263° capsule that has been removed and tested from St. Lucie Unit 2; however, the fluence value for this capsule has been updated. Table B-4 contains an updated calculation of the residual versus fast fluence.

Table B-7 St. Lucie Unit 2 Calculation of Residual versus Fast Fluence

Capsule	Capsule Fluence[(a)] (x 10^{19} n/cm^2, E > 1.0 MeV)	FF	Measured Shift[(b)] (°F)	RG 1.99 Shift (CF*FF)[(c)] (°F)	Residual Measured Shift (°F)
263°	1.02	1.006	131.2	136.9	5.7

Notes:

(a) Value taken from Table 4-2.

(b) Value taken from WCAP-18275-NP [Ref. B-9] Table B-5.

(c) Per WCAP-18275-NP [Ref. B-9] Table B-5, the Cu and Ni weight percent values for the St. Lucie Unit 2 correlation monitor material are 0.18 Cu and 0.66 Ni. This equates to a CF of 136.1°F from Regulatory Guide 1.99, Revision 2.

Table B-7 shows a 2σ uncertainty of less than 50°F, which is the allowable scatter in Figure 11 of NUREG/CR-6413. Hence, this criterion is met.

Conclusion

Based on the preceding responses to the five criteria of Regulatory Guide 1.99, Revision 2, Section B, the St. Lucie Unit 2 surveillance data for the Intermediate Shell Plate M-605-1 and Heat # 83637 are deemed credible.

B.4 REFERENCES

B-1. U.S. Nuclear Regulatory Commission, Office of Nuclear Regulatory Research, Regulatory Guide 1.99, Revision 2, "Radiation Embrittlement of Reactor Vessel Materials," May 1988. *[ADAMS Accession Number ML003740284]*

B-2. Code of Federal Regulations 10 CFR 50, Appendix G, "Fracture Toughness Requirements," U.S. Nuclear Regulatory Commission, Federal Register, December 12, 2013.

B-3. K. Wichman, M. Mitchell, and A. Hiser, USNRC, Generic Letter 92-01 and RPV Integrity Workshop Handouts, "NRC/Industry Workshop on RPV Integrity Issues," February 1998. *[ADAMS Accession Number ML110070570]*.

B-4. ASTM E185-82, "Standard Practice for Conducting Surveillance Tests for Light-Water Cooled Nuclear Power Reactor Vessels," American Society for Testing and Materials, 1982.

B-5. Westinghouse Report WCAP-15446, Revision 1, "Analysis of Capsule 284° from the Florida Power and Light St. Lucie Unit 1 Reactor Vessel Radiation Surveillance Program," January 2002.

B-6. Combustion Engineering Report CENPD-39, Revision 0, "Summary Report on Manufacture of Test Specimens and Assembly of Capsules for Irradiation Surveillance of Hutchinson Island Plant Unit 1 Reactor Vessel Materials," June 1972.

B-7. NUREG/CR-6413, ORNL/TM-13133, "Analysis of the Irradiation Data for A302B and A533B Correlation Monitor Materials," April 1996. *[ADAMS Accession Number ML20112B397]*

B-8. Westinghouse Report WCAP-17939-NP, Revision 0, "Analysis of Capsule 97° from the Florida Power & Light Company St. Lucie Unit 2 Reactor Vessel Radiation Surveillance Program," May 2015.

B-9. Westinghouse Report WCAP-18275-NP, Revision 0, "St. Lucie Unit 2 Heatup and Cooldown Limit Curves for Normal Operation through End of License Extension," November 2019.

Approval Information
Author Approval Lynch Donald Jul-15-2021 15:32:37
Reviewer Approval Mays Benjamin E Jul-15-2021 15:44:22
Reviewer Approval Hawk Andrew E Jul-15-2021 18:28:11
Approver Approval Patterson Lynn Jul-15-2021 22:02:22
Approver Approval Klingensmith Jesse J Jul-16-2021 08:48:01
Hold to Release Approval Mays Benjamin E Jul-16-2021 09:37:38

Files approved on Jul-16-2021

*** This record was final approved on 7/16/2021 9:37:38 AM. (This statement was added by the PRIME system upon its validation)

Enclosure 4

Non-proprietary Reference Documents and Redacted Versions of Proprietary Reference Documents (Public Version)

Attachment 5

Westinghouse Report LTR-SDA-II-20-32-NP, Revision 3, St. Lucie Units 1 & 2 Subsequent License Renewal: 80-Year Projected Transient Cycles, July 15, 2021

(14 Total Pages, including cover sheets)

Westinghouse

To: John T. Ahearn
cc: Eric J. Matthews

Date: July 15, 2021

From: Fluid Systems
Ext: 860-731-6388
Fax: 860-967-0822

Our ref: LTR-SDA-II-20-32-NP
Revision: 3

Subject: St. Lucie Units 1 & 2 Subsequent License Renewal: 80-Year Projected Transient Cycles

References:

1. Westinghouse Calculation Note CN-SDA-II-20-026, Revision 3, "St. Lucie Unit 1 and Unit 2 80-Year Transient Cycle Projections," July 15, 2021.
2. Westinghouse LTR-AMER-MKG-20-1686, Revision 6, "Westinghouse Final Revised Offer for Subsequent License Renewal for St. Lucie Units 1 & 2," July 6, 2021.
3. FPL St. Lucie Plant Administrative Procedure, ADM-17.43, Revision 2, "Component Cycles and Transients, April 4, 2018, with completed 2019 Attachment 2 – Annual Report of Cumulative Component Cycles and Transients," May 20, 2020.
4. Letter L-2002-165, from D. E. Jernigan, Vice President St. Lucie Plant to U.S. Nuclear Regulatory Commission, "St. Lucie Units 1 and 2 Docket Nos. 50-335 and 50-389 Response to NRC Request for Additional Information for Review of the St. Lucie Units 1 and 2 License Renewal Application," October 10, 2002. (ADAMS Accession No. ML022890450).
5. NUREG-1779, "Safety Evaluation Report Related to the License Renewal of St. Lucie Nuclear Plant, Units 1 and 2, Docket Nos. 50-335 and 50-389, Florida Power & Light Company," September 2003.
6. FPL Engineering Evaluation EC-284513, Revision 0, "Changes to Component Cyclic or Transient Limits based on fatigue re-evaluation of 2B RSG primary side components."
7. FPL St. Lucie Unit 2 Updated Final Safety Analysis Report, Amendment 26, Sections 3.9 and 5.0.
8. FPL Letter, PSLWEC-21-0008, "Design Input Transmittal for WS03 Internals Aging Management to Support the St. Lucie Unit 1 and Unit 2 Subsequent License Renewal," March 8, 2021.
9. FPL Letter PSLWEC-21-0069, "Design Input Transmittal for WS08(b) 80-Year Cycle Projections to Support the St. Lucie Unit 1 and Unit 2 Subsequent License Renewal," June 25, 2021.
10. Westinghouse Calculation Note CN-SDA-21-20, Revision 0, "St. Lucie Units 1 & 2 Subsequent License Renewal: Loss of Letdown Design Cycle Fatigue Reconciliation," July 8, 2021.
11. FPL Letter PSLWEC-21-0079, "Design Input Transmittal for WS08 80-Year Cycle Projections to Support the St. Lucie Unit 1 and Unit 2 Subsequent License Renewal," July 15, 2021.

This letter provides a summary of Westinghouse's evaluation of St. Lucie Units 1 and 2 80-Year Projected Transient Cycles, Reference 1, consistent with our Reference 2 offer.

In addition to listing of the transient events in the current St. Lucie fatigue monitoring program based on St. Lucie Plant Administrative Procedure, ADM-17.43, Revision 2, Reference 3, a complete list of events was created in Reference 1 including all UFSAR design transients consistent with the original PSL LRA, Reference 4, Tables 4.3.-1.1 through Table 4.3-1.4. The basis for exclusion of these additional events from fatigue monitoring has not been independently verified by Westinghouse but rather stated as such based on FPL responses contained in Reference 4. The results of this document provide 80-year cycle projections in support of current transient cycle counting activities and subsequent SLR TLAA evaluations. Projected 80-year cycles for transients previously included in the original PSL LRA for Units 1 and 2 are presented in Tables 1 and 2, respectively.

Events which are included in the current St. Lucie fatigue monitoring program based on St. Lucie Plant Administrative Procedure, ADM-17.43, Revision 2, Reference 3 but not previously included in the original PSL LRA for Units 1 and 2 are presented in Tables 3 and 4, respectively.

Revision 2 adds the following transients to the 80-year cycle projections to support the SLR TLAA evaluations: loading and unloading events, and operational basis earthquake and safe shutdown earthquake events. Revision 3 updates the Leak Tightness at Cold (torque cycles of 2B RSG primary manway) cycles in Table 4. Revision 3 additionally adds charging and letdown isolation events, updates the loading and unloading cycle subtotals in Table 5 and Table 6, provides an updated cycle limit for the loss of letdown transient, and adds the purification and boric acid dilution transients to the 80-year cycle projection scope. Preliminary assessments indicated that 80-year projected cycles are also required for these transients to support the SLR TLAA evaluations. These events for Units 1 and 2 are presented in Tables 5 and 6, respectively.

Sections 3.9 and 5.2.1.2 of the St. Lucie Unit 1 UFSAR and Section 3.9 of the St. Lucie Unit 2 UFSAR contain a listing of the design transients used in the design of the various Reactor Coolant System (RCS) Class 1 components. These design transients have been consolidated into Tables 1 and 2 for St. Lucie Units 1 and 2, respectively. However, each of these design transients is not necessarily a significant contributor to the overall Class 1 component fatigue usage. As part of the 60-year license renewal, a comprehensive review of each Reactor Coolant System Class 1 component fatigue analysis was performed to determine which design transients are a significant contributor to overall fatigue usage. A design transient was deemed to be significant if the transient contributed greater than 0.1 to the overall component cumulative usage factor (CUF). The transients included in the fatigue monitoring program for the PSL 60-year period of extended operation were determined to be appropriate as described in Section 4.3.2 of NUREG-1779 (Reference 5).

As discussed in Section 4.3.2 of NUREG-1779, the NRC requested the following data in RAI 4.3-1 of the original St. Lucie license renewal application:

- the current number of operating cycles and a description of the method used to determine the number and severity of the design transient from the plant operating history
- the number of operating cycles estimated for 60 years of plant operation and a description of the method used to estimate the number of cycles at 60 years

- a comparison of the design transients listed in the UFSAR with the transients monitored by the Fatigue Monitoring Program (FMP) as described in Section B3.2.7 of the LRA, identifying any transients listed in the UFSAR that are not monitored by the FMP and explaining why it is not necessary to monitor these transients.
- FPL provided the following responses to satisfy RAI 4.3-1:
    - Cycle counting has been performed since the startup of each unit.
    - The design calculations were reviewed, and design transients that result in a fatigue usage greater than 0.1 are monitored by the FMP.
    - Transients associated with plant loading and unloading events were not monitored because Units 1 and 2 are not load following plants and, therefore, the number of cycles used in the design is very conservative.
    - The original design transient assumptions were determined to be severe enough to bound all operating events.

FPL has implemented Fatigue Monitoring at both St. Lucie Units 1 and 2 to fulfill plant Technical Specification requirements and to ensure that the significant "fatigue-sensitive" design transient counts are not exceeded during plant operation. As described in Reference 4, a comprehensive review of each RCS Class 1 component fatigue analysis was performed as part of first license renewal to determine which design transients are a significant contributor to overall fatigue usage. Events which are included in the current St. Lucie fatigue monitoring program based on St. Lucie Plant Administrative Procedure, ADM-17.43, Revision 2, Reference 3 and previously included in the original PSL LRA for Units 1 and 2 are presented in Tables 1 and 2, respectively.

Note that some transients listed in Tables 1, 2, 3, and 4 are not fatigue-sensitive, but they are included in the Fatigue Monitoring Program because of plant Technical Specification requirements. Also note that some fatigue-sensitive transients identified from the CUF screening process performed for first license renewal have been excluded from the Fatigue Monitoring Program due to large margins that are present with respect to actual cycle counts versus allowable cycle counts.

Cycle counting has been performed since the startup of each St. Lucie unit. This program counts the design transients identified in Tables 1, 2, 3, and 4 by recording the actual number and types of transients imposed on the RCS components, and ensures that the design transient limits are not exceeded. As described in Reference 4, a comprehensive review of plant operating records was performed to validate that the transient counts included in the Fatigue Monitoring Program are accurate. This review concluded that the program accurately identifies and classifies plant design transients and provides an effective and consistent method for categorizing, counting, and tracking design transients. The current number of operating cycles (as of December 31, 2019) for each transient included in the Fatigue Monitoring Program is included in Tables 1, 2, 3, and 4.

As part of first license renewal, design basis transient severities were compared to the actual transients experienced at St. Lucie Units 1 and 2. This review was performed to demonstrate that the original design transient assumptions are severe enough to bound all operating events. Typical plant design transients were reviewed as part of the evaluation. The results of the review concluded that the original design transient assumptions are severe enough to bound all operating events.

Two cycle projection methods were considered. The first method calculated the projected 80-year cycles based on an extrapolation of the cycle counts accumulated from the time of the start of the respective transient monitoring period through December 31, 2019 consistent with the method used to calculate the projected 60-year cycles in Reference 4. The second method calculated the projected 80-year cycles based on cycle accumulation over the last 10 years of operation, or as applicable, the start of the transient monitoring pro-rated for years remaining to the 80 year projected life based on the assumption that recent plant operating history is generally a better predictor of future plant operation.

Method 1: PC = CC * POL/COL

Method 2: PC = CC + R10 * (POL - COL)

Where:

PC (Projected Cycles) = projected cycles over an 80-year operating life

CC (Current Cycles) = cycle counts to date

R10 = average cycle/year accumulation rate over the last 10 years (cycles/year)

POL (Projected Operating Life) = 80 years

COL (Current Operating Life) = current operating life to date (years)

The start dates correspond to the operating license issue dates:

- Unit 1: March 1, 1976
- Unit 2: April 6, 1983

If no cycles occurred over the last 10 years for a particular transient, the 80-year projected cycles were calculated by conservatively adding two more cycles to the cycle counts to date. Tables 1 and 2 report the maximum number of projected 80-year cycles between these two methods. In addition, if no cycles occurred since the start of plant operation, two cycles were added for that transient.

As illustrated by the results in Tables 1 and 2, the projected 80-year cycles for the transients identified in the license renewal application remain within the cycle limits.

The cycle limits for the Plant Heat-up, Plant Cooldown, and Primary Side Hydrostatic Test transients in Table 2 were reduced as follows per EC-284513, Reference 6, based on the fatigue re-evaluation of the 2B RSG primary side components. Plant Heat-up and Cooldown cycle limits were reduced from 500 cycles to 120 cycles and the Primary Side Hydrostatic Test cycle limit was reduced from 10 cycles to 1 cycle. The projected 80-year cycles for the Plant Heat-up, Plant Cooldown, and Primary Side Hydrostatic Test transients remain below the original cycle limits. Several component cyclic limits were affected by the fatigue reevaluation of the 2B RSG primary-side components due to a foreign object (FO) damage event at the end of the SL2-21 refueling outage per EC-284513, Reference 6. Plant Heat-up and Cooldown cycle limits for the 2B RSG primary-side components were reduced from 500 cycles to 120 cycles on the basis that 120 cycles remains bounding for a 60-year plant life and the Primary Side Hydrostatic Test cycle limit was reduced from 10 cycles to 1 cycle on the basis that this test was only performed once prior to installation and is not required to be repeated.

The projected 80-year cycles in Tables 1 and 2 for the Plant Heat-up and Cooldown transients reflect the period from plant startup to 80 years of operation. However, the 2B RSG was installed in the fall of 2007 per Section 5.0 of the UFSAR, Reference 7, so the 2B RSG would only experience a portion of the projected 80-year cycles. The projected cycles for the 2B RSG is 91 cycles for both the Plant Heat-up and Cooldown transients when considering only the period from RSG installation to 80 years of operation. Therefore, the Plant Heat-up and Cooldown projected cycles for the 2B RSG are expected to remain within the reduced cycle limit of 120 cycles through 80 years of plant operation.

One cycle of the Primary Side Hydrostatic Test transient has occurred through December 31, 2019. Per EC-284513, Reference 6, no additional primary side hydrostatic tests at the pressure and temperature conditions of the Primary Side Hydrostatic Test transient are permitted on the 2B RSG. Therefore, the Primary Side Hydrostatic Test transient cycles for the 2B RSG are expected to remain within the reduced cycle limit of one cycle through 80 years of plant operation.

Based on operating experience recorded in the recent period from the Fall of 2007 to the end of 2019, nine cycles of the Leak Tightness at Cold (torque cycles of 2B RSG primary manway) transient have occurred through December 31, 2019 for the 2B RSG. Per PSLWEC-21-0079, Reference 11, future occurrences of the Leak Tightness at Cold transient are highly likely to occur one cycle every other refueling outage. Therefore, the Leak Tightness at Cold transient cycles are expected to remain within the reduced cycle limit of 30 cycles through 80 years of plant operation. If a new degradation mechanism is identified in a future steam generator exam which necessitates more frequent opening of the 2B primary manway for steam generator exams, the information in PSLWEC-21-0079 and the 80-year cycle projections for the Leak Tightness at Cold transient should be reviewed accordingly.

Two new extrapolation techniques were used to project unit loading and unloading events, charging and letdown isolation events, and purification and boric acid dilution events due to the data for these transients covering a shorter timespan than the lifetime of each unit. These new techniques are consistent with Methods 1 and 2 except that an additional factor of 1.2 was applied to account for the possibility that transient cycles could be accumulated at a higher rate in early periods of plant operation. The more limiting result of the two cycle projection methods is credited herein. Additional design input to these evaluations was provided by References 8 and 9. These additional St. Lucie Units 1 and 2 Design Transients and transient cycle projections are presented in Table 5 and Table 6.

To ensure that the FMP remains adequate for SLR, the following actions are recommended:

1. The CUF screening process should be updated with the latest RCS Class 1 component fatigue analyses to determine if additional fatigue-sensitive transients should be included in the FMP.

2. The cycle limits for transients in the FMP should be updated to reflect the cycles listed in Tables 1 to 6 that were considered in the various SLR evaluations.

If there are any questions, please contact the undersigned.

Author: Mark R. Kulwich*
Fluid Systems

Verifier: Timothy P. Jaeger*
Fluid Systems

Manager: Jonathan C. Durfee*
Fluid Systems

***Electronically approved records are authenticated in the electronic document management system.*

Table 1: St. Lucie Unit 1 Design Transients Included in Fatigue Monitoring Program

Transient	Cycle Limit (1)	Cycle Counts as of 12/31/19	80-Year Projection	Margin
Reactor Trip	400	58	106	73%
Plant Heat-up	500	78	143	71%
Plant Cooldown	500	77	141	71%
Pressurizer Heat-up	500	71	130	74%
Pressurizer Cooldown	500	71	130	74%
Primary Side Hydrostatic Test	10	1	3 (2)	70%
Secondary Side Hydrostatic Test	10	1	3 (2)	70%
Primary Leak Test	200	0	2	99%
Secondary Leak Test	200	1	3 (2)	98%
Loss of Secondary Pressure	5	0	2	60%
Pressurizer Spray	1500(3)	296	597 (2)	60%
Inadvertent Auxiliary Spray	16	3	6	62%
Loss of Offsite Power (Loss of RCS Flow)	40	0	2	95%
Loss of Load	40	3	6	85%
Plant Loading, 5%/min.	15000	NC(4)	NC(4)	NA
Plant Unloading, 5%/min.	15000	NC(4)	NC(4)	NA
10% Step Load Increase	2000	NC(4)	NC(4)	NA
10% Step Load Decrease	2000	NC(4)	NC(4)	NA
Normal Plant Variations, +/- 100 psi, +/- 6ºF	1000000	NC(4)	NC(4)	NA
Primary Coolant Pump Starting/Stopping	4000	NC(4)	NC(4)	NA
Purification	1000	NC(4)	NC(4)	NA
Low Volume Control and Makeup	2000	NC(4)	NC(4)	NA
Boric Acid Dilution	8000	NC(4)	NC(4)	NA
Cold Feed Following Hot Standby	15000	NC(4)	NC(4)	NA
Actuation of Main or Auxiliary Spray	500	NC(4)	NC(4)	NA
Low Pressure Safety Injection, 40ºF Water into 300ºF Cold Leg	500	NC(4)	NC(4)	NA
Opening of Safety Injection Return Line Valves	2000	NC(4)	NC(4)	NA
Initiation of Shutdown Cooling	500	NC(4)	NC(4)	NA
Loss of Charging Flow	200	NC(4)	NC(4)	NA
Loss of Letdown Flow	50	NC(4)	NC(4)	NA
Regenerative Heat Exchanger Isolation Long Term	80	NC(4)	NC(4)	NA

Table 1: St. Lucie Unit 1 Design Transients Included in Fatigue Monitoring Program (continued)

Transient	Cycle Limit (1)(3)	Cycle Counts as of 12/31/19	80-Year Projection	Margin
Regenerative Heat Exchanger Isolation Short Term	40	NC(4)	NC(4)	NA
Loss of Feedwater Flow	8	NC(4)	NC(4)	NA
High Pressure Safety Injection, 40°F Water into 550°F Cold Leg	5	NC(4)	NC(4)	NA

Notes:

(1) Cycle Limits are from Section 3.9 of the UFSAR.

(2) Projection was based on operating experience recorded in the recent period from the end of 2009 to the end of 2019 versus extrapolation of events recorded from the time of plant startup.

(3) Per FPL's response to RAI 4.3-1 of the original PSL LRA, the number of cycles for this event was increased from the original number reported in the UFSAR based on additional plant-specific analysis of the pressurizer spray line.

(4) NC does not have cycles counted per FPL FMP. FPL's response to RAI 4.3-1 of the original LRA states that design transients were excluded from the FMP if they result in result in a fatigue usage less than 0.1 or large margins are present with respect to actual cycle counts versus allowable cycle counts.

Table 2: St. Lucie Unit 2 Design Transients Included in Fatigue Monitoring Program

Transient	Cycle Limit (1)	Cycle Counts as of 12/31/19	80-Year Projection	Margin
Reactor Trip	400	33	72	82%
Plant Heat-up	500	54	124(3)	75%
Reduced Limit for 2B Steam Generator	120(2)	21	914)	24%
Plant Cooldown	500	53	123(3)	75%
Reduced Limit for 2B Steam Generator	120(2)	21	91(4)	24%
Pressurizer Heat-up	500	49	107	78%
Pressurizer Cooldown	500	49	107	78%
Primary Side Hydrostatic Test	10	1	1	90%
Reduced Limit for 2B Steam Generator	1(2)	1	1	0%
Primary Leak Test	200	2	5	97%
Reduced Limit for 2B Steam Generator	30(2)	2	10(4)	67%
Loss of Secondary Pressure	5	0	2	60%
Pressurizer Spray	1500(5)	251	624(3)	58%
Loss of Offsite Power (Loss of RCS Flow)	40	0	2	95%
Loss of Load	40	1	3	92%
Plant Loading, 5%/min.	15000	NC(6)	NC(6)	NA
Plant Unloading, 5%/min.	15000	NC(6)	NC(6)	NA
10% Step Load Increase	2000	NC(6)	NC(6)	NA
10% Step Load Decrease	2000	NC(6)	NC(6)	NA
Normal Plant Variations, +/- 100 psi, +/- 6ºF	1000000	NC(6)	NC(6)	NA
Purification and Boron Dilution	24000	NC(6)	NC(6)	NA
Operating Basis Earthquake	200	NC(6)	NC(6)	NA
Loss of Charging Flow	20	NC(6)	NC(6)	NA
Loss of Letdown Flow	50	NC(6)	NC(6)	NA
Isolation Check Valve Leaks	40	NC(6)	NC(6)	NA
Loss of Secondary Pressure	5	NC(6)	NC(6)	NA

Notes:

(1) Cycle Limits are from Section 3.9 of the UFSAR.

(2) Several component cyclic limits were affected by the fatigue re-evaluation of the 2B RSG primary-side components due to a foreign object (FO) damage event at the end of the SL2-21 refueling outage per EC-284513, Reference 6. Plant Heat-up and Cooldown cycle limits were reduced from 500 cycles to 120 cycles on the basis that 120 cycles remains bounding for a 60-year plant life and the Primary Side Hydrostatic Test cycle limit was reduced from 10 cycles to 1 cycle on the basis that this test was only performed once prior to installation and is not required to be repeated.

(3) Projection was based on operating experience recorded in the recent period from either the end of 2009 or, where applicable, from the start of the transient monitoring period to the end of 2019 versus extrapolation of events recorded from the time of plant startup.
(4) The cycle counts as of 12/31/19 and 80-year projected cycles for the transients specific to the 2B RSG reflect the cycles that occurred after the RSG installation.
(5) Per FPL's response to RAI 4.3-1 of the original PSL LRA, the number of cycles for this event was increased from the original number reported in the UFSAR based on additional plant-specific analysis of the pressurizer spray line.
(6) NC does not have cycles counted per FPL FMP. FPL's response to RAI 4.3-1 of the original LRA states that design transients were excluded from the FMP if they result in result in a fatigue usage less than 0.1 or large margins are present with respect to actual cycle counts versus allowable cycle counts.

Table 3: Additional St. Lucie Unit 1 Design Transients Included in Fatigue Monitoring Program

Transient	Cycle Limit (1)	Cycle Counts as of 12/31/19	80-Year Projection	Margin
MSIV Spurious Closures after March 2013 Closure Event	10	0	2	80%

(1) The St. Lucie fatigue monitoring program tracks several transients that are not listed in the UFSAR, so 80-year projected cycles were performed for these transients in the event they would be needed for downstream evaluations.

Table 4: Additional St. Lucie Unit 2 Design Transients Included in Fatigue Monitoring Program

Transient	Cycle Limit (1)	Cycle Counts as of 12/31/19	80-Year Projection	Margin
PZR Main or Auxiliary Spray Actuation with Delta T greater than 200°F	1000	203	443	55%
PZR Spray Nozzle Cumulative Usage Factor	0.75	0.0212	0.0467(2)	93%
Permanent Cavity Seal Ring Experiences Reactor Heat-up and Cooldown	500	4	39	92%
Leak Tightness at Cold (torque cycles of 2B RSG primary manway)	30	9	24	20%

(1) The St. Lucie fatigue monitoring program tracks several transients that are not listed in the UFSAR, so 80-year projected cycles were performed for these transients in the event they would be needed for downstream evaluations.
(2) Projection was based on operating experience recorded in the recent period from either the end of 2009 or, where applicable, from the start of the transient monitoring period to the end of 2019 versus extrapolation of events recorded from the time of plant startup.

Table 5: Additional St. Lucie Unit 1 Design Transients[1]

Transient	Cycle Limit	80-Year Projection	Margin
Loading and Unloading Events			
Projected Cycles < 10%	NA	176	N/A
Projected Cycles ≥10 - < 30%	NA	159	N/A
Projected Cycles ≥30 - < 60%	NA	91	N/A
Projected Cycles ≥60 - 100%	NA	864	N/A
Total Cycles	15000	1290	91%
Charging and Letdown Isolation Events			
Loss of Charging Projection Summary	200	11	94%
Loss of Letdown Projection Summary	500[2]	279	44%
Loss of Regenerative Heat Exchanger (Short-Term)	40	29	27%
Loss of Regenerative Heat Exchanger (Long-Term)	80	20	75%
Operational Basis Earthquake Events	200	2	99%
Safe Shutdown Earthquake Events	1	1	N/A
Purification[3]	1000	3504	61%
Boric Acid Dilution[3]	8000		

(1) Transient data was provided by References 8 and 9

(2) The number of cycles for this event was increased from the original number reported in the UFSAR based on additional plant-specific analysis of the charging nozzle and piping in Reference 10.

(3) The 80-year projections for the Purification and Boric Acid Dilution transients were grouped together since the transient curves in the design specifications are similar for these transients and the plant data provided in Reference 9 was insufficient to differentiate between these transients. The margin was calculated based on the combined number of design cycles reported in the UFSAR.

Table 6: Additional St. Lucie Unit 2 Design Transients[1]

Transient	Cycle Limit	80-Year Projection	Margin
Loading and Unloading Events			
Projected Cycles < 10%	NA	142	N/A
Projected Cycles ≥10 - < 30%	NA	91	N/A
Projected Cycles ≥30 - < 60%	NA	113	N/A
Projected Cycles ≥60 - 100%	NA	938	N/A
Total Cycles	15000	1284	91%
Charging and Letdown Isolation Events			
Loss of Charging Projection Summary	20	11	45%
Loss of Letdown Projection Summary	500[2]	405	19%
Loss of Regenerative Heat Exchanger (Short-Term)	40	11	72%
Loss of Regenerative Heat Exchanger (Long-Term)	80	66	17%
Operational Basis Earthquake Events	200	2	99%
Safe Shutdown Earthquake Events	1	1	N/A
Purification and Boron Dilution	24000	1700	93%

(1) Transient data was provided by References 8 and 9
(2) The number of cycles for this event was increased from the original number reported in the UFSAR based on additional plant-specific analysis of the charging nozzle and piping in Reference 10.

Approval Information
Author Approval Kulwich Mark Jul-15-2021 12:51:33
Verifier Approval Jaeger Timothy Jul-15-2021 13:06:21
Manager Approval Durfee Jonathan C Jul-15-2021 14:42:34

Files approved on Jul-15-2021

Enclosure 4

Non-proprietary Reference Documents and Redacted Versions of Proprietary Reference Documents (Public Version)

Attachment 6

Westinghouse Report LTR-SDA-II-20-31-NP, Rev. 2, St. Lucie Units 1 & 2 Subsequent License Renewal: Primary Equipment and Piping Environmentally Assisted Fatigue Evaluations, July 14, 2021

(24 Total Pages, including cover sheets)

Westinghouse

1000 Westinghouse Drive
Cranberry Twp., PA 16066

To:	John T. Ahearn	Date:	July 14, 2021
cc:			
From:	Valve Engineering and Fatigue Aging Management	Ref:	LTR-SDA-II-20-31-NP, Rev. 2
Ext:	412-374-4474		
Fax:	724-940-8565		

Subject: St. Lucie Units 1 & 2 Subsequent License Renewal: Primary Equipment and Piping Environmentally Assisted Fatigue Evaluations

To support the St. Lucie Unit 1 and Unit 2 Subsequent License Renewal (SLR) program, environmentally assisted fatigue (EAF) evaluations were performed for the sentinel primary equipment and piping locations specified in the work scope described in LTR-AMER-MKG-20-1686 [1]. This letter report summarizes the results of those EAF evaluations.

Revisions 0 and 1 of this letter provide the results of EAF evaluations for the sentinel reactor vessel and safety injection nozzle locations. Revision 2 is a major revision that adds the results of the EAF evaluations for the remaining locations specified in LTR-AMER-MKG-20-1686 [1] and addresses the comments in the attached "LTR-SDA-II-20-31-P Rev 2 (DRAFT) - DCRF Rev D (signed).pdf" and "LTR-SDA-II-20-31-NP Rev 2 (DRAFT) - DCRF Rev D (signed).pdf" files.

Author: Eric J. Matthews*
Valve Engineering and Fatigue Aging Management

Verifier: Jamie L. Oakman*
Valve Engineering and Fatigue Aging Management

Manager: John Klimek*
Valve Engineering and Fatigue Aging Management

Foreword:

This document contains Westinghouse Electric Company LLC and Flowserve Corporation proprietary information and data. The proprietary information has been identified in brackets with coding (w) for Westinghouse and (fs) for Flowserve. In addition, coding (a,c,e) associated with the brackets sets forth the basis on which information is considered proprietary. These code letters are listed with their meanings in BMS-LGL-84, and are defined as follows:

a. The information reveals the distinguishing aspects of a process (or component, structure, tool, method, etc.) where the prevention of its use by any competitors without license from Westinghouse and Flowserve constitutes a competitive economic advantage over other companies.

c. The information, if used by a competitor, would reduce the competitor's expenditure of resources or improve the competitor's advantage in the design, manufacture, shipment, installation, assurance of quality, or licensing of a similar product.

e. The information reveals aspects of past, present, or future development plans and programs of potential commercial value to Westinghouse and Flowserve.

The proprietary information and data contained within the brackets of this document were obtained at considerable Westinghouse and Flowserve expense and its release could seriously affect competitive positions. This information is to be withheld from public disclosure in accordance with the Rules of Practice 10 CFR 2.390 and the information presented herein is to be safeguarded in accordance with 10 CFR 2.390. Withholding of this information does not affect the public interest.

This information has been provided for your internal use only and should not be released to persons or organizations outside the Directorate of Regulation and the ACRS (Advisory Committee on Reactor Safeguards) without the express written approval of Westinghouse and Flowserve. Should it become necessary to release this information to such persons as part of the review procedure, please contact Westinghouse and Flowserve, which will make the necessary arrangements required to protect proprietary interests.

The proprietary information in brackets has been deleted in this non-proprietary version. The deleted information is provided in the proprietary version of this report (LTR-SDA-II-20-31-P).

1.0 Introduction and Summary of Results

The St. Lucie Unit 1 and Unit 2 Subsequent License Renewal (SLR) program is intended to extend the operation license of these plants from 60 years to 80 years. Nuclear Regulatory Commission (NRC) guidance on the content of SLR applications is provided in NUREG-2191 [2.1] and NUREG-2192 [2.2]. Specifically, Section 4.3 of NUREG-2192 [2.2] provides the following guidance related to addressing the effects of a reactor water environment:

> *Applicants should include Cumulative Usage Factor including Reactor Water Environmental Effects (CUF_{en}) calculations for the limiting component locations exposed to the reactor water environment. This sample set includes the locations identified in NUREG/CR–6260 [2.3] and additional plant-specific component locations in the reactor coolant pressure boundary if they may be more limiting than those considered in NUREG/CR–6260. Plant-specific justification can be provided to demonstrate that calculations for the NUREG/CR–6260 locations do not need to be included. Environmental effects on fatigue for these critical components may be evaluated using the guidance in RG 1.207, Revision 1 [2.4]; NUREG/CR–6909, Revision 0 [2.5] (with "average temperature" used consistent with the clarification that was added to NUREG/CR–6909, Revision 1 [2.6]); or other subsequent NRC-endorsed alternatives.*

To address the concern that there may be additional component locations more limiting than those considered in NUREG/CR–6260 [2.3], Westinghouse performed an environmentally assisted fatigue (EAF) screening evaluation in CN-SDA-II-20-022 [3] for the Safety Class 1 reactor coolant pressure boundary components in major equipment and piping that meet the six criteria for time-limited aging analyses (TLAAs) in 10 CFR 54.3(a), including the locations listed in NUREG/CR–6260 [2.3]. The goal of the EAF screening evaluation was to eliminate locations for which environmental conditions are not a concern and provide a list of sentinel locations, which supplement those identified in NUREG/CR–6260 [2.3], to be addressed through separate aging management plans, such as EAF evaluations or inspections supported by fracture evaluations. This letter report summarizes the results of EAF evaluations performed for the following sentinel locations identified in CN-SDA-II-20-022 [3]. The remaining sentinel locations from CN-SDA-II-20-022 [3] are being evaluated by other vendors.

- Units 1 & 2 Reactor Vessel (RV) Outlet Nozzle
- Units 1 & 2 RV Inlet Nozzle
- Units 1 & 2 RV Wall Transition
- Unit 2 Control Element Drive Mechanism (CEDM) Upper Housing Tube
- Unit 2 CEDM Upper Housing Lower End Fitting
- Unit 2 CEDM Motor Housing Lower End Fitting
- Units 1 & 2 Reactor Coolant Pump (RCP) Cover
- Units 1 & 2 Reactor Coolant Loop (RCL) Suction Leg RCP Suction Nozzle
- Units 1 & 2 RCL Cold Leg RCP Discharge Nozzle
- Units 1 & 2 RCL Cold Leg Resistance Temperature Detector (RTD) Nozzle

- Units 1 and 2 RCL Cold Leg Spray Nozzle (Leading Carbon Steel (CS)/Low Alloy Steel (LAS) and Stainless Steel (SS) Locations)
- Unit 1 4" x 4" x 4" Main Spray/Auxiliary Spray Line Tee
- Unit 2 4" x 4" x 4" Main Spray Line Tee
- Unit 2 Pressurizer (PZR) Relief Valve Piping 4" x 4" x 4" Tee
- Units 1 & 2 RCL Letdown and Suction Leg Drain Nozzle (Leading CS/LAS and SS Locations)
- Unit 1 RCL Hot Leg Drain Nozzle (Leading SS Location)
- Unit 1 Loop 1B1 Charging Line Socket Weld at Elbow
- Unit 2 Loop 2A2 Charging Line Socket Welded Coupling
- Units 1 & 2 Cold Leg Safety Injection Nozzle (Leading CS/LAS and SS Locations)
- Unit 1 Loop 1B1 Safety Injection Line V3237 Valve Transition Weld
- Unit 1 Loop 1B1 Safety Injection Line 12" x 1" Branch
- Unit 2 Loop 2A1 Safety Injection Line V3227 Valve Transition Weld
- Unit 2 Loop 2A1 Safety Injection Line 12" x 12" x 6" Tee
- Unit 1 Shutdown Cooling Line 12" x 2" Branch
- Unit 1 Shutdown Cooling Line 10" x 1" Branch

2.0 Environmentally Assisted Fatigue Evaluation Methodology

In general, the EAF evaluations of the sentinel locations presented in this report can be categorized into the following groups:

1. Simplified EAF Evaluations
2. Comparative EAF Evaluations
3. Detailed EAF Evaluations

Each of these EAF evaluation groups are described in Sections 2.1 to 2.3. The general method to calculate the F_{en} factors is described in Sections 2.4 to 2.7. The transient cycles considered in the EAF evaluations are described in Section 2.8.

2.1 Simplified EAF Evaluations (Group 1)

The simplified EAF evaluations utilize the fatigue results from the existing analysis of record (AOR) along with the guidelines in RG 1.207 [2.4] and the F_{en} equations in NUREG/CR-6909 [2.6] to calculate a CUF_{en} less than 1.0. The process to perform this evaluation is summarized as follows:

1. A detailed review of the fatigue AOR is performed to determine the controlling regions based on stress results and materials of construction.
2. The design fatigue curves in Section A.2.1 of NUREG/CR-6909 [2.6] are applied to the fatigue results from the AOR to derive a cumulative usage factor (CUF).
3. The F_{en} equations in Section A.2 of NUREG/CR-6909 [2.6] are applied to the fatigue results from Step 2 to derive a CUF_{en}.

The goal of the simplified EAF evaluations is to calculate a CUF_{en} below 1.0 through typical linear elastic fatigue analysis techniques. Conservatisms in the stress and fatigue analyses in the AORs may be identified and removed in the CUF calculations. Conservatism reduction methods may include the use of 80-year projected cycles or reduced stress magnitudes based on actual transient severities.

The CUF_{en} is initially calculated by applying conservative constant F_{en} values to the CUF or partial fatigue usage factors of individual fatigue pairs. For any component locations that cannot accept this conservative method (i.e., $CUF_{en} > 1.0$), strain rate dependent F_{en} values may be calculated for significant fatigue pairs using the modified rate approach described in Section 4.4 of NUREG/CR-6909 [2.6].

2.2 Comparative EAF Evaluations (Group 2)

The comparative EAF evaluations compare sentinel locations across transient sections to demonstrate that a sentinel location is less limiting than a location from NUREG/CR-6260 [2.3] or another location for which a more detailed EAF evaluation will be performed. This comparison incorporates critical analysis items such as controlling thermal transient severity, transient occurrences, stress algorithms, and analysis methods used to evaluate components of interest.

2.3 Detailed EAF Evaluations (Group 3)

The general process to perform the detailed EAF evaluations is similar to the simplified EAF evaluations in described in Section 2.1 except that a detailed finite element model based on plant-specific geometry is utilized to support the evaluation. A finite element analysis is performed to generate transient stress time histories that will be used to determine the stress peaks and valleys for the fatigue evaluation, as well as the corresponding strain rates and temperature information needed for the F_{en} calculations. The stress peaks and valleys and applicable F_{en} factors will be used to determine the CUF_{en} for the limiting locations.

2.4 F_{en} Equations

The materials for the sentinel locations in the EAF evaluations include carbon steel (CS), low alloy steel (LAS), stainless steel (SS), and Ni-Cr-Fe alloy (NiA). The F_{en} for each of these materials was calculated using the equations in Section A.2 of NUREG/CR–6909 [2.6], which are presented in Equation 2-1 to Equation 2-3.

CS and LAS:

$$F_{en} = \exp\left((0.003 - 0.031\,\dot{\varepsilon}^*)\,S^*\,T^*\,O^*\right) \qquad \textbf{2-1}$$

Where:

$S^* = 2.0 + 98\,S$	$S \leq 0.015$ wt. %
$S^* = 3.47$	$S > 0.015$ wt. %
S = Sulfur Content (wt. %)	
$T^* = 0.395$	$T < 150°C\ (302°F)$
$T^* = (T - 75)/190$	$150°C\ (302°F) \leq T \leq 325°C\ (617°F)$
T = Service Temperature (°C)	for calculation of T^*
$O^* = 1.49$	$DO < 0.04$ ppm
$O^* = \ln(DO/0.009)$	$0.04 \text{ ppm} \leq DO \leq 0.5$ ppm
$O^* = 4.02$	$DO > 0.5$ ppm
DO = Dissolved Oxygen Content (ppm)	
$\dot{\varepsilon}^* = 0$	$\dot{\varepsilon} > 2.2$ %/s
$\dot{\varepsilon}^* = \ln(\dot{\varepsilon}/2.2)$	$0.0004\ \%/s \leq \dot{\varepsilon} \leq 2.2$ %/s
$\dot{\varepsilon}^* = \ln(0.0004/2.2)$	$\dot{\varepsilon} < 0.0004$ %/s
$\dot{\varepsilon}$ = Strain Rate (%/s)	

Wrought and Cast Austenitic SS:

$F_{en} = \exp(- T^* \dot{\varepsilon}^* O^*)$ **2-2**

Where:

$T^* = 0$	$T < 100°C$ (212°F)
$T^* = (T - 100)/250$	$100°C\ (212°F) \leq T \leq 325°C\ (617°F)$
T = Service Temperature (°C)	
$\dot{\varepsilon}^* = 0$	$\dot{\varepsilon} > 7.0$ %/s
$\dot{\varepsilon}^* = \ln(\dot{\varepsilon}/7.0)$	$0.0004\ \%/s \leq \dot{\varepsilon} \leq 7.0\ \%/s$
$\dot{\varepsilon}^* = \ln(0.0004/7.0)$	$\dot{\varepsilon} < 0.0004$ %/s
$\dot{\varepsilon}$ = Strain Rate (%/s)	

All wrought and cast SSs and heat treatments and SS weld metals:

$O^* = 0.29$	DO < 0.1 ppm

Sensitized high-carbon wrought and cast SSs:

$O^* = 0.29$	DO ≥ 0.1 ppm

All wrought SSs except sensitized high-carbon SSs:

$O^* = 0.14$	DO ≥ 0.1 ppm

DO = Dissolved Oxygen Content (ppm)

NiA (except Inconel 718):

$F_{en} = \exp(- T^* \dot{\varepsilon}^* O^*)$ **2-3**

Where:

$T^* = 0$	$T < 50°C$ (122°F)
$T^* = (T - 50)/275$	$50°C\ (122°F) \leq T \leq 325°C\ (617°F)$
T = Service Temperature (°C)	
$\dot{\varepsilon}^* = 0$	$\dot{\varepsilon} > 5.0$ %/s
$\dot{\varepsilon}^* = \ln(\dot{\varepsilon}/5.0)$	$0.0004\ \%/s \leq \dot{\varepsilon} \leq 5.0\ \%/s$
$\dot{\varepsilon}^* = \ln(0.0004/5.0)$	$\dot{\varepsilon} < 0.0004$ %/s
$\dot{\varepsilon}$ = Strain Rate (%/s)	
$O^* = 0.06$	NWC BWR water (i.e., DO ≥ 0.1 ppm)
$O^* = 0.14$	PWR or HWC BWR water (i.e., DO < 0.1 ppm)
DO = Dissolved Oxygen Content (ppm)	

2.5 Maximum F_{en} Values

[

] w-a,c,e

[

] w-a,c,e

2.6 Dissolved Oxygen Content

Per PSLWEC-21-0009 [4], the RCS DO content is controlled using 0-COP-05.04 [5]. When the RCS temperature is above 250°F, the DO content in the RCS is maintained below 5 ppb (0.005 ppm) in Modes 1 and 2 and 10 ppb (0.01 ppm) in Modes 3 and 4 as discussed in 0-COP-05.04 [5] and supported by data from 2010 to 2020 (contained in the "U1 RCS DO 10 years.xlsx" and "U2 RCS DO 10 years.xlsx" spreadsheets attached to PSLWEC-21-0009 [4]). When the RCS temperature is below 250°F, the DO content may exceed 10 ppb (0.01 ppm). Therefore, the following assumptions regarding the DO content are made in the EAF screening evaluation:

- When the RCS temperature is greater than 250°F, a constant DO content of 0.01 ppm is assumed.
- When the RCS temperature is less than or equal to 250°F, the DO content that maximizes the F_{en} is assumed.

2.7 Maximum Temperature for F_{en} Equations

Per Section A.2 of NUREG/CR-6909 [2.6], a maximum temperature limit of 325°C (617°F) is specified for the F_{en} equations as a reasonable bound to cover most anticipated light water reactor operating conditions when considering the use of average temperature. In cases where transient temperatures exceed 325°C (617°F), the guidelines in NUREG/CR-6909 [2.6] state that the analyst shall document the exceedance and justify its use in the F_{en} equations. The EAF evaluations assumed that [

] w-a,c,e

2.8 Transients

The design transients and cycles in the AORs were originally based on a 40-year operating period. However, the transient cycles analyzed herein must be applicable for an 80-year period of operation to support the St. Lucie Units 1 & 2 SLR program. 80-year transient cycle projections were developed in [6] for the transients included in the current St. Lucie Fatigue Monitoring Program as well as additional transients that were identified as fatigue-sensitive for the SLR TLAA evaluations. For transients where 80-year cycle projections were developed in [6], the design transients from the AORs remain bounding for an 80-year period of operation.

The design transient cycles from the AORs were initially considered in the EAF evaluations. However, the transient cycles considered in the EAF evaluations were reduced from those considered in the AOR for some locations to obtain a CUF_{en} less than 1.0. To inform potential changes to plant documents, Table 2-1 lists the minimum number of cycles analyzed for any transients where cycles were reduced in the EAF evaluations. Note that the reduced cycles in Table 2-1 bound the 80-year projected cycles developed in [6].

Table 2-1: Summary of Cycle Reductions for EAF Evaluations

Transient	80-Year Projected Cycles (1)		Minimum Reduced Cycles (2)		Margin (3)	
	Unit 1	Unit 2	Unit 1	Unit 2	Unit 1	Unit 2
Reactor Trip	106	72	142	95	25%	24%
Plant Heatup	143	124	193	245	26%	49%
Plant Cooldown	141	123	192	245	27%	50%
Primary Leak Test	2	5	5	150	60%	97%
Plant Loading	1290	1284	6500	6000	80%	79%
Plant Unloading	1290	1284	6500	6000	80%	79%
Purification and Boric Acid Dilution	3504	1700	8000	7000	56%	76%

Notes:
(1) The 80-year projected cycles are provided in Section 2.0 of [6].
(2) The minimum reduced cycles reflect the minimum number of cycles analyzed for any transients where cycles were reduced from the design cycles to obtain a CUF_{en} less than 1.0.
(3) The margin was calculated as follows:

$$\text{Margin} = \frac{\text{Reduced Cycles} - \text{Projected Cycles}}{\text{Reduced Cycles}}$$

3.0 Environmentally Assisted Fatigue Evaluation Results

The results of the EAF evaluations are presented in Table 3-1 and Table 3-2 for each of the sentinel equipment and piping locations listed in Section 1.0. These tables include the original AOR CUF, the reduced CUF for SLR, the F_{en} and CUF_{en}, and a summary of the conservatisms removed from the AOR. The EAF evaluations were performed using the guidelines in [2.4] and the F_{en} equations in [2.6]. The transient cycles considered in the EAF evaluations are bounding for an 80-year period of operation. The CUF_{en} for each location is less than the ASME Code limit of 1.0 and is therefore acceptable.

As described in Section 2.8, the transient cycles considered in the EAF evaluations were reduced from those considered in the AOR for some locations to obtain a CUF_{en} less than 1.0. Changes to plant documents (such as cycle counting procedures, FSAR, etc.) may be required to address the reduced transient cycles considered in these EAF evaluations to support the SLR program.

The CUF_{en} values for some locations in Table 3-1 and Table 3-2 are close to the ASME Code limit of 1.0. However, the CUF_{en} calculations included sufficient conservatism in both the analyzed transient cycles and F_{en} values. As shown in Table 2-1, the analyzed transient cycles include a margin of at least 24% above the 80-year projected cycles. In addition, the F_{en} values were calculated based on enveloping temperature, strain rate, dissolved oxygen content, and sulfur content values.

Table 3-1: Summary of EAF Results for Equipment Sentinel Locations

Line / System	Component / Location	Material Category	CUF		F_{en} (2)	CUF_{en}	EAF Evaluation Group	Reference	SLR CUF Conservatism Reduction Summary
			AOR (1)	SLR					
RV (Unit 1)	Outlet Nozzles	LAS	[ ]w-a,c,e	[ ]w-a,c,e	[ ]w-a,c,e	0.494	[ ]w-a,c,e	[7]	No conservatism reduction was required. The LAS ASME design fatigue curve considered in the AOR is more conservative than the fatigue curve in Section A.2.1 of [2.6]. The design cycles from the AOR were considered for all transients.
	Inlet Nozzles	LAS	[ ]w-a,c,e	[ ]w-a,c,e	[ ]w-a,c,e	0.311	[ ]w-a,c,e	[7]	No conservatism reduction was required. The LAS ASME design fatigue curve considered in the AOR is more conservative than the fatigue curve in Section A.2.1 of [2.6]. The design cycles from the AOR were considered for all transients.
	Vessel Wall Transition (3)	LAS	[ ]w-a,c,e	[ ]w-a,c,e	[ ]w-a,c,e	0.036	[ ]w-a,c,e	[7]	No conservatism reduction was required. The LAS ASME design fatigue curve considered in the AOR is more conservative than the fatigue curve in Section A.2.1 of [2.6]. The design cycles from the AOR were considered for all transients.
RV (Unit 2)	Outlet Nozzles	LAS	[ ]w-a,c,e	[ ]w-a,c,e	[ ]w-a,c,e	0.916	[ ]w-a,c,e	[7]	The LAS design fatigue curve in Section A.2.1 of [2.6] was applied. The cycles were reduced for the following transients: • Heatup: reduced from 500 cycles to 400 cycles • Cooldown: reduced from 500 cycles to 400 cycles The design cycles from the AOR were considered for all other transients.
	Inlet Nozzles	LAS	[ ]w-a,c,e	[ ]w-a,c,e	[ ]w-a,c,e	0.621	[ ]w-a,c,e	[7]	The LAS design fatigue curve in Section A.2.1 of [2.6] was applied. The design cycles from the AOR were considered for all transients.

Line / System	Component / Location	Material Category	CUF AOR (1)	CUF SLR	F_{en} (2)	CUF_{en}	EAF Evaluation Group	Reference	SLR CUF Conservatism Reduction Summary
	Vessel Wall Transition (3)	LAS	[ ]w-a,c,e	[ ]w-a,c,e	[ ]w-a,c,e	0.025	[ ]w-a,c,e	[7]	No conservatism reduction was required. The LAS ASME design fatigue curve considered in the AOR is more conservative than the fatigue curve in Section A.2.1 of [2.6]. The design cycles from the AOR were considered for all transients.
CEDM (Unit 2)	Upper Housing – Tube and Lower End Fitting	SS	[ ]w-a,c,e	[ ]w-a,c,e	[ ]w-a,c,e	0.991	[ ]w-a,c,e	[8]	The SS design fatigue curve in Section A.2.1 of [2.6] was applied. Temperature dependent F_{en} values were calculated for significant fatigue pairs. Refinements were made regarding the interaction of stress cycles between different transients when forming fatigue pairs. The cycles were reduced for the following transients: • Reactor Trip: reduced from 480 to 95 cycles The design cycles from the AOR were considered for all other transients.
	Motor Housing – Lower End Fitting	NiA	[ ]w-a,c,e	[ ]w-a,c,e	[ ]w-a,c,e	0.997	[ ]w-a,c,e	[8]	The Ni-Cr-Fe alloy (NiA) design fatigue curve in Section A.2.1 of [2.6] was applied. Temperature dependent F_{en} values were calculated for significant fatigue pairs. Refinements were made regarding the interaction of stress cycles between different transients when forming fatigue pairs. The cycles were reduced for the following transients: • Plant Unloading: reduced from 15000 to 13400 cycles The design cycles from the AOR were considered for all other transients.
RCP	Pump Cover	SS	[ ]fs-a,c,e	[ ]w-a,c,e	[ ]w-a,c,e	0.991	[ ]w-a,c,e	[8]	The SS design fatigue curve in Section A.2.1 of [2.6] was applied. Temperature

Line / System	Component / Location	Material Category	CUF		F_{en} (2)	CUF_{en}	EAF Evaluation Group	Reference	SLR CUF Conservatism Reduction Summary
			AOR (1)	SLR					
(Units 1 & 2)									dependent F_{en} values were calculated for significant fatigue pairs. The cycles were reduced for the following transients: • Heatup and Cooldown: reduced from 500 to 245 cycles The design cycles from the AOR were considered for all other transients.

Notes:
(1) The AOR CUFs are listed in Section 2.0 of [3].
(2) This F_{en} value represents a weighted average value, defined as the CUF_{en} divided by the SLR CUF. The actual F_{en} values may vary between individual fatigue pairs.
(3) CUF_{en} values for both the RV lower shell-to-bottom head transition and the upper shell transition were calculated. The reported value reflects the higher value for the upper shell transition.

Table 3-2: Summary of EAF Results for Piping Sentinel Locations

Line / System	Component / Location	Material Category	CUF		F_{en} (2)	CUF_{en}	EAF Evaluation Group	Reference	SLR CUF Conservatism Reduction Summary
			AOR (1)	SLR					
RCL (Units 1 & 2)	Suction Leg – RCP Suction Nozzle	SS	[ ]$^{w-a,c,e}$	[ ]$^{w-a,c,e}$	[ ]$^{w-a,c,e}$	0.730	[ ]$^{w-a,c,e}$	[8]	The SS design fatigue curve in Section A.2.1 of [2.6] was applied. The design cycles from the AOR were considered for all transients.
	Cold Leg – RCP Discharge Nozzle	SS	[ ]$^{w-a,c,e}$	]$^{w-a,c,e}$	[ ]$^{w-a,c,e}$	0.090	[ ]$^{w-a,c,e}$	[8]	The SS design fatigue curve in Section A.2.1 of [2.6] was applied. The design cycles from the AOR were considered for all transients.
	Cold Leg – RTD Nozzle	NiA	[ ]$^{w-a,c,e}$	[ ]$^{w-a,c,e}$	[ ]$^{w-a,c,e}$	0.498	[ ]$^{w-a,c,e}$	[8]	The NiA design fatigue curve in Section A.2.1 of [2.6] was applied. Strain rate dependent F_{en} values were calculated for significant fatigue pairs. The design cycles from the AOR were considered for all transients.
Spray and Aux. Spray	Cold Leg Spray Nozzle	SS	[ ]$^{w-a,c,e}$	[ ]$^{w-a,c,e}$	[ ]$^{w-a,c,e}$	0.512	[ ]$^{w-a,c,e}$	[8]	The SS design fatigue curve in Section A.2.1 of [2.6] was applied. Refinements

Line / System	Component / Location	Material Category	CUF AOR (1)	CUF SLR	F_{en} (2)	CUF_{en}	EAF Evaluation Group	Reference	SLR CUF Conservatism Reduction Summary
(Unit 1)	(Leading SS Location)								were made regarding the interaction of stress cycles between different transients when forming fatigue pairs. The design cycles from the AOR were considered for all transients.
	Cold Leg Spray Nozzle (Leading CS/LAS Location)	CS/LAS	[ ]w-a,c,e	[ ]w-a,c,e	[ ]w-a,c,e	0.157	[ ]w-a,c,e	[8]	The CS design fatigue curve in Section A.2.1 of [2.6] was applied. Refinements were made regarding the interaction of stress cycles between different transients when forming fatigue pairs. The design cycles from the AOR were considered for all transients.
	4" x 4" x 4" Main Spray/Auxiliary Spray Tee	SS	[ ]w-a,c,e	---	---	---	[ ]w-a,c,e	[8]	A comparative evaluation was performed to demonstrate that the Unit 1 PZR spray nozzle (leading SS location) is more limiting with respect to EAF than the Unit 1 4" x 4" x 4" main spray/auxiliary spray tee.
Spray and Aux. Spray (Unit 2)	Cold Leg Spray Nozzle (Leading SS Location)	SS	[ ]w-a,c,e	[ ]w-a,c,e	[ ]w-a,c,e	0.512	[ ]w-a,c,e	[8]	The SS design fatigue curve in Section A.2.1 of [2.6] was applied. Refinements were made regarding the interaction of stress cycles between different transients when forming fatigue pairs. The design cycles from the AOR were considered for all transients.
	Cold Leg Spray Nozzle (Leading CS/LAS Location)	CS	[ ]w-a,c,e	[ ]w-a,c,e	[ ]w-a,c,e	0.157	[ ]w-a,c,e	[8]	The CS design fatigue curve in Section A.2.1 of [2.6] was applied. Refinements were made regarding the interaction of stress cycles between different transients when forming fatigue pairs. The design cycles from the AOR were considered for all transients.
	4" x 4" x 4" Main Spray Tee	SS	[ ]w-a,c,e	---	---	---	[ ]w-a,c,e	[8]	A comparative evaluation was performed to demonstrate that the Unit 2 4" x 2" auxiliary spray reducer is more limiting

Line / System	Component / Location	Material Category	CUF		Fen (2)	CUFen	EAF Evaluation Group	Reference	SLR CUF Conservatism Reduction Summary
			AOR (1)	SLR					
									with respect to EAF than the Unit 2 4” x 4” x 4” main spray tee.
PZR Relief Valve Piping (Unit 2)	4” x 4” x 4” Tee	SS	0.053	---	---	---	[ ]w-a,c,e	[8]	A comparative evaluation was performed to demonstrate that the Unit 2 4” x 4” x 4” main spray tee is more limiting with respect to EAF than the Unit 2 4” x 4” x 4” PZR relief valve piping tee.
Letdown and Suction Leg Drain (Unit 1)	Suction Leg Drain Nozzle (Leading CS/LAS Location)	CS	[ ]w-a,c,e	[ ]w-a,c,e	[ ]w-a,c,e	0.170	[ ]w-a,c,e	[8]	The CS design fatigue curve in Section A.2.1 of [2.6] was applied. Strain rate dependent F_{en} values were calculated for significant fatigue pairs. Emergency and faulted condition transients were excluded from the fatigue evaluation. Refinements were made regarding the interaction of stress cycles between different transients when forming fatigue pairs. The design cycles from the AOR were considered for all transients.
	Suction Leg Drain Nozzle (Leading SS Location)	SS	[ ]w-a,c,e	[ ]w-a,c,e	[ ]w-a,c,e	0.902	[ ]w-a,c,e	[8]	The SS design fatigue curve in Section A.2.1 of [2.6] was applied. Temperature and strain rate dependent F_{en} values were calculated for significant fatigue pairs. Emergency and faulted condition transients were excluded from the fatigue evaluation. Refinements were made regarding the interaction of stress cycles between different transients when forming fatigue pairs. The cycles were reduced for the following transients: • Heatup: reduced from 500 to 130 cycles • Cooldown: reduced from 500 to 130 cycles • Reactor Trip: reduced from 400 to 95 cycles

Line / System	Component / Location	Material Category	CUF AOR (1)	CUF SLR	F_{en} (2)	CUF_{en}	EAF Evaluation Group	Reference	SLR CUF Conservatism Reduction Summary
									• Leak Test: reduced from 200 to 5 cycles Since the safe end was replaced in May 2010 per ISI-PSL-1-2010 [11], this location would only experience a portion of the cycles that occur for an 80-year plant life. To inform potential changes to plant documents with cycle limits based on an 80-year plant life, an equivalent number of 80-year cycles were calculated as follows by adding the cycles from the 2009 cycle counting report [13]: • Heatup: 193 cycles • Cooldown: 192 cycles • Reactor Trip: 142 cycles • Leak Test: 5 cycles The design cycles from the AOR were considered for all other transients.
Letdown and Suction Leg Drain (Unit 2)	Suction Leg Drain Nozzle (Leading CS/LAS Location)	CS	[ ]w-a,c,e	[ ]w-a,c,e	[ ]w-a,c,e	0.180	[ ]w-a,c,e	[8]	The CS design fatigue curve in Section A.2.1 of [2.6] was applied. Strain rate dependent F_{en} values were calculated for significant fatigue pairs. Emergency and faulted condition transients were excluded from the fatigue evaluation. Refinements were made regarding the interaction of stress cycles between different transients when forming fatigue pairs. The design cycles from the AOR were considered for all transients.
	Suction Leg Drain Nozzle (Leading SS Location)	SS	[ ]w-a,c,e	[ ]w-a,c,e	[ ]w-a,c,e	0.909	[ ]w-a,c,e	[8]	The SS design fatigue curve in Section A.2.1 of [2.6] was applied. Temperature and strain rate dependent F_{en} values were calculated for significant fatigue pairs. Emergency and faulted condition transients were excluded from the fatigue

Line / System	Component / Location	Material Category	CUF AOR (1)	CUF SLR	F_{en} (2)	CUF_{en}	EAF Evaluation Group	Reference	SLR CUF Conservatism Reduction Summary
									evaluation. Refinements were made regarding the interaction of stress cycles between different transients when forming fatigue pairs. The cycles were reduced for the following transients: • Heatup: reduced from 500 to 375 cycles • Cooldown: reduced from 500 to 375 cycles • Leak Test: reduced from 200 to 150 cycles The design cycles from the AOR were considered for all other transients.
Hot Leg Drain (Unit 1)	Hot Leg Drain Nozzle (Leading SS Location)	SS	[ ]w-a,c,e	[ ]w-a,c,e	[ ]w-a,c,e	0.976	[ ]w-a,c,e	[8]	The SS design fatigue curve in Section A.2.1 of [2.6] was applied. Temperature dependent F_{en} values were calculated for significant fatigue pairs. The design cycles from the AOR were considered for all transients.
Charging (Unit 1)	Socket Weld at Elbow (Loop 1B1)	SS	[ ]w-a,c,e	[ ]w-a,c,e	[ ]w-a,c,e	0.941	[ ]w-a,c,e	[9]	A finite element analysis was performed to refine the derived transient stresses and the corresponding CUF value. The SS design fatigue curve in Section A.2.1 of [2.6] was applied. Temperature dependent F_{en} values were calculated for significant fatigue pairs. The cycles were reduced for the following transients: • Plant Loading: reduced from 15000 to 6500 cycles • Plant Unloading: reduced from 15000 to 6500 cycles • Purification and Boric Acid Dilution: reduced from 9000 to 8000 cycles The cycles for the Loss of Letdown transient were increased from 50 to 500

Line / System	Component / Location	Material Category	CUF		F_{en} (2)	CUF_{en}	EAF Evaluation Group	Reference	SLR CUF Conservatism Reduction Summary
			AOR (1)	SLR					
									cycles based on the 80-year transient cycle projections performed in CN-SDA-II-20-026 [6] and the design cycle fatigue reconciliation performed in CN-SDA-21-20 [15]. The design cycles from the AOR were considered for all other transients.
Charging (Unit 2)	Socket Welded Coupling (Loop 2A2)	SS	[ ]$^{w-a,c,e}$	[ ]$^{w-a,c,e}$	[ ]$^{w-a,c,e}$	0.975	[ ]$^{w-a,c,e}$	[9]	A finite element analysis was performed to refine the derived transient stresses and the corresponding CUF value. The SS design fatigue curve in Section A.2.1 of [2.6] was applied. Temperature dependent F_{en} values were calculated for significant fatigue pairs. The cycles were reduced for the following transients: • Plant Loading: reduced from 15000 to 6000 cycles • Plant Unloading: reduced from 15000 to 6000 cycles • Purification and Boric Acid Dilution: reduced from 24000 to 7000 cycles The cycles for the Loss of Letdown transient were increased from 50 to 500 cycles based on the 80-year transient cycle projections performed in CN-SDA-II-20-026 [6] and the design cycle fatigue reconciliation performed in CN-SDA-21-20 [15]. The design cycles from the AOR were considered for all other transients.
Safety Injection (Unit 1)	Cold Leg Safety Injection Nozzle (Leading CS/LAS Location)	LAS	[ ]$^{w-a,c,e}$	[ ]$^{w-a,c,e}$	[ ]$^{w-a,c,e}$	0.653	[ ]$^{w-a,c,e}$	[7]	The LAS design fatigue curve in Section A.2.1 of [2.6] was applied. The design cycles from the AOR were considered for all transients.

Line / System	Component / Location	Material Category	CUF		F_{en} (2)	CUF_{en}	EAF Evaluation Group	Reference	SLR CUF Conservatism Reduction Summary
			AOR (1)	SLR					
	Cold Leg Safety Injection Nozzle (Leading SS Location)	SS	[ ]w-a,c,e	[ ]w-a,c,e	[ ]w-a,c,e	0.243	[ ]w-a,c,e	[7]	The SS design fatigue curve in Section A.2.1 of [2.6] was applied. The design cycles from the AOR were considered for all transients.
	V3237 Valve Transition Weld (Loop 1B1)	SS	0.0622	[ ]w-a,c,e	[ ]w-a,c,e	0.939	[ ]w-a,c,e	[8]	The SS design fatigue curve in Section A.2.1 of [2.6] was applied. Temperature dependent F_{en} values were calculated for significant fatigue pairs. The design cycles from the AOR were considered for all transients.
	12” x 1” Branch (Loop 1B1)	SS	0.0702	[ ]w-a,c,e	[ ]w-a,c,e	0.953	[ ]w-a,c,e	[8]	The SS design fatigue curve in Section A.2.1 of [2.6] was applied. Temperature dependent F_{en} values were calculated for significant fatigue pairs. The cycles were reduced for the following transients: • Cooldown: reduced from 500 to 450 cycles The design cycles from the AOR were considered for all other transients.
Safety Injection (Unit 2)	Cold Leg Safety Injection Nozzle (Leading CS/LAS Location) (3)	LAS	[ ]w-a,c,e	[ ]w-a,c,e	[ ]w-a,c,e	0.872	[ ]w-a,c,e	[7]	The LAS design fatigue curve in Section A.2.1 of [2.6] was applied. The design cycles from the AOR were considered for all transients.
	Cold Leg Safety Injection Nozzle (Leading SS Location) (3)	SS	[ ]w-a,c,e	[ ]w-a,c,e	[ ]w-a,c,e	0.743	[ ]w-a,c,e	[7]	The SS design fatigue curve in Section A.2.1 of [2.6] was applied. The design cycles from the AOR were considered for all transients.

Line / System	Component / Location	Material Category	CUF		F_{en} (2)	CUF_{en}	EAF Evaluation Group	Reference	SLR CUF Conservatism Reduction Summary
			AOR (1)	SLR					
	V3227 Valve Transition Weld (Loop 2A1)	SS	0.526	---	---	---	[ ]$^{w-a,c,e}$	[14]	A comparative evaluation was performed to demonstrate that the Unit 2 12” x 12” x 6” tee is more limiting with respect to EAF than the Unit 2 V3227 valve transition weld.
	12” x 12” x 6” Tee (Loop 2A1)	SS	0.526	[ ]$^{w-a,c,e}$	[ ]$^{w-a,c,e}$	0.877	[ ]$^{w-a,c,e}$	[10]	A finite element analysis was performed to refine the derived transient stresses and the corresponding CUF value. The SS design fatigue curve in Section A.2.1 of [2.6] was applied. Temperature dependent F_{en} values were calculated for significant fatigue pairs. The cycles were reduced for the following transients: • Heatup: reduced from 500 to 400 cycles • Cooldown: reduced from 500 to 400 cycles The design cycles from the AOR were considered for all other transients.
Shutdown Cooling (Unit 1)	12” x 2” Branch	SS	0.0086	[ ]$^{w-a,c,e}$	[ ]$^{w-a,c,e}$	0.384	[ ]$^{w-a,c,e}$	[8]	The SS design fatigue curve in Section A.2.1 of [2.6] was applied. The design cycles from the AOR were considered for all transients.
	10” x 1” Branch	SS	0.0100	[ ]$^{w-a,c,e}$	[ ]$^{w-a,c,e}$	0.384	[ ]$^{w-a,c,e}$	[8]	The SS design fatigue curve in Section A.2.1 of [2.6] was applied. The design cycles from the AOR were considered for all transients.

Notes:
(1) The AOR CUFs are listed in Section 2.0 of [3].
(2) This F_{en} value represents a weighted average value, defined as the CUF_{en} divided by the SLR CUF. The actual F_{en} values may vary between individual fatigue pairs.
(3) CUF_{en} values for configurations with and without thermal sleeves were calculated for the Unit 2 cold leg safety injection nozzles. The reported value reflects the higher value for the configuration without a thermal sleeve.

4.0 References

1. Westinghouse Letter, LTR-AMER-MKG-20-1686, Revision 6, "Westinghouse Final Revised Offer for Subsequent License Renewal for St. Lucie Units 1 & 2."
2. NRC Documents:
   - 2.1. NRC Document, NUREG-2191, Volumes 1 and 2, "Generic Aging Lessons Learned for Subsequent License Renewal (GALL-SLR) Report," July 2017 (Agencywide Documents Access and Management System (ADAMS) Accession Nos. ML17187A031 and ML17187A204).
   - 2.2. NRC Document, NUREG-2192, "Standard Review Plan for Review of Subsequent License Renewal Applications for Nuclear Power Plants," July 2017 (ADAMS Accession No. ML17188A158).
   - 2.3. NRC Document, NUREG/CR-6260, "Application of NUREG/CR-5999 Interim Fatigue Curves to Selected Nuclear Power Plant Components," February 1995.
   - 2.4. NRC Regulatory Guide, 1.207, Revision 1, "Guidelines for Evaluating the Effects of Light-Water Reactor Water Environments in Fatigue Analyses of Metal Components," (ADAMS Accession No. ML16315A130).
   - 2.5. NRC Document, NUREG/CR-6909, Revision 0, "Effect of LWR Coolant Environments on the Fatigue Life of Reactor Materials," (ADAMS Accession No. ML070660620).
   - 2.6. NRC Document, NUREG/CR-6909, Revision 1, "Effect of LWR Water Environments on the Fatigue Life of Reactor Materials," (ADAMS Accession No. ML16319A004).
3. Westinghouse Calculation Note, CN-SDA-II-20-022, Revision 1, "St. Lucie Units 1 & 2 Subsequent License Renewal: Primary Equipment and Piping Environmentally Assisted Fatigue Screening Evaluation."
4. Florida Power & Light Design Input Transmittal, PSLWEC-21-0059, Rev. 0, "Design Input Transmittal for WS04 Environmentally Assisted Fatigue (EAF) to Support the St. Lucie Unit 1 and Unit 2 Subsequent License Renewal," June 4, 2021.
5. Florida Power & Light Procedure, 0-COP-05.04, Revision 119, "Chemistry Department Surveillances and Parameters," August 12, 2020. (electronically attached to [4])
6. Westinghouse Calculation Note, CN-SDA-II-20-026, Revision 2, "St. Lucie Unit 1 and Unit 2 80-Year Transient Cycle Projections."
7. Westinghouse Calculation Note, CN-SDA-II-20-023, Revision 0, "St. Lucie Units 1 & 2 Subsequent License Renewal: Environmentally Assisted Fatigue Analysis of Reactor Vessel and Safety Injection Nozzles."
8. Westinghouse Calculation Note, CN-SDA-II-21-010, Revision 0, "St. Lucie Units 1 & 2 Subsequent License Renewal: Primary Equipment and Piping Environmentally Assisted Fatigue Evaluation."
9. Westinghouse Calculation Note, CN-SDA-II-21-007, Revision 0, "St. Lucie Units 1 & 2 Subsequent License Renewal: Environmentally Assisted Fatigue Evaluation for the Units 1 & 2 Charging Line Socket Weld Limiting Location."

10. Westinghouse Calculation Note, CN-SDA-II-21-009, Revision 0, "St. Lucie Units 1 & 2 Subsequent License Renewal: Unit 2 Loop 2A1 Safety Injection Line 12" x 12" x 6" Tee Environmentally Assisted Fatigue Evaluation."

11. ISI-PSL-1-2010, OAR-1 Owner's Activity Report for St. Lucie Nuclear Power Plant Unit 1 Refueling Outage SL-1-23, dated August 26, 2010 (ADAMS Accession No. ML102520487).

12. FPL Letter, PSLWEC-21-0014, Revision 0, "Design Input Transmittal for WS08 80-Year Cycle Projections to Support the St. Lucie Unit 1 and Unit 2 Subsequent License Renewal," February 11, 2021.

13. St. Lucie Plant Procedure, 0010134, Revision 24, "Component Cycles and Transients," with 2009 Appendix B, "Annual Report of Cumulative Component Cycles and Transients," February 1, 2010 (electronically attached to [12] as "2009 report.pdf").

14. Westinghouse Calculation Note, CN-SDA-II-21-008, Revision 0, "St. Lucie Unit 2 Subsequent License Renewal – Safety Injection Line Transients and ANSYS-WESTEMS Interface File Development."

15. Westinghouse Calculation Note, CN-SDA-21-20, Revision 0, "St. Lucie Units 1 & 2 Subsequent License Renewal: Loss of Letdown Design Cycle Fatigue Reconciliation."

This page was added to the quality record by the PRIME system upon its validation and shall not be considered in the page numbering of this document.

Approval Information
Author Approval Matthews Eric J Jul-14-2021 10:44:34
Verifier Approval Oakman Jamie L Jul-14-2021 11:25:40
Manager Approval Klimek John Jul-14-2021 13:23:55
Hold to Release Approval Matthews Eric J Jul-14-2021 15:50:36

Files approved on Jul-14-2021

*** This record was final approved on 7/14/2021 3:50:36 PM. (This statement was added by the PRIME system upon its validation)

Enclosure 4

Non-proprietary Reference Documents and Redacted Versions of Proprietary Reference Documents (Public Version)

Attachment 7

BWXT Report MSLEF-SR-01-NP, Revision 0, St. Lucie Unit 1 Replacement Steam Generator Environmentally Assisted Fatigue Report (Non-Proprietary), July 16, 2021

(21 Total Pages, including cover sheets)

BWXT Canada Ltd.

CUSTOMER COPY

WESTINGHOUSE ELECTRIC COMPANY

ST. LUCIE UNIT 1 REPLACEMENT STEAM GENERATOR ENVIRONMENTALLY ASSISTED FATIGUE REPORT (NON-PROPRIETARY)

BWXT CANADA
REPORT NO.: MSLEF-SR-01-NP
REVISION 0
JULY 2021

Engineering Specification: F-MECH-SP-002 Rev. 3

Prepared By: Digitally signed by Derek Hartman Date: 2021.07.16 10:23:09 -04'00' Date: See electronic signature
D. Hartman, P. Eng.
Manager, Engineering Analysis and Qualification

Verified By: Digitally signed by Adriana Cameron Date: 2021.07.16 10:52:29 -04'00' Date: See electronic signature
A. Cameron
Engineering Analyst

Approved By: Digitally signed by Derek Hartman Date: 2021.07.16 10:24:18 -04'00' Date: See electronic signature
D. Hartman, P. Eng.
Manager, Engineering Analysis and Qualification

Approved By: R. G. MacEacheron Digitally signed by R. G. MacEacheron DN: cn=R. G. MacEacheron, o=BWXT Canada Ltd., ou=Engineering Services, email=rmaceacheron@bwxt.com, c=CA Date: 2021.07.16 11:00:55 -04'00' Date: See electronic signature
R. MacEacheron, P. Eng.
Project Engineer

Approved By: on behalf of R. G. MacEacheron Digitally signed by R. G. MacEacheron DN: cn=R. G. MacEacheron, o=BWXT Canada Ltd., ou=Engineering Services, email=rmaceacheron@bwxt.com, c=CA Date: 2021.07.16 11:01:38 -04'00' Date: See electronic signature
S. Fluit, P. Eng.
Manager, Engineering Services

INDEPENDENT DESIGN VERIFICATION BY DESIGN REVIEW

NEF008 Rev. 01

Design Review Verification Criteria (as applicable)	Rev. 0	Rev. 1	Rev. 2	Rev. 3	Rev. 4	Rev. 5
1. Are the design inputs (including customer specification requirements and other customer supplied inputs, drawings or other analysis) correctly selected and incorporated into the design?	Yes					
2. Are the design inputs (including customer specification requirements and other customer supplied inputs, drawings or other analysis) verified?	Yes					
3. Are verified customer supplied design inputs located in either the CIS or project services database?	Yes					
4. Are assumptions necessary to perform the design activity reasonable and adequately described? Where necessary, are the assumptions identified for subsequent reverification when the detailed design activities are complete?	Yes					
5. Is the design method appropriate?	Yes					
6. Were all design inputs correctly incorporated into the design?	Yes					
7. Is the design output reasonable compared to design input?	Yes					
8. Are the necessary design inputs and verification requirements for interfacing organizations specified in the design documents or in supporting procedures or instructions?	N/A					

Rev	Verified By	Date	Rev	Verified By	Date
0	Adriana Cameron Digitally signed by Adriana Cameron Date: 2021.07.16 10:52:57 -04'00'	See electronic signature	3		
1			4		
2			5		

LIST OF REVISIONS

Rev.	Sec. / Page	Description
0	All	Original Release

TABLE OF CONTENTS

1.0 FORWARD 5
2.0 ABSTRACT 6
3.0 INTRODUCTION 7
4.0 ACCEPTANCE CRITERIA 8
5.0 LOADING CONDITIONS 8
6.0 MATERIALS 10
7.0 ANALYSIS LOCATIONS 11
8.0 ANALYSIS 13
9.0 VERIFICATION OF ASSUMPTIONS 17
10.0 CONCLUSIONS 17
11.0 REFERENCES, DESIGN DRAWINGS AND COMPUTER CODES 18
12.0 LIST OF DETAILED ANALYSIS CALCULATIONS 20

1.0 FORWARD

This document contains BWXT Canada Ltd. (BWXT) proprietary information and data which has been identified by brackets. Coding (a and c) associated with the brackets sets forth information which is considered proprietary.

The proprietary information and data contained within the brackets in this report were obtained at considerable BWXT expense and its release could seriously affect our competitive position. This information is to be withheld from public disclosure in accordance with the Rules of Practice 10 CFR 2.390 and the information presented herein is safeguarded in accordance with 10 CFR 2.390. Withholding of this information does not adversely affect the public interest.

This information has been provided for your internal use only and should not be released to persons or organizations outside the Directorate of Regulation and the Advisory Committee on Reactor Safeguards (ACRS) without the express written approval of BWXT. Should it become necessary to release this information to such persons as part of the review procedure, please contact BWXT, which will make the necessary arrangements required to protect the Company's proprietary interests.

Proprietary information is identified and bracketed. For each of the bracketed locations, the reason for the proprietary classification is provided, using a standardized system. The proprietary brackets are labeled with two (2) different letters, "a", and "c" which stand for:

a. The information reveals the distinguishing aspects of a process or component, structure, tool, method, etc. The prevention of its use by BWXT's competitors, without license from BWXT, gives BWXT a competitive economic advantage.
c. The information, if used by a competitor, would reduce the competitor's expenditure of resources or improve the competitor's advantage in the design, manufacture, shipment, installation, assurance of quality, or licensing of a similar product.

2.0 ABSTRACT

This report presents the environmentally assisted fatigue (EAF) assessment of the sentinel primary side wetted pressure boundary locations for the St. Lucie Unit 1 Replacement Steam Generator (RSG). The evaluation demonstrates the acceptability of the primary side wetted pressure boundary components for the projected 80-year operating transient cycles with primary coolant water environment, in accordance with the requirements defined in Regulatory Guideline 1.207 [R-7].

Stresses and fatigue pairs due to the Level A and B transients are extracted from the Extended Power Uprate (EPU) analysis documented in B&W/BWXT Canada Reports CM9021278-SR-01 [R-3] and 314Q-SR-01 [R-12]. The projected 80-year operating transient cycles and the environmental fatigue factor (F_{en}) are incorporated to calculate the cumulative fatigue usage factor in a water environment (CUF_{en}). The analysis concludes that:

1. All sentinel locations have cumulative fatigue usage factors with environmental effects considered (CUF_{en}) less than 1 for the projected 80-year operating transient cycles. Where an 80-year projected cycle has been provided, based on cycle counting to date, the cycles have been conservatively increased by 61% to demonstrate additional margin.

3.0 INTRODUCTION

The St. Lucie Unit 1 Replacement Steam Generator (RSG) at 3020 MWth (3034 MWth NSSS) Extended Power Uprate (EPU) conditions has been analyzed in B&W/BWXT Canada Reports CM9021278-SR-01 [R-3] and 314Q-SR-01 [R-12]. To support license extension efforts to an 80 year operating life, environmentally assisted fatigue (EAF) is considered for the primary side wetted pressure boundary components. The cumulative fatigue usage factor in a water environment (CUF_{en}) is calculated for the 80-year operating life [R-5] with a factor applied on the cycles, as per the requirements defined in Regulatory Guideline 1.207 [R-7].

Environmentally assisted fatigue is considered for sentinel (leading) locations for the primary side wetted pressure boundary components, based on the screening evaluation of the design cumulative fatigue usage factors (CUF) performed by Westinghouse [R-5]. The sentinel locations consider each of the primary side wetted pressure boundary material types and are discussed in detail in Section 7.0.

The environmental effects are considered through application of the environmental factor (F_{en}) described in Regulatory Guideline 1.207 [R-7] and NUREG/CR-6909 [R-8]. The design cumulative fatigue usage factor (CUF) is recalculated considering the analysis results summarized in B&W/BWXT Canada Reports CM9021278-SR-01 [R-3] and 314Q-SR-01 [R-12] and modified to account for the projected 80-year transient cycles as described in Section 5.0. The transient definitions and resultant transient stresses are unchanged from those analyzed in CM9021278-SR-01 [R-3] and therefore the fatigue stress pairs, stress amplitude and component metal temperatures are also extracted directly from the calculations supporting CM9021278-SR-01 [R-3]. The analysis supporting 314Q-SR-01 [R-12] for the tube-to-tubesheet weld is re-run using the same analysis approach to remove conservatism in the inputs as discussed in Section 8.0. More details on the analysis for the environmental effects are given in Section 8.0.

The report conclusions are described in Section 10.0. The references, design drawings and computer codes used in the detailed analysis calculation are described in Section 11.0. This detailed analysis calculation is identified in Section 12.0.

4.0 ACCEPTANCE CRITERIA

For Level A and B condition, the following cumulative fatigue usage factor (CUF) limits are applied as stipulated by NB-3222 and NB-3223 [R-10]:

$$CUF \leq 1.0$$

Based on Regulatory Guideline 1.207 [R-7] and NUREG/CR-6909 [R-8], the environmental CUF (CUF_{en}) is to be calculated by the application of the environmental fatigue factor (F_{en}) to the CUF calculated in air.

$$CUF_{en} \leq 1.0$$

5.0 LOADING CONDITIONS

5.1 Transient Conditions

The transient conditions for the St. Lucie Unit 1 Replacement Steam Generator (RSG) at 3020 MWth (3034 MWth NSSS) Extended Power Uprate (EPU) conditions are specified in the CDS [R-2] and FPL letter [R-1]. These Level A and B transient conditions have been analyzed for the steam generator in B&W/BWXT Canada Reports CM9021278-SR-01 [R-3] and 314Q-SR-01 [R-12]. To support license renewal to an 80 year operating period, projected 80-year operating life transient cycles are specified in a Westinghouse Letter [R-5]. The transients along with the CDS and 80-year projected transient cycles can be seen in Table 1.

The analysis in CM9021278-SR-01 [R-3] and 314Q-SR-01 [R-12] considered enveloping transients ('lumped') which bound multiple transients. The total transient cycles across all of the transients which are lumped together are considered. This approach is conservative. These same lumped transients have been considered in the current analysis. Additionally, based on CM9021278-SR-01 [R-3], some transients were determined to have negligible impact on the transient stress results for the components being assessed in this report and are therefore not considered in this report. The transients and lumped transients analyzed for the components considered in this report can be seen in Table 2. A factor is applied on these cycles to determine the maximum allowable number of cycles. The cycles are increased by 61% to demonstrate additional margin, with the final cycle values for each transient seen in Table 2. Note that only transients where an 80-year projected cycle is given are increased. Transients where 80-year projected cycles are not given and where the CDS cycle limits are used [R-5], are not increased.

The Cold Feedwater Following Hot Standby transient results in no cyclic stresses in the tubesheet assembly or tubes and is thus excluded [R-9][R-4]. The Operating Basic Earthquake (OBE) transient does not result in significant cyclic stresses in the tubesheet assembly and is thus excluded [R-9]. It is considered for the tube and tube-to-tubesheet weld analysis. The Primary Coolant pump starting and stopping does not cause significant cyclic stress in the tubesheet assembly and is not included. It is conservatively considered in the tube and tube-to-tubesheet weld analysis.

Table 1 Level A and B and Test Transients for St. Lucie Unit 1.

Transients	CDS Cycles [R-2]	80-Year Projected Cycles [R-5]
Plant Heatup	500	143
Plant Cooldown	500	141
Plant loading 5%/min	15,000	1,290
Plant unloading 5%/min	15,000	1,290
10% step load increase	2,000	2,000 (1)
10% step load decrease	2,000	2,000 (1)
Cold Feedwater following hot standby	15,000	15,000 (1)
Primary Coolant pump starting and stopping	4,000	4,000 (1)
Normal Plant Variation	10^6	10^6 (1)
Reactor Trip	400	106
Loss of reactor coolant flow	40	2
Loss of Load	40	6
Operation Basis Earthquake	200	2
Primary Side Hydrostatic Test	10	3
Secondary Side Hydrostatic Test	10	3
Primary Leak Test	200	2
Secondary Leak Test	200	3

Notes:

1. 80-year projected cycles not given. Therefore, the CDS cycles are considered [R-5].

Table 2 Analyzed Level A and B and Test Transients for St. Lucie Unit 1 Primary Side Wetted Components.

Transient Number	Transients	80-Year Projected Cycles	Acceptable 80-Year Projected Cycles
1	Plant Heatup/Cooldown	143	231
1 (1)	Primary Leak Test	2	4
2	Plant loading/Unloading	1,290	2,077
3	10% step load increase/decrease	2,000	2,000
4	Lumped Transient (2)	114	184
5	Normal Plant Variation	10^6	10^6
6	Secondary Leak Test	3	5
-- (3)	Primary Coolant pump starting and stopping	4,000	4,000
-- (3)	Operation Basis Earthquake	2	4

Notes:

1. Bounded by Plant Heat / Cooldown. Therefore, the total number of Plant Heatup / Cooldown plus Primary Leak Test cycles are considered for Plant Heatup / Cooldown (145 and 235 cycles for 80-year and acceptable 80-year cycles respectively).
2. Lumped transient includes 'Reactor Trip', 'Loss of Primary Flow' and 'Loss of Turbine Generator Load'. Total number of cycles across all three transients considered. This corresponds to: Reactor Trip (106 and 171 cycles), Loss of Primary Flow (2 and 3 cycles) and Loss of Turbine Generator Load (6 and 10 cycles) for 80-year and acceptable 80-year cycles respectively.
3. Does not result in significant cyclic stress for the primary head / tubesheet assembly. Considered for the tube and tube-to-tubesheet weld analysis.

6.0 MATERIALS

The material designations for the primary side wetted pressure boundary components for the St. Lucie Unit 1 RSG are specified in the B&W Canada Drawing 7612E151 and summarized in Table 3. Details of material mechanical properties used in a specific component/assembly analysis are given in the corresponding calculation for that component/assembly. The fatigue curves for the materials are taken from ASME B&PVC Section III, Appendix I. Note that the calculation of the F_{en} parameter is based on ASME Boiler and Pressure Vessel Code (B&PVC) 2013 Edition [R-11]. As such, the fatigue curves from the 2013 Edition of ASME B&PVC [R-11] are considered. If more conservative, the original fatigue design curves [R-10] are retained. This is discussed in more detail in Section 8.0.

Table 3 Primary Side Wetted Pressure Boundary Component Materials.

Component	Material
Tubesheet	[ ]c
Primary Head	[ ]c
Stay Cylinder	[ ]c
Tubesheet Divider Plate Seat Bar	[ ]c
Stay Cylinder Divider Plate Seat Bar	[ ]c
Primary Head Divider Plate Seat Bar	[ ]c
Inlet / Outlet Nozzle Dam Ring	[ ]c
Inlet / Outlet Nozzles	[ ]c
Manway Cover	[ ]c
Manway Diaphragm	[ ]c
Primary Side Instrument Taps	]c
Tubes	[ ]c
Tube-to-Tubesheet Weld (1)	[ ]c

Notes

1) [ ]c.

7.0 ANALYSIS LOCATIONS

The locations with the highest CUF based on material type are shown in Table 4. For the low alloy steels, a number of locations with higher CUF values are all presented. Based on this table and the screening F_{en} values provided by Westinghouse [R-5], the sentinel locations to be analyzed are discussed below. Other locations presented in the table are not analyzed as they consider a similar or more conservative level of analysis rigour as the sentinel locations analyzed. This is discussed in more detail below. In Table 4, dark shaded items are those items to be analyzed (sentinel locations). The lighter shaded items of the same colour are those that consider a similar analysis approach and level of analysis rigour but have a lower CUF.

Table 4: Primary Side Wetted Surface Pressure Boundary Cumulative Usage Factor by Material Type.

Location	Max CUF by Material			
	Stainless Steel	Carbon Steel	Low Alloy Steel	Ni-Cr-Fe Alloy
---(5)				
Tubes [R-3][R-4]	[ ]c	[ ]c	[ ]c	[ ]c
Tube-to-Tubesheet Weld [R-12]	[ ]c	[ ]c	[ ]c	[ ]c
Tubesheet Solid Rim (at Tubesheet Dome) [R-3]	[ ]c	[ ]c	[ ]c	[ ]c
Primary Head (4) [R-3]	[ ]c	[ ]c	[ ]c	[ ]c
Tubesheet Perforated (primary side) [R-3]	[ ]c	[ ]c	[ ]c	[ ]c
Inlet/Outlet Nozzle [R-3]	[ ]c	[ ]c	[ ]c	[ ]c
Primary Head at Divider Plate Seat Bar (1) [R-3]	[ ]c	[ ]c	[ ]c	[ ]c
Primary Head At Instrument / Accelerometer Taps (2) [R-3]	[ ]c	[ ]c	[ ]c	[ ]c
Primary Head at Inlet Nozzle Dam Ring Juncture (3) [R-3]	[ ]c	[ ]c	[ ]c	[ ]c
Primary Head at Outlet Nozzle Dam Ring Juncture (3) [R-3]	[ ]c	[ ]c	[ ]c	[ ]c
Primary Manway Cover [R-3]	[ ]c	[ ]c	[ ]c	[ ]c

Notes

1) [ ]a
2) [ ]a
3) [ ]a
4) Maximum CUF for primary head for other locations not listed.
5) [ ]a

Based on the results summarized in Table 4, the following are the sentinel locations to be analyzed for the environmentally assisted fatigue considerations.

1) Tube. Analyzed since it is Ni-Cr-Fe alloy and has screened in based on the potential F_{en} factor to be considered. It considers a different analysis approach compared to the tube-to-tubesheet weld.
2) Tube-to-Tubesheet Weld. Analyzed since it is Ni-Cr-Fe alloy and has screened in based on the potential F_{en} factor to be considered. It considers a different analysis approach compared to the tubes.
3) Primary Head at Divider Plate Seat Bar. Analyzed since it is the low alloy steel location with the highest CUF and has screened in based on the potential F_{en} factor to be considered. [ ]a
4) Tubesheet. Analyzed since it is the low alloy steel location with a high CUF and has screened in based on the potential F_{en} factor to be considered.

The following locations are considered to have a similar analysis approach as the sentinel locations discussed above, but have a lower CUF.

1) Inlet / Outlet Nozzle. The inlet and outlet nozzles are analyzed using a similar modeling and fatigue analysis approach as for the Tubesheet location. In addition, the inlet / outlet nozzles retain some additional conservatism due to consideration of conservative transients, that were then conservatively prorated to account for the St. Lucie Unit 1 EPU.
2) Primary Manway Cover. This location has a low CUF and will remain below 1 with the appropriate F_{en} applied. Therefore, it does not need to be analyzed.
3) Tubesheet Perforated Region. The tubesheet perforated region is analyzed using a similar modeling approach as the Tubesheet (solid) region.
4) Primary Head at Instrument /Accelerometer Tap. This location is analyzed using the same modeling and fatigue analysis approach as for the Primary Head at Divider Plate Seat Bar location. [ ]a
5) Primary Head at Inlet Nozzle Dam Ring location. The inlet nozzle dam ring location is analyzed using a similar modeling and fatigue analysis approach as for the Tubesheet location. In addition, the inlet nozzle dam ring retains some additional conservatism due to consideration of conservative transients, that were then conservatively prorated to account for the St. Lucie Unit 1 EPU. [ ]a
6) Primary Head at Outlet Nozzle Dam Ring location. Same approach and conservatism as the Primary Head at Inlet Nozzle Dam Ring location.
7) Primary Head. The primary head is analyzed using the same modeling and fatigue approach as the Tubesheet (solid) region.

8.0 ANALYSIS

Based on Regulatory Guideline 1.207 [R-7] and NUREG/CR-6909 [R-8], the environmental CUF (CUF_{en}), to account for the effects of water environments, is calculated by the application of the environmental fatigue factor (F_{en}) to the CUF calculated in air. It is noted in Regulatory Guideline 1.207 [R-7] that the CUF in air should be calculated considering the 2013 Edition (2013E) of the ASME B&PVC [R-11] fatigue design curves.

The analysis for the EPU as documented in CM9021278-SR-01 [R-3] and 314Q-SR-01 [R-12] considers the fatigue curves from the 1986 Edition (1986E) of the ASME B&PVC [R-10]. A comparison is made between the fatigue design curves of the two editions below.

1) For the low alloy steel (UTS < 80 ksi), fatigue design curve (Figure I-9.1), the 1986E [R-10] and 2013E [R-11] fatigue design curves are identical above a stress amplitude of 12.5 ksi (1E6 cycles). Beyond this point, the 2013E contains additional points not present in the 1986E. However, these points are below the strain threshold as presented in Section 8.1. Therefore, there is insignificant impact to the CUF in air documented in CM9021278-SR-01 [R-3] for low alloy steel materials.
2) For Ni-Cr-Fe alloy, fatigue design curve (Figure I-9.2.1 / I-9.2.2 and Figure I-9.2 respectively) the 1986E [R-10] and 2013E [R-11] fatigue design curves show some differences, with the 1986E being more conservative above a stress amplitude of approximately 201 ksi (2E2 cycles) and the 2013E being more conservative for stress amplitudes between approximately 14.1 ksi and 201 ksi (1E8 and 2E2 cycles). The two curves are the same below 14.1 ksi (1E8 cycles). As such, the 2013E of the fatigue design curve is considered, except for stress amplitudes above 201 ksi (if applicable).

8.1 Environmental Fatigue Factor (F_{en})

8.1.1 Carbon and Low Alloy Steels

The following are the environmental fatigue factor (F_{en}) equations given in Appendix A of NUREG/CR-6909 [R-8], as described in Regulatory Guideline 1.207 [R-7] for carbon and low alloy steels.

$$F_{en} = \exp((0.003 - 0.031\dot{\varepsilon}^*)\, S^* T^* O^*),$$

where S^*, T^*, O^*, and $\dot{\varepsilon}^*$ are transformed sulfur (S) content, material temperature, dissolved oxygen (DO) level, and strain rate, respectively, defined as follows:

$S^* = 2.0 + 98\,S$	$(S \le 0.015\ \text{wt.\%})$
$S^* = 3.47$	$(S > 0.015\ \text{wt.\%})$
$T^* = 0.395$	$(T < 150°C)$
$T^* = (T - 75)/190$	$(150°C \le T \le 325°C)$
$O^* = 1.49$	$(DO < 0.04\ \text{ppm})$
$O^* = \ln(DO/0.009)$	$(0.04\ \text{ppm} \le DO \le 0.5\ \text{ppm})$
$O^* = 4.02$	$(DO > 0.5\ \text{ppm})$
$\dot{\varepsilon}^* = 0$	$(\dot{\varepsilon} > 2.2\%/s)$
$\dot{\varepsilon}^* = \ln(\dot{\varepsilon}/2.2)$	$(0.0004\%/s \le \dot{\varepsilon} \le 2.2\%/s)$
$\dot{\varepsilon}^* = \ln(0.0004/2.2)$	$(\dot{\varepsilon} < 0.0004\%/s)$

A threshold value of 0.07% strain amplitude or 21.0 ksi stress amplitude is defined, below which the environmental effects for steel do not occur.

$$F_{en} = 1 \qquad (\varepsilon_a \le 0.07\% \text{ or } 145\ \text{MPa}\ \{21.0\ \text{ksi}\}\ \text{stress amplitude})$$

8.1.2 Ni-Cr-Fe Alloys

The following are the environmental fatigue factor (F_{en}) equations given in Appendix A of NUREG/CR-6909 [R-8], as described in Regulatory Guideline 1.207 [R-7] for Ni-Cr-Fe materials.

For all Ni-Cr-Fe alloys except Inconel 718,

$$F_{en} = \exp(-T^* \dot{\varepsilon}^* O^*)$$

where T^*, $\dot{\varepsilon}^*$, and O^* are transformed temperature, strain rate, and DO, respectively, defined as:

$T^* = 0$	$(T < 50°C)$
$T^* = (T - 50)/275$	$(50°C \le T \le 325°C)$
$\dot{\varepsilon}^* = 0$	$(\dot{\varepsilon} > 5.0\%/s)$
$\dot{\varepsilon}^* = \ln(\dot{\varepsilon}/5.0)$	$(0.0004\%/s \le \dot{\varepsilon} \le 5.0\%/s)$
$\dot{\varepsilon}^* = \ln(0.0004/5.0)$	$(\dot{\varepsilon} < 0.0004\%/s)$
$O^* = 0.06$	(NWC BWR water (i.e., ≥ 0.1 ppm DO)))
$O^* = 0.14$	(PWR or HWC BWR water (i.e., < 0.1 ppm DO))

A threshold value of 0.10% strain amplitude or 28.3 ksi stress amplitude is defined, below which the environmental effects for Ni-Cr-Fe do not occur.

$F_{en} = 1$ $(\varepsilon_a \le 0.10\%$ or a 195 MPa {28.3 ksi} stress amplitude)

8.2 Dissolved Oxygen and Sulfur Content

The Reactor Coolant System (RCS) dissolved oxygen (DO) content is controlled according to procedure 0-COP-05.04 [R-6]. When the RCS temperature is above 250°F, the DO content in the RCS is maintained below 5 ppb (0.005 ppm) in Modes 1 and 2 and 10 ppb (0.01 ppm) in Modes 3 and 4 as discussed in 0-COP-05.04 and supported by data from 2010 to 2020 [R-5]. When the RCS temperature is below 250°F, the DO content may exceed 10 ppb (0.01 ppm) [R-5]. Therefore, the following assumptions regarding the DO content are made in the EAF evaluation:

- When the RCS temperature is greater than 250°F, a constant DO content of 0.01 ppm is assumed.
- When the RCS temperature is less than or equal to 250°F, the DO content that maximizes the F_{en} is assumed.

This approach is applicable for the analysis of carbon and low alloy steel components. This approach is consistent with the standard approach employed by Westinghouse on the Subsequent License Renewal (SLR) project [R-5].

The sulfur content of pressure boundary materials, except for weld filler, is limited to 0.005% as described in Section 4.13.1 of the CDS [R-2]. For weld filler material, the sulfur content shall not exceed 0.010% [R-2]. Therefore, the sulfur content of 0.010% is considered in the analysis.

8.3 Cumulative Usage Factor in Water Environment

8.3.1 Low Alloy Steels

The low alloy steel locations discussed in Section 7.0 (tubesheet solid rim at tubesheet dome, primary head at divider plate seat bar) are analyzed for the effects of the water environment by incorporating the F_{en} factor for each stress pair to calculate the total CUF_{en} value. The fatigue analysis of these components for the EPU condition is documented in CM9021278-B02 [R-9]. Therefore, the fatigue pairs, stress amplitude and metal temperature are extracted directly from this calculation at the locations of interest. Based on the projected 80-year transient cycles as described in Table 2, the CUF in air is recalculated. Based on the temperature, dissolved oxygen content and strain rate which are calculated from the results in CM9021278-B02 [R-9], the F_{en} for each stress pair is calculated following the equations given in Section 8.1.1 and the total CUF_{en} is calculated. This is documented in BWXT Canada Calculation MSLEF-B001 (listed in Section 12.0). The F_{en} are calculated by conservatively considering the maximum temperature and dissolved oxygen from each peak and valley range and before applying to the stress pairs. For the Primary Head at Divider Plate Seat Bar location, the fatigue usage factor is calculated using the fatigue design curve for low alloy steel in CM9021278-B02 [R-9] as it is more conservative compared to the fatigue design curve for Ni-Cr-Fe alloy. For the F_{en} calculation, the equations for low alloy steel also lead to a higher F_{en} value and therefore this approach is appropriate.

The results are documented in Table 5 for the Tubesheet Solid Rim at the Tubesheet Dome location and in Table 6 for the Primary Head at Divider Plate Seat Bar location. Only the stress pairs that lead to a stress amplitude greater than the fatigue curve cutoff are shown. These CUF values consider the increase of 61% on the transient cycles, as detailed in Section 5.1.

Table 5: Fatigue Pass Table for Tubesheet Solid Rim near Dome.

Pair	Num. of Cycles		UF	F_{en}	UF*F_{en}
	Design	Allowed			
1	[ ]c	[ ]c	[ ]c	[ ]c	[ ]c
2	[ ]c	[ ]c	[ ]c	[ ]c	[ ]c
3	[ ]c	[ ]c	[ ]c	[ ]c	[ ]c
4	[ ]c	[ ]c	[ ]c	[ ]c	[ ]c
5	[ ]c	[ ]c	[ ]c	[ ]c	[ ]c
		CUF	[ ]c	CUF_{en}	[ ]c

Table 6: Fatigue Pass Table for Primary Head at Divider Plate Seat Bar Location.

Pair	Num. of Cycles		UF	F_{en}	UF*F_{en}
	Design	Allowed			
1	[ ]c	[ ]c	[ ]c	[ ]c	[ ]c
2	[ ]c	[ ]c	[ ]c	[ ]c	[ ]c
3	[ ]c	[ ]c	[ ]c	[ ]c	[ ]c
4	[ ]c	[ ]c	[ ]c	[ ]c	[ ]c
5	[ ]c	[ ]c	[ ]c	[ ]c	[ ]c
6	[ ]c	[ ]c	[ ]c	[ ]c	[ ]c
		CUF	[ ]c	CUF_{en}	[ ]c

8.3.2 Ni-Cr-Fe Alloys

The tube is analyzed in a conservative manner in the original analysis [R-3][R-4], where the maximum stress intensity range is calculated across all of the transients and then applied to the total number of cycles from all transients applicable to the tube. This conservative approach is maintained and a conservative F_{en} is calculated considering the maximum primary side temperature for the transients and the minimum strain rate, according to the equations given in Section 8.1.2, as documented in BWXT Canada Calculation MSLEF-B001 (listed in Section 12.0). As discussed in Section 8.0, the F_{en} is to be applied on the 2013E fatigue design curve [R-11]. Therefore, the number of allowed cycles is re-calculated compared to the original analysis, using the 2013E fatigue design curve [R-11], as shown in Table 7. These CUF values consider the increase of 61% on the transient cycles, as detailed in Section 5.1.

Table 7: Fatigue Pass Table for Tube Location.

Pair	Num. of Cycles		UF	F_{en}	UF*F_{en}
	Design	Allowed			
1	[ ]c	[ ]c	[ ]c	[ ]c	[ ]c
		CUF	[ ]c	CUF_{en}	[ ]c

The tube-to-tubesheet weld is analyzed in a conservative manner in the analysis given in BWXT Canada Report 314Q-SR-01 [R-12]. The analysis has been re-run to remove conservatism, in BWXT Canada Calculation MSLEF-B002 (listed in Section 12.0), to generate the transient stress results and the fatigue analysis has been performed using the 80-year projected transient cycles, including the increase of 61%, as described in Section 5.1. The 2013E fatigue design curve [R-11] is used as it is more conservative for the stress amplitudes seen in the analysis, as described in Section 8.0. A conservative F_{en} value is applied to each fatigue pair. The CUF value considering the 2013E fatigue design curve and the 61% increase on the 80-year projected transient cycles is seen in Table 8.

Table 8: Fatigue Pass Table for Tube-to-Tubesheet Weld Location.

Pair	Num. of Cycles		UF	F_{en}	UF*F_{en}
	Design	Allowed			
1	[ ]c	[ ]c	[ ]c	[ ]c	[ ]c
2	[ ]c	[ ]c	[ ]c	[ ]c	[ ]c
3	[ ]c	[ ]c	[ ]c	[ ]c	[ ]c
4	[ ]c	[ ]c	[ ]c	[ ]c	[ ]c
5	[ ]c	[ ]c	[ ]c	[ ]c	[ ]c
6	[ ]c	[ ]c	[ ]c	[ ]c	[ ]c
		CUF	[ ]c	CUF_{en}	[ ]c

9.0 VERIFICATION OF ASSUMPTIONS

There are no assumptions requiring verification made in the calculations listed in Section 12.0.

10.0 CONCLUSIONS

The identified sentinel locations for the primary side wetted pressure boundary components: Tubesheet Solid Rim at Tubesheet Dome, Primary Head at Divider Plate Seat Bar, U-Tubes and Tube-to-Tubesheet Welds, are analyzed for the environmental fatigue considerations per the requirements of Regulatory Guideline 1.207 [R-7] and NUREG/CR-6909 [R-8]. The cumulative usage factors for the analysis of record (AOR), subsequent license renewal (SLR) and with environmental effects considered (CUF_{en}) are summarized in Table 9 for the sentinel locations. As can be seen, all locations meet the requirements of Regulatory Guideline 1.207 [R-7] as the CUF_{en} is less than 1 for the 80-year projected transient cycles [R-5], with the cycles increased by 61% for all transients where a 80-year projected cycle was given, to demonstrate additional margin.

Table 9: Cumulative Usage Factors with Environmental Effects Considered for Sentinel Locations of Primary Side Wetted Pressure Boundary Components.

Location	Material Type	CUF		F_{en}	CUF_{en}	Analysis Method
		AOR	SLR			
Tubesheet Solid Rim (at Tubesheet Dome)	Low Alloy Steel	[ ]c	[ ]c	[ ]c	[ ]c	ASME NB-3200 analysis assuming design and projected allowable cycles from Table 1 and Table 2 respectively.
Primary Head at Divider Plate Seat Bar	Low Alloy Steel	[ ]c	[ ]c	[ ]c	[ ]c	
Tube	Ni-Cr-Fe	[ ]c	[ ]c	[ ]c	[ ]c	
Tube-to-Tubesheet Weld	Ni-Cr-Fe	[ ]c	[ ]c	[ ]c	[ ]c	

11.0 REFERENCES, DESIGN DRAWINGS AND COMPUTER CODES

11.1 References

[R-1] FPL Letter NP-EPU-09-0051, St. Lucie Plant – Extended Power Uprate Project, Transmittal of Westinghouse Results of the Steam Generator Design Transients for the St. Lucie Extended Power Uprate, dated January 15, 2009.

[R-2] FPL Certified Design Specification No. F-MECH-SP-002 Rev. 3, Engineering Specification for RSG Assemblies for FPL Co., St. Lucie Unit 1.

[R-3] Babcock & Wilcox Canada Ltd Report, CM9021278-SR-01, Rev. 2, Florida Power and Light St. Lucie Unit 1 Replacement Steam Generators Structural Integrity Qualification Report For Extended Power Uprate Operation with Core Power of 3020 MWth (Nuclear Steam Supply System Thermal Power Level of 3034 MWth).

[R-4] Babcock & Wilcox Canada Ltd Report, 222-7698-SR-07, Rev. 2, Florida Power and Light Company St. Lucie Nuclear Power Plant Unit 1 Replacement Steam Generators Tube Stress Report.

[R-5] Westinghouse Electric Company Letter, WEC-BWXT-PSL-SLR-21-001, Rev. 1, Transmittal of Inputs for EAF Evaluation of Sentinel Unit 1 RSG Locations, Florida Power & Light Company (FPL) St. Lucie – Unit 1 and 2, Subsequent License Renewal (SLR).

[R-6] FPL Procedure No. 0-COP-05.04, Rev. 119, St. Lucie Plant Chemistry Procedure: Chemistry Department Surveillances and Parameters.

[R-7] Regulatory Guide 1.207, Revision 1, Guidelines for Evaluating the Effects of Light-Water Reactor Water Environments in Fatigue Analysis of Metal Components.

[R-8] Regulatory Guide NUREG/CR-6909, Revision 1, Effect of the LWR Coolant Environments on Fatigue Life of Reactor Materials.

[R-9] Babcock & Wilcox Canada Ltd Calculation, CM9021278-B02, Rev. 0, St. Lucie Unit 1 –Primary Head / Stay Cylinder / Tubesheet / Secondary Shell Assembly Level A and B Analysis for EPU Conditions.

[R-10] ASME Boiler and Pressure Vessel Code, 1986 Edition, Section III, Division 1, Subsections NB Class 1 and Appendices.

[R-11] ASME Boiler and Pressure Vessel Code, 2013 Edition, Section III, Division 1, Subsections NB Class 1 and Appendices.

[R-12] BWXT Canada Ltd Report, 314Q-SR-01, Rev. 1, Florida Power and Light St. Lucie Unit 1 Nuclear Power Plant Replacement Steam Generators Tube-to-Tubesheet Weld Stress Analysis Report.

[R-13] BWXT Canada List of Approved Codes for Nuclear Analysis, June 11, 2021.

11.2 Design Drawings

The design drawings used in the analyses are the latest revisions and are listed in Table 10.

Table 10 List of Design Drawings

B&W Canada Design Drawings		
Drawing No.	**Rev. No.**	**Title**
7612E501	05	F.P.L. St. Lucie Unit 1 RSG General Arrangement
7612E151	06	F.P.L. St. Lucie Unit 1 RSG Material and Parts List (HX)

11.3 Computer Codes

The following computer codes are used in the analysis contained in this report.

Program Name	Program Version No.	User's Guide Rev. No.	Program Description	System
ANSYS	15.0	On-line Manuals	General Purpose Finite Element Program for structural, seismic and thermal analysis of various nuclear pressure vessel components	Windows 10 on DP T5810
ATAPP	2.1 with GUI 2.1	2.2	ANSYS Transient Analysis Post Processor for calculating stress ranges and fatigue usage factors	Windows 10 on DP T5810

These codes are qualified by BWXT for Nuclear Analysis. All User Guide limitations and computer program notifications, as applicable, have been reviewed to ensure there is no impact on this calculation. These computer codes are part of BWXT's List of Approved Codes for Nuclear Analysis [R-13].

12.0 LIST OF DETAILED ANALYSIS CALCULATIONS

Calculation	Rev.	Title
MSLEF-B001	0	St. Lucie Unit 1 Replacement Steam Generator Environmentally Assisted Fatigue Analysis of Primary Side Wetted Pressure Boundary.
MSLEF-B002	0	St. Lucie Unit 1 Replacement Steam Generator Environmentally Assisted Fatigue Analysis of Tube to Tubesheet Weld.

The detailed engineering analysis is proprietary to BWXT. They are available at BWXT Canada Cambridge office or via secure electronic data room, upon request, on a platform such as Firmex.

Enclosure 4

Non-proprietary Reference Documents and Redacted Versions of Proprietary Reference Documents (Public Version)

Attachment 8

Framatome Document No. 86-9329647-000, St. Lucie SLR CUFen Evaluations Summary – Non Proprietary, July 15, 2021

(21 Total Pages, including cover sheets)

framatome **CALCULATION SUMMARY SHEET (CSS)**

Document No. 86 - 9329647 - 000 Safety Related: ☒Yes ☐ No

Title St. Lucie SLR CUFen Evaluations Summary – Non Proprietary

PURPOSE AND SUMMARY OF RESULTS:

Purpose:

The purpose of this document is to summarize the Environmentally-Assisted Fatigue (EAF) Cumulative Usage Factor (CUF_{en}) calculations for St. Lucie, in support of FPL's Subsequent License Renewal Application (SLRA). In addition, the loading reconciliation for the Replacement Reactor Vessel Closure Head (RRVCH) Control Element Drive Mechanism (CEDM) and In-Core Instrumentation (ICI) Nozzles and the loading analysis for the Unit 2 Replacement Steam Generators (RSGs) will be summarized in this document.

Summary of Results:

Section 5.1 contains a summary of all the results from the CUF_{en} Evaluations. The change in external loads on the RRVCH CEDM and ICI Nozzles reflected in Reference [39] were shown to have no impact on the existing fatigue calculations (see Section 5.2) and Reference [40] shows that the breaks considered in the Framatome RSG structural loading analysis are consistent with the breaks considered in the Westinghouse analyses (see Section 5.3).

The proprietary version of this document is 86-9329644-001.

If the computer software used herein is not the latest version per the EASI list, AP 0402-01 requires that justification be provided. THE FOLLOWING COMPUTER CODES HAVE BEEN USED IN THIS DOCUMENT:		THE DOCUMENT CONTAINS ASSUMPTIONS THAT SHALL BE VERIFIED PRIOR TO USE
CODE/VERSION/REV	CODE/VERSION/REV	☐Yes
N/A		☒ No

Review Method: ☒ Design Review (Detailed Check)

☐ Alternate Calculation

Does this document establish design or technical requirements? ☐ YES ☒ NO

Does this document contain Customer Required Format? ☐ YES ☒ NO

Signature Block

Name and Title (printed or typed)	Signature	P/R/A/M and LP/LR	Date	Pages/Sections Prepared/Reviewed/Approved
CJ McGaughy Advisory Engineer	*CJ MCGAUGHY 7/15/2021*	LP		All
Tomas Straka Advisory Engineer	*T STRAKA 7/15/2021*	LR		All
David Cofflin Manager CAFM	*DR COFFLIN 7/15/2021*	A		All

Notes: P/R/A designates Preparer (P), Reviewer (R), Approver (A);
LP/LR designates Lead Preparer (LP), Lead Reviewer (LR);
M designates Mentor (M)

In preparing, reviewing and approving revisions, the lead preparer/reviewer/approver shall use 'All' or 'All except ___' in the pages/sections reviewed/approved. 'All' or 'All except ___' means that the changes and the effect of the changes on the entire document have been prepared/reviewed/approved. It does not mean that the lead preparer/reviewer/approver has prepared/reviewed/approved all the pages of the document.

With Approver permission, calculations may be revised without using the latest CSS form. This deviation is permitted when expediency and/or cost are a factor. Approver shall add a comment in the right-most column that acknowledges and justifies this deviation.

Project Manager Approval of Customer References and/or Customer Formatting (N/A if not applicable)

Name (printed or typed)	Title (printed or typed)	Signature	Date	Comments
N/A	N/A	N/A	N/A	N/A

Record of Revision

Revision No.	Pages/Sections/Paragraphs Changed	Brief Description / Change Authorization
000	All	Original Release
001	Sections TOC, List of Tables 1.0 2.0, 2.1, 2.2 3.2 4.0 5.1 7.0	Description of changes - Updated - Editorial changes - Editorial changes - Editorial changes - Revised Table 4-1, added Tables 4-2, 4-3 - Editorial changes, added U1 RPZR Heater Assembly and U2 PZR Heater Assembly to Table 5-1, Added U2 PZR Spray Nozzle and PZR Spray Line Reducer to Table 5-2, updated values, Added Table 5-3 - Updated references

Table of Contents

Page

SIGNATURE BLOCK 2

RECORD OF REVISION 3

LIST OF TABLES 5

1.0 INTRODUCTION AND PURPOSE 6

2.0 ANALYTICAL METHODOLOGY 6
- 2.1 Environmentally-Assisted Fatigue 6
  - 2.1.1 Carbon and Low Alloy Steel 7
  - 2.1.2 Wrought and Cast Austenitic Stainless Steel 7
  - 2.1.3 Ni-Cr-Fe Alloy 8
- 2.2 RRVCH CEDM and ICI Nozzles for U1/U2 Loading Reconciliation 8
  - 2.2.1 Approach for Updated External Loading 8
  - 2.2.2 Approach for Updated Design Transients 9
- 2.3 U2 Reactor Coolant Hydraulic and Structural Loading Evaluation 9

3.0 ASSUMPTIONS 9
- 3.1 Unverified Assumptions 9
- 3.2 Justified Assumptions 9
- 3.3 Modeling Simplifications 10

4.0 DESIGN INPUTS 10

5.0 RESULTS 13
- 5.1 Environmentally-Assisted Fatigue Results 13
- 5.2 RRVCH U1U2 CEDM Loading Reconciliation Results 18
- 5.3 U2 Reactor Coolant Hydraulic and Structural Loading Evaluation Results 18

6.0 CONCLUSION 18

7.0 REFERENCES 19

List of Tables

Page

Table 4-1: U1 Design Transients Included in Fatigue Monitoring Program 10

Table 4-2: U2 Design Transients Included in Fatigue Monitoring Program 11

Table 4-3: U2 RSG A Primary Manway Design Transients Included in Fatigue Monitoring Program 12

Table 5-1: CUF_{en} Summary (Design Cycles) 13

Table 5-2: CUF_{en} Summary (Limited Cycles) 15

1.0 INTRODUCTION AND PURPOSE

Florida Power & Light (FPL) intends to apply for Subsequent License Renewal (SLR = life to 80 years) for St. Lucie Unit 1 (PSL-1) and Unit 2 (PSL-2). Many evaluations were performed to obtain the results, listed below are the types of calculations completed by Framatome for FPL.

- Environmentally-Assisted Fatigue (EAF) at susceptible locations in the Reactor Coolant System (RCS) including the U2 Replacement Steam Generator's (RSG's), U1 and U2 Replacement Reactor Vessel Closure Head (RRVCH), U1 Replacement Pressurizer (RPZR), U2 Pressurizer (PZR) repairs, U2 weld overlays (WOL) and U2 Aux Spray Line Reducer.
- Loading reconciliation on the RRVCH Control Element Drive Mechanism (CEDM) and In-Core Instrumentation (ICI) Nozzles for PSL-1 and PSL-2.
- Structural loading analysis for the Replacement Steam Generators (RSGs) for PSL-2.

The purpose of this document is to summarize the EAF usage factor calculations, the RRVCH loading reconciliation, and the U2 pipe break loading evaluation for St. Lucie, in support of FPL's Subsequent License Renewal Application (SLRA).

2.0 ANALYTICAL METHODOLOGY

2.1 Environmentally-Assisted Fatigue

The F_{en} method is used to perform EAF calculations. The method is developed in Reference [1] is an acceptable approach in the EAF evaluation, in which the F_{en} factor is a nominal correction value defined as the ratio of fatigue life in-air at room temperature ($N_{air,RT}$) to that in LWR coolant environments at service temperature (N_{water}):

$$F_{en} = \frac{N_{air,RT}}{N_{water}}$$

The F_{en} methodology used in these calculations can be outlined as follows:

1. For either the simplified or detailed CUF_{en} calculation, the in-air CUF needs to be adjusted by using the S-N curve provided in Appendix A of Reference [1].
   a. For the detailed approach, the alternating stress (S_a) for each fatigue cycle is obtained from the related stress analysis. The alternating stress value is used to reference new allowable cycles (N) from the fatigue curves in Reference [1], with that the corresponding usage factor (U_i) can be calculated as follows:

$$U_i = \frac{Required\ Cycles}{Allowable\ Cycles}$$

   b. For the simplified approach, the maximum in-air CUF is adjusted by multiplying it by the maximum ratio of allowable cycles between the applicable ASME Code design fatigue curve and the Reference [1] design fatigue curve (R_{curve}):

$$Adjusted\ CUF = CUF_{air} * Maximum\ R_{curve}$$

2. Next, calculate the bounding F_{en} value from the relevant, material specific, F_{en} formula (Appendix A, Reference [1]). F_{en} equations are shown in Sections 2.1.1 through 2.1.3.
3. For a detailed approach, calculate the final fatigue usage considering EAF by:

$$CUF_{en} = F_{en,1} * U_1 + F_{en,2} * U_2 + F_{en,3} * U_3 + \cdots$$

Where U_i is the partial adjusted fatigue usage factor and $F_{en,i}$ is the local nominal correction value. For a simplified calculation the above equation simplifies to,

$$CUF_{en} = Adjusted\ CUF * F_{en}$$

Where F_{en} is the bounding (maximum) value of $F_{en,i}$ and the adjusted CUF is the cumulative usage factor based on the design fatigue curves in Reference [1].

4. Record results and note whether the criterion $CUF_{en} < 1.0$ is met.

$$F_{en} = \frac{N_{air,RT}}{N_{water}}$$

2.1.1 Carbon and Low Alloy Steel

From Reference [1], Appendix A, a summary of the F_{en} for carbon steel (CS) and low alloy steels (LAS) is expressed as:

$$F_{en} = \exp\left[(0.003 - 0.031\dot{\varepsilon}^*)S^*T^*O^*\right]$$

Where S^*, T^*, O^* and $\dot{\varepsilon}^*$ are the transformed sulfur content (S), material temperature (T), dissolved oxygen (DO) level, and strain rate ($\dot{\varepsilon}$), respectively, as defined as follows:

$$S^* = \begin{cases} 2.0 + 98S & S \le 0.015\ wt.\% \\ 3.47 & S > 0.015\ wt.\% \end{cases}$$

$$T^* = \begin{cases} 0.395 & T < 150°C \\ (T - 75)/190 & 150°C \le T \le 325°C \end{cases}$$

$$O^* = \begin{cases} 1.49 & DO < 0.04\ ppm \\ \ln(DO/0.009) & 0.04\ ppm \le DO \le 0.5\ ppm \\ 4.02 & DO > 0.5\ ppm \end{cases}$$

$$\dot{\varepsilon}^* = \begin{cases} 0 & \dot{\varepsilon} > 2.2\%/s \\ \ln(\dot{\varepsilon}/2.2) & 0.0004\% \le \dot{\varepsilon} \le 2.2\%/s \\ \ln(0.0004/2.2) & \dot{\varepsilon} < 0.0004\%/s \end{cases}$$

The equations above could yield a F_{en} between 1.0 and 6.279.

For carbon and low-alloy steels, a threshold value of 0.07% for strain amplitude (ε_a, one-half the strain range for the cycle) is defined in Reference [1], below which environmental effects on the fatigue lives of these steels may not occur:

$F_{en} = 1$ for $\varepsilon_a \le 0.07\%$.

2.1.2 Wrought and Cast Austenitic Stainless Steel

From Reference [1], Appendix A, a summary of the F_{en} for wrought and cast austenitic stainless steels (SS) is expressed as:

$$F_{en} = \exp(-T^*O^*\dot{\varepsilon}^*)$$

Where T^*, O^* and $\dot{\varepsilon}^*$ are the same parameters as explained above but defined as follows:

$$T^* = \begin{cases} 0 & T < 100°C \\ (T - 100)/250 & 100°C \le T \le 325°C \end{cases}$$

$$\dot{\varepsilon}^* = \begin{cases} 0 & \dot{\varepsilon} > 7\%/s \\ \ln(\dot{\varepsilon}/7) & 0.0004\%/s \le \dot{\varepsilon} \le 7\%/s \\ \ln(0.0004/7) & \dot{\varepsilon} < 0.0004\%/s \end{cases}$$

For PWR water, DO is usually less than 0.1 ppm and $O^* = 0.29$ given in Appendix A of Reference [1]. The equations above could yield a F_{en} factor between 1.0 and 12.807.

For wrought and cast austenitic stainless steels, a threshold value of 0.10% for strain amplitude is defined in Reference [1], below which environmental effects on the fatigue lives of these alloys do not occur:

$F_{en} = 1$ for $\varepsilon_a \le 0.10\%$.

2.1.3 Ni-Cr-Fe Alloy

From Reference [1], Appendix A, a summary of the F_{en} for Ni-Cr-Fe alloys with the exception of Inconel 718 is expressed as:

$$F_{en} = \exp(-T^* O^* \dot{\varepsilon}^*)$$

Where T^*,O^* and $\dot{\varepsilon}^*$ are the same parameters as explained above but defined as follows:

$$T^* = \begin{cases} 0 & T < 50°C \\ (T-50)/275 & 50°C \le T \le 325°C \end{cases}$$

$$\dot{\varepsilon}^* = \begin{cases} 0 & \dot{\varepsilon} > 5.0\%/s \\ \ln(\dot{\varepsilon}/5.0) & 0.0004\% \le \dot{\varepsilon} \le 5.0\%/s \\ \ln(0.0004/5.0) & \dot{\varepsilon} < 0.0004\%/s \end{cases}$$

For PWR water, DO is usually less than 0.1 ppm and $O^* = 0.14$ given in Appendix A of Reference [1]. The equations above could yield a F_{en} factor between 1.0 and 3.746.

For Ni-Cr-Fe alloys except Inconel 718, a threshold value of 0.10% for strain amplitude is defined in Reference [1], below which environmental effects on the fatigue lives of these alloys do not occur:

$F_{en} = 1$ for $\varepsilon_a \le 0.10\%$.

2.2 RRVCH CEDM and ICI Nozzles for U1/U2 Loading Reconciliation

The methodology for this analysis can be outlined as follows:

- Verified that the updated loads (Reference [3]) are bounded by the external loads used in original CEDM and ICI nozzle analyses.
- Verified that the updated transients (Reference [3]) were bounded by the Extended Power Uprate (EPU) transients.

The end result from this analysis is to demonstrate any differences between the design transients and the external loads that were previously used in PSL-1 and PSL-2 CEDM and ICI analyses (Section 2.2.1 and 2.2.2) remain bounding.

2.2.1 Approach for Updated External Loading

The external loads in the CEDM design specification have been updated since the CEDM and ICI nozzle ASME Section III analyses were originally performed. The CEDM loading specification for the PSL-1 RRVCH is provided in Reference [2]; additionally, these loads are conservatively applied to the ICI nozzle, hence the inclusion of ICI analyses.

The updated external loads communicated in Reference [3] are compared to the external loads used in the original analyses to determine the difference between them. The original input loads provided in Reference [2] must equal or exceed the updated loads to justify that there is no impact to the original Section III CEDM and ICI analyses. Stress and fatigue analyses performed using a larger applied external load will bound analyses performed with a lesser applied external load.

2.2.2 Approach for Updated Design Transients

Several design transients in the CEDM design specification have changed since the CEDM and ICI nozzle ASME Section III analyses were originally performed. These changes are due to Extended Power Uprate (EPU). The effects of EPU design transients have been justified to have a negligible or no impact on the original ASME Section III CEDM and ICI analyses for PSL-1 and PSL-2 in Reference [4] and Reference [5], respectively. The PSL-1 EPU design transients as originally communicated to Framatome are recorded in Reference [6] and the PSL-2 EPU design transients as originally communicated are recorded in Reference [7].

To determine that the updated design transients communicated in Reference [3] do not impact any Framatome analyses, they are compared directly with the EPU design transients in References [6] and [7] to verify that they are identical.

2.3 U2 Reactor Coolant Hydraulic and Structural Loading Evaluation

The evaluation of the attributes of the primary pipe breaks considering LBB between the Westinghouse analyses that are being performed and the Framatome analyses of record are discussed below.

Hot Leg Attached Pipe Breaks:

Framatome considered the following breaks:

- 12" Surge Line Break at Hot Leg Nozzle
- 12" Shutdown Cooling Outlet Line Break at the Hot Leg Nozzle

Cold Leg Attached Pipe Breaks:

Framatome considered the following breaks:

- 12" Safety Injection/Shutdown Cooling Inlet Line Break at Cold Leg Nozzle in Loop 1A
- 12" Safety Injection/Shutdown Cooling Inlet Line Break at Cold Leg Nozzle in Loop 1B

3.0 ASSUMPTIONS

3.1 Unverified Assumptions

There are no unverified assumptions within this calculation.

3.2 Justified Assumptions

The following assumptions are considered in the calculation of the Environmentally-Assisted Fatigue usage factor (CUF_{en}) in the documents referenced herein.

[ ]

[ ]

3.3 Modeling Simplifications

There are no modeling simplifications within this calculation.

4.0 DESIGN INPUTS

Tables 4-1 and 4-2 list the design and 80-year projected cycle counts for the U1 and U2 RCS, respectively, based on reference [8]. Table 4-3 lists the design and 80-year projected cycle counts specifically for the U2 RSG A primary manway, from reference [32].

Table 4-1: U1 Design Transients Included in Fatigue Monitoring Program

Transient No.	Transient Description	Design Cycles	80-Year Projection
1	Plant Heat-up (HU)	500	143
	Pressurizer Heat-up	500	130
2	Plant Cooldown (CD)	500	141
	Pressurizer Cooldown	500	130
3	Plant Loading 5%/min 15-100% (PL)	15000	N/A
4	Plant Unloading 5%/min 100-15% (UL)	15000	N/A
5	10% Step Load Increase (LI)	2000	N/A
6	10% Step Load Decrease (LD)	2000	N/A
7	Cold Feedwater Following Hot Standby	15000	N/A
8	Normal Plant Variations (NV)	10^6	N/A
9	Reactor Trip (RT)	400	106
10	Loss of Offsite Power (Loss of RCS Flow)	40	2
11	Loss of Turbine Generator Load (LL)	40	6
12	Primary Side Hydrostatic Test	10	3
13	Secondary Side Hydrostatic Test	10	3
14	Primary Side Leak Test	200	2

Transient No.	Transient Description	Design Cycles	80-Year Projection
15	Secondary Side Leak Test	200	3
16	Primary Coolant Pump Starting/Stopping (DP)	4000	N/A
OBE	Operation Basis Earthquake (OBE)	200	N/A

1) Reduced cycle counts are based on operating experience recorded in the recent period from either the end of 2009 or, where applicable, from the start of the transient monitoring period to the end of 2019 versus extrapolation of events recorded from the time of plant startup.
2) Some cycle counts are N/A, indicates that, per reference [8], these cycles are not counted due to low CUF.

Table 4-2: U2 Design Transients Included in Fatigue Monitoring Program

Transient No.	Transient Description	Design Cycles	80-Year Projection
1	Plant Heat-up (HU)	500	124
	Reduced Limit for 2B SG	120	91
	Pressurizer Heat-up	500	107
2	Plant Cooldown (CD)	500	123
	Reduced Limit for 2B SG	120	91
	Pressurizer Cooldown	500	107
3	Plant Loading 5%/min 15-100% (PL)	15000	N/A
4	Plant Unloading 5%/min 100-15% (UL)	15000	N/A
5	10% Step Load Increase (LI)	2000	N/A
6	10% Step Load Decrease (LD)	2000	N/A
7	Cold Feedwater Following Hot Standby	15000	N/A
8	Normal Plant Variations (NV)	10^6	N/A
9	Reactor Trip (RT)	400	72
10	Loss of Offsite Power (Loss of RCS Flow)	40	2
11	Loss of Turbine Generator Load (LL)	40	3
12	Primary Side Hydrostatic Test	10	1
	Reduced Limit for 2B SG	1	1
13	Secondary Side Hydrostatic Test	10	N/A

Transient No.	Transient Description	Design Cycles	80-Year Projection
14	Primary Side Leak Test	200	5
	Reduced Limit for 2B SG	30	10
15	Secondary Side Leak Test	200	N/A
16	Primary Coolant Pump Starting/Stopping (DP)	4000	N/A
OBE	Operation Basis Earthquake (OBE)	200	N/A

1) Reduced cycle counts are based on operating experience recorded in the recent period from either the end of 2009 or, where applicable, from the start of the transient monitoring period to the end of 2019 versus extrapolation of events recorded from the time of plant startup.
2) Some cycle counts are N/A, which indicates that, per reference [8], these cycles are not counted due to low CUF.

Table 4-3: U2 RSG A Primary Manway Design Transients Included in Fatigue Monitoring Program

Transient No.	Transient Description	Design Cycles	80-Year Projected cycles
1	Plant Heat-up	500	124
2	Plant Cooldown	500	123
3	Plant Loading 5%/min 15-100%	15000	N/A
4	Plant Unloading 5%/min 100-15%	15000	N/A
5	10% Step Load Increase	2000	N/A
6	10% Step Load Decrease	2000	N/A
7	Cold Feedwater at Hot Standby	15000	N/A
8	Normal Plant Variations	10^6	10^6
9	Reactor Trip	400	72
10	Loss of reactor coolant flow	40	N/A
11	Loss of Turbine Generator Load	40	3
12	Primary side hydrostatic test	10	1
13	Primary side leak test	200	N/A
14	Leaktightness at Cold T (0 - Lmax)	90	N/A
15	Leaktightness at Cold T (Lmax – Lres)	270	N/A

1) Reduced cycle counts are based on operating experience recorded in the recent period from either the end of 2009 or, where applicable, from the start of the transient monitoring period to the end of 2019 versus extrapolation of events recorded from the time of plant startup.
2) Some cycle counts are N/A, which indicates that, per reference [8], these cycles are not counted due to low CUF.

5.0 RESULTS

This section contains a summary of all the results from the CUF_{en} Evaluations.

5.1 Environmentally-Assisted Fatigue Results

Table 5-1 contains a summary of the CUF_{en} results that were calculated with design cycle limits (i.e. no cycle limitations). Table 5-2 contains a summary of the CUF_{en} results that contain limited cycles for at least one transient, meaning it could be from the 80-year projected cycles (Reference [8]) or limited to meet CUF_{en} criterion. Each transient is assumed to use the design cycle limits unless otherwise stated. Each CUF_{en} calculation is only listed in one table, i.e. either in Table 5-1 or Table 5-2. In cases where detailed EAF evaluations are performed, the listed F_{en} value is a weighted average and is determined as follows,

$$F_{en} = \frac{CUF_{en}}{SLR\ In\text{-}Air\ CUF}$$

Table 5-1: CUF_{en} Summary (Design Cycles)

Location	Material	AOR In-Air CUF	SLR In-Air CUF(4)	F_{en}	CUF_{en}	Reference
U2 RSG Primary Outlet Nozzles	LAS				0.659	[9]
U1 RRVCH Vent Nozzle	LAS				0.515	[10]
	Ni-Cr-Fe				0.618	
U1 RRVCH ICI Nozzle	LAS				0.584	[11]
	SS				0.020	
	Ni-Cr-Fe				0.506	
U1 RRVCH Closure Head to Vessel Joint	LAS				0.980	[12]
U2 RRVCH Vent Nozzle	LAS				0.527	[13]
	Ni-Cr-Fe				0.641	
U2 RRVCH ICI Nozzle	LAS				0.534	[14]
	SS				0.030	
	Ni-Cr-Fe				0.094	
U2 RRVCH Closure Head to Vessel Joint	LAS				0.848	[15]
U1 RPZR Surge Nozzle	LAS				0.276	[16]

Location	Material	AOR In-Air CUF	SLR In-Air CUF[4]	F_{en}	CUF_{en}	Reference
	SS				0.602	
U1 RPZR Safety Nozzle	LAS				0.766	[17]
	SS				0.530	
U1 RPZR Relief Nozzle	LAS				0.239	[18]
	SS				0.298	
U1 RPZR Heater Sleeve	LAS				0.119	[19]
	Ni-Cr-Fe				0.798	
U1 RPZR Manway	LAS				0.069	[20]
	SS				0.640	
U2 PZR Surge Nozzle WOL	LAS				0.593	[21]
	SS				0.756	
	Ni-Cr-Fe				0.111	
U2 PZR Relief Nozzle WOL	LAS				0.070	[22]
	SS				0.009	
	Ni-Cr-Fe				0.028	
U2 Hot Leg Shutdown Cooling Nozzle WOL	CS				0.230	[23]
	SS				0.001	
	Ni-Cr-Fe				0.011	
U2 Hot Leg Surge Nozzle WOL	CS				0.016	[24]
	SS				0.196	
	Ni-Cr-Fe				0.042	
U2 Hot Leg Drain Nozzle WOL	CS				0.062	[25]
	SS				0.000	
	Ni-Cr-Fe				0.0105	
U1 RPZR Upper Head Instrumentation Nozzle	LAS				0.157	[26]
	Ni-Cr-Fe				0.667	
U1 RPZR Temperature Nozzle	LAS				0.6879	[27]
	Ni-Cr-Fe				0.9200	
U1 RPZR Heater Assembly	SS				0.4903	[28]
	Ni-Cr-Fe				0.0036	
U2 PZR Heater Assembly	SS				0.7278	[29]
	Ni-Cr-Fe				N/A [5]	

[4]: This column lists the in-air CUF based on the NUREG/CR-6909 fatigue curves

Table 5-2: CUF_{en} Summary (Limited Cycles)

Location	Material	Cycle Adjustments	AOR In-Air CUF	SLR In-Air CUF	F_{en}	CUF_{en}	Reference
U1 RPZR Spray Nozzle	LAS	no cycles adjusted				0.364	[31]
	SS	Limiting cycle count to: 72 HUCD 1072 PLUL 500 LILD 10 LL				0.883	
U2 RSG-A: Primary Inlet Nozzle Drain Hole	LAS	Limiting cycle count to: 124 HUCD 7989 PLUL 72 RT 1 primary side hydrostatic test 5 primary side leak test				0.973	[32]
U2 RSG-A: Primary Manway Drain Hole	LAS	Limiting cycle count to: 124 HUCD 72 RT 10740 PLUL 3 LL 8899 Cold Feedwater at hot standby				0.972	
U2 RSG-A: Primary Manway	LAS	no cycles adjusted				0.099	
U2 RSG-A: Tube-to-Tube Sheet Weld	Ni-Cr-Fe	no cycles adjusted				0.562	
U2 RSG-B: Primary Inlet Nozzle Drain Hole	LAS	Limiting cycle count to: 91 HUCD 72 RT 3700 PLUL 1 primary side hydrostatic test 10 primary side leak test				0.977	[33]

Location	Material	Cycle Adjustments	AOR In-Air CUF	SLR In-Air CUF	F_{en}	CUF_{en}	Reference
U2 RSG-B: Primary Manway Drain Hole	LAS	Limiting cycle count to: 91 HUCD 72 RT 4700 PLUL 2826 Cold Feedwater at hot standby 3 LL				0.960	
U2 RSG-B: Primary Manway	LAS	Limiting cycle count to: 91 HUCD				0.540	
U2 RSG-B: Tube-to-Tube Sheet Weld	Ni-Cr-Fe	Limiting cycle count to: 91 HUCD 35 secondary side leak test 94 DP 3 LL				0.931	
U2 PZR Heater Sleeve	LAS	Limiting cycle count to: 124 HUCD				0.871	[34]
	SS	no cycles adjusted				0.404	
	Ni-Cr-Fe	Limiting cycle count to: 124 HUCD				0.926	
U2 PZR Spray Nozzle	SS	Limiting cycle count to: 107 HUCD 5 Primary Leak Test 2 Loss of Flow Transient 17A/B/C Allowable Cycles – as defined by current design basis methodology 17A Case 1 17B Case 2 n=0: 17B Case 2 n=2: 17B Case 2 n=4: 17B Case 2 n=6: 17B Case 2 n=7: 17C Case 3 n=0: 17C Case 3 n=2: 17C Case 3 n=4: 17C Case 3 n=6: 17C Case 3 n=7:				0.843	[35]

Location	Material	Cycle Adjustments	AOR In-Air CUF	SLR In-Air CUF	F_{en}	CUF_{en}	Reference
	LAS	no cycles adjusted				0.605	
U2 PZR Spray Line Reducer	SS	Limiting cycle count to: 124 HUCD 624 Main Spray Initiations 13 RCP Stop in Heatup 72 Reactor Trips 3 Loss of Load 2 Loss of Flow 10 Aux Spray at Power 1 10 Aux Spray at Power 2 124 Main Spray Term in Cooldown				0.9560	[36]

Table 5-3: Spray Nozzle Transients 17A/17B/17C Information

5.2 RRVCH U1U2 CEDM Loading Reconciliation Results

Per Reference [39], all external loads used as inputs in the original PSL-1 RRVCH CEDM and ICI nozzle analysis equal or exceed the external loads from the updated CEDM design specification. As such, there is no impact on those original calculations. All original Framatome ASME Section III CEDM and ICI analyses have been determined to not be impacted by changes to the CEDM design specification, they are suitable for providing inputs to the PSL-1 and PSL-2 SLRA environmentally assisted fatigue analyses.

5.3 U2 Reactor Coolant Hydraulic and Structural Loading Evaluation Results

The results from the primary pipe breaks considering LBB between the Westinghouse analyses and the Framatome analyses of record are discussed below.

Hot Leg Attached Pipe Breaks:

From Reference [40], the break size is 80.52 in^2. The break location is considered in the hot leg between the RV and the RSG, the exact location is not critical since losses are negligible.

Cold Leg Attached Pipe Breaks:

From Reference [40] the break size is 80.52 in^2. The break location is considered in the cold leg between the RV and the RC Pump, the exact location is not critical since losses are negligible.

Jet Impingement and Thrust Loads

These loads are considered in the Framatome analysis as appropriate based on the orientation of each break. From Reference [40], these types of component loads are negligible in the determination of the RSG internal loads (tube bundle and tubesheet) that are generated for the RSG structural analyses.

Per Reference [40], based on the loading evaluation, the breaks that were performed in the Framatome RSG structural loading analysis are consistent with the breaks in the Westinghouse analyses.

6.0 CONCLUSION

Section 5.1 contains a summary of all the results from the CUF_{en} Evaluations. The change in external loads on the RRVCH CEDM and ICI Nozzles reflected in Reference [39] were shown to have no impact on the existing fatigue calculations (see Section 5.2) and Reference [40] shows that the breaks considered in the Framatome RSG structural loading analysis are consistent with the breaks considered in the Westinghouse analyses (see Section 5.3).

7.0 REFERENCES

1. NUREG/CR-6909 "Effect of LWR Water Environments on the Fatigue Life of Reactor Materials," Rev.1, Final Report, May 2018
2. Framatome Document 18-5032328-004, "Design Transients and Loading Specification"
3. LTR-SDA-21-017, "St. Lucie Units 1 and 2 - Framatome Requested Documents - Updated CEDM Parameters" Rev. 0, as contained in Framatome Document 38-9324528-000, "St. Lucie SLR NDA with Westinghouse"
4. Framatome Document 51-9113813-000, "St. Lucie Unit 1 EPU Summary Document Evaluation for Bin 1 and Bin 2"
5. Framatome Document 51-9113814-000, "St. Lucie Unit 2 EPU Summary Document Evaluation for Bin 1, Bin 2, and Bin 3"
6. Framatome Document 38-2200691-000, "Pressurizer, Reactor Vessel Upper Head, and Steam Generator Design Transients for St. Lucie 1 EPU"
7. Framatome Document 38-2200692-000, "Transmittal of Areva's Document Reviews for Westinghouse Letter LTR-OA-08-119"
8. Westinghouse Non-Proprietary Class 3, LTR-SDA-II-20-32-NP, Rev. 1, dated April 26, 2021 and Rev. 2, dated June 7, 2021, "St. Lucie Units 1 & 2 Subsequent License Renewal: 80-Year Projected Transient Cycles," as contained in Framatome Document 38-9326609-000, "F.505511 St. Lucie Design Inputs from FPL"
9. Framatome Document 32-9323849-001, "St. Lucie SLR CUFen U2 RSG Primary Outlet Nozzles"
10. Framatome Document 32-9323861-000, "St. Lucie SLR CUFen U1 RRVCH Vent Nozzle"
11. Framatome Document 32-9323863-000, "St. Lucie SLR CUFen U1 RRVCH ICI Nozzle"
12. Framatome Document 32-9323866-000, "St. Lucie SLR CUFen U1 RRVCH Closure Head to Vessel Joint"
13. Framatome Document 32-9323868-000, "St. Lucie SLR CUFen U2 RRVCH Vent Nozzle"
14. Framatome Document 32-9323870-000, "St. Lucie SLR CUFen U2 RRVCH ICI Nozzle"
15. Framatome Document 32-9323873-000, "St. Lucie SLR CUFen U2 RRVCH Closure Head to Vessel Joint"
16. Framatome Document 32-9323874-000, "St. Lucie SLR CUFen U1 RPZR Surge Nozzle"
17. Framatome Document 32-9323876-000, "St. Lucie SLR CUFen U1 RPZR Safety Nozzle"
18. Framatome Document 32-9323877-000, "St. Lucie SLR CUFen U1 RPZR Relief Nozzle"
19. Framatome Document 32-9323878-000, "St. Lucie SLR CUFen U1 RPZR Heater Sleeve"
20. Framatome Document 32-9323879-000, "St. Lucie SLR CUFen U1 RPZR Manway"
21. Framatome Document 32-9328970-000, "St. Lucie SLR CUFen U2 PZR Surge Nozzle WOL"
22. Framatome Document 32-9328971-000, "St. Lucie SLR CUFen U2 PZR Relief Nozzle WOL"
23. Framatome Document 32-9328972-000, "St. Lucie SLR CUFen U2 Hot Leg Shutdown Cooling Nozzle WOL"
24. Framatome Document 32-9328973-000, "St. Lucie SLR CUFen U2 Hot Leg Surge Nozzle WOL"
25. Framatome Document 32-9328974-000, "St. Lucie SLR CUFen U2 Hot Leg Drain Nozzle WOL"
26. Framatome Document 32-9329318-000, "St. Lucie SLR CUFen U1 RPZR Upper Head Instrumentation Nozzle"
27. Framatome Document 32-9329319-000, "St. Lucie SLR CUFen U1 RPZR Temperature Nozzle"
28. Framatome Document 32-9332551-000, "St. Lucie SLR CUFen U1 RPZR Heater Assembly"
29. Framatome Document 32-9332552-000, "St. Lucie SLR CUFen U2 PZR Heater Assembly"
30. Framatome Document 32-5055722-02, "St. Lucie Nuclear Plant Unit 1 Replacement Pressurizer Temperature Nozzle Analysis"
31. Framatome Document 32-9323875-000, "St. Lucie SLR CUFen U1 RPZR Spray Nozzle"

32. Framatome Document 32-9329136-001, "St. Lucie SLR Detailed CUFen U2 RSG A"
33. Framatome Document 32-9329316-001, "St. Lucie SLR U2 RSG Detailed CUFen and Loose Parts Fatigue Analysis RSG B"
34. Framatome Document 32-9331253-000, "St. Lucie SLR CUFen U2 PZR Heater Sleeve"
35. Framatome Document 32-9331374-000, "St. Lucie SLR CUFen U2 PZR Spray Nozzle"
36. Framatome Document 32-9331377-000, "St. Lucie SLR CUFen U2 PZR Spray Line Reducer"
37. Framatome SAS, D02-ARV-01-180-868, "EAF Evaluation for the Saint Lucie Unit 2 Steam Generators on Primary Side." as contained in Framatome Document 38-9332683-000, "St. Lucie U2 RSG – Primary Side EAF Evaluation from SAS"
38. Framatome Document 32-9098372-003, "St. Lucie Unit 2 Pressurizer Heater Sleeve Replacement Analysis"
39. Framatome Document 51-9329320-000, "St. Lucie SLR RRVCH U1U2 CEDM Loading Reconciliation"
40. Framatome Document 51-9327029-000, "St. Lucie RSG – Reactor Coolant Hydraulic and Structural Loading Evaluation"

Enclosure 4

Non-proprietary Reference Documents and Redacted Versions of Proprietary Reference Documents (Public Version)

Attachment 9

Structural Integrity Report No. 2001262.403, Revision 0, Summary of Fatigue Usage for Charging Nozzle at St. Lucie, Units 1 and 2 for Subsequent License Renewal, June 25, 2021

(8 Total Pages, including cover sheets)

Structural Integrity Associates, Inc.
kwong@structint.com
5215 Hellyer Avenue, Suite 210, San Jose, CA 95138 | 408-978-8200

June 25, 2021
REPORT NO. 2001262.403
REVISION: 0
PROJECT NO. 2001262.00

Quality Program: ☒ Nuclear ☐ Commercial

Bill Maher
Florida Power & Light Co.
St. Lucie Nuclear Power Plant
6501 S. Ocean Dr.
Jenson Beach, FL 34957

Subject: Summary of Fatigue Usage for Charging Nozzle at St. Lucie, Units 1 and 2 for Subsequent License Renewal

Dear Bill,

This letter report documents the results of the fatigue usage analysis [1 - 4] for St. Lucie, Units 1 and 2, including environmentally assisted fatigue for subsequent license renewal (SLR) through eighty years of plant operation.

1.0 SUBSEQUENT LICENSE RENEWAL

For subsequent license renewal EAF evaluations, St. Lucie, Units 1 and 2 is following the methodology described in NUREG/CR-6909, Revision 1 [5]. Using ASME Code, Section III, NB-3200 [6], the EAF analyses for the charging nozzles of St. Lucie, Units 1 and 2 needed to be updated for eighty years of plant operation with the projected 80-year cycles shown in Table 1.

2.0 TECHNICAL APPROACH FOR CHARGING NOZZLE FATIGUE USAGE ANALYSIS

Design inputs including design transient definitions, piping interface loads, and projected 80-year cycles were compiled in the loads calculation [2] for both St. Lucie, Units 1 and 2. Heat transfer coefficients were calculated based on applicable geometry, flow and temperature conditions.

Two finite element models of charging nozzle were developed; one each for St. Lucie, Unit 1 [1.a] and St. Lucie, Unit 2 [1.b]. Stress analysis was performed for unit moment, unit pressure and thermal transients on each of the respective finite element models [3]. Linearized stresses were extracted at critical stress paths, as shown in Figure 1 for Unit 1 and Figure 2 for Unit 2. Stress Path 1 was at the location of the highest thermal stress. Stress Path 2 was in the dissimilar metal weld. Stress Path 3 was at the nozzle blend radius at the highest thermal stress location.

Fatigue usage analysis [4] followed the methodology in ASME Code, Section III [6, NB-3200]. Fatigue strength reduction factors were applied if required for specific locations by ASME Code, Section III [6, NB-3213.17]. The EAF analysis applied the fatigue usage curves and methods of NUREG/CR-6909 Revision 1 [5] for calculation of fatigue usage and F_{en} values.

3.0 RESULTS OF CHARGING NOZZLE FATIGUE USAGE ANALYSIS FOR SUBSEQUENT LICENSE RENEWAL TO EIGHTY YEARS OF OPERATION

Using 80-year projected cycles for St. Lucie, Unit 1, the results for the bounding locations are [4.a]:

- SS, path 1 inside: U=0.2474, and U_{en}=0.6474, yielding an average F_{en} of 2.6169.
- CS, path 3 inside: U=0.0053, and U_{en}=0.0247, based on a bounding F_{en} of 4.668.

The fatigue usage, U, and EAF usage factor, U_{en}, for the bounding locations on the St. Lucie Unit 1 charging nozzles are less than 1.0 and are therefore acceptable for subsequent license renewal for up to eighty years of plant operation.

Using 80-year projected cycles for St. Lucie, Unit 2, the results for the bounding locations are [4.b]:

- SS, path 1 inside: U=0.4420, and U_{en}=0.937, yielding an average F_{en} of 1.795.
- LAS, path 3 inside: U=0.0255, and U_{en}=0.119, based on a bounding F_{en} of 4.668.

The U and U_{en} for the bounding locations on the St. Lucie Unit 2 charging nozzles are less than 1.0 and are therefore acceptable for eighty years of plant operation.

5.0 REFERENCES

1. Finite Element Model Calculations
    a. Structural Integrity Associates Calculation No. 2001262.301, Revision 0, "St. Lucie Plant Unit 1 Charging Nozzle Finite Element Model," REDACTED.
    b. Structural Integrity Associates Calculation No. 2001262.302, Revision 0, "Charging Nozzle Finite Element Model, St. Lucie Unit 2," REDACTED.
2. Structural Integrity Associates Calculation No. 2001262.303, Revision 1, "Loading for St. Lucie Units 1 and 2 Charging Nozzles," REDACTED.
3. Stress Analysis Calculations
    a. Structural Integrity Associates Calculation No. 2001262.304, Revision 0, "Charging Nozzle Stress Analysis, St. Lucie Unit 1."
    b. Structural Integrity Associates Calculation No. 2001262.305, Revision 0, "Charging Nozzle Stress Analysis, St. Lucie Unit 2."
4. Fatigue Usage Analysis Calculations
    a. Structural Integrity Associates Calculation No. 2001262.306, Revision 0, "Charging Nozzle Fatigue Usage, St. Lucie Unit 1," REDACTED.
    b. Structural Integrity Associates Calculation No. 2001262.307, Revision 0, "Charging Nozzle Fatigue Usage, St. Lucie Unit 2," REDACTED.
5. NUREG/CR-6909, Revision 1, "Effect of LWR Water Environments on the Fatigue Life of Materials," U.S. NRC, May 2018
6. ASME Boiler and Pressure Vessel Code, 2007 Edition with Addenda through 2008.

Structural Integrity Associates, Inc.
info@structint.com 1-877-4SI-POWER structint.com

Table 1. Projected 80-Year Cycles

Source: Load Calculation [2, Table 1]

Transient	Unit 1	Unit 2
Plant Heat-up	143	124
Plant Cooldown	141	123
Loading, 5%/min.	1200	1200
Unloading, 5%/min.	1200	1200
Step Load Increase	520	520
Step Load Decrease	520	520
Reactor Trip	106	72
Loss of RCS Flow	2	2
Loss of Load	6	3
Loss of Secondary Pressure	2	2
Purification	381	277
Low Volume Control and Makeup	763	555
Boric Acid Dilution	3051	2219
Loss of Charging Flow	11	11
Loss of Letdown	279	405
Regenerative HX Isolation Long Term	20	66
Regenerative HX Isolation Short Term	29	11
Operating basis earthquake (OBE)	1	1
Hydrostatic Test (primary side)	3	1
Leak Test (primary side)	2	5

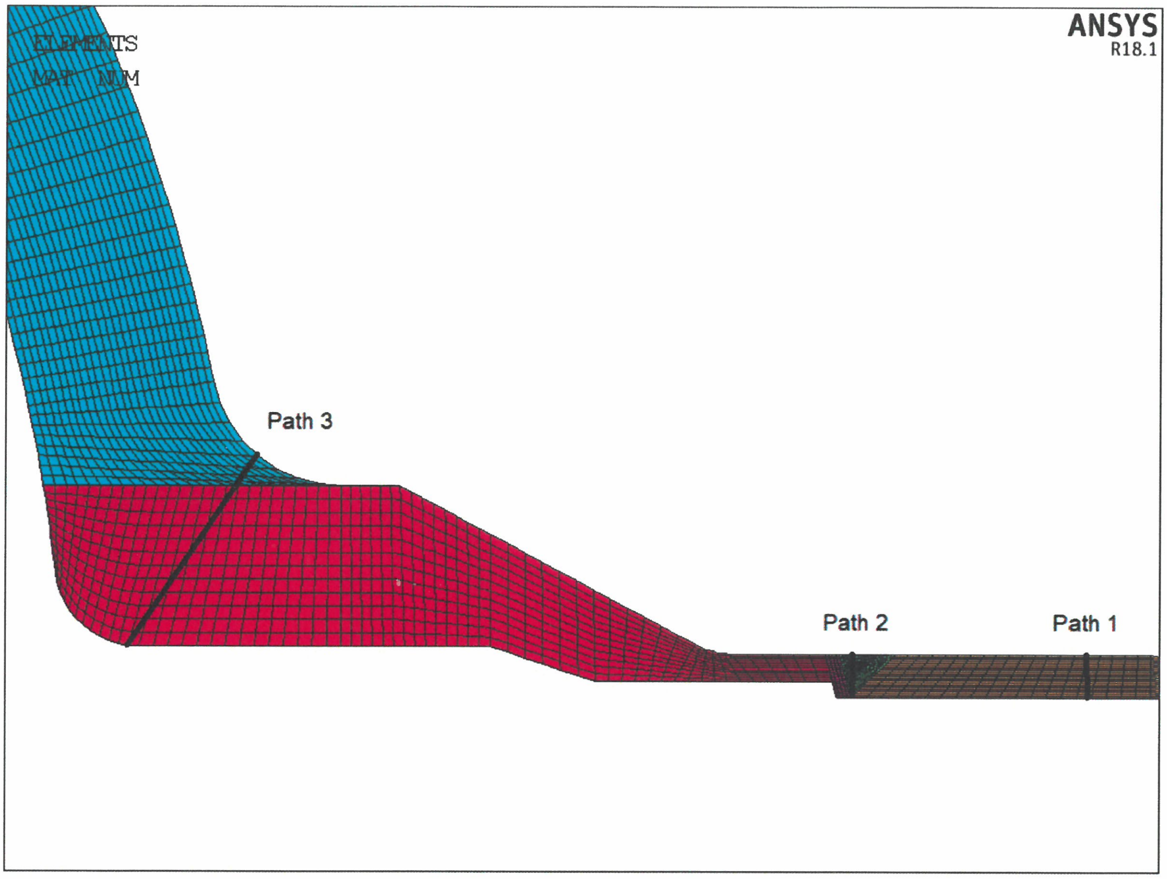

Figure 1. Unit 1 Stress Paths

Source: Unit 1 Stress Analysis Calculation [3.a, Figure 6]

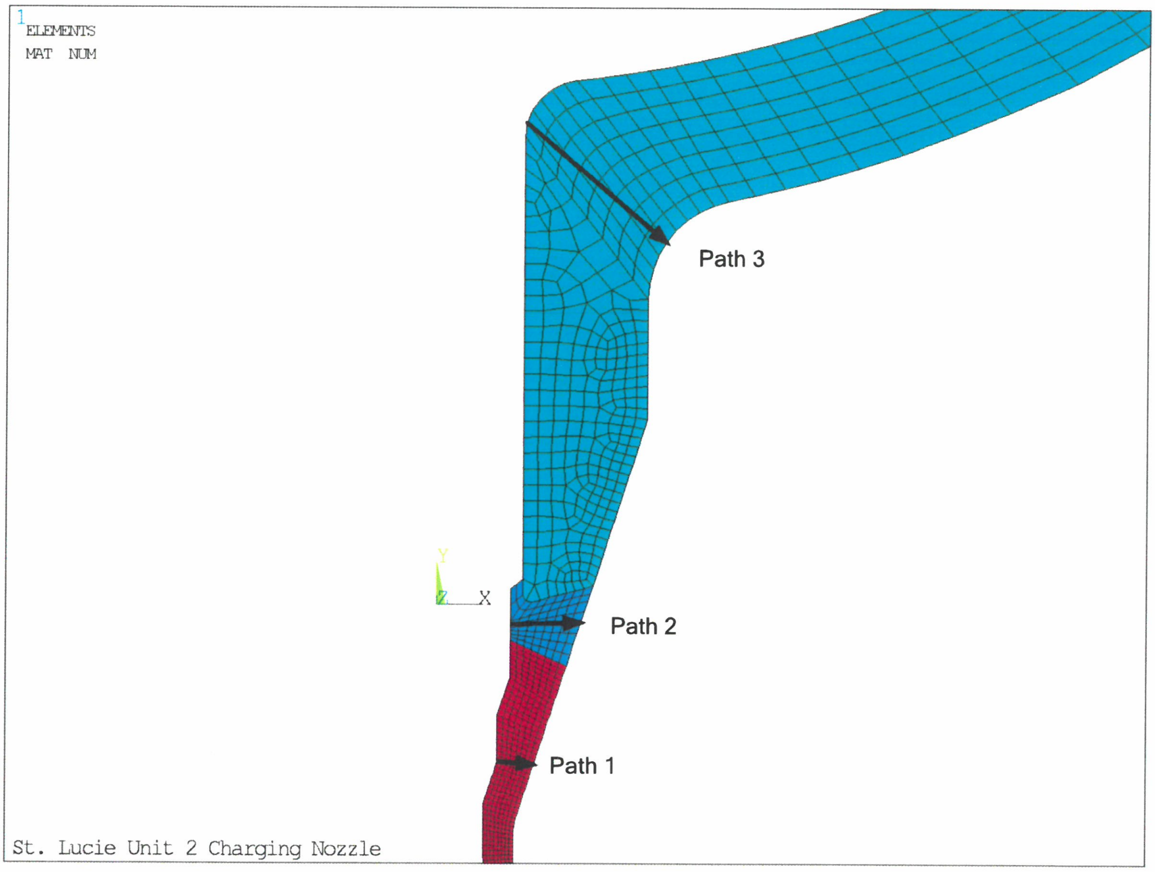

Figure 2. Unit 2 Stress Paths

Source: Unit 2 Stress Analysis Calculation [3.b, Figure 6]

Prepared by:

Kevin K. L. Wong
Consultant

06/25/2021
Date

Reviewed by:

Terry J. Herrmann
Senior Associate

06/25/2021
Date

Approved by:

David A. Gerber
Senior Associate

6/25/2021
Date

cc: Tim D. Gilman, Structural Integrity Associates

Structural Integrity Associates, Inc.
info@structint.com 1-877-4SI-POWER structint.com

Enclosure 4

Non-proprietary Reference Documents and Redacted Versions of Proprietary Reference Documents (Public Version)

Attachment 10

Westinghouse Report WCAP-18617-NP, Revision 1, St. Lucie Units 1 & 2 Subsequent License Renewal: Technical Justification for Eliminating Large Primary Loop Pipe Rupture as the Structural Design Basis, June 3, 2021

(69 Total Pages, including cover sheets)

Westinghouse Non-Proprietary Class 3

WCAP-18617-NP
Revision 1

June 2021

St. Lucie Units 1 & 2 Subsequent License Renewal: Technical Justification for Eliminating Large Primary Loop Pipe Rupture as the Structural Design Basis

Westinghouse

WCAP-18617-NP
Revision 1

St. Lucie Units 1 & 2 Subsequent License Renewal: Technical Justification for Eliminating Large Primary Loop Pipe Rupture as the Structural Design Basis

June 2021

Author: Gerrie W. Delport*
Structural Design Analysis

Reviewer: Momo Wiratmo*
Operating Plants Piping and Supports

Approved: Lynn A. Patterson*, Manager
Reactor Vessel and Containment
Vessel Design and Analysis

*Electronically approved records are authenticated in the electronic document management system.

Westinghouse Electric Company LLC
1000 Westinghouse Drive
Cranberry Township, PA 16066, USA

REVISION INDEX

Revision	Date	Remarks
0	4/2021	Original Issue
1	6/2021	Customer comments incorporated

TABLE OF CONTENTS

LIST OF TABLES v

LIST OF FIGURES vi

1 INTRODUCTION 1-1
 1.1 PURPOSE 1-1
 1.2 BACKGROUND INFORMATION 1-1
 1.3 SCOPE AND OBJECTIVES 1-2
 1.4 REFERENCES 1-3
2 OPERATION AND STABILITY OF THE REACTOR COOLANT SYSTEM 2-1
 2.1 STRESS CORROSION CRACKING 2-1
 2.2 WATER HAMMER 2-2
 2.3 LOW CYCLE AND HIGH CYCLE FATIGUE 2-3
 2.4 WALL THINNING, CREEP, AND CLEAVAGE 2-3
 2.5 REFERENCES 2-3
3 PIPE GEOMETRY AND LOADING 3-1
 3.1 INTRODUCTION TO METHODOLOGY 3-1
 3.2 CALCULATION OF LOADS AND STRESSES 3-1
 3.3 LOADS FOR LEAK RATE EVALUATION 3-2
 3.4 LOAD COMBINATION FOR CRACK STABILITY ANALYSES 3-2
 3.5 REFERENCES 3-3
4 MATERIAL CHARACTERIZATION 4-1
 4.1 PRIMARY LOOP PIPE, RCP SUCTION AND DISCHARGE MATERIALS 4-1
 4.2 TENSILE PROPERTIES 4-1
 4.3 FRACTURE TOUGHNESS PROPERTIES 4-3
 4.4 REFERENCES 4-7
5 CRITICAL LOCATION AND EVALUATION CRITERIA 5-1
 5.1 CRITICAL LOCATIONS 5-1
 5.2 EVALUATION CRITERIA 5-1
6 LEAK RATE PREDICTIONS 6-1
 6.1 INTRODUCTION 6-1
 6.2 GENERAL CONSIDERATIONS 6-1
 6.3 CALCULATION METHOD 6-1
 6.4 LEAK RATE CALCULATIONS 6-2
 6.5 REFERENCES 6-2
7 FRACTURE MECHANICS EVALUATION 7-1
 7.1 LOCAL FAILURE MECHANISM 7-1
 7.2 GLOBAL FAILURE MECHANISM 7-1
 7.3 REFERENCES 7-3
8 FATIGUE CRACK GROWTH ANALYSIS 8-1
 8.1 REFERENCES 8-4
9 ASSESSMENT OF MARGINS 9-1
10 CONCLUSIONS 10-1
APPENDIX A LIMIT MOMENT A-1

LIST OF TABLES

Table 3-1. Dimensions, Normal Loads and Stresses for St Lucie Unit 1 3-4

Table 3-2. Dimensions, Normal Loads and Stresses for St Lucie Unit 2 3-4

Table 3-3. Dimensions, Faulted Loads and Stresses for St. Lucie Unit 1 3-5

Table 3-4. Dimensions, Faulted Loads and Stresses for St. Lucie Unit 2 3-5

Table 4-1. Measured Tensile Properties for St. Lucie Units 1 & 2 (A351-CF8M) 4-8

Table 4-2. ASME Code Tensile Properties for Material A351-CF8M 4-9

Table 4-3. Tensile Properties for St. Lucie Units 1 and 2 A351-CF8M Material at Operating Temperatures 4-10

Table 4-4. Tensile Properties for St. Lucie Units 1 and 2 Alloy 82/182 Welds at Operating Temperatures 4-10

Table 4-5. St. Lucie Units 1 and 2 CF8M Chemical Composition 4-11

Table 4-6. St. Lucie Units 1 and 2 CF8M Fracture Toughness Properties 4-12

Table 4-7. Units 1 and 2 A351-CF8M Lowest Fracture Toughness Properties 4-13

Table 4-8. J_{IC}, J_{max}, T_{mat} Limiting Values NUREG/CR-4513 per Rev. 1 and Rev. 2 4-14

Table 5-1. Critical Analysis Locations for St. Lucie Units 1 and 2 RCL Lines 5-2

Table 6-1. Flaw Sizes for St. Lucie Units 1 and 2 Yielding a Leak Rate of 10 gpm for the Critical Analysis Locations with A351-CF8M CASS Material 6-3

Table 6-2. Flaw Sizes for St. Lucie Units 1 and 2 Yielding a Leak Rate of 10 gpm for the Critical Analysis Locations with Alloy 82/182 Welds 6-3

Table 7-1. Flaw Stability Results for St. Lucie Units 1 and 2 the Critical Analysis Locations Based on J-Integral Evaluations and CASS Thermal Aging 7-4

Table 7-2. Flaw Stability Results for St. Lucie Units 1 and 2 Yielding a Leak Rate of 10 gpm for the Critical Analysis Locations with A351-CF8M CASS Material 7-5

Table 7-3. Flaw Stability Results for St. Lucie Units 1 and 2 Yielding a Leak Rate of 10 gpm for Critical Analysis Locations with Alloy 82/182 Welds 7-5

Table 8-1. Summary of Transients (Representative 80-year Design) 8-5

Table 8-2. St. Lucie Fatigue Crack Growth at Hot and Cold Legs Carbon Steel Material 8-6

Table 8-3. Alloy 82/182 FCG and PWSCC Growth – Operating Time for a Surface Flaw to Grow Through-Wall 8-6

Table 9-1. Leakage Flaw Sizes, Critical Flaw Sizes and Margins for St. Lucie Units 1 and 2 for Critical Analysis Locations with A351-CF8M CASS Material 9-2

Table 9-2. Leakage Flaw Sizes, Critical Flaw Sizes and Margins for St. Lucie Units 1 and 2 for Critical Analysis Locations with Alloy 82/182 Welds 9-2

LIST OF FIGURES

Figure 3-1 St. Lucie Units 1 and 2 RCL Point Locator 3-6

Figure 3-2. RCP Suction Pipe 3-7

Figure 4-1. Pre-Service J vs. Δa for SA351-CF8M Cast Stainless Steel at 600°F 4-15

Figure 5-1. Schematic Diagram of St. Lucie Units 1 and 2 Primary Loop Showing RCP Nozzle Critical Analyzed Weld Locations 5-3

Figure 6-1. Analytical Predictions of Critical Flow Rates of Steam-Water Mixtures 6-4

Figure 6-2. [ ]^{a,c,e} Pressure Ratio as a Function of L/D 6-5

Figure 6-3. Idealized Pressure Drop Profile Through a Postulated Crack 6-6

Figure 7-1. [ ]^{a,c,e} Stress Distribution 7-6

Figure 8-1. Alloy 82/182 Weld Fatigue Crack Growth Rate Properties in a PWR Environment 8-7

Figure 8-2. Hot Leg Circumferential Fatigue Crack Growth 8-8

Figure 8-3. Hot Leg Axial Fatigue Crack Growth 8-9

Figure 8-4. Cold Leg Circumferential Fatigue Crack Growth 8-10

Figure 8-5. Cold Leg Axial Fatigue Crack Growth 8-11

Figure 8-6. RCP Discharge Fatigue Crack Growth (23% Circumferential Length, 20% Depth) 8-12

Figure 8-7. RCP Discharge Fatigue Crack Growth (23% Circumferential Length, 30% Depth) 8-13

Figure A-1. Pipe with a Through-Wall Crack in Bending A-2

1 INTRODUCTION

1.1 PURPOSE

This report applies to the St. Lucie Units 1 and 2 Reactor Coolant System (RCS) primary loop piping. It is intended to demonstrate that for the specific parameters of the St. Lucie Units 1 and 2 Nuclear Power Plants, RCS primary loop pipe breaks need not be considered in the structural design basis for the 80-year plant life subsequent license renewal (SLR) program. The specific parameters include normal operation temperature and internal pressure conditions for extended power uprate (EPU) programs and also NSSS design transient cycles for 80-year plant life.

In addition, this report also confirms the use of alloy 82/182 nickel-base materials which are susceptible to primary water stress corrosion cracking (PWSCC) at the dissimilar metal weld (DMW) locations. Both the suction and discharge sides of the reactor coolant pumps (RCPs) are joined to the piping with a cast austenitic stainless steel (CASS) safe-end and a dissimilar metal (DM) weld of Alloy 82/182 weld material. The remainder of the piping is carbon steel with stainless steel cladding.

1.2 BACKGROUND INFORMATION

The work performed in this calculation note is to update the LBB evaluations for the St. Lucie Units 1 and 2 primary loop piping to support the subsequent license renewal (SLR) program for the plant operation extension from 60 years to 80 years.

Originally, Combustion Engineering Owners Group performed the Leak-Before-Break (LBB) evaluation for the St. Lucie Units 1 and 2 primary loop piping in February 1991 (Reference 1-1), along with other Combustion Engineering designed nuclear steam supply systems of similar layouts.

For St. Lucie Unit 1, the LBB evaluation was updated in 2009, due to Replacement Steam Generators (RSG) / uprating. In comparing the revised plant-specific loads for the EPU to the evaluation performed in CEN-367-A (Reference 1-1), it was concluded that the St. Lucie Unit 1 Reactor Coolant loop (RCL) hot and cold leg pipes are qualified for the LBB under EPU conditions and that the existing LBB evaluation remained applicable for Unit 1.

For St. Lucie Unit 2, the LBB evaluation was updated in 2010, due to Replacement Steam Generators (RSG) / uprating. In comparing the revised plant-specific loads for the EPU to the evaluation performed in CEN-367-A (Reference 1-1), it was concluded that the St. Lucie Unit 2 RCL hot and cold leg pipes are qualified for the LBB under EPU conditions and that the existing LBB evaluation remained applicable for Unit 2.

For the Subsequent License Renewal (SLR) program, this report demonstrates that the conclusions reached in Reference 1-1 remains applicable in the structural design basis for the 80-year plant life for the specific parameters of the St. Lucie Units 1 and 2 Nuclear Power Stations.

1.3 SCOPE AND OBJECTIVES

The general purpose of this investigation is to demonstrate leak-before-break for the primary loops in St. Lucie Units 1 and 2 on a plant specific basis for the 80-year plant life. The primary loop consists of the Hot Leg, the Cold Leg Reactor Coolant Pump Suction and Discharge Piping Lines. The primary loop does not include the Pressurizer Surge Piping Line or any other auxiliary line branches attached to the primary loop. The recommendations and criteria proposed in References 1-2 and 1-3-are used in this evaluation. These criteria and resulting steps of the evaluation procedure can be briefly summarized as follows:

1. Calculate the applied loads. Identify the locations at which the highest stress occurs.
2. Identify the limiting material profiles and the associated material properties.
3. Postulate a surface flaw at the governing locations. Determine fatigue crack growth. Show that a through-wall crack will not result.
4. Postulate a through-wall flaw at the governing locations. The size of the flaw should be large enough so that the leakage is assured of detection with margin using the installed leak detection equipment when the pipe is subjected to normal operating loads. A margin of 10 is demonstrated between the calculated leak rate and the leak detection capability.
5. Using faulted loads, demonstrate that there is a margin of 2 between the leakage flaw size and the critical flaw size.
6. Review the operating history to ascertain that operating experience has indicated no particular susceptibility to failure from the effects of corrosion, water hammer or low and high cycle fatigue.
7. For the materials actually used in the plant provide the properties including toughness and tensile test data. Evaluate long term effects such as thermal aging.
8. Demonstrate margin on the calculated applied load value; margin of 1.4 using algebraic summation of loads or margin of 1.0 using absolute summation of loads.

This report provides a fracture mechanics demonstration of primary loop integrity for the St. Lucie Units 1 and 2 plants consistent with the NRC position for exemption from consideration of dynamic effects.

The LBB evaluation summarized in this report consider the limiting weld locations of the RCL piping. In general, the analyses consider the material properties of the piping base metal, which are more limiting than the weld materials. The re-evaluations were performed to ensure that the LBB evaluation conclusions remain valid for 80-year plant life in the SLR program.

It should be noted that the terms "flaw" and "crack" have the same meaning and are used interchangeably. "Governing location" and "critical location" are also used interchangeably throughout the report.

The computer codes used in this evaluation for leak rate and fracture mechanics calculations have been validated and used for all the LBB applications by Westinghouse.

1.4 REFERENCES

1-1 CEN-367-A, Revision 0, "Leak-Before-Break Evaluation of Primary Coolant Loop Piping in Combustion Engineering Designed Nuclear Steam Supply Systems," February 1991.

1-2 NUREG-0800 Revision 1, March 2007, Standard Review Plan: 3.6.3 Leak-Before-Break Evaluation Procedures.

1-3 Standard Review Plan: Public Comments Solicited; 3.6.3 Leak-Before-Break Evaluation Procedures; Federal Register/Vol. 52, No. 167/Friday August 28, 1987/Notices, pp. 32626-32633.

2 OPERATION AND STABILITY OF THE REACTOR COOLANT SYSTEM

2.1 STRESS CORROSION CRACKING

The reactor coolant system primary loops of Westinghouse and Combustion Engineering (CE) plants have an operating history that demonstrates the inherent operating stability characteristics of the design. This includes a low susceptibility to cracking failure from the effects of corrosion (e.g., intergranular stress corrosion cracking (IGSCC)). This operating history totals over 1400 reactor-years, including more than 16 plants each having over 30 years of operation, 10 other plants each with over 25 years of operation, 11 plants each with over 20 years of operation, and 12 plants each with over 15 years of operation.

In 1978, the United States Nuclear Regulatory Commission (USNRC) formed the second Pipe Crack Study Group. (The first Pipe Crack Study Group (PCSG) established in 1975, addressed cracking in boiling water reactors only.) One of the objectives of the second PCSG was to include a review of the potential for stress corrosion cracking in Pressurized Water Reactors (PWR's). The results of the study performed by the PCSG were presented in NUREG-0531 (Reference 2-1) entitled "Investigation and Evaluation of Stress Corrosion Cracking in Piping of Light Water Reactor Plants." In that report the PCSG stated:

> "The PCSG has determined that the potential for stress-corrosion cracking in PWR primary system piping is extremely low because the ingredients that produce IGSCC are not all present. The use of hydrazine additives and a hydrogen overpressure limit the oxygen in the coolant to very low levels. Other impurities that might cause stress-corrosion cracking, such as halides or caustic, are also rigidly controlled. Only for brief periods during reactor shutdown when the coolant is exposed to the air and during the subsequent startup are conditions even marginally capable of producing stress-corrosion cracking in the primary systems of PWRs. Operating experience in PWRs supports this determination. To date, no stress corrosion cracking has been reported in the primary piping or safe ends of any PWR."

During 1979, several instances of cracking in PWR feedwater piping led to the establishment of the third PCSG. The investigations of the PCSG reported in NUREG-0691 (Reference 2-2) further confirmed that no occurrences of IGSCC have been reported for PWR primary coolant systems.

As stated above, for the Westinghouse and CE plants there is no history of cracking failure in the reactor coolant system loop. The discussion below further qualifies the PCSG's findings.

For stress corrosion cracking (SCC) to occur in piping, the following three conditions must exist simultaneously: high tensile stresses, susceptible material, and a corrosive environment. Since some residual stresses and some degree of material susceptibility exist in any piping, the potential for stress corrosion is minimized by properly selecting a material resistant to SCC (e.g., internal stainless steel cladding on carbon steel pipes) as well as preventing the occurrence of a corrosive environment. The material specifications consider compatibility with the system's operating environment (both internal and external) as well as other material in the system, applicable ASME Code rules, fracture toughness, welding, fabrication, and processing.

The elements of a water environment known to increase the susceptibility of austenitic stainless steel to stress corrosion are: oxygen, fluorides, chlorides, hydroxides, hydrogen peroxide, and reduced forms of sulfur (e.g., sulfides, sulfites, and thionates). Strict pipe cleaning standards prior to operation and careful control of water chemistry during plant operation are used to prevent the occurrence of a corrosive environment. Prior to being put into service, the piping is cleaned internally and externally. During flushes and preoperational testing, water chemistry is controlled in accordance with written specifications. Requirements on chlorides, fluorides, conductivity, and pH are included in the acceptance criteria for the piping.

During plant operation, the reactor coolant water chemistry is monitored and maintained within very specific limits. Contaminant concentrations are kept below the thresholds known to be conducive to stress corrosion cracking with the major water chemistry control standards being included in the plant operating procedures as a condition for plant operation. For example, during normal power operation, oxygen concentration in the RCS is expected to be in the parts-per-billion (ppb) range by controlling charging flow chemistry and maintaining hydrogen in the reactor coolant at specified concentrations. Halogen concentrations are also stringently controlled by maintaining concentrations of chlorides and fluorides within the specified limits. Thus, during plant operation, the likelihood of stress corrosion cracking is minimized.

The potential susceptibility to primary water stress corrosion cracking (PWSCC) in materials such as alloy 82/182 in the dissimilar metal welds in the St. Lucie Units 1 and 2 RCS primary loop piping was investigated. St. Lucie Units 1 and 2 reactor coolant system primary loop piping contains alloy 82/182 dissimilar metal welds which are susceptible to PWSCC. Figure 3-1 show the locations of the alloy 82/182 welds are at the RCP Suction nozzle (locations 6 and 12) and RCP Discharge nozzles (locations 7 and 13).

2.2 WATER HAMMER

Overall, there is a low potential for water hammer in the RCS since it is designed and operated to preclude the voiding condition in normally filled lines. The reactor coolant system, including piping and primary components, is designed for normal, upset, emergency, and faulted condition transients. The design requirements are conservative relative to both the number of transients and their severity. Relief valve actuation and the associated hydraulic transients following valve opening are considered in the system design. Other valve and pump actuations are relatively slow transients with no significant effect on the system dynamic loads. To ensure dynamic system stability, reactor coolant parameters are stringently controlled. Temperature during normal operation is maintained within a narrow range; pressure is controlled by pressurizer heaters and pressurizer spray also within a narrow range for steady-state conditions. The flow characteristics of the system remain constant during a fuel cycle because the only governing parameters, namely system resistance and the reactor coolant pump characteristics, are controlled in the design process. Additionally, Westinghouse has instrumented typical reactor coolant systems to verify the flow and vibration characteristics of the system. Preoperational testing and operating experience have verified the Westinghouse approach. The operating transients of the RCS primary piping are such that no significant water hammer can occur.

2.3 LOW CYCLE AND HIGH CYCLE FATIGUE

An assessment of the low cycle fatigue loadings was carried out as part of this study in the form of a fatigue crack growth analysis, as discussed in Section 8.

High cycle fatigue loads in the system would result primarily from pump vibrations. These are minimized by restrictions placed on shaft vibrations during hot functional testing and operation. During operation, an alarm signals the exceedance of the vibration limits. Field vibration measurements have been made on the reactor coolant loop piping in a number of plants during hot functional testing, including plants similar to St. Lucie Units 1 and 2. Stresses in the elbow below the reactor coolant pump resulting from system vibration have been found to be very small. When vibrations are translated to the connecting auxiliary piping systems, these stresses would be even lower, well below the fatigue endurance limit for the piping material and would result in an applied stress intensity factor below the threshold for fatigue crack growth.

2.4 WALL THINNING, CREEP, AND CLEAVAGE

Wall thinning by erosion and erosion-corrosion effects should not occur in the primary loop piping due to the low velocity, typically less than 1.0 ft/sec and the stainless steel cladding material, which is highly resistant to these degradation mechanisms. The cause of wall thinning is related to high water velocity and is therefore clearly not a mechanism that would affect the primary loop piping.

Creep is typical experienced for temperatures over 700°F for stainless steel and carbon steel materials, and the maximum operating temperature of the primary loop piping is well below this temperature value; therefore, there would be no significant mechanical creep damage in stainless steel piping.

Cleavage type failures are not a concern for the operating temperatures and the stainless steel material used in the primary loop piping.

2.5 REFERENCES

2-1 Investigation and Evaluation of Stress-Corrosion Cracking in Piping of Light Water Reactor Plants, NUREG-0531, U.S. Nuclear Regulatory Commission, February 1979.

2-2 Investigation and Evaluation of Cracking Incidents in Piping in Pressurized Water Reactors, NUREG-0691, U.S. Nuclear Regulatory Commission, September 1980.

3 PIPE GEOMETRY AND LOADING

3.1 INTRODUCTION TO METHODOLOGY

The general approach is discussed first. As an example, a segment of the primary coolant RCP suction pipe is shown in Figure 3-2. The as-built outside diameter and minimum wall thickness of the pipe are 36.06 in. and 3.03 in for Unit 1, as shown in the figure. The as-built geometry for Unit 2 is slightly different at these locations which results in small differences in the stresses (Tables 3-2 and 3-4). The normal stresses at the weld locations are from the load combination as discussed in Section 3.3 whereas the faulted loads are as described in Section 3.4. The components for normal loads are pressure, deadweight and thermal expansion (Table 3-1 and Table 3-2). An additional component, Safe Shutdown Earthquake (SSE), is considered for faulted loads (Table 3-3 and Table 3-4). Tables 3-1 thru 3-4 show the enveloping loads for St. Lucie Units 1 and 2. As seen from Tables 3-3 and 3-4, the highest stressed location in the entire St. Lucie Units 1 and 2 reactor coolant loops is at Location 6 shown in Figure 3-1. This is one of the locations at which leak-before-break is to be established. Essentially a circumferential flaw is postulated to exist at this location which is subjected to both the normal loads and faulted loads to assess leakage and stability, respectively. The loads (developed below) at this location are also given in Figure 3-2.

St. Lucie Units 1 and 2 reactor coolant pump nozzle safe-ends are components made of A351-CF8M material. Locations other than the highest stressed pipe location were examined by taking into consideration both fracture toughness and stress. The four most critical locations among the entire primary loop are identified after the full analysis is completed (see Section 5). Once loads (this section) and fracture toughnesses (Section 4) are obtained, the critical locations are determined (Section 5). At these locations, leak rate evaluations (Section 6) and fracture mechanics evaluations (Section 7) are performed per the guidance of References 3-1 and 3-2.

For global failure mechanism, all critical locations are evaluated using A351-CF8M and alloy 82/182 material properties which present a limiting condition due to A351-CF8M susceptibility to the thermal aging at the reactor operating temperature, and alloy 82/182 susceptibility to Primary Water Stress Corrosion Cracking (PWSCC).

For local stability mechanism, the respective locations are evaluated using the A351-CF8M cast austenitic stainless steel (CASS) material properties which present a limiting condition not only due to their tensile properties in unaged condition but also the material fracture toughness and tearing modulus reductions due to the thermal aging effects for the entire 80-year plant life.

Fatigue crack growth (Section 8) assessment and stability margins are also evaluated (Section 9). All the weld locations considered for the LBB evaluation are those shown in Figure 3-2.

3.2 CALCULATION OF LOADS AND STRESSES

The stresses due to axial loads and bending moments are calculated by the following equation:

$$\sigma = \frac{F}{A} + \frac{M}{Z} \qquad (3\text{-}1)$$

where,

σ	=	stress, ksi
F	=	axial load, kips
M	=	bending moment, in-kips
A	=	pipe cross-sectional area, in^2
Z	=	section modulus, in^3

The total moments for the desired loading combinations are calculated by the following equation:

$$M = \sqrt{M_X^2 + M_Y^2 + M_Z^2} \tag{3-2}$$

where,

M	=	total moment for required loading
M_X	=	X component of moment (torsion)
M_Y	=	Y component of bending moment
M_Z	=	Z component of bending moment

NOTE: X-axis is along the center line of the pipe.

The axial load and bending moments for leak rate predictions and crack stability analyses are computed by the methods to be explained in Sections 3.3 and 3.4.

3.3 LOADS FOR LEAK RATE EVALUATION

The normal operating loads for leak rate predictions include pressure, deadweight and normal thermal expansion loads.

Load combinations are taken consistent with CEN-367-A (Reference 3-3). A review of the current RCL piping design specification has confirmed the loads from CEN-367-A (Reference 3-1) remain bounding for St. Lucie with the inclusion of EPU and branch line MSIP effects. The loads from CEN-367-A (Reference 3-3) represent the bounding conditions for both Loops A and B of St. Lucie Units 1 and 2.

The loads based on this method of combination are provided in Table 3-1 for Unit 1 and Table 3-2 for Unit 2 at all the critical weld locations (weld points 6, 7, 12, 13) identified in Figure 3-1.

3.4 LOAD COMBINATION FOR CRACK STABILITY ANALYSES

In accordance with Standard Review Plan 3.6.3 (References 3-1 and 3-2), the margin in terms of applied loads needs to be demonstrated by crack stability analysis. The faulted loads for crack stability analysis include the combined normal operating (NOP) loads and SEE loads, using formula: sqrt(2) x (NOP + SSE) loads.

Load combinations are taken consistent with CEN-367-A (Reference 3-3). A review of the current RCL piping design specification has confirmed the loads from CEN-367-A (Reference 3-1) remain bounding for St. Lucie with the inclusion of EPU and branch line MSIP effects. The loads from CEN-367-A (Reference 3-3) represent the bounding conditions for both Loops A and B of St. Lucie Units 1 and 2.

The loads based on this method of combination are provided in Table 3-3 for Unit 1 and Table 3-4 for Unit 2 at all the critical weld locations (weld points 6, 7, 12, 13) identified in Figure 3-1.

3.5 REFERENCES

3-1 Standard Review Plan: Public Comments Solicited; 3.6.3 Leak-Before-Break Evaluation Procedures; Federal Register/Vol. 52, No. 167/Friday, August 28, 1987/Notices, pp. 32626-32633.

3-2 NUREG-0800 Revision 1, March 2007, Standard Review Plan: 3.6.3 Leak-Before-Break Evaluation Procedures.

3-3 Westinghouse Report, CEN-367-A, Rev. 000, "Leak-Before-Break Evaluation of Primary Coolant Loop Piping in Combustion Engineering Designed Nuclear Steam Supply Systems," February 1991.

Table 3-1. Dimensions, Normal Loads and Stresses for St Lucie Unit 1

Location Weld Points[a]	Outside Diameter (in)	Minimum Thickness (in)	Axial Load[b] (lb)	Moment (in-lb)	Total Stress (psi)
6	36.06	3.03	1338640	17386000	11502
7	36.06	3.03	1630240	4954000	7248
12	36.06	3.03	1599040	3661000	6609
13	36.06	3.03	1504040	4427000	6627

Notes:
a. See Figure 3-1
b. Includes Pressure force from 2235 psig distributed over the 30" ID flow area

Table 3-2. Dimensions, Normal Loads and Stresses for St Lucie Unit 2

Location Weld Points[a]	Outside Diameter (in)	Minimum Thickness (in)	Axial Load[b] (lb)	Moment (in-lb)	Total Stress (psi)
6	36.13	3.06	1338640	17386000	11372
7	36.13	3.06	1630240	4954000	7166
12	36.13	3.06	1599040	3661000	6535
13	36.13	3.06	1504040	4427000	6552

Notes:
a. See Figure 3-1
b. Includes Pressure force from 2235 psig distributed over the 30" ID flow area

Table 3-3. Dimensions, Faulted Loads and Stresses for St. Lucie Unit 1

Location Weld Points[a]	Outside Diameter (in)	Minimum Thickness (in)	Axial Load[b] (lb)	Moment (in-lb)	Total Stress (psi)
6	36.06	3.03	2088285	47674553	26510
7	36.06	3.03	2527540	30798743	20872
12	36.06	3.03	2456546	28264472	19590
13	36.06	3.03	2349066	30053452	19994

Notes:

a. See Figure 3-1

b. Includes Pressure force from 2235 psig distributed over the 30" ID flow area

c. Calculated as (|P+NOP|+|SSE|)x(√2)

Table 3-4. Dimensions, Faulted Loads and Stresses for St. Lucie Unit 2

Location Weld Points[a]	Outside Diameter (in)	Minimum Thickness (in)	Axial Load[b] (lb)	Moment (in-lb)	Total Stress (psi)
6	36.13	3.06	2088285	47674553	26208
7	36.13	3.06	2527540	30798743	20636
12	36.13	3.06	2456546	28264472	19368
13	36.13	3.06	2349066	30053452	19768

Notes:

a. See Figure 3-1

b. Includes Pressure force from 2235 psig distributed over the 30" ID flow area

c. Calculated as (|P+NOP|+|SSE|)x(√2)

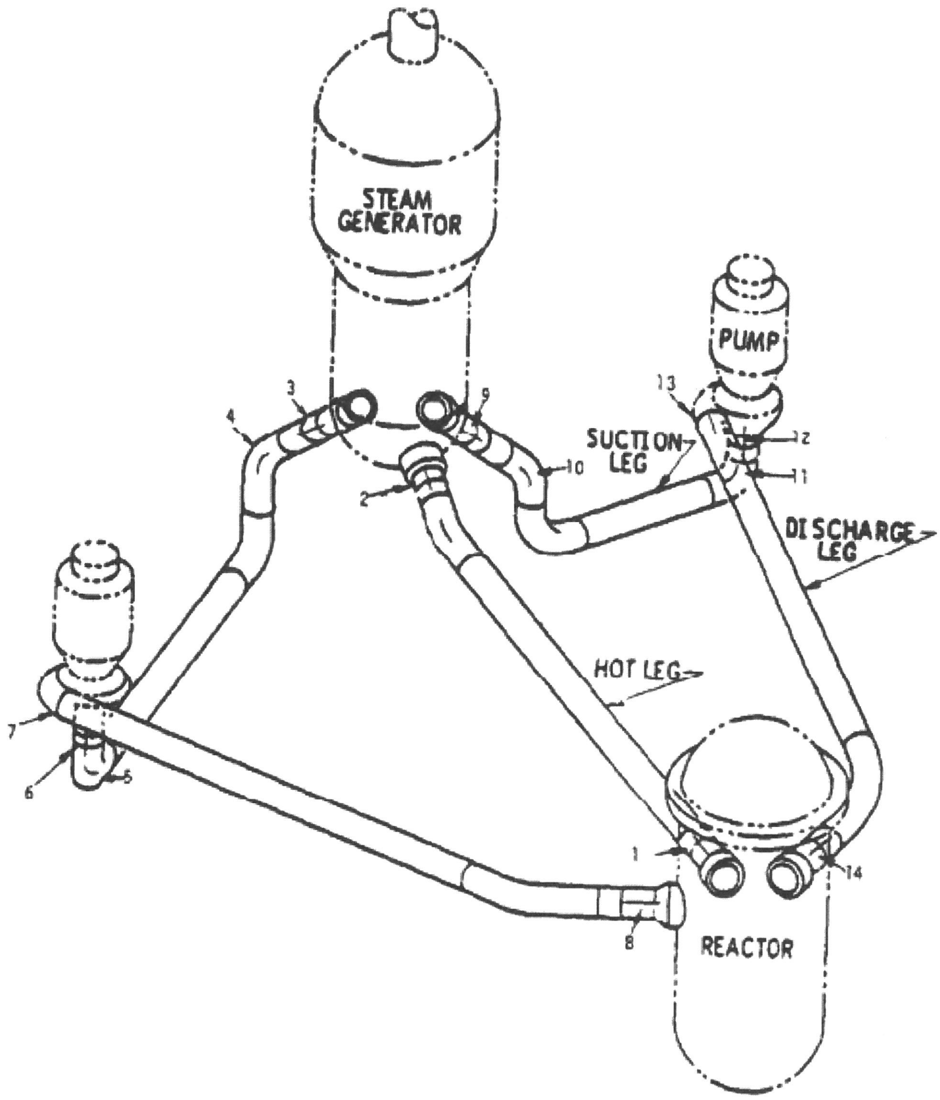

Figure 3-1. St. Lucie Units 1 and 2 RCL Point Locator

Note: This figure shows Loop A of the St. Lucie plant. Loop B is symmetrically mirrored across the Reactor Vessel.

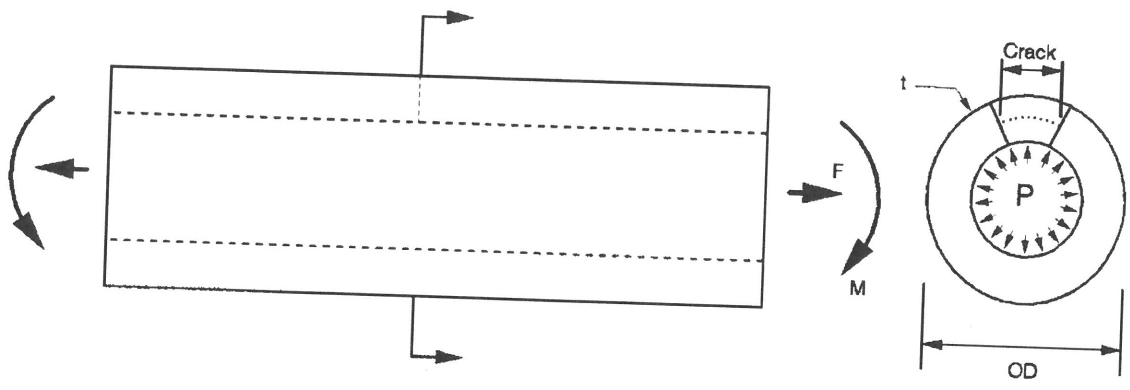

Location 6 (Unit 1)

OD[a] = 36.06 in
t[a] = 3.03 in
(Unit 1)

Normal Loads[a]		Faulted Loads[b]	
Force[c]:	1339 kips	Force[c]:	2088 kips
Bending Moment:	17386 in-kips	Bending Moment:	47675 in-kips

[a]See Table 3-1
[b]See Table 3-3
[c]Includes the force due to a pressure of 2235 psig

Figure 3-2. RCP Suction Pipe

4 MATERIAL CHARACTERIZATION

4.1 PRIMARY LOOP PIPE, RCP SUCTION AND DISCHARGE MATERIALS

The RCL piping for St. Lucie Units 1 and 2 is carbon steel (SA-516-70) with stainless steel cladding. Analyses for these locations are documented in CEN-367-A and remain applicable for the SLR.

As documented in CEN-367-A, the St. Lucie carbon steel cold leg piping which are joined to RCP Suction and Discharge nozzles for both Units 1 and 2. The four nozzle safe-ends contain A351-CF8M CASS material and Alloy 82/182 weld material. The A351-CF8M material is susceptible to the thermal aging at the reactor operating temperatures, and the DM weld of Alloy 82/182 material is susceptible to Primary Water Stress Corrosion Cracking (PWSCC).

This report documents the material characterization of A351-CF8M material at the RCP Suction and Discharge nozzle safe-ends with consideration for thermal aging, and the DM weld of alloy 82/182 material with consideration for primary water stress corrosion cracking (PWSCC).

The welding processes used at critical locations are assumed conservatively as Submerged Arc Weld (SAW).

For the Leak-Before-Break analyses, the tensile properties for both materials (A351-CF8M and Alloy 82/182) are described in Section 4.2. For the consideration of thermal aging, CF8M material fracture toughness properties are described in Section 4.3.

4.2 TENSILE PROPERTIES

For the CF8M material, the Certified Materials Test Reports (CMTRs) for the St. Lucie Units 1 and 2 Reactor Coolant System are used to establish the tensile properties as shown in Table 4-1 and summarized in Table 4-3.

For the 82/182 weld material, typical tensile properties are shown in Table 4-4.

The uprate program operating temperatures are used, i.e., 606.0°F for Hot Leg, 550.6°F for Cold Leg RCP Suction and 551.0°F for Cold Leg RCP Discharge.

Code tensile properties for CF8M CASS material at temperatures for the operating conditions considered in this LBB analysis are obtained by linear interpolation of tensile properties provided in the Section II of the 2007 ASME Boiler and Pressure Vessel Code (Reference 4-1). Tensile properties for alloy 82/182 welds at temperatures for the operating conditions considered in this LBB analysis are obtained by linear interpolation of tensile properties provided in Table 4-4.

Ratios of the Code tensile properties at the operating temperatures to the corresponding properties at the CMTR temperature are then applied to obtain the St. Lucie Units 1 and 2 line-specific properties at operating temperatures for the A351-CF8M material. No such ratios are used for the alloy 82/182 welds, which do not have CMTRs readily available.

For A351-CF8M material heats, CMTR data is available for the 70°F test temperatures. The representative properties at 550.6°F and 551.0°F are established from the tensile properties either at 70°F given in Table 4-1 by utilizing Section II of the 2007 ASME Boiler and Pressure Vessel Code (Reference 4-1).

Code tensile properties at temperatures for the operating conditions considered in this LBB analysis are obtained by linear interpolation of tensile properties provided in the Code. Ratios of the Code tensile properties at the operating temperatures to the corresponding properties at the CMTR temperature are then applied to obtain the St. Lucie Units 1 and 2 line-specific properties at operating temperatures.

It should be noted that there is no significant impact by using the 2007 ASME Code Section II edition for material properties for the LBB analysis, as compared to the St. Lucie ASME Code of record.

Material modulus of elasticity is also interpolated from ASME Code values for the operating temperatures considered, and Poisson's ratio is taken as 0.3. The temperature-dependent material properties from the ASME Code are shown in Table 4-2. The average and lower bound yield strengths, ultimate strengths, and elastic moduli for the pipe material at applicable operating temperatures are tabulated in Table 4-3 and Table 4-4.

For the SLR program that accounts for 80 years of plant operation, the more conservative material properties are used.

Conservative Evaluations:

For global failure mechanism based on limit load method, the stability of postulated cracks at critical locations for 80 years of plant operation are examined. To evaluate conservatively, it is desired to use lower tensile properties obtained from base-metals and weld materials, since lower tensile properties potentially reduce the critical flaw size/flaw size margins. Since lower tensile properties (S_u and S_y) are more conservative for the LBB evaluation because they increase the calculated J_{app} and T_{app} values, the unaged tensile properties as shown in Table 4-3 are used in calculation.

For local stability mechanism based on J-integral method, the stability of postulated cracks at A351-CF8M CASS material at the critical locations for 80 years of plant operation is examined based on the following parameter values: J_{Ic}, J_{max}, T_{mat}, J_{app} and T_{app} (see Section 5.2), where:

(1) If $J_{app} < J_{Ic}$, then the crack will not initiate, and the crack is stable;

(2) If $J_{app} \geq J_{Ic}$; and $T_{app} < T_{mat}$ and $J_{app} < J_{max}$, then the crack is stable.

The A351-CF8M material is susceptible to thermal aging. J_{app}, T_{app}, and T_{mat} values (which are dependent on aging tensile (S_u and S_y) properties) will be affected. To evaluate conservatively, both unaged and aged tensile properties are used for the following reasons: (a) lower tensile properties are more conservative for the LBB evaluation by increasing the calculated J_{app} and T_{app} values; therefore, the unaged tensile properties as shown in Table 4-3 are used to calculate those values; (b) higher tensile properties are more conservative for the LBB evaluation by lowering T_{mat} values; therefore, the aged tensile properties as shown in Table 4-6 are used just to calculate T_{mat}.

4.3 FRACTURE TOUGHNESS PROPERTIES

The pre-service fracture toughness (J) of cast austenitic stainless steel CASS) that are of interest are in terms of J_{Ic} (J at Crack Initiation) and have been found to be very high at 600°F. [ ]^{a,c,e} However, cast stainless steel is susceptible to thermal aging at the reactor operating temperature, that is, about 290°C (550°F). Thermal aging of cast stainless steel results in embrittlement, that is, a decrease in the ductility, impact strength, and fracture toughness of the material. Depending on the material composition, the Charpy impact energy of a cast stainless steel component could decrease to a small fraction of its original value after exposure to reactor temperatures during service.

In 1994, the Argonne National Laboratory (ANL) completed an extensive research program in assessing the extent of thermal aging of cast stainless steel materials. The ANL research program measured mechanical properties of cast stainless steel materials after they had been heated in controlled ovens for long periods of time. ANL compiled a database, both from data within ANL and from international sources, of about 85 compositions of cast stainless steel exposed to a temperature range of 290°–400°C (550°–750°F) for up to 58,000 hours (6.5 years). In 2015 the work done by ANL was augmented, and the fracture toughness database for CASS materials was aged to 100,000 hours at 290°–350°C (554°–633°F). The methodology for estimating fracture properties has been extended to cover CASS materials with a ferrite content of up to 40%. From this database (NUREG/CR-4513, Revision 2), ANL developed correlations for estimating the extent of thermal aging of cast stainless steel (Reference 4-2).

ANL developed the fracture toughness estimation procedures by correlating data in the database conservatively. After developing the correlations, ANL validated the estimation procedures by comparing the estimated fracture toughness with the measured value for several cast stainless steel plant components removed from actual plant service. The procedure developed by ANL was used to calculate the end of life fracture toughness values for this analysis. The ANL research program was sponsored and the procedure was accepted by the NRC.

The results from the ANL Research Program indicate that the lower-bound fracture toughness of thermally aged cast stainless steel is similar to that of submerged arc welds (SAWs). The applied value of the J-integral for a flaw in the weld regions will be lower than that in the base metal because the yield stress for the weld materials is much higher at the temperature.[1]

Therefore, weld regions are less limiting than the cast material.

Based on Reference 4-2, the fracture toughness correlations used for the full aged condition is applicable for plants operating at ≥15 EFPY (effective full-power years) for the A351-CF8M materials. For the SLR program that accounts for 80 years of plant operation, the materials will thermally age. Therefore, the use of the fracture toughness correlations described in the following sections is applicable for the fully aged or saturated condition of the St. Lucie Units 1 and 2 RCP Suction and Discharge nozzle safe-ends made of A351-CF8M material.

[1]In the report all the applied J values were conservatively determined by using base metal strength properties.

It is noted that both Revision 1 and Revision 2 of NUREG/CR-4513 were considered in evaluating the thermal aging of the St. Lucie CASS materials. Table 4-9 provides a comparison of the J_{Ic} values for each CASS material heat calculated using both Revision 1 and Revision 2 of NUREG/CR-4513. While Revision 1 may be limiting for some material heats, it was found that Revision 2 (Reference 4-2) resulted in the most limiting fracture toughness values for the critical material heats identified in Table 4-8.

Fracture Toughness Properties of Pipes and Elbows (CF8M)

The susceptibility of the material to thermal aging increases with increasing ferrite contents, and the molybdenum bearing CF8M shows increased susceptibility to thermal aging.

The chemical compositions and tensile properties of the St. Lucie Units 1 and 2 primary loop piping materials are available from CMTRs. The following equations 4-1 to 4-3 for delta ferrite calculations are taken from CMTRs and applicable for CF8M type materials.

$$Cr_{eq} = Cr + 1.21(Mo) + 0.48(Si) - 4.99 = \text{(Chromium equivalent)} \quad (4\text{-}1)$$

$$Ni_{eq} = (Ni) + 0.11(Mn) - 0.0086(Mn)^2 + 18.4(N) + 24.5(C) + 2.77 = \text{(Nickel equivalent)} \quad (4\text{-}2)$$

Note: N is not included for all CMTRs. Value of 0.04 is assumed per Reference 4-2.

$$\delta_c = 100.3(Cr_{eq} / Ni_{eq})^2 - 170.72(Cr_{eq} / Ni_{eq}) + 74.22 \quad (4\text{-}3)$$

where the elements are in percent weight and δ_c is ferrite in percent volume.

The saturation room temperature (RT at 77°F) impact energies of the cast stainless steel materials are determined from the chemical compositions available from CMTRs and shown in Table 4-5.

For CF8M steel with < 10% Ni, the saturation value of RT impact energy Cv_{sat} (J/cm^2) is the lower value determined from

$$\log_{10}Cv_{sat} = 0.27 + 2.81 \exp(-0.022\phi) \quad (4\text{-}4)$$

where the material parameter ϕ is expressed as

$$\phi = \delta_c (Ni + Si + Mn)^2 (C + 0.4N)/5.0 \quad (4\text{-}5)$$

and from

$$\log10Cv_{sat} = 7.28 - 0.011\delta_c - 0.185Cr - 0.369Mo - 0.451Si - 0.007Ni - 4.71(C + 0.4N) \quad (4\text{-}6)$$

For CF8M steel with $\geq$ 10% Ni, the saturation value of RT impact energy Cv_{sat} (J/cm^2) is the lower value determined from

$$\log_{10}Cv_{sat} = 0.84 + 2.54 \exp(-0.047\phi) \quad (4\text{-}7)$$

where the material parameter ϕ is expressed as

$$\phi = \delta_c\ (Ni + Si + Mn)^2(C + 0.4N)/5.0 \tag{4-8}$$

and from

$$\log_{10}Cv_{sat} = 7.28 - 0.011\delta_c - 0.185Cr - 0.369Mo - 0.451Si - 0.007Ni - 4.71(C + 0.4N) \tag{4-9}$$

$$Q = 10\ [74.52 - 7.20\theta - 3.46Si - 1.78Cr - 4.35Mn + 23N] \tag{4-10}$$

Per Reference 4-2: 65 < Q (kJ/mole) < 250 where actual %Mn < 1.2 and 536°F < T < 752°F. θ equals 2.9.

$$P = \log_{10}(t) - \frac{1000Q}{19.143} + \left(\frac{1}{T_s+273} - \frac{1}{673}\right) \tag{4-11]}$$

Where: t = aging time (hrs) and T_s = operating temperature in °C

Note: the value of Cv is conservatively taken equal to Cv_{sat} in the J_d calculation below:

For centrifugal-cast CF8M steel materials with RT impact energy values ≥ 35 J/cm², the J-R curve is given by

$$J_d = 20\ (Cv)^{0.67}(\Delta a)^n \tag{4-12}$$

for centrifugal-cast CF8M steel materials with RT impact energy values < 35 J/cm², the J-R curve is given by

$$J_d = 1.78\ (Cv)^{1.35}(\Delta a)^n \tag{4-13}$$

$$n = 0.20 + 0.08 \log_{10} (Cv) \tag{4-14}$$

where J_d is the "deformation J" in kJ/m² and Δa is the crack extension in mm.

For centrifugal-cast CF8M steel materials at 290°–320°C (554°–608°F) with impact energy values ≥ 41 J/cm², the J-R curve is given by

$$J_d = 57\ (Cv)^{0.41}(\Delta a)^n \tag{4-15}$$

For centrifugal-cast CF8M steel materials at 290°–320°C (554°–608°F) with impact energy values < 41 J/cm², the J-R curve is given by

$$J_d = 6.9\ (Cv)^{0.98}(\Delta a)^n \tag{4-16}$$

$$n = 0.19 + 0.07 \log_{10} (Cv) \tag{4-17}$$

where J_d is the "deformation J" in kJ/m² and Δa is the crack extension in mm.

J_{Ic} and J_{max} Calculations:

[

]a,c,e

T_{mat} Calculations:

The material tearing modulus, T_{mat}, is calculated as follows:

$$T_{mat} = dJ/da \times E/(\sigma_{fa})^2$$

Where: E = Elastic Modulus at operating temperature, psi.

σ_{fa} = aged flow stress (per Reference 4-2)

J_{app} and T_{app} Calculations:

The critical heat for CF8M with lowest fracture toughness property and lowest tearing modulus value from Table 4-6 on St. Lucie Units and 2 RCL are summarized in Table 4-7.

The applied J Integral value, J_{app}, is calculated and compared to the J_{Ic} and J_{max} values in Table 7-1 for Units 1 and 2.

Consideration of Dissimilar Metal Weld Material Profiles

St. Lucie Units 1 and 2 reactor coolant loop piping lines contain components made of A351-CF8M material. The A351-CF8M material is susceptible to the thermal aging at the reactor operating temperatures. Both the suction and discharge sides of the RCP nozzles are joined to the piping with a A351-CF8M cast austenitic stainless steel (CASS) safe-end and a dissimilar metal (DM) weld of Alloy 82/182 weld material. The remainder of the piping is carbon steel with stainless steel cladding, as evaluated in CEN-367-A.

For local failure mechanism, the RCP Suction and Discharge safe-end locations are evaluated using the cast stainless steel material properties (A351-CF8M) as shown in Table 4-7 which present a limiting condition due to the thermal aging effects. As stated in Reference 4-3,

> "The fracture resistance of Alloy 82 and 52 welds have been investigated by conducting fracture toughness J-R curve tests at 24 – 338 °C in deionized water [...]. The results indicate that these welds exhibit high fracture toughness in air and high-temperature water (> 93 °C)."

Since nickel alloys are known to have high toughness properties and because the CF8M CASS base metal of the RCP Suction and Discharge Nozzle safe-ends are susceptible to thermal aging degradation of the fracture toughness, it is determined that the CF8M CASS base metal presents the most limiting condition.

For the DMW locations , the evaluation is represented by J-integral evaluation for location 6 (RCP Suction and Discharge Nozzle safe-ends) and location 7 (RCP Discharge Nozzle safe-ends) based on

A351-CF8M CASS base metal (A351-CF8M) property that presents the most limiting condition. The evaluation results are presented in Table 7-1 and applicable for 80 year plant life period in SLR program.

4.4 REFERENCES

4-1 ASME Boiler and Pressure Vessel Code Section II, 2007 Edition through 2008 Addenda.

4-2 NUREG/CR-4513, Revision 2 (May 2016) and Revision 1 (May 1994), "Estimation of Fracture Toughness of Cast Stainless Steels During Thermal Aging in LWR Systems," O. K. Chopra, U.S. Nuclear Regulatory Commission, Washington, DC.

4-3 NUREG/CR-6721, "Effects of Alloy Chemistry, Cold Work, and Water Chemistry on Corrosion Fatigue and Stress Corrosion Cracking of Nickel Alloys and Welds," date published: April 2001.

Table 4-1. Measured Tensile Properties for St. Lucie Units 1 & 2 (A351-CF8M)

RCL	Heat Number	Serial Number	At Room Temperature (CMTRs)		At Operating Temperature (Interpolated)	
			Yield Strength (psi)	Ultimate Strength (psi)	Yield Strength (psi)	Ultimate Strength (psi)
1A1 Suction	A2137890-21	C4317-4	36970	76720	23838	73651
1A2 Suction	A2137890-18	C4317-3	36970	76720	23838	73651
1B1 Suction	A2137890	C4317-1	36970	76720	23838	73651
1B2 Suction	A2137890	C4317-2	36970	76720	23838	73651
1A1 Discharge	A2137890-22	C4317-5	36970	76720	23832	73651
1A2 Discharge	A1829012-25	C4317-8	36900	78100	23787	74976
1B1 Discharge	A2137890-23	C4317-6	36970	76720	23832	73651
1B2 Discharge	A2137890-24	C4317-7	36970	76720	23832	73651
2A1 Suction	D-419-3	M-9216-3	45300	85500	29209	82080
2A2 Suction	D-419-4	M-9216-4	45300	85500	29209	82080
2B1 Suction	D-423-3	M-9216-5	35600	75400	22954	72384
2B2 Suction	D-423-2	M-9216-6	35600	75400	22954	72384
2A1 Discharge	D-423-1	M-9216-7	35600	75400	22949	72384
2A2 Discharge	D-419-1	M-9216-1	45300	85500	29202	82080
2B1 Discharge	D-419-2	M-9216-2	45300	85500	29202	82080
2B2 Discharge	J-984	M-9216-8	46100	82300	29718	79008

Table 4-2. ASME Code Tensile Properties for Material A351-CF8M

Temperature (°F)	A351-CF8M Yield Strength (ksi)	Ultimate Strength (ksi)	Elastic Modulus (ksi)
70	30.000	70.000	28300
100	30.000	70.000	28300
150	27.300	70.000	27900
200	25.800	70.000	27500
250	24.500	69.000	27250
300	23.300	68.000	27000
400	21.400	67.200	26400
500	19.900	67.200	25900
550.6	19.343	67.200	25596
551.0	19.339	67.200	25594
600	18.800	67.200	25300
650	18.400	67.200	25050
700	18.100	67.200	24800

Notes:

1. Material properties are from the 2007 Edition of the ASME Boiler and Pressure Vessel Code (Reference 4-1).
2. Shaded cells are based on linear interpolation of the values provided in the ASME Code.

Table 4-3. Tensile Properties for St. Lucie Units 1 and 2 A351-CF8M Material at Operating Temperatures

RCL	Temperature (°F)	Average Yield Strength (ksi)	Lower Bound		Modulus of Elasticity (ksi)
			Yield Strength (ksi)	Ultimate Strength (ksi)	
Cold Leg RCP Suction	550.6	24.9594	22.9542	72.3840	25596.4
Cold Leg RCP Discharge	551.0	25.7942	22.9489	72.3840	25594.0

Table 4-4. Tensile Properties for St. Lucie Units 1 and 2 Alloy 82/182 Welds at Operating Temperatures

RCL	Temperature (°F)	Typical Yield* Strength (ksi)	Ultimate Strength (ksi)	Modulus of Elasticity (ksi)
Cold Leg RCP Suction	550.6	49.9645	84.7029	28897.6
Cold Leg RCP Discharge	551.0	49.9625	84.6976	28896.0

Note: * Typical Yield Strength is considered as the average yield strength

Table 4-5. St. Lucie Units 1 and 2 CF8M Chemical Composition

a,c,e

Table 4-6. St. Lucie Units 1 and 2 CF8M Fracture Toughness Properties

a,c.e

Table 4-7. Units 1 and 2 A351-CF8M Lowest Fracture Toughness Properties

a,c,e

Table 4-8. J_{IC}, J_{max}, T_{mat} Limiting Values NUREG/CR-4513 per Rev. 1 and Rev. 2

a,c,e

a,c,e

Figure 4-1. Pre-Service J vs. Δa for SA351-CF8M Cast Stainless Steel at 600°F

5 CRITICAL LOCATION AND EVALUATION CRITERIA

5.1 CRITICAL LOCATIONS

The governing or critical locations for the LBB evaluation are established not only based on the fracture toughness properties of the base metal at the weld points, but also on the basis of pipe geometry, welding process, operating temperature, operating pressure, and the highest faulted stresses at the welds.

Critical locations for LBB Evaluation as shown in Table 5-1 and Figure 5-1 are determined based on the maximum faulted stresses. Weld point 6 and 7, for both Units 1 and 2, bound the maximum faulted stresses for weld points 12 and 13. Based on slight geometrical differences in the pipe for Unit 1 and Unit 2, weld points 6 and 7 are evaluated for both units.

For LBB evaluation, Table 5-1 shows the critical locations bounding both St. Lucie Units 1 and 2. Figure 5-1 shows the locations of the critical welds for St. Lucie Units 1 and 2.

As noted in Section 4-1, CEN-367-A remains applicable for the LBB evaluation of the remaining carbon steel piping locations. The critical locations and corresponding results for the carbon steel piping are documented in CEN-367-A.

5.2 EVALUATION CRITERIA

As will be discussed later, fracture mechanics analyses are made based on local failure mechanism as described in Section 7.1 and based on global failure mechanism as described in Section 7.2.

For local failure mechanism, stability analysis is performed using J-integral evaluation method with the criteria as follows:

(1) If $J_{app} < J_{Ic}$; then the crack will not initiate, and the crack is stable;

(2) If $J_{app} \geq J_{Ic}$; and $T_{app} < T_{mat}$ and $J_{app} < J_{max}$, then the crack is stable.

where:

J_{app} = Applied J
J_{Ic} = J at Crack Initiation
T_{app} = Applied Tearing Modulus
T_{mat} = Material Tearing Modulus
J_{max} = Maximum J value of the material

For global failure mechanism, the stability analysis is performed using limit load method based on loads and postulated flaw sizes related to leakage, with the criteria as follows:

- Margin of 10 on the Leak Rate
- Margin of 2.0 on Flaw Size
- Margin of $\sqrt{2}$ on Loads, using (|P+NOP|+|SSE|)x($\sqrt{2}$) for faulted load combination.

Table 5-1. Critical Analysis Locations for St. Lucie Units 1 and 2 RCL Lines

Weld Pts.	D_o Pipe (in)	Thickness (in)	Welding Process	Operating Pressure (psia)	Operating Temperature (°F)	Maximum Faulted Stress (psi)
6	36.063	3.031	SAW	2250	550.6	26510 (Unit 1)
7	36.063	3.031	SAW	2250	551.0	20872 (Unit 1)
6	36.125	3.063	SAW	2250	550.6	26208 (Unit 2)
7	36.125	3.063	SAW	2250	551.0	20636 (Unit 2)

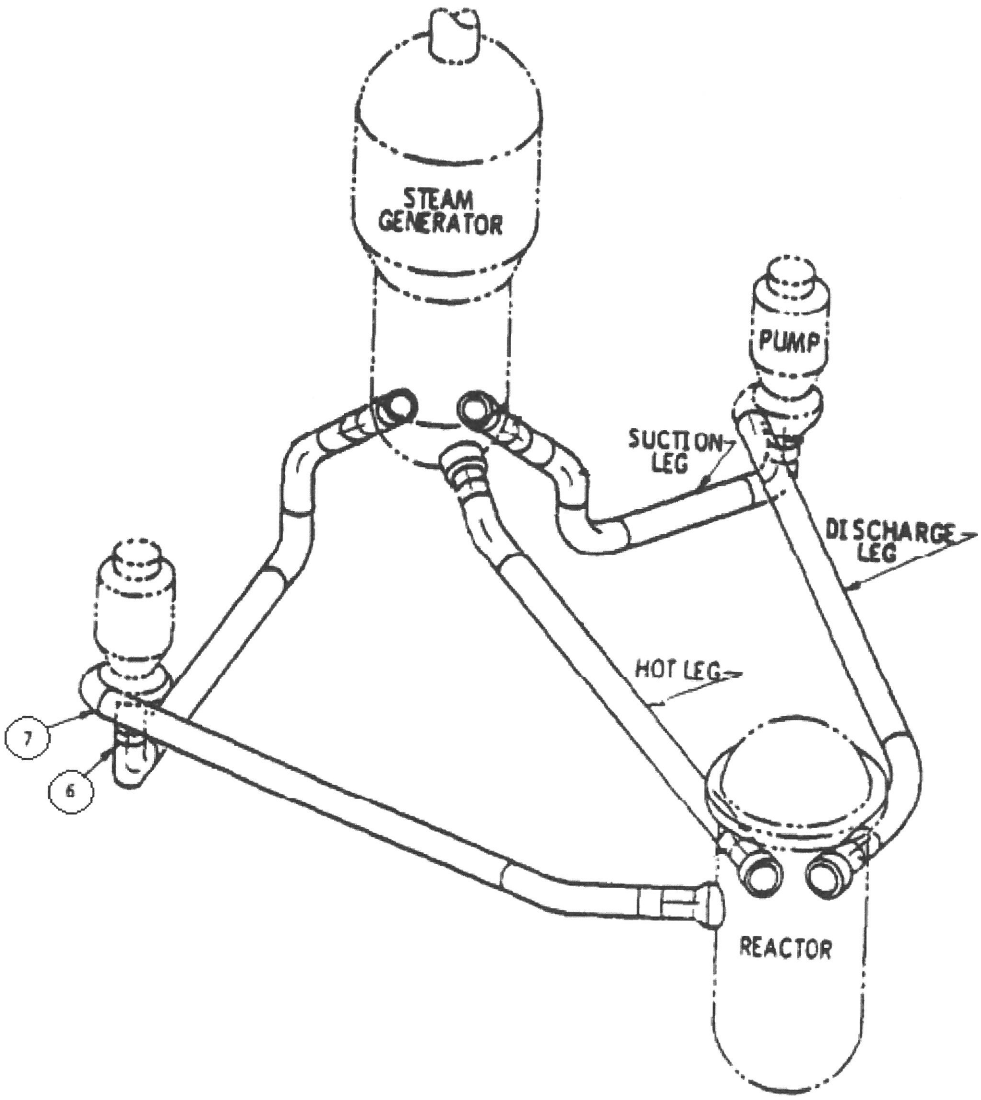

Figure 5-1. Schematic Diagram of St. Lucie Units 1 and 2 Primary Loop Showing RCP Nozzle Critical Analyzed Weld Locations

6 LEAK RATE PREDICTIONS

6.1 INTRODUCTION

The purpose of this section is to discuss the method which is used to predict the flow through postulated through-wall cracks and present the leak rate calculation results for through-wall circumferential cracks.

6.2 GENERAL CONSIDERATIONS

The flow of hot pressurized water through an opening to a lower back pressure causes flashing which can result in choking. For long channels where the ratio of the channel length, L, to hydraulic diameter, D_H, (L/D_H) is greater than [

]^{a,c,e}

6.3 CALCULATION METHOD

The basic method used in the leak rate calculations is the method developed by [

]^{a,c,e}

The flow rate through a crack was calculated in the following manner. Figure 6-1 from Reference 6-2 was used to estimate the critical pressure, P_c, for the primary loop enthalpy condition and an assumed flow. Once P_c was found for a given mass flow, the [ ]^{a,c,e} was found from Figure 6-2 (taken from Reference 6-2). For all cases considered, since [ ]^{a,c,e} Therefore, this method will yield the two-phase pressure drop due to momentum effects as illustrated in Figure 6-3, where P_o is the operating pressure. Now using the assumed flow rate, G, the frictional pressure drop can be calculated using

$$\Delta P_f = [\qquad]^{a,c,e} \tag{6-1}$$

where the friction factor f is determined using the [ ]^{a,c,e} The crack relative roughness, ε, was obtained from fatigue crack data on stainless steel samples. The relative roughness value used in these calculations was [ ]^{a,c,e}

The frictional pressure drop using equation 6-1 is then calculated for the assumed flow rate and added to the [ ]^{a,c,e} to obtain the total pressure drop from the primary system to the atmosphere. That is, for the primary loop:

$$\text{Absolute Pressure} - 14.7 = [\qquad]^{a,c,e} \tag{6-2}$$

for a given assumed flow rate G. If the right-hand side of equation 6-2 does not agree with the pressure difference between the primary loop and the atmosphere, then the procedure is repeated until equation 6-2 is satisfied to within an acceptable tolerance which in turn leads to flow rate value for a given crack size.

6.4 LEAK RATE CALCULATIONS

Leak rate calculations were made as a function of crack length at the governing locations previously identified in Section 5.1. The normal operating loads of Table 3-1 and Table 3-2 were applied in these calculations. The crack opening areas were estimated using the method of Reference 6-3, and the leak rates were calculated using the two-phase flow formulation described in the preceding section. The average material properties of Section 4 (see Table 4-3 for CF8M and Table 4-4 for 82/182 welds) were used for these calculations.

The flaw sizes to yield a leak rate of 10 gpm are calculated for the RCL Lines at the critical locations. The flaw sizes, so determined, are called leakage flaw sizes and are shown in Table 6-1 for Units 1 and 2 CASS material and Table 6-2 for Units 1 and 2 alloy 82/182 weld material. Based on the PWSCC crack morphology, a conservative factor of 1.69 between the PWSCC and fatigue crack morphologies (Reference 6-4) is applied the leakage flaw sizes for the alloy 82/182 material in Table 6-2.

The St. Lucie Units 1 and 2 RCS pressure boundary leak detection system capability is 1 gpm. Thus, to satisfy the margin of 10 on the leak rate, the flaw sizes (leakage flaw sizes) (crack lengths) are determined which yield a leak rate of 10 gpm.

6.5 REFERENCES

6-1 [ ][a,c,e]

6-2 M. M, El-Wakil, "Nuclear Heat Transport, International Textbook Company," New York, N.Y, 1971.

6-3 Tada, H., "The Effects of Shell Corrections on Stress Intensity Factors and the Crack Opening Area of Circumferential and a Longitudinal Through-Crack in a Pipe," Section II-1, NUREG/CR-3464, September 1983.

6-4 D. Rudland, R. Wolterman, G. Wilkowski, R. Tregoning, "Impact of PWSCC and Current Leak Detection on Leak-Before-Break," proceedings of Conference on Vessel Head Penetration, Inspection, Cracking, and Repairs, Sponsored by USNRC, Marriot Washingtonian Center, Gaithersburg, MD, September 29 to October 2, 2003. *(NRC ADAMS Accession Number ML052370273)*

Table 6-1. Flaw Sizes for St. Lucie Units 1 and 2 Yielding a Leak Rate of 10 gpm for the Critical Analysis Locations with A351-CF8M CASS Material

Weld Points	Leakage Flaw Size (in)
6	5.96 (Unit 1)
	6.02 (Unit 2)
7	8.03 (Unit 1)
	8.10 (Unit 2)

Table 6-2. Flaw Sizes for St. Lucie Units 1 and 2 Yielding a Leak Rate of 10 gpm for the Critical Analysis Locations with Alloy 82/182 Welds

Weld Points	Leakage Flaw Size (in)	Apply 1.69 Factor (in)
6	6.97 (Unit 1)	11.78 (Unit 1)
	7.03 (Unit 2)	11.88 (Unit 2)
7	8.90 (Unit 1)	15.04 (Unit 1)
	8.96 (Unit 2)	15.14 (Unit 2)

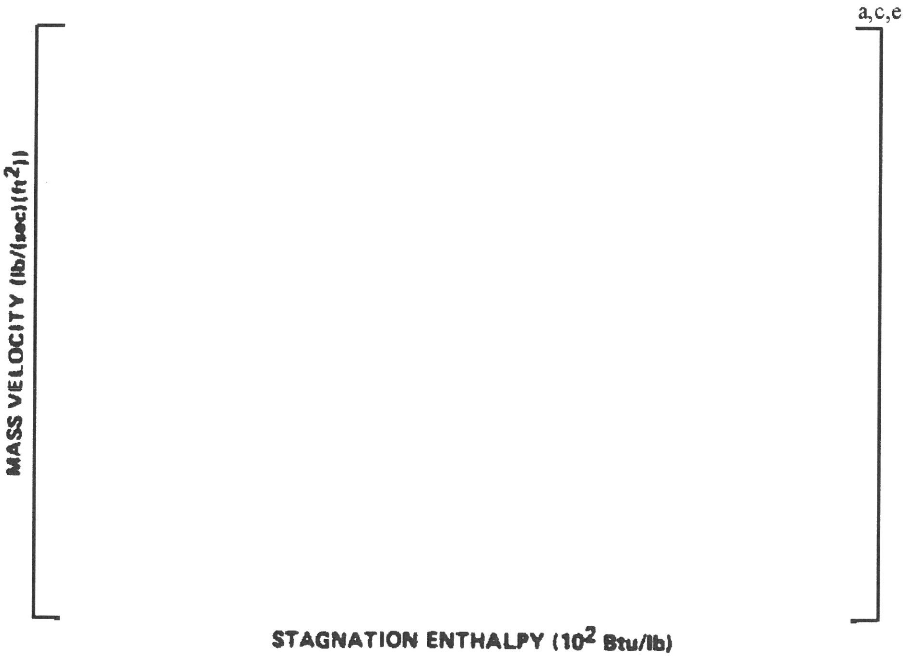

Figure 6-1. Analytical Predictions of Critical Flow Rates of Steam-Water Mixtures

Figure 6-2. [ ]^{a,c,e} Pressure Ratio as a Function of L/D

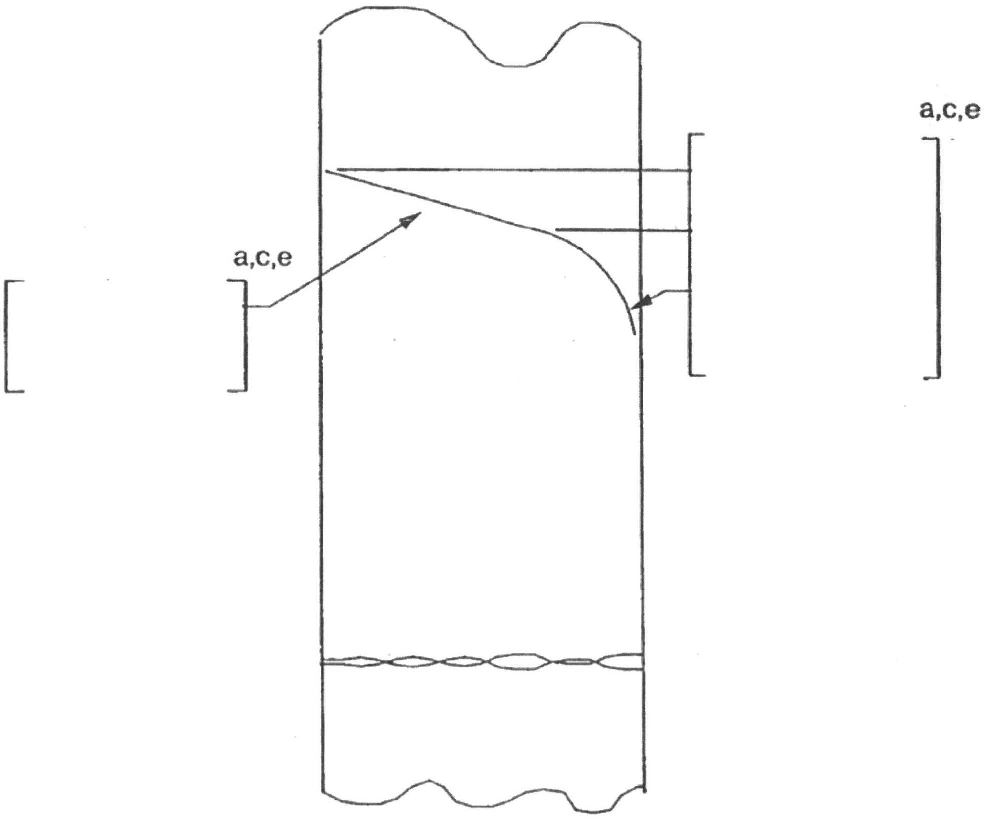

Figure 6-3. Idealized Pressure Drop Profile Through a Postulated Crack

7 FRACTURE MECHANICS EVALUATION

7.1 LOCAL FAILURE MECHANISM

The local mechanism of failure is primarily dominated by the crack tip behavior in terms of crack-tip blunting, initiation, extension, and final crack instability. The local stability will be assumed if the crack does not initiate at all. It has been accepted that the initiation toughness measured in terms of J_{Ic} from a J-integral resistance curve is a material parameter defining the crack initiation. If, for a given load, the calculated J-integral value is shown to be less than the J_{Ic} of the material, then the crack will not initiate. If the initiation criterion is not met, one can calculate the tearing modulus as defined by the following relation:

$$T_{app} = \frac{dJ}{da} x \frac{E}{\sigma_f^2} \tag{7-1}$$

where:

T_{app}	=	applied tearing modulus
E	=	modulus of elasticity
σ_f	=	$0.5\ (\sigma_y + \sigma_u)$ = flow stress
a	=	crack length
σ_y, σ_u	=	yield and ultimate strength of the material, respectively

Stability is said to exist when ductile tearing does not occur if T_{app} is less than T_{mat}, the experimentally determined tearing modulus. Since a constant T_{mat} is assumed a further restriction is placed in J_{app}. J_{app} must be less than J_{max} where J_{max} is the maximum value of J for which the experimental T_{mat} is greater than or equal to the T_{app} used.

As discussed in Section 5.2 the local crack stability criteria is a two-step process:

(1) If $J_{app} < J_{Ic}$, then the crack will not initiate, and the crack is stable;

(2) If $J_{app} \geq J_{Ic}$; and $T_{app} < T_{mat}$ and $J_{app} < J_{max}$, then the crack is stable.

The calculations of J_{app} and T_{app} values for the critical locations are performed following the methodology developed in References 7-2 and 7-3. The stability results based on elastic-plastic J-integral evaluations for St. Lucie Units 1 and 2 are provided in Table 7-1.

7.2 GLOBAL FAILURE MECHANISM

Determination of the conditions which lead to failure in stainless steel should be done with plastic fracture methodology because of the large amount of deformation accompanying fracture. One method for predicting the failure of ductile material is the plastic instability method, based on traditional plastic limit load concepts, but accounting for strain hardening and taking into account the presence of a flaw. The flawed pipe is predicted to fail when the remaining net section reaches a stress level at which a plastic hinge is formed. The stress level at which this occurs is termed as the flow stress. The flow stress is generally taken as the average of the yield and ultimate tensile strength of the material at the temperature of interest. This methodology has been shown to be applicable to ductile piping through a large number of experiments and will be used here to predict the critical flaw size in the primary coolant piping. The failure criterion has been obtained by requiring equilibrium of the section containing the flaw (Figure 7-1) when loads are applied. The detailed development is provided in Appendix A for a through-wall circumferential flaw in a pipe with internal pressure, axial force, and imposed bending moments. The limit moment for such a pipe is given by:

[

]^{a,c,e}

The analytical model described above accurately accounts for the piping internal pressure as well as imposed axial force as they affect the limit moment. Good agreement was found between the analytical predictions and the experimental results (Reference 7-1). For application of the limit load methodology, the material, including consideration of the configuration, must have a sufficient ductility and ductile tearing resistance to sustain the limit load.

A stability analysis based on limit load is performed to determine the critical flaw size. For the RCL Lines of St. Lucie Units 1 and 2, the SAW weld processes are conservatively assumed to be used for the CF8M CASS material. The "Z" correction factor (References 7-4 and 7-5) for SAW is as follows:

$$Z = 1.30\ [1.0 + 0.01\ (OD\text{-}4)] \qquad \text{for SAW} \qquad (7\text{-}4)$$

where OD is the outer diameter of the pipe in inches.

The Z-factors were calculated for the critical locations, using the dimensions given in Tables 3-1 and 3-2. The applied loads were increased by the Z factors. Table 7-2 and Table 7-3 summarizes the results of the stability analyses based on limit load. The leakage flaw sizes are also presented on the same table.

St. Lucie Units 1 and 2 reactor coolant system primary loop piping contains alloy 82/182 dissimilar metal welds which are susceptible to PWSCC. Locations of the alloy 82/182 welds are at the RCP Suction nozzles (locations 6 and 12) and RCP Discharge nozzles (locations 7 and 13). However, critical analysis locations are determined to be locations 6 and 7 for both Units 1 and 2, as shown in Figure 5-1.

The alloy 82/182 welds have not been mitigated to prevent PWSCC. For the SLR program, the RCP alloy 82/182 welds are evaluated for the postulated circumferential flaws.

Alloy 82/182 material has high toughness (see MRP-140 Section 3.1.1, Reference 7-6), similar to stainless steel weld materials and Tungsten Inert Gas (TIG) welds, limit load behavior is assured, such that no weld process Z-factors need be considered in computing critical flaw sizes. [

]a,c,e

In conclusion, the existence of alloy 82/182 welds at St. Lucie Units 1 and 2 RCP Suction and Discharge nozzles are acceptable for the SLR program (for 80 years of plant operation).

7.3 REFERENCES

7-1 Kanninen, M. F., et al., "Mechanical Fracture Predictions for Sensitized Stainless Steel Piping with Circumferential Cracks," EPRI NP-192, September 1976.

7-2 [
]a,c,e

7-3 [
] a,c,e

7-4 Standard Review Plan; Public Comment Solicited; 3.6.3 Leak-Before-Break Evaluation Procedures; Federal Register/Vol. 52, No. 167/Friday, August 28, 1987/Notices, pp. 32626-32633.

7-5 NUREG-0800 Revision 1, March 2007, Standard Review Plan: 3.6.3 Leak-Before-Break Evaluation Procedures.

7-6 Materials Reliability Program: Leak-Before-Break Evaluation for PWR Alloy 82/182 Welds (MRP-140). EPRI, 1011808, November 2005.

7-7 ASME Pressure Vessel and Piping Division Conference Paper PVP2008-61840, "Technical Basis for Revision to Section XI Appendix C for Alloy 600/82/182/132 Flaw Evaluation in Both PWR and BWR Environments," July 28-31, Chicago IL, USA.

Table 7-1. Flaw Stability Results for St. Lucie Units 1 and 2 the Critical Analysis Locations Based on J-Integral Evaluations and CASS Thermal Aging

a,c,e

Table 7-2. Flaw Stability Results for St. Lucie Units 1 and 2 Yielding a Leak Rate of 10 gpm for the Critical Analysis Locations with A351-CF8M CASS Material

Weld Points	Leakage Flaw Size (in)	Critical Flaw Size (in)
6	5.96 (Unit 1)	18.86 (Unit 1)
	6.02 (Unit 2)	19.26 (Unit 2)
7	8.03 (Unit 1)	24.73 (Unit 1)
	8.10 (Unit 2)	25.09 (Unit 2)

Table 7-3. Flaw Stability Results for St. Lucie Units 1 and 2 Yielding a Leak Rate of 10 gpm for Critical Analysis Locations with Alloy 82/182 Welds

Weld Points	Leakage Flaw Size (in)	Critical Flaw Size (in)
6	11.78 (Unit 1)	38.48 (Unit 1)
	11.88 (Unit 2)	38.80 (Unit 2)
7	15.04 (Unit 1)	42.35 (Unit 1)
	15.14 (Unit 2)	42.64 (Unit 2)

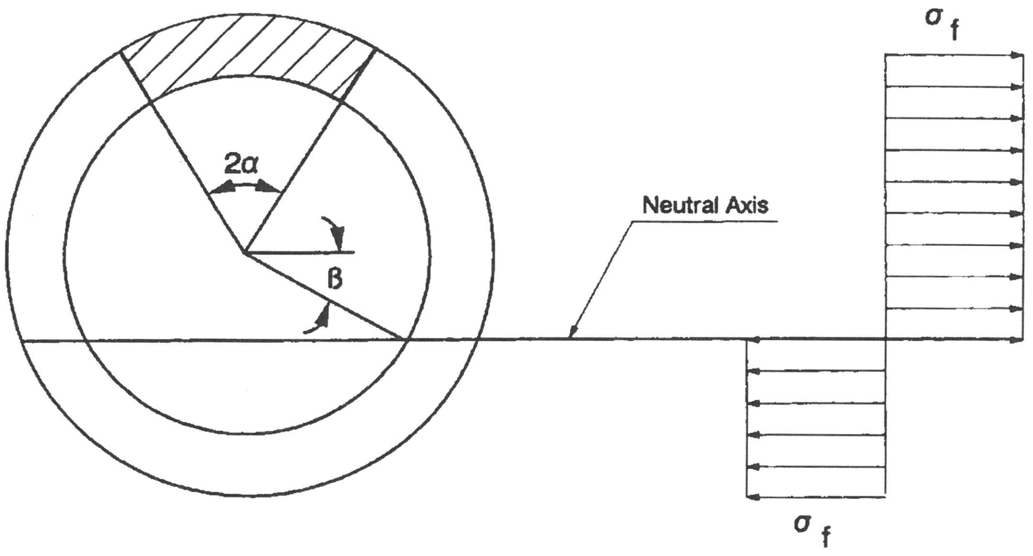

Figure 7-1. [ ]a,c,e Stress Distribution

8 FATIGUE CRACK GROWTH ANALYSIS

To determine the sensitivity of the primary coolant system to the presence of small cracks, a fatigue crack growth analysis has been performed in CEN-367-A (Reference 8-1) representative of St. Lucie hot leg (3.75" wall thickness) and cold leg (2.5" wall thickness) pipe regions. The calculated crack growth at the hot leg and cold leg will be typical of that in the entire primary loop. Crack growths calculated at other locations can be expected to show minimal variation.

St. Lucie hot leg and cold leg pipe is made of carbon steel material. The results of fatigue crack growth analysis are repeated in Table 8-2. The results indicate that the crack growth is insignificant for the calculated operating life.

Another fatigue crack growth (FCG) along with PWSCC growth analysis has been performed for St. Lucie RCP discharge nozzle dissimilar metal welds . The evaluated region is at the nozzle to safe-end weld that is made of alloy 82/182 material. The calculated crack growth at the RCP discharge will be typical of that in RCP discharge and suction nozzles. The results of FCG and PWSCC growth analysis are provided in Table 8-3. Based on Table 8-3, it can be shown that the conservative approximations of crack growth takes [ ]a,c,e before it reaches the RCP discharge nozzle outside diameter. The results indicate that the crack growth is very slow.

Fatigue crack growth rate laws were used from the ASME Section XI, Appendix A (Reference 8-2) for the carbon steel. For Alloy 82/182, PWSCC growth rate formula were used from EPRI (Reference 8-3) and FCG formula from NUREG/CR-6721 (Reference 8-4).

For carbon steel FCG analysis results (Table 8-2), the fatigue crack growth was analyzed using the following formula (Reference 8-1),

$$da/dn = c(\Delta K_I)^n \qquad \text{Eq. 8-1}$$

where:

c	=	a scaling constant = 1.95×10^{-7} to 7.88×10^{10} (Reference 8-1)
n	=	1.95 to 5.95 (Reference 8-1)
ΔK_I	=	range of stress intensity factor
da/dn	=	crack growth rate

For the Alloy 82-182, the combined PWSCC and FCG analysis results in Table 8-3 were calculated using the following PWSCC growth formula:

a,c,e

[ ]

a,c,e

[ ]

and the following the FCG formula, for Alloy 82/182 material in PWR environments:

a,c,e

[ ]

[ ]a,c,e

Based on the results reported in (Reference 8-4), the parameters for the FCG rate curve for Alloy 82/182 material are:

a,c,e

[ ]

a,c,e

[ ]

[

]a,c,e is shown in Figure 8-1.

Since it has been concluded that the fatigue crack growth for St. Lucie will not cause degradation of pressure boundary integrity for the operating service life and the crack growth will be very slow, the conclusion of the existing FCG analysis (Reference 8-1) and FCG+PWSCC analysis of the DM weld need to be reviewed to ensure that conclusions remain valid for 80-year service.

The enveloping design loading conditions for St. Lucie are unchanged from 40-year to 80-year service, except the plant specific transient and its cycles. However, CEN-367-A (Reference 8-1) has used generic design basis transient cycles that envelope the projected 80-year transient cycles listed in Table 8-1, to calculate the crack growth as provided in Table 8-2.

By comparing the St. Lucie plant specific transients and cycles presented in Table 8-1 against the FCG transient inputs, it is evident that the existing analyses envelope the design data for 80 years of St. Lucie plant service. If there are slight changes in the cycles for the 80-year design transients, they will not have a significant impact on the fatigue crack growth conclusions, since there is insignificant growth of small surface flaws as shown in Table 8-2.

It is, therefore, concluded that the generic fatigue crack growth analysis results as shown in Table 8-2 and the combined PWSCC growth and FCG analysis results as in Table 8-3 are representative of the St. Lucie plants fatigue crack growth and is applicable for 80 years.

Along with the above conclusion, the fatigue crack growth analysis is not a requirement for the LBB analysis (see References 8-5 and 8-6) since the LBB analysis is based on the postulation of through-wall flaws, whereas the FCG analysis is performed based on a surface flaw. In addition, Reference 8-7 has indicated that, "the Commission deleted the fatigue crack growth analysis in the proposed rule. This requirement was found to be unnecessary because it was bounded by the crack stability analysis." This evaluation of FCG is presented as a defense-in-depth justification in support of the demonstration of LBB.

The FCG evaluation results of the representative Reactor Coolant Loop (RCL) piping lines are presented in Table 8-2 and Table 8-3. Beyond showing that small surface flaws in the carbon steel piping material would not develop to through-wall flaw, the FCG evaluation also demonstrates that the growth of a flaw will be very slow. These results support the justification that flaw growth would be insignificant in between the time when leakage reaches 10 gpm and the time that the plant would be shutdown. Based on this justification, it is concluded that fatigue crack growth is not a concern for the St. Lucie Units 1 and 2 Reactor Coolant Loop piping lines.

8.1 REFERENCES

8-1 Westinghouse Report, CEN-367-A, Rev. 000, "Leak-Before-Break Evaluation of Primary Coolant Loop Piping in Combustion Engineering Designed Nuclear Steam Supply Systems," February 1991.

8-2 ASME Boiler and Pressure Vessel Code Section XI, 1986 Edition.

8-3 Materials Reliability Program: Crack Growth Rates for Evaluating Primary Water Stress Corrosion Cracking (PWSCC) of Alloy 82, 182, and 132 Welds (MRP-115), Electric Power Research Institute, Palo Alto, CA: September 2004. 1006696.

8-4 NUREG/CR-6721, ANL-01/07, "Effects of Alloy Chemistry, Cold Work, and Water Chemistry on Corrosion Fatigue and Stress Corrosion Cracking of Nickel Alloys and Welds," U.S. Nuclear Regulatory Commission, April 2001.

8-5 Standard Review Plan: Public Comments Solicited; 3.6.3 Leak-Before-Break Evaluation Procedures; Federal Register/Vol. 52, No. 167/Friday August 28, 1987/Notices, pp. 32626-32633.

8-6 NUREG-0800, Revision 1, "Standard Review Plan: 3.6.3 Leak-Before-Break Evaluation Procedures," March 2007.

8-7 Nuclear Regulatory Commission, 10 CFR 50, Modification of General Design Criteria 4 Requirements for Protection Against Dynamic Effects of Postulated Pipe Ruptures, Final Rule, Federal Register/Vol. 52, No. 207/Tuesday, October 27, 1987/Rules and Regulations, pp. 41288-41295.

Table 8-1. Summary of Transients (Representative 80-year Design)

Number	Typical Transient Identification	Number of Cycles					
		Carbon Steel	Alloy 82/182	Design Basis		80-year Projections	
				Unit 1	Unit 2	Unit 1	Unit 2
1	Plant Heatup 100°F/hr	500	500	500	120	143	124
2	Plant Cooldown 100°F/hr	500	500	500	120	141	123
3	Plant Loading 5%/min (1)	15000	15000	N/A	N/A	N/A	N/A
4	Plant Unloading 5%/min (1)	15000	15000	N/A	N/A	N/A	N/A
5	Normal Plant Variation (± 100 psi, ± 10°F) (2)	1000000	1000000	N/A	N/A	N/A	N/A
6	Leak Test, 2250 psi @ 100-400°F	200	N/A	200	30	2	5
7	Reactor Trip	400	400	400	400	106	72
8	Loss of Turbine Generator Load	40	40	40	40	6	3
9	Loss of Reactor Coolant Flow	40	40	40	40	2	2
10	Loss of Secondary Pressure	5	N/A	5	5	2	2

Notes:

1. Large margins are present with respect to actual cycle counts versus allowable cycle counts, i.e. plant loading/unloading events are not monitored because St. Lucie Units 1 & 2 are not load following plants. Therefore, such events rarely occur, and projections are not calculated.
2. The fatigue monitoring program for St. Lucie does not monitor Normal Plant Variation transients (also known as Steady State Fluctuations) because it produces negligible stress ranges that do not contribute to the fatigue crack growth.

Table 8-2. St. Lucie Fatigue Crack Growth at Hot and Cold Legs Carbon Steel Material

	Orientation	Assumed Initial Flaw Depth (in)	Computed Final Flaw Depth (in)	Final (a/t)
Hot Leg	Circumferential(1)	0.114	0.177	0.047
	Axial(2)	0.114	0.149	0.040
Cold leg	Circumferential(3)	0.110	0.161	0.064
	Axial(4)	0.110	0.157	0.063

Notes:
(1) See Figure 8-2
(2) See Figure 8-3
(3) See Figure 8-4
(4) See Figure 8-5

Table 8-3. Alloy 82/182 FCG and PWSCC Growth – Operating Time for a Surface Flaw to Grow Through-Wall

Assumed Initial Flaw		Operating Time (years)
Circumferential Length (%)	Depth (%)	
[		
		]a,c,e

Notes:
(1) See Figure 8-6
(2) See Figure 8-7

a,c,e

Figure 8-1. Alloy 82/182 Weld Fatigue Crack Growth Rate Properties in a PWR Environment

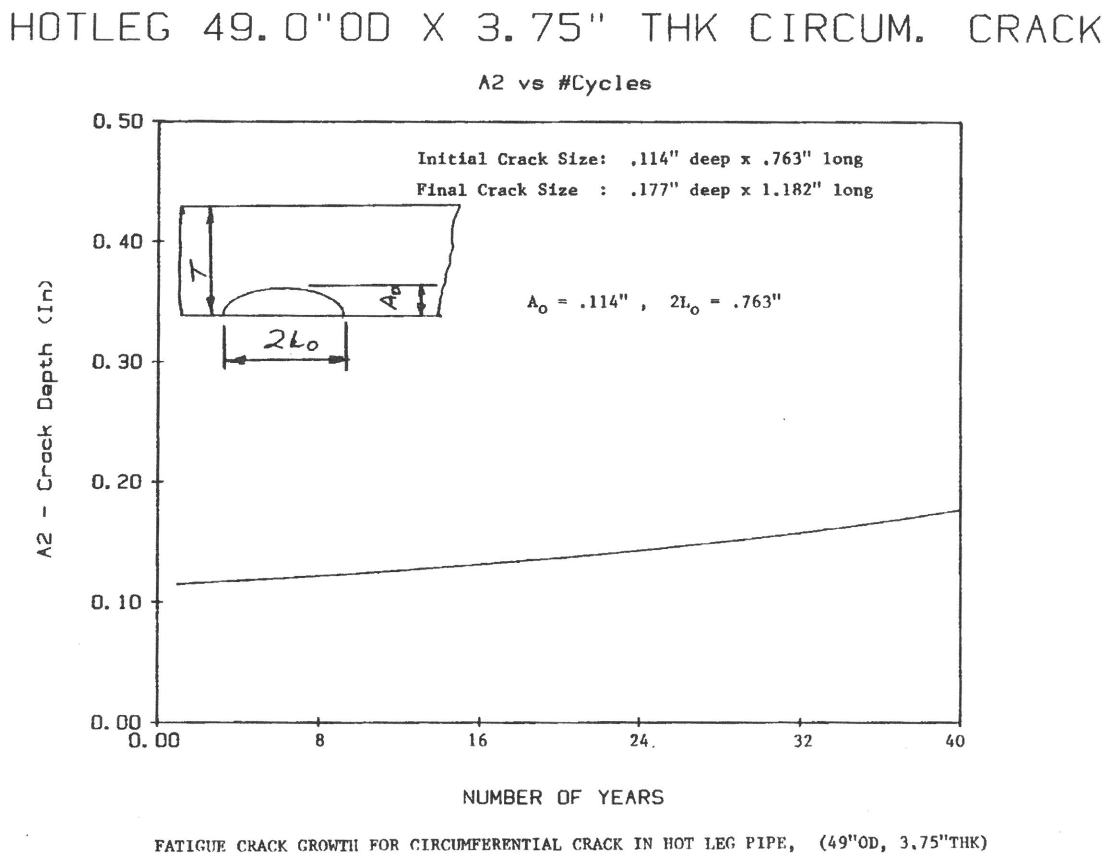

Figure 8-2. Hot Leg Circumferential Fatigue Crack Growth

Note: 40-year results are applicable for 80-years based on the transient comparisons in Table 8-1.

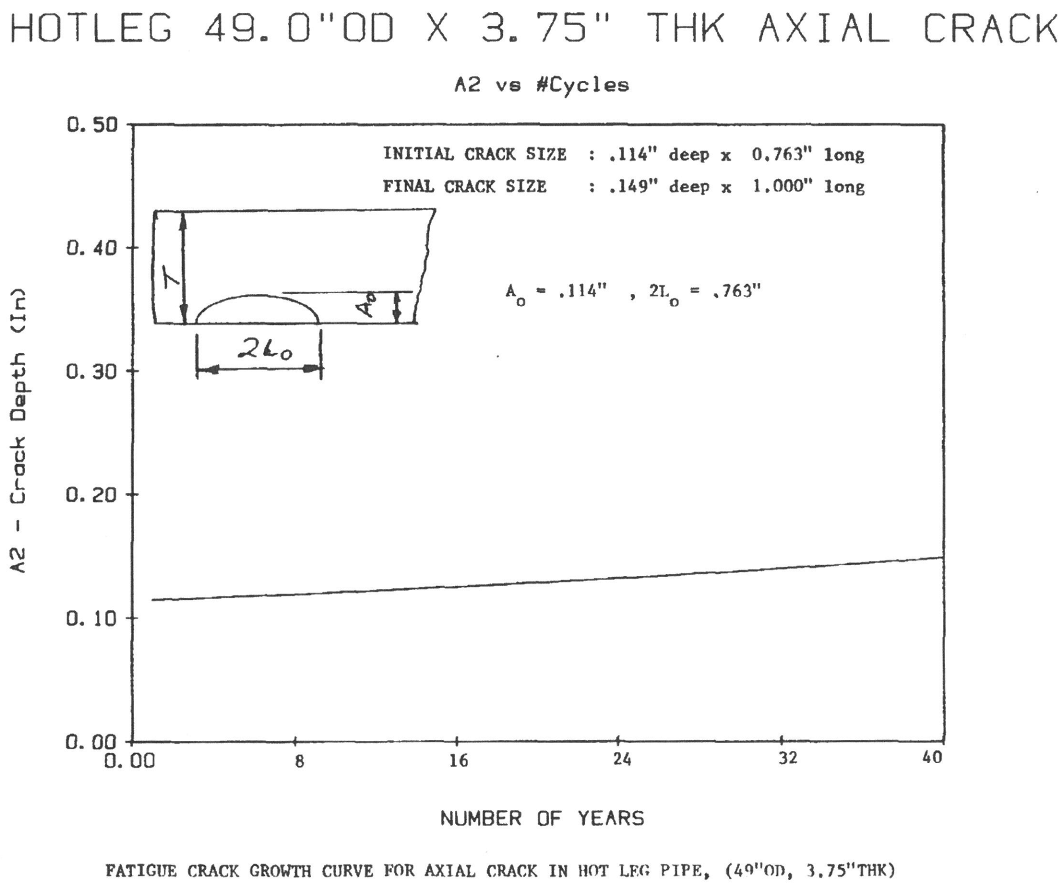

Figure 8-3. Hot Leg Axial Fatigue Crack Growth

Note: 40-year results are applicable for 80-years based on the transient comparisons in Table 8-1.

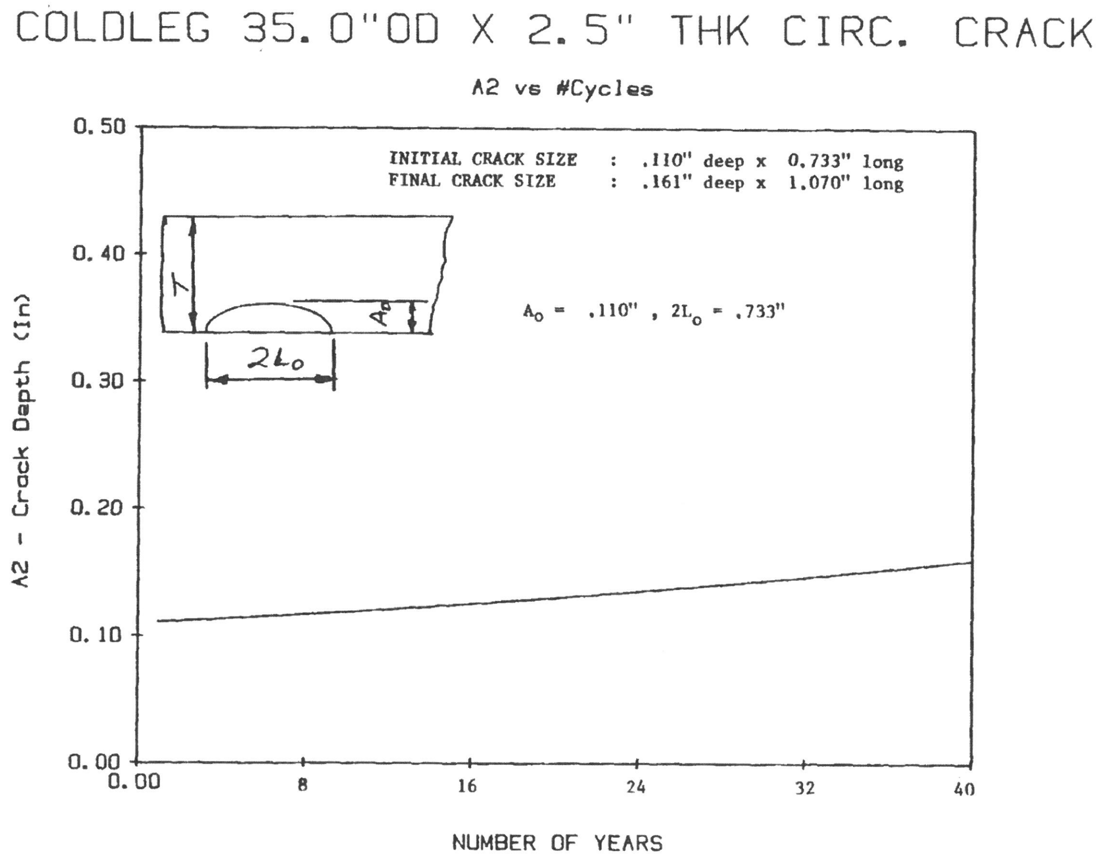

FATIGUE CRACK GROWTH CURVE FOR CIRCUMFERENTIAL CRACK IN COLD LEG PIPE, (35"OD, 2.5"THK)

Figure 8-4. Cold Leg Circumferential Fatigue Crack Growth

Note: 40-year results are applicable for 80-years based on the transient comparisons in Table 8-1.

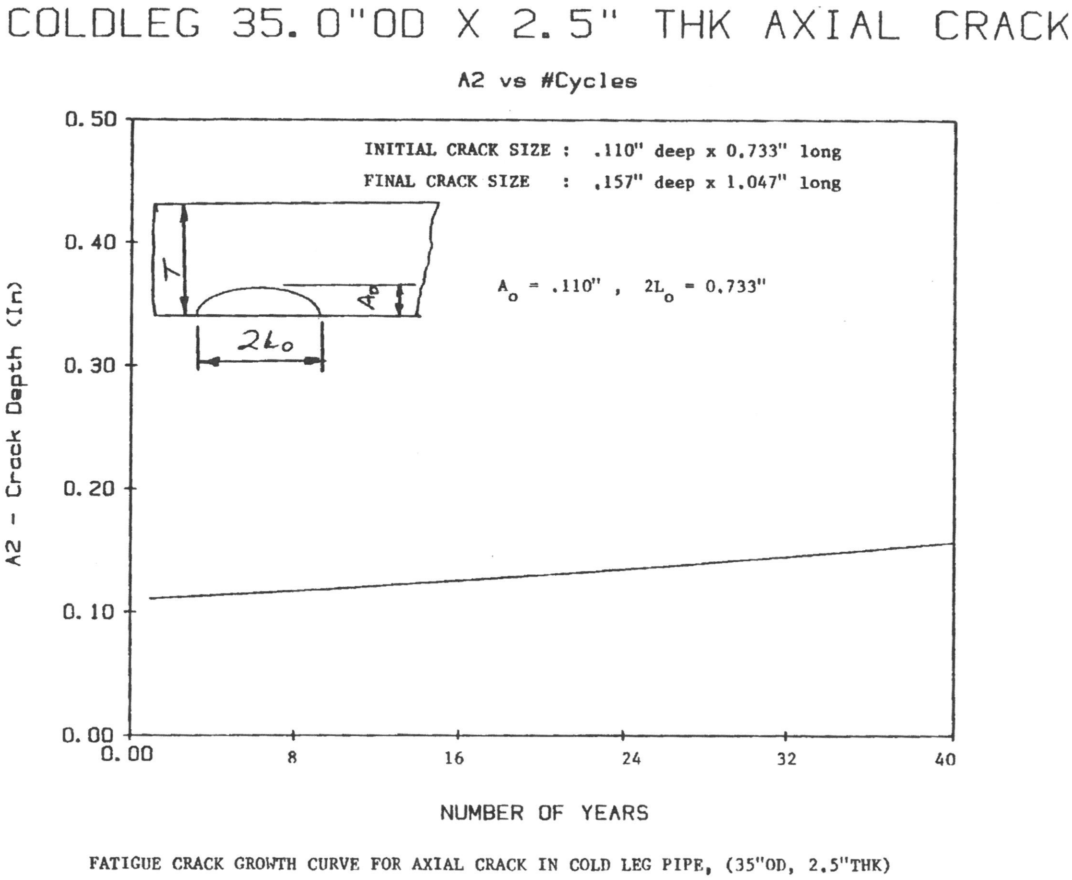

Figure 8-5. Cold Leg Axial Fatigue Crack Growth

Note: 40-year results are applicable for 80-years based on the transient comparisons in Table 8-1.

a,c,e

Figure 8-6. RCP Discharge Fatigue Crack Growth (23% Circumferential Length, 20% Depth)

a,c,e

Figure 8-7. RCP Discharge Fatigue Crack Growth (23% Circumferential Length, 30% Depth)

9 ASSESSMENT OF MARGINS

The results of the leak rates of Section 6.4 and the corresponding stability and fracture toughness evaluations of Sections 7.1 and 7.2 are used in performing the assessment of margins. Margins are shown in Table 9-1 and Table 9-2 for Units 1 and 2. All of the LBB recommended margins are satisfied. The LBB analyses results are acceptable for the subsequent license renewal program (80 years).

In summary, at all the critical locations relative to:

1. Flaw Size – Using faulted loads obtained by the absolute sum method, a margin of 2 or more exists between the critical flaw and the flaw having a leak rate of 10 gpm (the leakage flaw).

2. Leak Rate – A margin of 10 exists between the calculated leak rate from the leakage flaw and the plant leak detection capability of 1 gpm.

3. Loads – At the critical locations the leakage flaw was shown to be stable using the faulted loads obtained by the absolute sum method (i.e., a flaw twice the leakage flaw size is shown to be stable; hence the leakage flaw size is stable). A margin of 1 on loads using the absolute summation of faulted load combinations is satisfied.

Table 9-1. Leakage Flaw Sizes, Critical Flaw Sizes and Margins for St. Lucie Units 1 and 2 for Critical Analysis Locations with A351-CF8M CASS Material

Location	Leakage Flaw Size (in)	Critical Flaw Size (in)	Margin
6 (Unit 1)	5.96 in.	18.86[a] in.	3.16[a]
	5.96 in.	11.92[b] in.	>2.0[b]
7 (Unit 1)	8.03 in.	24.73[a] in.	3.08[a]
	8.03 in.	16.06[b] in.	>2.0[b]
6 (Unit 2)	6.02 in.	19.26[a] in.	3.20[a]
	6.02 in.	12.04[b] in.	>2.0[b]
7 (Unit 2)	8.10 in.	25.09[a] in.	3.10[a]
	8.10 in.	16.20[b] in.	>2.0[b]

[a]based on limit load

[b]based on J integral evaluation

Table 9-2. Leakage Flaw Sizes, Critical Flaw Sizes and Margins for St. Lucie Units 1 and 2 for Critical Analysis Locations with Alloy 82/182 Welds

Location	Leakage Flaw Size (in)*	Critical Flaw Size (in)	Margin
6 (Unit 1)	11.78	38.48	3.3
7 (Unit 1)	15.04	42.35	2.8
6 (Unit 2)	11.88	38.80	3.3
7 (Unit 2)	15.14	42.64	2.8

*Based on a conservative factor of 1.69 PWSCC crack morphology

10 CONCLUSIONS

This report justifies the elimination of RCS primary loop pipe breaks from the structural design basis for the 80-year plant life of St. Lucie Units 1 and 2 as follows:

a. Stress corrosion cracking is precluded by use of fracture resistant materials in the piping system and controls on reactor coolant chemistry, temperature, pressure, and flow during normal operation. Alloy 82/182 welds are present at the St. Lucie Unit 1 and Unit 2 RCP Suction and Discharge Nozzles. The alloy 82/182 welds are susceptible to PWSCC (Primary Water Stress Corrosion Cracking) and have been conservatively evaluated to consider the effects of PWSCC.

b. As stated in Section 3, for global failure mechanisms, all locations are evaluated using the limiting material properties. For local failure mechanisms, all locations are evaluated using the A351-CF8M cast stainless steel material properties which present a limiting condition due to the thermal aging effects.

c. Evaluation of the RCS piping considering the thermal aging effects for the 80-year plant life period of the SLR program and also the use of the most limiting fracture toughness properties ensures that each materials profile is appropriately bounded by the LBB results presented in this report.

d. Water hammer should not occur in the RCS piping because of system design, testing, and operational considerations.

e. The effects of low and high cycle fatigue on the integrity of the primary piping are negligible.

f. Ample margin exists between the leak rate of small stable flaws and the capability of the St. Lucie Units 1 and 2 reactor coolant system pressure boundary Leakage Detection System.

g. Ample margin exists between the small stable flaw sizes of item (f) and larger stable flaws.

h. Ample margin exists in the material properties used to demonstrate end-of-service life (fully aged) stability of the critical flaws.

For the critical locations, flaws are identified that will be stable because of the ample margins described in f, g, and h above.

The LBB analysis results for RCP Suction and Discharge nozzle safe-end locations are acceptable for A351-CF8M CASS material from thermal aging effect and for Alloy 82/182 DM weld material from PWSCC effect. All the LBB criteria are satisfied.

The results for the RCL remaining locations not evaluated herein remain bounded by the Analysis of Record, CEN-367-A (Reference 1-1).

It is therefore concluded that dynamic effects of RCS primary loop pipe breaks need not be considered in the structural design basis for St. Lucie Units 1 and 2 Nuclear Power Plants for the 80-year plant life (subsequent license renewal program). With the elimination of the RCS primary loop pipe breaks, it is expected that the next most limiting break sizes would be associated with the larger auxiliary piping systems, e.g., the 12-inch Pressurizer Surge Line, Safety Injection Tank Line, or Shutdown Cooling Line.

APPENDIX A
LIMIT MOMENT

[

]a,c,e

a,c,e

Figure A-1. Pipe with a Through-Wall Crack in Bending

Approval Information
Author Approval Delport Gerrie W Jun-03-2021 10:17:13
Reviewer Approval Wiratmo Momo Jun-03-2021 12:20:17
Manager Approval Patterson Lynn Jun-03-2021 12:40:29

Files approved on Jun-03-2021

Enclosure 4

Non-proprietary Reference Documents and Redacted Versions of Proprietary Reference Documents (Public Version)

Attachment 11

Westinghouse Report LTR-SDA-20-097-NP, Revision 2, St. Lucie Units 1 & 2 Subsequent License Renewal: Alloy 600 Half Nozzle Repair Flaw Evaluation, May 5, 2021

(23 Total Pages, including cover sheets)

Westinghouse Non-Proprietary Class 3

LTR-SDA-20-097-NP, Revision 2

St. Lucie Units 1 & 2 Subsequent License Renewal: Alloy 600 Half Nozzle Repair Flaw Evaluation

May 2021

Author: Xiaolan Song*, RV/CV Design & Analysis

Verifiers: B. Reddy Ganta*, Structural Design & Analysis

Reviewer: Gordon Z. Hall*, Structural Design & Analysis

Manager: Stephen P. Rigby*, Structural Design & Analysis

Forward

This document contains Westinghouse Electric Company LLC proprietary information and data which has been identified by brackets. Coding (a,c,e) associated with the brackets sets forth information which is considered proprietary.

The proprietary information and data contained within the brackets in this report were obtained at considerable Westinghouse expense and its release could seriously affect our competitive position. This information is to be withheld from public disclosure in accordance with the Rules of Practice 10 CFR 2.390 and the information presented herein is safeguarded in accordance with 10 CFR 2.390. Withholding of this information does not adversely affect the public interest.

This information has been provided for your internal use only and should not be released to persons or organizations outside the Directorate of Regulation and the Advisory Committee on Reactor Safeguards (ACRS) without the express written approval of Westinghouse Electric Company LLC. Should it become necessary to release this information to such persons as part of the review procedure, please contact Westinghouse Electric Company LLC, which will make the necessary arrangements required to protect the Company's proprietary interests.

Several locations in this topical report contain proprietary information. Proprietary information is identified and bracketed. For each of the bracketed locations, the reason for the proprietary classification is provided, using a standardized system. The proprietary brackets are labeled with three (3) different letters, "a", "c", and "e" which stand for:

a. The information reveals the distinguishing aspects of a process or component, structure, tool, method, etc. The prevention of its use by Westinghouse's competitors, without license from Westinghouse, gives Westinghouse a competitive economic advantage.

c. The information, if used by a competitor, would reduce the competitor's expenditure of resources or improve the competitor's advantage in the design, manufacture, shipment, installation, assurance of quality, or licensing of a similar product.

e. The information reveals aspects of past, present, or future Westinghouse- or customer-funded development plans and programs of potential commercial value to Westinghouse.

1.0 Introduction

Small diameter Alloy 600 nozzles, such as pressurizer and Reactor Coolant System hot-leg instrumentation nozzles in Combustion Engineering (CE) designed pressurized water reactors (PWR) have developed leaks or partial through-wall cracks as a result of primary water stress corrosion cracking (PWSCC). The residual stresses imposed by the partial-penetration "J" welds between the nozzles and the low alloy or carbon steel pressure boundary components are the driving force for crack initiation and propagation.

St. Lucie Units 1 and 2 have experienced instances of Alloy 600 instrument nozzle leakage over the design life of the plants. Therefore, repair has been done to the alloy 600 small bore nozzles for both St. Lucie Units 1 and 2 by relocating the partial penetration attachment weld from the interior surface of the pipe or pressurizer to the outside surface of the pipe or pressurizer. Preventative repairs were also preformed to prevent the leakage. Table 1 of L-2018-027 [1] and L-2014-252 [2] summarize the alloy 600 small bore nozzle repairs for St. Lucie Unit 1 and Unit 2, respectively. These tables are reproduced in Tables 1-1 and 1-2. Note that there are two methods of repair:

1) Half Nozzle Repair shown as Design A and Design B in Figure 1-1; In the half nozzle repair technique, the Alloy 600 nozzle is cut outboard of the partial-penetration weld and replaced with a short Alloy 690 nozzle section that is welded to the outside surface of the pressure boundary component. This repair leaves a short section of the original nozzle attached to the inside surface with the "J" weld.
2) Sleeve Repair shown as Design C and Design D in Figure 1-1; In the sleeve repair technique, the entire Alloy 600 nozzle is removed by machining and the bore diameter is slightly enlarged. An alloy 690 nozzle is inserted into the bore and rolled into place. A sleeve is placed between the Alloy 690 nozzle and the bore. The end of the sleeve at the interior surface of the piping or the pressurizer is either roll expanded or welded to the interior surface of the piping or pressurizer.

Alloy 600 small bore nozzle repairs were evaluated based on fracture mechanics analysis justifying the acceptability of indications in the "J" weld based on a conservative postulated flaw size and flaw growth considering the applicable design cycles. The evaluation was performed based on the fracture mechanics analysis provided in Combustion Engineering Owners Group (CEOG) Topical Report CE NPSD-1198-P [3] and WCAP-15973 [4 and 5].

Reports [3] and [4 and 5] provides a bounding flaw evaluation that covers all small diameter Alloy 600/690 nozzle repairs in accordance with ASME Section XI requirements. The flaw growth analysis included in the report assumes the total number of design cycles, consistent with the St. Lucie Units 1 and 2 Updated Final Safety Analysis Reports (UFSAR). The analyses associated with the flaw growth analysis of the Unit 1 and Unit 2 Alloy 600 instrument nozzle repairs was evaluated for St. Lucie Units 1 and 2 first license renewal application (see Subsection 4.6.4 of [6]) and determined to remain valid for the period of extended operation (i.e., 60 years design life), in accordance with 10 CFR 54.21(c)(1)(i).

The purpose of this letter is to reassess the Alloy 600 half nozzle repairs for the St. Lucie Units 1 and 2 subsequent license renewal (SRL) including the following topics, in accordance with the request in USNRC Safety Evaluation Report (SER) related to St. Lucie Units 1 and 2 first license renewal [7]:

1. Calculate the maximum bore diameter at the end of 80 years operation considering the carbon and low-alloy steel borated water corrosion to demonstrate that the limiting allowable bore diameters are not exceeded.
2. Reconcile that the fatigue crack growth and flaw stability evaluation in WCAP-15973 [4 and 5] remain valid for the 80 years operation of St. Lucie Units 1 and 2 plants to demonstrate that the ASME code acceptance criteria for crack growth and crack stability are met for the rest of the plant life including the extended operation.
3. Provide acceptable bases and arguments for concluding that unacceptable growth of the existing flaw by stress corrosion into the vessels or piping is improbable.

Note that Alloy 600 weld pad is used at the outer wall in some repairs for St. Lucie Unit 2 as noted in Table 1-2. These Alloy 600 weld pads at the outer wall are managed by the Alloy 600 inspection program [8] and is thus outside of the evaluation scope of this calculation note.

Revision 1 of this letter incorporates the editorial comments from the customer. The changes are marked using a change bar at the left side of the page.

Revision 2 of this letter corrects the ADAMS Access number for reference [5]. For clarity, a separate reference [5.a] is added for the US NRC Safety Evaluation Report with its own ADAMS Access number. The changes are marked using a change bar at the left side of the page.

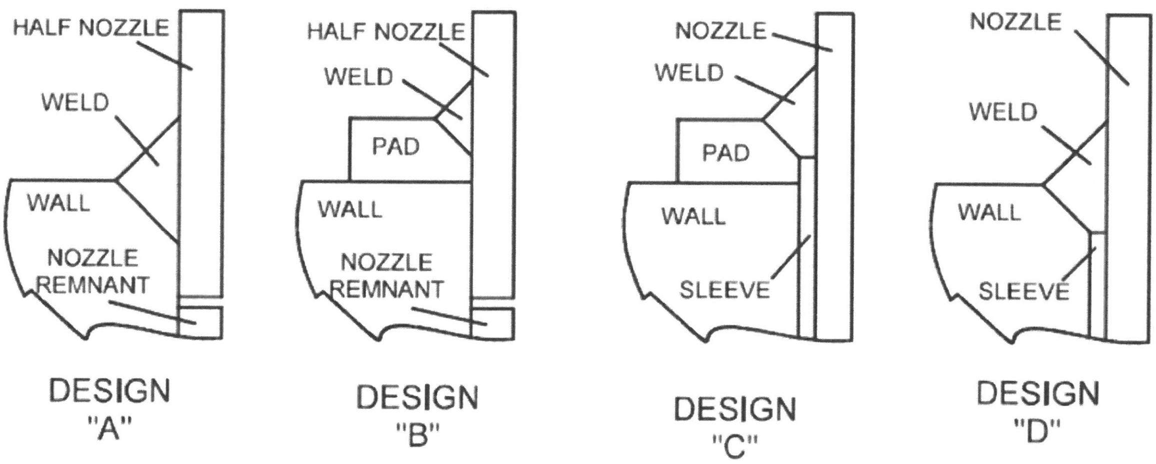

Figure 1-1 Nozzle Repair Designs

Table 1-1 St. Lucie Unit 1 Replacement history Alloy 600 Small Bore Nozzles on Hot Leg Piping

Tag ID	Hot Leg A or B	Replacement Date	Replacement Method (Figure 1-1 Design A)	Reason for Replacement
PDT-1121D	B	2001	1/2 Nozzle Repair	Leakage
TE-1112HA	A	2005	1/2 Nozzle Repair	Preventative
TE-1112HB	A	2005	1/2 Nozzle Repair	Preventative
TE-1112HC	A	2005	1/2 Nozzle Repair	Preventative
TE-1112HD	A	2005	1/2 Nozzle Repair	Preventative
TE-1111X	A	2005	1/2 Nozzle Repair	Preventative
TE-1122HA	B	2005	1/2 Nozzle Repair	Preventative
TE-1122HB	B	2005	1/2 Nozzle Repair	Preventative
TE-1122HC	B	2005	1/2 Nozzle Repair	Preventative
TE-1122HD	B	2005	1/2 Nozzle Repair	Preventative
TE-1121X	B	2005	1/2 Nozzle Repair	Preventative
PDT-1111A	A	2005	1/2 Nozzle Repair	Preventative
PDT-1111B	A	2005	1/2 Nozzle Repair	Preventative
PDT-1111C	A	2005	1/2 Nozzle Repair	Preventative
PDT-1111D	A	2005	1/2 Nozzle Repair	Preventative
PDT-1121A	B	2005	1/2 Nozzle Repair	Preventative
PDT-1121B	B	2005	1/2 Nozzle Repair	Preventative
PDT-1121C	B	2005	1/2 Nozzle Repair	Preventative
RC-143	A	2005	1/2 Nozzle Repair	Preventative

Table 1-2 St. Lucie Unit 2 Replacement history Alloy 600 Small Bore Nozzles on Hot Leg Piping

Location	Tag ID	Repair Date	Repair Method (Figure 1-1 Design)	Reason for Repair
PZR Stm Space Upper Head	A	1994	1/2 Nozzle Repair(1) (B)	Linear Indications
PZR Stm Space Upper Head	B	1994	1/2 Nozzle Repair(1) (B)	Linear Indications
PZR Stm Space Upper Head	C	1994	1/2 Nozzle Repair(1) (B)	Leakage / Linear Indications
PZR Stm Space Upper Head	D	1994	1/2 Nozzle Repair(1) (B)	Preventative
PZR Wtr Space Lower Head	RC-105	1995(2)	Sleeve Repair(1) (C)	Preventative
PZR Wtr Space Lower Head	RC-130	1995	Sleeve Repair(1) (C)	Preventative
PZR Wtr Space Side Shell	TE-1101	1995	Sleeve Repair(1) (C)	Preventative
RCS Hot Leg RTD Nozzle	TE-1112HA	1989	Sleeve Repair(1)(3) (C)	Preventative
RCS Hot Leg RTD Nozzle	TE-1111X	1989	Sleeve Repair(1)(3) (C)	Preventative
RCS Hot Leg RTD Nozzle	TE-1122HC	1989	Sleeve Repair(1)(3) (C)	Preventative
RCS Hot Leg RTD Nozzle	TE-1122HD	1989	Sleeve Repair(1)(3) (C)	Preventative
RCS Hot Leg RTD Nozzle	TE-1121X	1989	Sleeve Repair(1)(3) (C)	Preventative
RCS Hot Leg RTD Nozzle	TE-1112HB	2003	1/2 Nozzle Repair (A)	Preventative
RCS Hot Leg RTD Nozzle	TE-1112HC	2003	1/2 Nozzle Repair (A)	Preventative
RCS Hot Leg RTD Nozzle	TE-1112HD	2003	1/2 Nozzle Repair (A)	Preventative
RCS Hot Leg RTD Nozzle	TE-1122HA	2003	1/2 Nozzle Repair (A)	Preventative
RCS Hot Leg RTD Nozzle	TE-1122HB	2003	1/2 Nozzle Repair (A)	Preventative

Table 1-2 St. Lucie Unit 2 Replacement history Alloy 600 Small Bore Nozzles on Hot Leg Piping - Continued

Location	Tag ID	Repair Date	Repair Method (Figure 1-1 Design)	Reason for Repair
RCS Hot Leg Flow Nozzle	PDT-1121B	1995	Sleeve Repair (D)	Leakage
RCS Hot Leg Flow Nozzle	PDT-1111A	1995	Sleeve Repair (D)	Preventative
RCS Hot Leg Flow Nozzle	PDT-1111B	1995	Sleeve Repair (D)	Preventative
RCS Hot Leg Flow Nozzle	PDT-1111C	1995	Sleeve Repair (D)	Preventative
RCS Hot Leg Flow Nozzle	PDT-1111D	1995	Sleeve Repair (D)	Preventative
RCS Hot Leg Flow Nozzle	PDT-1121A	1995	Sleeve Repair (D)	Preventative
RCS Hot Leg Flow Nozzle	PDT-1121C	1995	Sleeve Repair (D)	Preventative
RCS Hot Leg Flow Nozzle	PDT-1121D	1995	Sleeve Repair (D)	Preventative
RCS Hot Leg Flow Nozzle	Sample Line	1995	Sleeve Repair (D)	Preventative
PZR Heater Sleeves	30	2011	1/2 Nozzle Repair(1) (B)	Preventative

Notes:

1. Nozzle welded to a nickel alloy weld pad.
2. Per [8], this location was repaired again in 2018 with a similar design. The only difference is that the nickel alloy weld pad was changed from Alloy 600 equivalent to Alloy 690 equivalent weld metal.
3. Alloy 600 weld pad was used at the outer wall. Per [8], any Alloy 600 material at the outer wall of the repair is managed by the Alloy 600 inspection program, and is beyond the scope of the evaluation in this calculation note.

2.0 Method Discussion

WCAP-15973 [4 and 5] evaluated the half-nozzle repair for the Alloy 600 nozzles of all the CE designed PWRs from a corrosion, fatigue crack growth and stress corrosion assessment perspective. It was concluded that corrosion of carbon and low alloy steels would be within Code limits and it would be acceptable to leave a flaw in place in small diameter Alloy 600 nozzles and partial penetration for the 40-year plant design life. This calculation note reconciles the evaluation in WCAP-15973 [4 and 5] for the 80-year plant operation of St. Lucie Units 1 and 2 considering the actual plant operation and plant specific geometries. The reconciliation in Section 5.0 shows that the conclusions in WCAP-15973 [4 and 5] remain valid for the period of extended operation.

3.0 Discussion of Significant Assumptions

1. The corrosion rate calculated in Section 2.3 of WCAP-15973-P [4] was based on [

   ]^{a,c,e}

   The plant specific corrosion rates based on the generation data review were calculated to be 1.20 mpy [1] and 1.34 mpy [2] for Unit 1 and Unit 2, respectively. Therefore, the corrosion rate of [ ]^{a,c,e} bounds the corrosion rate based on St. Lucie Unit 1 and Unit 2 power generation data. It is assumed that the corrosion rate of [ ]^{a,c,e} remains bounding for the rest of the 80 year operation.

2. In order to use the stress corrosion assessment in WCAP-15973 [4 and 5], NRC requires that the plants demonstrate that the contaminant concentrations in the reactor coolant have been typically maintained at levels below 10 ppb for dissolved oxygen, 150 ppb for halide ions and 150 ppb for sulfate ions. Per reference [1] and [2], plant chemistry reviews show that for both St. Lucie Unit 1 and Unit 2, typical contaminant concentrations for dissolved oxygen, halide ions and sulfate ions are maintained at less than 5 ppb, far below the NRC requirement. It is assumed that the contaminant concentrations is maintained below the NRC requirement for the 80 year operation.

The assumptions above will be examined every ten years when the plant submits the plants request relief from Code requirements for existing and future half nozzle repair technique that leaves the cracks in place which is in conflict with ASME Code Section XI requirements. The most recent relief requests [1 and 2] were submitted and approved in 2018 for St. Lucie Unit 1 and 2014 for St. Lucie Unit 2.

4.0 Acceptance Criteria

Acceptance criteria for crack growth and stability are based on ASME Code 2007 Edition with 2008 Addenda, Section XI, IWB-3600 [9] and the acceptance criteria specified in RG 1.161 for the Elastic-Plastic Fracture Mechanics (EFPM) evaluation.

For the corrosion evaluation, ASME Code requirements for the maximum allowable hole size cannot be exceeded considering the corrosion that may occur in the crevice region of the replaced nozzles. The allowable diameter of a corroded hole is calculated based on the allowable shear stress of the weld in accordance with paragraph NB-3227.2(a) and the reinforcement requirement in NB-3332.2 of ASME Code 1989 Edition, Section III [10]. The maximum allowable corroded hole diameter for small Alloy 600 partial penetration welded nozzles is calculated in A-CEOG-9449-1242 Rev. 00 [11].

5.0 Carbon and Low-Alloy Steel Borated Water Corrosion Evaluations

As shown in Figure 1-1, four designs (Design A, B, C, and D) were used for half nozzle repair in St. Lucie Unit 1 and 2 plants. The corrosion evaluation for Design A/B and Design C/D are discussed separately as below.

Design A/B Corrosion Evaluation

For Designs A and B, a small gap remains between the remnant of the original alloy 600 component and the new alloy 690 component. As a result, primary coolant (borated water) will fill the crevice between the nozzle or heater sleeve and the pipe or the pressurizer wall. Since a crevice exists, the low alloy and carbon steels are exposed to borated water and corrosion could occur.

The corrosion rate evaluation was performed in Section 2.3 of WCAP-15973-P [4] considering all the CE designed PWR plants. [

]a,c,e Reference [1] reviewed St. Lucie Unit 1 generation data from 4/15/2001 (oldest half nozzle repair for Unit 1) to 12/31/2017. Reference [2] reviewed St. Lucie Unit 2 generation data from 1/1/1995 to 2/28/2014; note that the oldest half nozzle repair with Design A/B occurred in 1994. The plant specific corrosion rates based on the generation data review were calculated to be 1.20 mpy [1] and 1.34 mpy [2] for Unit 1 and Unit 2, respectively. The corrosion rate of [ ]a,c,e calculated in Section 2.3 of [4] bounds the corrosion rate calculated for St. Lucie Unit 1 and Unit 2, [

]a,c,e

The corrosion rate of [ ]a,c,e from [4] is thus conservatively used herein to calculate the amount of general corrosion based thinning for the vessels or piping over the life of the plant considering 80 years of operation. Note that with the approval of subsequent license renewal application, the plant licenses for St. Lucie Unit 1 and Unit 2 will be extended to 2056 and 2063, respectively.

Table 5-1 calculates the maximum repair bore diameter at the end of 80 years operation for all the design A/B half-nozzle repairs and compares the results to the corresponding limiting allowable diameter. It shows that repair bore diameter at the end of 80 years operation is below the limiting allowable diameter for all the design A/B half-nozzle repairs. Therefore, these repairs have acceptable wall thickness until the end of 80 years operation.

Table 5-1 Summary of Limiting Allowable Diameter Calculations for Half-Nozzle Repair – Design A and B

St. Lucie Unit 1 Corrosion Evaluation for 80 Years Operation						
Nozzle Location(1)	**Repair Method (Figure 1-1 Design)(1)**	**Earliest Repair Year(1)**	**Nozzle Repair Bore Diameter (inch)(2)**	**Diameter Corrosion Loss (inch)(3)**	**Repair Bore Diameter at the end of 80 years operation (inch)(4)**	**Limiting Allowable Diameter (inch)(5)**
Hot Leg Piping	A	2001	1.063	[ ]a,c,e	[ ]a,c,e	1.27
St. Lucie Unit 2 Corrosion Evaluation for 80 Years Operation						
Nozzle Location(6)	**Repair Method (Figure 1-1 Design)(6)**	**Earliest Repair Year(6)**	**Nozzle Repair Bore Diameter (inch)(7)**	**Diameter Corrosion Loss (inch)(8)**	**Repair Bore Diameter at the end of 80 years operation (inch)(4)**	**Limiting Allowable Diameter (inch)(5)**
PZR Stm Space Upper Head	B	1994	1.325	[ ]a,c,e	[ ]a,c,e	2.26
RCS Hot Leg RTD Nozzle	A	2003	1.063	[ ]a,c,e	[ ]a,c,e	1.27
Pressurizer Heater Sleeve	B	2011	1.693	[ ]a,c,e	[ ]a,c,e	2.26

Notes:

1. Information from Table 1-1.
2. See St. Lucie Unit 1 relief request [1].
3. [ ]a,c,e
4. Repair bore diameter at the end of 80 years operation is equal to the sum of nozzle repair bore diameter and diameter corrosion loss.
5. Limiting Allowable diameter is from Table 2 of A-CEOG-9449-1242 [11].
6. Information from Table 1-2.
7. See St. Lucie Unit 2 relief request [2].
8. [ ]a,c,e

Design C/D Corrosion Evaluation

For Designs C and D, the end of the Alloy 690 sleeve at the interior surface of the piping or the pressurizer is either roll expanded or welded to the interior surface of the piping or pressurizer to eliminate corrosion of the carbon steel by stopping the replenishment of borated solution in contact with the carbon steel. As discussed in Section 2.5 of WCAP-15973 [4], since the borated solution confined in the tight crevice between the sleeve and the interior surface of the piping or pressurizer cannot be replenished, the crevice region will fill with corrosion products when corrosion occurs. The presence of corrosion products in the crevice will prevent access of the corrodent (borated water) to the carbon and low alloy steel, reducing the corrosion rate. Further corrosion will result in the crevice corrosion products becoming denser and less permeable to the primary coolant. Eventually, the corrosion process will stifle because the steel will become isolated from the coolant. The lifetime maximum diametrical loss for the tight crevice like sleeve repair in Design C/D is conservatively assessed as [ ]^{a,c,e} in Section 2.5 of WCAP-15973 [4].

Table 5-2 calculates the maximum repair bore diameter at the end of 80 years operation for all the design C/D half-nozzle repairs and compares the results to the corresponding limiting allowable diameter. It shows that repair bore diameter at the end of 80 years operation is below the limiting allowable diameter for all the design C/D half-nozzle repairs. Note that Design C/D repairs were only performed in St. Lucie Unit 2 plant. Therefore, these repairs have acceptable wall thickness until the end of 80 years operation.

Table 5-2 Summary of Limiting Allowable Diameter Calculations for Half-Nozzle Repair – Design C and D

St. Lucie Unit 2 Corrosion Evaluation for 80 Years Operation						
Nozzle Location(1)	**Repair Method (Figure 1-1 Design)(1)**	**Earliest Repair Date(1)**	**Nozzle Repair Bore Diameter (inch)(2)**	**Diameter Corrosion Loss (inch)**	**Repair Bore Diameter at the end of 80 years operation (inch)(3)**	**Limiting Allowable Diameter (inch)(4)**
PZR Wtr Space Lower Head	C	1995	1.5	[ ]a,c,e	[ ]a,c,e	2.26
PZR Wtr Space Side Shell	C	1995	1.325	[ ]a,c,e	[ ]a,c,e	1.62
RCS Hot Leg RTD Nozzle	C	1989	1.129	[ ]a,c,e	[ ]a,c,e	1.27
RCS Hot Leg Flow Nozzle	D	1995	1.178	[ ]a,c,e	[ ]a,c,e	1.27

Notes:

1. Information from Table 1-2.
2. See St. Lucie Unit 2 relief request [2].
3. Repair bore diameter at the end of 80 years operation is equal to the sum of nozzle repair bore diameter and diameter corrosion loss.
4. Limiting Allowable diameter is from Table 2 of A-CEOG-9449-1242 [11].

6.0 Carbon and Low Alloy Steel Fatigue Crack Growth and Flaw Stability

Fatigue crack growth evaluation for half nozzle repair was performed to bound all the CE PWRs in WCAP-15973 [4 and 5]. Calculations were performed assuming that a crack had propagated through the nozzle and associated weld metal and had reached the interface with the carbon or low alloy steel. The postulated flaws were subjected to anticipated (Level A/B) transients for the plant evaluation period to determine the final flaw size using the guidance outlined in ASME Code Section XI, Appendix A. The final flaw size was then used in subsequent flaw stability calculations. WCAP-15973 [4 and 5] provided the results of fatigue crack growth evaluations and crack stability analyses for pressurizer heater sleeves and instrument nozzles and hot leg pipe nozzles, including the effects of the support skirt and pressurizer in-surges. The details of the calculation are in CN-CI-02-71 [12]. The results indicate that the ASME code acceptance criteria for crack growth and crack stability are met.

In addition, a plant specific fatigue crack growth and flaw stability evaluation for postulated flaws at small-bore locations in the pressurizer and Hot Leg Piping for St. Lucie Units 1 & 2 was performed in CN-CI-02-69, Rev. 0 [13] using the same methods as CN-CI-02-71 [12] to support a 60 year fatigue life. The results in CN-CI-02-69, Rev. 0 [13] also demonstrate that the ASME code acceptance criteria for crack growth and crack stability are met.

The NRC SE to WCAP-15973-P-A [5, 5.a] states that Licensees seeking to reference this topical report for future licensing applications need to demonstrate the following:

1. The geometry of the leaking penetration is bounded by the corresponding penetration reported in calculation report CN-CI-02-71, Revision 01.
2. The plant-specific pressure and temperature profiles in the pressurizer water space for the limiting curves (cooldown curves) do not exceed the analyzed profile shown in Figure 6-2 of Calculation Report CN-CI-02-71, Revision 01.
3. The plant-specific Charpy upper-shelf energy (USE) data shows a USE value of at least 70 ft-lb to bound the USE value used in the analysis. If the plant-specific Charpy USE data does not exist and the licensee plans to use Charpy USE data from other plants pressurizers and hot leg piping, then justification (e.g., based on statistical or lower bound analysis) has to be provided.
4. If the licensee plans on using this alternative beyond the 40 years and through the license renewal period, the thermal fatigue crack growth analysis shall be re-evaluated to include the extended period, as applicable, and submitted as a time limited aging analysis in their license renewal application as required by 10 CFR 54.21(c)(1).

Note that CN-CI-02-71, Revision 01 was later revised to Revision 02, but only editorial changes were made in Revision 02 (see Reference [12]). No technical change was made to CN-CI-02-71, Revision 01.

The four NRC requests are addressed correspondingly in the following paragraphs:

1. The fatigue crack growth and flaw stability analyses specific for St. Lucie plants geometry were performed in CN-CI-02-69, Rev. 0 [13], which was submitted to NRC as part of the St. Lucie License Renewal activity. An extended license was approved for St. Lucie Unit 1 and Unit 2. The calculation and results in CN-CI-02-69, Rev. 0 [13] are equivalent to that

shown in CN-CI-02-71, Rev. 1. It is recognized that the calculations of CN-CI-02-69, Rev. 0 [13] did not address the pressurizer heater sleeves since the half nozzle repair of the small diameter nozzle at the heater sleeve location at St. Lucie Unit 2 occurred about 9 years after the study in CN-CI-02-69, Rev. 0 [13]. However, the geometry of the St. Lucie Unit 2 pressurizer heater sleeves with half nozzle repair was reviewed and determined to be equivalent to that shown in CN-CI-02-71, Rev. 1. Therefore, the half nozzle repairs for St. Lucie plants as listed in Table 1-1 and Table 1-2 are addressed by the analyses in CN-CI-02-71 [12] and CN-CI-02-69 [13].

2. As discussed in [1], since Figure 6-2 of [12] applies to the pressurizer and the hot leg piping does not see the transients experienced by the pressurizer, the evaluation of the pressurizer limiting curves is considered not applicable to the hot leg nozzles per [1]. All the half nozzle repair locations for St. Lucie Unit 1 are on the hot leg piping. Therefore, this request does not apply to St. Lucie Unit 1.

   The pressurizer cooldown transient used in CN-CI-02-71 Rev. 1 and Rev. 2 [12] as shown in Figure 6-2 of [12] has [

   ]^{a,c,e} Per [2], cooldown of the pressurizer water space for St. Lucie Unit 2 is administratively controlled by a plant procedure to a maximum rate of 75°F per hour for normal operation, which is within the rates shown in Figure 6-2 of CN-CI-02-71 [12].

3. Charpy USE value of 70 ft-lb was used in Section 6.3.3.2 of CN-CI-02-71 [12] to support an elastic-plastic fracture mechanics (EPFM) analysis of the pressurizer lower shell and lower head. The analysis was not performed on the pressurizer upper head and the hot leg piping because the pressurizer upper head and hot leg piping are not affected by the large in-surge transient or thermal stress that occurs at the pressurizer lower head and lower shell. All the half nozzle repair locations for St. Lucie Unit 1 are on the hot leg piping. Therefore, the evaluation of the plant-specific Charpy USE data is only applicable to pressurizer lower shell and lower head of St. Lucie Unit 2 plant. As discussed in [2], Charpy USE data for the pressurizer was not required when the pressurizer was built and thus was not determined. However, the Charpy impact data for the two lower shell plates, the upper head, and the bottom head of the pressurizer was reviewed in [2] along with the Charpy impact data and USE for six plates in the reactor vessel (RV) shell. The pressurizer lower shell plates, upper head and bottom head are made to the same alloy specification, SA-533 Grade B Class 1, as the six RV plates. The four pressurizer items and the six RV items have similar chemistry and received similar heat treatment. Therefore, it can be reasonably expected that the USE data for the pressurizer material should be comparable to that of the RV plates [2]. The review of the Charpy impact data for the pressurizer items along with the Charpy impact data and USE for the RV items in [2] demonstrated that the St. Lucie Unit 2 pressurizer lower shell and lower head is expected to exhibit USE well in excess of 70 ft-lb and is bounded by the analysis in CN-CI-01-71 [12].

4. The fatigue crack growth and flaw stability analyses in CN-CI-02-71 [12] were performed using design cycles that were specified in the plant design process. These design cycles were intended to be conservative and bounding for all foreseeable plant operational conditions. Experience has shown that actual plant operation is often very conservatively

represented by these design cycles. The use of actual operating history data allows the quantification of these conservatisms. [

]a,c,e Therefore, the design cycles used in CN-CI-02-71 [12] are bounding for the period of extended 80 years operation.

It is noted that the analyses in CN-CI-02-71 [12] were based on the 1992 Edition of ASME Code, Section XI [15] while the Section XI Code year for St. Lucie Unit 1 and Unit 2 is currently 2007 Edition with 2008 Addenda [9]. The comparison of 1992 Edition and 2007 Edition with 2008 Addenda ASME Code, Section XI is performed herein regarding the fatigue crack growth and flaw stability analyses in CN-CI-02-71 [12]. It shows that the flaw characterization in IWA-3300, guidance outlined in Appendix A for the fatigue crack growth analysis, and the flaw stability acceptance criteria in IWB-3610 are the same in the two versions of ASME Code Section XI. It is noted that in ASME Code Section XI, 2007 Edition with 2008 Addenda, it is added in IWA-3300 that combination of multiple planar flaws is not required for fatigue or stress corrosion cracking analysis. This does not affect the analyses in CN-CI-02-71 [12], which didn't need to address the combination of multiple planar flaws.

Based on the evaluation above, the conclusion from the fatigue crack growth and flaw stability analyses in WCAP-15973 [4 and 5] and CN-CI-02-71 [12] remains valid for the 80 years of operation. The ASME code acceptance criteria for crack growth and crack stability are met for the rest of the plant life including the extended operation.

7.0 Carbon and Low Alloy Steel Stress Corrosion Cracking Assessment

Section 3.6 of WCAP-15973 [4 and 5] evaluated the possibility that a crack that had propagated through an Alloy 600 nozzle and weld metal would continue to propagate by a stress corrosion mechanism through the carbon or low alloy steel component. Stress corrosion cracking (SCC) is dependent on the simultaneous presence of three elements: an aggressive environment, a susceptible material condition, and a stress (applied plus residual) in excess of some threshold value. If any element is missing, SCC will not occur. WCAP-15973 [4 and 5] concluded that the environmental conditions expected in PWRs indicate that SCC initiation and propagation in the carbon or low alloy steels component base metals as a result of cracked Alloy 600 nozzles left in place during nozzle repair is not a concern. In addition, the tests conducted indicated that there was no SCC growths of existing defects even at high stress intensity factor levels for low potential (PWR) conditions. WCAP-15973 [4 and 5] also reviewed the field experience and concluded that PWR field experience is consistent with laboratory observations and confirms that SCC of carbon and low alloy steel components as a result of nozzle repairs is not likely for CE plants.

The NRC SE to WCAP-15973-P-A [5, 5.a] states that Licensees seeking to implement half-nozzle replacements may use the stress corrosion assessment in WCAP-15973 [4 and 5] as the bases for concluding that existing flaws in the weld metal will not grow by stress corrosion if the following conditions are met:

1. Conduct appropriate plant chemistry reviews and demonstrate that a sufficient level of hydrogen overpressure has been implemented for the RCS and that the contaminant concentrations in the reactor coolant have been typically maintained at levels below 10 ppb for dissolved oxygen, 150 ppb for halide ions and 150 ppb for sulfate ions.
2. During the outage in which the half-nozzle repairs are scheduled to be implemented, licensees adopting the stress corrosion crack growth arguments will need to review their plant specific RCS coolant chemistry histories over the last two operating cycles for their plants and confirm that these conditions have been met over the last two operating cycles.

Per reference [1] and [2], plant chemistry reviews show that for both St. Lucie Unit 1 and Unit 2, typical contaminant concentrations for dissolved oxygen, halide ions and sulfate ions are maintained at less than 5 ppb.

Therefore, the conclusion in WCAP-15973 [4 and 5] remains valid for 80 years of operation and the existing flaws in the weld metal will not grow by stress corrosion.

8.0 Summary and Conclusion

The Alloy 600 half nozzle repairs for the St. Lucie Units 1 and 2 are reassessed for the subsequent license renewal (SRL). The results for the evaluation of corrosion, fatigue crack growth and flaw stability, and corrosion stress cracking are summarized below:

1. For Design A/B of half nozzle repair in Figure 1-1, the corrosion rate of [ ]^{a,c,e} from WCAP-15973 [4 and 5] is determined to bound the corrosion rate of 1.20 mpy [1] for St. Lucie Unit 1 and 1.34 mpy [2] for St. Lucie Unit 2 based on the plant power generation data. Table 5-1 summarizes the amount of general corrosion based thinning at the half nozzle repair locations over the life of the plant considering 80 years of operation, which is calculated by conservatively using the [ ]^{a,c,e} corrosion rate from WCAP-15973 [4 and 5]. The results in Table 5-1 show that the repair bore diameter at the end of 80 years operation is below the limiting allowable diameter for all the design A/B half-nozzle repairs. Therefore, these repairs have acceptable wall thickness until the end of 80 years operation.

2. For Design C/D of half nozzle repair in Figure 1-1, since the borated solution confined in the tight crevice between the sleeve and the interior surface of the piping or pressurizer cannot be replenished, the crevice region will fill with corrosion products when corrosion occurs. The presence of corrosion products in the crevice will prevent access of the corrodent (borated water) to the carbon and low alloy steel, reducing the corrosion rate. Further corrosion will result in the crevice corrosion products becoming denser and less permeable to the primary coolant. Eventually, the corrosion process will stifle because the steel will become isolated from the coolant. The lifetime maximum diametrical loss for the tight crevice like sleeve repair in Design C/D is conservatively assessed as [ ]^{a,c,e} in Section 2.5 of WCAP-15973 [4]. Table 5-2 shows that the maximum repair bore diameter at the end of 80 years operation is below the limiting allowable diameter for all the design C/D half-nozzle repairs. Therefore, these repairs are also acceptable for 80 years of operation regarding the corrosion evaluation.

3. Section 6 reconciled the fatigue crack growth and flaw stability evaluation in WCAP-15973 [4 and 5] for the extended 80 years operation of St. Lucie Unit 1 and Unit 2 plants. The design cycles used in the fatigue crack growth analysis in [4 and 5] are conservative and bound the projected transient cycles for 80 years of operation. The geometry of half-nozzle repair locations in St. Lucie Unit 1 and Unit 2 is bounded by what analyzed in CN-CI-02-71 [12]. The plant-specific pressurizer cooldown curves are also bounded by the profile analyzed in CN-CI-02-71 [12]. The review of the Charpy impact data for the plant specific pressurizer items along with the Charpy impact data and upper shelf energy (USE) for the RV items in [2] demonstrated that the St. Lucie Unit 2 pressurizer lower shell and lower head is expected to exhibit USE well in excess of 70 ft-lb and is bounded by the analysis in CN-CI-01-71 [12]; the pressurizer lower head and lower shell flaw stability evaluation based on elastic-plastic fracture mechanics (EPFM) analysis in CN-CI-01-71 [12] thus can be used to demonstrate the acceptability of the half nozzle repairs performed at St. Lucie 2 pressurizer locations. Therefore, the conclusion from the fatigue crack growth and flaw stability analyses in WCAP-15973 [4 and 5] and CN-CI-02-71 [12] remains valid for the 80 years of operation. The ASME code acceptance criteria for crack

growth and crack stability are met for the rest of the plant life including the extended operation.

4. As discussed in WCAP-15973 [4 and 5], cracks that may be present in Alloy 600 remnants left in place following a half-nozzle repair or cracks that may initiate after completion of the repair will not propagate by stress corrosion cracking (SCC) through the carbon or low alloy steel components. Per [1] and [2], plant chemistry reviews show that for both St. Lucie Unit 1 and Unit 2, typical contaminant concentrations for dissolved oxygen, halide ions and sulfate ions are maintained at less than 5 ppb. The very low primary side oxygen levels that result in corrosion potentials is well below the critical cracking potentials for the carbon or low alloy steel materials.

Therefore, the alloy 600 half nozzle repairs in the St. Lucie Unit 1 and Unit 2 plants are evaluated to be acceptable regarding corrosion, fatigue crack growth and flaw stability, and stress corrosion cracking for 80 years of operation. The conditions for using the topical report, WCAP-15973 [5], listed in the NRC SER [5.a] Sections 3.1, 3.2 and 3.3 are satisfied. Note that the evaluation herein also confirms that the conclusions in the responses to NRC request for additional information (RAI) 4.6.4-1 and 4.6.4-2 for the original St. Lucie Units 1 and 2 license renewal application in ML022890457 [16] remain valid for 80 years of operation.

9.0 References

1. FPL Letter, L-2018-027, "St. Lucie Unit 1 Docket No. 50-335 Inservice Inspection Plan, Fifth Ten-Year Interval Unit 1 Relief Request No. 5, Revision 0," February 8, 2018. (ADAMS Access Number ML18039A437)
2. FPL Letter, L-2014-252, "St. Lucie Unit 2 Docket No. 50-389 In-Service Inspection Plan, Fourth Ten-Year Interval Unit 2 Relief Request 2," August 1, 2014. (ADAMS Access Number ML14224A010)
3. CE Owners Group Topical Report, CE NPSD-1198-P, Rev. 00, "Low-Alloy Steel Component Corrosion Analysis Supporting Small-Diameter Alloy 600/690 Nozzle Repair/Replacement Programs CEOG," February 8, 2001.
4. Westinghouse Report, WCAP-15973-P, Rev. 1, "Low-Alloy Steel Component Corrosion Analysis Supporting Small-Diameter Alloy 600/690 Nozzle Repair/Replacement Programs," May 2004.
5. Westinghouse Report, WCAP-15973-P-A, Rev. 0 (NRC approved version of WCAP-15973-P, Revision 1 with SER and resolved questions), "Low-Alloy Steel Component Corrosion Analysis Supporting Small-Diameter Alloy 600/690 Nozzle Repair/Replacement Programs," February 2005. (ADAMS Access Number ML050700431)
    a. USNRC SER, "Final Safety Evaluation for Topical Report WCAP-15973-P, Revision 01, "Low-Alloy Steel Component Corrosion Analysis Supporting Small-Diameter Alloy 600/690 Nozzle Repair/Replacement Program" (TAC No. MB6805)," January 12, 2005. (ADAMS Access Number ML050180528)
6. License Renewal Application, St. Lucie Units 1 and 2, November 30, 2011 (Renewed License Issued 10/02/2003). https://www.nrc.gov/reactors/operating/licensing/renewal/applications/st-lucie.html
7. NUREG-1779, "Safety Evaluation Report Related to the License Renewal of St Lucie Nuclear Plant, Units 1 and 2," September 2003. (ADAMS Accession Number ML032940205).
8. FPL Letter, PSLWEC-21-0005, Revision 0, "Design Input Transmittal for WS09a Alloy 600 Locations to Support the St. Lucie Unit 1 and Unit 2 Subsequent License Renewal," February 4, 2021.
9. ASME Boiler and Pressure Vessel Code, 2007 Edition with 2008 Addenda, Section XI, "Rules for Inservice Inspection of Nuclear Power Plant Components."
10. ASME Boiler and Pressure Vessel Code, 1989 Edition, Section III, "Rules for Construction of Nuclear Facility Components."
11. CE Design Analysis, A-CEOG-9449-1242 Rev. 00, "Evaluation of the Corrosion Allowance for Reinforcement and Effective Weld to Support Small Ally 600 Nozzle Repairs," June 13, 2000.
12. Westinghouse Calculation Note, CN-CI-02-71, Rev. 2, "Summary of Fatigue Crack Growth Evaluation Associated with Small Diameter Nozzles in CEOG Plants," December 9, 2005.
13. Westinghouse Calculation Note, CN-CI-02-69, Rev. 0, "Evaluation of Fatigue Crack Growth Associated with Small Diameter Nozzles for St. Lucie 1 & 2," October 9, 2002 (Attached to FPL Letter L2002-222, Adams Accession # ML023380149).
14. Westinghouse Calculation Note, CN-SDA-II-20-026, Rev. 0, "St. Lucie Unit 1 and Unit 2 80-Year Transient Cycle Projections," February 25, 2021.
15. ASME Boiler and Pressure Vessel Code, 1992 Edition, Section XI, "Rules for Inservice Inspection of Nuclear Power Plant Components."

16. FPL Letter, L-2002-165, "Response to NRC Request for Additional Information for Review of the St. Lucie Units1 and 2 License Renewal Application," October 10, 2002 (Adams Accession # ML022890450).

Approval Information
Author Approval Song Xiaolan May-04-2021 17:16:23
Verifier Approval Ganta B Reddy May-04-2021 17:53:33
Reviewer Approval Hall Gordon Z May-05-2021 09:02:54
Manager Approval Hall Gordon Z for Rigby Stephen May-05-2021 09:11:49

Files approved on May-05-2021

<u>Enclosure 4</u>

<u>Non-proprietary Reference Documents and Redacted Versions of Proprietary Reference Documents (Public Version)</u>

<u>Attachment 12</u>

Westinghouse Report LTR-SDA-20-104-NP, Rev. 2, St. Lucie Units 1&2 Subsequent License Renewal: Evaluation of Time-Limited Aging Analysis of the Reactor Vessel Internals, July 9, 2021

(11 Total Pages, including cover sheets)

Westinghouse

1000 Westinghouse Drive
Cranberry Twp., PA 16066

To: John T. Ahearn
cc:

Date: July 9, 2021

From: Structural Design and Analysis
Ext: 207-550-7671

Ref: LTR-SDA-20-104-NP, Rev. 2

Subject: St. Lucie Units 1&2 Subsequent License Renewal: Evaluation of Time-Limited Aging Analysis of the Reactor Vessel Internals

Core support barrel (CSB) repair plugs were installed at the end of cycle (EOC) 5 as part of the overall St. Lucie Unit 1 CSB repair effort. This repair effort was undertaken to repair damage incurred following malfunction of the thermal shield support system and subsequent removal of the thermal shield assembly. A calculation was completed to re-calculate the minimum plug-flange deflection requirements of the Unit 1 CSB repair plugs using revised fluence input over the increased plant lifetime for Subsequent License Renewal (SLR). As-measured deflections are then evaluated against these revised minimum requirements. In addition, the PSL Unit 1 and Unit 2 RVI Fatigue Analyses were evaluated with the design transient event occurrences projected for SLR in this report. The analysis performed for St. Lucie Unit 1 CSB repair plug preload relaxation considering added fluence exposure is acceptable for 80 years of plant operation. Therefore, the analysis is projected through the subsequent period of extended operation in accordance with 10 CFR 54.21(c)(1)(ii). Furthermore, the current RVI aging management program for the repair plugs remains appropriate to support a 10 CFR 54.21(c)(1)(iii) disposition.

The purpose of revision 2 of this letter is to update relevant results utilizing fluence with a +10% bias on the peripheral and re-entrant corner assembly relative powers, as well as an additional 10% increase on all fluence values to address uncertainties.

Author: Michael A. DiFiore
Structural Design and Analysis

Verifier: Gerrie W. Delport
Structural Design and Analysis

Manager: Stephen Rigby
Structural Design and Analysis

Foreword:

This document contains Westinghouse Electric Company LLC proprietary information and data which has been identified in brackets. Coding (a,b,c,e) associated with the brackets sets forth the basis on which information is considered proprietary. These code letters are listed with their meanings in BMS-LGL-84, and are defined as follows:

a. The information reveals the distinguishing aspects of a process (or component, structure, tool, method, etc.) where the prevention of its use by any of Westinghouse's competitors without license from Westinghouse constitutes a competitive economic advantage over other companies.

b. The information consists of supporting data, including test data, relative to a process (or component, structure, tool, method, etc.), the application of which secures a competitive economic advantage, e.g., by optimization or improved marketability.

c. The information, if used by a competitor, would reduce the competitor's expenditure of resources or improve the competitor's advantage in the design, manufacture, shipment, installation, assurance of quality, or licensing of a similar product.

e. The information reveals aspects of past, present, or future Westinghouse or customer funded development plans and programs of potential commercial value to Westinghouse.

The proprietary information and data contained within the brackets of this document were obtained at considerable Westinghouse expense and its release could seriously affect our competitive position. This information is to be withheld from public disclosure in accordance with the Rules of Practice 10 CFR 2.390 and the information presented herein is to be safeguarded in accordance with 10 CFR 2.390. Withholding of this information does not affect the public interest.

This information has been provided for your internal use only and should not be released to persons or organizations outside the Directorate of Regulation and the ACRS (Advisory Committee on Reactor Safeguards) without the express written approval of Westinghouse Electric Company LLC. Should it become necessary to release this information to such persons as part of the review procedure, please contact Westinghouse Electric Company LLC, which will make the necessary arrangements required to protect the Company's proprietary interests.

1.0 Introduction and Summary of Results

The critical plug locations are determined from the previous two calculations that evaluated the required preload of the U1 CSB repair plugs, [1] and [2]. The 3 plugs with the smallest previously calculated margins are the critical CSB repair plug locations. The calculation results encompass the evaluation of all plugs.

In accordance with the original evaluation of CSB repair plug flange deflection measurements documented in [9], actual CSB repair plug flange deflection measurement tool readings must be greater than or equal to the minimum required values. The minimum required deflection value is described in the detailed evaluation method in Section 2.1 and calculated in Section 2.2. Satisfaction of this criterion demonstrates that the plugs have sufficient preload to perform their intended function over the operating life of the plant.

Actual CSB repair plug flange deflection measurement tool readings exceed the minimum required values in all cases. Therefore, the acceptance criterion outlined in the calculation note is met, and the CSB repair plugs will perform their intended function for the remainder of the plant service life considering SLR. This calculation addressed the time-limited aging analysis (TLAA) performed for license extension in [1] and shows that the TLAA is acceptable with Extended Power Uprate (EPU) for 72 effective full power years (EFPY). The CSB repair plug results are provided in Table 1-1. The minimum margin is [ ]^{b,c,e} for plug ID 17-5 based on the measurement tool readings from EOC 6. For comparison, the minimum margin was [ ]^{b,c,e} at Plug ID 14-2 calculated for 54 EFPY in [2]. The minor difference of [ ]^{b,c,e} is reasonable since the relaxation factor as a function of fluence decreases exponentially, so the added fluence due to SLR has a minor effect on the relaxation of the plugs.

Additionally, the fatigue analysis of the Unit 1 damaged core support barrel, along with other fatigue analyses performed for the EPU on reactor vessel internals (RVI) components for both units (Unit 1 and Unit 2) are addressed to encompass all time-limited aging analysis (TLAA) on the RVI. The number of occurrences for the design transients remain conservatively applicable for SLR as confirmed by the 80-year cycle projections performed in [6]. The fatigue analyses evaluations are discussed in Sections 2.3 and 2.4 of this letter. The EPU thermal and hydraulic loads on the RVI are applicable to SLR per Item 2 in the Attachment to the design input transmittal [7]. Therefore, the fatigue analysis results in the analyses of record remain applicable to SLR.

Table 1-1: Summary of Calculation Results for Selected Plugs

Plug ID	Fluence at Plug at 72 EFPY	Req. Plug Flange Deflection for EOC 6 to EOL	Minimum Plug-Flange Deflection Actual Measurement at EOC 6	Required Minimum Plug-Flange Deflection Measurement Tool Reading for EOC 6 to EOL	Overall Margin at EOL at 54 EFPY	Overall Margin at EOL at 72 EFPY	Margin Difference
6 – 12	[ ]^{b,c,e}	[ ]^{b,c,e}	[ ]^{b,c,e}	[ ]^{b,c,e}	[ ]^{b,c,e}	[ ]^{b,c,e}	[ ]^{b,c,e}
17 – 5	[ ]^{b,c,e}	[ ]^{b,c,e}	[ ]^{b,c,e}	[ ]^{b,c,e}	[ ]^{b,c,e}	[ ]^{b,c,e}	[ ]^{b,c,e}
14 – 2	[ ]^{b,c,e}	[ ]^{b,c,e}	[ ]^{b,c,e}	[ ]^{b,c,e}	[ ]^{b,c,e}	[ ]^{b,c,e}	[ ]^{b,c,e}

2.0 Evaluation Methodology and Analyses

2.1 Evaluation Method

[

]a,c,e

In summary, the method of evaluation consists of calculating the plug preloads, then necessary adjustment factors are calculated and applied. Additionally, tool readings are calculated and compared to the minimum deflection measurement tool readings. The evaluation is limited to critical plug locations. This methodology is consistent with first license renewal (as clarified in RAI 4.6.3-2 of [10]) and considers iron atom displacements for a 10% bias on the peripheral and re-entrant corner assembly relative powers, as well as a 10% increase to account for fluence uncertainty at 72 EFPY.

2.2 Unit 1 CSB Plug Calculations

Calculation of Plug Preloads Required to Resist Hydraulic Drag Forces

[ ]a,c,e

Calculation of Irradiation-Induced Relaxation Factors

Fluence at Plug ID 6-12: $Fluence_{6L_1} := mean(DPA_{EFPY72\_6\_12} - DPA_{EOC6\_6\_12})$

Fluence at Plug ID 17-5: $Fluence_{6L_2} := mean(DPA_{EFPY72\_17\_5} - DPA_{EOC6\_17\_5})$

Fluence at Plug ID 14-2: $Fluence_{6L_3} := mean(DPA_{EFPY72\_14\_2} - DPA_{EOC6\_14\_2})$

Relaxation Factor in Plug Flange from EOC 6 Through EOL

[

]a,c,e

Calculation of Required Plug Flange Deflection

[

]a,c,e

Calculation of Required Minimum Plug Flange Deflection Measurement Tool Reading

[

]a,b,c,e

2.3 Evaluation of Unit 1 RVI Fatigue Analyses

The Unit 1 RVI fatigue analyses are performed for the EPU in calculation note CN-RIDA-09-9, [3]. The EPU thermal and hydraulic loads are applicable to SLR per Item 2 in the Attachment to the design input transmittal [7]. The number of design transient event occurrences projected for SLR in [6] is bounded by the number of design transient event occurrences used in the fatigue analysis of [3]. Since the inputs to the fatigue analysis performed for EPU are not affected by SLR, the Unit 1 RVI fatigue analyses performed for the EPU in calculation note CN-RIDA-09-9, [3], remain applicable. This evaluation meets the fatigue criteria specified in the May 1972 draft of Section III, Subsection NG of the ASME Boiler and Pressure Vessel Code to address RAI 4.6.3-1 of [10].

2.4 Evaluation of Unit 2 RVI Fatigue Analyses

The Unit 2 RVI fatigue analyses are performed for the EPU in calculation note CN-RIDA-14-114, [8]. The EPU thermal and hydraulic loads are applicable to SLR per Item 2 in the Attachment to the design input transmittal [7]. The number of design transient event occurrences projected for SLR in [6] is bounded by the number of design transient event occurrences used in the fatigue analysis of [8]. Since the inputs to the fatigue analysis performed for EPU are not affected by SLR, the Unit 2 RVI fatigue analyses performed for the EPU in calculation note CN-RIDA-14-114, [8], remain applicable. This evaluation meets the fatigue criteria specified in the May 1971 Edition with Addenda through Winter 1973 of Section III, Subsection NG of the ASME Boiler and Pressure Vessel Code.

3.0 Comparison of Actual Plug Flange Deflection Versus Minimum Required Results

The minimum margin [ ]b,c,e at Plug ID 17-5. For comparison, the minimum margin was [ ]b,c,e at Plug ID 14-2 calculated for 54 EFPY in [2]. The minor difference of [ ]b,c,e is reasonable since the relaxation factor as a function of fluence decreases exponentially, so the added fluence due to SLR has a minor effect on the relaxation of the plugs.

4.0 References

1. Westinghouse Calculation Note, F-ME-C-000019, Rev. 00, "Evaluation of CSB Repair Plug Preloads for RSG and License Renewal," September 20, 2001.
2. Westinghouse Calculation Note, CN-RIDA-09-4, Rev. 0, "St. Lucie Unit 1 EPU Evaluation of CSB Repair Plug Preload," March 31, 2009.
3. Westinghouse Calculation Note, CN-RIDA-09-9, Rev. 1, "St. Lucie Unit 1 EPU Reactor Vessel Internals Stress Analysis," August 30, 2013, as modified by:
   (a) Assessment Record, CN-RIDA-09-9-R1-ASMT-1.
4. Combustion Engineering Calculation, 19367-640-60, Rev. 01, "Calculation of Minimum Allowable Plug Flange Deflections," September 10, 1985.
5. Combustion Engineering Document, 19367-MD-GI-01, Rev. 05, "Guidelines for Post Installation Inspection of Core Support Barrel Plugs and Patches," October 23, 1985.
6. Westinghouse Calculation Note, CN-SDA-II-20-026, Rev. 1, "St. Lucie Unit 1 and Unit 2 80-Year Transient Cycle Projections," June 4, 2021.
7. Florida Power & Light Company Letter, PSLWEC-21-0013, Rev. 0, "Design Input Transmittal for WS07a Other TLAAs to Support the St. Lucie Unit 1 and Unit 2 Subsequent License Renewal," February 24, 2021.
8. Westinghouse Calculation Note, CN-RIDA-14-114, Rev. 1, "Design Reconciliation of St. Lucie Unit 2 Reactor Vessel Internals under Normal Operating plus Upset Conditions with AREVA Fuel," March 19, 2015.
9. Combustion Engineering Report, CEN-324 (F), "Engineering Overview Report of St. Lucie Unit One Post Cycle Six Inspection," May 12, 1986.
10. Florida Power & Light Company Letter, L-2002-165, "St. Lucie Units 1 and 2 Docket Nos. 50-335 and 50-389 Response to NRC Request for Additional Information for Review of the St. Lucie Units 1 and 2 License Renewal Application," October 10, 2002. (ADAMS Accession Number ML022890450).

Approval Information
Author Approval DiFiore Michael A Jul-09-2021 13:00:37
Verifier Approval Delport Gerrie W Jul-09-2021 13:46:28
Manager Approval Rigby Stephen Jul-09-2021 15:03:21

Files approved on Jul-09-2021

Enclosure 4

Non-proprietary Reference Documents and Redacted Versions of Proprietary Reference Documents (Public Version)

Attachment 13

Westinghouse Report LTR-SDA-20-099-NP, Revision 1, St. Lucie Units 1&2 Subsequent License Renewal: Task 9E RCP Casing Code Case N-481 Evaluation, April 7, 2021

(21 Total Pages, including cover sheets)

Westinghouse Non-Proprietary Class 3

LTR-SDA-20-099-NP, Revision 1

St. Lucie Units 1&2 Subsequent License Renewal: Task 9E RCP Casing Code Case N-481 Evaluation

April 7, 2021

Author: Gordon Z. Hall*, Structural Design & Analysis

Author: Jennifer J. Zhang*, Concrete/Re-bar Design & Seismic Analysis

Verifiers: B. Reddy Ganta*, Structural Design & Analysis

Manager: Stephen P. Rigby*, Structural Design & Analysis

Forward

This document contains Westinghouse Electric Company LLC proprietary information and data which has been identified by brackets. Coding (a,c,e) associated with the brackets sets forth information which is considered proprietary.

The proprietary information and data contained within the brackets in this report were obtained at considerable Westinghouse expense and its release could seriously affect our competitive position. This information is to be withheld from public disclosure in accordance with the Rules of Practice 10 CFR 2.390 and the information presented herein is safeguarded in accordance with 10 CFR 2.390. Withholding of this information does not adversely affect the public interest.

This information has been provided for your internal use only and should not be released to persons or organizations outside the Directorate of Regulation and the Advisory Committee on Reactor Safeguards (ACRS) without the express written approval of Westinghouse Electric Company LLC. Should it become necessary to release this information to such persons as part of the review procedure, please contact Westinghouse Electric Company LLC, which will make the necessary arrangements required to protect the Company's proprietary interests.

Several locations in this topical report contain proprietary information. Proprietary information is identified and bracketed. For each of the bracketed locations, the reason for the proprietary classification is provided, using a standardized system. The proprietary brackets are labeled with three (3) different letters, "a", "c", and "e" which stand for:

a. The information reveals the distinguishing aspects of a process or component, structure, tool, method, etc. The prevention of its use by Westinghouse's competitors, without license from Westinghouse, gives Westinghouse a competitive economic advantage.

c. The information, if used by a competitor, would reduce the competitor's expenditure of resources or improve the competitor's advantage in the design, manufacture, shipment, installation, assurance of quality, or licensing of a similar product.

e. The information reveals aspects of past, present, or future Westinghouse- or customer-funded development plans and programs of potential commercial value to Westinghouse.

1.0 Background and Purpose

Loss-of-fracture toughness due to thermal aging embrittlement of cast austenitic stainless streel (CASS) Reactor Coolant Pump (RCP) casings is identified as an aging effect/mechanism in GALL-SLR report NUREG-2191, Volume 2, AMP XI.M12 [1]. Specifically, GALL-SLR provides an allowance for continued use of flaw evaluations performed as part of implementation of Code Case N-481:

> *For pump casings, as an alternative to the screening, no further actions are needed if applicants demonstrate that the original flaw tolerance evaluation performed as part of the ASME Code Case N-481 implementation remains bounding and applicable for the subsequent license renewal (SLR) period or the evaluation is revised to be applicable for 80 years.*

Furthermore, based on the latest Public Meeting #2 on USNRC Lessons Learned on SLR [2], the aging management program (AMP) on Thermal Aging Embrittlement of CASS will be updated to include plant specific reviews of the pump casings.

In 1993, the Combustion Engineering (CE) Owners group performed Code Case N-481 flaw evaluations for several CE NSSS fleet pumps, including St. Lucie Units 1 and 2 Byron-Jackson RCPs in the report CEN-412, Revision 2 [3]. The Code Case N-481 allows visual inspections in lieu of volumetric inspections of the pump casing base metal and welds based on a fracture mechanics evaluation. The USNRC received the CEN-412 report, but did not approve it generically and requested that utilities retain a copy at site for future audits as needed [4].

In 2003, for St. Lucie Units 1 and 2 first license renewal, the USNRC accepted the use of ASME Section XI IWB in-service inspection program to manage the reduction of fracture toughness for the RCP CASS components (see subsection 3.1.5.2.1 of Reference 5). However, as described above, for subsequent license renewal, the USNRC requires an AMP on Thermal Aging Embrittlement of CASS for RCP casings for the SLR period of 80 years. Thus, the description provided herein addresses the scope for pressure boundary RCP CASS components for SLR.

The purpose of this letter report is to summarize the Code Case N-481 RCP casing flaw evaluation for the St. Lucie Units 1 & 2 Subsequent License Renewal (SLR), Task 9e of LTR-AMER-MKG-20-1686 [9].

Revision 1 of this letter incorporates the editorial comments from the customer. The changes are marked by change bars. Customer comment resolution forms are electronically attached in PRIME.

2.0 Method Discussion

The overall methodology is to perform a reconciliation analysis for St. Lucie Units 1 and 2 to the evaluation completed in CEN-412 in support of SLR. The latest piping loads, and 80-year design transients and cycles will be considered for the reconciliation. The fracture toughness evaluated in CEN-412 was based on NUREG-4513, Rev. 0 [6.a]. Since then Revision 1 and Revision 2 of NUREG/CR-4513 have been published [6.b and 6.c], a confirmatory check is performed for St. Lucie RCP casings per NUREG/CR-4513 Rev. 1 and 2. For fatigue crack growth evaluation, St. Lucie Units 1 and 2 considered growth rates based on older industry accepted models as discussed in Section 5.1 of CEN-412. For the SLR scope, a comparison to the more recently accepted fatigue crack growth rates are considered for stainless steel in air environment from Appendix C of the ASME Section XI code [8], with a PWR environment factor of 2 applied, per [7].

3.0 Acceptance Criteria

As discussed in CEN-412 [3], the calculated RCP casing material fracture toughness provide a basis for calculating the end-point crack size limits for the two failure modes related to thermal embrittlement: non-ductile propagation and ductile tearing. The third criterion for establishing end-point crack size is based on the flow stress of the material. An end-point crack size was determined by these three criteria:

1. The crack becomes unstable against non-ductile propagation.
2. The crack becomes unstable against ductile tearing.
3. The remaining ligament cannot carry its original loading, based on its flow stress.

Acceptance criteria are based on ASME Section XI IWB-3600 [8].

4.0 Input

Combustion Engineering (CE) Owners Group report, CEN-412 [3], contains detailed information of the St. Lucie Units 1 and 2 RCPs. Generic descriptions of the RCP casing design, fabrication, and materials are discussed in Section 3 of the main body of CEN-412. The St. Lucie Units 1 and 2 specific inputs including CMTR chemistry, yield and tensile strength, transients and cycles are in Appendix E of CEN-412. The FPL design input transmittal [17] confirmed the design reports [10, 11], design specifications [12, 13], the ASME Section XI [8], and that there have been no indications identified in the pump casings.

5.0 Fatigue Crack Growth

The fatigue crack growth evaluation in the CEN-412 [3] is reassessed and reconciled in this section for St. Lucie Units 1 and 2 SLR. The main body of CEN-412 report discussed the general methodology for CE plants. Appendix E of CEN-412 is specific for the St. Lucie Units 1 and 2.

Design Transients and Loads

CEN-412, Appendix E referenced the Byron-Jackson company stress reports [10 and 11] and the corresponding RCP specifications 19367-31-3, Rev. 4 [12] for Unit 1, and 13172-PE-480, Rev. 05 [13] for Unit 2. FPL confirmed these stress reports are applicable for St. Lucie Units 1 and 2 in [17]. The Unit 1 RCP specification referenced in CEN-412 is consistent with the stress report, TCF-1017-STR, Vol. 1, Rev. 1 [10]. However, the Unit 2 stress report, TCF-1024-STR, Vol. 1, Rev. 1 [11] referenced the original issue, Rev. 0 of the engineering specification 13172-PE-480, where CEN-412 referenced Rev. 5 of the Unit 2 RCP specification. Comparison of the specification 13172-PE-480, Rev. 0 vs. Rev. 5 concluded the transient definitions and cycles are identical. The dead weight, thermal and accident RCP nozzle loads in Rev. 5 are identical to Rev. 0. Since the maximum seismic loads in Rev. 0 of the specification are all greater than the envelop SSE loads in Rev. 5, the Unit 2 stress report [11] is conservative, applicable to evaluations in CEN-412 and the SLR application.

Critical Locations

Per CEN-412, Appendix E, Section 5.3, the high stress locations are:

(1) Diffuser Vane 8

(2) Discharge Nozzle, Section C, adjacent to Crotch Region

(3) Suction Nozzle

(4) Junction, Volute with Lower Flange

(5) Hanger Bracket #1 Vicinity

As discussed in Section 5.1.1 of CEN-412, the critical locations were determined by reviewing stresses in the Byron-Jackson company stress reports, which are [10 and 11] for St. Lucie Units 1 and 2. These are the applicable stress reports for SLR per [17]. Therefore, these critical locations remain applicable for the SLR application.

Initial Flaw Size

As discussed in CEN-412, Sections 4.4, 4.5 and 5.1.2, the postulated initial flaw size is 8% of the section thickness for all cases. Since any detectable cracks in the pump casings would have been required to be repaired as part of preoperational inspection, and the radiographic detection sensitivity was 2% section thickness, the assumed 8% initial flaw size is a conservative estimate of the largest undetectable crack. The length to depth aspect ratio (AR) for the postulated flaw is assumed to be 6:1. Additionally, the fatigue crack growth evaluation assumed the AR remain unchanged throughout the growth history. These assumptions discussed in CEN-412 remain valid for the St. Lucie SLR application.

Stress Intensity Factor

The surface flaw stress intensity factors (K_I) were calculated per Equation 5-1 of CEN-412:

$$K_I = (\sigma_m M_m + \sigma_b M_b)\sqrt{\frac{\pi a}{Q}}$$

The parameters M_m, M_b and Q are calculated and listed in Table 5.1-1 of CEN-412, per Figures A-3300-3, A-3300-5 and A-3300-1 in pre-1994 editions of ASME Section XI, Appendix A. Per ASME record XI-1-A94 (94-90), Appendix A, A-3300 was revised. It modified A-3000 to allow the user to use a more accurate and less conservative formulation for determining stress intensity factors for any gradient stress distribution over the flaw face. The comparison made between the new method and existing methods are documented in a paper by Lawrence and Hechmer and [16] published in the ASME Journal of Pressure Technology in June 1991. Therefore, the K_I calculated in the CEN-412 remain applicable for St. Lucie SLR application.

Fatigue Crack Growth Rate

As discussed in CEN-412 [3], section 5.1.4, the fatigue crack growth rate (CGR) is the Bernard & Slama equation:

$$\frac{da}{dN} = 4.306 \times 10^{-11}\left(\frac{\Delta K_I}{1 - {}^{R}/_{2}}\right)^4$$

where $R = K_{I\_min}/K_{I\_max}$ through the cycle. A simplifying and conservative assumption of $K_{I\_min} = 0$, i.e., the RCP is not running, at room temperature and zero stress. The crack growth rate is then simplifies to:

$$\frac{da}{dN} = 4.306 \times 10^{-11}(K_I)^4$$

The simplified CGR used in CEN-412 is compared to the ASME Section XI [8], Appendix C, C-8410, stainless steel CGR with a factor of 2 for water environment. As shown in Figure 5-1, the CGR used in CEN-412 is lower than the ASME XI rate until delta K_I at about 25 ksi√in. It is clearly shown that the CGR in CEN-412 is higher for $\Delta K_I > 30$ ksi√in. Since $K_{I\_min} = 0$, ΔK_I is just the maximum K_I at operating condition. As summarized in CEN-412, Appendix E, Table 5-1 through Table 5-5, all K_I are greater than 30 ksi√in. Therefore, the fatigue CGR in CEN-412 is more conservative than the CGR per ASME Section XI, C-8410 for the analyzed locations and conditions, and remain valid for the St. Lucie SLR application.

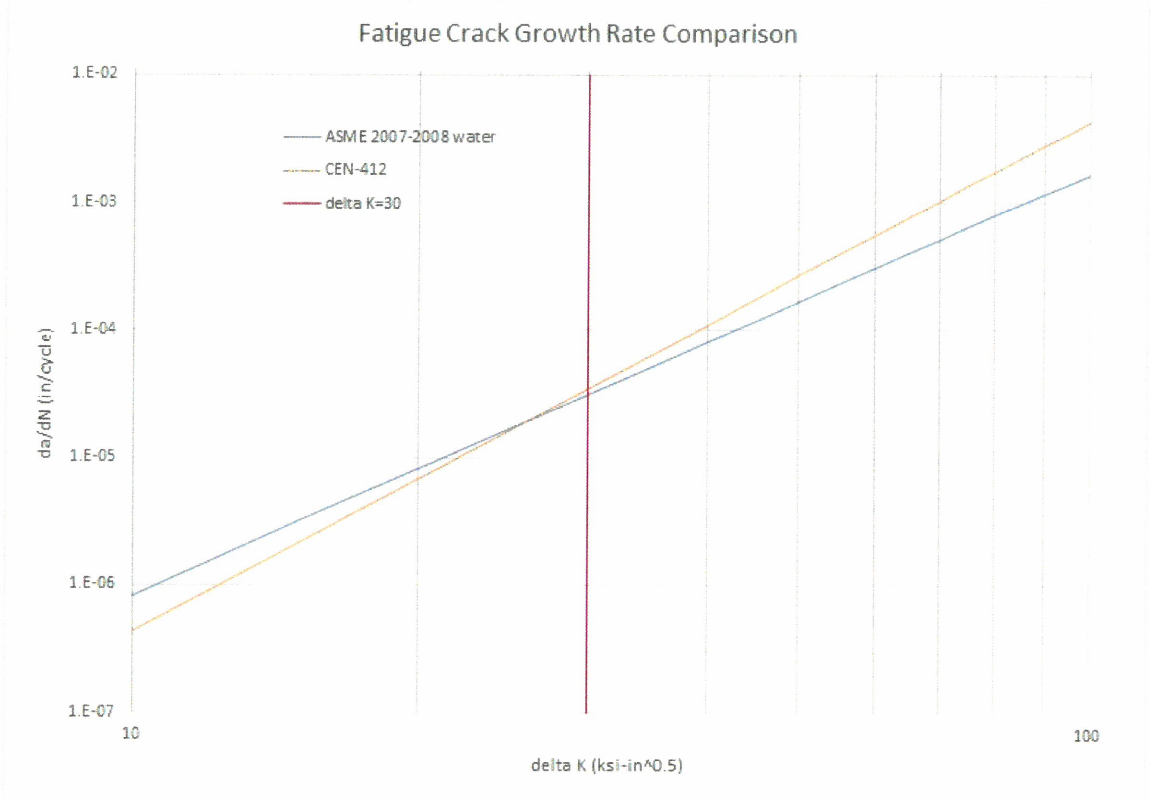

Figure 5-1: CEN-412 vs. ASME XI C-8410 Fatigue Crack Growth Rate Comparison

<u>Transients and Cycles</u>

As discussed in the generic portion of CEN-412, Section 5.1.4, and the St. Lucie plant specific, Appendix E, Section 3, the stress cycles are between atmospheric and operating pressures during heatup and cooldown over the nominal 40-year life of the plants. The Byron Jackson stress analyses in [10 and 11] used 500 cycles for heatup and cooldown. The fatigue crack growth analysis in CEN-412 used 500 cycles of heatup and cooldown plus 5 cycles of Loss of Secondary Pressure. CEN-412, Appendix E, Section 3.3 stipulates that heat-up-plus-cooldown, constitute one cycle. Based on the cycle data ending in mid-1991, it was averaged less than 3.3 cycle per year for Unit 1 and less than 3.1 cycles per year for Unit 2. At the same rate over an 80-year operation period, there will be 264 and 248 cycles for Units 1 and 2, respectively. The FCG cycles used in CEN-412 is about twice the projected cycle based on the 1991 data. Based the latest plant data, Westinghouse performed an updated 80-year cycle projection in [14]. The projected transient cycles are less than the 505 cycles analyzed in CEN-412. Therefore, the transient cycles analyzed in CEN-412 remain valid and conservative for the St. Lucie SLR application.

Based on the review of the aforementioned input and methodology, the St. Lucie Units 1 and 2 plant specific FCG evaluation in CEN-412 [3] remain valid for the 80-year SLR application.

6.0 Fracture Toughness of St. Lucie Units 1 and 2 RCP Casings

For the St. Lucie Units 1 and 2 SLR of 80 years, the plant-specific saturation (fully aged) fracture toughness values of the RCP casings are determined based on fracture toughness correlations for thermal aging of CASS from both of Rev. 1 and 2 of NUREG/CR-4513 [6.b and 6.c].

In CEN-412 [3], Section 5, the fracture toughness properties were predicted for the aged material of St. Lucie Units 1 and 2 RCP casings per NUREG/CR-4513, Rev. 0 [6.a], using chemistry compositions data from certified material test reports (CMTR). The deformation J integral (J_d) are recalculated per the updated NUREG/CR-4513, Rev.1 and Rev.2 [6.b and 6.c] using St. Lucie specific CMTR chemistry data provided in Appendix E of CEN-412, Rev.2 [3]. The chemical compositions and the aged flow stress values at Room Temperature (70°F) and 550°F of each heat are provided in Appendix E of CEN-412, Rev.2 [3]. The material chemistry and the aged flow stress values are replicated in Table 6-1 and Table 6-2 for St. Lucie Units 1 and 2, respectively. J-integral resistance (J-R) curves are then created by J_d at various flaw extensions.

In CEN-412, Rev.2 [3], J_{Ic} is determined from the saturation J-R curve equation according to the methods of ASTM E 813-89 [15], which is shown in Figure 6-1. J_{Ic} is defined as the intersection of the 0.2 mm offset line with the power law equation of the J-R Curve. ASTM E 813 uses a slope of two times the flow stress (σ_f) for the blunting, data exclusion and offset lines. The flow stress is defined as the average of the yield strength and tensile strength. As described in Appendix B of NUREG/CR-4513, Rev.2 [6.c], J-R curve tests on CASS materials indicate that a slope of four times the flow stress for the blunting line expresses the J-vs.-Δa data better than the slope of two times the flow stress as defined in ASTM E 813-89 [15]. The fracture toughness J_{Ic} values are determined with the slope ($4\sigma_f$) for the blunting line and the 0.2 mm offset line per NUREG/CR-4513, Rev.2 [6.c], using the iteration procedure described in Section 9.2.6 of ASTM E 813-89 [15].

The elastic-plastic fracture toughness, J_{Ic}, can be converted to an equivalent linear-elastic fracture toughness, K_{Jc}. When plane strain conditions predominate, the relationship between J and K is given by the equation,

$$J = K^2/[E/(1-v^2)]$$

where E is the elastic modulus and v is Poisson's ratio. Per CEN-412, Rev.2 [3], E at Room Temperature (70°F) and 550°F are equal to 2.83×10^7 psi and 2.56×10^7 psi, respectively. The aged flow stress values at room temperature (70°F) and 550°F of each heat are provided in Appendix E of CEN-412, Rev.2 [3]. J_{Ic} and K_{Jc} of the critical heat of RCPs at St. Lucie Unit 1 and Unit 2 are summarized in Table 6-3 and Table 6-4, respectively.

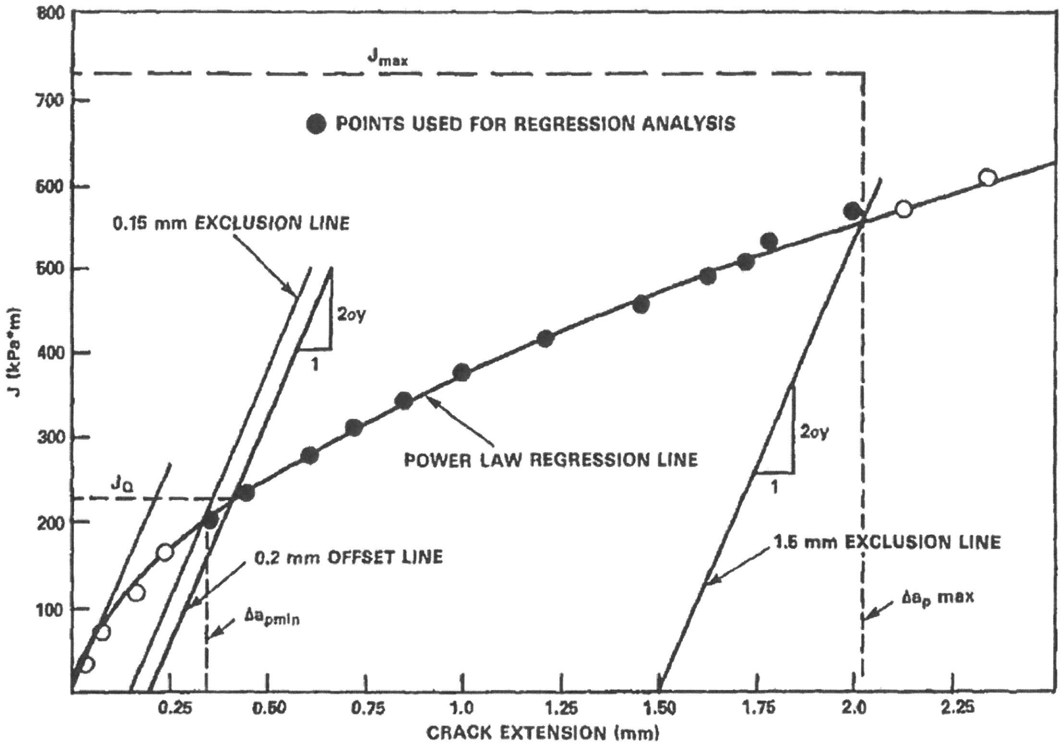

Figure 6-1: Curves to Define J_{IC} per ASTM E-813 [15] and CEN-412 [3]

Note:

The slope of the blunting line is generically illustrated as $2\sigma_y$, or 2 times flow stress. Flow stress is denoted as σ_f in this report for clarity. Per NUREG/CR-4531, Rev. 2 [6.c], $4\sigma_f$ will be used for the blunting line slope to calculate J_{Ic} herein.

Table 6-1: St. Lucie Unit 1 RCP Casings Chemistry and Aged Flow Stress

	Heat #	%Ni	%C	%Mn	%Cr	%Si	%Mo	%N	Aged Flow Stress	
									RT (ksi)	550°F (ksi)
Pump 681-N-0445										
CASING WELD	4146	9.96	0.02	1.84	20.48	1.47	2.7	0.04	78.6	58
HUB/DIFFUSER	40116	9.48	0.06	0.67	19.15	0.96	2.48	0.04	76.215	55.621
CASING WELD	3063	10.29	0.04	1.7	19.89	0.53	2.81	0.04	78.6	58
CASE SCROLL	46737	9.33	0.06	0.7	18.66	1.22	2.29	0.04	81.44	60.846
CASING WELD	X43439	9.1	0.03	1.39	19.9	0.36	2.31	0.04	78.6	58
CASING WELD	4367	9.78	0.02	1.64	19.01	1.37	2.98	0.04	78.6	58
CASING WELD	4459	9.44	0.02	0.91	19.82	0.51	2.46	0.04	78.6	58
CASING WELD	3036	9.7	0.03	1.53	19.01	0.47	2.81	0.04	78.6	58
CASING WELD	4313	9.93	0.02	0.91	19.59	0.52	2.59	0.04	78.6	58
CASING WELD	03036A	9.89	0.04	1.52	18.69	0.47	2.84	0.04	78.6	58
CASING WELD	4455	9.86	0.02	0.95	18.87	0.51	2.46	0.04	78.6	58
CASING WELD	4286	10.12	0.02	0.9	18.83	0.52	2.41	0.04	78.6	58
Pump 681-N-0446										
HUB/DIFFUSER	46993	9.54	0.06	0.72	19.45	1.16	2.24	0.04	77.878	57.284
CASE SCROLL	48368	9.19	0.04	0.78	19.06	1.07	2.28	0.04	78.749	58.155
CASING WELD	X43439	9.1	0.03	1.39	19.9	0.36	2.31	0.04	78.6	58
CASING WELD	4460	10	0.02	1	20.35	0.51	2.37	0.04	78.6	58
CASING WELD	4459	9.44	0.02	0.91	19.82	0.51	2.46	0.04	78.6	58
CASING WELD	4509	9.75	0.02	0.94	19.67	0.45	2.51	0.04	78.6	58
CASING WELD	4313	9.93	0.02	0.91	19.59	0.52	2.59	0.04	78.6	58
CASING WELD	03036A	9.89	0.04	1.52	18.69	0.47	2.84	0.04	78.6	58
CASING WELD	4635	10	0.02	1	19.4	0.49	2.71	0.04	78.6	58
CASING WELD	T03951	10.03	0.04	1.55	19.02	0.5	2.44	0.04	78.6	58
CASING WELD	1953	9.69	0.02	1.68	19.11	0.44	2.83	0.04	78.6	58
CASING WELD	4455	9.86	0.02	0.95	18.87	0.51	2.46	0.04	78.6	58
CASING WELD	57203	10.2	0.02	0.66	18.65	0.48	2.41	0.04	78.6	58

Table 6-1: St. Lucie Unit 1 RCP Casings Chemistry and Aged Flow Stress (Continued)

	Heat #	%Ni	%C	%Mn	%Cr	%Si	%Mo	%N	Aged Flow Stress	
									RT (ksi)	550°F (ksi)
Pump 681-N-0447										
CASING WELD	4146	9.96	0.02	1.84	20.48	1.47	2.7	0.04	78.6	58
CASE SCROLL	45920	9.63	0.05	0.78	19.88	1.13	2.19	0.04	80.965	60.371
HUB/DIFFUSER	45871	9.77	0.06	0.68	19.15	1.08	2.17	0.04	77.007	56.413
CASING WELD	X43439	9.1	0.03	1.39	19.9	0.36	2.31	0.04	78.6	58
CASING WELD	4367	9.78	0.02	1.64	19.01	1.37	2.98	0.04	78.6	58
CASING WELD	4509	9.75	0.02	0.94	19.67	0.45	2.51	0.04	78.6	58
CASING WELD	3036	9.7	0.03	1.53	19.01	0.47	2.81	0.04	78.6	58
CASING WELD	4313	9.93	0.02	0.91	19.59	0.52	2.59	0.04	78.6	58
CASING WELD	03036A	9.89	0.04	1.52	18.69	0.47	2.84	0.04	78.6	58
CASING WELD	T03951	10.03	0.04	1.55	19.02	0.5	2.44	0.04	78.6	58
CASING WELD	4455	9.86	0.02	0.95	18.87	0.51	2.46	0.04	78.6	58
Pump 681-N-0448										
HUB/DIFFUSER	46406	9.17	0.08	0.96	19	0.94	2.21	0.04	75.345	54.751
CASE SCROLL	47380	9.33	0.06	0.7	18.66	1.22	2.29	0.04	79.699	59.106
CASING WELD	X43439	9.1	0.03	1.39	19.9	0.36	2.31	0.04	78.6	58
CASING WELD	4460	10	0.02	1	20.35	0.51	2.37	0.04	78.6	58
CASING WELD	4459	9.44	0.02	0.91	19.82	0.51	2.46	0.04	78.6	58
CASING WELD	4509	9.75	0.02	0.94	19.67	0.45	2.51	0.04	78.6	58
CASING WELD	3036	9.7	0.03	1.53	19.01	0.47	2.81	0.04	78.6	58
CASING WELD	4313	9.93	0.02	0.91	19.59	0.52	2.59	0.04	78.6	58
CASING WELD	03036A	9.89	0.04	1.52	18.69	0.47	2.84	0.04	78.6	58
CASING WELD	T03951	10.03	0.04	1.55	19.02	0.5	2.44	0.04	78.6	58
CASING WELD	1953	9.69	0.02	1.68	19.11	0.44	2.83	0.04	78.6	58
CASING WELD	4455	9.86	0.02	0.95	18.87	0.51	2.46	0.04	78.6	58
CASING WELD	57203	10.2	0.02	0.66	18.65	0.48	2.41	0.04	78.6	58

Table 6-2: St. Lucie Unit 2 RCP Casings Chemistry and Aged Flow Stress

	Heat #	%Ni	%C	%Mn	%Cr	%Si	%Mo	%N	Aged Flow Stress	
									RT (ksi)	550°F (ksi)
Pump 741-N-0001										
HUB/DIFFUSER	91097-1	9.14	0.06	0.72	19.76	1.18	2.62	0.04	86.665	66.071
CASING WELD	6074	9.84	0.06	1.29	20.92	0.55	2.52	0.04	78.6	58
CASE SCROLL	91402-1	9.5	0.05	0.62	19.38	1.28	2.18	0.04	80.411	59.817
CASING WELD	7174	10.2	0.03	1.26	19.65	0.62	2.65	0.04	78.6	58
CASING WELD	5952C	10.8	0.06	1.2	19.08	0.58	2.87	0.04	78.6	58
CASING WELD	5929	9.62	0.02	0.91	19.7	0.72	2.54	0.04	78.6	58
CASING WELD	5733	10.6	0.03	1.33	19.33	0.41	2.9	0.04	78.6	58
CASING WELD	9317-051	9.98	0.02	1.1	19.7	0.6	2.28	0.04	78.6	58
CASING WELD	5280	10.36	0.03	1.26	19.6	0.47	2.3	0.04	78.6	58
CASING WELD	5936	9.66	0.01	0.87	19.6	0.76	2.3	0.04	78.6	58
CASING WELD	5386	10.03	0.03	1.19	18.76	0.53	2.6	0.04	78.6	58
CASING WELD	7242	10.06	0.01	0.91	19.38	0.52	2.58	0.04	78.6	58
Pump 741-N-0002										
CASING WELD	6074	9.84	0.06	1.29	20.92	0.55	2.52	0.04	78.6	58
CASE SCROLL	97947-1	9.59	0.06	0.5	19.5	1.23	2.25	0.04	80.965	60.371
HUB/DIFFUSER	95211-1	9.43	0.06	0.58	19	1.09	2.1	0.04	74.395	53.801
CASING WELD	7174	10.2	0.03	1.26	19.65	0.62	2.65	0.04	78.6	58
CASING WELD	5929	9.62	0.02	0.91	19.7	0.72	2.54	0.04	78.6	58
CASING WELD	5733	10.6	0.03	1.33	19.33	0.41	2.9	0.04	78.6	58
CASING WELD	6546	10.39	0.03	1.42	20.01	0.38	2.39	0.04	78.6	58
CASING WELD	9317-051	9.98	0.02	1.1	19.7	0.6	2.28	0.04	78.6	58
CASING WELD	7553A	10.52	0.05	1.24	18.91	0.42	2.74	0.04	78.6	58
CASING WELD	7242	10.06	0.01	0.91	19.38	0.52	2.58	0.04	78.6	58

Table 6-2: St. Lucie Unit 2 RCP Casings Chemistry and Aged Flow Stress (Continued)

	Heat #	%Ni	%C	%Mn	%Cr	%Si	%Mo	%N	Aged Flow Stress	
									RT (ksi)	550°F (ksi)
Pump 741-N-0003										
CASING WELD	6074	9.84	0.06	1.29	20.92	0.55	2.52	0.04	78.6	58
HUB/DIFFUSER	99346-1	9.57	0.06	0.67	19.14	1.27	2.26	0.04	74.395	53.81
CASING WELD	7174	10.2	0.03	1.26	19.65	0.62	2.65	0.04	78.6	58
CASING WELD	6546	10.39	0.03	1.42	20.01	0.38	2.35	0.04	78.6	58
CASING WELD	5733	10.6	0.03	1.33	19.33	0.41	2.9	0.04	78.6	58
CASE SCROLL	99918-1	9.85	0.04	0.49	18.76	1.21	2.11	0.04	73.999	53.405
CASING WELD	7553A	10.52	0.05	1.24	18.91	0.42	2.74	0.04	78.6	58
CASING WELD	7242	10.06	0.01	0.91	19.38	0.52	2.58	0.04	78.6	58
Pump 741-N-0004										
CASING WELD	6074	9.84	0.06	1.29	20.92	0.55	2.52	0.04	78.6	58
HUB/DIFFUSER	99161-1	9.5	0.06	0.66	19.21	1.27	2.13	0.04	77.403	56.809
CASE SCROLL	00233-1	9.42	0.07	0.58	18.85	1.21	2.11	0.04	71.149	50.555
CASING WELD	6546	10.39	0.03	1.42	20.01	0.38	2.35	0.04	78.6	58
CASING WELD	5733	10.6	0.03	1.33	19.33	0.41	2.9	0.04	78.6	58
CASING WELD	5280	10.36	0.03	1.26	19.6	0.47	2.3	0.04	78.6	58
CASING WELD	7553A	10.52	0.05	1.24	18.91	0.42	2.74	0.04	78.6	58
CASING WELD	5386	10.03	0.03	1.19	18.76	0.53	2.6	0.04	78.6	58
CASING WELD	7242	10.06	0.01	0.91	19.38	0.52	2.58	0.04	78.6	58

Table 6-3: St. Lucie Unit 1 RCP Casings Critical J_{Ic} and K_{Jc}

[ ]a,c,e

Table 6-4: St. Lucie Unit 2 RCP Casings Critical J_{Ic} and K_{Jc}

[ ]a,c,e

As shown in Table 6-3 and Table 6-4, the limiting fracture toughness, K_{Jc} is [ ]a,c,e for normal operation at 550°F.

7.0 Critical Flaw Size and Acceptable Period of Operation

As discussed in CEN-412 [3], the calculated RCP casing material fracture toughness provide a basis for calculating the end-point crack size limits for the two failure modes related to thermal embrittlement: non-ductile propagation and ductile tearing. The third criterion for establishing end-point crack size is based on the flow stress of the material. An end-point crack size was determined by these three criteria:

1. The crack is unstable against non-ductile propagation.
2. The crack is unstable against ductile tearing.
3. The remaining ligament cannot carry its original loading, based on its flow stress.

In all cases analyzed in CEN-412 [3], the end-point crack depth is limited by the flow stress, not the fracture toughness criteria. The end-point crack depth will be referred to as critical flaw size in this calculation note.

7.1 Critical Flaw Size Based on Non-Ductile Propagation

As discussed in CEN-412 [3], the non-ductile propagation criterion is met if applied K_I is less than the aged material toughness, K_{Jc}. The limiting location for St. Lucie Units 1 and 2 is the Vane number 8. As shown in CEN-412, Appendix E, Table 5-1, reproduced here in Table 7-1, the applied $K_I = 99.35$ ksi√in at a/t of 0.40, for 130 years of crack growth, which is bounding of the 80-year of SLR. The applied K_I for a/t = 0.40 is 99.35 ksi√in, less than the minimum K_{Jc} = [ ]^{a,c,e}. Therefore, the non-ductile crack propagation criterion is met for a flaw depth of 40% wall thickness in a hypothetical crack growth of nearly 130 years.

$$K_I = 99.35\ ksi\sqrt{in} < K_{Jc} = [\qquad\qquad]^{a,c,e}\text{, at 130 years, a/t = 0.40}$$

Table 7-1: St. Lucie Units 1 and 2 Crack Growth Results at Vane Number 8

a/t Interval (fraction)	K_I (KSI √IN)	da/dT (IN/YEAR)	ΔTime (YEARS)	
0.08 -- 0.10	49.98	3.39×10^{-3}	28.0	
0.10 -- 0.15	60.08	7.08×10^{-3}	45.6*	129.9
0.15 -- 0.20	68.76	1.21×10^{-2}	24.4*	years
0.20 -- 0.25	76.76	1.89×10^{-2}	12.5	
0.25 -- 0.30	84.17	2.73×10^{-2}	8.7	
0.30 -- 0.35	91.69	3.84×10^{-2}	6.2	
0.35 -- 0.40	99.35	5.29×10^{-2}	4.5	
0.40 -- 0.45	108.3	7.48×10^{-2}	3.2	
0.45 -- 0.50	118.4	0.107	2.2	

(σ_m = 20.95, σ_b = 19.87, t = 4.75")

* Sum of five time steps through 1% a/t increments using interpolated K_I values.

7.2 Critical Flaw Size Based on Unstable Ductile Tearing

As discussed in CEN-412, Section 5.3.2, stability against ductile tearing is ordinarily demonstrated by comparing applied J-integrals ($J_{applied}$) for a series of crack depths to the tearing modulus slope, and demonstrating that after a given crack extension, the J_d of the material exceeds the $J_{applied}$, i.e., $\frac{\partial J_{applied}}{\partial a} < \frac{dJ_d}{da}$. However, this flaw stability criteria are only necessary only when the $J_{applied}$ exceeds the J_{Ic}, J-integral required for the initial ductile tearing. Here the condition is satisfied because the applied $K_I < K_{Jc}$ as shown in Section 7.1. Therefore, the stability against ductile tearing criteria is satisfied, and the fatigue cycles is the only crack growth mechanism.

7.3 Critical Flaw Size Based on Flow Stress Limit

As discussed in Sections 5.3.3 and 5.3.4 of CEN-412 [3], the remaining ligament (uncracked segment of the thickness) in a cracked section must remain capable of carrying the applied force and moment. A conservative, two-dimensional approximation method was used to establish the limiting crack depth for which this would no longer be possible. Once the flow stress limited crack depth is reached, any subsequent crack growth renders the remaining ligament incapable of supporting the load application. The critical flaw sizes based on flow stress for St. Lucie Units 1 and 2 RCP casing under design, emergency and faulted conditions were conservatively calculated and shown in CEN-412 Figures 5.3-5, 5.3-10 and 5.3-15. These results are reproduced in Figure 7-1, Figure 7-2 and Figure 7-3. The critical flaw sizes based on the flow stress criterion is a/t=0.44 for design; a/t > 0.5 for emergency; and a/t = 0.38 faulted conditions. The most limiting critical flaw sizes is a/t = 0.385 for faulted conditions at 130 years, consistent with CEN-412.

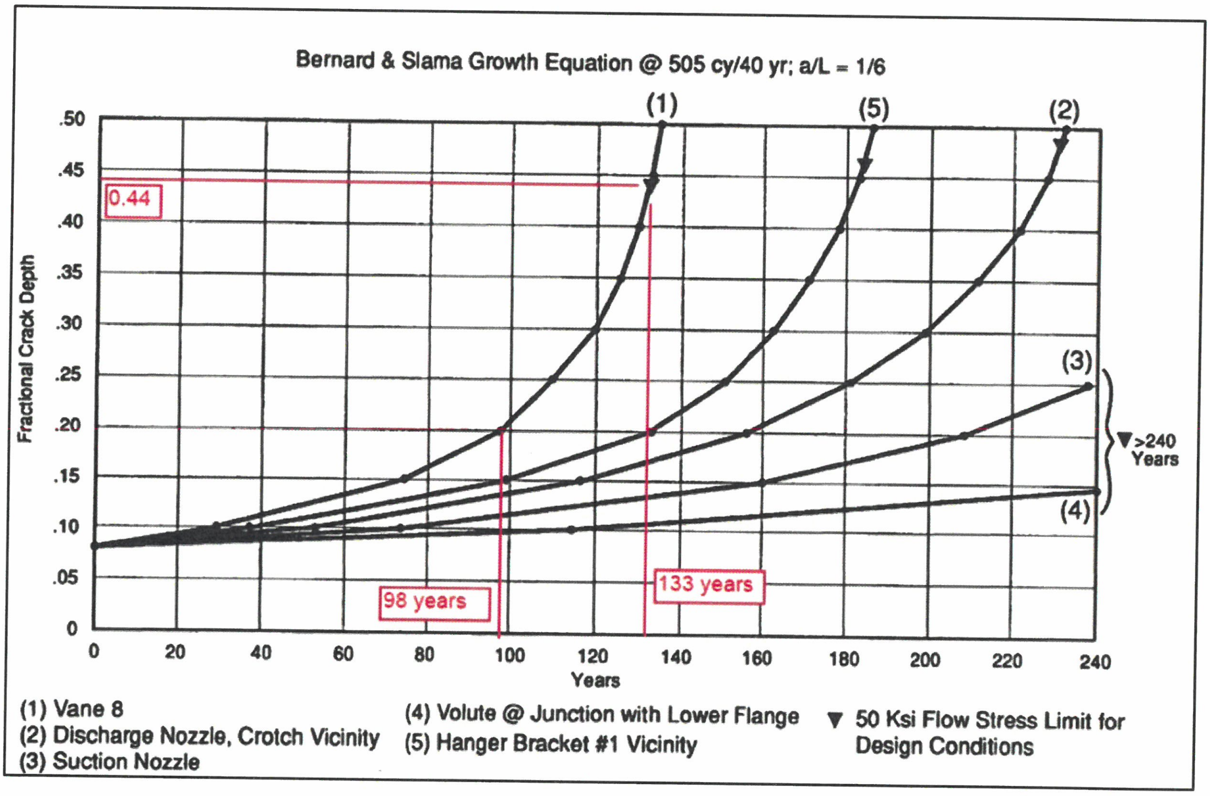

Figure 7-1: St. Lucie Units 1 and 2 FCG with Flow Stress Limit for Design Conditions

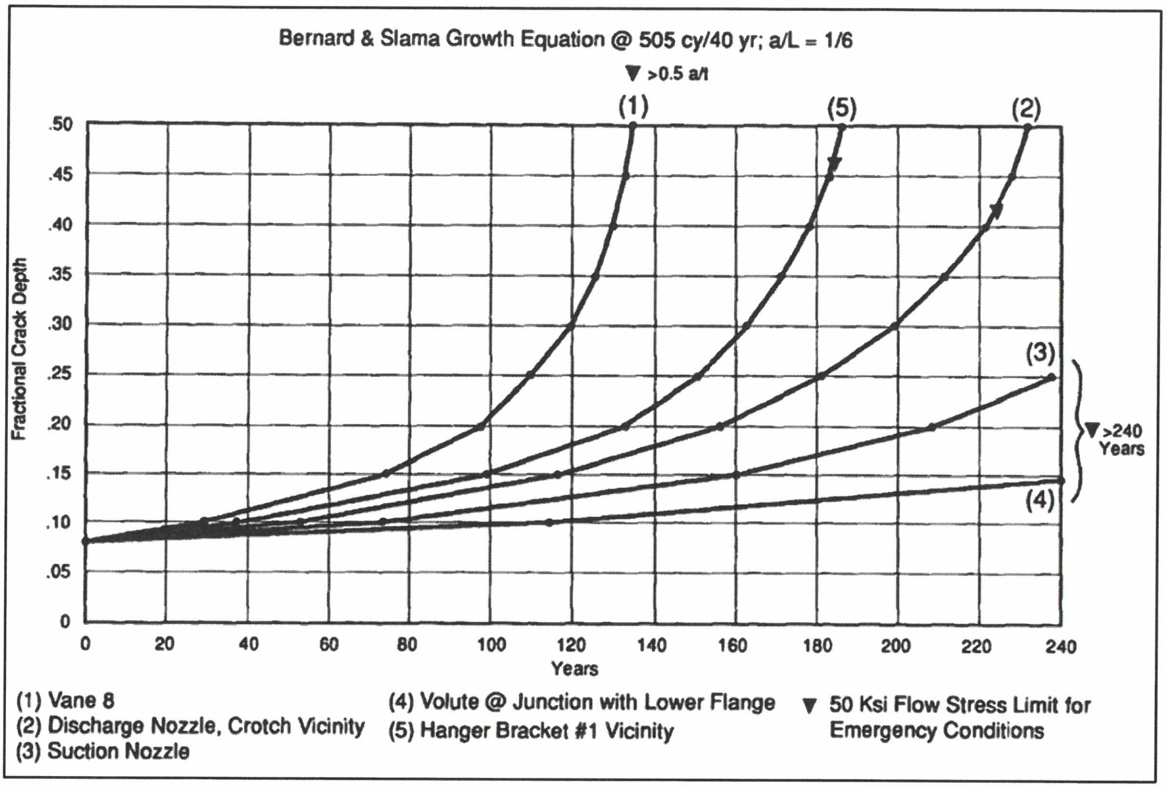

Figure 7-2: St. Lucie Units 1 and 2 FCG with Flow Stress Limit for Emergency Conditions

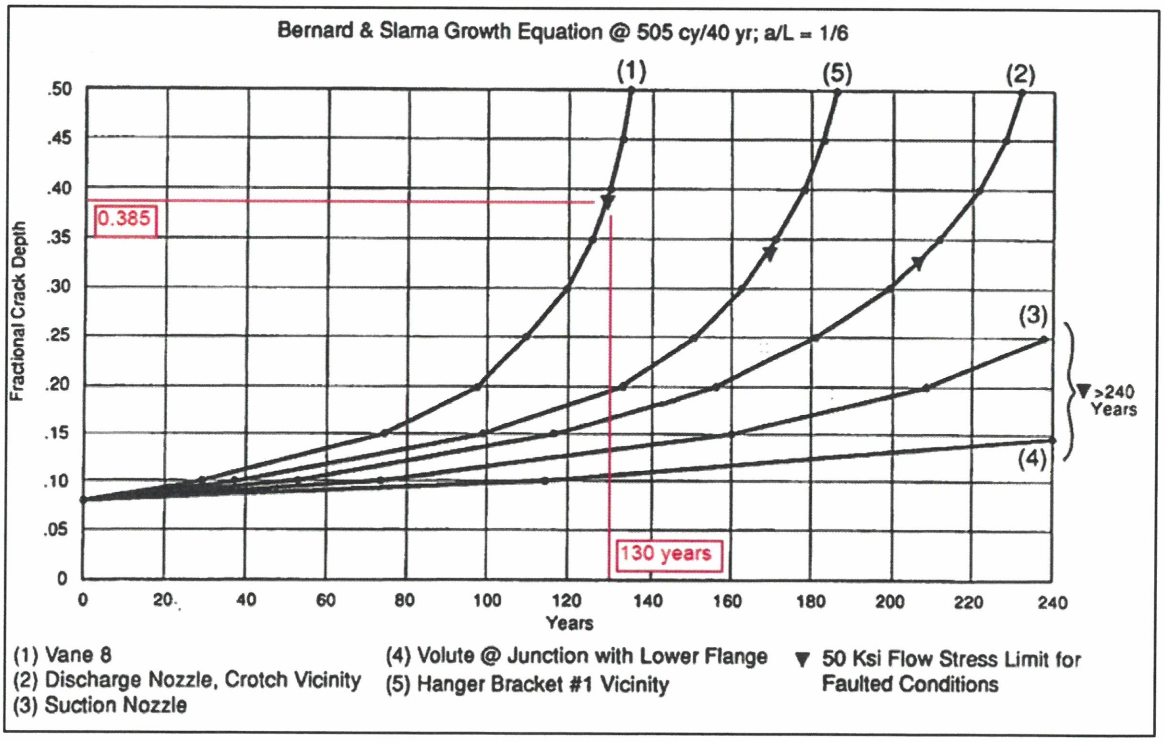

Figure 7-3: St. Lucie Units 1 and 2 FCG with Flow Stress Limit for Faulted Conditions

8.0 Summary and Conclusion

The fatigue crack growth evaluations for St. Lucie Units 1 and 2 RCP casing were reconciled for the 80-year SLR operation in Section 7.1 and the current ASME Section XI crack growth rate [8]. Section 7.2 updates for the fracture toughness for RCP casings were per NUREG/CR-4513, Revisions 1 and 2 [6.b, 6.c]. As discussed in CEN-412 [3] and Section 7.2, since the applied $K_I < K_{Jc}$, the stability against ductile tearing criteria is satisfied, and the fatigue cycles is the only crack growth mechanism. Section 7.3 evaluated the critical flaw sizes and acceptable period of operation based on non-ductile propagation, ductile tearing, and flow stress limit.

The conclusions in CEN-412 [3] remain valid for 80-year SLR operation. A postulated initial flaw depth of 8% wall thickness will grow to 25% in about 110 years while satisfying the non-ductile propagation and ductile tearing criteria of $K_I < K_{Jc}$. The postulated flaw will continue to grow until reaching the critical flaw size of 38%, limited by the flow stress in about 130 years.

Therefore, the St. Lucie Units 1 and 2 RCP casings meet the material criteria in ASME Code Case N-481 for waiving volumetric examinations of cast austenitic pump casings. A postulated 25% thickness reference flaw will remain stable under governing design, emergency and faulted conditions stresses. All calculated endpoint (critical) flaw depths are greater than the 25% thickness reference flaw postulated in Code Case N-481. Base on this evaluation, it is concluded that inservice volumetric examination of these RCP casings are not necessary for the 80-year SLR period of operation. However, visual (VT-3) examinations of casing inside surfaces, to the extent practical, are prudent whenever an RCP is disassembled for maintenance. The St. Lucie Units 1 and 2 RCP casing integrity is shown to be retained for a total of 130 years from initial operation.

9.0 References

1. NUREG-2191, Volume 2, "Generic Aging Lessons Learned for Subsequent License Renewal (GALL-SLR) Report," July 2017. (ADAMS Accession Number ML17187A204).
2. USNRC Presentation on December 12, 2019, "Subsequent License Renewal (SLR) Lessons Learned Public Meeting #2." ML19345F191.
3. CE Owners Group Report, CEN-412, Revision 2, "Relaxation of Reactor Coolant Pump Casing Inspection Requirements," April 1993. CEOG Task 678.
4. FPL Letter L-92-320, "St. Lucie Unit 1 Docket No. 50-335, ASME Boiler and Pressure Vessel Code Case N-481, "Alternative Exam Requirements for Cast Austenitic Pump Casing" in place of Relief Request 7 in second 10-year inspection plan, December 1, 1992. (ADAMS No. ML17227A644)
5. NUREG-1779, "Safety Evaluation Report Related to the License Renewal of St. Lucie Nuclear Plant, Units 1 and 2" Florida Power & Light Company, Docket Nos. 50-335 and 50-389. September 2003.
6. O. K. Chopra, "Estimation of Fracture Toughness of Cast Stainless Steels during Thermal Aging in LWR Systems,"
    a. NUREG/CR-4513, ANL-90/42, Rev.0, June 1991.
    b. NUREG/CR-4513, ANL-93/22, Rev.1 August 1994.
    c. NUREG/CR-4513, ANL-15/08, Rev. 2, May 2016.
7. "Evaluation of Flaws in Austenitic Steel Piping," Trans ASME, Journal of Pressure Vessel Technology, Vol. 108, Aug. 1986, pp. 352-366.
8. ASME Boiler and Pressure Vessel Code, Section XI, 2007 Edition through 2008 Addenda.
9. Westinghouse Letter, LTR-AMER-MKG-20-1686, Rev. 2, "Westinghouse Revised Offer for Subsequent License Renewal for St. Lucie Unit 1 & 2," November 13, 2020.
10. Pump Case Structural Analysis for Florida Power and Light Co. (CE Contract 19367) (i.e., St. Lucie 1), TCF-1017-STR, Vol. 1, Rev. 1, August 7, 1974.
11. Pump Casing Structural Analysis for Florida Power and Light, St. Lucie Plant, Unit 2, TCF-1024-STR, Vol. 1, Rev. 1, March 22, 1977.
12. 19367-31-3, Rev. 4, "Engineering Specification for Reactor Coolant Pumps for Florida Power and Light Company Hutchinson Island Plant Unit #1 – 1974 – 890 MW Installation," May 20, 1971.
13. 13172-PE-480, Rev. 5, "Project Engineering Specification for Reactor Coolant Pumps for St. Lucie Plant – Unit No. 2 1978-890 MW Extension," October 12, 1983.
14. Westinghouse Calculation Note, CN-SDA-II-20-026, Rev. 0, "St. Lucie Unit 1 and Unit 2 80-Year Transient Cycle Projections," February 25, 2021.
15. ASTM E 813-89, "Standard Test Method for J_{IC}, A Measure of Fracture Toughness," April 1991.
16. PVP-Vol. 213/MPC-Vol. 32, Pressure Vessel Integrity ASME 1991, "Closed Form Stress Intensity Factors for a Semi-Elliptical Crack in a Flat Plate Under a Gradient Stress Field," J. M. Lawrence and J. L. Hechmer.
17. FPL Design Input Transmittal, PSLWEC-21-0015, Rev. 0, "Design Input Transmittal for WS09e N-481 Pump Casing to Support the St. Lucie Unit 1 and Unit 2 Subsequent License Renewal," February 12, 2021.

This page was added to the quality record by the PRIME system upon its validation and shall not be considered in the page numbering of this document.

Approval Information
Author Approval Hall Gordon Z Apr-07-2021 19:23:55
Author Approval Zhang Jennifer J Apr-07-2021 20:52:16
Verifier Approval Ganta B Reddy Apr-07-2021 21:51:49
Manager Approval Rigby Stephen Apr-08-2021 09:51:49

Files approved on Apr-08-2021

*** This record was final approved on 4/8/2021 9:51:49 AM. (This statement was added by the PRIME system upon its validation)

Enclosure 4

Non-proprietary Reference Documents and Redacted Versions of Proprietary Reference Documents (Public Version)

Attachment 14

Structural Integrity Report No. 2001262.402, Revision 1, Flaw Tolerance Evaluation of St. Lucie Units 1 and 2 CASS Components for SLR, July 15, 2021

(32 Total Pages, including cover sheets)

Structural Integrity Associates, Inc.

dgerber@structint.com
5215 Hellyer Avenue, Suite 210, San Jose, CA 95138 | 408-978-8200

July 15, 2021
REPORT NO. 2001262.402
REVISION: 1
PROJECT NO. 2001262.00

Quality Program: ☒ Nuclear ☐ Commercial

Bill Maher
Florida Power & Light Co.
St. Lucie Nuclear Power Plant
6501 S. Ocean Dr.
Jenson Beach, FL 34957

Subject: Flaw Tolerance Evaluation of St. Lucie Units 1 and 2 CASS Components for SLR

Dear Bill,

This letter report documents the results of the flaw tolerance evaluation of CASS components to support the aging management program (AMP) at St. Lucie Units 1 and 2 by demonstrating that CASS components potentially susceptible to Thermal Aging Embrittlement (TAE) have adequate toughness to be flaw tolerant for 80 years of plant operation, consistent with the requirements of Section X1.M12 of the GALL-SLR Report [1].

For Revision 1 of this report, LTR-SDA-II-20-32-NP (Reference 11) was updated to Revision 1. Table 8 and associated notes were updated for Plant Heatup and Plant Cooldown cycles, and OBE was added. The supporting files for the Appendix L reevaluation in Section 6.0 were rerun, and the results in Table 9 were updated. Revision 1 changes are noted with revision lines in the right margin.

1.0 BACKGROUND

As part of the Plant St. Lucie (PSL) Nuclear Power Plant license renewal process for Units 1 and 2, FPL committed to manage the reduction in fracture toughness due to thermal aging of CASS components through an aging management program (AMP) which will be consistent with the recommendations of NUREG-1801 (GALL Report), Chapter XI, Program XI.M12, *Thermal Aging Embrittlement of Cast Austenitic Stainless Steel (CASS)* [2]. The purpose of the PSL CASS Thermal Aging Embrittlement (TAE) Aging Management Program (AMP) is to manage reduction of fracture toughness due to TAE of CASS RCS pressure boundary components [3]. The commitments for managing thermal aging of CASS components are documented as Item 8 for Unit 1 and Item 7 for Unit 2 in the NRC SER Report [4].

PSL Unit 1 (from Appendix D, Table 1 of Reference 4)

Item	Commitment	UFSAR Supplement Location (LRA Appendix A1)	Implementation Schedule	Source
8	Implement the Thermal Aging Embrittlement of CASS Program.	18.1.6, Thermal Aging Embrittlement of CASS Program	Prior to the end of the initial operating license term.	LRA Appendix B, Subsection 3.1.6

PSL Unit 2 (from Appendix D, Table 2 of Reference 4)

Item	Commitment	UFSAR Supplement Location (LRA Appendix A2)	Implementation Schedule	Source
7	Implement the Thermal Aging Embrittlement of CASS Program.	18.1.5, Thermal Aging Embrittlement of CASS Program	Prior to the end of the initial operating license term.	LRA Appendix B, Subsection 3.1.6

The PSL Thermal Aging Embrittlement of CASS Program License Renewal Basis Document [13] and the FP&L AMP (Administrative Procedure No. ADM-17.36, current Revision No. 2) [3] credits the flaw tolerance evaluation that was performed by Structural Integrity Associates (SI) for the initial license renewal period of 60 years [5] which concluded that the susceptible CASS components at PSL, Units 1 and 2 are very flaw tolerant.

The AMP of CASS piping components includes determination of the susceptibility of CASS components to thermal aging embrittlement and augmented inspection or flaw tolerance evaluation. A screening process was performed in the previous evaluation [5] to determine the susceptibility to TAE of the CASS piping components and identify the susceptible materials. There are no additional inspections or evaluations required for those components that were determined to not be susceptible to thermal aging. However, for the components with susceptible materials, aging management is required either through volumetric examination or alternatively, component-specific flaw tolerance evaluation, consistent with the guidelines of the GALL Report [2] and the Grimes Letter [6]. The component-specific flaw tolerance evaluation was used to demonstrate compliance with the attributes in the ISG on CASS dated May 19, 2000, and later GALL Report, Rev. 2 [2], for the susceptible CASS components at St. Lucie Units 1 and 2. In the Safety Evaluation [4], NRC accepted the commitments for management of TAE at PSL (Item 8 for PSL Unit 1 and Item 7 for PSL Unit 2) and the proposed approach for meeting the criteria in the GALL Report [2] and the Grimes Letter for managing TAE of CASS for 60 years of plant operation [6] as documented in the CASS LR Basis Document [13] and the

Structural Integrity Associates, Inc.
info@structint.com 1-877-4SI-POWER structint.com

AMP for PSL Units 1 and 2 [3]. On October 3, 2014, FP&L submitted letter L-2014-304 to the NRC (ADAMS Accession Number ML14294A448) stating that they will follow the guidance in GALL Report, Revision 2, and informed NRC that FP&L opted to manage thermal aging embrittlement through flaw tolerance evaluations of susceptible components, consistent with the 10 attributes of program X1.M12 in GALL Report, Revision 2. NRC subsequently reviewed this plan and commitment for managing TAE of CASS, including the use of a flaw tolerance evaluation. From the review of a sampling of the flaw tolerance evaluation results documented in procedure ADM-17.36, "Cast Austenitic Stainless Steel Aging Management Program, Saint Lucie Plant," NRC verified that the limiting susceptible locations identified in the AMP were being evaluated for the 60-year period of extended operation (PEO) [14, 15].

For the SLR period, FP&L intends to update the CASS AMP (Administrative Procedure No. ADM-17.36, Revision No. 2) [3]. Using a similar approach documented in the AMP, the results of the present study will demonstrate that the CASS components in St. Lucie Units 1 and 2 remain flaw tolerant by the criteria in the GALL-SLR [1]. Acceptable margins are maintained even with the long-term effects of thermal aging of susceptible CASS components. Therefore, the CASS flaw tolerance evaluation performed for the 60-year operating period is updated for SLR (i.e., 80-year operating period) in this report to demonstrate equivalent margins as shown in the previous SI report [5].

There is new information since the publication of Reference [5] in 2015 that needs to be considered for this study for SLR. The flaw tolerance evaluation in Reference [5] for 60 years consisted of probabilistic fracture mechanics (PFM) evaluation to determine the tolerable flaw sizes and then performance of a crack growth evaluation with a postulated flaw to show that the tolerable flaws sizes would not be exceeded during the period of extended operation (an additional 20 years for 60 to 80 years of plant life). The evaluations were performed consistent with the methodology outlined in MRP-362 [7] and consisted of determining the tolerable flaw sizes for the susceptible CASS components.

An important aspect in determining the tolerable flaw size is the fracture toughness of the CASS material. In Reference [5], the saturated fracture toughness was determined using correlations provided in NUREG/CR-4513 Revision 1 [8]. The correlations in Reference [8] are valid up to a ferrite content of 25%. As will be shown later, the ferrite content of some of the CASS components at PSL, Units 1 and 2 exceed 25%. However, a procedure was developed in Reference [5] for addressing the CASS components with ferrite content greater than 25%. Subsequently, NUREG/CR-4513, Revision 2 [9], which was published after the Reference [5] report, permits the use of the fracture toughness correlations up to 40% ferrite which therefore does not require the procedure adopted in the Reference [5] report for components with ferrite levels greater than 25%. In addition, the previous crack growth model has been reexamined and extended for an additional 20-year operating period to show acceptability using 80-year cycle projections and the latest reference crack growth rates in ASME Code Case N-809 [10].

2.0 OBJECTIVES

The objectives of this letter report are as follows:

1. Perform updated analyses using current technical information and design inputs to supplement the evaluations in Reference [5] to address plant operation from 60 to 80 years for the SLR period.
2. Provide recommendations for updating the AMP for thermal aging embrittlement of CASS piping at PSL Units 1 and 2 for SLR.

3.0 REVIEW OF PRIOR ANALYSES FOR 60-YEAR OPERATION

Details of the evaluation for the 60-year operation are provided in Reference [5] and as such only a summary is provided herein. A flaw tolerance evaluation consistent with the requirements of the GALL Report [2] and the Grimes Letter [6] was performed for the CASS piping components at PSL Units 1 and 2, which were found to be potentially susceptible to TAE. The evaluation consisted of determining the maximum tolerable flaw sizes on a location-specific basis using probabilistic fracture mechanics (PFM) techniques and methodology in MRP-362 [7], and then determining the operating period it would take a postulated initial flaw to reach the tolerable flaw sizes. The sequence of the evaluation is summarized below.

3.1 Identification of CASS components potentially susceptible to TAE which require augmented Inspection or analyses

The CASS components at PSL Units 1 and 2 are provided in Tables 4-1 of the Reference [5] SER. The CASS components evaluated included the surge line piping for Units 1 and 2, the safety injection nozzle safe ends for Unit 1 and the RCP safe ends for Unit 2. The CASS grade for all these components is CF8M as shown in Table 3-1 of the Reference [5] report. The centrifugal cast process was used in fabricating these components. The delta ferrite contents of these materials were determined using the Hull's equivalent factor method recommended in the Grimes Letter [6]. Using the ferrite content and the guidance provided in the Grimes Letter [6], the components susceptible to TAE were determined and presented in Table 4-4 of Reference [5]. Per the guidance provided in the Grimes Letter [6], for centrifugally cast CF8M CASS, components with ferrite content greater than 20% are considered susceptible to TAE. For evaluation purposes, the centrifugally cast CF8M CASS components at PSL Units 1 and 2 were further subdivided into three parts in Tables 4-5, 4-6 and 4-7 of Reference [5] as follows:

1. Delta ferrite content between 20 and 25%
2. Delta ferrite content between 25 and 30%
3. Delta ferrite content greater than 30%

For reference, the CASS components that were determined to be susceptible to TAE at PSL Units 1 and 2 are reproduced in Tables 1 and 2 of this report.

3.2 Determination of Saturated Fracture Toughness

In the previous evaluation for 60 years, the saturated fracture toughness distributions used in the PFM analyses were determined using the correlations in NUREG-4513 Revision1 [8] for the three groups of ferrite levels determined above as follows [5]:

1) Delta ferrite between 20 and 25% (Mean = 22.5, Standard Deviation = 2.5%),

2) Delta ferrite between 25 and 30%, (Mean = 27.5, Standard Deviation = 2.5%),

3) Delta ferrite exceeding 30%. For this group, the lower bound saturation fracture toughness for Grade CF8M in NUREG-4513 Revision 1 [8] was conservatively used.

These toughness distributions were demonstrated to be conservative using all the data and information that was available for aged CASS materials at the time [5].

3.3 Determine Stresses on the Components at The Susceptible Locations

Operating transients at the susceptible locations were determined in Section 5 of Reference [5]. Pertinent loads and transients/cycles are provided in Tables 5-1 through 5-7 and 5-9 through 5-13 of Reference [5].

3.4 Determine the Maximum Tolerable Flaw Depths

The maximum tolerable flaw depths were determined using PFM methods by employing the methodology in MRP-362 [7] using the saturated fracture toughness distributions for the three groups of delta ferrite above, a fracture mechanics model for circumferential crack as described in Section 4 of Reference [5] and the loads discussed above. The maximum tolerable flaw sizes were determined for ASME Code, Service levels A, B, C and D and presented in Tables 7-7 through 7-10 of Reference [5]. For reference, these are reproduced as Table 3 through 6 of this report. It can be seen from these tables that the tolerable flaw depths are very large (75% of wall thickness) at all locations.

3.5 Perform Crack Growth Evaluation

Crack growth evaluations were performed to determine how long it would take an initial postulated flaw to reach the tolerable flaw sizes determined above. An initial postulated flaw of one quarter the thickness with length six times the depth was assumed in the analyses. The results of the crack growth evaluation are presented in Tables 7-7 through 7-10 of Reference [5] and shown in Tables 3 through 6 of this report. It can be seen from these tables that for the limiting location (corresponding to the PSL Units 1 and 2 surge lines), it takes 252 months (greater than 20 years) for the initial postulated flaw to grow to exceed the tolerable flaw size. At all locations on the safety injection piping and the reactor coolant pumps, it takes at least 480 months (40 years) for the initial postulated flaws to exceed the tolerable flaw sizes. Since PSL performed volumetric inspections of the CASS locations prior to the first extended operating period as part of a one-time inspection for license renewal, this flaw tolerance evaluation confirmed that all the CASS components exhibited adequate toughness for 20 years of operation for the entire license renewal period (40 to 60 years of plant life) without the need for any additional inspections.

4.0 TECHNICAL ASPECTS TO BE ADDRESSED FOR 80-YEAR OPERATION

The following technical aspects from the previous SI report for license renewal needed to be addressed in this revised evaluation for subsequent license renewal:

1. The fracture toughness distributions derived in Reference [5] used the correlations in NUREG/CR-4513, Rev.1 [8] for the CF8M materials at PSL, Units 1 and 2. The fracture correlations in NUREG/CR-4513, Rev.1 are applicable to ferrite level of 25%. As discussed previously for ferrite levels greater than 25%, a conservative procedure was developed in Reference [5] as described in Section 6.1. With the publication of NUREG/CR-4513, Revision 2 [9], which has saturation fracture toughness correlations up to 40% ferrite, the procedures used in Reference [5] for component with ferrite greater than 25% have been compared to those in NUREG/CR-4513, Revision 2 to see if they are still bounding.

2. An essential part of the flaw tolerance evaluation in Reference [5] is a crack growth evaluation which considered the growth of a hypothetical flaw from plant operation up to the end of the first period of extended operation (20 years after the last inspection). Since the SLR period will be 40 years after the last inspection, the crack growth evaluation has been revisited for the SLR period of 80 years using the most recent crack growth laws available in ASME Code Case N-809 [10] to determine the safe operating period.

3. Based on Items 1 and 2, determine if any significant changes are required for the TAE of CASS Program at PSL Units 1 and 2 for SLR.

5.0 TECHNICAL APPROACH

To extend the existing 60-year flaw tolerance evaluation in Reference [5] to 80 years, two issues are addressed in this report related to the reevaluation study for 80 years:

1. The saturated fracture toughness for the three groups of delta ferrite were recalculated using the correlations in NUREG/CR-4513 Revision 2 [9]. They were then compared to those previously evaluated in Reference [5] to determine applicability of the Reference [5] Report to 80 years.
2. The fatigue crack growth evaluations were reperformed using an updated crack growth law for Type 316 stainless steel provided in Code Case N-809 [10] using the annual transient cycles for 80 years to determine the extended applicability of the Reference [5] results for SLR.

Using the results of the above evaluations, recommendations are provided for updating the AMP at PSL Units 1 and 2 for SLR.

6.0 EVALUATION

6.1 Fracture Toughness For 80 Years of Operation

The previous SI report used the equations and methodology from NUREG/CR-4513, Revision 1 [8] to determine the saturated J-R curve properties for aged CASS materials in the flaw tolerance evaluation [5, Section 4.2]. The stated range of applicability in NUREG/CR-4513, Revision 1 is for CASS materials with ferrite content less than 25%. However, because the ferrite content of some of the CASS components at PSL Units 1 and 2 are greater than 25%, conservative distributions of those with ferrite content greater than 25% ferrite were derived resulting in three distributions of fully saturated *J-R curve* toughness as a function of delta ferrite content:

- CASS materials with ferrite content between 20% - 25% are within the range of applicability and hence use the equations from NUREG/CR-4513, Rev. 1.

- For CASS materials with ferrite content between 25% and 30%, the equations from NUREG/CR-4513, Rev.1 are extended slightly beyond the maximum applicability of 25% ferrite content.

- For CASS materials with ferrite content greater than 30%, the lower bound J-R curve from NUREG/CR-4513, Rev. 1 for materials with unknown chemical composition was used.

Subsequently, the fracture toughness correlations for aged CASS materials were updated in NUREG/CR-4513, Rev. 2 [9]. Revision 2 updated the procedure and correlations used for predicting the change in fracture toughness and tensile properties of CASS components due to thermal aging. The methodology was extended to include CASS components with ferrite content up to 40% which covers the ferrite range of the CASS components at PSL Units 1 and 2. The effects of these changes to the PFM evaluation were examined to determine if the fracture toughness distribution in the Reference [5] for ferrite content greater than 25% in the Reference [5] report are still bounding. A comparison of the fracture toughness of those components studied in the Reference [5] report was performed using the revised NUREG/CR-4513, Rev. 2 correlations for extended applicability for 80 years.

The comparison of the key equations in NUREG/CR-4513, Revision 1 and Revision 2 are shown in Table 7 for centrifugally cast Grade CF8M CASS components. As shown in Tables 1 and 2, the nickel content of all the CASS components at St. Lucie Units 1 and 2 except one are less than 10% and so the comparison in Table 7 was made using correlations in NUREG/CR-4513, Revision 2 for such nickel content. The comparison is also made at plant operating temperature of 290ºC and 350ºC (550ºF to 662ºF). Table 7 shows that the main differences between Revision 1 and Revision 2 of NUREG-4513 is in the correlation for Cv_{sat} (Item 4 of Table 7) and the J-R curve parameters in Items 6 and 7. There is also a slight difference in the power law for the lower bound J-R curves for CASS with unknown chemical composition in Item 7. Since the correlations in NUREG/CR-4513, Revision 2 are applicable up to 40% ferrite, which covers the

CASS components at PSL Units 1 and 2, there is no need to use the lower bound J-R curve provided in NUREG/CR-4513 Revision 2 for materials with unknown chemical composition.

The use of NUREG/CR-4513, Rev. 1 in the previous SI report was reconciled with NUREG/CR-4513, Rev. 2 as follows:

- For CASS materials with ferrite content between 20% - 25%, the J-R curves for the minimum and maximum ferrite content of this range were compared to those derived from NUREG-4513, Revision 2 correlations. This will correspond to Heat A25823 (Ferrite = 24.69%) and Heat S-250 (Ferrite = 20.45%). A comparison of the J-R curves is shown in Figure 1. As shown in this figure there is negligible difference between NUREG-4513 Revision 1 and Revision 2 J-R curves for ferrite levels in this range. As such, the CASS evaluation results using NUREG/CR-4513, Rev. 1 in the previous SI report [5] remain valid for all components with ferrite content between 20% and 25%.

- For CASS materials with ferrite content between 25% - 30%, there were two components (Pieces 505-03-1 and 505-04) with the same material composition (i.e., same heat A2562). Figure 2 compares the J-R curves using the heat-specific material composition and equations from Revision 1 and Revision 2 of NUREG/CR-4513. The figure shows that the differences between the J-R curves for Revision 1 and Revision 2 are negligible. As such, the CASS evaluation results using NUREG/CR-4513, Rev. 1 in the previous SI report [5] remain valid for the two components.

- For CASS materials with ferrite content greater than 30%, there were six components with three heats - Heat A2611 (Piece 505-02-2), Heat A2612 (Pieces 508-04-1, 508-04-2, 508-04-3, and 508-04-4), and Heat W-050 (Piece 751-102). Figure 3 shows that lower bound J-R curve toughness from NUREG/CR-4513, Rev. 1 bounds the J-R curve toughness using three heat-specific material compositions and the equations from NUREG/CR-4513, Rev. 2. As such, the CASS evaluation results using NUREG/CR-4513, Rev. 1 in the previous SI report [5] remain valid for the six components.

-

Thus, the fracture toughness for the CASS components at PSL Units 1 and 2 using the updated correlations in NUREG/CR-4513, Revision 2 are comparable to those derived using the correlations NUREG/CR-4513 Revision 1. Therefore, the J-R curves used in the Reference [5] report are still applicable for the extended operating period to 80 years.

6.3 Maximum Tolerable Flaw Sizes for 80 Years Operation

The J-R curves distributions are an important input in the PFM evaluation methodology used to determine the maximum tolerable flaw size in Reference [5]. It has been shown above that the J-R curves derived in Reference [5] for 60-year operation remain applicable for 80 years of operation as well. Since the other inputs used in the determination of the tolerable flaw size (stresses and geometry) remain unchanged from the previous evaluation in Reference [5], the maximum tolerable flaw sizes determined in Reference [5] and presented in Tables 3 through 6 also remain applicable for 80-year operation (through SLR).

Structural Integrity Associates, Inc.
info@structint.com 1-877-4SI-POWER structint.com

6.3 Cycles Used in Determining Fatigue Crack Growth for 80 Years of Operation

The objective of the fatigue crack evaluation is to ensure that crack growth with a postulated initial flaw size will not exceed the tolerable flaw size during the extended operating period. The previous SI report used projected 60-year cycles for thermal transients to calculate the annual cycles for fatigue crack growth analysis [5, Tables 7-1 thru 7-3]. The projected total 80-year cycles for thermal transients are provided in Reference [11]. Table 8 compares the projected annual cycles for 60-year cycles used in the CASS evaluation in Reference [5] and the projected 80-year cycles for SLR.

As shown in Table 8, for most of the thermal transients, the use of projected 60-year cycles on an annual basis in the CASS evaluation bounds the projected 80-year cycles on an annual basis for SLR. It should be noted that thermal stratification cycles for the surge line evaluation [5, Table 7-1] were calculated based on plant heatup and plant cooldown cycles, and as such, the conclusion for plant heatup and plant cooldown is applicable for thermal stratification events.

Updated fatigue crack growth evaluations were performed using the 80-year projected cycles and applying the fatigue crack growth law of ASME Section XI Code Case N-809 [10]. This ASME Code-approved Code Case contains the reference crack growth rate curves for CASS materials. The analyses were performed assuming an initial postulated flaw of 25% of wall thickness with length 6 times the depth, the same reference flaw used in the Reference [5] analysis. The same stresses used in the Reference [5] report were also utilized in this updated analysis. In this updated analysis, pc-Crack Version 5.0 [12] was used. This newer version of pc-Crack allows the user to include rise time and metal temperature for each loading block, thus eliminating some of the unnecessary conservatisms in the previous analysis in Reference [5]. The fatigue crack growth for PSL Units 1 and 2 surge line piping, Unit 1 safety injection nozzle safe ends and Unit 2 RCP safe ends are evaluated as follows.

PSL Units 1 and 2 Surge Lines

The previous analysis for the PSL Units 1 and 2 surge line in Reference [5] for 60 years yielded an operating period of 252 months at the limiting stress location at the elbow base metal (Stress Path 4). The updated analysis was performed for this limiting stress path. The results of this updated analysis indicate that the number of years to reach the tolerable flaw size is more than 960 months (80 years) from the time of the most recent inspection. Since the most critical stress location was used in the fatigue crack growth analysis, it will take at least 960 months for an initial postulated flaw to reach the tolerable flaw sizes at any location on the surge line from the time of the most recent inspection at that location. The updated fatigue crack growth evaluation results in comparison to the tolerable flaw sizes are provided in Table 9.

PSL Unit 1 Safety Injection Nozzle Safe Ends

The previous analysis for the PSL Unit 1 safety injection nozzle safe-ends n Reference [5] for 60 years yielded an operating period of 480 months at the limiting location (Stress Path SI3). The updated analysis was performed for the limiting location. The results of this updated analysis,

Structural Integrity Associates, Inc.
info@structint.com 1-877-4SI-POWER structint.com

presented in Table 9, indicate that the number of years to reach the tolerable flaw size is more than 960 months (80 years) from the time of the most recent inspection. Since the most critical location was used in the fatigue crack growth analysis, it will take at least 960 months for an initial postulated flaw to reach the tolerable flaw sizes for any of the Unit 1 safety injection nozzle safe-ends from the time of the most recent inspection.

PSL Unit 2 RCP Safe Ends

The previous analysis for the PSL Unit 2 RCP discharge and suction safe-ends in Reference [5] for 60 years yielded an operating period of 480 months at the limiting location (Stress Path CL1). The updated analysis was performed for the limiting location. The results of this updated analysis, shown in Table 9, indicate that the number of years to reach the tolerable flaw size is more than 960 months (80 years) from the time of the most recent inspection. Since the most critical location was used in the fatigue crack growth analysis, it will take at least 960 months for an initial postulated flaw to reach the tolerable flaw sizes for any of the PSL Unit 2 RCP suction and discharge safe-ends from the time of the most recent inspection.

The results of the above updated analyses indicate that for the PSL Units 1 and 2 surge line, the PSL Unit 1 safety injection nozzle safe-end and PSL Unit 2 RCP suction and discharge safe-end locations, no further inspections are required for 80 years from the time when the last qualified inspections were performed of these CASS components. PSL Unit 1 Baseline UTs were completed just prior to PEO (the last outage prior in April 2015, approximately one year before PEO of March 1, 2016). PSL Unit 2 Baseline UTs were completed in March 2017, approximately 6 years before PEO of April 6, 2023. Eighty years from these most recent inspections at PSL Units 1 and 2 indicate that no additional inspections are required to be performed on these CASS components at PSL Units 1 and 2 during the second period of extended operation (approximately 79 additional years for PSL Unit 1 and 74 additional years for PSL Unit 2 from the most recent inspections).

7.0 CONCLUSIONS AND RECOMMENDATIONS FOR CHANGES IN AMP FOR SLR

Evaluations have been performed as documented in this letter report to address two key technical aspects relative to the flaw tolerance evaluation of the CASS piping components at PSL Units 1 and 2 and to confirm whether the conclusions of existing SI Report No. 1301079.402, Revision 0 [5], which was prepared to address 60-year license renewal, remain applicable to SLR (80-year operation). The two technical aspects that have been addressed are fracture toughness and fatigue crack growth. The conclusions related to these two issues are as follows:

- The aged fracture toughness was determined using the updated NUREG/CR-4513, Revision 2 saturated fracture correlations which are applicable to CASS materials with ferrite contents up to 40%. The fracture toughness considering 80 years of operation was found comparable to or lower than the fracture toughness used in the Reference [5] report. Since the stresses and other inputs used in the determination of the tolerable flaw sizes remain unchanged, the tolerable flaw sizes determined in the Reference [5] report for 60 years remain applicable to 80 years of plant operation.

- The crack evaluation performed using updated crack growth law for Type 316 stainless steel and annualized transients for 80 years at PSL Units 1 and 2 show that with an initial postulated quarter thickness flaw with length six times the depth, the tolerable flaw sizes are not reached until after 960 months (80 years) of operation for the PSL Units 1 and 2 surge lines, PSL Unit 1 safety injection nozzle safe-ends and PSL Unit 2 RCP suction and discharge safe ends at all the susceptible CASS locations since the most recent inspection of these components at PSL Units 1 and 2 (approximately 79 additional years for PSL Unit 1 and 74 additional years for PSL Unit 2 from the most recent inspections).
- These results confirm that the aged CASS components in PSL Units 1 and 2 are demonstrated to be flaw tolerant. Furthermore, since inspections of the CASS components were performed as part of the one-time inspections prior to entering the first PEO, no further inspections are required to manage TAE of CASS for at least an additional 80 years of plant operation from the time of the most recent inspection which would allow operation to the end of the subsequent PEO.

It is recommended that the AMP for CASS base metal components at PSL Units 1 and 2 be updated to include the findings of this report. Specifically, the following recommendations are provided:

1. The AMP should indicate that the saturated fracture toughness previously derived using the correlations from NUREG-4513 Revision 1 (which are applicable to delta ferrite content up to 25%) have been compared to those of NUREG/CR-4513, Revision 2 (which are applicable to delta ferrite content of 40%) and the existing calculations based on NUREG/CR-4513, Revision 1 remain applicable and therefore the tolerable flaw sizes remain unchanged from the previous evaluation in Reference [5].
2. The crack growth results show that an additional 80 years of operation from the last inspection of the CASS components at PSL Units 1 and 2 (performed as part of the onetime inspections just prior to entering the first PEO) is acceptable and, therefore, no further inspection of the aged CASS components is required for operation through the subsequent PEO.
3. The flaw tolerance results in Table 7 of the AMP should be replaced by Table 9 of this report which show that the allowable operating period evaluated is a minimum of 960 months (80 years) from the time of the last inspection for all CASS components at PSL Units 1 and 2.

8.0 REFERENCES

1. Generic Aging Lessons Learned for Subsequent License Renewal (GALL-SLR) Report, NUREG-2191, Vol. 2, Chapter XI, Program XI.M12, *Thermal Aging Embrittlement of Cast Austenitic Stainless Steel (CASS)*, U. S. Nuclear Regulatory Commission, July 2017. [ADAMS Accession No. ML17187A204].
2. Generic Aging Lessons Learned (GALL) Report, NUREG-1801, Rev. 2, Chapter XI, Program XI.M12, *Thermal Aging Embrittlement of Cast Austenitic Stainless Steel*

(CASS), U. S. Nuclear Regulatory Commission, December 2010. [ADAMS Accession No. ML103490041].
3. "Cast Austenitic Stainless Steel (CASS) Aging Management Program, St. Lucie Plant," FP&L Administrative Procedure No. ADM-17.36, Revision No. 2, December 3, 2019.
4. Safety Evaluation Report Related to the License Renewal of St. Lucie Nuclear Plant, Units 1 and 2, NUREG-1779, Docket Nos. 50-335 and 50-389, U. S. Nuclear Regulatory Commission, Office of Nuclear Reactor Regulation, Wash. D. C., September 2003. [ADAMS Accession No. ML032940205].
5. SI Report No. 1301079.402, Revision 0, "Flaw Tolerance Evaluation of St. Lucie Units 1 and 2 CASS Components, Task 5 Report, Aging Management Program Final Report at St. Lucie Units 1 & 2," September 2015.
6. Letter from C. Grimes, USNRC dated May 19, 2000, Subject: License Renewal Issue No. 98-0030, "Thermal Aging Embrittlement of Cast Austenitic Stainless Steel Components."
7. *Materials Reliability Program: Technical Basis for ASME Section XI Code Case N-838–Flaw Tolerance Evaluation of Cast Austenitic Stainless Steel (CASS) Piping Components (MRP-362).* EPRI, EPRI, Palo Alto, CA: 2013. 3002000672.
8. Chopra, O. K., "Estimation of Fracture Toughness of Cast Stainless Steels During Thermal Aging in LWR Systems," NUREG/CR-4513, Rev. 1, May 1994.
9. Chopra, O. K., "Estimation of Fracture Toughness of Cast Stainless Steels during Thermal Aging in LWR Systems," NUREG/CR-4513, Rev. 2, May 2016. [ADAMS Accession No. ML16145A082].
10. ASME Section XI Code Case N-809, "Reference Fatigue Crack Growth Rate Curves for Austenitic Stainless Steels in Pressurized Water Reactor Environments Section XI, Division 1," Approval date June 23, 2015.
11. Westinghouse Letter LTR-SDA-II-20-32-NP, Revision 1, "St. Lucie Units 1 and 2 Subsequent License Renewal: 80-Year Projected Transient Cycles," SI File No. 200126.201.
12. **pc-CRACK**, Version 5.0 CS, Structural Integrity Associates, Inc., December 30, 2020.
13. "St. Lucie Thermal Aging Embrittlement of CASS Program License Renewal Basis Document," PSL-ENG-LRAM-01-022, Rev. 3, Engineering Evaluation Form, Latest Revision.
14. Letter from Mr. Shakur A. Walker (NRC) to Mr. Mano Nazur (NextEra Energy), "Saint Lucie Plant, Unit 1 - U. S. Nuclear Regulatory Commission Post-Approval Site Inspection for License Renewal, Inspection Report 05000335/2015010, January 4, 2016. [ADAMS Accession No. ML16004A248].
15. Letter from Mr. Brian R. Bosner (NRC) to Mr. Mano Nazur (NextEra Energy), "Saint Lucie Plant, Unit 2 - U. S. Nuclear Regulatory Commission Post-Approval Site Inspection for License Renewal, Inspection Report 05000389/2017009, November 30. 2017 [ADAMS Accession No. ML17334308].

Table 1. List of TAE Susceptible CF-8M Components Based on Screening for Delta Ferrite for at St. Lucie Unit 1

Piece	Assembly	Code	Heat		Cr	Ni	Mo	Si	N	Mn	C	Cr_{eq}	Ni_{eq}	Ferrite %
20 – 25% Ferrite [5, Table 4-5(a)]														
505-08-1	505-06	C4320-1	A18412	L	20.50	9.00	2.50	0.50	0.063	0.93	0.06	18.78	14.59	20.61
				C	19.80	8.96	2.32	0.44	0.040	0.83	0.08	17.83	14.46	16.19
505-08-2	505-06	C4320-2	A25823	L	20.02	9.46	2.62	0.70	0.042	0.75	0.05	18.54	14.40	20.63
				C	20.40	9.50	2.79	0.68	0.040	0.75	0.05	19.11	14.36	24.69
25 – 30% Ferrite [5, Table 4-6(a)]														
505-03-1	505-01	C4322-1	A2562	L	20.00	9.06	2.70	0.72	0.055	0.63	0.04	18.62	13.89	25.64
				C	19.60	8.95	2.62	0.66	0.040	0.65	0.05	18.10	13.75	23.28
505-04	505-01	C4322-2	A2562	L	20.00	9.06	2.70	0.72	0.055	0.63	0.04	18.62	13.89	25.64
				C	19.60	8.95	2.62	0.66	0.040	0.65	0.05	18.10	13.75	23.28
> 25% Ferrite [5, Table 4-7(a)]														
505-02-2	505-01	C4319-2	A2611	L	21.00	9.66	2.74	0.69	0.034	0.78	0.03	19.66	13.87	33.71
				C	20.75	9.50	2.63	0.64	0.040	0.73	0.04	19.25	13.96	29.48
508-04-1	504-01	C4318-1	A2612	L	20.70	9.36	2.78	0.66	0.035	0.75	0.03	19.39	13.59	34.87
				C	20.50	9.55	2.85	0.70	0.040	0.75	0.04	19.29	14.16	27.80
508-04-2	504-04	C4318-1	A2612	L	20.70	9.36	2.78	0.66	0.035	0.75	0.03	19.39	13.59	34.87
				C	20.50	9.55	2.85	0.70	0.040	0.75	0.04	19.29	14.16	27.80
508-04-3	504-03	C4318-1	A2612	L	20.70	9.36	2.78	0.66	0.035	0.75	0.03	19.39	13.59	34.87
				C	20.50	9.55	2.85	0.70	0.040	0.75	0.04	19.29	14.16	27.80
508-04-4	504-05	C4318-1	A2612	L	20.70	9.36	2.78	0.66	0.035	0.75	0.03	19.39	13.59	34.87
				C	20.50	9.55	2.85	0.70	0.040	0.75	0.04	19.29	14.16	27.80

Table 2. List of TAE Susceptible CF-8M Components Based on Screening for Delta Ferrite at St. Lucie Unit 2

Piece	Assembly	Code	Heat		Cr	Ni	Mo	Si	N	Mn	C	Cr_{eq}	Ni_{eq}	Ferrite %
20 – 25% Ferrite [5, Table 4-5(b)]														
751-110	771-1609	M-9229-2	W-051	L	20.16	9.01	2.34	0.97	0.060	0.82	0.06	18.47	14.44	19.95
				C	20.20	9.01	2.50	0.91	0.040	0.82	0.06	18.67	14.07	24.30
751-104	771-1609	M-9231-1	S-249	L	19.28	9.98	2.71	0.70	0.060	0.72	0.05	17.91	15.15	12.53
				C	20.37	9.42	2.58	0.84	**0.040**	0.81	0.05	18.91	14.23	**24.40**
751-107	751-106	M-9231-2	S-250	L	20.29	9.60	2.55	0.79	0.050	0.83	0.06	18.76	14.85	18.68
				C	19.88	9.27	2.56	0.85	0.040	0.69	0.06	18.4	14.32	20.45
751-109	751-106	M-9231-3	S-251	L	19.83	10.29	2.74	0.89	0.060	0.97	0.06	18.58	15.73	12.50
				C	20.26	9.36	2.57	0.89	**0.040**	0.84	0.06	18.81	14.42	**22.15**
731-101	771-701	M-9216-1	D-419-1	L	20.22	9.17	2.37	0.60	0.040	0.87	0.06	18.39	14.24	21.04
				C	19.12	9.50	2.46	0.60	0.040	0.85	0.07	17.39	14.81	12.08
731-101	771-901	M-9216-2	D-419-2	L	20.22	9.17	2.37	0.60	0.040	0.87	0.06	18.39	14.24	21.04
				C	19.12	9.50	2.46	0.60	0.040	0.85	0.07	17.39	14.81	12.08
731-101	771-1501	M-9216	D-419	L	20.22	9.17	2.37	0.60	0.040	0.87	0.06	18.39	14.24	21.04
				C	19.12	9.50	2.46	0.60	0.040	0.85	0.07	17.39	14.81	12.08
731-101	771-1501	M-9216	D-419	L	20.22	9.17	2.37	0.60	0.040	0.87	0.06	18.39	14.24	21.04
				C	19.12	9.50	2.46	0.60	0.040	0.85	0.07	17.39	14.81	12.08
731-101	771-1301	M-9216-8	J-984	L	20.53	9.74	2.33	0.60	0.049	0.60	0.03	18.65	14.22	22.85
				C	20.79	9.82	2.32	0.52	0.040	0.82	0.07	18.86	15.13	17.28
25 – 30% Ferrite [5, Table 4-6(b) Note]														
None														
>30% Ferrite [5, Table 4-7(b)]														
751-102	**771-1609**	M-9229-1	W-050	L	19.79	9.38	2.64	1.05	0.050	0.80	0.04	18.5	14.13	22.60
				C	20.30	9.03	2.50	0.98	0.040	0.78	0.03	18.81	13.35	32.74

Table 3: 60-Year Results from Previous CASS Evaluation for Unit 1 Safety Injection Nozzle Safe Ends [5, Table 7-7]

Unit	Piece Component	Tolerable Flaw Size for (θ/n = 0.15)			Crack Growth Results(1)		Operating Period Evaluated
		Service Level	Tolerable Flaw Depth		Final Flaw Depth		
			[a/t]	in	[a/t]	in	months
Unit 1	508-04-1 Safety Injection P5	A	0.75	0.984	0.6937	0.9102	480
		B	0.75	0.984			
		C/D	0.75	0.984			
	508-04-2 Safety Injection P9	A	0.75	0.984	0.6862	0.9003	480
		B	0.75	0.984			
		C/D	0.75	0.984			
	508-04-3 Safety Injection P14	A	0.75	0.984	0.6944	0.9110	480
		B	0.75	0.984			
		C/D	0.75	0.984			
	508-04-4 Safety Injection P18	A	0.75	0.984	0.6868	0.9011	480
		B	0.75	0.984			
		C/D	0.75	0.984			

Note:

(1) Crack growth is evaluated for up to 40 years. The postulated flaw did not grow beyond the tolerable flaw size during that time period, and therefore, the final flaw depth at 40 years is reported.

Table 4: 60-Year Results from Previous CASS Evaluation for Unit 1 Surge Line [5, Table 7-8]

Unit	Piece Component	Tolerable Flaw Size for (θ/π = 0.15)			Crack Growth Results(1)			Operating Period Evaluated
		Service Level	Tolerable Flaw Depth		Stress Path	Final Flaw Depth		
			[a/t]	in		[a/t]	in	months
Unit 1	505-03-1 Surge Line Elbow Point 30 (Hot Leg End)	A	0.75	0.98	1	0.7481	0.9815	432
		B	0.75	0.98				
		C/D	0.75	0.98				
		A	0.75	0.98	2	0.7241	0.9500	624
		B	0.75	0.98				
		C/D	0.75	0.98				
		A	0.75	0.98	3	0.7327	0.9613	384
		B	0.75	0.98				
		C/D	0.75	0.98				
		A	0.75	0.98	4	0.7394	0.9701	**252**
		B	0.75	0.98				
		C/D	0.75	0.98				
Unit 1	505-03-1 Surge Line Elbow Point 50B (Pressurizer End)	A	0.75	0.98	1	0.7481	0.9815	432
		B	0.75	0.98				
		C/D	0.75	0.98				
		A	0.75	0.98	2	0.7241	0.9500	624
		B	0.75	0.98				
		C/D	0.75	0.98				
		A	0.75	0.98	3	0.7327	0.9613	384
		B	0.75	0.98				
		C/D	0.75	0.98				
		A	0.75	0.98	4	0.7394	0.9701	**252**
		B	0.75	0.98				
		C/D	0.75	0.98				

Notes:

(1) The crack growth analysis is bounding for Units 1 and 2 and uses the highest stresses at the bounding surge line location, namely the elbow directly attached to the hot leg surge nozzle, to calculate the maximum crack growth rate.

Table 4: 60-Year Results from Previous CASS Evaluation for Unit 1 Surge Line [5, Table 7-8] (Continued)

Unit	Piece Component	Tolerable Flaw Size for (θ/n = 0.15)			Crack Growth Results(1)			Operating Period Evaluated
		Service Level	Tolerable Flaw Depth		Stress Path	Final Flaw Depth		
			[a/t]	in		[a/t]	in	months
Unit 1	505-02-2 Surge Line Pipe Point 70 (Hot Leg End)	A	0.75	0.98	1	0.7481	0.9815	432
		B	0.75	0.98				
		C/D	0.75	0.98				
		A	0.75	0.98	2	0.7241	0.9500	624
		B	0.75	0.98				
		C/D	0.75	0.98				
		A	0.75	0.98	3	0.7327	0.9613	384
		B	0.75	0.98				
		C/D	0.75	0.98				
		A	0.75	0.98	4	0.7394	0.9701	**252**
		B	0.75	0.98				
		C/D	0.75	0.98				
Unit 1	505-02-2 Surge Line Pipe Point 100 (Pressurizer End)	A	0.75	0.98	1	0.7481	0.9815	432
		B	0.75	0.98				
		C/D	0.75	0.98				
		A	0.75	0.98	2	0.7241	0.9500	624
		B	0.75	0.98				
		C/D	0.75	0.98				
		A	0.75	0.98	3	0.7327	0.9613	384
		B	0.75	0.98				
		C/D	0.75	0.98				
		A	0.75	0.98	4	0.7394	0.9701	**252**
		B	0.75	0.98				
		C/D	0.75	0.98				
Unit 1	505-04 Surge Line Elbow Point 100 (Hot Leg End)	A	0.75	0.98	1	0.7481	0.9815	432
		B	0.75	0.98				
		C/D	0.75	0.98				
		A	0.75	0.98	2	0.7241	0.9500	624
		B	0.75	0.98				
		C/D	0.75	0.98				
		A	0.75	0.98	3	0.7327	0.9613	384
		B	0.75	0.98				
		C/D	0.75	0.98				
		A	0.75	0.98	4	0.7394	0.9701	**252**
		B	0.75	0.98				
		C/D	0.75	0.98				

Table 4: 60-Year Results from Previous CASS Evaluation for Unit 1 Surge Line [5, Table 7-8] (Continued)

Unit	Piece Component	Tolerable Flaw Size for (θ/π = 0.15)			Crack Growth Results[(1)]			Operating Period Evaluated
		Service Level	Tolerable Flaw Depth		Stress Path	Final Flaw Depth		
			[a/t]	in		[a/t]	in	months
Unit 1	505-04 Surge Line Elbow Point 100B (Pressurizer End)	A	0.75	0.98	1	0.7481	0.9815	432
		B	0.75	0.98				
		C/D	0.75	0.98				
		A	0.75	0.98	2	0.7241	0.9500	624
		B	0.75	0.98				
		C/D	0.75	0.98				
		A	0.75	0.98	3	0.7327	0.9613	384
		B	0.75	0.98				
		C/D	0.75	0.98				
		A	0.75	0.98	4	0.7394	0.9701	**252**
		B	0.75	0.98				
		C/D	0.75	0.98				
Unit 1	505-08-2 Surge Line Pipe Point 100B (Hot Leg End)	A	0.75	0.98	1	0.7481	0.9815	432
		B	0.75	0.98				
		C/D	0.75	0.98				
		A	0.75	0.98	2	0.7241	0.9500	624
		B	0.75	0.98				
		C/D	0.75	0.98				
		A	0.75	0.98	3	0.7327	0.9613	384
		B	0.75	0.98				
		C/D	0.75	0.98				
		A	0.75	0.98	4	0.7394	0.9701	**252**
		B	0.75	0.98				
		C/D	0.75	0.98				
Unit 1	505-08-2 Surge Line Pipe Point 120 (Pressurizer End)	A	0.75	0.98	1	0.7481	0.9815	432
		B	0.75	0.98				
		C/D	0.75	0.98				
		A	0.75	0.98	2	0.7241	0.9500	624
		B	0.75	0.98				
		C/D	0.75	0.98				
		A	0.75	0.98	3	0.7327	0.9613	384
		B	0.75	0.98				
		C/D	0.75	0.98				
		A	0.75	0.98	4	0.7394	0.9701	**252**
		B	0.75	0.98				
		C/D	0.75	0.98				

Table 4: 60-Year Results from Previous CASS Evaluation for Unit 1 Surge Line [5, Table 7-8] (Concluded)

Unit	Piece Component	Tolerable Flaw Size for (θ/π = 0.15) Service Level	Tolerable Flaw Depth [a/t]	Tolerable Flaw Depth in	Crack Growth Results(1) Stress Path	Final Flaw Depth [a/t]	Final Flaw Depth in	Operating Period Evaluated months
Unit 1	505-08-1 Surge Line Pipe Point 120 (Hot Leg End)	A	0.75	0.98	1	0.7481	0.9815	432
		B	0.75	0.98				
		C/D	0.75	0.98				
		A	0.75	0.98	2	0.7241	0.9500	624
		B	0.75	0.98				
		C/D	0.75	0.98				
		A	0.75	0.98	3	0.7327	0.9613	384
		B	0.75	0.98				
		C/D	0.75	0.98				
		A	0.75	0.98	4	0.7394	0.9701	**252**
		B	0.75	0.98				
		C/D	0.75	0.98				
Unit 1	505-08-1 Surge Line Pipe Point 150 (Pressurizer End)	A	0.75	0.98	1	0.7481	0.9815	432
		B	0.75	0.98				
		C/D	0.75	0.98				
		A	0.75	0.98	2	0.7241	0.9500	624
		B	0.75	0.98				
		C/D	0.75	0.98				
		A	0.75	0.98	3	0.7327	0.9613	384
		B	0.75	0.98				
		C/D	0.75	0.98				
		A	0.75	0.98	4	0.7394	0.9701	**252**
		B	0.75	0.98				
		C/D	0.75	0.98				

Table 5: 60-Year Results from Previous CASS Evaluation for Unit 2 Reactor Coolant Pump Safe Ends [5, Table 7-9]

Unit	Piece (Assembly) Component	Tolerable Flaw Size for (θ/π = 0.15)			Crack Growth Results(1)		Operating Period Evaluated
		Service Level	Tolerable Flaw Depth		Final Flaw Depth		
			[a/t]	in	[a/t]	in	months
Unit 2	731-101 (771-701) Cold Leg P5-A Pump 2A2 Discharge	A	0.75	2.400	0.2728	0.8730	480
		B	0.75	2.400			
		C/D	0.75	2.400			
	731-101 (771-901) Cold Leg P14-A Pump 2B1 Discharge	A	0.75	2.400	0.2723	0.8713	480
		B	0.75	2.400			
		C/D	0.75	2.400			
	731-101 (771-1301) Cold Leg P18-A Pump 2B2 Discharge	A	0.75	2.400	0.2706	0.8661	480
		B	0.75	2.400			
		C/D	0.75	2.400			
	731-101 (771-1501) Cold Leg P4-B Pump 2A2 Suction	A	0.75	2.400	0.2719	0.8702	480
		B	0.75	2.400			
		C/D	0.75	2.400			
	731-101 (771-1501) Cold Leg P13-B Pump 2B1 Suction	A	0.75	2.400	0.2716	0.8692	480
		B	0.75	2.400			
		C/D	0.75	2.400			

Note:

(1) Crack growth is evaluated for up to 40 years. The postulated flaw did not grow beyond the tolerable flaw size during that time period, and therefore, the final flaw depth at 40 years is reported.

Table 6: 60-Year Results from Previous CASS Evaluation for Unit 2 Surge Line [5, Table 7-10]

Unit	Piece Component	Tolerable Flaw Size for (θ/π = 0.15)			Crack Growth Results[(1)]			Operating Period Evaluated
		Service Level	Tolerable Flaw Depth		Stress Path	Final Flaw Depth		
			[a/t]	in		[a/t]	in	Months
Unit 2	751-107 Surge Line Elbow Point 30 (Hot Leg End)	A	0.75	0.98	1	0.7481	0.9815	432
		B	0.75	0.98				
		C/D	0.75	0.98				
		A	0.75	0.98	2	0.7241	0.9500	624
		B	0.75	0.98				
		C/D	0.75	0.98				
		A	0.75	0.98	3	0.7327	0.9613	384
		B	0.75	0.98				
		C/D	0.75	0.98				
		A	0.75	0.98	4	0.7394	0.9701	**252**
		B	0.75	0.98				
		C/D	0.75	0.98				
Unit 2	751-107 Surge Line Elbow Point 50B (Pressurizer End)	A	0.75	0.98	1	0.7481	0.9815	432
		B	0.75	0.98				
		C/D	0.75	0.98				
		A	0.75	0.98	2	0.7241	0.9500	624
		B	0.75	0.98				
		C/D	0.75	0.98				
		A	0.75	0.98	3	0.7327	0.9613	384
		B	0.75	0.98				
		C/D	0.75	0.98				
		A	0.75	0.98	4	0.7394	0.9701	**252**
		B	0.75	0.98				
		C/D	0.75	0.98				

Notes:

(1) The crack growth analysis is bounding for Units 1 and 2 and uses the highest stresses at the bounding surge line location, namely the elbow directly attached to the hot leg surge nozzle, to calculate the maximum crack growth rate.

Table 6: 60-Year Results from Previous CASS Evaluation for Unit 2 Surge Line [5, Table 7-10] (Continued)

Unit	Piece Component	Tolerable Flaw Size for (θ/π = 0.15)			Crack Growth Results(1)			Operating Period Evaluated
		Service Level	Tolerable Flaw Depth		Stress Path	Final Flaw Depth		
			[a/t]	in		[a/t]	in	months
Unit 2	751-109 Surge Line Elbow Point 100 (Hot Leg End)	A	0.75	0.98	1	0.7481	0.9815	432
		B	0.75	0.98				
		C/D	0.75	0.98				
		A	0.75	0.98	2	0.7241	0.9500	624
		B	0.75	0.98				
		C/D	0.75	0.98				
		A	0.75	0.98	3	0.7327	0.9613	384
		B	0.75	0.98				
		C/D	0.75	0.98				
		A	0.75	0.98	4	0.7394	0.9701	**252**
		B	0.75	0.98				
		C/D	0.75	0.98				
Unit 2	751-109 Surge Line Elbow Point 100B (Pressurizer End)	A	0.75	0.98	1	0.7481	0.9815	432
		B	0.75	0.98				
		C/D	0.75	0.98				
		A	0.75	0.98	2	0.7241	0.9500	624
		B	0.75	0.98				
		C/D	0.75	0.98				
		A	0.75	0.98	3	0.7327	0.9613	384
		B	0.75	0.98				
		C/D	0.75	0.98				
		A	0.75	0.98	4	0.7394	0.9701	**252**
		B	0.75	0.98				
		C/D	0.75	0.98				
Unit 2	751-102 Surge Line Pipe Point 100B (Hot Leg End)	A	0.75	0.98	1	0.7481	0.9815	432
		B	0.75	0.98				
		C/D	0.75	0.98				
		A	0.75	0.98	2	0.7241	0.9500	624
		B	0.75	0.98				
		C/D	0.75	0.98				
		A	0.75	0.98	3	0.7327	0.9613	384
		B	0.75	0.98				
		C/D	0.75	0.98				
		A	0.75	0.98	4	0.7394	0.9701	**252**
		B	0.75	0.98				
		C/D	0.75	0.98				

Table 6: 60-Year Results from Previous CASS Evaluation for Unit 2 Surge Line [5, Table 7-10] (Continued)

Unit	Piece Component	Tolerable Flaw Size for (θ/π = 0.15)			Crack Growth Results(1)			Operating Period Evaluated
		Service Level	Tolerable Flaw Depth		Stress Path	Final Flaw Depth		
			[a/t]	in		[a/t]	in	months
Unit 2	751-102 Surge Line Pipe Point 120 (Pressurizer End)	A	0.75	0.98	1	0.7481	0.9815	432
		B	0.75	0.98				
		C/D	0.75	0.98				
		A	0.75	0.98	2	0.7241	0.9500	624
		B	0.75	0.98				
		C/D	0.75	0.98				
		A	0.75	0.98	3	0.7327	0.9613	384
		B	0.75	0.98				
		C/D	0.75	0.98				
		A	0.75	0.98	4	0.7394	0.9701	**252**
		B	0.75	0.98				
		C/D	0.75	0.98				
Unit 2	751-110 Surge Line Pipe Point 120 (Hot Leg End)	A	0.75	0.98	1	0.7481	0.9815	432
		B	0.75	0.98				
		C/D	0.75	0.98				
		A	0.75	0.98	2	0.7241	0.9500	624
		B	0.75	0.98				
		C/D	0.75	0.98				
		A	0.75	0.98	3	0.7327	0.9613	384
		B	0.75	0.98				
		C/D	0.75	0.98				
		A	0.75	0.98	4	0.7394	0.9701	**252**
		B	0.75	0.98				
		C/D	0.75	0.98				
Unit 2	751-110 Surge Line Pipe Point 150 (Pressurizer End)	A	0.75	0.98	1	0.7481	0.9815	432
		B	0.75	0.98				
		C/D	0.75	0.98				
		A	0.75	0.98	2	0.7241	0.9500	624
		B	0.75	0.98				
		C/D	0.75	0.98				
		A	0.75	0.98	3	0.7327	0.9613	384
		B	0.75	0.98				
		C/D	0.75	0.98				
		A	0.75	0.98	4	0.7394	0.9701	**252**
		B	0.75	0.98				
		C/D	0.75	0.98				

Structural Integrity Associates, Inc.
info@structint.com 1-877-4SI-POWER structint.com

Table 6: 60-Year Results from Previous CASS Evaluation for Unit 2 Surge Line [5, Table 7-10] (Concluded)

Unit	Piece Component	Tolerable Flaw Size for (θ/π = 0.15)			Crack Growth Results(1)			Operating Period Evaluated
		Service Level	Tolerable Flaw Depth		Stress Path	Final Flaw Depth		
			[a/t]	in		[a/t]	in	months
Unit 2	751-104 Surge Line Pipe Point 150 (Hot Leg End)	A	0.75	0.98	1	0.7481	0.9815	432
		B	0.75	0.98				
		C/D	0.75	0.98				
		A	0.75	0.98	2	0.7241	0.9500	624
		B	0.75	0.98				
		C/D	0.75	0.98				
		A	0.75	0.98	3	0.7327	0.9613	384
		B	0.75	0.98				
		C/D	0.75	0.98				
		A	0.75	0.98	4	0.7394	0.9701	**252**
		B	0.75	0.98				
		C/D	0.75	0.98				
Unit 2	751-104 Surge Line Pipe Point 150B (Pressurizer End)	A	0.75	0.98	1	0.7481	0.9815	432
		B	0.75	0.98				
		C/D	0.75	0.98				
		A	0.75	0.98	2	0.7241	0.9500	624
		B	0.75	0.98				
		C/D	0.75	0.98				
		A	0.75	0.98	3	0.7327	0.9613	384
		B	0.75	0.98				
		C/D	0.75	0.98				
		A	0.75	0.98	4	0.7394	0.9701	**252**
		B	0.75	0.98				
		C/D	0.75	0.98				

Table 7 - Comparison of Key Correlations in NUREG-4513 Revision 1 and Revision 2 for Centrifugal CASS, Grade CF8M (554°F to 608°F)

Item	Parameter	NUREG-4513 Revision 1 [8]	NUREG-4513 Revision 2 [9]
1	Chromium Eq	$Cr_{eq} = (Cr) + 1.21(Mo) + 0.48(Si) - 4.99$	$Cr_{eq} = (Cr) + 1.21(Mo) + 0.48(Si) - 4.99$
2	Nickel Eq	$Ni_{eq} = (Ni) + 0.11(Mn) - 0.0086(Mn)^2 + 18.4(N) + 24.5(C) + 2.77$	$Ni_{eq} = (Ni) + 0.11(Mn) - 0.0086(Mn)^2 + 18.4(N) + 24.5(C) + 2.77$
3	Ferrite Content	$FC = 100.3(Cr_{eq}/Ni_{eq})^2 - 170.72(Cr_{eq}/Ni_{eq}) + 74.22$	$FC = 100.3(Cr_{eq}/Ni_{eq})^2 - 170.72(Cr_{eq}/Ni_{eq}) + 74.22$
4	Cvsat	$\mathrm{Log}_{10}\, Cv_{sat} = 1.10 + 2.12\exp(-0.041\,\Phi)$	$\mathrm{Log}_{10}\, Cv_{sat} = 0.27 + 2.81\exp(-0.022\,\Phi)$
	Phi	$\Phi = \delta_c (Ni + Si + Mn)^2 (C + 0.4N)/5$	$\Phi = \delta_c (Ni + Si + Mn)^2 (C + 0.4N)/5$
5	Cvsat	$\mathrm{Log}_{10}\, Cv_{sat} = 7.28 - 0.011\,(\delta_c) - 0.185\,(Cr) - 0.369\,(Mo) - 0.451\,(Si) - 0.007\,(Ni) - 4.71\,(C + 0.4N)$	$\mathrm{Log}_{10}\, Cv_{sat} = 7.28 - 0.011\,(\delta_c) - 0.185\,(Cr) - 0.369\,(Mo) - 0.451\,(Si) - 0.007\,(Ni) - 4.71\,(C + 0.4N)$
6	J-R Curve	$J_d = C[\Delta a]^n$	$J_d = C\,[Cv_{sat}]^m\,[\Delta a]^n$
	C for Cv_{sat} > 20.7 ft-lb	$404[25.4]^n\,[Cv_{sat}]^{0.41}$	$404[25.4]^n\,[Cv_{sat}]^{0.41}$
	C for Cv_{sat} < 20.7 ft-lb	$404[25.4]^n\,[Cv_{sat}]^{0.41}$	$65[25.4]^n\,[Cv_{sat}]^{0.98}$
	n	$n = 0.244 + 0.06\,\log_{10} Cv_{sat}$	$n = 0.190 + 0.07\,\log_{10} Cv_{sat}$
7	Lower Bound J-R Curve	$Jd = 2474[\Delta a]^{0.33}$	$Jd = 2474[\Delta a]^{0.29}$

Table 8. Projected 60-Year Cycles in the CASS Evaluation Versus Projected 80-Year Cycles for SLR

Thermal Transients	60-Year Cycles [5]		80 Year Cycles [11]	
	Total Projected Cycles [4]	Annual Projected Cycles	Total Projected Cycles [13]	Annual Projected Cycles
Plant Heatup(1)	143	2.4	143	1.788
Plant Cooldown(1)	143	2.4	141	1.763
Plant Loading A	900	15	1200	15
Plant Loading B	900	15	1200	15
Plant Unloading A	900	15	1200	15
Plant Unloading B	900	15	1200	15
10% Step Increase	390	6.5	520	6.5
10% Step Decrease	390	6.5	520	6.5
Reactor Trip	115	1.9	106	1.325
Loss of Flow	1	0.017	2	0.025
Loss of Load	8	0.133	6	0.075
Loss of Secondary Pressure	1	0.017	2	0.025
Safety Injection II	500(2)	8.33	N/A(2)	N/A
Hydrostatic Test	13	0.217	6	0.075
Leak Test Up	116	1.93	5	0.063
Leak Test Down	116	1.93	5	0.063
OBE	40	0.67	80(3)	1

Notes:

1. Thermal stratification cycles for the surge line evaluation [5, Table 7-1] were calculated based on plant heatup and plant cooldown cycles. As such, the conclusion for plant heatup and plant cooldown is applicable for thermal stratification events.
2. For Safety Injection II, the design cycles for 40 years were used in the CASS evaluation [5, Table 7-3, Note 2], and the projected 80-year cycles are not available.
3. Two OBE events with forty internal cycles each are assumed for a total of eighty projected cycles over the 80-year plant life.

Table 9: 80-Year Results of CASS Reevaluation for Units 1 and 2

Unit	Component	Tolerable Flaw Size for (θ/π = 0.15)			Reevaluated 80-Year Crack Growth Results			Operating Period Evaluated
		Service Level	Tolerable Flaw Depth		Stress Path	Final Flaw Depth		
			[a/t]	in		[a/t]	in	months
Unit 1 Unit 2	All Surge Line Components	A	0.75	0.98	P4 (Bounding)	0.3396	0.4455	960
		B	0.75	0.98				
		C/D	0.75	0.98				
Unit 1	Safety Injection Nozzle Safe-Ends	A	0.75	0.98	SI3 (Bounding)	0.3293	0.4321	960
		B	0.75	0.98				960
		C/D	0.75	0.98				960
Unit 2	RCP Suction and Discharge Safe-Ends	A	0.75	2.40	CL1 (Bounding)	0.2559	0.8190	960
		B	0.75	2.40				960
		C/D	0.75	2.40				960

Structural Integrity Associates, Inc.
info@structint.com 1-877-4SI-POWER structint.com

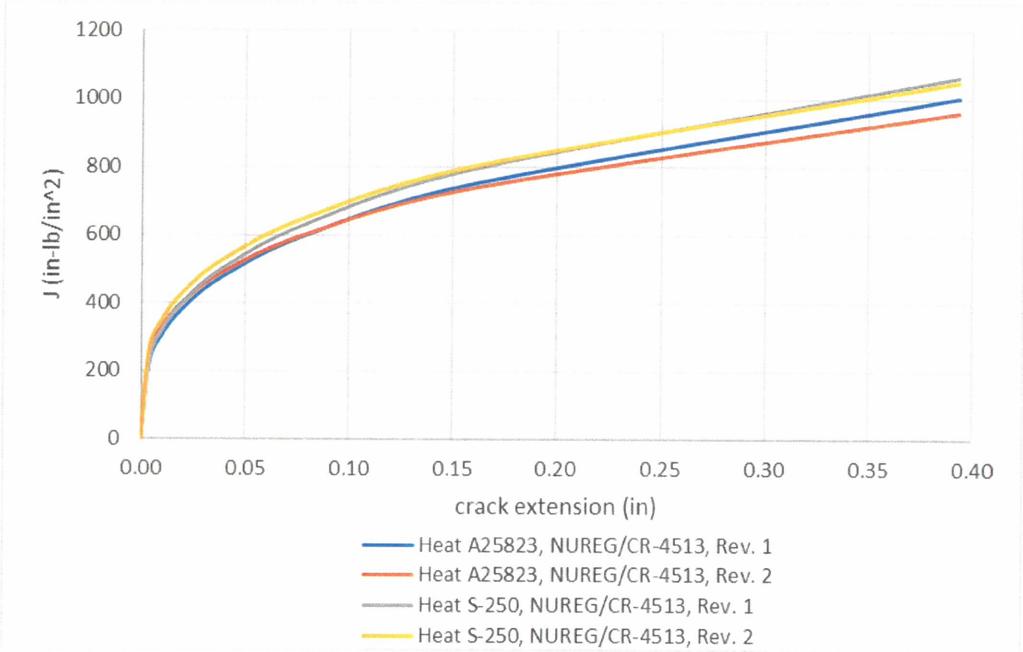

Figure 1: Comparison of J-R Distribution from NUREG/CR-4513, Revisions 1 and 2 for Delta Ferrite between 20 - 25% (554°F to 608°F)

.

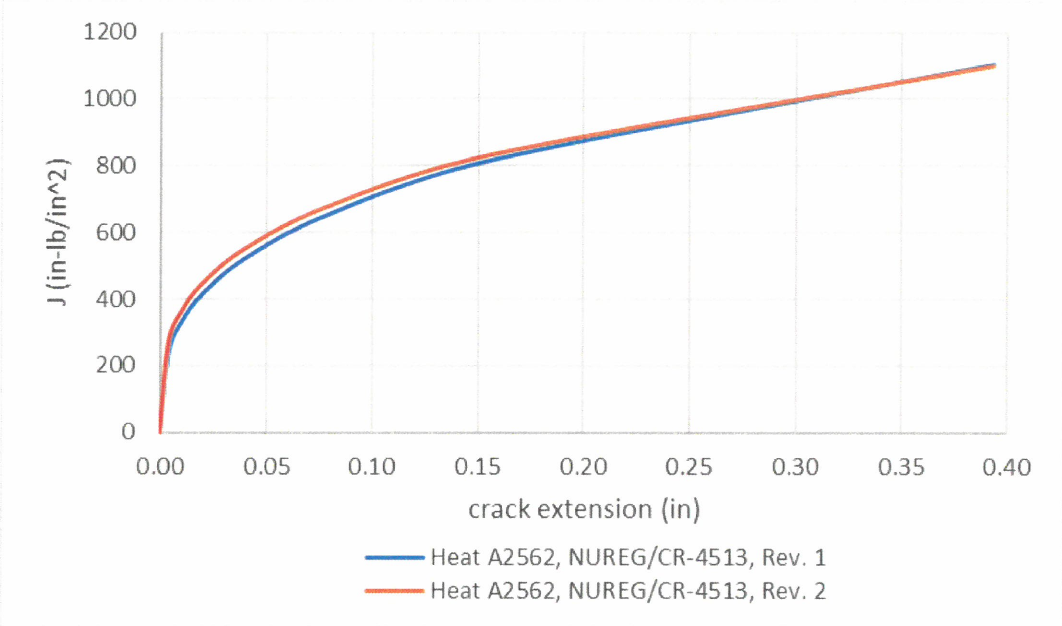

Figure 2: Comparison of J-R Distribution from NUREG/CR-4513, Revisions 1 and 2 for Delta Ferrite between 25 - 30% (554°F to 608°F)

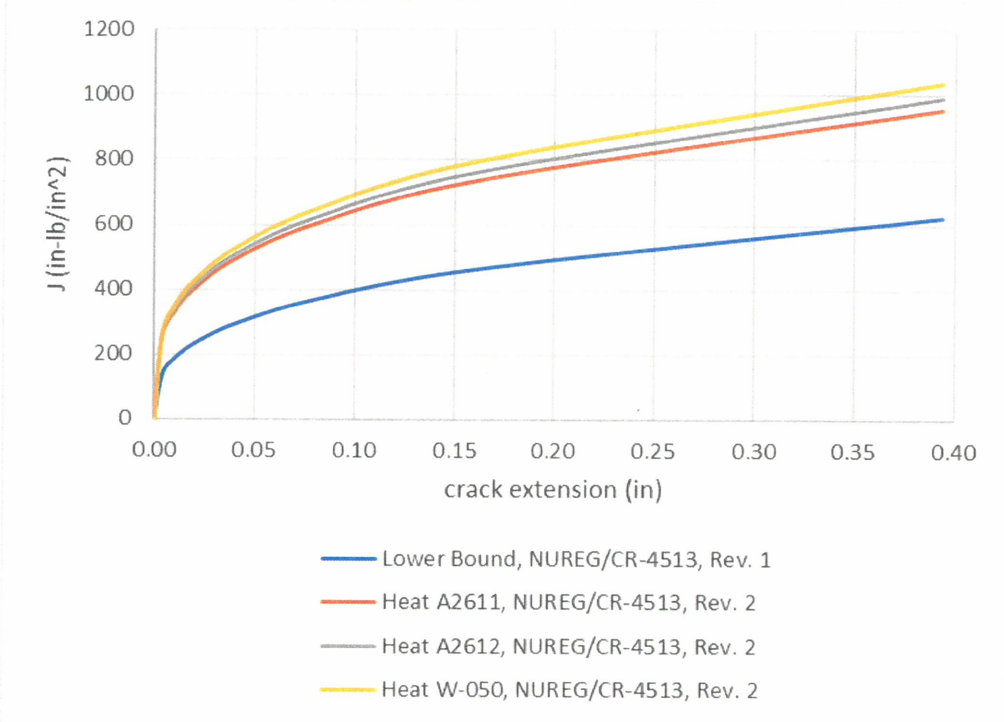

Figure 3: Comparison of J-R Distribution of NUREG/CR-4513, Revisions 1 and 2 for Delta Ferrite > 30% (554°F to 608°F)

Terry J. Herrmann Senior Associate	7/15/21 Date	Nathaniel Cofie Senior Associate	7/15/21 Date
Kevin L. Wong Consultant	7/15/21 Date	David A. Gerber Senior Associate	7/15/21 Date
Gary Dominguez Engineer	7/15/21 Date		

Revision	Section	Preparer	Reviewers	PM Reviewer
0	1	Timothy Griesbach	Nathaniel Cofie, Terry Herrmann	Dave Gerber
	2	Timothy Griesbach	Nathaniel Cofie, Terry Herrmann	
	3	Nathaniel Cofie	Timothy Griesbach, Terry Herrmann	
	4	Nathaniel Cofie	Timothy Griesbach, Terry Herrmann	
	5	Nathaniel Cofie	Timothy Griesbach, Terry Herrmann	
	6	Kevin Wong	Nathaniel Cofie, Terry Herrmann	
	7	Nathaniel Cofie	Timothy Griesbach, Terry Herrmann	
	8	Timothy Griesbach	Nathaniel Cofie, Terry Herrmann	
	Supporting Files	Gary Dominguez	Kevin Wong	
1	All	Kevin Wong	Nathaniel Cofie, Terry Herrmann	Dave Gerber
	Supporting Files	Gary Dominguez	Kevin Wong	

Enclosure 4

Non-proprietary Reference Documents and Redacted Versions of Proprietary Reference Documents (Public Version)

Attachment 15

Framatome Document No. 86-9329648-000, St. Lucie SLR Crack Growth Analysis Summary - Non Proprietary, July 2, 2021

(19 Total Pages, including cover sheets)

framatome **CALCULATION SUMMARY SHEET (CSS)**

Document No. 86 - 9329648 - 000 Safety Related: ☒Yes ☐ No

Title St. Lucie SLR Crack Growth Analysis Summary - Non Proprietary

PURPOSE AND SUMMARY OF RESULTS:

Purpose:

The purpose of this document is to summarize the results of the fatigue and primary water stress corrosion crack growth of postulated, inside surface-connected, 360° circumferential and semi-elliptical axial flaws in the weld overlays at St. Lucie Unit 2 in order to establish the acceptable period of operation between inspections based on the predicted crack growth calculated by the guidelines of Non-Mandatory Appendix C of the ASME Code Section XI for FPL's Subsequent License Renewal Application (SLRA).

The locations summarized in this document are as follows:

- Pressurizer (PZR) Surge Nozzle Weld Overlay (WOL)
- PZR Relief Nozzle WOL
- Hot Leg (HL) Shutdown Cooling Nozzle WOL
- HL Surge Nozzle WOL
- HL Drain Nozzle WOL

Summary of Results:

The results from the fracture mechanics analysis were to evaluate worst case flaws in the overlaid configurations and to establish the acceptable period of operation between inspections, Table 5-1 provides the results from this analysis. The most limiting acceptable period of operation between inspections for the 80 year SLR period is 18.10 years, which occurs for the Unit 2 Hot Leg Surge Nozzle.

The proprietary version of this document is 86-9329645-000.

If the computer software used herein is not the latest version per the EASI list, AP 0402-01 requires that justification be provided.

THE FOLLOWING COMPUTER CODES HAVE BEEN USED IN THIS DOCUMENT:

CODE/VERSION/REV	CODE/VERSION/REV
N/A	

THE DOCUMENT CONTAINS ASSUMPTIONS THAT SHALL BE VERIFIED PRIOR TO USE

☐Yes

☒ No

Review Method: ☒ Design Review (Detailed Check)

☐ Alternate Calculation

Does this document establish design or technical requirements? ☐ YES ☒ NO

Does this document contain Customer Required Format? ☐ YES ☒ NO

Signature Block

Name and Title (printed or typed)	Signature	P/R/A/M and LP/LR	Date	Pages/Sections Prepared/Reviewed/Approved
John Cosso Engineer I	*JD COSSO* *7/2/2021*	P		All
Jennifer Nelson Principal Engineer	*JA NELSON* *7/2/2021*	R		All
David Cofflin Supervisory Engineer	*DR COFFLIN* *7/2/2021*	A		All

Notes: P/R/A designates Preparer (P), Reviewer (R), Approver (A);
LP/LR designates Lead Preparer (LP), Lead Reviewer (LR);
M designates Mentor (M)

In preparing, reviewing and approving revisions, the lead preparer/reviewer/approver shall use 'All' or 'All except ___' in the pages/sections reviewed/approved. 'All' or 'All except ___' means that the changes and the effect of the changes on the entire document have been prepared/reviewed/approved. It does not mean that the lead preparer/reviewer/approver has prepared/reviewed/approved all the pages of the document.

With Approver permission, calculations may be revised without using the latest CSS form. This deviation is permitted when expediency and/or cost are a factor. Approver shall add a comment in the right-most column that acknowledges and justifies this deviation.

Project Manager Approval of Customer References and/or Customer Formatting (N/A if not applicable)

Name (printed or typed)	Title (printed or typed)	Signature	Date	Comments
N/A	N/A	N/A	N/A	N/A

Record of Revision

Revision No.	Pages/Sections/Paragraphs Changed	Brief Description / Change Authorization
000	All	Original Release

Table of Contents

Page

SIGNATURE BLOCK 2

RECORD OF REVISION 3

LIST OF TABLES 5

LIST OF FIGURES 6

1.0 INTRODUCTION AND PURPOSE 7

2.0 ANALYTICAL METHODOLOGY 7
- 2.1 Postulated Flaws 8
- 2.2 Stress Intensity Factors (SIF) Solutions 9
- 2.3 Fatigue Crack Growth Mechanisms 9
- 2.4 PWSCC Crack Growth Mechanisms 10
- 2.5 Methodology for Flaw Growth Analysis 10
- 2.6 Acceptance Criteria 11

3.0 ASSUMPTIONS 12
- 3.1 Unverified Assumptions 12
- 3.2 Justified Assumptions 12
- 3.3 Modeling Simplifications 12

4.0 GEOMETRY 13

5.0 RESULTS 15

6.0 REFERENCES 17

List of Tables

Page

Table 2-1: Relevant Sources of Stress for Fatigue and PWSCC Flaw Growth Analysis 10

Table 5-1: Flaw Evaluation Summary 16

List of Figures

Page

Figure 2-1: Inside Surface-Connected, Partial Through-Wall, 360° Circumferential Flaw 8
Figure 2-2: Inside Surface-Connected, Partial Through-Wall, Semi-Elliptical Axial Flaw 9
Figure 4-1: U2 PZR Surge Nozzle Path Lines 13
Figure 4-2: U2 PZR Relief Nozzle Geometry Path Lines 14
Figure 4-3: U2 HL Shutdown Cooling Nozzle Path Lines 14
Figure 4-4: U2 HL Surge Nozzle Path Lines 15
Figure 4-5: U2 HL Drain Nozzle Lines 15

1.0 INTRODUCTION AND PURPOSE

Florida Power & Light (FPL) intends to apply for a Subsequent License Renewal Application (SLRA) at St. Lucie Unit 2 (PSL-2) to extend operating life to 80 years. Therefore, in support of the SLRA, flaw tolerance analyses are done to determine the acceptable period of operation between inspections at susceptible locations in the Reactor Coolant System (RCS). The time between inspections is determined to satisfy footnote 10 of Code Case N-770-2 (Reference [1]), which requires that inspections be performed within the mitigation evaluation period. The susceptible locations are as follows:

- Pressurizer (PZR) Surge Nozzle Weld Overlay (WOL)
- PZR Relief Nozzle WOL
- Hot Leg (HL) Shutdown Cooling Nozzle WOL
- HL Surge Nozzle WOL
- HL Drain Nozzle WOL

The purpose of this document is to provide FPL with a summary of the acceptable period of operation (APO) between inspections per location based on the crack growth analyses (CGA) performed for SLR based on the guidelines of Non-Mandatory Appendix C of the ASME Code Section XI [15]. The acceptable period of operation between inspections is investigated to address the possibility of fatigue and primary water stress corrosion crack (PWSCC) growth using:

- PWSCC growth and fatigue crack growth evaluations for the Alloy 182 dissimilar metal weld (DMW) and butter, extending into the Alloy 52M SWOL, as required, using Non-Mandatory Appendix C of the 2007 Edition with 2008 Addenda of the ASME Code Section XI [15] with the use of applicable operating transients and associated cycles.
- Fatigue crack growth evaluations for the stainless steel weld portion of this nozzle, as required, using Non-Mandatory Appendix C of the 2007 Edition with 2008 Addenda of the ASME Code Section XI [15] with the use of applicable operating transients and associated cycles.

It is postulated that an inside surface-connected, partial through-wall, 360° circumferential flaw(s) and a semi-elliptical axial flaw(s) would propagate by PWSCC and fatigue through the thickness of the DMW/Butter region and by fatigue through the thickness of the safe end stainless steel weld. If the postulated flaws propagate through the original weld materials, PWSCC and fatigue crack growth analysis is also performed to determine the amount of crack growth into the Alloy 52M structural weld overlay.

Additionally, paragraph 2(a) of ASME Code Case N-740-2, Reference [2], states that if the flaw is at or near the boundary of two different materials, evaluation of the flaw growth in both materials is required. Therefore, the path line near the boundary with the Low Alloy Steel (LAS) or Carbon Steel (CS) nozzle is also evaluated for the LAS/CS nozzle material. Fatigue crack growth evaluation for the postulated circumferential and axial flaws at this location is conducted using Non-Mandatory Appendix C of the 2007 Edition with 2008 Addenda of the ASME Code Section XI Reference [15] with use of applicable operating transients and associated cycles.

This document summarizes the methodology used to perform the SLR CGA (life to 80 years) for St. Lucie Unit 2. In addition, the results from the original crack growth evaluations (CGE) for 60 year life are summarized in Section 5.0.

2.0 ANALYTICAL METHODOLOGY

A fracture mechanics analysis is performed to determine potential worst case flaws that could develop within a component. The high-level methodology that was used to determine the acceptable period of operation between inspections is listed below. See Section 2.0 of References [17], [19], [21], [23], and [25]) for the complete methodology for each specific CGA.

2.1 Postulated Flaws

An inside surface-connected, partial through-wall, full (360°) circumferential flaw in a cylinder, as shown in Figure 2-1, or an inside surface-connected, partial through-wall, semi elliptical axial flaw, as shown in Figure 2-2, is postulated to exist at the time the overlay is applied.

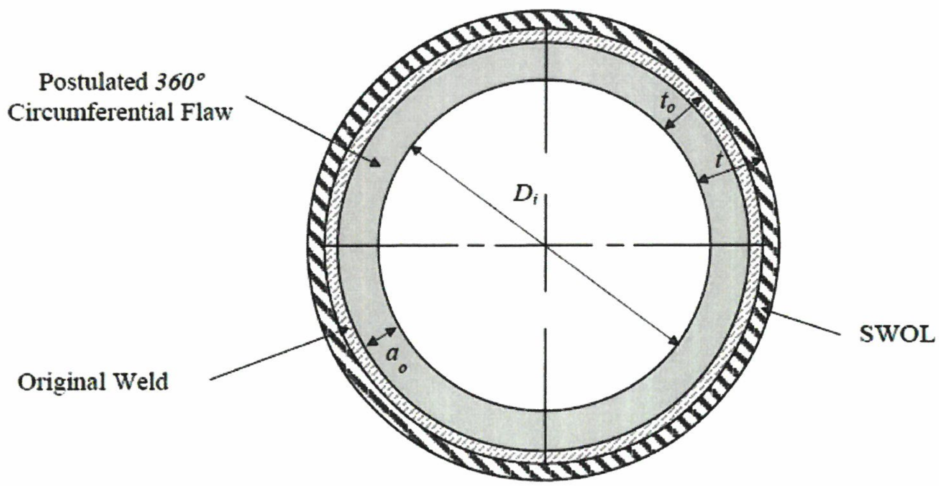

Where,

a_o = initial flaw depth
D_i = diameter of inside surface
t_o = wall thickness prior to weld overlay
t = overall wall thickness post weld overlay

Figure 2-1: Inside Surface-Connected, Partial Through-Wall, 360° Circumferential Flaw

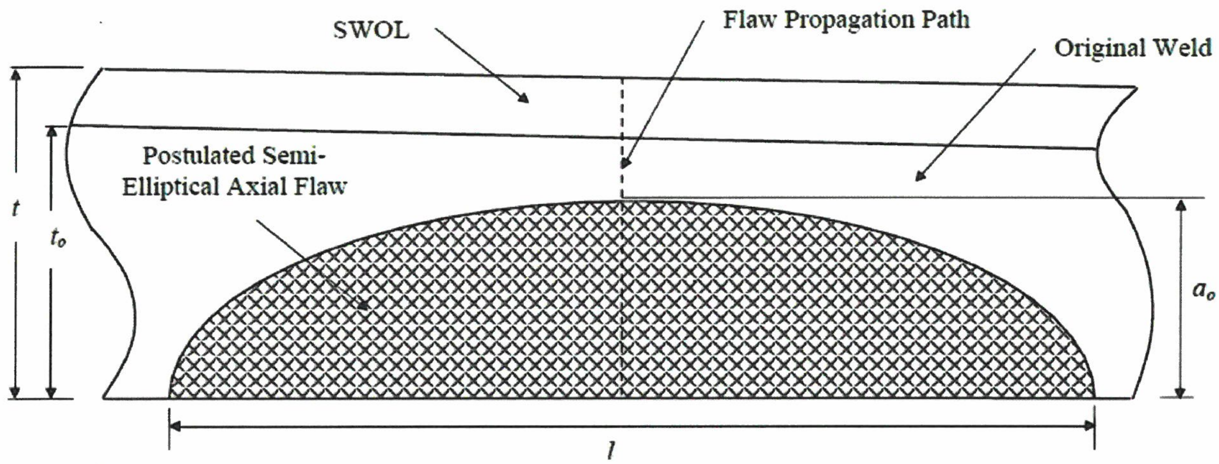

Where,

a_o = initial flaw depth
l = flaw length
t_o = wall thickness prior to weld overlay
t = overall wall thickness post weld overlay

Figure 2-2: Inside Surface-Connected, Partial Through-Wall, Semi-Elliptical Axial Flaw

2.2 Stress Intensity Factors (SIF) Solutions

[

]

This is a well-established fracture mechanics methodology which Framatome has implemented in a Microsoft Excel macro. The technical basis for this implementation is given in Reference [3] and [4].

2.3 Fatigue Crack Growth Mechanisms

The crack growth analysis is conducted on a cycle by cycle basis to the end of the mitigation evaluation period. Each material has a specific fatigue crack growth equation which is used to determine the crack growth rate. Listed below are the component materials found in the CGAs, with a general summary of the references used to calculate the crack growth rate.

- **Alloy 182**: Flaw growth in the Alloy 182 weld material in water environment due to cyclic loading is calculated using [

  ]

- **Stainless Steel Welds (Type 304L and 316L)**: The fatigue crack growth rate for Type 304L and Type 316L austenitic stainless steel and associated weld metals in water environment is obtained from [ ]

- **Alloy 52M**: Flaw growth in the Alloy 52M in water environment due to cyclic loading is calculated using the fatigue crack growth model presented in [ ]
- **LAS/CS**: The flaw growth due to fatigue of the LAS/CS material is [ ]

2.4 PWSCC Crack Growth Mechanisms

Each material has a specific PWSCC crack growth equation, which is used to determine the crack growth rate. Listed below are the component materials found in the CGAs, with a general summary of references used to calculate the crack growth rate.

- **Alloy 182**: For the Alloy 182 material, the PWSCC crack growth rate is per [ ]
- **Alloy 52M**: PWSCC crack growth in Alloy 52M is also assessed using [ ]

2.5 Methodology for Flaw Growth Analysis

For the crack growth analysis, the applied stress intensity factor is driven by axial stresses for the *360°* circumferential flaws, and by hoop stresses for the axial flaws. The relevant sources of stress for fatigue and PWSCC crack growth analyses are summarized in Table 2-1.

Table 2-1: Relevant Sources of Stress for Fatigue and PWSCC Flaw Growth Analysis

Inside Surface-Connected, Partial Through-Wall, 360° Circumferential Flaw	
Fatigue Crack Growth	[
PWSCC Crack Growth	]
Inside Surface-Connected, Partial Through-Wall, Semi-Elliptical Axial Flaw	
Fatigue Crack Growth	[
PWSCC Crack Growth	]

For each transient, the cycles are assumed to be uniformly distributed through the end of the mitigation evaluation period. The cycles from all the transients are sorted based on the time that they are assumed to occur. Fatigue flaw growth is calculated by considering the assumed sequence of total transient stresses which may consist of a collection of sub-cycles (peaks and valleys) within any transient. The service life is conservatively taken to be 56 years of plant operation following the installation of the structural weld overlay (SWOL) during the Fall of 2007 that corresponds to the end of the 80-year license period through the Spring of 2063 for St. Lucie Unit 2.

The PWSCC and fatigue crack growth mechanisms are considered to be active simultaneously. Following the guidance in article [ ] the PWSCC and fatigue crack growths are coupled in an incremental manner at selected time points throughout the service life (i.e., in approximate chronological order).

The PWSCC and fatigue crack growth of the inside surface-connected, partial through-wall, semi-elliptical axial flaw is controlled by the values of [ ]

2.6 Acceptance Criteria

The objective of the flaw growth analysis is to establish the acceptable period of operation between inspections based on the predicted crack growth calculated by the guidelines of Non-Mandatory Appendix C.

Per C-2610 of the ASME B&PV Code, Section XI, Reference [15], analytical evaluation procedures can be used to demonstrate acceptability for continued service during the evaluation period if the flaw parameters satisfy either the Flaw Size Criteria in C-2611 or the Applied Stress Criteria in C-2612.

The Applied Stress Criteria of C-2612 of Reference [15] requires that the calculated pipe stresses have to be less than the allowable stresses for the flawed pipe, which are a function of pipe stresses, required structural factors, pipe material properties, end-of-evaluation-period flaw length and depth, flaw orientation, and pipe failure mode. In addition, for axially-oriented flaws, C-2612 requires that the final flaw length, l_f shall not exceed the corresponding allowable flaw length l_{allow} for the postulated flaws. [ ]

According to C-4210, Reference [15], the sequence used to determine the failure mode and analysis method for austenitic piping is given in Figure C-4210-1 of Reference [15]. Based on Figure C-4210-1 of Reference [15], for a flaw in austenitic/Ni-Cr-Fe weld material, Sections C-5000 and C-6000 of Reference [15] are to be used as the analysis methods for Non-flux and Flux welds, respectively.

The Alloy 182 dissimilar metal welds and the stainless steel welds in are considered to be flux welds. Therefore, for the postulated flaws in austenitic/Ni-Cr-Fe and austenitic stainless steel weld materials, allowable stresses and flaw lengths are determined from the analysis method defined in C-6000 of Reference [15].

The Alloy 52M SWOLs in the St. Lucie Unit 2 nozzles are considered to be non-flux welds. Therefore, if the postulated flaws propagate into the Alloy 52M weld material, allowable stresses and flaw lengths are determined from the analysis method defined in C-5000 of Reference [15].

[ ]

Additionally, paragraph 2(a) of ASME Code Case N-740-2, Reference [2], states that if the flaw is at or near the boundary of two different materials, evaluation of flaw growth in both materials is required. Therefore, the path line on the butter weld near the boundary with the LAS or CS nozzle is also evaluated considering the LAS/CS nozzle material properties. Per C-4230 of Reference [15], for fusion-line flaws in Ni-Cr-Fe buttered welds, the piping flaw evaluation procedures of C-4220 for the adjacent base metal shall be used. Based on Figure C 4220-1, the screening criteria from C-4300 shall be applied to determine the applicable method of analysis (i.e., C-5000, C-6000, or C-7000 of Reference [15]).

3.0 ASSUMPTIONS

3.1 Unverified Assumptions

There are no unverified assumptions within the 80 year SLR CGA calculations (see Section 3.1 of References [17], [19], [21], [23], and [25]).

3.2 Justified Assumptions

Listed below are general assumptions for the crack growth analyses, for a complete list of justified assumptions see Section 3.2 of References [17], [19], [21], [23], and [25]).

3.3 Modeling Simplifications

For complete lists of modeling simplifications see Section 3.3 of References [17], [19], [21], [23], and [25]).

4.0 GEOMETRY

This section outlines the geometry of each component. Depicted below are figures that describe the path lines for each component used from the fracture mechanics evaluations. These path lines are selected as they are representative stress states in the DMW and butter region (Paths FR1, FR2 and FR3), and the stainless steel weld (Path FR4).

The orientation of path lines FR1 and FR3 along the interface of the butter/weld with the base material is chosen to obtain stresses in a region where cracks are likely to occur. Since the crack plane of the postulated 360° circumferential flaw is perpendicular to the axial direction of the nozzle, the stress state along the "slant" path lines FR1 through FR3 are mapped directly on to the auxiliary path lines, which are perpendicular to the axial direction of the nozzle.

Figure 4-1: U2 PZR Surge Nozzle Path Lines

[ ]

Figure 4-2: U2 PZR Relief Nozzle Geometry Path Lines

[ ]

Figure 4-3: U2 HL Shutdown Cooling Nozzle Path Lines

Figure 4-4: U2 HL Surge Nozzle Path Lines

Figure 4-5: U2 HL Drain Nozzle Lines

5.0 RESULTS

Table 5-1 provides the worst case flaw results from the fracture mechanics analyses. Each analysis was performed to establish the acceptable period of operation (APO) between inspection, based on the predicted crack growth acceptance criteria within the Non-Mandatory Appendix C of the 2007 Edition with 2008 Addenda of the ASME Code Section XI (Reference [15]) for the 80 year SLR period. The values listed for the acceptable period of operation between inspections are the most limiting values, with their associated path line(s), and flaw description from the fracture mechanic analyses.

In addition, the results from the original crack growth evaluations (CGE) for 60 year life are summarized in Table 5-1.

Table 5-1: Flaw Evaluation Summary

Location	Path Line(s) 60 Year CGE APO between Inspections (years)	CGE Reference	Path Line(s) 80 Year SLR APO between Inspections (years)	Limiting Flaw	SLR Reference
U2 PZR Surge Nozzle	[	[16]	FR1/FR2/FR3 (Figure 4-1) 18.95	360° Circumferential	[17]
U2 PZR Relief Nozzle		[18]	FR1/FR2/FR3 (Figure 4-2) 22.7	Semi-Elliptical Axial	[19]
U2 HL Shutdown Cooling Nozzle		[20]	ALL (Figure 4-3) 56	N/A	[21]
U2 HL Surge Nozzle		[22]	FR4 (Figure 4-4) 18.10	360° Circumferential	[23]
U2 HL Drain Nozzle	]	[24]	ALL (Figure 4-5) 56	N/A	[25]

1) [ ]
2) SLR APO maximum value = 56 years

6.0 REFERENCES

1. ASME Code Case N-770-2, "ASME/BPVC CASE N-770-2, "Alternative Examination Requirements and Acceptance Standards for Class 1 PWR Piping and Vessel Nozzle Butt Welds Fabricated With UNS N06082 or UNS W86182 Weld Filler Material With or Without Application of Listed Mitigation Activities Section XI, Division 1."
2. ASME Code Case N-740-2, "Full Structural Dissimilar Metal Weld Overlay for Repair or Mitigation of Class 1, 2, and 3 Items Section XI, Division 1."
3. Framatome Document 32-9052958-005, "Evaluation of Stress Intensity Factors Using the Weight Function Method."
4. Framatome Document 32-9055891-007, "Fatigue and PWSCC Crack Growth Evaluation Tool AREVACGC" (Proprietary Document).
5. NUREG/CR-6907, "Crack Growth Rates of Nickel Alloy Welds in a PWR Environment", May 2006.
6. ASME Code Case N-809, "Reference Fatigue Crack Growth Rate Curves for Austenitic Stainless Steels in Pressurized Water Reactor Environments Section XI, Division 1."
7. NRC Letter from Richard Barrett, Director Division of Engineering, Office of NRR to Alex Marion of Nuclear Energy Institute, "Flaw Evaluation Guidelines," April 11, 2003, Accession Number ML030980322.
8. Enclosure 2 to Reference [7], "Appendix A: Evaluation of Flaws in PWR Reactor Vessel Upper Head Penetration Nozzles," Accession Number ML030980333.
9. NUREG/CR-6721, "Effects of Alloy Chemistry, Cold Work, and Water Chemistry on Corrosion Fatigue and Stress Corrosion Cracking of Nickel Alloys and Welds," U.S. Nuclear Regulatory Commission (Argonne National Laboratory), April 2001.
10. Materials Reliability Program: Crack Growth Rates for Evaluating Primary Water Stress Corrosion Cracking (PWSCC) of Thick-Wall Alloy 600 Materials and Alloy 82, 182, and 132 Welds (MRP-420, Revision 1), July 2018.
11. Materials Reliability Program: Recommended Factors of Improvement for Evaluating Primary Water Stress Corrosion Cracking (PWSCC) Growth Rates of Thick- Wall Alloy 690 Materials and Alloy 52, 152, and Variants Welds (MRP 386), December 2017.
12. Materials Reliability Program: Crack Growth Rates for Evaluating Primary Water Stress Corrosion Cracking (PWSCC) of Alloy 82, 182, and 132 Welds (MRP-115), November 2004.
13. Materials Reliability Program: Technical Basis for Reexamination Interval Extension for Alloy 690 PWR Reactor Vessel Top Head Penetration Nozzles (MRP-375), February 2014.
14. ASME Boiler and Pressure Vessel Code Section XI, "Rules for Inservice Inspection of Nuclear Power Plant Components," 2017 Edition.
15. ASME Boiler and Pressure Vessel Code Section XI, "Rules for Inservice Inspection of Nuclear Power Plant Components," 2007 Edition with 2008 Addenda.
16. Framatome Document 32-9054154-001, "Saint Lucie Unit 2 PZR Surge Nozzle Weld Overlay Crack Growth Evaluation."
17. Framatome Document 32-9323851-000, "St. Lucie SLR WOL CGA U2 Pressurizer Surge Nozzle – APP C."
18. Framatome Document 32-9042953-000, "Saint Lucie Unit 2 Pressurizer Relief Nozzle Weld Overlay Crack Growth Evaluation."
19. Framatome Document 32-9323852-000, "St. Lucie SLR WOL CGA U2 PZR Relief Nozzle – APP C."
20. Framatome Document 32-9054503-001, "Saint Lucie Unit 2 Hot Leg Shutdown Cooling Outlet Nozzle Weld Overlay Crack Growth Evaluation."
21. Framatome Document 32-9323853-000, "St. Lucie SLR WOL CGA U2 Hot Leg Shutdown Cooling Nozzle – APP C."

22. Framatome Document 32-9054974-001, "Saint Lucie Unit 2 Hot Leg Surge Nozzle Weld Overlay Crack Growth Evaluation."
23. Framatome Document 32-9323854-000, "St. Lucie SLR WOL CGA U2 Hot Leg Surge Nozzle – APP C."
24. Framatome Document 32-9042954-001, "Saint Lucie Unit 2 Hot Leg Drain Nozzle Weld Overlay Crack Growth Evaluation."
25. Framatome Document 32-9323855-000, "St. Lucie SLR WOL CGA U2 Hot Leg Drain Nozzle – App C."

Enclosure 4

Non-proprietary Reference Documents and Redacted Versions of Proprietary Reference Documents (Public Version)

Attachment 16

Structural Integrity Report No. 2001262.401, Revision 1, Flaw Tolerance Evaluation of St. Lucie, Units 1 and 2 Surge Line Using ASME Code, Section XI, Appendix L for Subsequent License Renewal, July 15, 2021

(9 Total Pages, including cover sheets)

Structural Integrity Associates, Inc.

kwong@structint.com
5215 Hellyer Avenue, Suite 210, San Jose, CA 95138 | 408-978-8200

July 15, 2021
REPORT NO. 2001262.401
REVISION: 1
PROJECT NO. 2001262.00

Quality Program: ☒ Nuclear ☐ Commercial

Bill Maher
Florida Power & Light Co.
St. Lucie Nuclear Power Plant
6501 S. Ocean Dr.
Jenson Beach, FL 34957

Subject: Flaw Tolerance Evaluation of St. Lucie, Units 1 and 2 Surge Line Using ASME Code, Section XI, Appendix L for Subsequent License Renewal

Dear Bill,

This letter report documents the results of a flaw tolerance evaluation in accordance with ASME Code, Section XI, Appendix L [1] to manage fatigue at the critical locations of the St. Lucie, Units 1 and 2 pressurizer surge line for subsequent license renewal (SLR) up to eighty years of plant operation. Differences between the guidance used for initial License Renewal and SLR are addressed as part of this evaluation.

For Revision 1 of this report, the supporting analysis (Reference 4) and CASS Report (Reference 11) were revised to Revision 1. Table 1 and associated notes were updated for Plant Heatup, Plant Cooldown, and stratification cycles, and OBE was added. The results in Table 2 were updated from the supporting analysis. Wording was added to Section 3.0 to clarify the scope of this evaluation. Revision 1 changes are noted with revision lines in the right margin.

1.0 BACKGROUND

For St. Lucie Units 1 and 2 license renewal for up to sixty years of plant operation, a flaw tolerance evaluation [3] was previously performed for the surge line using the ASME Code, Section XI, Appendix L methodology in the 2001 Edition with 2003 Addenda [2]. The previous report concluded that a postulated flaw would take 21 years to reach the allowable flaw size at the bounding surge line location at the elbow adjacent to the hot leg surge nozzle for Units 1 and 2.

For subsequent license renewal for up to eighty years of plant operation, the previous flaw tolerance evaluation [3] was revised in Reference [4] using the ASME Code, Section XI, Appendix L methodology in the 2007 Edition with 2008 Addenda [1], which is the Code edition specified for the St. Lucie, Units 1 and 2 subsequent license renewal.

In addition to technical changes to the Appendix L methodology between the two ASME Code editions, the revised flaw tolerance evaluation will also incorporate the projected 80-year cycles for the St. Lucie SLR [5] and latest austenitic stainless steel crack growth rates from ASME Code Case N-809 [6].

2.0 PREVIOUS APPENDIX L EVALUATION FOR LICENSE RENEWAL TO SIXTY YEARS OF OPERATION

The surge line components are fabricated from either cast austenitic stainless steel (CASS) [3, Section 5.2] or forged stainless steel. For the CASS components, the CASS base metal of the surge line components needs to be managed for thermal aging embrittlement under Program X1.M12 of the aging management program (AMP) [9] whereas Appendix L is under Program X.M1, in accordance with the NUREG-1801, Revision 2 - Generic Aging Lessons Learned (GALL) Report [8] for license renewal. In support of both AMP programs, the previous Appendix L report evaluated the weld metal and the CASS base metal and supplemented the Appendix L methodology with technical aspects from the EPRI technical basis document for CASS flaw tolerance evaluation [10], as noted.

The previous Appendix L evaluation performed a screening of surge line components [3, Section 3.0] to address environmentally assisted fatigue (EAF) in accordance with NUREG-1801, Revision 2 - Generic Aging Lessons Learned (GALL) Report [8, X.M1]. The pressurizer surge nozzle and hot leg surge nozzles were both acceptable for license renewal, but accounting for EAF, all three elbows in the surge line piping failed to meet the allowable cumulative usage factor when considering the reactor coolant environment (U_{en}) of 1.0.

To model stratification, fluid insurges in the horizontal sections of the surge line produce slowly developing thermally stratified conditions. During an outsurge from the pressurizer, hot fluid flows over a stationary cold fluid. During an insurge into the pressurizer, cold fluid flows below hot stationary fluid. A stress analysis was performed for the entire surge line and concluded that the elbow adjacent to the hot leg surge nozzle was the EAF bounding location for the surge line [3, Section 5.0]. Through-wall stresses in the base metal (Stress Paths 1-4) and welds (Stress Paths 9 - 12) [3, Figure 5-4] of the bounding elbow were extracted for the flaw tolerance evaluation.

For fatigue crack growth in both the base metal and weld metal, an initial flaw depth of 25% of the wall thickness was used from the EPRI CASS methodology [10, Section 4.0]. The CASS initial flaw depth is conservative relative to the initial flaw depths (maximum a/t = 11%) from Table IWB-3514-2 of the ASME Code, Section XI, Appendix L methodology.

The previous Appendix L evaluation [3] concluded that the allowable operating period is 21 years from the time of the last inspection at the bounding surge line location (i.e., Stress Path 4 in the base metal of the elbow adjacent to the hot leg surge nozzle, bounding for both St. Lucie Units 1 and 2), and the inservice inspection interval for the surge line locations is ten years [3, Section 7.4].

3.0 TECHNICAL ASPECTS TO ADDRESS FOR SUBSEQUENT LICENSE RENEWAL TO EIGHTY YEARS OF OPERATION

A revised screening was performed for subsequent license renewal to address EAF in accordance with NUREG-2191 - Generic Aging Lessons Learned for Subsequent License Renewal (GALL-SLR) Report [7]. The screening identified the elbow adjacent to the hot leg surge nozzle as the sentinel location for the surge line for both units. As such, the revised Appendix L evaluation was performed for the same bounding surge line location as the previous Appendix L evaluation.

The following plant modifications were made to the surge line after license renewal and are dispositioned to not impact this Appendix L evaluation:

- The Unit 1 hot leg surge nozzle had a structural weld overlay (SWOL) installed and is screened out by the revised screening performed by others.
- The Unit 1 pressurizer surge nozzle, safe end, and forged elbow adjacent to the pressurizer surge nozzle were replaced and are addressed by others in a separate evaluation.
- The Unit 2 pressurizer surge nozzle had a SWOL installed and is screened out by the revised screening performed by others.
- The Unit 2 hot leg surge nozzle had a SWOL installed and is being addressed in a separate evaluation performed by others.

The revised screening and separate evaluations by others were not reviewed for this Appendix L evaluation, and Florida Power & Light will reconcile this Appendix L evaluation with the revised screening and separate evaluations by others for SLR.

The revised Appendix L evaluation for subsequent license renewal [4] evaluated the elbow adjacent to the hot leg surge nozzle, which bounds the surge lines for both Units 1 and 2. The revised evaluation uses the same design inputs (i.e., surge line geometry, design transients, piping loads, etc.) [3, Section 4.0] and stress analysis [3, Section 5.0] as the previous Appendix L evaluation with the following technical changes:

1. For subsequent license renewal, the CASS base metal of the surge line components was evaluated in a separate evaluation [11] in support of Program X1.M12 for the SLR AMP. As such, the scope of the revised Appendix L flaw tolerance evaluation for

subsequent license renewal is only for the weld metal of the surge line in support of Program X.M1 for the SLR AMP [7]. The St. Lucie in-service inspection program does not inspect the CASS base metal, and thus, only the surge lines welds are inspected for Appendix L.

2. For fatigue crack growth in the weld metal, the initial flaw depth [4, Section 5.2] was determined from the applicable inservice inspection acceptance standard in ASME Code Section XI Table IWB-3410-1 per the Appendix L methodology [1, L-3212].

3. Projected 80-year cycles for the St. Lucie, Units 1 and 2 subsequent license renewal [4] in Table 1 [4, Table 1] were used to establish an estimate of the average number per year for calculating fatigue crack growth.

4. The latest crack growth curves for Type 304 and Type 316 stainless steels [4, Section 2.1] from ASME Code Case N-809 [6] were used for fatigue crack growth. ASME Code Case N-809 has been approved by ASME and has been used in previous Appendix L evaluations for license renewal and subsequent license renewal.

4.0 RESULTS OF REVISED APPENDIX L EVALUATION FOR SUBSEQUENT LICENSE RENEWAL TO EIGHTY YEARS OF OPERATION

The revised Appendix L evaluation for subsequent license renewal [4] evaluated the same stress paths in the weld (i.e., Stress Paths 9 - 12 [4, Figure 2]) of the bounding elbow adjacent to the hot leg surge nozzle as the previous Appendix L evaluation [3].

The revised Appendix L evaluation results are shown in Table 2 [4, Table 5] and concluded that the allowable operating period is 47 years at the bounding surge line weld location (i.e., Stress Path 12 in the weld metal of the elbow adjacent to the hot leg surge nozzle, bounding for both St. Lucie, Units 1 and 2) [4, Table 5]. Furthermore, the bounding evaluation implies that the allowable operating period for every surge line weld is 47 years from the time of the last inspection of that weld for subsequent license renewal.

Following the guidelines of Table L-3420-1 of Appendix L and IWB-2410 of ASME Code, Section XI [1], the inservice inspection interval for every surge line weld including those for the pressurizer surge nozzle and hot leg surge nozzle at St. Lucie, Units 1 and 2 is **ten years** from the time of the last inspection of that weld for subsequent license renewal.

5.0 REFERENCES

1. ASME Boiler & Pressure Vessel Code, Section XI, 2007 Edition with Addenda through 2008.
2. ASME Boiler & Pressure Vessel Code, Section XI, 2001 Edition with Addenda through 2003.
3. Structural Integrity Associates Report No. 1301103.401, Revision 0, "Flaw Tolerance Evaluation of St. Lucie Surge Line Welds Using ASME Code Section XI, Appendix L."
4. Structural Integrity Associates Calculation 2001262.320P, Revision 1, "Flaw Tolerance Evaluation for St. Lucie Nuclear Plant, Units 1 and 2."
5. Westinghouse Letter LTR-SDA-II-20-32-NP, Revision 1, "St. Lucie Units 1 and 2 Subsequent License Renewal: 80-Year Projected Transient Cycles," SI File No. 2001262.201.
6. ASME Code Case N-809, "Reference Fatigue Crack Growth Rate Curves for Austenitic Stainless Steels in Pressurized Water Reactor Environments Section XI, Division 1," Cases the ASME Boiler and Pressure Vessel Code, June 23, 2015.
7. Generic Aging Lessons Learned for Subsequent License Renewal (GALL-SLR) Report, NUREG-2191, U. S. Nuclear Regulatory Commission, July 2017. [ADAMS Accession No. ML17187A204].
8. Generic Aging Lessons Learned (GALL) Report, NUREG-1801, Revision. 2, U. S. Nuclear Regulatory Commission, December 2010. [ADAMS Accession No. ML103490041].
9. "Cast Austenitic Stainless Steel (CASS) Aging Management Program, St. Lucie Plant," FP&L Administrative Procedure No. ADM-17.36, Revision No. 2, December 3, 2019.
10. *Materials Reliability Program: Technical Basis for ASME Section XI Code Case on Flaw Tolerance Evaluation of Cast Austenitic Stainless Steel (CASS) Piping (MRP-362).* EPRI, Palo Alto, CA: 2013. 3002000672.
11. Structural Integrity Associates Report No. 2001262.402, Revision 1, "Flaw Tolerance Evaluation of St. Lucie Units 1 and 2 CASS Components for SLR."

Structural Integrity Associates, Inc.
info@structint.com 1-877-4SI-POWER structint.com

Table 1. Projected 80-Year Cycles for Subsequent License Renewal

Source: Revised Appendix L Evaluation [4, Table 1]

Description	Projected Cycles (80 years)
Plant Heatup	143(2)
Plant Cooldown	141(2)
Plant Loading A	1200(3)
Plant Loading B	1200(3)
Plant Unloading A	1200(3)
Plant Unloading B	1200(3)
10% Step Increase	520(3)
10% Step Decrease	520(3)
Reactor Trip, Loss of Flow, Loss of Load	114(2)
Hydrostatic Test	6(2)
Leak Test Up	5(2)
Leak Test Down	5(2)
Low Pressure Stratification at Δ320°F	42(1)
High Pressure Stratification at Δ320°F	42(1)
Low Pressure Stratification at Δ250°F	214(1)
High Pressure Stratification at Δ250°F	214(1)
Low Pressure Stratification at Δ200°F	228(1)
High Pressure Stratification at Δ200°F	228(1)
Low Pressure Stratification at Δ150°F	286(1)
High Pressure Stratification at Δ150°F	286(1)
Hot Standby Stratification at Δ90°F	50170(1)
OBE	80(4)

Notes:

(1) Stratification cycles are scaled to the Plant Heatup cycles. Since the 60-year projected Plant Heatup cycles [3, Table 7-1] are the same as the 80-year projected Plant Heatup cycles [5, Table 1], these values are unchanged from Reference [3, Table 7-1].
(2) Transient cycles are based on 80-year projected cycles for St. Lucie, Units 1 and 2 SLR [5]. The projected cycles for Unit 1 are higher than those of Unit 2 and are therefore, considered bounding for both units.
(3) 80-year projections are calculated by scaling 60-year projections [3, Table 7-1] by a factor of 80/60.
(4) Two OBE events with forty internal cycles each are assumed for a total of eighty projected cycles over the 80-year plant life [4, Assumption 8].

Table 2. Crack Growth Results for Revised Appendix L Evaluation for St. Lucie Units 1 and 2 Surge Line for Subsequent License Renewal

Source: Revised Appendix L Evaluation [4, Table 4]

Analysis Section Number (ASN) (Note 1)	Flaw Configuration (Note 2)	Appendix L Calculated Aspect Ratio	Initial Flaw Size, Acceptable Standards Flaw Size Table Section XI Table IWB-3410-1 (a/t)	Final Flaw Size (a/t)	Maximum Allowable End-of-Evaluation Flaw Size (a/t)	Allowable Operating Period (years)
Stress Path P9	360-Degree Circumferential Flaw	N/A	0.1097	0.2197	0.2214	55
Stress Path P10	360-Degree Circumferential Flaw	N/A	0.1097	0.2195	0.2214	73
Stress Path P11	360-Degree Circumferential Flaw	N/A	0.1097	0.2180	0.2214	51
Stress Path P12	360-Degree Circumferential Flaw	N/A	0.1097	0.2174	0.2214	47

Notes:

(1) Stress paths are in the weld of the elbow adjacent to the hot leg surge nozzle. The location has been identified as the sentinel location for the surge line of both Units 1 and 2.
(2) A 360-degree circumferential flaw bounds a semi-elliptical axial flaw and a semi-elliptical circumferential flaw.

Prepared by:

Kevin K. L. Wong
Consultant

7/15/21
Date

Reviewed by:

Garivalde S. Dominguez
Engineer

7/15/21
Date

Approved by:

David A. Gerber
Senior Associate

7/15/21
Date

cc: Terry J. Herrmann, Structural Integrity Associates
Tim D. Gilman, Structural Integrity Associates